ISSN: 2152-7385 Volume 6, Number 2, February 2015

Scientific Research Publishing

Applied Mathematics

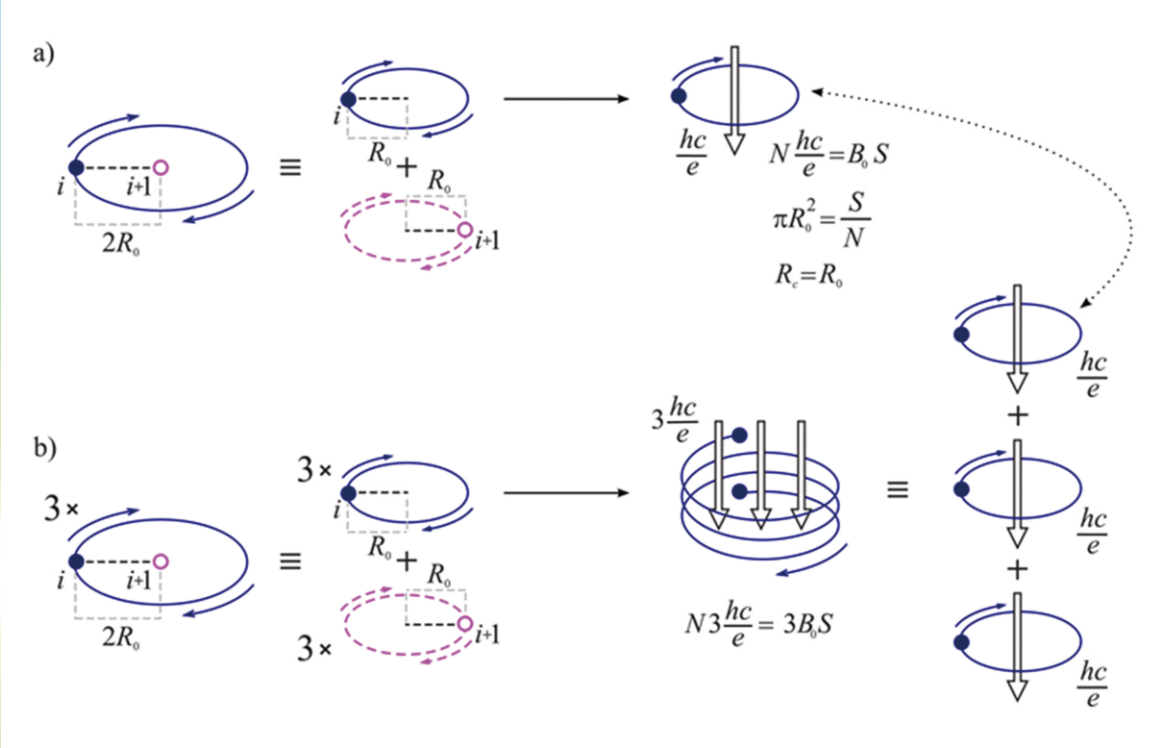

ISSN: 2152-7385

www.scirp.org/journal/am

Journal Editorial Board

ISSN Print: 2152-7385 ISSN Online: 2152-7393

http://www.scirp.org/journal/am

Editor-in-Chief

Applied Mathematics, 2015, 6, 221-446
Published Online February 2015 in SciRes. http://www.scirp.org/journal/am

Scientific Research Publishing

Table of Contents

Volume 6 Number 2 February 2015

Applied Mathematics, 2015, 6, 221-446
Published Online February 2015 in SciRes. http://www.scirp.org/journal/am

The figure on the front cover is from the article published in Applied Mathematics, 2015, Vol. 6, No. 2, pp. 345-358 by Janusz Jacak, Patrycja Łydżba and Lucjan Jacak.

Applied Mathematics (AM)

Journal Information

SUBSCRIPTIONS

The *Applied Mathematics* (Online at Scientific Research Publishing, www.SciRP.org) is published monthly by Scientific Research Publishing, Inc., USA.

Subscription rates:

Print: $89 per copy.
To subscribe, please contact Journals Subscriptions Department, E-mail: sub@scirp.org

SERVICES

Advertisements
Advertisement Sales Department, E-mail: service@scirp.org

Reprints (minimum quantity 100 copies)
Reprints Co-ordinator, Scientific Research Publishing, Inc., USA.
E-mail: sub@scirp.org

COPYRIGHT

PRODUCTION INFORMATION

For manuscripts that have been accepted for publication, please contact:
E-mail: am@scirp.org

Applied Mathematics, 2015, 6, 221-227
Published Online February 2015 in SciRes. http://www.scirp.org/journal/am
http://dx.doi.org/10.4236/am.2015.62021

Scientific Research Publishing

Information Worth of MinMaxEnt Models for Time Series

Aladdin Shamilov[1], Cigdem Giriftinoglu[1,2]

[1]Department of Statistics Anadolu University, Eskisehir, Turkey
[2]Department of Economics, University of Illinois, Urbana-Champaign, USA
Email: asamilov@anadolu.edu.tr, cgiriftinoglu@anadolu.edu.tr, giriftin@illinois.edu

Received 9 January 2015; accepted 27 January 2015; published 3 February 2015

Abstract

In this study, by starting from Maximum entropy (MaxEnt) distribution of time series, we introduce a measure that quantifies information worth of a set of autocovariances. The information worth of autocovarience is measured in terms of entropy difference of MaxEnt distributions subject to different autocovariance sets due to the fact that the information discrepancy between two distributions is measured in terms of their entropy difference in MaxEnt modeling. However, MinMaxEnt distributions (models) are obtained on the basis of MaxEnt distributions dependent on parameters according to autocovariances for time series. This distribution is the one which has minimum entropy and maximum information out of all MaxEnt distributions for family of time series constructed by considering one or several values as parameters. Furthermore, it is shown that as the number of autocovariances increases, the entropy of approximating distribution goes on decreasing. In addition, it is proved that information worth of each model defined on the basis of MinMaxEnt modeling about stationary time series is equal to sum of all possible information increments corresponding to each model with respect to preceding model starting with first model in the sequence of models. The fulfillment of obtained results is demonstrated on an example by using a program written in Matlab.

Keywords

Maximum Entropy Distribution, Time Series, Estimation of Missing Values, MinMaxEnt Distribution, Information Worth

1. Introduction

In many instances, the type of data available for modeling and that used for optimization is a set of observations measured over time of system variable(s) of interest [1]-[4]. A time series stated as only one realization of a

stochastic process is a set of data measured through time. In many areas from engineering to economics, patterns of time series are encountered. It is difficult to find a science program not required to study with a data set in form of time series. The characteristic property of a time series is that its future behavior can not be exactly estimated. It is not uncommon in economic analysis to develop a model and perform empirical analysis by assuming that economic agents make decisions based on a set of available information [5]. In empirical analyses, however, the information is usually designated by a generic information set $\mathbb{S}$. There is no attempt to quantify the amount of information in $\mathbb{S}$. A quantification of the worth of such a set would not be an easy task even if one could identify all elements of $\mathbb{S}$ [6]. In this paper, we view the flow of information to a stochastic process from the autocovariance sets and consider measuring the amount of information when $\mathbb{S}$ is a set which consists of autocovariances obtained from the time series. For this reason, it is concerned with the analysis of the ordered data using the principle of maximum entropy when the information about the times series is given by autocovariances up to a lag m. According to the maximum entropy approach, given time series can be viewed as single trial from a stochastic process that is stationary up to its second-order statistics and has a zero mean. It is known that MaxEnt distribution of an observed time series is determined as a multivariate normal distribution whose dimension is equal to the number of observations [1]. By virtue of the entropy of normal distribution, entropy optimization (EO) functional is constructed as $H_{\max}$. It can be shown that as the number of constraints generated by autocovariances increases, value of $H_{\max}$ decreases. In this investigation, firstly MaxEnt distribution for stationary time series subject to constraints generated by autocovariances set $\{r_0, r_1, \cdots, r_m\}$ is considered. It is proved that as number of lags of successive autocovariances increases, the entropy value of this distribution goes on decreasing but its information worth goes on increasing. Furthermore, by starting from MaxEnt distribution dependent on parameters, MinMaxEnt distribution which has minimum entropy and maximum information out of all MaxEnt distributions is defined. It should be noted that MinMaxEnt and MaxMaxEnt distributions as solutions of Generalized Entropy Optimization (GEO) problem firstly are defined and generally investigated in [7]-[9]. In [10], GEO distribution dependent on parameters in time series is introduced and via this distribution an estimation method of missing value is proposed. In this study, it is shown that entropy value and information worth of MinMaxEnt distribution obtained on the bases of MaxEnt distribution dependent on parameters has the same above expressed properties at each fixed value of parameters as MaxEnt distribution. In addition, it is proved that information worth of each model defined on the basis of MinMaxEnt modeling about stationary time series is equal to the sum of all possible information increments corresponding to each model with respect to preceding model starting with first model in the sequence of models. The fulfillment of obtained results is demonstrated on an example by the use of a program written in Matlab.

2. Information Worth of Autocovariances Set in MaxEnt Modeling

In this section, MaxEnt distributions according to different number of autocovariances are considered and it is proved that the entropy values of these distributions constitute a monotonically decreasing sequence when the number of autocovariances increases. Moreover it is shown that the information generated by autocovariances set is expressed as sum of information worth of each autocovariance taken separately.

Theorem 1. *Let* $r_0, r_1, \cdots, r_m$ *be autocovariances with* $0,1,\cdots,m$ *lags of observed stationary time series* $\{y_0, y_1, \cdots, y_N\}$, $P_{r_k}(y)$ *be MaxEnt distribution subject to constraints generated by autocovariances set* $\{\mathbf{r}_k\} = \{r_0, r_1, \cdots, r_k\}$, $k = 1, \cdots, m$; $m < N$ *and* $H_{\max}(r_k)$ *be the entropy value of this distribution. Then, entropy values of mentioned MaxEnt distributions form a monotonically decreasing sequence of the following form*:

$$H_{\max}(r_0) > H_{\max}(r_1) > H_{\max}(r_2) > \cdots > H_{\max}(r_m) \tag{1}$$

Proof. The Shannon entropy measure subject to constraints generated by autocovariances $r_0, r_1, \cdots, r_m$ with $0,1,\cdots,m$ of stationary time series $\{y_0, y_1, \cdots, y_N\}$ is multivariate normal [1]. Therefore by increasing of the number of k of autocovariances vector $\{\mathbf{r}_k\} = \{r_0, r_1, \cdots, r_k\}$, the conditions to maximize Shannon measure is increased and the domain of entropy measure becomes narrow. Consequently, entropy value of $H_{\max}(r_k)$ is strongly decreased and the inequalities (1) are satisfied. Theorem 1 is proved.

If we denote by $I(r_k)$ information worth of autocovariance r_k, due to the fact that the information discrepancy between two distributions is measured in terms of their entropy difference in MaxEnt modeling, then

$$I(r_k) = H_{\max}(r_{k-1}) - H_{\max}(r_k), \quad k = 1, \cdots, m. \tag{2}$$

Furthermore, if information worth generated by autocovariances set $\{r_1,\cdots,r_k\}$ in the aggregate is denoted by $I(r_1,\cdots,r_k)$, $k=1,\cdots,m$, then

$$I(r_1,\cdots,r_k)=H_{\max}(r_0)-H_{\max}(r_k). \tag{3}$$

Remark 1. *The information $I(r_1,\cdots,r_k)$, $k=1,\cdots,m$, generated by autocovariances set $\{r_1,\cdots,r_k\}$ is expressed as sum of information worths of each autocovariances taken separately,*

$$I(r_1,\cdots,r_k)=I(r_1)+\cdots+I(r_k). \tag{4}$$

From (3) by virtue of formula (2) follows

$$\begin{aligned} I(r_1,\cdots,r_k) &= H_{\max}(r_0)-H_{\max}(r_k)\\ &= H_{\max}(r_0)-H_{\max}(r_1)+H_{\max}(r_1)-H_{\max}(r_2)+\cdots+H_{\max}(r_{k-1})-H_{\max}(r_k)\\ &= I(r_1)+\cdots+I(r_k), \end{aligned}$$

consequently

$$I(r_1,\cdots,r_k)=I(r_1)+\cdots+I(r_k).$$

3. Information Worth of Dependent on Parameters

In this section, according to different number of autocovariances MaxEnt distributions dependent on parameters are considered and it is proved that at each value of parameter, these distributions and their entropies possess the same properties as in section 2.

Theorem 2. *Let $P_{r_k}(y)$ be MaxEnt distribution generated by autocovariances set $\{r_0,r_1,\cdots,r_m\}$ of given stationary time series $\{y_0,\cdots,y_{s-1},\gamma,y_{s+1},\cdots,y_N\}$ with missing value $\gamma\in[\alpha,\beta]$, where $\alpha=\min_{j\neq i}\{y_j\}$, $\beta=\max_{j\neq i}\{y_j\}$. Since $r_0,r_1,\cdots,r_m$ depend on γ, MaxEnt distribution $P_{r_k}(y)$ is also dependent on γ. Thereafter, autocovariances set $\{r_0,r_1,\cdots,r_m\}$ will be represented as $r_0(\gamma),\cdots,r_m(\gamma)$, MaxEnt distribution as $P_{r_k(\gamma)}(y)$ and entropy of this distribution as $H_{\max}(r_k(\gamma))$. Thus, we have a family of time series dependent on γ.*

Between entropy values $H_{\max}(r_k(\gamma))$ of MaxEnt distributions $P_{r_k(\gamma)}(y)$, $k=0,1,\cdots,m$ the following inequalities are fulfilled:

$$H_{\max}(r_0(\gamma))>H_{\max}(r_1(\gamma))>H_{\max}(r_2(\gamma))>\cdots>H_{\max}(r_m(\gamma)) \tag{5}$$

In other words, entropy values of MaxEnt distributions dependent on γ constitute a monotonically decreasing sequence.

Proof. According to Theorem 1, entropy values $H_{\max}(r_k)$ of MaxEnt distributions form a monotonically decreasing sequence of the form (1). Since $r_0(\gamma),\cdots,r_m(\gamma)$ depend on γ. Consequently, inequalities (5) are satisfied. Theorem 2 is proved.

Information worth $I(r_k(\gamma))$ of autocovariance r_k dependent on γ is determined by the following equation similarly to (2),

$$I(r_k(\gamma))=H_{\max}(r_{k-1}(\gamma))-H_{\max}(r_k(\gamma)),\ k=1,\cdots,m. \tag{6}$$

Then, information worth generated by autocovariances set $\{r_1(\gamma),\cdots,r_k(\gamma)\}$ is denoted by $I(r_1(\gamma),\cdots,r_k(\gamma))$, $k=1,\cdots,m$, and

$$I(r_1(\gamma),\cdots,r_k(\gamma))=H_{\max}(r_0(\gamma))-H_{\max}(r_k(\gamma)),\ k=1,\cdots,m. \tag{7}$$

Remark 2. *The information $I(r_1(\gamma),\cdots,r_k(\gamma))$, $k=1,\cdots,m$, generated by autocovariances set $\{r_1(\gamma),\cdots,r_k(\gamma)\}$ is expressed as sum of information worths of each autocovariances taken separately,*

$$I(r_1(\gamma),\cdots,r_k(\gamma))=I(r_1(\gamma))+\cdots+I(r_k(\gamma)). \tag{8}$$

From (7) by virtue of formula (6) follows

$$\begin{aligned} I\left(r_1(\gamma),\cdots,r_k(\gamma)\right) &= H_{\max}\left(r_0(\gamma)\right)-H_{\max}\left(r_1(\gamma)\right) \\ &= H_{\max}\left(r_0(\gamma)\right)-H_{\max}\left(r_1(\gamma)\right)+H_{\max}\left(r_1(\gamma)\right)-H_{\max}\left(r_2(\gamma)\right) \\ &\quad +\cdots+H_{\max}\left(r_{k-1}(\gamma)\right)-H_{\max}\left(r_k(\gamma)\right) \\ &= I\left(r_1(\gamma)\right)+\cdots+I\left(r_k(\gamma)\right) \end{aligned}$$

$$I\left(r_1(\gamma),\cdots,r_k(\gamma)\right) = I\left(r_1(\gamma)\right)+\cdots+I\left(r_k(\gamma)\right).$$

4. Information Worth of MinMaxEnt Models Dependent on Autocovariances

In this section, MinMaxEnt distributions (models) are obtained on the basis of MaxEnt distributions dependent on parameters and it is shown that as the number of autocovariances k goes on increasing, the entropy of approximating distribution (model) goes on decreasing. Furthermore, it is proved that information worth of each model defined on the basis of MinMaxEnt modeling about stationary time series is equal to the sum of all possible information increments corresponding to each model with respect to preceding model starting with first model in the sequence of models.

Theorem 3. *Let* $P_{r_k(\gamma)}(y)$ *be MaxEnt distribution generated by autocovariances set* $\{r_0(\gamma), r_1(\gamma),\cdots,r_k(\gamma)\}$ *of given stationary time series* $\{y_0,\cdots,y_{s-1},\gamma,y_{s+1},\cdots,y_N\}$ *with parameter* $\gamma\in[\alpha,\beta]$, *at position s, where* $\alpha=\min_{j\neq i}\{y_j\}$, $\beta=\max_{j\neq i}\{y_j\}$ *and entropy value of this distribution be* $H_{\max}\left(r_k(\gamma)\right)$. *Moreover, let* γ_k, $k=1,\cdots,m$ *be the value* $\gamma_k\in[\alpha,\beta]$ *realizing MinMaxEnt distribution* $P_{r_k(\gamma)}(y)$, *in other words*

$$\min_{\gamma\in[\alpha,\beta]} H_{\max}\left(r_k(\gamma)\right)=H_{\max}\left(r_k(\gamma_k)\right),\ k=1,\cdots,m \tag{9}$$

Then, between entropy values of MinMaxEnt distributions the inequalities

$$H_{\max}\left(r_0(\gamma_0)\right)>H_{\max}\left(r_1(\gamma_1)\right)>H_{\max}\left(r_2(\gamma_2)\right)>\cdots>H_{\max}\left(r_m(\gamma_m)\right) \tag{10}$$

are satisfied.

Proof. According to Theorem 2 *for any* γ, $\gamma\in[\alpha,\beta]$, *the inequalities* (5) *hold. For this reason,*

$$\min_{\gamma\in[\alpha,\beta]} H_{\max}\left(r_0(\gamma)\right)=H_{\max}\left(r_0(\gamma_0)\right)>H_{\max}\left(r_1(\gamma_0)\right) \tag{11}$$

On the other hand,

$$\min_{\gamma\in[\alpha,\beta]} H_{\max}\left(r_1(\gamma)\right)=H_{\max}\left(r_1(\gamma_1)\right) \tag{12}$$

$$\min_{\gamma\in[\alpha,\beta]} H_{\max}\left(r_1(\gamma_0)\right)>H_{\max}\left(r_1(\gamma_1)\right) \tag{13}$$

From inequality (11) *by taken into account* (12) *and* (13), *the inequality*

$$H_{\max}\left(r_0(\gamma_0)\right)>H_{\max}\left(r_1(\gamma_1)\right) \tag{14}$$

is got. If this process is consecutively repeated, then it is easy to get to the inequalities (10). *Theorem* 3 *is proved.*

Remark 3. *By using Theorem* 3, *it is possible to obtain information worth of MinMaxEnt distributions with the different number of autocovariances.*

By using Theorem 3, it is possible to obtain information worth of MinMaxEnt distributions with the different number of autocovariances. However, in order to simplify the description of results, we introduce the following symbols. Let Y_k, $(k=1,\cdots,m)$ be a model representing MinMaxEnt distribution $P_{\mathbf{r}_k(\gamma_k)}(\mathbf{y})$ for a stationary time series $\{y_0,\cdots,y_{s-1},\gamma,y_{s+1},\cdots,y_N\}$. Moreover, let $I(k)$, $(k=1,\cdots,m)$ be the information contained by model Y_k about this time series, then

$$I^{(k)}=H\left(Y_0\right)-H\left(Y_k\right),\ k=1,\cdots,m \tag{15}$$

and

$$I^{(k-1)} = H(Y_0) - H(Y_{k-1}),\ k = 1, \cdots, m \tag{16}$$

From (15) and (16),

$$\begin{aligned} I^{(k)} - I^{(k-1)} &= H(Y_0) - H(Y_k) - \left(H(Y_0) - H(Y_{k-1})\right) \\ &= H(Y_{k-1}) - H(Y_k) = I_k,\ k = 1, \cdots, m \\ &= I_k \end{aligned}$$

$$I^{(k)} - I^{(k-1)} = I_k \tag{17}$$

where I_k is the information increment corresponding to each model Y_k with respect to preceding model Y_{k-1}. By virtue of the obtained results, the following theorem can be asserted.

Theorem 4. *Information worth $I^{(m)}$ of model Y_m defined on the basis of MinMaxEnt modelling about stationary time series $\{y_0, \cdots, y_{s-1}, \gamma, y_{s+1}, \cdots, y_N\}$ is equal to sum of all possible information increments $I_k = I^{(k)} - I^{(k-1)} = H(Y_{k-1}) - H(Y_k)$, $k = 1, \cdots, m$ corresponding to each model with respect to preceding model Y_{k-1} starting with first model $(1 \le k \le m)$ in the sequence of models $Y_0, Y_1, \cdots, Y_m$.*

Proof. By using the new notations $Y_0, Y_1, \cdots, Y_m$ inequalities (10) *can be represented as*

$$H(Y_0) > H(Y_1) > H(Y_2) > \cdots > H(Y_m) \tag{18}$$

Equation (10) *shows that as the number of autocovariances k increases, the entropy of approximating distribution* (*model*) *goes on decreasing but it never goes below the entropy of probability distribution satisfying the same conditions as MinMaxEnt distribution. According to* (15) *and* (17)

$$\begin{aligned} I^{(m)} &= H(Y_0) - H(Y_1) \\ &= H(Y_0) - H(Y_1) + H(Y_1) - H(Y_2) + \cdots + H(Y_{m-1}) - H(Y_m) \\ &= I_1 + I_2 + \cdots + I_m \end{aligned}$$

or

$$I^{(m)} = I_1 + I_2 + \ldots + I_m \tag{19}$$

According to (18) *in* (19), $I_k > 0$, $k = 1, \cdots, m$. *Theorem* 4 *is proved.*

5. Applications

The developed MinMaxEnt models $Y_0, Y_1, \cdots, Y_m$ can be applied to estimate the missing value in time series. According to Theorem 4, information worth generated by Y_m is greater than information worth generated by Y_{m-1}. Consequently, γ_m generating the model Y_m is the better estimation than γ_{m-1} generating the model Y_{m-1} in the sense of information worth. On an example it is shown that mentioned estimated value is the best also in the sense of mean square error (MSE). To realize required operations, a program in MATLAB is written. For this purpose, we have considered data set generated from autoregressive process $AR(4)$ as follows:

$$X_t = 1.90X_{t-1} - 2.01X_{t-2} + 1.84X_{t-3}6 - 0.80X_{t-4} + \varepsilon_t,\ \varepsilon_t \sim N(0, 0.5) \tag{20}$$

and the data set is given in **Table 1**. By using the data in **Table 1**, estimations based on MinMaxEnt models are obtained for missing values in each position via constraints generated by r_0, r_1, r_2 autocovariances and r_0, r_1, r_2, r_3 autocovariances. From **Table 1** it is seen that, MinMaxEnt estimations γ_{3t} determined by the set consisting of r_0, r_1, r_2, r_3 autocovariances are better than MinMaxEnt estimations γ_{2t} determined by the set consisting of r_0, r_1, r_2 autocovariances in each position. Moreover, $(MSE)_{r_0, r_1, r_2, r_3}$ calculated by MinMaxEnt estimations with autocovariances is 0.2564 and it is lower than $(MSE)_{r_0, r_1, r_2} = 3.6605$ calculated by MinMaxEnt estimations with r_0, r_1, r_2 autocovariances and $(MSE)_{r_0, r_1} = 8.0426$ calculated by MinMaxEnt estimations with r_0, r_1 autocovariances.

Furthermore, in **Table 2** the entropy and information worth of different autocovariance sets are given. These quantities calculated from the data set verify Theorem 4. It can be seen that as the number of constraints which is generated by autocovariances increases, the value of $H_{\max}$ decreases.

Table 1. The data generated from AR(4) and its estimations with different autocovariance sets.

t	$X(t)$	γ_{2t}	γ_{3t}	t	$X(t)$	γ_{2t}	γ_{3t}
1	−7.6164	−3.7049	−4.5863	26	−2.5809	−0.4340	−2.2861
2	−7.9251	−5.9152	−8.2637	27	−1.8546	0.0249	−1.8094
3	−2.3466	−3.1335	−1.5912	28	4.7113	2.7239	4.5856
4	−1.0788	−2.6884	−1.1953	29	5.2406	2.9464	5.1481
5	−6.3050	−4.4728	−6.1961	30	−1.0943	0.4262	−0.8107
6	−7.7206	−4.9192	−7.7193	31	−2.4052	−0.1378	−2.3785
7	−2.2376	−2.6242	−2.2308	32	4.0709	3.0661	4.3309
8	0.33865	−1.6810	−0.0090	33	7.9505	4.9433	7.7333
9	−4.5611	−3.2248	−4.3121	34	3.5777	3.7644	3.5249
10	−7.3435	−4.7417	−7.6510	35	0.8252	3.1348	0.8623
11	−3.3723	−2.9111	−3.2169	36	−2.4052	−0.1378	−2.3785
12	0.13548	−1.8088	−0.0447	37	4.0709	3.0661	4.3309
13	−3.7786	−3.4259	−3.7174	38	7.9505	4.9433	7.7333
14	−8.2637	−5.3028	−8.1113	39	3.5777	3.7644	3.5249
15	−5.2458	−4.0749	−4.8305	40	0.8252	3.1348	0.8623
16	−0.2230	−2.2286	−0.1069	41	11.292	8.1259	11.159
17	−2.1272	−2.2977	−1.8858	42	7.5889	6.6536	7.3807
18	−5.4257	−2.6645	−5.2509	43	3.3139	5.2987	3.5224
19	−1.0920	−0.1997	−1.3106	44	6.5842	6.0319	6.2192
20	5.5526	3.1233	5.2295	45	10.412	7.5539	10.267
21	4.5110	3.1064	3.9525	46	7.2051	6.1065	7.1059
22	−0.8572	1.2503	−0.9899	47	2.0869	3.6081	2.1044
23	0.0716	1.1921	−0.2413	48	3.1468	3.5739	3.1619
24	4.7447	2.7488	4.8959	49	7.1153	5.0748	7.1544
25	3.4163	1.6973	3.3217	50	5.9239	4.4184	4.9659

Table 2. Entropy and information worth of different autocovariance sets.

$H_{\max}(r_0)$	$H_{\max}(r_0,r_1)$	$H_{\max}(r_0,r_1,r_2)$	$H_{\max}(r_0,r_1,r_2,r_3)$	$I(r_1)$	$I(r_2)$	$I(r_3)$	$I(r_1,r_2,r_3)$
171.94	155.74	153.80	117.37	16.20	1.94	36.43	54.57

6. Conclusions

In this study, the following results are established.

- MaxEnt distributions according to different number of autocovariances are considered and it is proved that the entropy values of these distributions constitute a monotonically decreasing sequence when the number of autocovariances increases. Moreover it is shown that the information generated by autocovariances set is expressed as sum of information worth of each autocovariance taken separately.
- According to different number of autocovariances, MaxEnt distributions dependent on parameters are considered and it is proved that at each value of parameter these distributions and their entropies possess the

same properties as the MaxEnt distributions.

- MinMaxEnt distributions (models) are obtained on the basis of MaxEnt distributions dependent on parameters and it is shown that as the number of autocovariances k goes on increasing, the entropy of approximating distribution (model) goes on decreasing. Furthermore, it is proved that information worth of each model defined on the basis of MinMaxEnt modeling about stationary time series is equal to the sum of all possible information increments corresponding to each model with respect to preceding model starting with first model in the sequence of models.
- Information worth of autocovariances in time series and values generating MinMaxEnt distributions can be applied in solving many problems. One of the mentioned problems is the problem of estimation of missing value in time series. It is proved that the value generating MinMaxEnt distribution independence on position represents the best estimation of the missing value in the sense of information worth.
- The fulfillment of the obtained results is demonstrated on an example by using a program written in Matlab.

Acknowledgements

We thank the Editor and the referee for their comments. This support is greatly appreciated.

References

[1] Kapur, J.N. and Kesavan, H.K. (1992) Entropy Optimization Principles with Applications. Academic Press, New York.

[2] Wei, W.S. (2006) Time Series Analysis, Univariate and Multivariate Methods. Pearson, United States.

[3] Box, G.E.P. and Jenkins, G. (1976) Time Series Analysis: Forecasting and Control. Holden-Day, United States.

[4] Little, R. and Rubin, D. (1987) Statistical Analysis with Missing Data. Wiley, New York.

[5] Pourahmadi, M. and Soofi, E. (1998) Prediction Variance and Information Worth of Observations in Time Series. *Journal of Time Series Analysis*, **21**, 413-434. http://dx.doi.org/10.1111/1467-9892.00191

[6] Pourahmadi, M. (1989) Estimation and Interpolation of Missing Values of a Stationary Time Series. *Journal of Time Series Analysis*, **10**, 149-169. http://dx.doi.org/10.1111/j.1467-9892.1989.tb00021.x

[7] Shamilov, A. (2006) A Development of Entropy Optimization Methods. *WSEAS Transaction on Mathematics*, **5**, 568-575.

[8] Shamilov, A. (2007) Generalized Entropy Optimization Problems and the Existence of Their Solutions. *Physica A: Statistical Mechanics and its Applications*, **382**, 465-472. http://dx.doi.org/10.1016/j.physa.2007.04.014

[9] Shamilov, A. (2010) Generalized Entropy Optimization Problems with Finite Moment Functions Sets. *Journal of Statistics and Management Systems*, **13**, 595-603,. http://dx.doi.org/10.1080/09720510.2010.10701489

[10] Shamilov, A. and Giriftinoglu, C. (2010) Generalized Entropy Optimization Distributions Dependent on Parameter in Time Series. *WSEAS Transactions on Information Science and Applications*, **1**, 102-111.

Applied Mathematics, 2015, 6, 228-234
Published Online February 2015 in SciRes. http://www.scirp.org/journal/am
http://dx.doi.org/10.4236/am.2015.62022

Setting the Linear Oscillations of Structural Heterogeneity Viscoelastic Lamellar Systems with Point Relations

Ismail Ibrahimovich Safarov, Maqsud Sharipovich Akhmedov, Zafar Ihterovich Boltaev

Bukhara Technological-Institute of Engineering, Bukhara, Republic of Uzbekistan
Email: maqsud.axmedov.1985@mail.ru, maqsud.axmedov.1985@mail.ru, lazizbek.axmedov.2011@mail.ru

Received 9 January 2015; accepted 27 January 2015; published 3 February 2015

Abstract

The paper solves the problem of the variation formulation of the steady-linear oscillations of structurally inhomogeneous viscoelastic plate system with point connections. Under the influence of surface forces, range of motion and effort varies harmonically. The problem is reduced to solving a system of algebraic equations with complex parameters. The system of inhomogeneous linear equations is solved by the Gauss method with the release of the main elements in columns and rows of the matrix. For some specific problems, the amplitude-frequency characteristics are obtained.

Keywords

Plates, The Ability to Move, The Complex Amplitude

1. Introduction

Currently, in many technical designs there are widely used shell and plate structures. Thin-walled tubes and panels in real conditions usually interact with other structures and bodies, which are based on resilient supports and also have hinge supports and associated masses. As in [1], we present a generalized interpretation of the statement of the problem of forced oscillations for a certain class of thin deformable bodies, as well as mechanical systems consisting of these elements. Support was adopted from the hinge or of entrapped type that connects elements of the system. The location supports linkages and concentrated masses arbitrarily [2]-[4]. Elements of the system can be both elastic and viscoelastic, on the edge of the elements given by the homogeneous boundary conditions. The case when the operating system on the driving force subordinates to the harmonic law is required to determine the frequency response of the system.

How to cite this paper: Safarov, I.I., Akhmedov, M.S. and Boltaev, Z.I. (2015) Setting the Linear Oscillations of Structural Heterogeneity Viscoelastic Lamellar Systems with Point Relations. *Applied Mathematics*, **6**, 228-234.
http://dx.doi.org/10.4236/am.2015.62022

2. The Mathematical Formulation of the Problem of Forced Vibrations Viscoelastic Systems with Point Connections

Consider a homogeneous isotropic a resilient plate of constant thickness *h*, limited to the size of a rectangular contour *a*, *b*. Suppose on the plate is *Q* dot added mass $M_q\left(q=1,\cdots,Q\right)$ and it is elastically and, accordingly, simply supported rigidly in *L'* and correspondingly *S* internal points. Swivel bearing plate at the point may be combined with jamming in any direction, layout of point masses and in the plane of the plate arbitrarily. The boundary condition on each side of the plate can be one of the following: hinge-support, jamming or free edge. This paper considers the package of plates (consisting of n-plates (n = 1, ···, N)). It is required to determine the steady-linear oscillations of the plate. Assume that the perturbing forces applied to the *n*-mu body have the same frequency but different amplitude; Then they change the law can be written as

$$\overline{P}_{nj}\left(t\right)=\overline{P}_{nj}^{0}\mathrm{e}^{-i\omega t}\left(n=1,\cdots,N,\ j=1,\cdots,J\right), \tag{1}$$

where ω—given real frequency of the disturbing force, $\overline{P}_{nj}^{0}$—Vector amplitude of the disturbing force directed at *j*-th component of the displacement vector $U_{nj}\left(\overline{x},t\right)$, *N*—the number of elements of the system, *J*—number of components of the displacement vector. Assuming the validity of Kirchhoff-Love hypotheses, we write the known from the theory of elasticity relationship between displacements and strains [5]:

$$\varepsilon_x=-z\frac{\partial^2 W}{\partial x^2},\quad \varepsilon_y=-z\frac{\partial^2 W}{\partial y^2},\quad \varepsilon_{xy}=-2z\frac{\partial^2 W}{\partial x\partial y}$$

Here *z*—coordinate of a point in a direction perpendicular to the middle surface, ε_x, ε_y, ε_{xy}—components of the strain tensor of the plate. To describe the relaxation processes occurring in the viscoelastic elements or point connections system, we adopt a linear Boltzmann theory of heredity:

$$\sigma_{mk}^{n}\left(t\right)=E_n\left[\varepsilon_{mk}^{n}\left(t\right)-\int_{-\infty}^{t}R^n\left(t-\tau\right)\varepsilon_{mk}^{n}\left(\tau\right)\mathrm{d}\tau\right], \tag{2}$$

where $R^n\left(t\right)$—relaxation kernel *n*-th viscoelastic element or connection point, E_n—instantaneous modulus of elasticity. To stress was periodic function of time, in a ratio heredity (2) the lower limit of integration taken to be negative infinity. If the lower limit is zero, the voltage will contain a periodic additive which decreases with time. On the influence function $R\left(t-\tau\right)$ the usual requirements imposed inerrability, continuity (except $t=\tau$), fixed sign and monotonicity:

$$R>0,\quad \frac{\mathrm{d}R\left(t\right)}{\mathrm{d}t}\le 0,\quad 0<\int_0^{\infty}R\left(t\right)\mathrm{d}t<1.$$

In contrast to the problems of the natural oscillations [1], the conditions (a little) kernel parameters of relaxation not put.

If $R\left(t\right)=0$, the elastic body. Stress components are equal

$$\begin{aligned}
G_x&=-\frac{E_z}{1-\nu^2}\left[\frac{\partial^2 W}{\partial x^2}+\nu\frac{\partial^2 W}{\partial y^2}\right],\\
G_y&=-\frac{E_z}{1-\nu^2}\left[\frac{\partial^2 W}{\partial y^2}+\nu\frac{\partial^2 W}{\partial x^2}\right],\\
G_{xy}&=G_{yx}=-\frac{E_z}{1-\nu^2}\frac{\partial^2 W}{\partial x\partial y},
\end{aligned} \tag{3}$$

where *E*—Young's modulus, and *v*-Poisson's ratio, which is assumed to be constant. The normal components G_z transverse rupture is small compared to G_x and G_y, therefore believe G_z = 0. The potential energy stored during the elastic deformation of the plate is given by:

$$G=\frac{1}{2}\int\int\int_V\left(G_x\varepsilon_x+G_y\varepsilon_y+G_{xy}\varepsilon_{xy}\right)\mathrm{d}x\mathrm{d}y\mathrm{d}z\ , \tag{4}$$

where *V*—the volume of the plate. Substituting in (4) the values of the components of deformation and stress (2),

(3) and taking into account the potential energy of elastic supports, we obtain

$$G^* = \frac{D}{2}\int_0^a\int_0^b\left[\left(\frac{\partial^2 W}{\partial x^2}+\frac{\partial^2 W}{\partial y^2}\right)^2 - 2(1-\nu)\left(\frac{\partial^2 W}{\partial x^2}\frac{\partial^2 W}{\partial y^2}-\left(\frac{\partial^2 W}{\partial x\partial y}\right)^2\right)\right]\mathrm{d}x\mathrm{d}y + \frac{1}{2}\sum_{l'=1}^{L'} c_1' W^2\left(x^{l'}, y^{l'}\right), \tag{5}$$

here $D = Eh^3\left[12\left(1-\nu^2\right)\right]^{-1}$—stiffness of the plate cylinder, and $C^{l'}x^{l'}$, $y^{l'}$—stiffness and the coordinates of the elastic support. Double integrals in (5) is taken over the surface of the neutral layer. The kinetic energy of the plate, taking into account the added mass is given by

$$T = \frac{\rho h}{2}\int_0^a\int_0^b\left(\frac{\partial W}{\partial t}\right)^2 \mathrm{d}x\mathrm{d}y + \frac{1}{2}\sum_{q=1}^{Q} M_q\left(\frac{\partial W\left(x^q, y^q, t\right)}{\partial t}\right)^2, \tag{6}$$

where ρ—the density of the plate material, x^q, y^q—coordinates q-th associated mass. We formulate the problem in terms of the method of virtual displacements, according to which the sum of the work of all active forces in the possible displacement δU, satisfies the boundary conditions, is equal to zero:

$$\delta A_\sigma + \delta A_u + \delta A_m + \delta A_p = 0 \tag{7}$$

here δA_σ, δA_u, δA_m, δA_p—virtual work of internal forces shell, elastic supports, inertia forces, taking into account the concentrated loads and virtual work surface forces. These works are calculated by the formulas

$$\begin{aligned}
\delta A_\sigma &= -\int_V \sigma_{ij}\delta\varepsilon_{ij}\mathrm{d}v,\\
\delta A_u &= -\sum_{l'=1}^{L'}\sigma_{l'}\delta\varepsilon_{l'},\\
\delta A_m &= -\rho h\int_\Omega \bar{U}\left(X_1, X_2, t\right)\delta\bar{U}\mathrm{d}\Omega - \sum_{q=1}^{Q} M_q\bar{U}\left(X_1^q, X_2^q, t\right)\delta\bar{U},\\
\delta A_p &= \sum_{n=1}^{N}\sum_{j=1}^{J}\bar{P}_{nj}(t)\int_{\Omega_n}\delta U_{nj}\left(\bar{x}, t\right)\mathrm{d}\Omega,
\end{aligned} \tag{8}$$

where ρ, h—density and thickness of the shell, M_q-q-I added mass, L'—number-the elastic supports, Q—the number of additional masses, V, Ω—volume and lateral surface of the shell, σ_{ij}, ε_{ij}—components of stress and strain tensors shell, $\sigma_{l'}$, $\varepsilon_{l'}$—Stress and strain l'-th elastic support, δ—variation on the generalized displacements $\left(\bar{U}, \varepsilon_{ij}, \varepsilon_{l'}\right)$. All terms in Equations (7) are calculated by the formula (8). Steady-state oscillations of n-th element of the system will be sought in the form

$$U_{nj}\left(\bar{x}, t\right) = U_{nj}^0\left(\bar{x}\right)\mathrm{e}^{-i\omega t} \tag{9}$$

where $U_{nj}^0\left(\bar{x}\right)$—complex amplitude of forced oscillations. It is clear that all the generalized coordinates of the system should be changed with a single frequency equal to (ω real) viscoelastic forces. Transform variation equation (9) as well as in [1], *i.e.* substitute in a series of (2), (3), (4), (5), while expressing the deformation of the components of the displacement vector $U_{nj}\left(\bar{x}, t\right)$. Contained in the equation of integral expressions of type (2) by replacing the variable $t-\tau = z$ into the form [6]

$$\int_\infty^t R(t-\tau)\varphi(\tau)\mathrm{d}\tau = \left[\Gamma_c(\omega) + is(\omega)\right]\varphi(t),$$

where $\Gamma^C\left(\omega_R\right) = \int_0^\infty R(\tau)\cos\omega_R\tau\mathrm{d}\tau$, $\Gamma^s\left(\omega_R\right) = \int_0^\infty R(\tau)\sin\omega_R\tau\mathrm{d}\tau$—respectively, the cosine and sine Fourier transforms relaxation kernel material. This will eliminate the function of time $\varphi(t)$, which in this case has the form $\varphi(t) = \mathrm{e}^{-i\omega t}$, obtain the variation equation for the displacement vector. Imposed on the system of rigid connection point, as in the problem of the natural vibrations, made under the sign of the variation by the method of Lagrange multipliers. The final form of the variation equation is as follows:

$$\delta\left\{G\left(U_{nj}^{0}\left(\overline{x}\right),\omega^{2}\right)+F\left(\lambda_{nj}^{s},\kappa_{nj}^{s},\mu_{nj}^{r}\right)\right\}=0\,, \tag{10}$$

where G—total virtual works of the system, and F—kinematic conditions of rigid point constraints imposed on the system.

The task is now formulated as follows:

- Let the driving force $\overline{P}_{nj}\left(t\right)$ satisfies the relation (1);
- Required depending on the frequency of the driving force to find a module of the displacement vector $U_{nj}^{0}\left(\overline{x}\right)$ (the amplitude of the forced oscillations) satisfying Equation (10) and specify the homogeneous boundary conditions. When studies have established processes, the initial conditions are not put here. If necessary, you can define and Lagrange multipliers, the physical meaning of which - the reaction of hard point connections.

3. Evaluation of the Practical Convergence of the Method

In this paper we do not address the question of convergence of the method with a rigorous mathematical point of view, since it is not crucial for the following reasons. Energy approach used in the formulation of the problem is essentially the Ritz method, the convergence is strictly proved, for example, in [7] [8]. Accounting using Lagrange point constraints imposed on the plate, there is also a well-known method of finding a conditional extremum.

4. Construction of Resolving Equations of Linear Problems of Forced Vibrations of Viscoelastic Systems with Point Connections

The solution of the variation Equation (10) is sought in the form of a superposition of orthogonal basis functions. It is proposed that the elements are free from localized masses and all point connections (poles, posts) are known. Then as the desired displacement field satisfies the variation Equation (10) and specify the homogeneous boundary conditions, we assume a finite sum of these fundamental functions:

$$U_{nj}^{0}\left(\overline{x}\right)=\sum_{k=1}^{K}\gamma_{nj}^{k}\Phi_{nj}^{k}\left(\overline{x}\right)\quad\left(n=1,\cdots,N,\ j=1,\cdots,J\right), \tag{11}$$

where γ_{nj}^{k} —unknown coefficients.

After substituting the sum (11) into Equation (10) coefficients γ_{nj}^{k} and Lagrange multipliers λ_{nj}^{s}, κ_{nj}^{s}, μ_{nj}^{r} will be the generalized coordinates. The dimensionality of the system is the same as in the case of free oscillation [1]. In matrix for it can be written as

$$\left(A+\sum_{n=1}^{N_n}f_n\left(\omega\right)A_n^n+\sum_{n=1}^{N-1}\sum_{l=1}^{L_n}f_{ln}\left(\omega\right)A_{ln}^n+\sum_{n=1}^{N-1}\sum_{l'=1}^{L'}f_{l'n}\left(\omega\right)A_{l'n}^n-\omega^2B\right)\overline{\xi}=\overline{\hat{P}}_{nj}^{0}\,. \tag{12}$$

Symbols of all the quantities in the left part of the system of equations (12) coincide with the notation of [1]. The program that implements the algorithm, the formation of all the matrices A, A_n^n, A_{ln}^n, $A_{l'n}^n$, B produced by the same routines that are used in the problem of natural oscillations [1]. Vector-Column $\overline{\hat{P}}_{nj}^{0}$ structurally consists of two sub vectors. If equation (10) is differentiated with respect Lagrange multiplier first λ_{nj}^{s}, κ_{nj}^{s}, μ_{nj}^{r}, them the upper subvector vector $\overline{\hat{P}}^{0}$ will be zero, and its dimension is equal to the total number of Lagrange multipliers. Lower subvector is the vector amplitude of the driving forces $\overline{\hat{P}}_{nj}^{0}$. In formula (9) it is assumed that the disturbing force is distributed nature. Merits will not change if the applied force is concentrated. Then the virtual work space element is replaced by the virtual work of the concentrated force. Ultimately, the change shall be subject only vector amplitudes $\overline{\hat{P}}_{nj}^{0}$, which, apart from the amplitude of a force filled with zeros. The system (12) is solved by the Gauss method with the release of the main elements in columns and rows. Note that the initial system of equations (8) has complex coefficients, so the program that implements the algorithm is written for the general case, *i.e.*, for systems with complex numerical coefficients and complex unknowns. Right side of the system, *i.e.* vector $\overline{\hat{P}}_{nj}^{0}$, must be specified as

$$\overline{\hat{P}}_{nj}^{0}=\overline{RP}_{nj}^{0}+i\overline{IP}_{nj}^{0}\,,$$

where $\overline{RP}_{nj}^{0}$, $\overline{IP}_{nj}^{0}$—the real and imaginary parts of the load vector, and, $\overline{IP}_{nj}^{0}=0$.

The calculated components of the vector of unknowns, are complex quantities, *i.e.* vector $\overline{\xi}'$ represented in the for $\overline{\xi}'=\overline{\xi}_R+i\overline{\xi}_I$. To the amplitude of the forced vibrations and reactions bonds had a real sense, it is necessary to take $\overline{\xi}'=\left|\overline{\xi}\right|$, *i.e.*, as generalized coordinates λ_{nj}^{s}, κ_{nj}^{s}, μ_{nj}^{r}, γ_{nj}^{k} take modules of the corresponding components of the vector $\overline{\xi}$. After this, the components of the displacement vector $U_{nj}^{0}\left(\overline{x}\right)$ unambiguously be identified through γ_{nj}^{k} Formula (11). Substituting the last formula the coordinates of any point of the system, we obtain the vibration amplitude for a given driving frequency ω.

5. Numerical Implementation of the Algorithm for Solving Problems of Steady Oscillations with the Analysis of the Results

This part presents the solution of several problems, which are received and analyzed by the frequency-amplitude characteristics for the displacements of individual points of structurally inhomogeneous viscoelastic systems. The purpose of research is to confirm (or refute) the mechanical effects described in [1]. For this purpose, the distribution of forces perturbing is selected so that the resonant cases of components of the displacement field get values close to their own forms. Definition of a sufficient number of basic functions in approximating the sum is as follows. For a selected point of the system builds the frequency-amplitude characteristics at $K=K_1,K_1+1,\cdots$, where K_1—some fixed positive integer. The process ends after the transition from a $K+1$ results in a change of the resonance curve, which is not more than 1% of the maximum in the vicinity of the resonance, or in any other region of interest.

Problem 1. Consider the design is a package of two parallel square plates with elastic shock absorber and the associated mass. This task determines the frequency-amplitude characteristics of the mechanical system depending on its geometrical parameters. The system is a package of two elastic square plates connected at the center of a weightless viscoelastic damper. Kernel for relaxation absorber selected as

$$R(t)=A\exp\left(-\beta t\right)t^{\alpha-1},$$

where A, β, α—Kernel parameters.

This corresponds to approximately 60% surge creep contribution to the overall deformation of the viscoelastic body under quasi-static loading process. With the damper stiffness is fixed and taken to be 10.

For this case, the kernel parameters as follows: $A=0.078$; $\alpha=0.1$; $\beta=0.05$. In both plates has one attached mass. Plate simply supported along a contour similar to mechanical and geometrical parameters, $E=2\times10^{11}$ н/м^2; $\rho=7.8\times10^{3}$ кг/м^3; $\nu=0.3$; $a=b=0.2$ м; $h=0.001$ м. Weights are equal to each other ($M_1=M_2=0.05$ кг), one of them (M_1) fixed on the bottom plate at a point $x_{M_1}=0.14$ м, $y_{M_1}=0.1$ м, and another (M_2) can move through the central axis of the structure $\left(y_{M_1}=0.1\text{ м}\right)$. As the load harmonic excitation is considered uniformly distributed over the area of the two plates driving force vector R. The amplitude of this force is equated to the unit vector. Depending on the position of the load M_2 were the amplitude of forced oscillations of the system of plates. The amplitudes have been constructed for the central points of the two plates ($x=y=0.1$ m). **Figure 1** shows the case where the mass M_2 located as the point $x_{M_2}=0.02$ м, $y_{M_2}=0.1$ м or $x_{M_2}=0.18$ м, $y_{M_2}=0.1$ м the upper plate. Under these conditions of the masses M_2 frequency-amplitude characteristics of the upper and lower plates are similar and therefore show on the same graph. Given in [1] of Figure 3.1 shows that the damping capacity of the structure at the specified coordinates mass M_2 one and the same. Thus, coincidence plots frequency amplitude characteristics at various locations weight M_2 Figure 3.1 confirms the symmetry [1]. Analysis **Figure 1** shows that when the driving frequency coincides with the natural frequencies ω_1, ω_2 a jump in amplitude as that lower and the upper plates, wherein the absolute value of these resonant amplitude lower and upper plates are different. Here and further the equality of natural and forced frequencies relative, since due to the dissipative properties of the structure of the jump amplitude maximum shifted somewhat to the left of their own (and hence disturbing) frequency. Let us analyze the behavior of the graphs in **Figure 1**. Resonant amplitude of the central points of the two plates takes large values in the case of the first resonance compared to the second. This is because the load applied to the plates at the first resonance is in phase oscillations. Thus, when forced oscillations qualitatively identical displacement field of the central points of the plates at $\omega=\omega_1$ и $\omega=\omega_2$ differ in terms of quantity, *i.e.* in the resonance amplitude. This fact is also consistent with Figure 3.1 [1], in which all and, in particular, in these points, $\left|\omega_I^1\right|<\left|\omega_I^2\right|$. **Figure 2** shows the case when the mass M_2

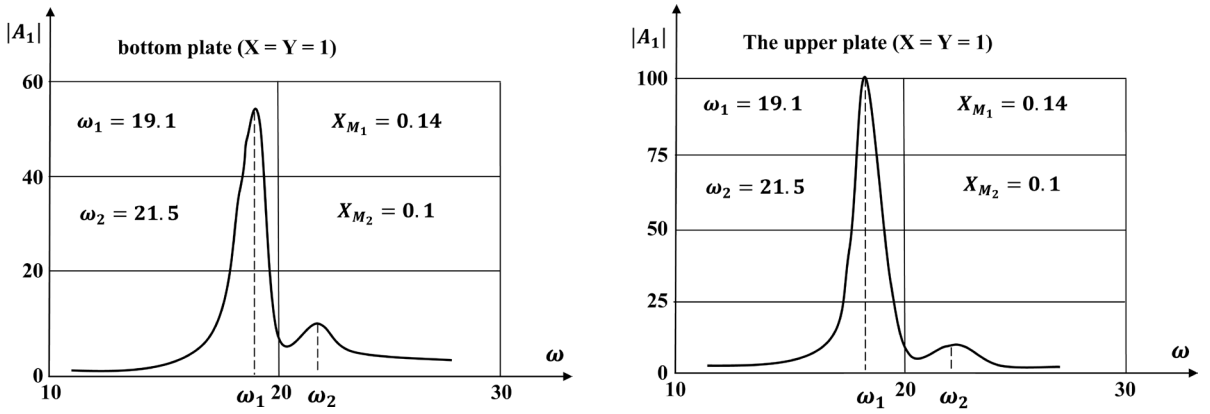

Figure 1. Amplitude of forced oscillations of the system.

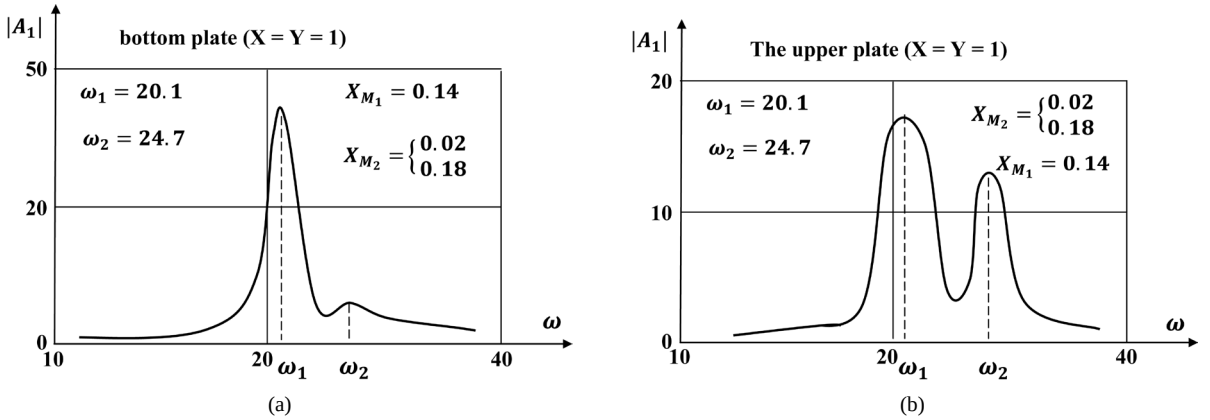

Figure 2. Amplitude of forced oscillations of the system.

located at $x_{M_2} = 0.1$ м, $y_{M_2} = 0.1$ м, *i.e.*, in the center.

The behavior of the resonant amplitudes for the top and bottom plates is qualitatively different from **Figure 1**. However, in the latter case, the resonant amplitude of the first two plates is greater than the corresponding amplitudes shown in **Figure 1**. This is also consistent with the results obtained in [1], namely, the fact that these positions weight M_2 damping coefficients of the first global forms are different. It should be noted that here, as in the previous embodiments, the task number for the resonance amplitude plates plays a determinant role oscillation phase relative to each other, the first resonance occurs when the two plates oscillations in phase (with different or equal amplitudes), the second resonance occurs when vibrations of plates are in antiphase (shift for the period). Displacement field at forced oscillations separate plate within these resonant frequencies qualitatively unchanged—it is close to its own form.

Task 2. Two identical mechanical properties elastic plate ($E = 28$; $\rho = 4$; $\nu = 0.3$) are connected in the center of one weightless viscoelastic damper (spring). The mass of the spring $M_0 = 0.05$, square plate ($a = b = 1$), supported along the contour, the thickness of the lower plate $h_1 = 0.1$; and upper $h_2 = 0.046$ on the bottom plate is attached at the center point mass. Recall that we consider two parallel hinged plates connected at the center of a viscoelastic damper. Plates are elastic square and thicknesses. On one of them (thicker) is fixed in the center of the concentrated mass. Parameters his relaxation kernel absorber (spring) determines the value $A = 0.078$; $\alpha = 0.1$; $\beta = 0.05$ (higher viscosity). The design is distributed over the area of the two plates of the disturbing nature of the harmonic load. Vector amplitudes of these forces have components equal to one. For the case of forced oscillations is required to evaluate the dissipative properties of structurally inhomogeneous viscoelastic system in general, depending on the magnitude of the instantaneous stiffness of the shock absorber. Assessment methodology is as follows. Selected characteristic point of the system and for her with fixed parameter instantaneous

damping built—frequency amplitude characteristic. In this case, the damping capacity of the system is determined by the maximum of the resonance amplitude. Then the parameter varies, and with all the defining (maximum) resonance amplitude is selected minimum. This parameter value and will fit most case dissipation system. As the feature points are selected as two of the central ($x = y = 0.5$) point on the bottom and top plates. Point to other coordinates gives qualitatively the same results. In [1], it was shown that the natural frequency of the global damping factor reaches its maximum. Thus, the effect of the interaction of natural forms is confirmed once again the problem of forced oscillations [1] [3] [4]. The difference in the optimal values of the instantaneous damping for forced and natural ($C^* = 3.4 \times 10^{-3}$ *и* $C^* = 5.4 \times 10^{-3}$) explains the difference between the viscosities of shock absorbers.

References

[1] Safarov, I.I., Teshaev, M.K.H. and Madjidov, M. (2014) Damping Dissipation—Inhomogeneous Mechanical Systems. Lambert Academic Publishing (LAP), Germany, 217 p.

[2] Chen, Y. (1963) On the Vibrations of Beams or Rods Carrying a Concentrated Mass. *Journal of Applied Mechanics*, **30**, 310-311.

[3] Bazarov, M.B., Safarov, I.I. and Shokin, Y.M. (1996) Numerical Simulation Fluctuations Dissipative Heterogeneous and Homogeneous Mechanical Systems. Siberian Branch, Novosibirsk, 189 p.

[4] Safarov, I.I. (1992) Oscillations and Waves in Dissipative Inhomogeneous Media and Designs. Publishing “Science”, Tashkent.

[5] Timoshenko, S.P. and Voynovskiy, S. (1966) Krieger Plates and Shells. McGran Hill Book Company, Inc., New York, Toronto, London, 636 p.

[6] Sachenkov, A.V. and Hemp, Y.G. (1975) Vibrations of Rectangular Plates on Point Support. *Applied Mehanika. Kiev*, T.XI, 37-41.

[7] Sunchaliev, R.M. and Filatov, A.N. (1972) On Some Methods for the Study of Nonlinear Problems in the Theory of Viscoelasticity. *Journal of Academy of Sciences Reports, Moscow*, **206**, 201-203.

[8] Jilin, P.A. (2006) Fundamentals of the Theory of Shells. Publishing House of the Polytechnic, University Press, St. Petersburg, 167 p.

Applied Mathematics, 2015, 6, 235-241
Published Online February 2015 in SciRes. http://www.scirp.org/journal/am
http://dx.doi.org/10.4236/am.2015.62023

Scientific Research Publishing

Global Convergence of a Modified Tri-Dimensional Filter Method

Bei Gao, Ke Su, Zixing Rong

Department of Mathematics and Information Science, Hebei University, Baoding, China
Email: shuiguogaobei@163.com, pigeonsk@163.com, rongzixingcn@163.com

Received 9 January 2015; accepted 27 January 2015; published 3 February 2015

Abstract

In this paper, a tri-dimensional filter method for nonlinear programming was proposed. We add a parameter into the traditional filter for relaxing the criterion of iterates. The global convergent properties of the proposed algorithm are proved under some appropriate conditions.

Keywords

Tri-Dimensional, NCP Function, Global Convergence, QP-Free

1. Introduction

This paper is concerned with finding a solution of a Nonlinear Programming (NLP) problem, as following

$$\begin{aligned} &\min\ f(x) \\ &s.t.\, c(x) \le 0, \end{aligned} \tag{1}$$

where $f(x): R^n \to R$, $c(x) = (c_1(x), \cdots, c_m(x))^{\mathrm{T}}: R^n \to R^m$ are second-order continuously differentiable. The Lagrangian function associated with problem (1) is the function

$$L(x, \lambda) = f(x) + \lambda c(x)$$

where $\lambda = (\lambda_1, \lambda_2, \cdots, \lambda_m)^{\mathrm{T}} \in R^m$ is the multiplier vector. For simplicity, we denote the column vector $(x^{\mathrm{T}}, \lambda^{\mathrm{T}})^{\mathrm{T}}$ as (x, λ). A point $(x^*, \lambda^*) \in R^{n \times m}$ is called a *Karush-Kuhn-Tucker* (KKT) point if it satisfies the following conditions:

$$\nabla_x L(x^*, \lambda^*) = 0, \quad c(x^*) \le 0, \ \lambda^* \ge 0, \ \lambda^* c(x^*) = 0, \tag{2}$$

we also say that $x^* \in D$ is a KKT point of problem (1) if there exists a $\lambda^* \in R^m$ such that (x^*, λ^*) satisfied

How to cite this paper: Gao, B., Su, K. and Rong, Z.X. (2015) Global Convergence of a Modified Tri-Dimensional Filter Method. *Applied Mathematics*, **6**, 235-241. http://dx.doi.org/10.4236/am.2015.62023

(2).

Traditionally, this question has been answered by using penalty function. But it is difficult to find a suitable penalty parameter. In order to avoid the pitfalls of penalty function, Nonlinear programming problems (NLP) filter methods were first proposed by Fletcher in a plenary talk at the SIAM Optimization Conference in Victoria in May 1996; the methods are described in [1]. And soon, Global convergence proof of filter method was given in [2]. Because of good global convergence and numerical results, filter methods have quickly become popular in other areas such as nonsmooth optimization, nonlinear equations and so on [3] [4].

Motivated by the ideas of filter methods above, a tri-dimensional filter method for nonliner programming was proposed as acceptance criterion to judge whether to accept a trial step in our algorithm. We have following advantages:

1) By enhancing the flexibility of filter, motivated by [5], we increase a dimension by introducing a parameter to relax the criterion of iterates.

2) The Maratos effect that makes good progress toward the solution may be rejected and has been avoided by using tri-dimensional filter method as acceptance criterion.

3) Tri-dimensional filter method can make full use of the information we get along the algorithm process.

This paper is divided into 4 sections. The next section introduces the concept of a Modified tri-dimensional filter and the NCP function. In Section 3, an algorithm of line search filter is given. The global convergence properties are proved in the last section.

2. Preliminaries

2.1. NCP Function

The method that based on the Fischer-Burmeister NCP function are efficient, both theoretical results and computational experience. The Fischer-Burmeister function has a very simple structure

$$\psi(a,b)=\sqrt{a^2+b^2}-a-b.$$

We know that: ψ is continuously differentiable everywhere except at the origin, but it is strongly semismooth at the origin. *i.e.* if $a\neq 0$ or $b\neq 0$, then ψ is continuously differentiable at $(a,b)\in R^2$, and

$$\nabla\psi(a,b)=\left(\frac{a}{\sqrt{a^2+b^2}}-1,\frac{b}{\sqrt{a^2+b^2}}-1\right);$$

if $a=0$ and $b=0$, then the generalized Jacobian of ψ at $(0,0)$ is

$$\partial\psi(0,0)=\left\{\xi-1,\eta-1\middle|\xi^2+\eta^2=1\right\}.$$

Let

$$\phi_i(x,\mu)=\psi(-c_i(x),\mu_i),\ 1\le i\le m$$

We denote $\Phi(x,\mu)=\left(\left(\nabla_x L(x,\mu)\right)^{\mathrm{T}},\left(\Phi_1(x,\mu)\right)^{\mathrm{T}}\right)^{\mathrm{T}}$, where $\Phi_1(x,\mu)=\left(\phi_1(x,\mu),\cdots,\phi_m(x,\mu)\right)^{\mathrm{T}}$.

Clearly, the KKT optimality conditions (2) can be equivalently reformulated as the nonsmooth equations $\Phi(x,\mu)=0$.

If $(c_i(x),\mu_i)\neq(0,0)$, then ϕ_i is continuously differentiable at $(x,\mu)\in R^{n+m}$. In this case, we have

$$\nabla_x\phi_i=\left(\frac{-c_i(x)}{\sqrt{\left(c_i(x)\right)^2+\mu_i^2}}+1\right)\nabla c_i(x);\ \nabla_\mu\phi_i=\left(\frac{\mu_i}{\sqrt{\left(c_i(x)\right)^2+\mu_i^2}}-1\right)e_i$$

where $e_i=(0,\cdots,0,1,0\cdots,0)^{\mathrm{T}}\in R^m$ is the ith column of the unit matrix, its ith element is 1, and other elements are 0.

If $c_i(x)=0$ and $\mu_i=0,1\le i\le m$, then $\phi_i(x,\mu)$ is strongly semismooth and directionally differentiable at (x,μ). We have

$$\partial_x \phi_i(x,\mu) = \left\{ (\xi+1)\nabla c_i(x) \middle| -1 \le \xi \le 1 \right\}$$

and

$$\partial_{\mu_i} \phi_i(x,\mu) = \left\{ (\xi-1) \middle| -1 \le \xi \le 1 \right\}.$$

We may reformulated the KKT (at point x^*, λ^*, μ^*) conditions as a system of equations.

$$\nabla_x L(x^*, \lambda^*, \mu^*) = 0, \ \Phi_1(x^*, \mu^*) = 0,$$

where $\lambda = (\lambda_1, \lambda_2, \cdots, \lambda_p)^{\mathrm{T}} \in R^p$ and $\mu = (\mu^1, \mu^2, \cdots, \mu^m)^{\mathrm{T}} \in R^m$ are the multiplier vectors, $\phi_i(x,\mu_j) = \psi(-g_i(x), \mu_j)$, $\phi(x^*, \mu^*) = (\phi_1(x,\mu_1^*), \phi_2(x,\mu_2^*), \cdots, \phi_m(x,\mu_m^*))$.

Replace the violation constrained function $p(G(x))$ in filter F of Fletcher and Leyffer method, we use the violation constrained function $p(G(x),\mu) = \|\Phi_1(x,\mu)\|^2$.

If $(c(x^k), \mu^k) \ne (0,0)$, let

$$\xi_j^k = \xi_j(x^k,\mu^k) = \frac{-c_j^k}{\sqrt{(c_j^k)^2 + (\mu_j^k)^2}} + 1; \ \eta_j^k = \eta_j(x^k,\mu^k) = \frac{\mu_j^k}{\sqrt{(c_j^k)^2 + (\mu_j^k)^2}} - 1;$$

otherwise we denote

$$\xi_j^k = \xi_j(x^k,\mu^k) = 1 + \frac{\sqrt{2}}{2}; \ \eta_j^k = \eta_j(x^k,\mu^k) = -1 + \frac{\sqrt{2}}{2}.$$

Let

$$V_k = \begin{pmatrix} V_{11}^k & V_{12}^k \\ V_{21}^k & V_{22}^k \end{pmatrix} = \begin{pmatrix} H^k & \nabla c^k \\ \mathrm{diag}(\xi^k)(\nabla c^k)^{\mathrm{T}} & \mathrm{diag}(\eta^k) \end{pmatrix}.$$

where H^k is a positive matrix which may be modified by BFGS update. $\mathrm{diag}(\xi^k)$ or $\mathrm{diag}(\eta^k)$ denotes the diagonal matrix whose j diagonal element is ξ^k or η^k respectively.

Definition 1.1 [1] A pair (f_j, h_j) is said to dominate another pair (f_l, h_l) if and only if both $f_j \le f_l$ and $h_j \le h_l$.

Definition 1.2 [1] A filter is a list of pairs (f_l, h_l) such that no pair dominates any other. A point (f_j, h_j) is said to be acceptable for inclusion in the filter if it is not dominated by any point in the filter.

Definition 1.3 NCP pair and NCP functions [6] We call a pair $(a,b) \in R^2$ to be an NCP pair if $a \ge 0$, $b \ge 0$ and $ab = 0$ a function $\psi : R^2 \to R$ is called an NCP function if $(a,b) = 0$ if and only if (a,b) is an NCP pair.

Denote $h(x) = \|\Phi_1(x,\mu)\|^2$ in the following context. It is straightforward to see that the constraint (1) is equivalent to the following equation: $h(x) = 0$.

2.2. Tri-Dimensional Filter

A two dimensional filter is often used in traditional filter method, some information about convergent like the positions of iterates are neglected. Therefore, we aim to enhance its flexibility of filter. Motivated by [5], we adopt (h, f, δ) in which a parameter δ is used to relax the criterion of iterates. We denote the filter by $\mathcal{F}_k$ for each iteration k. Flexible exact penalty function is introduced to promote convergence refer to [7]. Given a prescribed interval, penalty parameter can be chosen as any number from it and it is extends classical penalty function methods. We generalized the idea to filter which we called Tri-dimensional filter. Different from the original two dimensional filter, we increase a dimension by introducing a parameter.

We use pairs (h_j, f_j, δ_j) to constitute the elements of filter, where δ_j is a non-negative parameter. Our strategy for setting δ_j depends on the region in $h - f - \delta$ space to which s_k moves into. **Figure 1** is Distinct regions defined by the current iterate.

If s_k moves into region I, which is defined as

$$I = \left\{ (h, f, \delta) : h > 1.1h_k \text{ and } f + \delta_k h < f_k + \delta_k h_k, \delta_k \ge 0 \right\},$$

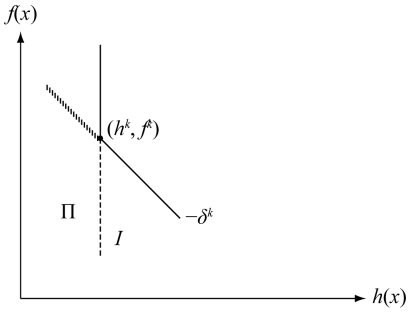

Figure 1. Distinct regions defined by the current iterate.

We say that the algorithm does not make good improvement since we do not want to accept points with larger constraint violation. Thus, we try to impose stricter acceptance criterion. Meanwhile, we do not permit δ_k larger than σ_k. In our algorithm, we increase δ^k in the following way

$$\delta_{k+1} = \min\left\{\sigma_k, \delta_k + \max\left\{0.001, 0.1\left(\left|\frac{f_k - f\left(x_k + s_k\right)}{h_k - h\left(x_k + s_k\right)}\right| - \delta_k\right)\right\}\right\}. \tag{3}$$

If s_k moved into region Π which is defined as

$$\Pi = \left\{\left(h, f, \delta\right) : h < 0.9h_k \text{ and } f + \delta_k h < f_k + \delta_k h_k, \delta_k \geq 0\right\},$$

We say that the algorithm makes good improvement since it reduces not only the constraint violation, but also the penalty function value. So, we may loosen the acceptance criterion to wish more improvement. Here, we achieve this goal by reducing δ_k by setting

$$\delta_{k+1} = \max\left\{0, \sigma_k - \max\left\{0.001, 0.1\left(\left|\frac{f_k - f\left(x_k + s_k\right)}{h_k - h\left(x_k + s_k\right)}\right| - \delta_k\right)\right\}\right\}. \tag{4}$$

In our algorithm, the trial step s_k is accepted by filter if

$$h\left(x_k + s_k\right) \leq \gamma h_j \quad \text{or} \quad f\left(x_k + s_k\right) + \delta_j h\left(x_k + s_k\right) \leq \gamma\left(f_j + \delta_j\right) \text{ and } \delta_k \geq 0 \tag{5}$$

For all $\left(h_j, f_j, \delta_j\right) \in \mathcal{F}_k$. The parameter $\gamma \in (0,1)$ is a constant close to 1 which sets an "envelope" around the border of the dominated part of the $\left(h, f, \delta\right)$-space in which the trial step is rejected. And also in the filter if

$$h_j > h_k \text{ and } h_j + \delta_k f_j > h_k + \delta_k f_k \text{ and } \delta_k \geq 0 \tag{6}$$

then we say x_j is dominated by x_k.

3. Description of the Algorithm

In this section we hope that the Lagrange multiplier λ_k will converge to the Lagrange multiplier λ^* at the solution x^*. From the KKT system of (1), a good estimate of the Lagrange multiplier is the least square solution of $c(x) - A(x)\lambda = 0$, namely $\lambda = \left(A(x)\right)^+ c(x)$. In our algorithm, λ_k is updated only after a trial step is accepted, and is set componentwise as

$$\lambda_k^i = \begin{cases} A_k^+ c_k^i, & l^i = u^i, \\ \max\left\{\left(A_k^+ c_k\right)^i, 0\right\}, & l^i = 0, u^i = +\infty, \\ \min\left\{\left(A_k^+ c_k\right)^i, 0\right\}, & l^i = -\infty, u^i = 0, \end{cases} \tag{7}$$

Now, we consider how to update the penalty parameter. Let x^* be a solution of (1) at which the LICQ is

satisfied, and the second order sufficient conditions are satisfied. Then when $\sigma > \left\|\lambda^*\right\|_1$, x^* is the strict local minimizer of penalty function. So we force the condition at each iteration: $\sigma_{k+1} \geq \left\|\lambda_{k+1}\right\|_1$.

And also, since the penalty term aims to reduce the constraint violation we double the penalty parameter if the constraint violation could not reduce by half, that is

$$\sigma_{k+1} = 2\sigma_k, \text{ if } h\left(x_k + s_k\right) \geq 0.5h_k.$$

To summarize, we update the penalty parameter in the following formula:

$$\sigma_{k+1} = \begin{cases} \max\left\{2\sigma_k, \left\|\lambda_{k+1}\right\|_1\right\}, & h\left(x_k + s_k\right) \geq 0.5h_k, \\ \max\left\{\sigma_k, \left\|\lambda_{k+1}\right\|_1\right\}, & \text{otherwise.} \end{cases} \tag{8}$$

The improved algorithm is presented as following.

Algorithm

Step 0. Initialization: Give a starting point $x_0 \in R^n$, μ_0, λ_0 and a initial positive definite matrix H_0, $\tau \in (0,1)$, $k = 0$. compute h_0, f_0, g_0, A_0.

Step 1. Terimination test. If $h_k + \left\|g_k - A_k\lambda_k\right\|_\infty < \varepsilon$ then returing x_k as a solution and stop.

Step 2. Computation of the search direction. compute d^{k_0} and λ^{k_0} by solving the following linear system in (d, λ):

$$V_k \begin{pmatrix} d \\ \lambda \end{pmatrix} = \begin{pmatrix} -\nabla f^k \\ 0 \end{pmatrix}. \tag{9}$$

where $\nabla f^k = \nabla f\left(x^k\right)$.

If $d^{k_0} = 0$, then stop otherwise, compute $\left(d^{k_1}, \lambda^{k_1}\right)$ by solving the following linear system in (d, λ):

$$V_k \begin{pmatrix} d \\ \lambda \end{pmatrix} = \begin{pmatrix} -\nabla L^k \\ -\Phi_1^k \end{pmatrix}. \tag{10}$$

where $\nabla L^k = \nabla L\left(x^k, \lambda^k\right)$ and $\Phi_1^k = \Phi_1\left(x^k, \lambda^k\right)$.

Step3. Liner search with filter

If $\Phi_1^k = 0$ then let $b^k = 1$ and $\rho^k = 0$, otherwise if $d^{k_0} = 0$ then let $b^k = 0$ and $\rho^k = 1$, otherwise denote $b^k = \left(1 - \rho^k\right)$ and

$$\rho^k = \begin{cases} 1 & \text{if } \left(d^{k_1}\right)^{\mathrm{T}} \nabla f^k \leq \theta\left(d^{k_0}\right)^{\mathrm{T}} \nabla f^k \\ (1-\theta)\dfrac{\left(d^{k_0}\right)^{\mathrm{T}} \nabla f^k}{\left(d^{k_0} - d^{k_1}\right)^{\mathrm{T}} \nabla f^k} & \text{otherwise} \end{cases} \tag{11}$$

and let

$$\begin{pmatrix} d^k \\ \lambda^k \end{pmatrix} = b^k \begin{pmatrix} d^{k_0} \\ \lambda^{k_0} \end{pmatrix} + \rho^k \begin{pmatrix} d^{k_1} \\ \lambda^{k_1} \end{pmatrix},$$

Step 4. Acceptance criterion of the trial step

Let $x^+ = x_k + s_k$, evalute h^+ and f^+ and δ^+; If x^+ is accepted by filter, $x_{k+1} = x^+$ and go to step 5; $x_{k+1} = x_k$, and $k = k+1$; go to step 2.

Step 5. Paramenters update

Update λ_{k+1} by (7); Update σ_{k+1} by (8); Update δ_{k+1} by (3) or (4); $k = k+1$ go to step 1.

4. The Convergence Properties

To present a proof of global convergence of algorithm, in this section, we always assume that the following conditions hold.

A1 The level set $\left\{x \middle| F(x) \leq f\left(x^0\right)\right\}$ is bounded, and for sufficiently large *k*, $\left\|\mu^k + \lambda^{k_0} + \lambda^{k_1}\right\| < \mu$

A2 f and g_i are twice Lipschitz continuously differentiable, and for all $y, z \in R^{n+m}$,

$$\left\|\nabla L(y)-\nabla L(z)\right\| \le m_3\|y-z\|, \quad \left\|\Phi(y)-\Phi(z)\right\| \le m_3\|y-z\|,$$

where $m_3 > 0$ is the Lipschitz constant.

A3 H^k is positive definite and there exist positive numbers m_1 and m_2 such that

$$m_1\|d\|^2 \le d^{\mathrm{T}} H^k d \le m_2\|d\|^2$$

for all $d \in R^n$ and all k.

Lemma 1. *If* $\Phi^k \ne 0$ *then* V^k *and* V^* *are nonsingular.*

Proof. If $V_k\begin{pmatrix} u \\ \vartheta \end{pmatrix} = 0$, for some $(u,\vartheta) \in R^n$, where $\vartheta = (\vartheta_1,\cdots,\vartheta)^{\mathrm{T}}$, $u = (u_1,\cdots,u_n)^{\mathrm{T}}$, then we have

$$H^k u + \nabla c^k v = 0 \tag{12}$$

and

$$\operatorname{diag}(\xi^k)(\nabla c^k)^{\mathrm{T}} u + \operatorname{diag}(\eta^k) v = 0 \tag{13}$$

From the definition of ξ_j^k and η_j^k, we know that $\xi_j^k \ge 0$ and $\eta_j^k \ne 0$ for all j. So, diag η^k is nonsingular. We have

$$v = -\left(\operatorname{diag}(\eta^k)\right)^{-1}\operatorname{diag}(\xi^k)(\nabla c^k)^{\mathrm{T}} u \tag{14}$$

Putting (14) into (12), we have

$$u^{\mathrm{T}}\left(H^k u + \nabla c^k v\right) = u^{\mathrm{T}} H^k u - u^{\mathrm{T}}\nabla c^k \operatorname{diag}(\xi^k)\left(\operatorname{diag}(\eta^k)\right)^{-1}(\nabla c^k)^{\mathrm{T}} u = 0$$

The fact that $-\nabla c^k \operatorname{diag}(\xi^k)\left(\operatorname{diag}(\eta^k)\right)^{-1}(\nabla c^k)^{\mathrm{T}}$ is positive semidefinite implies $u = 0$, and then $v = 0$ by (14). V^k is nonsingular. And if (x^*,μ^*) is an accumulation point of $\{(x^k,\mu^k)\}$, $\{(x^k,\mu^k)\} \to (x^*,\mu^*)$, $\Phi^k \to \Phi^*$ and $V^K \to V^*$. If $\Phi^* \ne 0$ then Φ^* is nonsingular. This lemma holds. □

The lemma 2 hold (see [8] Lemma 2)

Lemma 2. *If* $d^{k_0} = 0$, *then* $\nabla f(x^k) = 0$. *and* x^k *is KKT point of problem* (*NLP*).

Lemma 3. *Consider an infinite sequence iterations on which* $\left\{\left\|\Phi_1^k\right\|^2, f^k\right\}$ *entered into filter, where* $\left\|\Phi_1^k\right\|^2 > 0$ *and* $\{f^k\}$ *is bounded below. It follows that* $\Phi_1^k \to 0$.

Proof. Suppose the theorem is not true, then exists an $\varepsilon > 0$ and an infinitely members of index set K such that either $\left\|\Phi_1(x^k,\mu^k)\right\| \ge \varepsilon > 0$ and $\left\|\Phi_1(x^{k+1},\mu^{k+1})\right\| \le \eta\Phi_1(x^k,\mu^k)$ for any $k \in K$. then we obtain that $\left\{\left\|\Phi_1(x^k,\mu^k)\right\|\right\}_{k\in K} \to 0$, or $\{f_k\}_{k\in K}$ is monotonically decreasing, then lemma 5.1 implies $\left\|\Phi_1(x^k,\mu^k)\right\| \to 0$. So, the lemma holds. □

The following lemma 4 - 5 hold (see [9])

Lemma 4. $d^k \to 0$.

Lemma 5. *If* (x^*,μ^*) *is an accumulation point of* $\{(x^k,\mu^k)\}$ *then* $d^* = 0$, *and* d^*, λ^* *is the solution of*:

$$V_*\begin{pmatrix} d \\ \lambda \end{pmatrix} = \begin{pmatrix} -\nabla f^* \\ 0 \end{pmatrix}.$$

and $\nabla L(x^*,\mu^*) = 0$.

Theorem 1. *If* (x^*,μ^*) *is an accumulation point of* $\{(x^k,\mu^k)\}$ *then* x^* *is a KKT point of Problem* (*NLP*).

It is obviously to prove the conclusion holds according to the above lemmas.

Acknowledgements

We thank the Editor and the referee for their comments. This work is supported by the National Natural Science

Foundation of China (No. 11101115), the Natural Science Foundation of Hebei Province (No. 2014201033) and the Science and Technology project of Hebei province (No. 13214715).

References

[1] Fletcher, R. and Leyyfer, S. (2002) Nonlinear Programming without a Penalty Function. *Mathematical Programming*, **91**, 239-269. http://dx.doi.org/10.1007/s101070100244

[2] Fletcher, R., Leyffer, S. and Toint, P.L. (1998) On the Global Convergence of an SLP-Filter Algorithm. Numerical Analysis Report NA/183, University of Dundee, Dundee.

[3] Fletcher, R., Leyffer, S., *et al.* (2006) A Brief History of Filter Methods. Mathematics and Computer Science Division, Preprint ANL/MCSP1372-0906, Argonne National Laboratory.

[4] Chin, C.M., Rashid, A.H.A. and Nor, K.M. (2007) Global and Local Convergence of a Filter Line Search Method for Nonlinear Programming. *Optimization Method Software*, **22**, 365-390. http://dx.doi.org/10.1080/10556780600565489

[5] Wang, X. (2010) A New Filter Trust Region Method for Nonlinear Programming. *Journal of the Operations Research of China*, **10**, 133-140.

[6] Zhou, Y. and Pu, D. (2007) A New QP-Free Feasible Method for Inequality Constrained Optimization. *OR Transactions*, **11**, 31-43.

[7] Curtis, F.E. and Nocedal, J.(2008) Flexible Penalty Function for Nonlinear Constrained Optimization. *IMA Journal of Numerical Analysis*, **28**, 749-769. http://dx.doi.org/10.1093/imanum/drn003

[8] Su, K. (2008) A New Globally and Superlinearly Convergent QP-Free Method for Inequality Constrained Optimization. *Journal of Tongji University*, **36**, 265-272.

[9] Pu, D.G., Li, K. and Xue, W. (2005) Convergence of QP-Free Infeasible Methods for Nonlinear Inequality Constrained Optimization Problems. *Journal of Tongji University*, **33**, 525-529.

Applied Mathematics, 2015, 6, 242-264
Published Online February 2015 in SciRes. http://www.scirp.org/journal/am
http://dx.doi.org/10.4236/am.2015.62024

U-Type Designs via New Generalized Partially Balanced Incomplete Block Designs with m = 4, 5 and 7 Associated Classes

Imane Rezgui[1], Zebida Gheribi-Aoulmi[1], Hervé Monod[2]

[1]Department of Mathematics, University of Constantine 1, Constantine, Algeria
[2]INRA, UR MaIAGE, Jouy-en-Josas, Paris, France
Email: rezgui_imane@yahoo.fr, gheribiz@yahoo.fr, herve.monod@jouy.inra.fr

Received 10 January 2015; accepted 28 January 2015; published 4 February 2015

Abstract

The traditional combinatorial designs can be used as basic designs for constructing designs of computer experiments which have been used successfully till now in various domains such as engineering, pharmaceutical industry, etc. In this paper, a new series of generalized partially balanced incomplete blocks PBIB designs with m associated classes (m = 4, 5 and 7) based on new generalized association schemes with number of treatments v arranged in w arrays of n rows and l columns ($w \geq 2$, $n \geq 2$, $l \geq 2$) is defined. Some construction methods of these new PBIB are given and their parameters are specified using the Combinatory Method (s). For n or l even and s divisor of n or l, the obtained PBIB designs are resolvable PBIB designs. So the Fang RBIBD method is applied to obtain a series of particular U-type designs U (wnl; $\frac{wnl^r}{2s}$) (r is the repetition number of each treatment in our resolvable PBIB design).

Keywords

Association Scheme, Combinatory Method (s), Resolvable Partially Balanced Incomplete Block Design, U-Type Design

1. Introduction

Designs of computer experiments drew a wide attention in the previous two decades and were still being used

How to cite this paper: Rezgui, I., Gheribi-Aoulmi, Z. and Monod, H. (2015) U-Type Designs via New Generalized Partially Balanced Incomplete Block Designs with m = 4, 5 and 7 Associated Classes. *Applied Mathematics*, **6**, 242-264.
http://dx.doi.org/10.4236/am.2015.62024

successfully till now in various domains. Among the various construction methods of these designs, the traditional combinatorial designs can be used as basic designs (example: [1] [2]) and particularly the PBIB designs. The association schemes of two or three associated classes have been widely studied, while it is not the case of those over three associated classes. However, some association schemes with five associated classes have been studied (example: [3]). Besides, a method to obtain new association schemes by crossing or nesting other association schemes was given by Bailey [4] using the character tables and strata of the initial association schemes to find the parameters of the obtained association schemes.

In this paper, new association schemes with 4, 5 and 7 associated classes are described starting by a geometric representation. The parameter expressions of these association schemes are given. Moreover, some methods to construct the PBIB designs based on these association schemes are explained using an accessible construction method called the Combinatory Method (*s*) [5], which allows obtaining a series of PBIB designs by only using these association schemes. The parameters expressions of these new designs are given. In addition, for *n* or *l* even and *s* divisor of *n* or *l*, the obtained PBIB are resolvable PBIB. Then, a series of *U*-type designs $U\left(wnl;\frac{wnl}{2s}^{r}\right)$ (*r* is the repetition number of each treatment in the resolvable PBIB design) is obtained by applying the RBIBD method [6] on these designs.

The paper is organized as follows. In Section 2, we give new definitions of generalized association schemes with *m* (= 4, 5 and 7) associated classes, starting by geometric representation and we give their parameters as properties. Section 3 describes a series of construction method using the Combinatory Method (s) for obtaining the PBIB designs associated to our generalized association schemes. We give the series of the *U*-type designs associated to our constructed PBIB designs in Section 4. We achieve our paper with a Conclusion.

Recall some definitions:

Definition 1. *An m-association scheme* ($m \geq 2$) *of v treatments* [7] *is a relation satisfying the following conditions*:

1) *Any two treatments are either* 1^{st}, 2^{nd}, ⋯, *or* m^{th} *associates. The relation of association is symmetric, i.e., if the treatment* α *is an* i^{th} *associate of* β, *then* β *is an* i^{th} *associate of* $\alpha\left(i=1,2,\cdots m\right)$.

2) *Each treatment* α *has* n_i i^{th} *associates, the number* n_i *being independent of* $\alpha\left(i=1,2,\cdots m\right)$.

3) *If any two treatments* α *and* β *are* i^{th} *associates, then the number of treatments that are* j^{th} *associates of* α *and* k^{th} *associates of* β *is* p_{jk}^{i} *and is independent of the pair of* i^{th} *associates* α *and* β $\left(i,j,k=1,2,\cdots m\right)$.

The numbers v, n_i $\left(i=1,2,\cdots m\right)$ *and* p_{jk}^{i} $\left(i,j,k=1,2,\cdots m\right)$ *are called the parameters of the association scheme.*

Definition 2. *A PBIB design* [7], *based on an m-association scheme* ($m \geq 2$), *with parameters v, b, r, k,* λ_i, $i=1,2,\cdots m$, *is a block design with v treatments and b blocks of size k each such that every treatment occurs in* r *blocks and any two distinct treatments being* i^{th} *associate occur together in exactly* λ_i *blocks. The number* λ_i *is independent of the pair of* i^{th} *associates* $\left(i=1,2,\cdots m\right)$.

A parallel class of PBIB is a collection of disjoint blocks from the b blocks whose union is V. A partition of the b blocks into $q=b/r$ *parallel classes is called a resolution, and PBIB design is resolvable if it has at least one resolution and it denoted by RPBIB design.*

The Combinatory Method (*s*) [5]:

Let an array of *n* rows and *l* columns as follows:

a_{11}	a_{12}	⋯	a_{1j}	⋯	a_{1l}
a_{21}	a_{22}	⋯	a_{2j}	⋯	a_{2l}
⋮	⋮	⋮	⋮	⋮	⋮
a_{i1}	a_{i2}	⋯	a_{ij}	⋯	a_{il}
⋮	⋮	⋮	⋮	⋮	⋮
a_{n1}	a_{n2}	⋯	a_{nj}	⋯	a_{nl}

Consider s different elements of the same row i $(2 \le s < l)$, and associate with them s other elements of a row i' $(i' \ne i)$, respecting the correspondence between the elements a_{ij} and $a_{i'j}$. Bringing together the $2s$ elements in the same block and making all possible combinations, we obtain a partially balanced incomplete block design of size $k = 2s$.

Definition 3. *Let U $(v; q_1, \cdots, q_r)$ denote a design of v runs and r factors with respective $q_1, \cdots, q_r$ levels. This design corresponds to an $v \times r$ matrix $X = (x^1, \cdots, x^r)$ such that the i^{th} column x^i takes values from a set of q_i elements, say $\{1, \cdots, q_i\}$, equally often. The set of all such designs, called U-type designs in the statistical literature, is denoted by U $(v; q_1, \cdots, q_r)$. Obviously, v must be a multiple of q_i $(1 \le i \le r)$. When all the q_i $(1 \le i \le r)$ are equal to q, we denote it by U $(v; q^r)$. Note that the rows and columns of X are identified with the runs and factors respectively* [6].

2. Generalized Rectangular Right Angular Association Schemes (m) (m = 4, 5 and 7 Associated Classes)

2.1. Generalized Rectangular Right Angular Association Scheme (4)

Let V be a set of $v = wnl$ treatments, ($w \ge 2$, $n \ge 2$, $l \ge 2$), to which we associate a geometrical representation in the following way:

Each treatment of V is associated with a unique triplet of the set $A^1 \cup \cdots \cup A^g \cup \cdots \cup A^w$ where:

$$A^g = \{(x, y, z) \in \mathbb{N}^3 / 1 \le x \le l,\ 1 \le y \le n,\ z = g\}, \quad g = 1, \cdots, w$$

Let α be a treatment of coordinates $(x, y, z) \in A^g$

- $A_1^g = \{(x', y', z') \in A^g / x' \ne x, y' = y\}$ corresponds to the treatments 1st associated to α
- $A_2^g = \{(x', y', z') \in A^g / x' = x, y' \ne y\}$ corresponds to the treatments 2nd associated to α.
- $A_3^g = \{(x', y', z') \in A^g / x' \ne x, y' \ne y\}$ corresponds to the treatments 3rd associated to α.
- $A_4^g = \{(x', y', z') \in A^{g'}, g' \ne g\}$ corresponds to the treatments 4th associated to α.

This geometric representation describes a new association scheme, we call it for convenience, generalized rectangular right angular association scheme (4) with four associated classes, to which we give the following equivalent definition:

Definition 4. *A generalized rectangular right angular association scheme* (4) *is an arrangement of $v = wnl$* ($w \ge 2$, $n \ge 2$, $l \ge 2$) *treatments in w arrays of n rows and l columns such that, with respect to each treatment α*:

1) *The first associates of α are the other treatments of the same row in the same array.*
2) *The second associates of α are the other treatments of the same column in the same array.*
3) *The third associates of α are the remaining treatments in the same array.*
4) *The fourth associates of α are the other treatments of the other arrays.*

Property 1. *The parameters of generalized rectangular right angular association schemes* (4) *are*:

$$v = wnl,\ n_1 = l - 1,\ n_2 = n - 1,\ n_3 = (n-1)(l-1),\ n_4 = (w-1)nl$$

$$P_1 = \begin{pmatrix} l-2 & 0 & 0 & 0 \\ 0 & 0 & n-1 & 0 \\ 0 & n-1 & (l-2)(n-1) & 0 \\ 0 & 0 & 0 & (w-1)ln \end{pmatrix}$$

$$P_2 = \begin{pmatrix} 0 & 0 & l-1 & 0 \\ 0 & n-2 & 0 & 0 \\ l-1 & 0 & (l-1)(n-2) & 0 \\ 0 & 0 & 0 & (w-1)ln \end{pmatrix}$$

$$P_3=\begin{pmatrix} 0 & 1 & l-2 & 0 \\ 1 & 0 & n-2 & 0 \\ l-2 & n-2 & (l-2)(n-2) & 0 \\ 0 & 0 & 0 & (w-1)ln \end{pmatrix}$$

$$P_4=\begin{pmatrix} 0 & 0 & 0 & l-1 \\ 0 & 0 & 0 & n-1 \\ 0 & 0 & 0 & (l-1)(n-1) \\ l-1 & n-1 & (l-1)(n-1) & (w-2)ln \end{pmatrix}$$

Definition 5. *A PBIB design based on a generalized rectangular right angular association scheme* (4) *is called generalized rectangular right angular GPBIB*$_4$ *design*.

2.2. Generalized Rectangular Right Angular Association Scheme (5)

Let V be a set of $v = wnl$ treatments, ($w \geq 2$, $n \geq 2$, $l \geq 2$), to which we associate a geometrical representation in the following way:

Each treatment of V is associated with a unique triplet (of coordinates) of the set $A^1 \cup \cdots \cup A^g \cup \cdots \cup A^w$ where:

$$A^g = \{(x,y,z) \in \mathbb{N}^3 / 1 \leq x \leq l,\ 1 \leq y \leq n,\ z = g\}, \quad g = 1, \cdots, w$$

Let α be a treatment of coordinates $(x,y,z) \in A^g$

- $A_1^g = \{(x',y',z') \in A^g / x' \neq x, y' = y\}$ corresponds to the treatments 1st associated to α
- $A_2^g = \{(x',y',z') \in A^g / x' = x, y' \neq y\}$ corresponds to the treatments 2nd associated to α.
- $A_3^g = \{(x',y',z') \in A^g / x' \neq x, y' \neq y\}$ corresponds to the treatments 3rd associated to α.
- $A_4^g = \{(x',y',z') \in A^{g'}, g' \neq g / y' = y\}$ corresponds to the treatments 4th associated to α.
- $A_5^g = \{(x',y',z') \in A^{g'}, g' \neq g / y' \neq y\}$ corresponds to the treatments 5th associated to α.

This geometric representation describes a new association scheme, we call it for convenience, generalized rectangular right angular association scheme (5) with five associated classes, to which we give the following equivalent definition:

Definition 6. *A generalized rectangular right angular association scheme* (5) *is an arrangement of* $v = wnl$ ($w \geq 2$, $n \geq 2$, $l \geq 2$) *treatments in* w ($n \times l$) *rectangular arrays such that, with respect to each treatment* α :

1) The first associates of α are the other treatments of the same row in the same array.
2) The second associates of α are the other treatments of the same column in the same array.
3) The third associates of α are the remaining treatments in the same array.
4) The fourth associates of α are the treatments of same row as α, of the other arrays.
5) The fifth associates of α are the remaining treatments in the other arrays.

Property 2. *The parameters of the generalized rectangular right angular association schemes* (5) *are*:

$$v = wnl,\ n_1 = l-1,\ n_2 = n-1,\ n_3 = (n-1)(l-1),\ n_4 = (w-1)l,\ n_5 = (w-1)(n-1)l$$

$$P_1=\begin{pmatrix} l-2 & 0 & 0 & 0 & 0 \\ 0 & 0 & n-1 & 0 & 0 \\ 0 & n-1 & (l-2)(n-1) & 0 & 0 \\ 0 & 0 & 0 & l & 0 \\ 0 & 0 & 0 & 0 & (w-1)(n-1)l \end{pmatrix}$$

$$P_2=\begin{pmatrix} 0 & 0 & l-1 & 0 & 0 \\ 0 & n-2 & 0 & 0 & 0 \\ l-1 & 0 & (l-1)(n-2) & 0 & 0 \\ 0 & 0 & 0 & 0 & l \\ 0 & 0 & 0 & l & (w-1)(n-2)l \end{pmatrix}$$

$$P_3=\begin{pmatrix} 0 & 1 & l-2 & 0 & 0 \\ 1 & 0 & n-2 & 0 & 0 \\ l-2 & n-2 & (l-2)(n-2) & 0 & 0 \\ 0 & 0 & 0 & 0 & l \\ 0 & 0 & 0 & l & (w-2)(n-2)l \end{pmatrix}$$

$$P_4=\begin{pmatrix} 0 & 0 & 0 & l-1 & 0 \\ 0 & 0 & 0 & 0 & n-1 \\ 0 & 0 & 0 & 0 & (l-1)(n-1) \\ l-1 & 0 & 0 & (w-2)l & 0 \\ 0 & n-1 & (l-1)(n-1) & 0 & (w-2)(l-1)(n-1) \end{pmatrix}$$

$$P_5=\begin{pmatrix} 0 & 0 & 0 & 0 & l-1 \\ 0 & 0 & 0 & 1 & n-2 \\ 0 & 0 & 0 & l-1 & (l-1)(n-2) \\ 0 & 1 & l-1 & 0 & (w-2)l \\ l-1 & n-2 & (l-1)(n-2) & (w-2)l & (w-2)(n-2)l \end{pmatrix}$$

Definition 7. *A PBIB design based on a generalized rectangular right angular association scheme* (5) *is called generalized rectangular right angular GPBIB*$_5$ *design.*

2.3. Generalized Rectangular Right Angular Association Scheme (7)

Let V be a set of $v = wnl$ treatments, ($w \geq 2$, $n \geq 2$, $l \geq 2$), to which we associate a geometrical representation in the following way:

Each treatment of V is associated with a unique triplet of the set $A^1 \cup \cdots \cup A^g \cup \cdots \cup A^w$ where:

$$A^g = \{(x,y,z) \in \mathbb{N}^3 / 1 \leq x \leq l,\ 1 \leq y \leq n,\ z = g\}, \quad g = 1, \cdots, w$$

Let α be a treatment of coordinates $(x,y,z) \in A^g$

- $A_1^g = \{(x',y',z') \in A^g / x' \neq x, y' = y\}$ corresponds to the treatments 1st associated to α
- $A_2^g = \{(x',y',z') \in A^g / x' = x, y' \neq y\}$ corresponds to the treatments 2nd associated to α.
- $A_3^g = \{(x',y',z') \in A^g / x' \neq x, y' \neq y\}$ corresponds to the treatments 3th associated to α.
- $A_4^g = \{(x',y',z') \in A^{g'}, g' \neq g / x' = x, y' = y\}$ corresponds to the treatments 4th associated to α.
- $A_5^g = \{(x',y',z') \in A^{g'}, g' \neq g / x' \neq x, y' = y\}$ corresponds to the treatments 5th associated to α.
- $A_6^g = \{(x',y',z') \in A^{g'}, g' \neq g / x' = x, y' \neq y\}$ corresponds to the treatments 6th associated to α.
- $A_7^g = \{(x',y',z') \in A^{g'}, g' \neq g / x' \neq x, y' \neq y\}$ corresponds to the treatments 7th associated to α.

This geometric representation describes a new association scheme, we call it for convenience, generalized rectangular right angular association scheme (7) with seven associated classes, to which we give the following equivalent definition:

Definition 8. *A generalized rectangular right angular association scheme* (7) *is an arrangement of* $v = wnl$

($w \geq 2$, $n \geq 2$, $l \geq 2$) *treatments in w arrays of n rows and l columns such that, with respect to each treatment* α:

1) *The first associates of* α *are the other treatments of the same row in the same array.*

2) *The second associates of* α *are the other treatments of the same column in the same array.*

3) *The third associates of* α *are the remaining treatments in the same array.*

4) *The fourth associates of* α *are the treatments in the same row and the same column as* α, *of the other arrays.*

5) *The fifth associates of* α *are the treatments of the same row as* α *in the other arrays, that are different from the fourth associates of* α.

6) *The sixth associates of* α *are the treatments of the same column as* α *in the other arrays, that are different from the fourth associates of* α.

7) *The seventh associates of* α *are the remaining treatments in the other arrays.*

Property 3. *the parameters of generalized rectangular right angular association schemes* (7) *are*:

$$v = wnl,\ \ n_1 = l-1,\ \ n_2 = n-1,\ \ n_3 = (n-1)(l-1),\ \ n_4 = w-1,$$

$$n_5 = (w-1)(l-1),\ \ n_6 = (w-1)(n-1),\ \ n_7 = (w-1)(n-1)(l-1)$$

$$P_1 = \begin{pmatrix} l-2 & 0 & 0 & 0 & 0 & 0 & 0 \\ 0 & 0 & n-1 & 0 & 0 & 0 & 0 \\ 0 & n-1 & (l-2)(n-1) & 0 & 0 & 0 & 0 \\ 0 & 0 & 0 & 0 & w-1 & 0 & 0 \\ 0 & 0 & 0 & w-1 & (w-1)(l-2) & 0 & 0 \\ 0 & 0 & 0 & 0 & 0 & 0 & (w-1)(n-1) \\ 0 & 0 & 0 & 0 & 0 & (w-1)(n-1) & (w-1)(n-1)(l-2) \end{pmatrix}$$

$$P_2 = \begin{pmatrix} 0 & 0 & l-1 & 0 & 0 & 0 & 0 \\ 0 & n-2 & 0 & 0 & 0 & 0 & 0 \\ l-1 & 0 & (l-1)(n-2) & 0 & 0 & 0 & 0 \\ 0 & 0 & 0 & 0 & 0 & w-1 & 0 \\ 0 & 0 & 0 & 0 & 0 & 0 & (w-1)(l-1) \\ 0 & 0 & 0 & w-1 & 0 & (w-1)(n-2) & 0 \\ 0 & 0 & 0 & 0 & (w-1)(l-1) & 0 & (w-1)(l-1)(n-2) \end{pmatrix}$$

$$P_3 = \begin{pmatrix} 0 & 1 & l-2 & 0 & 0 & 0 & 0 \\ 1 & 0 & n-2 & 0 & 0 & 0 & 0 \\ l-2 & n-2 & (l-2)(n-2) & 0 & 0 & 0 & 0 \\ 0 & 0 & 0 & 0 & 0 & 0 & w-1 \\ 0 & 0 & 0 & 0 & 0 & w-1 & (w-1)(l-2) \\ 0 & 0 & 0 & 0 & w-1 & 0 & (w-1)(n-2) \\ 0 & 0 & 0 & w-1 & (w-1)(l-2) & (w-1)(n-2) & (w-1)(l-2)(n-2) \end{pmatrix}$$

$$P_4 = \begin{pmatrix} 0 & 0 & 0 & 0 & l-1 & 0 & 0 \\ 0 & 0 & 0 & 0 & 0 & n-1 & 0 \\ 0 & 0 & 0 & 0 & 0 & 0 & (l-1)(n-1) \\ 0 & 0 & 0 & w-2 & 0 & 0 & 0 \\ l-1 & 0 & 0 & 0 & (w-2)(l-1) & 0 & 0 \\ 0 & n-1 & 0 & 0 & 0 & (w-2)(n-1) & 0 \\ 0 & 0 & (l-1)(n-1) & 0 & 0 & 0 & (w-2)(l-1)(n-1) \end{pmatrix}$$

$$P_5=\begin{pmatrix}0&0&0&1&l-2&0&0\\0&0&0&0&0&0&n-1\\0&0&0&0&0&n-1&(l-2)(n-1)\\1&0&0&0&w-2&0&0\\l-2&0&0&w-2&(w-2)(l-2)&0&0\\0&0&n-1&0&0&0&(w-2)(n-1)\\0&n-1&(l-2)(n-1)&0&0&(w-2)(n-1)&(w-2)(l-2)(n-1)\end{pmatrix}$$

$$P_6=\begin{pmatrix}0&0&0&0&0&0&l-1\\0&0&0&1&0&n-2&0\\0&0&0&0&l-1&0&(l-1)(n-2)\\0&1&0&0&0&w-2&0\\0&0&l-1&0&0&0&(w-2)(l-1)\\0&n-2&0&w-2&0&(w-2)(n-2)&0\\l-1&0&(l-1)(n-2)&0&(w-2)(l-1)&0&(w-2)(l-1)(n-2)\end{pmatrix}$$

$$P_7=\begin{pmatrix}0&0&0&0&0&1&l-2\\0&0&0&0&1&0&n-2\\0&0&0&1&l-2&n-2&(l-2)(n-2)\\0&0&1&0&0&0&w-2\\0&1&l-2&0&0&w-2&(w-2)(l-2)\\1&0&n-2&0&w-2&0&(w-2)(n-2)\\l-2&n-2&(l-2)(n-2)&w-2&(w-2)(l-2)&(w-2)(n-2)&(w-2)(n-2)(l-2)\end{pmatrix}$$

Definition 9. *A PBIB design based on a generalized rectangular right angular association scheme* (7) *is called generalized rectangular right angular GPBIB$_7$ design.*

3. Construction Method of *GPBIB$_m$* Designs (*m* = 4, 5 and 7 Associated Classes)

Let $v = wnl$ ($w \geq 2$, $n \geq 2$, $l \geq 2$) treatments be arranged in w arrays of n rows and l columns $A^{(1)}$, ..., $A^{(w)}$ and written as follows $\forall g = 1,\cdots,w$:

	$C_1^{(g)}$	$C_2^{(g)}$	$\cdots$	$C_j^{(g)}$	$\cdots$	$C_l^{(g)}$
$R_1^{(g)}$	$a_{11}^{(g)}$	$a_{12}^{(g)}$	$\cdots$	$a_{1j}^{(g)}$	$\cdots$	$a_{1l}^{(g)}$
$R_2^{(g)}$	$a_{21}^{(g)}$	$a_{22}^{(g)}$	$\cdots$	$a_{2j}^{(g)}$	$\cdots$	$a_{2l}^{(g)}$
$\vdots$	$\vdots$	$\vdots$	$\vdots$	$\vdots$	$\vdots$	$\vdots$
$R_i^{(g)}$	$a_{i1}^{(g)}$	$a_{i2}^{(g)}$	$\cdots$	$a_{ij}^{(g)}$	$\cdots$	$a_{il}^{(g)}$
$\vdots$	$\vdots$	$\vdots$	$\vdots$	$\vdots$	$\vdots$	$\vdots$
$R_n^{(g)}$	$a_{n1}^{(g)}$	$a_{n2}^{(g)}$	$\cdots$	$a_{nj}^{(g)}$	$\cdots$	$a_{nl}^{(g)}$

$A^{(g)}$

3.1. Construction Method of *GPBIB$_4$* Designs

3.1.1. First Construction Method of *GPBIB$_4$* Designs

Applying the Combinatory Method (s) on each of the w arrays, with chosen $s \in \{2,\cdots,l-1\}$, then we obtain w rectangular PBIB designs. The set of all blocks gives a PBIB design with 4 associated classes.

Theorem 1. *The partially balanced incomplete block designs with the parameters*:

$v = wnl$, $b = wn(n-1)C_s^l/2$, $r = (n-1)C_{s-1}^{l-1}$, $k = 2s$, $\lambda_1 = (n-1)C_{s-2}^{l-2}$, $\lambda_2 = C_{s-1}^{l-1}$, $\lambda_3 = C_{s-2}^{l-2}$, $\lambda_4 = 0$

are generalized rectangular right angular GPBIB$_4$ designs.

Proof. For each array of the *w* arrays, we obtain a rectangular design with parameters: $v^* = nl$, $b^* = n(n-1)C_s^l/2$, $r = (n-1)C_{s-1}^{l-1}$, $k = 2s$, $\lambda_1 = (n-1)C_{s-2}^{l-2}$, $\lambda_2 = C_{s-1}^{l-1}$, $\lambda_3 = C_{s-2}^{l-2}$. (see [5]).

For the *w* arrays we obtain a generalized rectangular right angular GPBIB$_4$ design with parameters: $v = wnl$, $b = wn(n-1)C_s^l/2$, $r = (n-1)C_{s-1}^{l-1}$, $k = 2s$, $\lambda_1 = (n-1)C_{s-2}^{l-2}$, $\lambda_2 = C_{s-1}^{l-1}$, $\lambda_3 = C_{s-2}^{l-2}$.

λ_4: Two treatments $a_{ij}^{(g)}$ and $a_{i'j'}^{(g')}$ from the arrays $A^{(g)}$ and $A^{(g')}$ respectively $\left(g \neq g' \in \{1, \cdots, w\}\right)$ they never appear together in the same block thus $\lambda_4 = 0$. □

Lemma 1. *For the special case s = l, the previous method can also be used for the construction of nested group divisible designs, with parameters*:

$$v = wnl,\ b = wn(n-1)/2,\ r = (n-1),\ k = 2l,\ \lambda_1 = n-1,\ \lambda_2 = 1 = \lambda_3,\ \lambda_4 = 0$$

Remark 1.

- *For w* = 1, *the GPBIB$_4$ design of Theorem* 1 *is a rectangular design with parameters as in the Theorem* 1 *of* [5].
- *For w* = 2, the *GPBIB$_4$ design of Theorem* 1 *is a rectangular right angular PBIB$_4$ design with parameters as in Proposition* 1 *of* [8].

Proposition 2. *Let GPBIB$_4$ be a design with parameters*:

$v = wnl$, $b = wn(n-1)C_s^l/2$, $r = (n-1)C_{s-1}^{l-1}$, $k = 2s$, $\lambda_1 = (n-1)C_{s-2}^{l-2}$, $\lambda_2 = C_{s-1}^{l-1}$, $\lambda_3 = C_{s-2}^{l-2}$, $\lambda_4 = 0$.

For n or l even and s divisor of l or s, the GPBIB$_4$ design is a resolvable PBIB designs (*RGPBIB$_4$*) *with r parallel classes where each parallel classes contain* $q = w\dfrac{nl}{2s}$ *blocks.*

Proof.

$$q = b/r = \frac{wn(n-1)C_s^l}{2(n-1)C_{s-1}^{l-1}} = \frac{wn(n-1)lC_{s-1}^{l-1}}{2s(n-1)C_{s-1}^{l-1}} = \frac{wnl}{2s}$$

n or *l* is even and *s* is divisor of *n* or *l*, then $q \in \mathbf{N}$.

Example 1. *Let v* = 3 × 4 × 4 *treatments be arranged in the three following arrays*:

1	2	3	4
5	6	7	8
9	10	11	12
13	14	15	16

17	18	19	20
21	22	23	24
25	26	27	28
29	30	31	32

33	34	35	36
37	38	39	40
41	42	43	44
45	46	47	48

The construction method for (*s* = 2), give the following resolvable generalized rectangular right angular *GPBIB$_4$* design, with the parameters:

$$v = 48,\ b = 108,\ r = 9,\ k = 4,\ q = 12$$

PC_1			
1	2	5	6
9	10	13	14
3	4	7	8
11	12	15	16
17	18	21	22
25	26	29	30
19	20	23	24
27	28	31	32
33	34	37	38
35	36	39	40
41	42	45	46
43	44	47	48

PC_2			
1	2	9	10
5	6	13	14
3	4	11	12
7	8	15	16
17	18	25	26
21	22	29	30
19	20	27	28
23	24	31	32
33	34	41	42
37	38	45	46
35	36	43	44
39	40	47	48

PC_3			
1	2	13	14
5	6	9	10
3	4	15	16
7	8	11	12
17	18	29	30
21	22	25	26
19	20	31	32
23	24	27	28
33	34	45	46
37	38	41	42
35	36	47	48
39	40	43	44

PC_4			
1	3	5	7
9	11	13	15
2	4	6	8
10	12	14	16
17	19	21	23
25	27	29	31
18	20	22	24
26	28	30	32
33	35	37	39
34	37	38	40
41	43	45	47
42	44	46	48

PC_5			
1	3	9	11
5	7	13	15
2	4	10	12
6	8	14	16
17	19	25	27
21	23	29	31
18	20	26	28
22	24	30	32
33	35	41	43
37	39	45	47
34	36	42	44
38	40	46	48

PC_6			
1	3	13	15
5	7	9	11
2	4	14	16
6	8	10	12
17	19	29	31
21	23	25	27
18	20	30	32
22	24	26	28
33	35	45	47
37	39	41	43
34	36	46	48
38	40	42	44

PC_7			
1	4	5	8
9	12	13	16
2	3	6	7
10	11	14	15
17	20	21	24
25	28	29	32
18	19	22	23
26	27	30	31
33	36	37	40
34	35	38	39
41	44	45	48
42	43	46	47

PC_8			
1	4	9	12
5	8	13	16
2	3	10	11
6	7	14	15
17	20	25	28
21	24	29	32
18	19	26	27
22	23	30	31
33	36	41	44
37	40	45	48
34	35	42	43
38	39	46	47

PC_9			
1	4	13	16
5	8	9	12
2	3	14	15
6	7	10	11
17	20	29	32
21	24	25	28
18	19	30	31
22	23	26	27
33	36	45	48
37	40	41	44
34	35	46	47
38	39	42	43

3.1.2. Second Construction Method of *GPBIB*$_4$ Designs with $\lambda_4 \neq 0$

Let $C_j^{(g)} = \left(a_{1j}^{(g)}, a_{2j}^{(g)}, \cdots, a_{nj}^{(g)}\right)'$, $C_j^{(g)1} = C_j^{(g)}$ and $C_j^{(g)h} = \left(a_{hj}^{(g)}, a_{(h+1)j}^{(g)}, \cdots, a_{nj}^{(g)}, a_{1j}^{(g)}, \cdots, a_{(h-1)j}^{(g)}\right)'$, $h = 2,3,\cdots,n$. Applying the Combinatory Method (s) with chosen $s \in \{3,\cdots,l\}$ on each array of the form $C_j^{(g)h} \cup A^{(g')}$ $(g' \neq g)$ for $j = 1,\cdots,l$, $h = 1,\cdots,n$ and $g = 1,\cdots,w$, by only considering the combinations of s treatments that always contain a component of the vector $C_j^{(g)h}$, the set of all the obtained blocks provides a PBIP with 4 associated classes.

Theorem 3. *The partially balanced incomplete block designs with the parameters*:

$$v = wnl,\ b = w(w-1)ln^2(n-1)C_{s-1}^l/2,\ r = s(w-1)n(n-1)C_{s-1}^l,\ k = 2s,\ \lambda_1 = (w-1)ln(n-1)C_{s-3}^{l-2},$$

$$\lambda_2 = s(w-1)nC_{s-1}^l,\ \lambda_3 = (w-1)nlC_{s-3}^{l-2},\ \lambda_4 = 4(n-1)C_{s-2}^{l-1}$$

are generalized rectangular right angular GPBIB$_4$ *designs.*

Proof.

- The v and k values are obvious.
- r: For each treatment $a_{ij_0}^{(g)}$ of the array $A^{(g)}$ $g = 1,\cdots,w$, we have:
  - On an array $C_{j_0}^{(g)h} \cup A^{(g')}$ $(g' \neq g)$, applying the procedure with the l other elements of the same row. There is C_{s-1}^l possibilities, each one being repeated $(n-1)$ times, with n permutations $(h = 1,\cdots,n)$, then we have $n(n-1)C_{s-1}^l$ repetitions. Therefore, we have $w-1$ arrays of the form $C_{j_0}^{(g)h} \cup A^{(g')}$ $(g' \neq g)$; so we have $(w-1)n(n-1)C_{s-1}^l$ repetitions of the treatment $a_{ij_0}^{(g)}$.
  - On an array $A^{(g)} \cup C_j^{(g')h}$ $(g' \neq g)$, $j = 1,\cdots,l$ and $h = 1,\cdots,n$, applying the procedure with the $l-1$ other elements of the same row. There is C_{s-2}^{l-1} possibilities each one being repeated $(n-1)$ times, with n permutations $(h = 1,\cdots,n)$, then we have $(n-1)C_{s-2}^{l-1}$ appearances repeated themselves n times. Therefore, for an array $A^{(g)} \cup C_j^{(g')h}$ we have $n(n-1)C_{s-2}^{l-1}$ repetitions of a_{ij_0}. Considering all the arrays $A^{(g)} \cup C_j^{(g')h}$ $(g' \neq g)$ for $j = 1,\cdots,l$ and $g' = 1,\cdots,w$; so we have $(w-1)\ln(n-1)C_{s-2}^{l-1}$ repetitions of a_{ij_0}.

  Thus: $r = (w-1)n(n-1)\left[C_{s-1}^l + lC_{s-2}^{l-1}\right] = s(w-1)n(n-1)C_{s-1}^l$.
- λ_1: Consider two treatments $a_{ij_0}^{(g)}$ and $a_{ij_0'}^{(g)}$ from the array $A^{(g)}$ ($g = 1,\cdots,w$ and $j_0 \neq j_0'$), they appear together $(n-1)C_{s-3}^{l-2}$ times with the other $l-2$ elements of the same row i of the arrays $A^{(g)} \cup C_j^{(g')h}$ $(g' \neq g)$, with n permutations $(h = 1,\cdots,n)$, we obtain $n(n-1)C_{s-3}^{l-2}$ times in which the two treatments appear together. Considering all the arrays $A^{(g)} \cup C_j^{(g')h}$ $(g' \neq g)$ for $j = 1,\cdots,l$ and $g' = 1,\cdots,w$; then we have $(w-1)ln(n-1)C_{s-3}^{l-2}$ times where the two treatments a_{ij_0} and $a_{ij_0'}$ appear together.
- λ_2: Consider two treatments $a_{ij_0}^{(g)}$ and $a_{i'j_0}^{(g)}$ from the array $A^{(g)}$, ($g = 1,\cdots,w$ and $i \neq i'$), we have:
  - In an array $A^{(g)} \cup C_j^{(g')h}$ $(g' \neq g)$: the two treatments appear together C_{s-2}^{l-1} times, with the n permutations $(h = 1,\cdots,n)$ they appear together nC_{s-2}^{l-1} times. Considering all the arrays of the form $A^{(g)} \cup C_j^{(g')h}$ $(g' \neq g)$ for $j = 1,\cdots,l$ and $g' = 1,\cdots,w$, they appear together $(w-1)\ln C_{s-2}^{l-1}$ times.
  - In the array $C_{j_0}^{(g)h} \cup A^{(g')}$: both treatments appear together C_{s-1}^l times, with the n permutations $(h = 1,\cdots,n)$ they appear nC_{s-1}^l times. Considering all the arrays of the form $C_{j_0}^{(g)h} \cup A^{(g')}$ $(g' \neq g)$ for $g' = 1,\cdots,w$; they appear together $(w-1)nC_{s-1}^l$ times.

  In total $\lambda_2 = (w-1)n\left[lC_{s-2}^{l-1} + C_{s-1}^l\right] = sn(w-1)C_{s-1}^l$.
- λ_3: Consider two treatments $a_{ij_0}^{(g)}$ and $a_{i'j_0'}^{(g)}$ from the array $A^{(g)}$ ($g = 1,\cdots,w$, $i \neq i'$ and $j_0 \neq j_0'$), they appear together C_{s-3}^{l-2} times for each array of the form $A^{(g)} \cup C_j^{(g')h}$ $(g' \neq g)$, with the n permutations $(h = 1,\cdots,n)$ they appear together nC_{s-3}^{l-2} times. Considering all the arrays $A^{(g)} \cup C_j^{(g')h}$ $(g' \neq g)$ for $j = 1,\cdots,l$ and $g' = 1,\cdots,w$, then the two treatments $a_{ij_0}^{(g)}$ and $a_{i'j_0'}^{(g)}$ appear together $(w-1)\ln C_{s-3}^{l-2}$ times.
- λ_4: Consider two treatments $a_{ij}^{(g)}$ and $a_{i'j'}^{(g')}$ from the arrays $A^{(g)}$ and $A^{(g')}$ respectively (g, $g' = 1,\cdots,w$):
  - If $i = i'$, for the array $A^{(g)} \cup C_j^{(g')h}$ $(g' \neq g)$ and h = 1 the two treatments appear together $(n-1)C_{s-2}^{l-1}$ times. For the array $C_j^{(g)h} \cup A^{(g')}$ $(g' \neq g)$ and h = 1 they also appear together $(n-1)C_{s-2}^{l-1}$ time, so we have $2(n-1)C_{s-2}^{l-1}$ times. On the other hand, for $h = 2,\cdots,n$, the two treatments appear together C_{s-2}^{l-1} times for the array $A^{(g)} \cup C_j^{(g')h}$ and C_{s-2}^{l-1} times for the array $C_j^{(g)h} \cup A^{(g')}$, so we have $2C_{s-2}^{l-1}$ for one value of h. Taking all the values of $h = 2,\cdots,n$, we obtain $2(n-1)C_{s-2}^{l-1}$ times where the two treatments appear together.

In total $\lambda_4 = 2(n-1)C_{s-2}^{l-1} + 2(n-1)C_{s-2}^{l-1} = 4(n-1)C_{s-2}^{l-1}$.

- If $i \neq i'$, then the two treatments appear together C_{s-2}^{l-1} times for the array of the form $A^{(g)} \cup C_{j'}^{(g)h}$ $(g' \neq g)$ and appear together C_{s-2}^{l-1} times for the array of the form $C_j^{(g)h} \cup A^{(g')}$ $(g' \neq g)$ for $h=1$, so we have $2C_{s-2}^{l-1}$ times. For $h = 2,\cdots,n$, among the $(n-1)$ permutations of the vector $C_{j'}^{(g)h}$, and for a given value of h, the treatment $a_{i'j'}^{(g')}$ takes the same row as $a_{ij}^{(g)}$ then the two treatments appear together $(n-1)C_{s-2}^{l-1}$ times, for the remaining values the two treatments appear together C_{s-2}^{l-1} times. For $h = 2,\cdots,n$, among the $(n-1)$ permutations of the vector $C_{j'}^{(g)}$ and for a given value of h, the treatment $a_{ij}^{(g)}$ takes the same row as $a_{i'j'}^{(g')}$ then the two treatments appear together $(n-1)C_{s-2}^{l-1}$ times, for the remaining values the two treatments appear together C_{s-2}^{l-1} times.

  In total $\lambda_4 = 2C_{s-2}^{l-1} + (n-1)C_{s-2}^{l-1} + (n-1)C_{s-2}^{l-1} + (n-1)C_{s-2}^{l-1} + (n-1)C_{s-2}^{l-1} = 4(n-1)C_{s-2}^{l-1}$.

- b: Using the above construction method on each array of the form: $A^{(g)} \cup C_{j'}^{(g)h}$ $(g' \neq g)$, we obtain $n(n-1)C_{s-1}^{l}/2$ blocks. So for the l arrays of the form $A \cup C_j^{(g)h}$ we have $ln(n-1)C_{s-1}^{l}/2$ blocks, with the n permutations $(h=1,\cdots,n)$ we obtain $ln^2(n-1)C_{s-1}^{l}/2$ blocks. Considering all the arrays $A^{(g)} \cup C_j^{(g')h}$ for $g' = 1,\cdots,w$, then in total we have $(w-1)\ln^2(n-1)C_{s-1}^{l}/2$ blocks. Considering all the arrays $A^{(g)} \cup C_j^{(g')h}$ for $g = 1,\cdots,w$, then in total we have $w(w-1)\ln^2(n-1)C_{s-1}^{l}/2$ blocks. □

Remark 2. *For w = 2, the GPBIB$_4$ design of Theorem 3 is a rectangular right angular PBIB$_4$ design with parameters as in Proposition 2 of* [8].

Proposition 4 *Let GPBIB$_4$ be a design with parameters*:

$$v = wnl,\ b = w(w-1)ln^2(n-1)C_{s-1}^{l}/2,\ r = s(w-1)n(n-1)C_{s-1}^{l},\ k = 2s,\ \lambda_1 = (w-1)ln(n-1)C_{s-3}^{l-2},$$

$$\lambda_2 = s(w-1)nC_{s-1}^{l},\ \lambda_3 = (w-1)nlC_{s-3}^{l-2},\ \lambda_4 = 4(n-1)C_{s-2}^{l-1}$$

For n or l even and s divisor of l or s, the GPBIB$_4$ design is a resolvable PBIB designs (RGPBIB$_4$) with r parallel classes where each parallel classes contain $q = w\dfrac{nl}{2s}$ *blocks.*

3.2. Construction Method of *GPBIB$_5$* Designs

Let $C_j^{(g)} = \left(a_{1j}^{(g)}, a_{2j}^{(g)}, \cdots, a_{nj}^{(g)}\right)'$ be the j^{th} column of the g^{th} array $g \in \{1,\cdots,w\}$. Applying the Combinatory Method (s) with s chosen $s \in \{3,\cdots,l\}$, on each array in the form $C_j^{(g)} \cup A^{(g')}$ $(g \neq g')$ for $j = 1,\cdots,l$ and $j = 1,\cdots,w$ by only considering the combinations of s treatments that contain a component of the vector $C_j^{(g)}$, then the set of all the blocks obtained, gives a *PBIB* design with 5 associated classes.

Theorem 5. *The incomplete block designs with parameters*:

$$v = wnl,\ b = w(w-1)ln(n-1)C_{s-1}^{l}/2,\ r = s(w-1)(n-1)C_{s-1}^{l},\ k = 2s,\ \lambda_1 = (w-1)l(n-1)C_{s-3}^{l-2},$$

$$\lambda_2 = (w-1)sC_{s-1}^{l},\ \lambda_3 = (w-1)lC_{s-3}^{l-2},\ \lambda_4 = 2(n-1)C_{s-2}^{l-1},\ \lambda_5 = 2C_{s-2}^{l-1}$$

are generalized rectangular right angular GPBIB$_5$ designs.

Remark 3. *For w = 2, the GPBIB$_5$ design of Theorem 5 is a rectangular right angular PBIB$_5$ design with parameters as in Proposition 3 of* [8].

Proposition 6. *Let GPBIB$_5$ be a design with parameters*:

$$v = wnl,\ b = w(w-1)ln(n-1)C_{s-1}^{l}/2,\ r = s(w-1)(n-1)C_{s-1}^{l},\ k = 2s,\ \lambda_1 = (w-1)l(n-1)C_{s-3}^{l-2},$$

$$\lambda_2 = (w-1)sC_{s-1}^{l},\ \lambda_3 = (w-1)lC_{s-3}^{l-2},\ \lambda_4 = 2(n-1)C_{s-2}^{l-1},\ \lambda_5 = 2C_{s-2}^{l-1}$$

For n or l even and s divisor of l or s, the GPBIB$_5$ design is a resolvable PBIB designs (RGPBIB$_5$) with r parallel classes where each parallel classes contain $q = w\dfrac{nl}{2s}$ *blocks.*

Example 2. *Let v = 3 × 2 × 3 treatments be arranged in the two following arrays*:

1	2	3
4	5	6

7	8	9
10	11	12

13	14	15
16	17	18

The construction method for (s = 3), give the following generalized rectangular right angular $GPBIB_5$ design, with parameters:

$$v = 18,\ \ b = 54,\ \ r = 18,\ \ k = 6,\ \ q = 6$$

PC_1					
1	7	8	4	10	11
9	13	14	12	16	17
15	2	3	18	5	6

PC_2					
1	7	9	4	10	12
8	13	15	11	16	18
14	2	3	17	5	6

PC_3					
1	8	9	4	11	12
7	14	15	10	17	18
13	2	3	16	5	6

PC_4					
2	7	8	5	10	11
9	13	15	12	16	18
14	1	3	17	4	6

PC_5					
2	7	9	5	10	12
13	1	3	16	4	6
8	14	15	11	17	18

PC_6					
2	8	9	5	11	12
7	13	14	10	16	17
15	1	3	18	4	6

PC_7					
3	7	8	6	10	11
9	14	15	12	17	18
13	1	2	16	4	5

PC_8					
3	7	9	6	10	12
8	13	14	11	16	17
15	1	2	18	4	5

PC_9					
3	8	9	6	11	12
7	13	15	10	16	18
14	1	2	17	4	5

PC_{10}					
13	7	8	16	10	11
9	1	2	12	4	5
3	14	15	6	17	18

PC_{11}					
13	7	9	16	10	12
8	1	3	11	4	6
2	14	15	5	17	18

PC_{12}					
13	8	9	16	11	12
7	2	3	10	5	6
1	14	15	4	17	18

PC_{13}					
14	7	8	17	10	11
9	2	3	12	5	6
1	13	15	4	16	18

PC_{14}					
14	7	9	17	10	12
8	1	2	11	4	5
3	13	15	6	16	18

PC_{15}					
14	8	9	17	11	12
7	1	3	10	4	6
2	13	15	5	16	18

PC_{16}					
15	7	8	18	10	11
9	1	3	12	4	6
2	13	14	5	16	17

PC_{17}					
15	7	9	18	10	12
8	2	3	11	5	6
1	13	14	4	16	17

PC_{18}					
15	8	9	18	11	12
7	1	2	10	4	5
3	13	14	6	16	17

3.3. Construction Method of *GPBIB*$_7$ Designs

3.3.1. First Construction Method of *GPBIB*$_7$ Designs

Applying the Combinatory Method (*s*) on each of the *w* arrays, with chosen and fixed $s \in \{2,\cdots,l-1\}$, then we obtain *w* rectangular PBIB designs. The juxtaposition of the blocks of the *w* rectangular PBIB designs, such that the blocks containing treatment $a_{ij}^{(g)}$ and $a_{ij}^{(g')}$ $\left(g \neq g' \in \{1,\cdots,w\}\right)$ are put side by side, gives a *PBIB* design with 7 associated classes.

Theorem 7. *The incomplete block designs with parameters*:

$$v = wnl,\quad b = \frac{n(n-1)C_s^l}{2},\quad \lambda_0 = r = (n-1)C_{s-1}^{l-1} = \lambda_4,\quad k = 2sw,$$

$$\lambda_1 = (n-1)C_{s-2}^{l-2} = \lambda_5,\quad \lambda_2 = C_{s-1}^{l-1} = \lambda_6,\quad \lambda_3 = C_{s-2}^{l-2} = \lambda_7$$

are generalized rectangular right angular GPBIB$_7$ *designs*.

Proof. The design parameters are deduced from the construction method. □

Remark 4.

- *For w* = 1, *the GPBIB*$_7$ *design of Theorem* 7 *is a rectangular design with parameters as in Theorem* 1 *of* [5].
- *For w* = 2, *the GPBIB*$_7$ *design of Theorem* 7 *is a rectangular right angular PBIB*$_7$ *design with parameters as in Proposition* 4 *of* [8].

Proposition 8. *Let GPBIB*$_7$ *be a design with parameters*:

$$v = wnl,\quad b = \frac{n(n-1)C_s^l}{2},\quad \lambda_0 = r = (n-1)C_{s-1}^{l-1} = \lambda_4,\quad k = 2sw,$$

$$\lambda_1 = (n-1)C_{s-2}^{l-2} = \lambda_5,\quad \lambda_2 = C_{s-1}^{l-1} = \lambda_6,\quad \lambda_3 = C_{s-2}^{l-2} = \lambda_7$$

For n or l even and s divisor of l or s, the GPBIB$_7$ *design is a resolvable PBIB designs* (*RGPBIB*$_7$) *with r*

parallel classes where each parallel classes contain $q = \frac{nl}{2s}$ *blocks.*

Example 3. *Let* $v = 3 \times 4 \times 4$ *treatments be arranged in the three following arrays*:

1	2	3	4
5	6	7	8
9	10	11	12
13	14	15	16

17	18	19	20
21	22	23	24
25	26	27	28
29	30	31	32

33	34	35	36
37	38	39	40
41	42	43	44
45	46	47	48

The construction method for (s = 2), give the following resolvable generalized rectangular right angular $GPBIB_7$ design, with the parameters:

$$v = 48,\ \ b = 36,\ \ r = 9,\ \ k = 12,\ \ q = 4$$

PC_1											
1	2	5	6	17	18	21	22	33	34	37	38
9	10	13	14	25	26	29	30	41	42	45	46
3	4	7	8	19	20	23	24	35	36	39	40
11	12	15	16	27	28	31	32	43	44	47	48

PC_2											
1	2	9	10	17	18	25	26	33	34	41	42
5	6	13	14	21	22	29	30	37	38	45	46
3	4	11	12	19	20	27	28	35	36	43	44
7	8	15	16	23	24	31	32	39	40	47	48

PC_3											
1	2	13	14	17	18	29	30	33	34	45	46
5	6	9	10	21	22	25	26	37	38	41	42
3	4	15	16	19	20	31	32	35	36	47	48
7	8	11	12	23	24	27	28	39	40	43	44

PC_4											
1	3	5	7	17	19	21	23	33	35	37	39
9	11	13	15	25	27	29	31	34	37	38	40
2	4	6	8	18	20	22	24	41	43	45	47
10	12	14	16	26	28	30	32	42	44	46	48

PC_5											
1	3	9	11	17	19	25	27	33	35	41	43
5	7	13	15	21	23	29	31	37	39	45	47
2	4	10	12	18	20	26	28	34	36	42	44
6	8	14	16	22	24	30	32	38	40	46	48

PC_6											
1	3	13	15	17	19	29	31	33	35	45	47
5	7	9	11	21	23	25	27	37	39	41	43
2	4	14	16	18	20	30	32	34	36	46	48
6	8	10	12	22	24	26	28	38	40	42	44

PC_7											
1	4	5	8	17	20	21	24	33	36	37	40
9	12	13	16	25	28	29	32	34	35	38	39
2	3	6	7	18	19	22	23	41	44	45	48
10	11	14	15	26	27	30	31	42	43	46	47

PC_8											
1	4	9	12	17	20	25	28	33	36	41	44
5	8	13	16	21	24	29	32	37	40	45	48
2	3	10	11	18	19	26	27	34	35	42	43
6	7	14	15	22	23	30	31	38	39	46	47

PC_9											
1	4	13	16	17	20	29	32	33	36	45	48
5	8	9	12	21	24	25	28	37	40	41	44
2	3	14	15	18	19	30	31	34	35	46	47
6	7	10	11	22	23	26	27	38	39	42	43

3.3.2. Second Construction Method of $GPBIB_7$ Designs with $\lambda_i \neq \lambda_{i+4}$ $(i=0,\cdots,4)$

Let $C_j^{(g)}=\left(a_{1j}^{(g)},a_{2j}^{(g)},\cdots,a_{nj}^{(g)}\right)'$ be the j^{th} column of the g^{th} array and let $R_i^{(g)}=\left(a_{i1}^{(g)},a_{i2}^{(g)},\cdots,a_{il}^{(g)}\right)$ be the i^{th} row of the g^{th} array $\left(g\in\{1,\cdots,w\}\right)$. Then applying the Combinatory Method (s) with chosen $s\in\{2,\cdots,l\}$ on each

array of the form $C_j^{(g)} \cup \left[A^{(g')} \setminus C_j^{(g')} \right]$ $(g' \neq g)$ for $j = 1, \cdots, l$ and g, $g' = 1, \cdots, w$ (respectively $R_i^{(g)} \cup \left[A^{(g')} \setminus R_i^{(g')} \right]$ $(g' \neq g)$ for $i = 1, \cdots, n$ and g, $g' = 1, \cdots, w$), by only considering the combinations of s treatments that always contain a component of the column $C_j^{(g)h}$ (respectively the row $R_i^{(g)}$), the set of all the obtained blocks provides a PBIP with 7 associated classes.

Theorem 9. *The partially balanced incomplete block designs with the parameters*:

$$v = wnl, \quad b = w(w-1)n(n-1)(s+2)C_s^l/2, \quad \lambda_0 = r = (w-1)(n-1)C_{s-1}^{l-1}(s+2), \quad k = 2s,$$

$$\lambda_1 = s(n-1)(w-1)C_{s-2}^{l-2}, \quad \lambda_2 = s(w-1)C_{s-1}^{l-1}, \quad \lambda_3 = (w-1)(l-2)C_{s-3}^{l-3}, \quad \lambda_4 = 0,$$

$$\lambda_5 = 2(n-1)C_{s-2}^{l-2}, \quad \lambda_6 = 2C_{s-1}^{l-1}, \quad \lambda_7 = 4C_{s-2}^{l-2}$$

are generalized rectangular right angular GPBIB$_7$ designs.

Proof. The design parameters are deduced from the construction method. □

Remark 5. *For w = 2, the GPBIB$_7$ design of Theorem* 9 *is a rectangular right angular PBIB$_7$ design with parameters as in Proposition* 5 *of* [8].

Proposition 10. *Let GPBIB$_7$ be a design with parameters*:

$$v = wnl, \quad b = w(w-1)n(n-1)(s+2)C_s^l/2, \quad \lambda_0 = r = (w-1)(n-1)C_{s-1}^{l-1}(s+2), \quad k = 2s,$$

$$\lambda_1 = s(n-1)(w-1)C_{s-2}^{l-2}, \quad \lambda_2 = s(w-1)C_{s-1}^{l-1}, \quad \lambda_3 = (w-1)(l-2)C_{s-3}^{l-3}, \quad \lambda_4 = 0,$$

$$\lambda_5 = 2(n-1)C_{s-2}^{l-2}, \quad \lambda_6 = 2C_{s-1}^{l-1}, \quad \lambda_7 = 4C_{s-2}^{l-2}$$

For n or l even and s divisor of l or s, the GPBIB$_7$ design is a resolvable PBIB designs (*RGPBIB$_7$*) *with r parallel classes where each parallel classes contain* $q = w\dfrac{nl}{2s}$ *blocks.*

Example 4. *Let v = 3 × 3 × 3 treatments be arranged in the three following arrays*:

1	2	3
4	5	6
7	8	9

10	11	12
13	14	15
16	17	18

19	20	21
22	23	24
25	2	27

The construction method for (s = 3), give a generalized rectangular right angular *GPBIB$_7$* design with parameters:

$$v = 27, \quad b = 90, \quad r = 20, \quad k = 6, \quad \lambda_1 = 12, \quad \lambda_2 = 6,$$
$$\lambda_3 = 4, \quad \lambda_4 = 0, \quad \lambda_5 = 4, \quad \lambda_6 = 2, \quad \lambda_7 = 4$$

To illustrate the method, we applying the construction method for the columns and rows of the first array, where each column represents a block:

b_1	b_2	b_3	b_4	b_5	b_6	b_7	b_8	b_9	b_{10}
1	1	4	2	2	5	3	3	6	1
11	11	14	10	10	13	10	10	13	20
12	12	15	12	12	15	11	11	14	21
4	7	7	5	8	8	6	9	9	4
14	17	17	13	16	16	13	16	16	23
15	18	18	15	18	18	14	17	17	24

b_{11}	b_{12}	b_{13}	b_{14}	b_{15}	b_{16}	b_{17}	b_{18}	b_{19}	b_{20}
1	4	2	2	5	3	3	6	1	1
20	23	19	19	22	19	19	22	2	2
21	24	21	21	24	20	20	23	3	3
7	7	5	8	8	6	9	9	13	16
26	26	22	25	25	22	25	25	14	17
27	27	24	27	27	23	26	26	15	18

b_{21}	b_{22}	b_{23}	b_{24}	b_{25}	b_{26}	b_{27}	b_{28}	b_{29}	b_{30}
4	4	7	7	1	1	4	4	7	7
5	5	8	8	2	2	5	5	8	8
6	6	9	9	3	3	6	6	9	9
10	16	10	13	22	25	19	25	19	22
11	17	11	14	23	26	20	26	20	23
12	18	12	15	24	27	21	27	21	24

4. Construction of the U-Type Designs Based on Resolvable *GPBIB*$_m$ Designs (m = 4, 5 and 7)

In this section we apply the RBIBD method (see [6]) on our resolvable rectangular right angular RGPBIB$_m$ designs (m = 4, 5 and 7) to obtain a series of U-type designs $U\left(v;q^r\right)$.

Let a resolvable GPBIB$_m$ designs (m = 4, 5 and 7) with r parallel classes $\mathrm{PC}_1,\cdots,\mathrm{PC}_r$ where each j-th class contains $q=b/r$ blocks ($1\le j\le r$). Then we can construct a U-type design $U\left(v;q^r\right)$ from resolvable *GPBIB*$_m$ designs (m = 4, 5 and 7) as follows:

Algorithm *RGPBIB*$_m$ – *UD*

- Step 1. Give a natural order $1,\cdots,q$ to the q blocks in each parallel class PC_j, $j=1,\cdots,r$.
- Step 2. For each PC_j, construct a q-level column $x^j=\left(x_{\alpha j}\right)$ as follows: Set $x_{\alpha j}=u$, if treatment α is contained in the u-th block of PC_j, $u=1,2,\cdots,q$
- Step 3. The r q-level columns constructed from PC_j, $j=1,\cdots,r$ form a $U\left(v;q^r\right)$.

Proposition 11. *For v = wnl runs ($w\ge 2$, $n\ge 2$, $l\ge 2$), a series of U-type* $U\left(v;q^r\right)$ *designs exist*:

- $U\left(wnl;\dfrac{wnl^{(n-1)C_{s-1}^{l-1}}}{2s}\right)$, n or l even and s divisor of n or l.
- $U\left(wnl;\dfrac{wnl^{s(w-1)n(n-1)C_{s-1}^{l}}}{2s}\right)$, n or l even and s divisor of n or l.

- $U\left(wnl;\frac{wnl^{s(w-1)(n-1)C_{s-1}^{l}}}{2s}\right)$, n or l even and s divisor of n or l.
- $U\left(wnl;\frac{nl^{(n-1)C_{s-1}^{l-1}}}{2s}\right)$, n or l even and s divisor of n or l.
- $U\left(wnl;\frac{wnl^{(s+2)(w-1)(n-1)C_{s-1}^{l-1}}}{2s}\right)$, n or l even and s divisor of n or l.

Proof. applying the $RGPBIB_m - UD$ Algorithm on each resolvable rectangular right angular $GPBIB_m$ (m = 4, 5 and 7) of the Proposition 1, 5. □

Example 5. *Applying the* $RGPBIB_m - UD$ *Algorithm on the resolvable rectangular right angular* $GPBIB_7$ *of Example* 1, *we obtain the following U-type U* (48, 4^9) *with* 48 *runs and nine* 4*-level factors.*

Runs	$Factor_1$	$Factor_2$	$Factor_3$	$Factor_4$	$Factor_5$	$Factor_6$	$Factor_7$	$Factor_8$	$Factor_9$
1	1	1	1	1	1	1	1	1	1
2	1	1	1	3	3	3	3	3	3
3	3	3	3	1	1	1	3	3	3
4	3	3	3	3	3	3	1	1	1
5	1	2	2	1	2	2	1	2	2
6	1	2	2	3	4	4	3	4	4
7	3	4	4	1	2	2	3	4	4
8	3	4	4	3	4	4	1	2	2
9	2	1	2	2	1	2	2	1	2
10	2	1	2	4	3	4	4	3	4
11	4	3	4	2	3	4	4	3	4
12	4	3	4	4	3	4	2	1	2
13	2	2	1	2	2	1	2	2	1
14	2	2	1	4	4	3	4	4	3
15	4	4	3	2	2	1	4	4	3
16	4	4	3	4	4	3	2	2	1
17	1	1	1	1	1	1	1	1	1
18	1	1	1	3	3	3	3	3	3
19	3	3	3	1	1	1	3	3	3
20	3	3	3	3	3	3	1	1	1
21	1	2	2	1	2	2	1	2	2
22	1	2	2	3	4	4	3	4	4
23	3	4	4	1	2	2	3	4	4
24	3	4	4	3	4	4	1	2	2
25	2	1	2	2	1	2	2	1	2
26	2	1	2	4	3	4	4	3	4

Continued

27	4	3	4	2	3	4	4	3	4
28	4	3	4	4	3	4	2	1	2
29	2	2	1	2	2	1	2	2	1
30	2	2	1	4	4	3	4	4	3
31	4	4	3	2	2	1	4	4	3
32	4	4	3	4	4	3	2	2	1
33	1	1	1	1	1	1	1	1	1
34	1	1	1	3	3	3	3	3	3
35	3	3	3	1	1	1	3	3	3
36	3	3	3	3	3	3	1	1	1
37	1	2	2	1	2	2	1	2	2
38	1	2	2	3	4	4	3	4	4
39	3	4	4	1	2	2	3	4	4
40	3	4	4	3	4	4	1	2	2
41	2	1	2	2	1	2	2	1	2
42	2	1	2	4	3	4	4	3	4
43	4	3	4	2	3	4	4	3	4
44	4	3	4	4	3	4	2	1	2
45	2	2	1	2	2	1	2	2	1
46	2	2	1	4	4	3	4	4	3
47	4	4	3	2	2	1	4	4	3
48	4	4	3	4	4	3	2	2	1

5. Conclusions

New association schemes with $m = 4$, 5 and 7 associated classes called generalized rectangular right angular association schemes for $v = wnl$ treatments arranged in $w \geq 2$ ($n \times l$) arrays were described and their parameters expressions were given exactly and directly. Some construction methods of *PBIB* designs based on these association schemes accommodated by accessible method called the Combinatory Method (s) which facilitates the construction application were explained. Moreover, a series of U-type designs $U\left(wnl; \frac{wnl^{r}}{2s}\right)$, by applying the Fang *RBIBD* method on resolvable generalized rectangular right angular $GPBIB_m$ designs ($m = 4$, 5 and 7) was constructed.

We note that all the construction methods described in this article were programmed with the R-package "CombinS" [9] (the ameliorated version).

References

[1] Fang, K.T., Ge, G.N., Liu, M. and Qin, H. (2004) Construction of Uniform Designs via Super-Simple Resolvable *t*-Designs. *Utilitas Mathematica*, **66**, 15-32.

[2] Fang, K.T., Tang, Y. and Yin, J.X. (2005) Resolvable Partially Pairwise Balanced Designs and Their Applications in Computer Experiments. *Utilitas Mathematica*, **70**, 141-157.

[3] Benmatti, A. (1983) Un schéma d'association partiellement équilibré appliqué aux croisements dialléles. Magister

Thesis. http://biblio.cca-paris.com/index.php?lvl=author_see&id=1181

[4] Bailey, R.A. (2004) Association Schemes: Designed Experiments, Algebra and Combinatorics. Cambridge University Press, Cambridge. www.cambridge.org/9780521824460

[5] Rezgui, I. and Gheribi-Aoulmi, Z. (2014) New Construction Method of Rectangular PBIB Designs and Singular Group Divisible Designs. *Journal of Mathematics and Statistics*, **10**, 45-48. http://dx.doi.org/10.3844/jmssp.2014.45.48

[6] Fang, K.T., Li, R. and Sudjianto, A. (2006) Design and Modeling for Computer Experiments. Taylor & Francis Group, LLC, London.

[7] Bose, R.C. and Nair, K.R. (1939) Partially Balanced Incomplete Block Designs. *Sankhya*, **4**, 337-372.

[8] Rezgui, I., Gheribi-Aoulmi, Z. and Monod, H. (2013) New Association Schemes with 4, 5 and 7 Associate Classes and Their Associated Partially Balanced Incomplete Block Designs. *Advances and Applications in Discrete Mathematics*, **12**, 207-215.

[9] Laib, M., Rezgui, I., Gheribi-Aoulmi, Z. and Monod, H. (2013) Package "CombinS": Constructions Method of Rectangular PBIB and Rectangular Right Angular PBIB(m) (m = 4, 5 and 7) Designs. Version 1.0. http://cran.r-project.org/web/packages/CombinS/CombinS.pdf

Applied Mathematics, 2015, 6, 265-273
Published Online February 2015 in SciRes. http://www.scirp.org/journal/am
http://dx.doi.org/10.4236/am.2015.62025

Energy Identities of ADI-FDTD Method with Periodic Structure

Rengang Shi[1,2], Haitian Yang[3]

[1]Department of Applied Mathematics, Dalian University of Technology, Dalian, China
[2]College of Science, China University of Petroleum, Qingdao, China
[3]Department of Engineering Mechanics, Dalian University of Technology, Dalian, China
Email: srg831@163.com, haitian@dlut.edu.cn

Received 10 January 2015; accepted 28 January 2015; published 4 February 2015

Abstract

In this paper, a new kind of energy identities for the Maxwell equations with periodic boundary conditions is proposed and then proved rigorously by the energy methods. By these identities, several modified energy identities of the ADI-FDTD scheme for the two dimensional (2D) Maxwell equations with the periodic boundary conditions are derived. Also by these identities it is proved that 2D-ADI-FDTD is approximately energy conserved and unconditionally stable in the discrete L^2 and H^1 norms. Experiments are provided and the numerical results confirm the theoretical analysis on stability and energy conservation.

Keywords

Stability, Energy Conservation, ADI-FDTD, Maxwell Equations

1. Introduction

The alternative direction implicit finite difference time domain (ADI-FDTD) methods, proposed in [1] [2], are interesting and efficient methods for numerical solutions of Maxwell equations in time domain, and cause many researchers' work since ADI-FDTD overcomes the stability constraint of the FDTD scheme [3]. For example, it was proved by Fourier methods in [4]-[8] that the ADI-FDTD methods are unconditionally stable and have reasonable numerical dispersion error; Reference [9] studied the divergence property; Reference [10] studied ADI-FDTD in a perfectly matched medium; Reference [11] gave an efficient PML implementation for the ADI-FDTD method. By Poynting's theorem, Energy conservation is an important property for Maxwell equations and good numerical method should conform it. In 2012, Gao [12] proposed several new energy identities of the two dimensional (2D) Maxwell equations with the perfectly electric conducting (PEC) boundary condi-

How to cite this paper: Shi, R.G. and Yang, H.T. (2015) Energy Identities of ADI-FDTD Method with Periodic Structure. *Applied Mathematics*, **6**, 265-273. http://dx.doi.org/10.4236/am.2015.62025

tions and proved that ADI-FDTD is approximately energy conserved and unconditionally in the discrete L^2 and H^1 norms. Is there any other structure which can keep energy conservation for Maxwell equations? Is there any other energy identity for ADI-FDTD method? This two interesting questions promote us to find other energy-conservation structure.

In this paper, we focus our attention on structure with periodic boundary conditions and propose energy identities in L^2 and H^1 norms of the 2D Maxwell equations with periodic boundary conditions. We derive the energy identities of ADI-FDTD for the 2D Maxwell equations (2D-ADI-FDTD) with periodic boundary conditions by a new energy method. Several modified energy identities of 2D-ADI-FDTD in terms of the discrete L^2 and H^1 norms are presented. By these identities it is proved that 2D-ADI-FDTD with the periodic boundary conditions is unconditionally stable and approximately energy conserved under the discrete L^2 and H^1 norms. To test the analysis, experiments to solve a simple problem with exact solution are provided. Computational results of the energy and error in terms of the discrete L^2 and H^1 norms confirm the analysis on the energy conservation and the unconditional stability.

The remaining parts of the paper are organized as follows. In Section 2, energy identities of the 2D Maxwell equations with periodic conditions in L^2 and H^1 norms are first derived. In Section 3, several modified energy identities of the 2D-ADI-FDTD method are derived, the unconditional stability and the approximate energy conservation in the discrete L^2 and H^1 norms are then proved. In Section 4, the numerical experiments are presented.

2. Energy Conservation of Maxwell Equations and 2D-ADI-FDTD

Consider the two-dimensional (2D) Maxwell equations:

$$\varepsilon\frac{\partial E_x}{\partial t}=\frac{\partial H_z}{\partial y},\ \varepsilon\frac{\partial E_y}{\partial t}=-\frac{\partial H_z}{\partial x}\ \text{and}\ \mu\frac{\partial H_z}{\partial t}=\frac{\partial E_x}{\partial x}-\frac{\partial E_y}{\partial y} \tag{2.1}$$

in a rectangular domain with electric permittivity ε and magnetic permeability μ, where ε and μ are positive constants; $\boldsymbol{E}=\left(E_x\left(x,y,t\right),E_y\left(x,y,t\right)\right)$ and $H_z=H_z\left(x,y,t\right)$ denote the electric and magnetic fields, $t\in\left(0,T\right]$, $\left(x,y\right)\in\Omega=\left[0,a\right]\times\left[0,b\right]$.

We assume that the rectangular region Ω is surrounded by periodic boundaries, so the boundary conditions can be written as

$$E_x\left(0,y,t\right)=E_x\left(a,y,t\right),\ E_x\left(x,0,t\right)=E_x\left(x,b,t\right),\ E_y\left(0,y,t\right)=E_y\left(a,y,t\right), \tag{2.2}$$

$$E_y\left(x,0,t\right)=E_y\left(x,b,t\right),\ H_z\left(0,y,t\right)=H_z\left(a,y,t\right),\ H_z\left(x,0,t\right)=H_z\left(x,b,t\right). \tag{2.3}$$

We also assume the initial conditions

$$\boldsymbol{E}\left(x,y,0\right)=\boldsymbol{E}_0\left(x,y\right)=\left(E_{x0}\left(x,y\right),E_{y0}\left(x,y\right)\right),\ H_z\left(x,y,0\right)=H_{z0}\left(x,y\right). \tag{2.4}$$

It can be derived by integration by parts and the periodic boundary conditions (2.2)-(2.3) that the above Maxwell equations have the energy identities:

Lemma 2.1 Let $\boldsymbol{E}\left(t\right)=\left(E_x\left(x,y,t\right),E_y\left(x,y,t\right)\right)$ and $H_z\left(t\right)=H_z\left(x,y,t\right)$ be the solution of the Maxwell-systems (2.1)-(2.4). Then

$$\left\|\boldsymbol{E}\left(t\right)\right\|^2+\left\|H_z\left(t\right)\right\|^2=\left\|\boldsymbol{E}\left(0\right)\right\|^2+\left\|H_z\left(0\right)\right\|^2, \tag{2.5}$$

where and in what follows, $\left\|\bullet\right\|$ denotes the L^2 norm with the weights ε (corresponding electric field) or μ (magnetic field). For example,

$$\left\|\boldsymbol{E}\left(t\right)\right\|^2=\left\|E_x\left(t\right)\right\|^2+\left\|E_y\left(t\right)\right\|^2,\ \left\|E_x\left(t\right)\right\|^2=\int_0^a\int_0^b\varepsilon E_x^2\left(x,y,t\right)\mathrm{d}y\mathrm{d}x. \tag{2.6}$$

Identity (2.5) is called the Poynting Theorem and can be seen in many classical physics books. Besides the above energy identities, we found new ones below.

Theorem 2.2 Let $\boldsymbol{E}\left(t\right)$ and $H_z\left(t\right)$ be the solution of the Maxwell systems (2.1)-(2.4), the same as those in Lemma 2.1. Then, the following energy identities hold

$$\left\|\frac{\partial \boldsymbol{E}(t)}{\partial u}\right\|^2+\left\|\frac{\partial H_z(t)}{\partial u}\right\|^2=\left\|\frac{\partial \boldsymbol{E}(0)}{\partial u}\right\|^2+\left\|\frac{\partial H_z(0)}{\partial u}\right\|^2, \tag{2.7}$$

$$\left\|\boldsymbol{E}(t)\right\|_1^2+\left\|H(t)\right\|_1^2=\left\|\boldsymbol{E}(0)\right\|_1^2+\left\|H_z(0)\right\|_1^2, \tag{2.8}$$

where $u = x$ or y, and $\|\bullet\|_1$ is the H^1 norm (the H^1 norm of f is defined by $\|f\|_1^2=\|f\|^2+|f|_{1/2}^2$, where $|f|_{1/2}^2=\|f_x\|^2+\|f_y\|^2$, $f_x=\partial f/\partial x$, $f_y=\partial f/\partial y$. $|f|_{1/2}$ is also called the H^1-semi norm of f).

Proof. First, we prove Equation (2.7) with $u = x$. Differentiating each of the Equations in (2.1) with respect to x leads to

$$\varepsilon\frac{\partial^2 E_x}{\partial x\partial t}=\frac{\partial^2 H_z}{\partial x\partial y},\quad \varepsilon\frac{\partial^2 E_y}{\partial x\partial t}=-\frac{\partial^2 H_z}{\partial x\partial x}\ \text{ and }\ \mu\frac{\partial^2 H_z}{\partial x\partial t}=\frac{\partial^2 E_x}{\partial x\partial y}-\frac{\partial^2 E_y}{\partial x\partial x}. \tag{2.9}$$

By the integration by parts and the periodic boundary conditions (2.2)-(2.3), we have

$$\begin{aligned}&\int_0^a\int_0^b\frac{\partial^2 E_x}{\partial x\partial y}\cdot\frac{\partial H_z}{\partial x}\mathrm{d}x\mathrm{d}y=-\int_0^a\int_0^b\frac{\partial E_x}{\partial x}\cdot\frac{\partial^2 H_z}{\partial x\partial y}\mathrm{d}x\mathrm{d}y,\\&\int_0^a\int_0^b\frac{\partial^2 E_y}{\partial x^2}\cdot\frac{\partial H_z}{\partial x}\mathrm{d}x\mathrm{d}y=r(t)-\int_0^a\int_0^b\frac{\partial E_y}{\partial x}\cdot\frac{\partial^2 H_z}{\partial x^2}\mathrm{d}x\mathrm{d}y\end{aligned} \tag{2.10}$$

where

$$r(t)=\int_0^b\left(\frac{\partial E_y}{\partial x}(a,y,t)\frac{\partial H_z}{\partial x}(a,y,t)-\frac{\partial E_y}{\partial x}(0,y,t)\frac{\partial H_z}{\partial x}(0,y,t)\right)\mathrm{d}y. \tag{2.11}$$

Multiplying the Equations (2.9) by $\varepsilon\partial E_x/\partial x$, $\varepsilon\partial E_y/\partial x$ and $\mu\partial H_z/\partial x$ respectively, integrating both sides over $[0,a]\times[0,b]$ and using (2.10), we have

$$\frac{1}{2}\frac{\mathrm{d}}{\mathrm{d}t}\left(\left\|\frac{\partial E_x}{\partial x}\right\|^2+\left\|\frac{\partial E_y}{\partial x}\right\|^2+\left\|\frac{\partial H_z}{\partial x}\right\|^2\right)=-r(t). \tag{2.12}$$

From (2.1) and the boundary conditions (2.2)-(2.3) we note that

$$\begin{aligned}\frac{\partial E_y}{\partial x}\frac{\partial H_z}{\partial x}(0,y,t)&=\lim_{x\to 0}\frac{\partial E_y}{\partial x}\frac{\partial H_z}{\partial x}(x,y,t)=-\lim_{x\to 0}\varepsilon\left(\frac{\partial E_x}{\partial y}-\mu\frac{\partial H_z}{\partial t}\right)\frac{\partial E_y}{\partial t}(x,y,t)\\&=-\lim_{x\to a}\varepsilon\left(\frac{\partial E_x}{\partial y}-\mu\frac{\partial H_z}{\partial t}\right)\frac{\partial E_y}{\partial t}(x,y,t)=\lim_{x\to a}\frac{\partial E_y}{\partial x}(x,y,t)\frac{\partial H_z}{\partial x}(x,y,t)\\&=\frac{\partial E_y}{\partial x}(a,y,t)\frac{\partial H_z}{\partial x}(a,y,t).\end{aligned} \tag{2.13}$$

So, $r(t)=0$. Then, by integrating (2.12) with respect to time over $[0,T]$, we get equation (2.7) with $u = x$. Similarly, the identity (2.7) with $u = y$ can be proved. Combining (2.5) and (2.7) leads to (2.8). □

The 2D-ADI-FDTD Scheme

The alternating direction implicit FDTD method for the 2D Maxwell equations (denoted by 2D-ADI-FDTD) was proposed by (Namiki, 1999). For convenience in analysis of this scheme, next we give some notations. Let

$$\begin{aligned}&x_i=i\Delta x, x_{i+\frac{1}{2}}=x_i+\frac{\Delta x}{2}, y_j=j\Delta y, y_{j+\frac{1}{2}}=y_j+\frac{\Delta y}{2},\ t^n=n\Delta t, t^{n+\frac{1}{2}}=t^n+\frac{\Delta t}{2},\\&i=0,1,\cdots,I-1,\ x_I=a,\ j=0,1,\cdots,J-1,\ y_J=b,\ n=0,1,\cdots,N-1,\ N\Delta t=T.\end{aligned}$$

where Δx and Δy are the mesh sizes along x and y directions, Δt is the time step, I, J and N are positive integers. For a grid function $f_{\alpha,\beta}^m=f\left(x_\alpha,y_\beta,t^m\right)$, define

$$\delta_x f^m_{\alpha,\beta} = \frac{f^m_{\alpha+\frac{1}{2},\beta} - f^m_{\alpha-\frac{1}{2},\beta}}{\Delta x}, \delta_y f^m_{\alpha,\beta} = \frac{f^m_{\alpha,\beta+\frac{1}{2}} - f^m_{\alpha,\beta-\frac{1}{2}}}{\Delta y},$$

$$\delta_t f^m_{\alpha,\beta} = \frac{f^{m+\frac{1}{2}}_{\alpha,\beta} - f^{m-\frac{1}{2}}_{\alpha,\beta}}{\Delta t}, \delta_u \delta_v f^m_{\alpha,\beta} = \delta_u \left(\delta_v f^m_{\alpha,\beta}\right), \Delta u^2 = \left(\Delta u\right)^2,$$

where $u = x, y$ or t. For $\boldsymbol{V} = \left(V_{x_{i+1/2,j}}, V_{y_{i,j+1/2}}\right)$, $W_{i+1/2,j+1/2}$, $\Delta v = \Delta x \Delta y$, define some discrete energy norms based on the Yee staggered grids (Yee, 1966),

$$\|V_x\|^2_{E_x} = \sum_{i=0}^{I-1}\sum_{j=0}^{J-1} \varepsilon \left(V_{x_{i+\frac{1}{2},j}}\right)^2 \Delta v, \|V_y\|^2_{E_y} = \sum_{i=0}^{I-1}\sum_{j=0}^{J-1} \varepsilon \left(V_{y_{i,j+\frac{1}{2}}}\right)^2 \Delta v, \|W\|^2_{H_z} = \sum_{i=0}^{I-1}\sum_{j=0}^{J-1} \mu \left(W_{z_{i+\frac{1}{2},j+\frac{1}{2}}}\right)^2 \Delta v,$$

$$\|\delta_x \boldsymbol{V}\|^2_{\delta_x \boldsymbol{E}} = \|\delta_x V_x\|^2_{\delta_x E_x} + \|\delta_x V_y\|^2_{\delta_x E_y}, \|\delta_x V_x\|^2_{\delta_x E_x} = \sum_{i=0}^{I-1}\sum_{j=0}^{J-1} \varepsilon \left(\delta_x V_{x_{i,j}}\right)^2 \Delta v, \|\delta_x V_y\|^2_{\delta_x E_y} = \sum_{i=0}^{I-1}\sum_{j=0}^{J-1} \varepsilon \left(\delta_x V_{y_{i+\frac{1}{2},j+\frac{1}{2}}}\right)^2 \Delta v.$$

Other norms: $\|\delta_y V_x\|_{\delta_y E_x}$, $\|\delta_y V_y\|_{\delta_y E_y}$ and $\|\delta_y H_z\|_{\delta_y H_z}$ are similarly defined. Denote by $E^m_{u_{\alpha,\beta}}$ and $H^m_{z_{\alpha,\beta}}$ the approximations of $E_u\left(x_\alpha, y_\beta, t^m\right)$ ($u = x, y$) and $H_z\left(x_\alpha, y_\beta, t^m\right)$, respectively. Then the 2D-ADI-FDTD scheme for (2.1) is written as

Stage 1:

$$\frac{E^{n+\frac{1}{2}}_{x_{i+\frac{1}{2},j}} - E^n_{x_{i+\frac{1}{2},j}}}{\Delta t/2} = \frac{\delta_y H^n_{z_{i+\frac{1}{2},j}}}{\varepsilon} \tag{2.14}$$

$$\frac{E^{n+\frac{1}{2}}_{y_{i,j+\frac{1}{2}}} - E^n_{y_{i,j+\frac{1}{2}}}}{\Delta t/2} = -\frac{\delta_x H^{n+\frac{1}{2}}_{z_{i,j+\frac{1}{2}}}}{\varepsilon} \tag{2.15}$$

$$\frac{H^{n+\frac{1}{2}}_{z_{i+\frac{1}{2},j+\frac{1}{2}}} - H^n_{z_{i+\frac{1}{2},j+\frac{1}{2}}}}{\Delta t/2} = \frac{1}{\mu}\left(\delta_y E^n_{x_{i+\frac{1}{2},j+\frac{1}{2}}} - \delta_x E^{n+\frac{1}{2}}_{y_{i+\frac{1}{2},j+\frac{1}{2}}}\right) \tag{2.16}$$

Stage 2:

$$\frac{E^{n+1}_{x_{i+\frac{1}{2},j}} - E^{n+\frac{1}{2}}_{x_{i+\frac{1}{2},j}}}{\Delta t/2} = \frac{\delta_y H^{n+1}_{z_{i+\frac{1}{2},j}}}{\varepsilon} \tag{2.17}$$

$$\frac{E^{n+1}_{y_{i,j+\frac{1}{2}}} - E^{n+\frac{1}{2}}_{y_{i,j+\frac{1}{2}}}}{\Delta t/2} = -\frac{\delta_x H^{n+\frac{1}{2}}_{z_{i,j+\frac{1}{2}}}}{\varepsilon} \tag{2.18}$$

$$\frac{H^{n+1}_{z_{i+\frac{1}{2},j+\frac{1}{2}}} - H^{n+\frac{1}{2}}_{z_{i+\frac{1}{2},j+\frac{1}{2}}}}{\Delta t/2} = \frac{1}{\mu}\left(\delta_y E^{n+1}_{x_{i+\frac{1}{2},j+\frac{1}{2}}} - \delta_x E^{n+\frac{1}{2}}_{y_{i+\frac{1}{2},j+\frac{1}{2}}}\right) \tag{2.19}$$

For simplicity in notations, we sometimes omit the subscripts of these field values without causing any ambiguity. By the definition of cross product of vectors, the boundary conditions for (2.2)-(2.3) become

$$\begin{cases} E^m_{x_{i+\frac{1}{2},0}} = E^m_{x_{i+\frac{1}{2},J}}, E^m_{x_{\frac{1}{2},j}} = E^m_{x_{I+\frac{1}{2},j}}, E^m_{x_{-\frac{1}{2},j}} = E^m_{x_{I-\frac{1}{2},j}}, E^m_{y_{0,j+\frac{1}{2}}} = E^m_{y_{I,j+\frac{1}{2}}}, E^m_{y_{i,\frac{1}{2}}} = E^m_{y_{i,J+\frac{1}{2}}}, E^m_{y_{i,-\frac{1}{2}}} = E^m_{y_{i,J-\frac{1}{2}}}, \\ H^m_{z_{\frac{1}{2},j+\frac{1}{2}}} = H^m_{z_{I+\frac{1}{2},j+\frac{1}{2}}}, H^m_{z_{-\frac{1}{2},j+\frac{1}{2}}} = H^m_{z_{I-\frac{1}{2},j+\frac{1}{2}}}, H^m_{z_{i+\frac{1}{2},\frac{1}{2}}} = H^m_{z_{i+\frac{1}{2},J+\frac{1}{2}}}, H^m_{z_{i+\frac{1}{2},-\frac{1}{2}}} = H^m_{z_{i+\frac{1}{2},J-\frac{1}{2}}}, \end{cases} \tag{2.20}$$

where $m = n$ or $m = n + 1/2$. Finally, the initial values $\boldsymbol{E}^0_{\alpha,\beta}$ and $H^0_{z_{\alpha,\beta}}$ of the2D-ADI-FDTD scheme are obtained by the initial condition (2.4).

3. Modified Energy Identities and Stability of 2D-ADI-FDTD in H^1 Norm

In this Section we derive modified energy identities of 2D-ADI-FDTD and prove its energy conservation and unconditional stability in the discrete H^1 norm.

Theorem 3.1 Let $n > 0$, $\boldsymbol{E}^n = \left(E^n_{x_{i+1/2,j}}, E^n_{y_{i,j+1/2}}\right)$ and $H^n_{z_{i+1/2,j+1/2}}$ be the solution of the ADI-FDTD scheme (2.14)-(2.19). Then the following modified energy identities hold,

$$\begin{aligned} &\left\|\delta_x \boldsymbol{E}^n\right\|^2_{\delta_x \boldsymbol{E}} + \left\|\delta_x H^n_z\right\|^2_{\delta_x H_z} + \frac{\Delta t^2}{4\mu\varepsilon}\left(\left\|\delta_x\delta_y H^n_z\right\|^2_{\delta_x E_x} + \left\|\delta_x\delta_y E^n_x\right\|^2_{\delta_x H_z}\right) \\ &= \left\|\delta_x \boldsymbol{E}^0\right\|^2_{\delta_x \boldsymbol{E}} + \left\|\delta_x H^0_z\right\|^2_{\delta_x H_z} + \frac{\Delta t^2}{4\mu\varepsilon}\left(\left\|\delta_x\delta_y H^0_z\right\|^2_{\delta_x E_x} + \left\|\delta_x\delta_y E^0_x\right\|^2_{\delta_x H_z}\right), \end{aligned} \tag{3.1}$$

$$\begin{aligned} &\left\|\delta_y \boldsymbol{E}^n\right\|^2_{\delta_y \boldsymbol{E}} + \left\|\delta_y H^n_z\right\|^2_{\delta_y H_z} + \frac{\Delta t^2}{4\mu\varepsilon}\left(\left\|\delta_y\delta_y H^n_z\right\|^2_{\delta_y E_x} + \left\|\delta_y\delta_y E^n_x\right\|^2_{\delta_y H_z}\right) \\ &= \left\|\delta_y \boldsymbol{E}^0\right\|^2_{\delta_y \boldsymbol{E}} + \left\|\delta_y H^0_z\right\|^2_{\delta_y H_z} + \frac{\Delta t^2}{4\mu\varepsilon}\left(\left\|\delta_y\delta_y H^0_z\right\|^2_{\delta_y E_x} + \left\|\delta_y\delta_y E^0_x\right\|^2_{\delta_y H_z}\right), \end{aligned} \tag{3.2}$$

where for $u = x, y$, and $m = n$ or 0

$$\left\|\delta_u \boldsymbol{E}^m\right\|^2_{\delta_u \boldsymbol{E}} = \left\|\delta_u E^m_x\right\|^2_{\delta_u E_x} + \left\|\delta_u E^m_y\right\|^2_{\delta_u E_y}.$$

Proof. First we prove (3.1). Applying δ_x to the Equations (2.14)-(2.19), and rearranging the terms by the time levels, we have

$$\delta_x E^{n+\frac{1}{2}}_{x_{i,j}} = \delta_x E^n_{x_{i,j}} + \frac{\Delta t}{2\varepsilon}\delta_x\delta_y H^n_{z_{i,j}}, \tag{3.3}$$

$$\delta_x E^{n+\frac{1}{2}}_{y_{i+\frac{1}{2},j+\frac{1}{2}}} + \frac{\Delta t}{2\varepsilon}\delta_x\delta_x H^{n+\frac{1}{2}}_{z_{i+\frac{1}{2},j+\frac{1}{2}}} = \delta_x E^n_{y_{i+\frac{1}{2},j+\frac{1}{2}}}, \tag{3.4}$$

$$\delta_x H^{n+\frac{1}{2}}_{z_{i,j+\frac{1}{2}}} + \frac{\Delta t}{2\mu}\delta_x\delta_x E^{n+\frac{1}{2}}_{y_{i,j+\frac{1}{2}}} = \delta_x H^n_{z_{i,j+\frac{1}{2}}} + \frac{\Delta t}{2\mu}\delta_x\delta_y E^n_{x_{i,j+\frac{1}{2}}}, \tag{3.5}$$

$$\delta_x E^{n+1}_{x_{i,j}} - \frac{\Delta t}{2\varepsilon}\delta_x\delta_y H^{n+1}_{z_{i,j}} = \delta_x E^{n+\frac{1}{2}}_{x_{i,j}}, \tag{3.6}$$

$$\delta_x E^{n+1}_{y_{i+\frac{1}{2},j+\frac{1}{2}}} = \delta_x E^{n+\frac{1}{2}}_{y_{i+\frac{1}{2},j+\frac{1}{2}}} - \frac{\Delta t}{2\varepsilon}\delta_x\delta_x H^{n+\frac{1}{2}}_{z_{i+\frac{1}{2},j+\frac{1}{2}}}, \tag{3.7}$$

$$\delta_x H^{n+1}_{z_{i,j+\frac{1}{2}}} - \frac{\Delta t}{2\mu}\delta_x\delta_y E^{n+1}_{x_{i,j+\frac{1}{2}}} = \delta_x H^{n+\frac{1}{2}}_{z_{i,j+\frac{1}{2}}} - \frac{\Delta t}{2\mu}\delta_x\delta_x E^{n+\frac{1}{2}}_{y_{i,j+\frac{1}{2}}}. \tag{3.8}$$

Multiplying both sides of the equations, (3.3)-(3.4) by $\sqrt{\varepsilon}$ respectively, and those of (3.5) by $\sqrt{\mu}$, and taking the square of the updated equations lead to

$$\varepsilon\left(\delta_x E_{x_{i,j}}^{n+\frac{1}{2}}\right)^2=\varepsilon\left(\delta_x E_{x_{i,j}}^{n}\right)^2+\frac{\Delta t^2}{4\mu\varepsilon}\mu\left(\delta_x\delta_y H_{z_{i,j}}^{n}\right)^2+\Delta t\delta_x E_{x_{i,j}}^{n}\delta_x\delta_x H_{z_{i,j}}^{n},\tag{3.9}$$

$$\varepsilon\left(\delta_x E_{y_{i+\frac{1}{2},j+\frac{1}{2}}}^{n+\frac{1}{2}}\right)^2+\frac{\Delta t^2}{4\mu\varepsilon}\mu\left(\delta_x\delta_x H_{z_{i+\frac{1}{2},j+\frac{1}{2}}}^{n+\frac{1}{2}}\right)^2+\Delta t\delta_x E_{y_{i+\frac{1}{2},j+\frac{1}{2}}}^{n+\frac{1}{2}}\delta_x\delta_x H_{z_{i+\frac{1}{2},j+\frac{1}{2}}}^{n+\frac{1}{2}}=\varepsilon\left(\delta_x E_{y_{i+\frac{1}{2},j+\frac{1}{2}}}^{n}\right)^2,\tag{3.10}$$

$$\begin{aligned}&\mu\left(\delta_x H_{z_{i,j+\frac{1}{2}}}^{n+\frac{1}{2}}\right)^2+\frac{\Delta t^2}{4\mu\varepsilon}\varepsilon\left(\delta_x\delta_x E_{y_{i,j+\frac{1}{2}}}^{n+\frac{1}{2}}\right)^2+\Delta t\delta_x H_{z_{i,j+\frac{1}{2}}}^{n+\frac{1}{2}}\delta_x\delta_x E_{y_{i,j+\frac{1}{2}}}^{n+\frac{1}{2}}\\&=\mu\left(\delta_x H_{z_{i,j+\frac{1}{2}}}^{n}\right)^2+\frac{\Delta t^2}{4\mu\varepsilon}\varepsilon\left(\delta_x\delta_y E_{x_{i,j+\frac{1}{2}}}^{n}\right)^2+\Delta t\delta_x H_{z_{i,j+\frac{1}{2}}}^{n}\delta_x\delta_y E_{x_{i,j+\frac{1}{2}}}^{n},\end{aligned}\tag{3.11}$$

Applying summation by parts, we see that

$$\begin{aligned}\sum_{i=0}^{I-1}\sum_{j=0}^{J-1}\delta_x H_z^n\cdot\delta_x\delta_y E_x^n\Big|_{i,j+\frac{1}{2}}&=\frac{1}{\Delta y}\sum_{i=0}^{I-1}\delta_x E_{x_{i,0}}^{n}\left(\delta_x H_{z_{i,J-\frac{1}{2}}}^{n}-\delta_x H_{z_{i,-\frac{1}{2}}}^{n}\right)-\sum_{i=1}^{I-1}\sum_{j=1}^{J-1}\delta_x E_x^n\cdot\delta_x\delta_y H_z^n\Big|_{i,j}\\&=-\sum_{i=0}^{I-1}\delta_x E_{x_{i,0}}^{m}\delta_x\delta_y H_{z_{i,0}}^{m}-\sum_{i=0}^{I-1}\sum_{j=1}^{J-1}\delta_x E_x^m\cdot\delta_x\delta_y H_z^m\Big|_{i,j}\\&=-\sum_{i=0}^{I-1}\sum_{j=0}^{J-1}\delta_x E_x^m\cdot\delta_x\delta_y H_z^m\Big|_{i,j},\end{aligned}\tag{3.12}$$

where we have used that $\delta_x E_{x_{i,0}}^{n}=\delta_x E_{x_{i,J}}^{n}$ and that $\delta_x H_{x_{i,J-\frac{1}{2}}}^{n}=\delta_x H_{x_{i,-\frac{1}{2}}}^{n}$, which can be obtained from the periodic boundary conditions. Similarly, we get that

$$\sum_{i=0}^{I-1}\sum_{j=0}^{J-1}\delta_x E_y^{n+\frac{1}{2}}\cdot\delta_x\delta_x H_z^{n+\frac{1}{2}}\Big|_{i+\frac{1}{2},j+\frac{1}{2}}=-\sum_{i=0}^{I-1}\sum_{j=0}^{J-1}\delta_x H_z^{n+\frac{1}{2}}\cdot\delta_x\delta_x E_y^{n+\frac{1}{2}}\Big|_{i,j+\frac{1}{2}}.\tag{3.13}$$

So, if summing each of the Equalities (3.9)-(3.11) over their subscripts, adding the updated equations, multiplying both sides by $\Delta x\Delta y$, and using the two identities, (3.12) and (3.13), together with the norms defined in Subsection 2.2, we arrive at

$$\begin{aligned}&\left\|\delta_x E_x^{n+\frac{1}{2}}\right\|_{\delta_x E_x}^2+\left\|\delta_x E_y^{n+\frac{1}{2}}\right\|_{\delta_x E_y}^2+\left\|\delta_x H_z^{n+\frac{1}{2}}\right\|_{\delta_x H_z}^2+\frac{\Delta t^2}{4\mu\varepsilon}\left(\left\|\delta_x\delta_y H_z^{n+\frac{1}{2}}\right\|_{\delta_x E_x}^2+\left\|\delta_x\delta_y E_x^{n+\frac{1}{2}}\right\|_{\delta_x H_z}^2\right)\\&=\left\|\delta_x E_x^{n}\right\|_{\delta_x E_x}^2+\left\|\delta_x E_y^{n}\right\|_{\delta_x E_y}^2+\left\|\delta_x H_z^{n}\right\|_{\delta_x H_z}^2+\frac{\Delta t^2}{4\mu\varepsilon}\left(\left\|\delta_x\delta_y H_z^{n}\right\|_{\delta_x E_x}^2+\left\|\delta_x\delta_y E_x^{n}\right\|_{\delta_x H_z}^2\right).\end{aligned}\tag{3.14}$$

Similar argument is applied to the second Stage (3.6)-(3.8), we have

$$\begin{aligned}&\left\|\delta_x E_x^{n+1}\right\|_{\delta_x E_x}^2+\left\|\delta_x E_y^{n+1}\right\|_{\delta_x E_y}^2+\left\|\delta_x H_z^{n+1}\right\|_{\delta_x H_z}^2+\frac{\Delta t^2}{4\mu\varepsilon}\left(\left\|\delta_x\delta_y H_z^{n+1}\right\|_{\delta_x E_x}^2+\left\|\delta_x\delta_y E_x^{n+1}\right\|_{\delta_x H_z}^2\right)\\&=\left\|\delta_x E_x^{n+\frac{1}{2}}\right\|_{\delta_x E_x}^2+\left\|\delta_x E_y^{n+\frac{1}{2}}\right\|_{\delta_x E_y}^2+\left\|\delta_x H_z^{n+\frac{1}{2}}\right\|_{\delta_x H_z}^2+\frac{\Delta t^2}{4\mu\varepsilon}\left(\left\|\delta_x\delta_y H_z^{n+\frac{1}{2}}\right\|_{\delta_x E_x}^2+\left\|\delta_x\delta_y E_x^{n+\frac{1}{2}}\right\|_{\delta_x H_z}^2\right).\end{aligned}\tag{3.15}$$

Combination of (3.14) and (3.15) leads to the identity (3.1). Identity (3.2) is similarly derived by repeating the above argument from the operated Equations (2.14)-(2.19) by δ_y. This completes the proof of Theorem 3.1. □

In the above proof, if taking δ_x as the identity operator, we obtain that

Theorem 3.2 Let $n>0$, $\boldsymbol{E}^n$ and H_z^n be the solution of 2D-ADI-FDTD. Then, the following energy identities hold

$$\begin{aligned}&\left\|E_x^n\right\|_{E_x}^2+\left\|E_y^n\right\|_{E_y}^2+\left\|H_z^n\right\|_{H_z}^2+\frac{\Delta t^2}{4\mu\varepsilon}\left(\left\|\delta_y E_x^n\right\|_{H_z}^2+\left\|\delta_y H_z^n\right\|_{E_x}^2\right)\\&=\left\|E_x^0\right\|_{E_x}^2+\left\|E_y^0\right\|_{E_y}^2+\left\|H_z^0\right\|_{H_z}^2+\frac{\Delta t^2}{4\mu\varepsilon}\left(\left\|\delta_y E_x^0\right\|_{H_z}^2+\left\|\delta_y H_z^0\right\|_{E_x}^2\right),\end{aligned}\tag{3.16}$$

Combining the results in Theorems 3.1 and 3.2 we have

Theorem 3.3 If the discrete H^1 semi-norm and H^1 norm of the solution of 2D-ADI-FDTD are denoted respectively by

$$\begin{aligned}&\left\|\boldsymbol{E}^n\right\|_{1/2}^2=\left\|\delta_x E_x^n\right\|_{\delta_x E_x}^2+\left\|\delta_x E_y^n\right\|_{\delta_x E_y}^2+\left\|\delta_y E_x^n\right\|_{\delta_y E_x}^2+\left\|\delta_y E_y^n\right\|_{\delta_y E_y}^2,\\&\left\|\boldsymbol{E}^n\right\|^2=\left\|E_x^n\right\|_{E_x}^2+\left\|E_y^n\right\|_{E_y}^2,\left\|\boldsymbol{E}^n\right\|_1^2=\left\|\boldsymbol{E}^n\right\|_{1/2}^2+\left\|\boldsymbol{E}^n\right\|_{\boldsymbol{E}}^2,\\&\left\|\delta_y E_x^n\right\|_1^2=\left\|\delta_x\delta_y E_x^n\right\|_{\delta_x H_z}^2+\left\|\delta_y\delta_y E_x^n\right\|_{\delta_y H_z}^2+\left\|\delta_y E_x^n\right\|_{H_z}^2,\\&\left\|H_z^n\right\|_1^2=\left\|\delta_x H_z^n\right\|_{\delta_x H_z}^2+\left\|\delta_y H_z^n\right\|_{\delta_y H_z}^2+\left\|H_z^n\right\|_{H_z}^2,\\&\left\|\delta_y H_z^n\right\|_1^2=\left\|\delta_x\delta_y H_z^n\right\|_{\delta_x E_x}^2+\left\|\delta_y\delta_y H_z^n\right\|_{\delta_y E_x}^2+\left\|\delta_y H_z^n\right\|_{E_x}^2,\end{aligned}$$

then, the following energy identities for 2D-ADI-FDTD hold

$$\left\|\boldsymbol{E}^n\right\|_{1/2}^2+\left\|H_z^n\right\|_{1/2}^2+\frac{\Delta t^2}{4\mu\varepsilon}\left(\left\|\delta_y E_x^n\right\|_{1/2}^2+\left\|\delta_y H_z^n\right\|_{1/2}^2\right)=\left\|\boldsymbol{E}^0\right\|_{1/2}^2+\left\|H_z^0\right\|_{1/2}^2+\frac{\Delta t^2}{4\mu\varepsilon}\left(\left\|\delta_y E_x^0\right\|_{1/2}^2+\left\|\delta_y H_z^0\right\|_{1/2}^2\right).\tag{3.17}$$

$$\left\|\boldsymbol{E}^n\right\|_1^2+\left\|H_z^n\right\|_1^2+\frac{\Delta t^2}{4\mu\varepsilon}\left(\left\|\delta_y E_x^n\right\|_1^2+\left\|\delta_y H_z^n\right\|_1^2\right)=\left\|\boldsymbol{E}^0\right\|_1^2+\left\|H_z^0\right\|_1^2+\frac{\Delta t^2}{4\mu\varepsilon}\left(\left\|\delta_y E_x^0\right\|_1^2+\left\|\delta_y H_z^0\right\|_1^2\right).\tag{3.18}$$

Remark 3.4 It is easy to see that the identities in Theorems 3.1, 3.2 and 3.3converge to those in Lemma 2.1 and Theorem 2.2 as the discrete step sizes approach zero. This means that2D-ADI-FDTD is approximately energy-conserved and unconditionally stable in the modified discrete form of the L^2 and H^1 norms**.**

4. Numerical Experiments

In this section we solve a model problem by 2D-ADI-FDTD, and then test the analysis of the stability and energy conservation in Section 3 by comparing the numerical solution with the exact solution of the model. The model considered is the Maxwell equations (2.1) with $\varepsilon=\mu=1$, $\Omega=[0,1]\times[0,1]$, $t\in(0,T]$, and its exact solution is: $E_x=E_x(t)=\cos\left(2\pi(x+y)-2\sqrt{2}\pi t\right)$, $E_y=E_y(t)=-E_x$, $H_z=H_z(t)=-\sqrt{2}E_x$.

It is easy to compute the norms of this solution are

$$\begin{aligned}&\left\|\left(E(t),H_z(t)\right)\right\|=\sqrt{\left\|\boldsymbol{E}(t)\right\|^2+\left\|H_z(t)\right\|^2}=\sqrt{2},\\&\left\|\left(E(t),H_z(t)\right)\right\|_1=\left(\left\|\boldsymbol{E}(t)\right\|_1^2+\left\|H_z(t)\right\|_1^2\right)^{1/2}=\left(2+8\pi^2\right)^{1/2}.\end{aligned}$$

4.1. Simulation of the Error and Stability

To show the accuracy of 2D-ADI-FDTD, we define the errors:

$$\mathcal{E}_{x_{i+1/2,j}}^n=E_x\left(t^n\right)_{i+1/2,j}-E_{x_{i+1/2,j}}^n,\ \mathcal{E}_{y_{i,j+1/2}}^n=E_y\left(t^n\right)_{i,j+1/2}-E_{y_{i,j+1/2}}^n\ \text{and}\ \mathcal{H}_{z_{i+1/2,j+1/2}}^n=H_z\left(t^n\right)_{i+1/2,j+1/2}-H_{z_{i+1/2,j+1/2}}^n,$$

where $E_x\left(t^n\right)$, $E_x\left(t^n\right)$, $H_z\left(t^n\right)$ are the true values of the exact solution. Denote the error and relative error in the norms defined in Section 3 by ErL_2, $R\text{-}ErL_2$, ErH_1 and $R\text{-}ErH_1$, *i.e.*

$$ErL_2=\sqrt{\left\|\mathcal{E}_x^n\right\|_{E_x}^2+\left\|\mathcal{E}_y^n\right\|_{E_y}^2+\left\|\mathcal{H}_z^n\right\|_{H_z}^2},\ R\text{-}ErL_2=\frac{ErL_2}{\left\|\left(\boldsymbol{E}(t),H_z(t)\right)\right\|}$$

$$ErH_1 = \left(\left(ErL_2\right)^2 + \left\|\delta_x \mathcal{E}_x^n\right\|_{\delta_x E_x}^2 + \left\|\delta_x \mathcal{E}_y^n\right\|_{\delta_x E_y}^2 + \left\|\delta_x \mathcal{H}_z^n\right\|_{\delta_x H_z}^2 + \left\|\delta_y \mathcal{E}_x^n\right\|_{\delta_y E_x}^2 + \left\|\delta_y \mathcal{E}_y^n\right\|_{\delta_y E_y}^2 + \left\|\delta_y \mathcal{H}_z^n\right\|_{\delta_y H_z}^2 \right)^{1/2},$$

$$R\text{-}ErH_1 = \frac{ErH_1}{\left\|\left(\boldsymbol{E}(t), H_z(t)\right)\right\|_1}, \quad \text{Rate} = \log_2 \frac{\text{Error}(h)}{\text{Error}(h/2)},$$

where log is the logarithmic function.

Table 1 gives the error and relative error of the numerical solution of the model problem computed by 2D-ADI-FDTD in the norms, and the convergence rates with different time step sizes $\Delta t = 4h$, $2h$ and h, when $\Delta x = \Delta y = h = 0.01$ is fixed and $T = 1$. From these results we see that the convergence rate of 2D-ADI-FDTD with respect to time is approximately 2 and that 2D-ADI-FDTD is unconditionally stable (when $\Delta t = \Delta x = \Delta y = h$, the CFL number $c\Delta t\sqrt{1/\Delta x^2 + 1/\Delta y^2} = \sqrt{2} > 1$).

Table 2 lists the similar results to **Table 1** when $\Delta t = 0.1h$ is fixed, $\Delta x = \Delta y$ varies from $2h$, h and $0.5h$, and the time length $T = 1$. From the columns "Rate" we see that 2D-ADI-FDTD is of second order in space under the discrete L^2 and H^1 norm.

4.2. Simulation of the Energy Conservation of 2D-ADI-FDTD

In this subsection we check the energy conservation of 2D-ADI-FDTD by computing the modified energy norms derived in Section 3 for the solution to the scheme. Denote these modified energy norms by

$$I_u\left(\boldsymbol{E}^n, H_z^n\right) = \sqrt{\left\|\delta_u \boldsymbol{E}^n\right\|_{\delta_u \boldsymbol{E}}^2 + \left\|\delta_u H_z^n\right\|_{\delta_u H_z}^2 + \frac{\Delta t^2}{4\mu\varepsilon}\left(\left\|\delta_u \delta_y H_z^n\right\|_{\delta_u E_x}^2 + \left\|\delta_u \delta_y E_x^n\right\|_{\delta_u H_z}^2\right)},$$

$$I_0\left(\boldsymbol{E}^n, H_z^n\right) = \sqrt{\left\|\boldsymbol{E}^n\right\|_{\boldsymbol{E}}^2 + \left\|H_z^n\right\|_{H_z}^2 + \frac{\Delta t^2}{4\mu\varepsilon}\left(\left\|\delta_y E_x^n\right\|_{H_z}^2 + \left\|\delta_y H_z^n\right\|_{E_x}^2\right)},$$

$$I_1\left(\boldsymbol{E}^n, H_z^n\right) = \sqrt{\left|I_x\left(\boldsymbol{E}^n, H_z^n\right)\right|^2 + \left|I_y\left(\boldsymbol{E}^n, H_z^n\right)\right|^2 + \left|I_0\left(\boldsymbol{E}^n, H_z^n\right)\right|^2}.$$

In **Table 3** are presented the energy norms $I_u\left(\boldsymbol{E}^n, H_z^n\right)(u = x, y, 0, 1)$ of the solution of the 2D-ADI-FDTD scheme at the time levels $n = 0$, $n = 1000$ and $n = 4000$ (the third to fifth rows), and the absolute values of their difference (the last two rows), where the sizes of the spatial and time steps are $\Delta x = \Delta y = 0.01$, $\Delta t = 0.04$. The second row shows the four kind of energies of the exact solution computed by using the definitions of $I_u(u = 0, x, y)$. From these value we see that 2D-ADI-FDTD is approximately energy-conserved.

Table 1. Error of $\left(\boldsymbol{E}^n, H_z^n\right)$ in L^2 and H^1 with $\Delta x = \Delta y = h$ and different Δt.

Δt	$R\text{-}ErL_2$	ErL_2	Rate	$R\text{-}ErH_1$	ErH_1	Rate
$4h$	6.0284e−2	8.5254e−2		6.0287e−2	7.6675e−1	
$2h$	1.6264e−2	2.3001e−2	1.8901	1.6265e−2	2.0595e−1	1.8901
h	5.1571e−3	7.2932e−3	1.6571	5.1571e−3	6.5229e−2	1.3182

Table 2. Error of $\left(\boldsymbol{E}^n, H_z^n\right)$ in L^2 and H^1 with $\Delta t = 0.1h$ and different spatial step sizes.

$\Delta x = \Delta y$	$R\text{-}ErL_2$	ErL_2	Rate	$R\text{-}ErH_1$	ErH_1	Rate
$2h$	5.0019e−3	8.3182e−3		5.0019e−3	7.4333e−3	
h	1.4981e−3	2.1186e−3	1.7393	1.4981e−3	1.8942e−3	1.7393
$0.5h$	4.0200e−4	5.6851e−4	1.8979	4.0200e−4	5.0834e−4	1.8978

Table 3. Energy of $\left(\boldsymbol{E}^n, H_z^n\right)$ and its error when $\Delta x = \Delta y = h = 0.01$, $\Delta t = 4h$ and $n = 0, 1000, 4000$.

Fields\Norms	$I_x(\cdot)$	$I_y(\cdot)$	$I_0(\cdot)$	$I_1(\cdot)$
$\left(\boldsymbol{E}(t), H_z(t)\right)$	8.9367	8.9367	1.4226	12.7183
$\left(\boldsymbol{E}^0, H_z^0\right)$	8.9367	8.9367	1.4226	12.7183
$\left(\boldsymbol{E}^{1000}, H_z^{1000}\right)$	8.9367	8.9367	1.4226	12.7183
$\left(\boldsymbol{E}^{4000}, H_z^{4000}\right)$	8.9367	8.9367	1.4226	12.7183
$\left(\boldsymbol{E}^{1000}, H_z^{1000}\right)-\left(\boldsymbol{E}^0, H_z^0\right)$	3.2685e−13	3.2685e−13	5.2403e−14	4.6718e−13
$\left(\boldsymbol{E}^{4000}, H_z^{4000}\right)-\left(\boldsymbol{E}^0, H_z^0\right)$	3.2685e−13	3.2685e−13	5.2403e−14	4.6718e−13

5. Conclusion

In this paper, the modified energy identities of the 2D-ADI-FDTD scheme with the periodic boundary conditions in the discrete L^2 and H^1 norms are established which show that this scheme is approximately energy conserved in terms of the two energy norms. By the deriving methods for the energy identities, new kind of energy identities of the Maxwell equations are proposed and proved by the new energy method. Numerical experiments are provided and confirm the analysis of 2D-ADI-FDTD.

References

[1] Namiki, T. (1999) A New FDTD Algorithm Based on Alternating-Direction Implicit Method. *IEEE Transactions on Microwave Theory and Techniques*, **47**, 2003-2007. http://dx.doi.org/10.1109/22.795075

[2] Zheng, F., Chen, Z. and Zhang, J. (2000) Toward the Development of a Three-Dimensional Unconditionally Stable Finite-Difference Time-Domain Method. *IEEE Transactions on Microwave Theory and Techniques*, **48**, 1550-1558. http://dx.doi.org/10.1109/22.869007

[3] Yee, K. (1966) Numerical Solution of Initial Boundary Value Problems Involving Maxwell's Equations in Isotropic Media. *IEEE Transactions on Antennas and Propagation*, **14**, 302-307. http://dx.doi.org/10.1109/TAP.1966.1138693

[4] Namiki, T. and Ito, K. (2000) Investigation of Numerical Errors of the Two-Dimensional ADI-FDTD Method [for Maxwell's Equations Solution]. *IEEE Transactions on Microwave Theory and Techniques*, **48**, 1950-1956. http://dx.doi.org/10.1109/22.883876

[5] Zheng, F. and Chen, Z. (2001) Numerical Dispersion Analysis of the Unconditionally Stable 3D ADI-FDTD Method. *IEEE Transactions on Microwave Theory and Techniques*, **49**, 1006-1009. http://dx.doi.org/10.1109/22.920165

[6] Zhao, A.P. (2004) Consistency of Numerical Dispersion Relation Expressed in Different Forms for the ADI-FDTD Method. *Microwave and Optical Technology Letters*, **40**, 12-13. http://dx.doi.org/10.1002/mop.11272

[7] Garcia, S.G., Rubio, R.G., Bretones, A.B. and Martin, R.G. (2006) On the Dispersion Relation of ADI-FDTD. *IEEE Microwave and Wireless Components Letters*, **16**, 354-356. http://dx.doi.org/10.1109/LMWC.2006.875619

[8] Fu, W. and Tan, E.L. (2007) Stability and Dispersion Analysis for ADI-FDTD Method in Lossy Media. *IEEE Transactions on Antennas and Propagation*, **55**, 1095-1102. http://dx.doi.org/10.1109/TAP.2007.893378

[9] Smithe, D.N., Cary, J.R. and Carlsson, J.A. (2009) Divergence Preservation in the ADI Algorithms for Electromagnetics. *Journal of Computational Physics*, **228**, 7289-7299. http://dx.doi.org/10.1016/j.jcp.2009.06.025

[10] Gedney, S.D., Liu, G., Roden, J.A. and Zhu, A. (2001) Perfectly Matched Layer Media with CFS for an Unconditional Stable ADI-FDTD Method. *IEEE Transactions on Antennas and Propagation*, **49**, 1554-1559. http://dx.doi.org/10.1109/8.964091

[11] Wang, S. and Teixeira, F.L. (2003) An Efficient PML Implementation for the ADI-FDTD Method. *IEEE Microwave and Wireless Components Letters*, **13**, 72-74. http://dx.doi.org/10.1109/LMWC.2003.808705

[12] Gao, L. (2012) Stability and Super Convergence Analysis of ADI-FDTD for the 2D Maxwell Equations in a Lossy Medium. *Acta Mathematica Scientia*, **32**, 2341-2368. http://dx.doi.org/10.1016/S0252-9602(12)60184-2

Applied Mathematics, 2015, 6, 274-294
Published Online February 2015 in SciRes. http://www.scirp.org/journal/am
http://dx.doi.org/10.4236/am.2015.62026

Complete Semigroups of Binary Relations Defined by Semilattices of the Class $\Sigma_1(X,10)$

Shota Makharadze[1], Neşet Aydın[2], Ali Erdoğan[3]

[1]Shota Rustavelli University, Batum, Georgia
[2]Çanakkale Onsekiz Mart University, Çanakkale, Turkey
[3]Hacettepe University, Ankara, Turkey
Email: shota59@mail.ru, neseta@comu.edu.tr, alier@hacettepe.edu.tr

Received 10 January 2015; accepted 28 January 2015; published 4 February 2015

Abstract

In this paper we give a full description of idempotent elements of the semigroup $B_X(D)$, which are defined by semilattices of the class $\Sigma_1(X, 10)$. For the case where X is a finite set we derive formulas by means of which we can calculate the numbers of idempotent elements of the respective semigroup.

Keywords

Semilattice, Semigroup, Binary Relation

1. Introduction

Let X be an arbitrary nonempty set, D be an X-semilattice of unions, *i.e.* such a nonempty set of subsets of the set X that is closed with respect to the set-theoretic operations of unification of elements from D, f be an arbitrary mapping of the set X in the set D. To each such a mapping f we put into correspondence a binary relation α_f on the set X that satisfies the condition

$$\alpha_f = \bigcup_{x\in X}\left(\{x\}\times f(x)\right)$$

The set of all such α_f $\left(f: X\to D\right)$ is denoted by $B_X(D)$. It is easy to prove that $B_X(D)$ is a semigroup with respect to the operation of multiplication of binary relations, which is called a complete semigroup of binary relations defined by an X-semilattice of unions D.

How to cite this paper: Makharadze, S., Aydın, N. and Erdoğan, A. (2015) Complete Semigroups of Binary Relations Defined by Semilattices of the Class $\Sigma_1(X,10)$. *Applied Mathematics*, **6**, 274-294. http://dx.doi.org/10.4236/am.2015.62026

Recall that we denote by $\varnothing$ an empty binary relation or empty subset of the set X. The condition $(x,y)\in\alpha$ will be written in the form $x\alpha y$. Further let $x, y\in X$, $Y\subseteq X$, $\alpha\in B_X(D)$, $T\in D$, $\varnothing\neq D'\subseteq D$, $\breve{D}=\cup D$ and $t\in\breve{D}$. Then by symbols we denoted the following sets:

$$y\alpha=\{x\in X\,|\,y\alpha x\},\quad Y\alpha=\bigcup_{y\in Y}y\alpha,\quad 2^X=\{Y|Y\subseteq X\},\quad X^*=2^X\setminus\{\varnothing\},$$
$$V(D,\alpha)=\{Y\alpha|Y\in D\},\quad D'_T=\{T'\in D'|T\subseteq T'\},\quad \ddot{D}'_T=\{T'\in D'|T'\subseteq T\},$$
$$D'_t=\{Z'\in D'|t\in Z'\},\quad l(D',T)=\cup(D'\setminus D'_T).$$

By symbol $\Lambda(D,D')$ is denoted an exact lower bound of the set D' in the semilattice D.

Definition 1. *We say that the complete X-semilattice of unions D is an XI-semilattice of unions if it satisfies the following two conditions*:

a) $\Lambda(D,D_t)\in D$ *for any* $t\in\breve{D}$;

b) $Z=\bigcup_{t\in Z}\Lambda(D,D_t)$ *for any nonempty element Z of the semilattice D.*

Definition 2. *We say that a nonempty element T is a nonlimiting element of the set D′ if* $T\setminus l(D',T)\neq\varnothing$ *and a nonempty element T is a limiting element of the set D′ if* $T\setminus l(D',T)=\varnothing$.

Definition 3. *Let* $\alpha\in B_X(D)$, $T\in V(X^*,\alpha)$, $Y_T^\alpha=\{y\in X\,|\,y\alpha=T\}$. *A representation of a binary relation* α *of the form* $\alpha=\bigcup_{T\in V(X^*,\alpha)}(Y_T^\alpha\times T)$ *is called quasinormal.*

Note that, if $\alpha=\bigcup_{T\in V(X^*,\alpha)}(Y_T^\alpha\times T)$ is a quasinormal representation of the binary relation α, then the following conditions are true:

1) $X=\bigcup_{T\in V(X^*,\alpha)}Y_T^\alpha$;

2) $Y_T^\alpha\cap Y_{T'}^\alpha=\varnothing$ for $T, T'\in V(X^*,\alpha)$ and $T\neq T'$.

Let $\sum_n(X,m)$ denote the class of all complete X-semilattices of unions where every element is isomorphic to a fixed semilattice D.

The following Theorems are well know (see [1] and [3]).

Theorem 4. *Let X be a finite set; δ and q be respectively the number of basic sources and the number of all automorphisms of the semilattice D. If* $|X|=n\geq\delta$ *and* $|\Sigma_n(X,m)|=s$, *then*

$$s=\frac{1}{q}\cdot\sum_{p=\delta}^{m}\left(\sum_{i=1}^{p+1}\left(\frac{(-1)^{p+i+1}\cdot C_{m-\delta}^{p-\delta}\cdot C_p^\delta\cdot(\delta!)\cdot((p-\delta)!)\cdot i^n}{(i-1)!\cdot(p-i+1)!}\right)\right)$$

where $C_j^k=\dfrac{j!}{(k!)\cdot(j-k)!}$ (*see Theorem* 11.5.1 [1]).

Theorem 5. *Let D be a complete X-semilattice of unions. The semigroup* $B_X(D)$ *possesses right unit iff D is an XI-semilattice of unions* (*see Theorem* 6.1.3 [1]).

Theorem 6. *Let X be a finite set and* $D(\alpha)$ *be the set of all those elements T of the semilattice* $Q=V(D,\alpha)\setminus\{\varnothing\}$ *which are nonlimiting elements of the set* $\ddot{Q}_T$. *A binary relation* α *having a quasinormal representation* $\alpha=\bigcup_{T\in V(D,\alpha)}(Y_T^\alpha\times T)$ *is an idempotent element of this semigroup iff*

a) $V(D,\alpha)$ *is complete XI-semilattice of unions*;

b) $\bigcup_{T'\in\ddot{D}(\alpha)_T}Y_{T'}^\alpha\supseteq T$ *for any* $T\in D(\alpha)$;

c) $Y_T^\alpha\cap T\neq\varnothing$ *for any nonlimiting element of the set* $\ddot{D}(\alpha)_T$ (*see Theorem* 6.3.9 [1]).

Theorem 7. *Let D,* $\Sigma(D)$, $E_X^{(r)}(D')$ *and I denote respectively the complete X-semilattice of unions, the set of all XI-subsemilatices of the semilattice D, the set of all right units of the semigroup* $B_X(D')$ *and the set of all idempotents of the semigroup* $B_X(D)$. *Then for the sets* $E_X^{(r)}(D')$ *and I the following statements are true*:

1) *if* $\varnothing\in D$ *and* $\Sigma_\varnothing(D)=\{D'\in\Sigma(D)|\varnothing\in D'\}$ *then*

a) $E_X^{(r)}(D')\cap E_X^{(r)}(D'')=\varnothing$ for any elements D' and D'' of the set $\Sigma_\varnothing(D)$ that satisfy the condition $D'\neq D''$;

b) $I=\bigcup_{D'\in\Sigma_\varnothing(D)}E_X^{(r)}(D')$

c) *the equality* $|I|=\sum_{D'\in\Sigma_\varnothing(D)}|E_X^{(r)}(D')|$ *is fulfilled for the finite set X.*

2) if $\varnothing \notin D$, then

a) $E_X^{(r)}(D') \cap E_X^{(r)}(D'') = \varnothing$ *for any elements* D' *and* D'' *of the set* $\Sigma(D)$ *that satisfy the condition* $D' \neq D''$;

b) $I = \bigcup_{D' \in \Sigma(D)} E_X^{(r)}(D')$

c) *the equality* $|I| = \sum_{D' \in \Sigma(D)} \left| E_X^{(r)}(D') \right|$ *is fulfilled for the finite set X* (*see Theorem* 6.2.3 [1]).

Corollary 1. *Let* $Y = \{y_1, y_2, \cdots, y_k\}$ *and* $D_j = \{T_1, T_2, \cdots, T_j\}$ *be some sets, where* $k \geq 1$ *and* $j \geq 1$. *Then the number* $s(k, j)$ *of all possible mappings of the set Y into any such subset* D_j' *of the set* D_j *that* $T_j \in D_j'$ *can be calculated by the formula* $s(k, j) = j^k - (j-1)^k$ (*see Corollary* 1.18.1 [1]).

2. Idempotent Elements of the Semigroups $B_X(D)$ Defined by Semilattices of the Class $\Sigma_1(X, 10)$

Let X and $\Sigma_1(X, 10)$ be respectively an arbitrary nonempty set and a class X-semilattices of unions, where each element is isomorphic to some X-semilattice of unions $D = \{Z_9, Z_8, Z_7, Z_6, Z_5, Z_4, Z_3, Z_2, Z_1, \breve{D}\}$ that satisfies the conditions:

$$
\begin{aligned}
&Z_9 \subset Z_4 \subset Z_1 \subset \breve{D},\ Z_9 \subset Z_5 \subset Z_1 \subset \breve{D},\\
&Z_9 \subset Z_6 \subset Z_1 \subset \breve{D},\ Z_9 \subset Z_6 \subset Z_2 \subset \breve{D},\\
&Z_9 \subset Z_6 \subset Z_3 \subset \breve{D},\ Z_9 \subset Z_7 \subset Z_3 \subset \breve{D},\\
&Z_9 \subset Z_8 \subset Z_3 \subset \breve{D},\ Z_1 \setminus Z_2 \neq \varnothing,\ Z_2 \setminus Z_1 \neq \varnothing,\\
&Z_1 \setminus Z_3 \neq \varnothing,\ Z_3 \setminus Z_1 \neq \varnothing,\ Z_2 \setminus Z_3 \neq \varnothing,\\
&Z_3 \setminus Z_2 \neq \varnothing,\ Z_4 \setminus Z_5 \neq \varnothing,\ Z_5 \setminus Z_4 \neq \varnothing,\\
&Z_4 \setminus Z_6 \neq \varnothing,\ Z_6 \setminus Z_4 \neq \varnothing,\ Z_4 \setminus Z_7 \neq \varnothing,\\
&Z_7 \setminus Z_4 \neq \varnothing,\ Z_4 \setminus Z_8 \neq \varnothing,\ Z_8 \setminus Z_4 \neq \varnothing,\\
&Z_5 \setminus Z_6 \neq \varnothing,\ Z_6 \setminus Z_5 \neq \varnothing,\ Z_5 \setminus Z_7 \neq \varnothing,\\
&Z_7 \setminus Z_5 \neq \varnothing,\ Z_5 \setminus Z_8 \neq \varnothing,\ Z_8 \setminus Z_5 \neq \varnothing,\\
&Z_6 \setminus Z_7 \neq \varnothing,\ Z_7 \setminus Z_6 \neq \varnothing,\ Z_6 \setminus Z_8 \neq \varnothing,\\
&Z_8 \setminus Z_6 \neq \varnothing,\ Z_7 \setminus Z_8 \neq \varnothing,\ Z_8 \setminus Z_7 \neq \varnothing,\\
&Z_1 \cup Z_2 = Z_1 \cup Z_3 = Z_2 \cup Z_3 = Z_4 \cup Z_2\\
&\qquad = Z_4 \cup Z_3 = Z_4 \cup Z_7 = Z_4 \cup Z_8 = Z_5 \cup Z_2\\
&\qquad = Z_5 \cup Z_3 = Z_5 \cup Z_7 = Z_5 \cup Z_8 = Z_7 \cup Z_1\\
&\qquad = Z_7 \cup Z_2 = Z_8 \cup Z_1 = Z_8 \cup Z_2 = \breve{D},\\
&Z_4 \cup Z_5 = Z_4 \cup Z_6 = Z_5 \cup Z_6 = Z_1,\\
&Z_6 \cup Z_7 = Z_6 \cup Z_8 = Z_7 \cup Z_8 = Z_3.
\end{aligned}
\tag{1}
$$

An X-semilattice that satisfies conditions (1) is shown in **Figure 1**.

Let $C(D) = \{P_0, P_1, P_2, P_3, P_4, P_5, P_6, P_7, P_8, P_9\}$ be a family of sets, where P_0, P_1, P_2, P_3, P_4, P_5, P_6, P_7, P_8, P_9

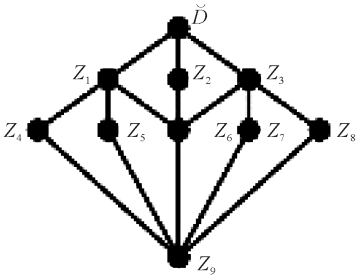

Figure 1. Diagram of D.

are pairwise disjoint subsets of the set X and $\varphi = \begin{pmatrix} \breve{D} & Z_1 & Z_2 & Z_3 & Z_4 & Z_5 & Z_6 & Z_7 & Z_8 & Z_9 \\ P_0 & P_1 & P_2 & P_3 & P_4 & P_5 & P_6 & P_7 & P_8 & P_9 \end{pmatrix}$ be a mapping of the semilattice D onto the family sets $C(D)$. Then for the formal equalities of the semilattice D we have a form:

$$\begin{aligned} \breve{D} &= P_0 \cup P_1 \cup P_2 \cup P_3 \cup P_4 \cup P_5 \cup P_6 \cup P_7 \cup P_8 \cup P_9, \\ Z_1 &= P_0 \cup P_2 \cup P_3 \cup P_4 \cup P_5 \cup P_6 \cup P_7 \cup P_8 \cup P_9, \\ Z_2 &= P_0 \cup P_1 \cup P_3 \cup P_4 \cup P_5 \cup P_6 \cup P_7 \cup P_8 \cup P_9, \\ Z_3 &= P_0 \cup P_1 \cup P_2 \cup P_4 \cup P_5 \cup P_6 \cup P_7 \cup P_8 \cup P_9, \\ Z_4 &= P_0 \cup P_2 \cup P_3 \cup P_5 \cup P_6 \cup P_7 \cup P_8 \cup P_9, \\ Z_5 &= P_0 \cup P_2 \cup P_3 \cup P_4 \cup P_6 \cup P_7 \cup P_8 \cup P_9, \\ Z_6 &= P_0 \cup P_4 \cup P_5 \cup P_7 \cup P_8 \cup P_9, \\ Z_7 &= P_0 \cup P_1 \cup P_2 \cup P_4 \cup P_5 \cup P_6 \cup P_8 \cup P_9, \\ Z_8 &= P_0 \cup P_1 \cup P_2 \cup P_4 \cup P_5 \cup P_6 \cup P_7 \cup P_9, \\ Z_9 &= P_0. \end{aligned} \tag{2}$$

Here the elements P_1, P_2, P_3, P_4, P_5, P_6, P_7, P_8 are basis sources, the elements P_0, P_6, P_9 are sources of completeness of the semilattice D. Therefore $|X| \geq 7$ and $\delta = 7$ (see [2]).

Lemma 1. *Let* $D \in \Sigma_1(X,10)$, $|\Sigma_1(X,10)| = s$ *and* $|X| \geq \delta \geq 7$. *If X is a finite set, then*

$$s = \frac{1}{8}\left((-1)\times 4^n + 7\times 5^n - 21\times 6^n + 35\times 7^n - 35\times 8^n + 21\times 9^n + 11^n\right).$$

Proof. In this case we have: $m = 10$, $\delta = 7$. Notice that an X-semilattice given in **Figure 1** has eight automorphims. By Theorem 1.1 it follows that

$$s = \frac{1}{8}\cdot\sum_{p=7}^{10}\left(\sum_{i=1}^{p+1}\left(\frac{(-1)^{p+i+1}\cdot C_3^{p-7}\cdot C_p^7\cdot(7!)\cdot((p-7)!)\cdot i^n}{(i-1)!\cdot(p-i+1)!}\right)\right),$$

where $C_j^k = \dfrac{j!}{k!\cdot(j-k)!}$ and that

$$s = \frac{1}{8}\left((-1)\times 4^n + 7\times 5^n - 21\times 6^n + 35\times 7^n - 35\times 8^n + 21\times 9^n + 11^n\right).$$

Example 8. *Let* $n = 7, 8, 9, 10$ *Then*:

$$|B_X(D)| = 10^7,\ 10^8,\ 10^9,\ 10^{10}.$$

Lemma 2. *Let* $D \in \Sigma_1(X,10)$. *Then the following sets are all proper subsemilattices of the semilattice* $D = \{Z_9, Z_8, Z_7, Z_6, Z_5, Z_4, Z_3, Z_2, Z_1, \breve{D}\}$:

1) $\{Z_9\}$, $\{Z_8\}$, $\{Z_7\}$, $\{Z_6\}$, $\{Z_5\}$, $\{Z_4\}$, $\{Z_3\}$, $\{Z_2\}$, $\{Z_1\}$, $\{\breve{D}\}$
(*see diagram* 1 *of the* ***Figure 2***);

2) $\{Z_9,Z_8\}$, $\{Z_9,Z_7\}$, $\{Z_9,Z_6\}$, $\{Z_9,Z_5\}$, $\{Z_9,Z_4\}$, $\{Z_9,Z_3\}$, $\{Z_9,Z_2\}$, $\{Z_9,Z_1\}$, $\{Z_9,\breve{D}\}$, $\{Z_8,Z_3\}$, $\{Z_8,\breve{D}\}$, $\{Z_7,Z_3\}$, $\{Z_7,\breve{D}\}$, $\{Z_6,Z_3\}$, $\{Z_6,Z_2\}$, $\{Z_6,Z_1\}$, $\{Z_6,\breve{D}\}$, $\{Z_5,Z_1\}$, $\{Z_5,\breve{D}\}$, $\{Z_4,Z_1\}$, $\{Z_4,\breve{D}\}$, $\{Z_3,\breve{D}\}$, $\{Z_2,\breve{D}\}$, $\{Z_1,\breve{D}\}$
(*see diagram* 2 of the ***Figure 2***);

3) $\{Z_9,Z_8,Z_3\}$, $\{Z_9,Z_8,\breve{D}\}$, $\{Z_9,Z_7,Z_3\}$, $\{Z_9,Z_7,\breve{D}\}$, $\{Z_9,Z_6,Z_3\}$, $\{Z_9,Z_6,Z_2\}$, $\{Z_9,Z_6,Z_1\}$, $\{Z_9,Z_6,\breve{D}\}$, $\{Z_9,Z_5,Z_1\}$, $\{Z_9,Z_5,\breve{D}\}$, $\{Z_9,Z_4,Z_1\}$, $\{Z_9,Z_4,\breve{D}\}$, $\{Z_9,Z_3,\breve{D}\}$, $\{Z_9,Z_2,\breve{D}\}$,

$\{Z_9, Z_1, \breve{D}\}$, $\{Z_8, Z_3, \breve{D}\}$, $\{Z_7, Z_3, \breve{D}\}$, $\{Z_6, Z_3, \breve{D}\}$, $\{Z_6, Z_2, \breve{D}\}$, $\{Z_6, Z_1, \breve{D}\}$, $\{Z_5, Z_1, \breve{D}\}$, $\{Z_4, Z_1, \breve{D}\}$
(see *diagram* 3 of the **Figure 2**);

4) $\{Z_9, Z_4, Z_1, \breve{D}\}$, $\{Z_9, Z_5, Z_1, \breve{D}\}$, $\{Z_9, Z_6, Z_1, \breve{D}\}$, $\{Z_9, Z_6, Z_2, \breve{D}\}$, $\{Z_9, Z_6, Z_3, \breve{D}\}$, $\{Z_9, Z_7, Z_3, \breve{D}\}$, $\{Z_9, Z_8, Z_3, \breve{D}\}$
(*see diagram* 4 *of the* **Figure 2**);

5) $\{Z_9, Z_5, Z_4, Z_1\}$, $\{Z_9, Z_6, Z_4, Z_1\}$, $\{Z_9, Z_6, Z_5, Z_1\}$, $\{Z_9, Z_7, Z_6, Z_3\}$, $\{Z_9, Z_8, Z_6, Z_3\}$, $\{Z_9, Z_8, Z_7, Z_3\}$, $\{Z_9, Z_8, Z_4, \breve{D}\}$, $\{Z_9, Z_8, Z_5, \breve{D}\}$, $\{Z_9, Z_7, Z_2, \breve{D}\}$, $\{Z_9, Z_7, Z_4, \breve{D}\}$, $\{Z_9, Z_7, Z_5, \breve{D}\}$, $\{Z_9, Z_8, Z_1, \breve{D}\}$, $\{Z_9, Z_8, Z_2, \breve{D}\}$, $\{Z_9, Z_4, Z_2, \breve{D}\}$, $\{Z_9, Z_4, Z_3, \breve{D}\}$, $\{Z_9, Z_5, Z_2, \breve{D}\}$, $\{Z_9, Z_5, Z_3, \breve{D}\}$, $\{Z_9, Z_7, Z_1, \breve{D}\}$, $\{Z_9, Z_2, Z_1, \breve{D}\}$, $\{Z_9, Z_3, Z_1, \breve{D}\}$, $\{Z_9, Z_3, Z_2, \breve{D}\}$, $\{Z_6, Z_2, Z_1, \breve{D}\}$, $\{Z_6, Z_3, Z_1, \breve{D}\}$, $\{Z_6, Z_3, Z_2, \breve{D}\}$;
(*see diagram* 5 of the **Figure 2**);

6) $\{Z_9, Z_5, Z_4, Z_1, \breve{D}\}$, $\{Z_9, Z_6, Z_4, Z_1, \breve{D}\}$, $\{Z_9, Z_6, Z_5, Z_1, \breve{D}\}$, $\{Z_9, Z_7, Z_6, Z_3, \breve{D}\}$, $\{Z_9, Z_8, Z_6, Z_3, \breve{D}\}$, $\{Z_9, Z_8, Z_7, Z_3, \breve{D}\}$
(*see diagram* 6 *of the* **Figure 2**);

7) $\{Z_9, Z_6, Z_2, Z_1, \breve{D}\}$, $\{Z_9, Z_6, Z_3, Z_1, \breve{D}\}$, $\{Z_9, Z_6, Z_3, Z_2, \breve{D}\}$
(*see diagram* 7 *of the* **Figure 2**);

8) $\{Z_9, Z_8, Z_6, Z_3, Z_2, \breve{D}\}$, $\{Z_9, Z_8, Z_6, Z_3, Z_1, \breve{D}\}$, $\{Z_9, Z_7, Z_6, Z_3, Z_2, \breve{D}\}$, $\{Z_9, Z_7, Z_6, Z_3, Z_1, \breve{D}\}$, $\{Z_9, Z_6, Z_5, Z_3, Z_1, \breve{D}\}$, $\{Z_9, Z_6, Z_5, Z_2, Z_1, \breve{D}\}$, $\{Z_9, Z_6, Z_4, Z_3, Z_1, \breve{D}\}$, $\{Z_9, Z_6, Z_4, Z_2, Z_1, \breve{D}\}$
(*see diagram* 8 *of the* **Figure 2**);

9) $\{Z_8, Z_7, Z_3\}$, $\{Z_8, Z_6, Z_3\}$, $\{Z_8, Z_6, \breve{D}\}$, $\{Z_8, Z_5, \breve{D}\}$, $\{Z_8, Z_4, \breve{D}\}$, $\{Z_8, Z_2, \breve{D}\}$, $\{Z_8, Z_1, \breve{D}\}$, $\{Z_7, Z_6, Z_3\}$, $\{Z_7, Z_5, \breve{D}\}$, $\{Z_7, Z_4, \breve{D}\}$, $\{Z_7, Z_2, \breve{D}\}$, $\{Z_7, Z_1, \breve{D}\}$, $\{Z_6, Z_5, Z_1\}$, $\{Z_6, Z_4, Z_1\}$, $\{Z_5, Z_4, Z_1\}$, $\{Z_5, Z_3, \breve{D}\}$, $\{Z_5, Z_2, \breve{D}\}$, $\{Z_4, Z_3, \breve{D}\}$, $\{Z_4, Z_2, \breve{D}\}$, $\{Z_3, Z_2, \breve{D}\}$, $\{Z_3, Z_1, \breve{D}\}$, $\{Z_2, Z_1, \breve{D}\}$
(*see diagram* 9 *of the* **Figure 2**);

10) $\{Z_8, Z_6, Z_3, \breve{D}\}$, $\{Z_8, Z_7, Z_3, \breve{D}\}$, $\{Z_7, Z_6, Z_3, \breve{D}\}$, $\{Z_5, Z_4, Z_1, \breve{D}\}$, $\{Z_6, Z_4, Z_1, \breve{D}\}$, $\{Z_6, Z_5, Z_1, \breve{D}\}$
(*see diagram* 10 *of the* **Figure 3**);

11) $\{Z_6, Z_5, Z_3, Z_1, \breve{D}\}$, $\{Z_6, Z_5, Z_2, Z_1, \breve{D}\}$, $\{Z_6, Z_4, Z_3, Z_1, \breve{D}\}$, $\{Z_6, Z_4, Z_2, Z_1, \breve{D}\}$, $\{Z_7, Z_6, Z_3, Z_2, \breve{D}\}$, $\{Z_7, Z_6, Z_3, Z_1, \breve{D}\}$, $\{Z_8, Z_6, Z_3, Z_2, \breve{D}\}$, $\{Z_8, Z_6, Z_3, Z_1, \breve{D}\}$
(*see diagram* 11 *of the* **Figure 2**);

12) $\{Z_6, Z_5, Z_4, Z_1\}$, $\{Z_8, Z_7, Z_6, Z_3\}$, $\{Z_8, Z_2, Z_1, \breve{D}\}$, $\{Z_3, Z_2, Z_1, \breve{D}\}$, $\{Z_4, Z_3, Z_2, \breve{D}\}$, $\{Z_5, Z_3, Z_2, \breve{D}\}$, $\{Z_7, Z_2, Z_1, \breve{D}\}$, $\{Z_7, Z_4, Z_2, \breve{D}\}$, $\{Z_7, Z_5, Z_2, \breve{D}\}$, $\{Z_8, Z_4, Z_2, \breve{D}\}$, $\{Z_8, Z_5, Z_2, \breve{D}\}$
(*see diagram* 12 *of the* **Figure 2**);

13) $\{Z_7, Z_5, Z_3, \breve{D}\}$, $\{Z_4, Z_2, Z_1, \breve{D}\}$, $\{Z_8, Z_3, Z_1, \breve{D}\}$, $\{Z_8, Z_3, Z_2, \breve{D}\}$, $\{Z_8, Z_4, Z_1, \breve{D}\}$, $\{Z_4, Z_3, Z_1, \breve{D}\}$, $\{Z_5, Z_2, Z_1, \breve{D}\}$, $\{Z_5, Z_3, Z_1, \breve{D}\}$, $\{Z_7, Z_3, Z_1, \breve{D}\}$, $\{Z_7, Z_3, Z_2, \breve{D}\}$, $\{Z_7, Z_4, Z_1, \breve{D}\}$, $\{Z_7, Z_4, Z_3, \breve{D}\}$, $\{Z_7, Z_5, Z_1, \breve{D}\}$, $\{Z_8, Z_4, Z_3, \breve{D}\}$, $\{Z_8, Z_5, Z_1, \breve{D}\}$, $\{Z_8, Z_5, Z_3, \breve{D}\}$
(*see diagram* 13 *of the* **Figure 2**);

14) $\{Z_9, Z_6, Z_5, Z_4, Z_1\}$, $\{Z_9, Z_8, Z_7, Z_6, Z_3\}$, $\{Z_6, Z_3, Z_2, Z_1, \breve{D}\}$, $\{Z_9, Z_3, Z_2, Z_1, \breve{D}\}$, $\{Z_9, Z_4, Z_3, Z_2, \breve{D}\}$,

$\{Z_9, Z_5, Z_3, Z_2, \breve{D}\}$, $\{Z_9, Z_7, Z_2, Z_1, \breve{D}\}$, $\{Z_9, Z_7, Z_4, Z_2, \breve{D}\}$, $\{Z_9, Z_7, Z_4, Z_3, \breve{D}\}$, $\{Z_9, Z_7, Z_5, Z_2, \breve{D}\}$, $\{Z_9, Z_8, Z_2, Z_1, \breve{D}\}$, $\{Z_9, Z_8, Z_4, Z_2, \breve{D}\}$, $\{Z_9, Z_8, Z_5, Z_2, \breve{D}\}$
(*see diagram* 14 *of the* ***Figure 2***);

15) $\{Z_9, Z_4, Z_2, Z_1, \breve{D}\}$, $\{Z_9, Z_4, Z_3, Z_1, \breve{D}\}$, $\{Z_9, Z_5, Z_2, Z_1, \breve{D}\}$, $\{Z_9, Z_5, Z_3, Z_1, \breve{D}\}$, $\{Z_9, Z_7, Z_3, Z_1, \breve{D}\}$, $\{Z_9, Z_7, Z_3, Z_2, \breve{D}\}$, $\{Z_9, Z_7, Z_4, Z_1, \breve{D}\}$, $\{Z_9, Z_7, Z_5, Z_1, \breve{D}\}$, $\{Z_9, Z_7, Z_5, Z_3, \breve{D}\}$, $\{Z_9, Z_8, Z_3, Z_1, \breve{D}\}$, $\{Z_9, Z_8, Z_3, Z_2, \breve{D}\}$, $\{Z_9, Z_8, Z_4, Z_1, \breve{D}\}$, $\{Z_9, Z_8, Z_4, Z_3, \breve{D}\}$, $\{Z_9, Z_8, Z_5, Z_1, \breve{D}\}$, $\{Z_9, Z_8, Z_5, Z_3, \breve{D}\}$
(*see diagram* 15 *of the* ***Figure 2***);

16) $\{Z_5, Z_4, Z_3, Z_1, \breve{D}\}$, $\{Z_5, Z_4, Z_2, Z_1, \breve{D}\}$, $\{Z_7, Z_5, Z_4, Z_1, \breve{D}\}$, $\{Z_8, Z_5, Z_4, Z_1, \breve{D}\}$, $\{Z_8, Z_7, Z_3, Z_2, \breve{D}\}$, $\{Z_8, Z_7, Z_3, Z_1, \breve{D}\}$, $\{Z_8, Z_7, Z_5, Z_3, \breve{D}\}$, $\{Z_8, Z_7, Z_4, Z_3, \breve{D}\}$
(*see diagram* 16 *of the* ***Figure 2***);

17) $\{Z_5, Z_3, Z_2, Z_1, \breve{D}\}$, $\{Z_4, Z_3, Z_2, Z_1, \breve{D}\}$, $\{Z_7, Z_4, Z_2, Z_1, \breve{D}\}$, $\{Z_7, Z_3, Z_2, Z_1, \breve{D}\}$, $\{Z_7, Z_5, Z_3, Z_2, \breve{D}\}$, $\{Z_7, Z_5, Z_2, Z_1, \breve{D}\}$, $\{Z_7, Z_4, Z_3, Z_2, \breve{D}\}$, $\{Z_8, Z_3, Z_2, Z_1, \breve{D}\}$, $\{Z_8, Z_5, Z_3, Z_2, \breve{D}\}$, $\{Z_8, Z_5, Z_2, Z_1, \breve{D}\}$, $\{Z_8, Z_4, Z_3, Z_2, \breve{D}\}$, $\{Z_8, Z_4, Z_2, Z_1, \breve{D}\}$
(*see diagram* 17 *of the* ***Figure 2***);

18) $\{Z_7, Z_4, Z_3, Z_1, \breve{D}\}$, $\{Z_7, Z_5, Z_3, Z_1, \breve{D}\}$, $\{Z_8, Z_5, Z_3, Z_1, \breve{D}\}$, $\{Z_8, Z_4, Z_3, Z_1, \breve{D}\}$
(*see diagram* 18 *of the* ***Figure 2***);

19) $\{Z_6, Z_5, Z_4, Z_1, \breve{D}\}$, $\{Z_8, Z_7, Z_6, Z_3, \breve{D}\}$.
(*see diagram* 19 *of the* ***Figure 2***);

20) $\{Z_8, Z_7, Z_5, Z_3, Z_2, \breve{D}\}$, $\{Z_8, Z_7, Z_4, Z_3, Z_2, \breve{D}\}$, $\{Z_8, Z_5, Z_4, Z_2, Z_1, \breve{D}\}$, $\{Z_7, Z_5, Z_4, Z_2, Z_1, \breve{D}\}$, $\{Z_8, Z_7, Z_3, Z_2, Z_1, \breve{D}\}$, $\{Z_5, Z_4, Z_3, Z_2, Z_1, \breve{D}\}$
(*see diagram* 20 *of the* ***Figure 2***);

21) $\{Z_6, Z_5, Z_4, Z_2, Z_1, \breve{D}\}$, $\{Z_8, Z_7, Z_6, Z_3, Z_2, \breve{D}\}$, $\{Z_8, Z_7, Z_6, Z_3, Z_1, \breve{D}\}$, $\{Z_6, Z_5, Z_4, Z_3, Z_1, \breve{D}\}$
(*see diagram* 21 *of the* ***Figure 2***);

22) $\{Z_9, Z_5, Z_4, Z_2, Z_1, \breve{D}\}$, $\{Z_9, Z_8, Z_7, Z_4, Z_3, \breve{D}\}$, $\{Z_9, Z_8, Z_7, Z_3, Z_1, \breve{D}\}$, $\{Z_9, Z_8, Z_5, Z_4, Z_1, \breve{D}\}$, $\{Z_9, Z_7, Z_5, Z_4, Z_1, \breve{D}\}$, $\{Z_9, Z_5, Z_4, Z_3, Z_1, \breve{D}\}$, $\{Z_9, Z_8, Z_7, Z_3, Z_2, \breve{D}\}$, $\{Z_9, Z_8, Z_7, Z_5, Z_3, \breve{D}\}$
(*see diagram* 22 *of the* ***Figure 2***);

23) $\{Z_9, Z_8, Z_7, Z_6, Z_3, \breve{D}\}$, $\{Z_9, Z_6, Z_5, Z_4, Z_1, \breve{D}\}$
(*see diagram* 23 *of the* ***Figure 2***);

24) $\{Z_9, Z_8, Z_5, Z_3, Z_2, \breve{D}\}$, $\{Z_9, Z_8, Z_5, Z_2, Z_1, \breve{D}\}$, $\{Z_9, Z_8, Z_4, Z_3, Z_2, \breve{D}\}$, $\{Z_9, Z_8, Z_4, Z_2, Z_1, \breve{D}\}$, $\{Z_9, Z_8, Z_3, Z_2, Z_1, \breve{D}\}$, $\{Z_9, Z_7, Z_5, Z_3, Z_2, \breve{D}\}$, $\{Z_9, Z_7, Z_5, Z_2, Z_1, \breve{D}\}$, $\{Z_9, Z_7, Z_4, Z_3, Z_2, \breve{D}\}$, $\{Z_9, Z_7, Z_4, Z_2, Z_1, \breve{D}\}$, $\{Z_9, Z_7, Z_3, Z_2, Z_1, \breve{D}\}$, $\{Z_9, Z_5, Z_3, Z_2, Z_1, \breve{D}\}$, $\{Z_9, Z_4, Z_3, Z_2, Z_1, \breve{D}\}$
(*see diagram* 24 *of the* ***Figure 2***);

25) $\{Z_9, Z_8, Z_5, Z_3, Z_1, \breve{D}\}$, $\{Z_9, Z_8, Z_4, Z_3, Z_1, \breve{D}\}$, $\{Z_9, Z_7, Z_5, Z_3, Z_1, \breve{D}\}$, $\{Z_9, Z_7, Z_4, Z_3, Z_1, \breve{D}\}$
(*see diagram* 25 *of the* ***Figure 2***);

26) $\{Z_9, Z_6, Z_3, Z_2, Z_1, \breve{D}\}$
(*see diagram* 26 *of the* ***Figure 2***);

27) $\{Z_8, Z_7, Z_5, Z_3, Z_1, \breve{D}\}$, $\{Z_8, Z_7, Z_4, Z_3, Z_1, \breve{D}\}$, $\{Z_8, Z_5, Z_4, Z_3, Z_1, \breve{D}\}$, $\{Z_7, Z_5, Z_4, Z_3, Z_1, \breve{D}\}$
(*see diagram* 27 *of the* ***Figure 2***);

28) $\{Z_8, Z_6, Z_5, Z_3, Z_1, \breve{D}\}$, $\{Z_8, Z_6, Z_4, Z_3, Z_1, \breve{D}\}$, $\{Z_8, Z_5, Z_3, Z_2, Z_1, \breve{D}\}$, $\{Z_7, Z_6, Z_5, Z_3, Z_1, \breve{D}\}$, $\{Z_7, Z_6, Z_4, Z_3, Z_1, \breve{D}\}$
(*see diagram* 28 *of the* ***Figure 2***);

29) $\{Z_8, Z_6, Z_3, Z_2, Z_1, \breve{D}\}$, $\{Z_7, Z_6, Z_3, Z_2, Z_1, \breve{D}\}$, $\{Z_6, Z_5, Z_3, Z_2, Z_1, \breve{D}\}$, $\{Z_6, Z_4, Z_3, Z_2, Z_1, \breve{D}\}$
(*see diagram* 29 *of the* ***Figure 2***);

30) $\{Z_8, Z_4, Z_3, Z_2, Z_1, \breve{D}\}$, $\{Z_7, Z_5, Z_3, Z_2, Z_1, \breve{D}\}$, $\{Z_7, Z_4, Z_3, Z_2, Z_1, \breve{D}\}$
(*see diagram* 30 *of the* ***Figure 2***);

31) $\{Z_8, Z_7, Z_5, Z_4, Z_3, Z_1, \breve{D}\}$
(*see diagram* 31 *of the* ***Figure 2***);

32) $\{Z_6, Z_5, Z_4, Z_3, Z_2, Z_1, \breve{D}\}$, $\{Z_8, Z_7, Z_6, Z_3, Z_2, Z_1, \breve{D}\}$
(*see diagram* 32 *of the* ***Figure 2***);

33) $\{Z_7, Z_5, Z_4, Z_3, Z_2, Z_1, \breve{D}\}$, $\{Z_8, Z_5, Z_4, Z_3, Z_2, Z_1, \breve{D}\}$, $\{Z_8, Z_7, Z_4, Z_3, Z_2, Z_1, \breve{D}\}$, $\{Z_8, Z_7, Z_5, Z_3, Z_2, Z_1, \breve{D}\}$
(*see diagram* 33 *of the* ***Figure 2***);

34) $\{Z_7, Z_6, Z_5, Z_4, Z_3, Z_1, \breve{D}\}$, $\{Z_8, Z_6, Z_5, Z_4, Z_3, Z_1, \breve{D}\}$, $\{Z_8, Z_7, Z_6, Z_4, Z_3, Z_1, \breve{D}\}$, $\{Z_8, Z_7, Z_6, Z_5, Z_3, Z_1, \breve{D}\}$
(*see diagram* 34 *of the* ***Figure 2***);

35) $\{Z_9, Z_6, Z_4, Z_3, Z_2, Z_1, \breve{D}\}$, $\{Z_9, Z_6, Z_5, Z_3, Z_2, Z_1, \breve{D}\}$, $\{Z_9, Z_7, Z_6, Z_3, Z_2, Z_1, \breve{D}\}$, $\{Z_9, Z_8, Z_6, Z_3, Z_2, Z_1, \breve{D}\}$, $\{Z_9, Z_8, Z_6, Z_3, Z_2, Z_1, \breve{D}\}$
(*see diagram* 35 *of the* ***Figure 2***);

36) $\{Z_9, Z_6, Z_5, Z_4, Z_3, Z_1, \breve{D}\}$, $\{Z_9, Z_8, Z_7, Z_6, Z_3, Z_1, \breve{D}\}$, $\{Z_9, Z_8, Z_7, Z_6, Z_3, Z_1, \breve{D}\}$
(*see diagram* 36 *of the* ***Figure 2***);

37) $\{Z_9, Z_7, Z_4, Z_3, Z_2, Z_1, \breve{D}\}$, $\{Z_9, Z_7, Z_5, Z_3, Z_2, Z_1, \breve{D}\}$, $\{Z_9, Z_8, Z_4, Z_3, Z_2, Z_1, \breve{D}\}$, $\{Z_9, Z_8, Z_5, Z_3, Z_2, Z_1, \breve{D}\}$
(*see diagram* 37 *of the* ***Figure 2***);

38) $\{Z_9, Z_7, Z_5, Z_4, Z_3, Z_1, \breve{D}\}$, $\{Z_9, Z_8, Z_5, Z_4, Z_3, Z_1, \breve{D}\}$, $\{Z_9, Z_8, Z_7, Z_4, Z_3, Z_1, \breve{D}\}$
(*see diagram* 38 *of the* ***Figure 2***);

39) $\{Z_9, Z_7, Z_6, Z_5, Z_3, Z_1, \breve{D}\}$
(*see diagram* 39 *of the* ***Figure 2***);

40) $\{Z_9, Z_7, Z_5, Z_4, Z_2, Z_1, \breve{D}\}$, $\{Z_9, Z_8, Z_5, Z_4, Z_2, Z_1, \breve{D}\}$, $\{Z_9, Z_8, Z_7, Z_4, Z_3, Z_2, \breve{D}\}$, $\{Z_9, Z_8, Z_7, Z_5, Z_3, Z_2, \breve{D}\}$, $\{Z_9, Z_5, Z_4, Z_3, Z_2, Z_1, \breve{D}\}$
(*see diagram* 40 *of the* ***Figure 2***);

41) $\{Z_9, Z_6, Z_5, Z_4, Z_2, Z_1, \breve{D}\}$, $\{Z_9, Z_8, Z_7, Z_6, Z_3, Z_2, \breve{D}\}$
(*see diagram* 41 *of the* ***Figure 2***);

42) $\{Z_7, Z_6, Z_5, Z_4, Z_3, Z_2, Z_1, \breve{D}\}$
(*see diagram* 42 *of the* **Figure 2**);

43) $\{Z_8, Z_6, Z_5, Z_4, Z_3, Z_2, Z_1, \breve{D}\}$, $\{Z_8, Z_7, Z_6, Z_4, Z_3, Z_2, Z_1, \breve{D}\}$, $\{Z_8, Z_7, Z_6, Z_5, Z_3, Z_2, Z_1, \breve{D}\}$
(*see diagram* 43 *of the* **Figure 2**);

44) $\{Z_8, Z_7, Z_5, Z_4, Z_3, Z_2, Z_1, \breve{D}\}$
(*see diagram* 44 *of the* **Figure 2**);

45) $\{Z_9, Z_8, Z_7, Z_5, Z_4, Z_3, Z_1, \breve{D}\}$
(*see diagram* 45 *of the* **Figure 2**);

46) $\{Z_9, Z_6, Z_5, Z_4, Z_3, Z_2, Z_1, \breve{D}\}$, $\{Z_9, Z_8, Z_7, Z_6, Z_3, Z_2, Z_1, \breve{D}\}$
(*see diagram* 46 *of the* **Figure 2**);

47) $\{Z_9, Z_7, Z_5, Z_4, Z_3, Z_2, Z_1, \breve{D}\}$, $\{Z_9, Z_8, Z_7, Z_5, Z_3, Z_2, Z_1, \breve{D}\}$, $\{Z_9, Z_7, Z_5, Z_4, Z_3, Z_2, Z_1, \breve{D}\}$, $\{Z_9, Z_8, Z_7, Z_4, Z_3, Z_2, Z_1, \breve{D}\}$
(*see diagram* 47 *of the* **Figure 2**);

48) $\{Z_9, Z_7, Z_6, Z_5, Z_4, Z_3, Z_1, \breve{D}\}$, $\{Z_9, Z_8, Z_6, Z_5, Z_4, Z_3, Z_1, \breve{D}\}$, $\{Z_9, Z_8, Z_7, Z_6, Z_4, Z_3, Z_1, \breve{D}\}$, $\{Z_9, Z_8, Z_7, Z_6, Z_5, Z_3, Z_1, \breve{D}\}$
(*see diagram* 48 *of the* **Figure 2**);

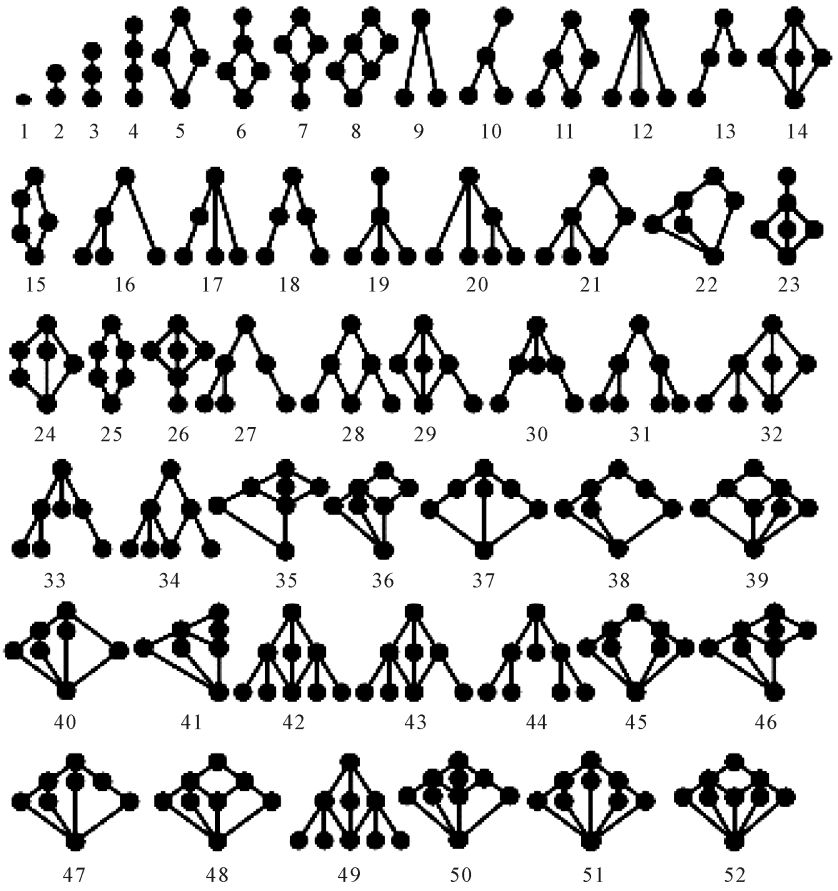

Figure 2. Diagram of all subsemilattices of *D*.

49) $\{Z_8, Z_7, Z_6, Z_5, Z_4, Z_3, Z_2, Z_1, \breve{D}\}$
(*see diagram* 49 *of the* ***Figure 2***);

50) $\{Z_9, Z_7, Z_6, Z_5, Z_4, Z_3, Z_2, Z_1, \breve{D}\}$, $\{Z_9, Z_8, Z_6, Z_5, Z_4, Z_3, Z_2, Z_1, \breve{D}\}$, $\{Z_9, Z_8, Z_7, Z_6, Z_4, Z_3, Z_2, Z_1, \breve{D}\}$, $\{Z_9, Z_8, Z_7, Z_6, Z_5, Z_3, Z_2, Z_1, \breve{D}\}$
(*see diagram* 50 *of the* ***Figure 2***);

51) $\{Z_9, Z_8, Z_7, Z_5, Z_4, Z_3, Z_2, Z_1, \breve{D}\}$
(*see diagram* 51 *of the* ***Figure 2***);

52) $\{Z_9, Z_8, Z_7, Z_6, Z_5, Z_4, Z_3, Z_1, \breve{D}\}$
(*see diagram* 52 *of the* ***Figure 2***);

Diagrams of subsemilattices of the semilattice *D*.

Lemma 3. *Let* $D \in \Sigma_1(X, 10)$. *Then the following sets are all XI-subsemi-lattices of the given semilattice D*:

1) $\{Z_9\}$, $\{Z_8\}$, $\{Z_7\}$, $\{Z_6\}$, $\{Z_5\}$, $\{Z_4\}$, $\{Z_3\}$, $\{Z_2\}$, $\{Z_1\}$, $\{\breve{D}\}$
(*see diagram* 1 *of the* ***Figure 2***);

2) $\{Z_9, \breve{D}\}$, $\{Z_9, Z_8\}$, $\{Z_9, Z_7\}$, $\{Z_9, Z_6\}$, $\{Z_9, Z_5\}$, $\{Z_9, Z_4\}$, $\{Z_9, Z_3\}$, $\{Z_9, Z_2\}$, $\{Z_9, Z_1\}$, $\{Z_8, Z_3\}$, $\{Z_8, \breve{D}\}$, $\{Z_7, Z_3\}$, $\{Z_7, \breve{D}\}$, $\{Z_6, Z_3\}$, $\{Z_6, Z_2\}$, $\{Z_6, Z_1\}$, $\{Z_6, \breve{D}\}$, $\{Z_5, Z_1\}$, $\{Z_5, \breve{D}\}$, $\{Z_4, Z_1\}$, $\{Z_4, \breve{D}\}$, $\{Z_3, \breve{D}\}$, $\{Z_2, \breve{D}\}$, $\{Z_1, \breve{D}\}$
(*see diagram* 2 *of the* ***Figure 2***);

3) $\{Z_9, Z_8, \breve{D}\}$, $\{Z_9, Z_7, \breve{D}\}$, $\{Z_9, Z_6, \breve{D}\}$, $\{Z_9, Z_5, \breve{D}\}$, $\{Z_9, Z_4, \breve{D}\}$, $\{Z_9, Z_3, \breve{D}\}$, $\{Z_9, Z_2, \breve{D}\}$, $\{Z_9, Z_1, \breve{D}\}$, $\{Z_9, Z_8, Z_3\}$, $\{Z_9, Z_7, Z_3\}$, $\{Z_9, Z_6, Z_3\}$, $\{Z_9, Z_6, Z_2\}$, $\{Z_9, Z_6, Z_1\}$, $\{Z_9, Z_5, Z_1\}$, $\{Z_9, Z_4, Z_1\}$, $\{Z_8, Z_3, \breve{D}\}$, $\{Z_7, Z_3, \breve{D}\}$, $\{Z_6, Z_3, \breve{D}\}$, $\{Z_6, Z_2, \breve{D}\}$, $\{Z_6, Z_1, \breve{D}\}$, $\{Z_5, Z_1, \breve{D}\}$, $\{Z_4, Z_1, \breve{D}\}$
(*see diagram* 3 *of the* ***Figure 2***);

4) $\{Z_9, Z_4, Z_1, \breve{D}\}$, $\{Z_9, Z_5, Z_1, \breve{D}\}$, $\{Z_9, Z_6, Z_1, \breve{D}\}$, $\{Z_9, Z_6, Z_2, \breve{D}\}$, $\{Z_9, Z_6, Z_3, \breve{D}\}$, $\{Z_9, Z_7, Z_3, \breve{D}\}$, $\{Z_9, Z_8, Z_3, \breve{D}\}$
(*see diagram* 4 *of the* ***Figure 2***);

5) $\{Z_9, Z_5, Z_4, Z_1\}$, $\{Z_9, Z_6, Z_4, Z_1\}$, $\{Z_9, Z_6, Z_5, Z_1\}$, $\{Z_9, Z_7, Z_6, Z_3\}$, $\{Z_9, Z_8, Z_6, Z_3\}$, $\{Z_9, Z_8, Z_7, Z_3\}$, $\{Z_9, Z_8, Z_4, \breve{D}\}$, $\{Z_9, Z_8, Z_5, \breve{D}\}$, $\{Z_9, Z_7, Z_2, \breve{D}\}$, $\{Z_9, Z_7, Z_4, \breve{D}\}$, $\{Z_9, Z_7, Z_5, \breve{D}\}$, $\{Z_9, Z_8, Z_1, \breve{D}\}$, $\{Z_9, Z_8, Z_2, \breve{D}\}$, $\{Z_9, Z_4, Z_2, \breve{D}\}$, $\{Z_9, Z_4, Z_3, \breve{D}\}$, $\{Z_9, Z_5, Z_2, \breve{D}\}$, $\{Z_9, Z_5, Z_3, \breve{D}\}$, $\{Z_9, Z_7, Z_1, \breve{D}\}$, $\{Z_9, Z_2, Z_1, \breve{D}\}$, $\{Z_9, Z_3, Z_1, \breve{D}\}$, $\{Z_9, Z_3, Z_2, \breve{D}\}$, $\{Z_6, Z_2, Z_1, \breve{D}\}$, $\{Z_6, Z_3, Z_1, \breve{D}\}$, $\{Z_6, Z_3, Z_2, \breve{D}\}$
(*see diagram* 5 *of the* ***Figure 2***);

6) $\{Z_9, Z_5, Z_4, Z_1, \breve{D}\}$, $\{Z_9, Z_6, Z_4, Z_1, \breve{D}\}$, $\{Z_9, Z_6, Z_5, Z_1, \breve{D}\}$, $\{Z_9, Z_7, Z_6, Z_3, \breve{D}\}$, $\{Z_9, Z_8, Z_6, Z_3, \breve{D}\}$, $\{Z_9, Z_8, Z_7, Z_3, \breve{D}\}$
(*see diagram* 6 *of the* ***Figure 2***);

7) $\{Z_9, Z_6, Z_2, Z_1, \breve{D}\}$, $\{Z_9, Z_6, Z_3, Z_1, \breve{D}\}$, $\{Z_9, Z_6, Z_3, Z_2, \breve{D}\}$
(*see diagram* 7 *of the* ***Figure 2***);

8) $\{Z_9, Z_8, Z_6, Z_3, Z_2, \breve{D}\}$, $\{Z_9, Z_8, Z_6, Z_3, Z_1, \breve{D}\}$, $\{Z_9, Z_7, Z_6, Z_3, Z_2, \breve{D}\}$, $\{Z_9, Z_7, Z_6, Z_3, Z_1, \breve{D}\}$, $\{Z_9, Z_6, Z_5, Z_3, Z_1, \breve{D}\}$, $\{Z_9, Z_6, Z_5, Z_2, Z_1, \breve{D}\}$, $\{Z_9, Z_6, Z_4, Z_3, Z_1, \breve{D}\}$, $\{Z_9, Z_6, Z_4, Z_2, Z_1, \breve{D}\}$ (*see diagram* 8 *of the* **Figure 2**);

Proof. It is well know (see [1]), that the semilattices 1 to 8, which are given by lemma 2 are always *XI*-semilattices. The semilattices 9 and 10 which are given by Lemma 2

$$\{Z_8, Z_7, Z_3\},\ \{Z_8, Z_6, Z_3\},\ \{Z_8, Z_6, \breve{D}\},\ \{Z_8, Z_5, \breve{D}\},\ \{Z_8, Z_4, \breve{D}\},$$
$$\{Z_8, Z_2, \breve{D}\},\ \{Z_8, Z_1, \breve{D}\},\ \{Z_7, Z_6, Z_3\},\ \{Z_7, Z_5, \breve{D}\},\ \{Z_7, Z_4, \breve{D}\},$$
$$\{Z_7, Z_2, \breve{D}\},\ \{Z_7, Z_1, \breve{D}\},\ \{Z_6, Z_5, Z_1\},\ \{Z_6, Z_4, Z_1\},\ \{Z_5, Z_4, Z_1\},$$
$$\{Z_5, Z_3, \breve{D}\},\ \{Z_5, Z_2, \breve{D}\},\ \{Z_4, Z_3, \breve{D}\},\ \{Z_4, Z_2, \breve{D}\},\ \{Z_3, Z_2, \breve{D}\},$$
$$\{Z_3, Z_1, \breve{D}\},\ \{Z_2, Z_1, \breve{D}\}.$$

(see diagram 9 of the **Figure 2**);

$$\{Z_8, Z_6, Z_3, \breve{D}\},\ \{Z_8, Z_7, Z_3, \breve{D}\},\ \{Z_7, Z_6, Z_3, \breve{D}\},\ \{Z_5, Z_4, Z_1, \breve{D}\},\ \{Z_6, Z_4, Z_1, \breve{D}\},\ \{Z_6, Z_5, Z_1, \breve{D}\}$$

(see diagram 10 of the **Figure 2**);
are *XI*-semilattices iff the intersection of minimal elements of the given semilattices is empty set. From the formal equalities (1) of the given semilattice *D* we have

$$Z_8 \cap Z_7 = (P_0 \cup P_1 \cup P_2 \cup P_4 \cup P_5 \cup P_6 \cup P_7 \cup P_9) \cup (P_0 \cup P_1 \cup P_2 \cup P_4 \cup P_5 \cup P_6 \cup P_8 \cup P_9) \neq \varnothing$$
$$Z_8 \cap Z_6 = (P_0 \cup P_1 \cup P_2 \cup P_4 \cup P_5 \cup P_6 \cup P_7 \cup P_9) \cup (P_0 \cup P_4 \cup P_5 \cup P_7 \cup P_8 \cup P_9) \neq \varnothing$$
$$Z_8 \cap Z_5 = (P_0 \cup P_1 \cup P_2 \cup P_4 \cup P_5 \cup P_6 \cup P_7 \cup P_9) \cup (P_0 \cup P_2 \cup P_3 \cup P_4 \cup P_6 \cup P_7 \cup P_8 \cup P_9) \neq \varnothing$$
$$Z_8 \cap Z_4 = (P_0 \cup P_1 \cup P_2 \cup P_4 \cup P_5 \cup P_6 \cup P_7 \cup P_9) \cup (P_0 \cup P_2 \cup P_3 \cup P_5 \cup P_6 \cup P_7 \cup P_8 \cup P_9) \neq \varnothing$$
$$Z_8 \cap Z_2 = (P_0 \cup P_1 \cup P_2 \cup P_4 \cup P_5 \cup P_6 \cup P_7 \cup P_9) \cup (P_0 \cup P_1 \cup P_3 \cup P_4 \cup P_5 \cup P_6 \cup P_7 \cup P_8 \cup P_9) \neq \varnothing$$
$$Z_8 \cap Z_1 = (P_0 \cup P_1 \cup P_2 \cup P_4 \cup P_5 \cup P_6 \cup P_7 \cup P_9) \cup (P_0 \cup P_2 \cup P_3 \cup P_4 \cup P_5 \cup P_6 \cup P_7 \cup P_8 \cup P_9) \neq \varnothing$$
$$Z_7 \cap Z_6 = (P_0 \cup P_1 \cup P_2 \cup P_4 \cup P_5 \cup P_6 \cup P_8 \cup P_9) \cup (P_0 \cup P_4 \cup P_5 \cup P_7 \cup P_8 \cup P_9) \neq \varnothing$$
$$Z_7 \cap Z_5 = (P_0 \cup P_1 \cup P_2 \cup P_4 \cup P_5 \cup P_6 \cup P_8 \cup P_9) \cup (P_0 \cup P_2 \cup P_3 \cup P_4 \cup P_6 \cup P_7 \cup P_8 \cup P_9) \neq \varnothing$$
$$Z_7 \cap Z_4 = (P_0 \cup P_1 \cup P_2 \cup P_4 \cup P_5 \cup P_6 \cup P_8 \cup P_9) \cup (P_0 \cup P_2 \cup P_3 \cup P_5 \cup P_6 \cup P_7 \cup P_8 \cup P_9) \neq \varnothing$$
$$Z_7 \cap Z_2 = (P_0 \cup P_1 \cup P_2 \cup P_4 \cup P_5 \cup P_6 \cup P_8 \cup P_9) \cup (P_0 \cup P_1 \cup P_3 \cup P_4 \cup P_5 \cup P_6 \cup P_7 \cup P_8 \cup P_9) \neq \varnothing$$
$$Z_7 \cap Z_1 = (P_0 \cup P_1 \cup P_2 \cup P_4 \cup P_5 \cup P_6 \cup P_8 \cup P_9) \cup (P_0 \cup P_2 \cup P_3 \cup P_4 \cup P_5 \cup P_6 \cup P_7 \cup P_8 \cup P_9) \neq \varnothing$$
$$Z_6 \cap Z_5 = (P_0 \cup P_4 \cup P_5 \cup P_7 \cup P_8 \cup P_9) \cup (P_0 \cup P_2 \cup P_3 \cup P_4 \cup P_6 \cup P_7 \cup P_8 \cup P_9) \neq \varnothing$$
$$Z_6 \cap Z_4 = (P_0 \cup P_4 \cup P_5 \cup P_7 \cup P_8 \cup P_9) \cup (P_0 \cup P_2 \cup P_3 \cup P_5 \cup P_6 \cup P_7 \cup P_8 \cup P_9) \neq \varnothing$$
$$Z_5 \cap Z_4 = (P_0 \cup P_2 \cup P_3 \cup P_4 \cup P_6 \cup P_7 \cup P_8 \cup P_9) \cup (P_0 \cup P_2 \cup P_3 \cup P_5 \cup P_6 \cup P_7 \cup P_8 \cup P_9) \neq \varnothing$$
$$Z_5 \cap Z_3 = (P_0 \cup P_2 \cup P_3 \cup P_4 \cup P_6 \cup P_7 \cup P_8 \cup P_9) \cup (P_0 \cup P_1 \cup P_2 \cup P_4 \cup P_5 \cup P_6 \cup P_7 \cup P_8 \cup P_9) \neq \varnothing$$
$$Z_5 \cap Z_2 = (P_0 \cup P_2 \cup P_3 \cup P_4 \cup P_6 \cup P_7 \cup P_8 \cup P_9) \cup (P_0 \cup P_1 \cup P_3 \cup P_4 \cup P_5 \cup P_6 \cup P_7 \cup P_8 \cup P_9) \neq \varnothing$$
$$Z_4 \cap Z_3 = (P_0 \cup P_2 \cup P_3 \cup P_5 \cup P_6 \cup P_7 \cup P_8 \cup P_9) \cup (P_0 \cup P_1 \cup P_2 \cup P_4 \cup P_5 \cup P_6 \cup P_7 \cup P_8 \cup P_9) \neq \varnothing$$

$$Z_4 \cap Z_2 = \left(P_0 \cup P_2 \cup P_3 \cup P_5 \cup P_6 \cup P_7 \cup P_8 \cup P_9\right) \cup \left(P_0 \cup P_1 \cup P_3 \cup P_4 \cup P_5 \cup P_6 \cup P_7 \cup P_8 \cup P_9\right) \neq \varnothing$$

$$Z_3 \cap Z_2 = \left(P_0 \cup P_1 \cup P_2 \cup P_4 \cup P_5 \cup P_6 \cup P_7 \cup P_8 \cup P_9\right) \cup \left(P_0 \cup P_1 \cup P_3 \cup P_4 \cup P_5 \cup P_6 \cup P_7 \cup P_8 \cup P_9\right) \neq \varnothing$$

$$Z_3 \cap Z_1 = \left(P_0 \cup P_1 \cup P_2 \cup P_4 \cup P_5 \cup P_6 \cup P_7 \cup P_8 \cup P_9\right) \cup \left(P_0 \cup P_2 \cup P_3 \cup P_4 \cup P_5 \cup P_6 \cup P_7 \cup P_8 \cup P_9\right) \neq \varnothing$$

$$Z_2 \cap Z_1 = \left(P_0 \cup P_1 \cup P_3 \cup P_4 \cup P_5 \cup P_6 \cup P_7 \cup P_8 \cup P_9\right) \cup \left(P_0 \cup P_2 \cup P_3 \cup P_4 \cup P_5 \cup P_6 \cup P_7 \cup P_8 \cup P_9\right) \neq \varnothing$$

From the equalities given above it follows that the semilattices 9 and 10 are not *XI*-semilattices. □

The semilattices 11

$$\left\{Z_6, Z_5, Z_3, Z_1, \breve{D}\right\},\ \left\{Z_6, Z_5, Z_2, Z_1, \breve{D}\right\},\ \left\{Z_6, Z_4, Z_3, Z_1, \breve{D}\right\},\ \left\{Z_6, Z_4, Z_2, Z_1, \breve{D}\right\},$$
$$\left\{Z_7, Z_6, Z_3, Z_2, \breve{D}\right\},\ \left\{Z_7, Z_6, Z_3, Z_1, \breve{D}\right\},\ \left\{Z_8, Z_6, Z_3, Z_2, \breve{D}\right\},\ \left\{Z_8, Z_6, Z_3, Z_1, \breve{D}\right\}.$$

(see diagram 1-8 of the **Figure 3**);
are not *XI*-semilattice since we have the following inequalities

$$Z_5 \cap Z_3 \neq \varnothing,\ Z_5 \cap Z_2 \neq \varnothing,\ Z_4 \cap Z_3 \neq \varnothing,\ Z_4 \cap Z_2 \neq \varnothing,$$
$$Z_7 \cap Z_2 \neq \varnothing,\ Z_7 \cap Z_1 \neq \varnothing,\ Z_8 \cap Z_2 \neq \varnothing,\ Z_8 \cap Z_1 \neq \varnothing.$$

The semilattices 12 to 52 are never *XI*-semilattices. We prove that the semilattice, diagram 52 of the **Figure 2**, is not an *XI*-semilattice (see **Figure 4**). Indeed, let $Q = \left\{T_0, T_1, T_2, T_3, T_4, T_5, T_6, T_7, T_8\right\}$ and

$$C\left(Q\right) = \left\{P_0', P_1', P_2', P_3', P_4', P_5', P_6', P_7', P_8'\right\}$$

be a family of sets, where P_0', P_1', P_2', P_3', P_4', P_5', P_6', P_7', P_8' are pairwise disjoint subsets of the set *X*. Let

$$\varphi = \begin{pmatrix} T_0 & T_1 & T_2 & T_3 & T_4 & T_5 & T_6 & T_7 & T_8 \\ P_0' & P_1' & P_2' & P_3' & P_4' & P_5' & P_6' & P_7' & P_8' \end{pmatrix}$$

be a mapping of the semilattice *Q* onto the family of sets $C\left(Q\right)$. Then for the formal equalities of the semilattice *Q* we have a form:

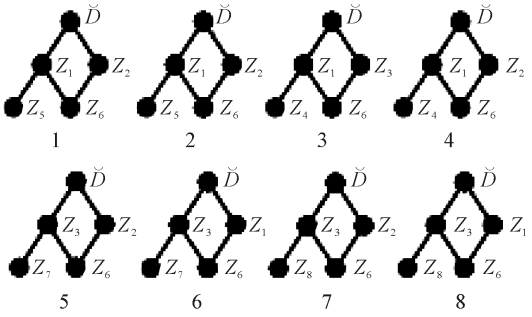

Figure 3. Diagram of all subsemilattices which are isomorphic to 11 in **Figure 2**.

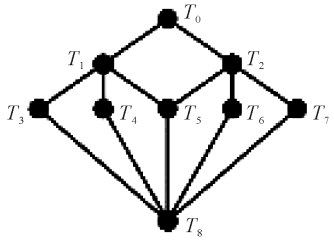

Figure 4. Diagram of subsemilattice 52 in **Figure 2**.

$$\begin{aligned}
T_0 &= P_0' \cup P_1' \cup P_2' \cup P_3' \cup P_4' \cup P_5' \cup P_6' \cup P_7' \cup P_8',\\
T_1 &= P_0' \cup P_2' \cup P_3' \cup P_4' \cup P_5' \cup P_6' \cup P_7' \cup P_8',\\
T_2 &= P_0' \cup P_1' \cup P_3' \cup P_4' \cup P_5' \cup P_6' \cup P_7' \cup P_8',\\
T_3 &= P_0' \cup P_2' \cup P_4' \cup P_5' \cup P_6' \cup P_7' \cup P_8',\\
T_4 &= P_0' \cup P_2' \cup P_3' \cup P_5' \cup P_6' \cup P_7' \cup P_8',\\
T_5 &= P_0' \cup P_3' \cup P_4' \cup P_6' \cup P_7' \cup P_8',\\
T_6 &= P_0' \cup P_1' \cup P_3' \cup P_4' \cup P_5' \cup P_7' \cup P_8',\\
T_7 &= P_0' \cup P_1' \cup P_3' \cup P_4' \cup P_5' \cup P_6' \cup P_8',\\
T_8 &= P_0'.
\end{aligned} \tag{3}$$

Here the elements $P_1', P_2', P_3', P_4', P_6', P_7'$ are basis sources, the elements P_0', P_5', P_8' are sources of completeness of the semilattice D. Therefore $|X| \geq 6$ and $\delta = 7$ (see [2]). Then of the formal equalities we have:

$$Q_t = \begin{cases}
Q, & \text{if } t \in P_0',\\
\{T_7, T_6, T_2, T_0\}, & \text{if } t \in P_1',\\
\{T_4, T_3, T_1, T_0\}, & \text{if } t \in P_2',\\
\{T_7, T_6, T_5, T_4, T_2, T_1, T_0\}, & \text{if } t \in P_3',\\
\{T_7, T_6, T_5, T_3, T_2, T_1, T_0\}, & \text{if } t \in P_4',\\
\{T_7, T_6, T_4, T_3, T_2, T_1, T_0\}, & \text{if } t \in P_5',\\
\{T_7, T_5, T_4, T_3, T_2, T_1, T_0\}, & \text{if } t \in P_6',\\
\{T_6, T_5, T_4, T_3, T_2, T_1, T_0\}, & \text{if } t \in P_7',\\
\{T_8, T_7, T_6, T_5, T_4, T_3, T_2, T_1, T_0\}, & \text{if } t \in P_8'.
\end{cases}$$

$$\Lambda(Q, Q_t) = \begin{cases}
T_8, & \text{if } t \in P_0',\\
T_8, & \text{if } t \in P_1',\\
T_8, & \text{if } t \in P_2',\\
T_8, & \text{if } t \in P_3',\\
T_8, & \text{if } t \in P_4',\\
T_8, & \text{if } t \in P_5',\\
T_8, & \text{if } t \in P_6',\\
T_8, & \text{if } t \in P_7',\\
T_8, & \text{if } t \in P_8'.
\end{cases}$$

We have, that $Q^{\wedge} = \{T_8\}$ and $\Lambda(Q, Q_t) \in Q$ for any $t \in Q$. But elements T_7, T_6, T_5, T_4, T_3, T_2, T_1, T_0 are not union of some elements of the set $Q^{\wedge}$. Therefore from the Definition 1 it follows that Q is not an *XI*-semilattice of unions. Statements 12 to 51 can be proved analogously.

We denoted the following semitattices by symbols:

a) $Q_1 = \{T\}$, where $T \in D$ (see diagram 1 of the **Figure 5**);

b) $Q_2 = \{T, T'\}$, where $T,\ T' \in D$ and $T \subset T'$ (see diagram 2 of the **Figure 5**);

c) $Q_3 = \{T, T', T''\}$, where $T,\ T',\ T'' \in D$ and $T \subset T' \subset T''$ (see diagram 3 of the **Figure 5**);

d) $Q_4 = \{Z_9, T, T', \breve{D}\}$, where $T,\ T' \in D$ and $Z_9 \subset T \subset T' \subset \breve{D}$ (see diagram 4 of the **Figure 5**);

e) $Q_5 = \{T, T', T'', T' \cup T''\}$ where $T,\ T',\ T'' \in D$, $T \subset T'$, $T \subset T''$, $T' \setminus T'' \neq \varnothing$, $T'' \setminus T' \neq \varnothing$, (see diagram 5 of the **Figure 5**);

f) $Q_6 = \{Z_9, T, T', T \cup T', \breve{D}\}$, where $T,\ T' \in D$, $Z_9 \subset T$, $Z_9 \subset T'$, $T \setminus T' \neq \varnothing$, $T' \setminus T \neq \varnothing$ (see diagram 6 of the **Figure 5**);

g) $Q_7 = \{Z_9, Z_6, T, T', \breve{D}\}$, where $T,\ T' \in D$, $Z_6 \subset T$, $Z_6 \subset T'$, $T \setminus T' \neq \varnothing$, $T' \setminus T \neq \varnothing$, $T \cup T' = \breve{D}$ (see diagram 7 of the **Figure 5**);

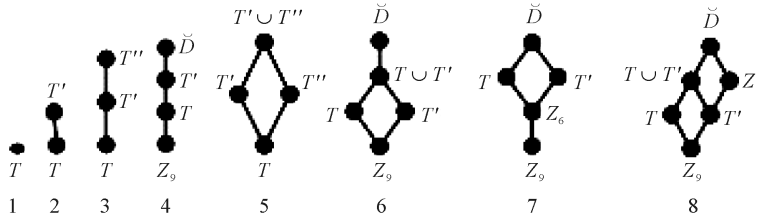

Figure 5. Diagram of all *XI*-subsemilattices of *D*.

h) $Q_8=\{Z_9,T,T',T\cup T',Z,\breve{D}\}$, where $Z_9\subset T'\subset Z$, $T\setminus T'\neq\varnothing$, $T'\setminus T\neq\varnothing$, $(T\cup T')\setminus Z\neq\varnothing$, $Z\setminus(T\cup T')\neq\varnothing$ (see diagram 8 of the **Figure 5**);

Note that the semilattices in **Figure 5** are all *XI*-semilattices (see [1] and Lemma 1.2.3).

Definition 9. *Let us assume that by the symbol* $\Sigma'_{XI}(X,D)$ *denote a set of all XI-subsemilatices of X-semilatices of unions D that every element of this set contains an empty set if* $\varnothing\in D$ *or denotes a set of all XI-subsemilatices of D.*

Further, let D', $D''\in\Sigma'_{XI}(X,D)$ and $\vartheta_{XI}\subseteq\Sigma'_{XI}(X,D)\times\Sigma'_{XI}(X,D)$. It is assumed that $D'\vartheta_{XI}D''$ iff there exists some complete isomorphism φ between the semilatices D' and D''. One can easily verify that the binary relation ϑ_{XI} is an equivalence relation on the set $\Sigma'_{XI}(X,D)$.

By the symbol $Q_i\vartheta_{XI}$ denote the ϑ_{XI}-equivalence class of the set $\Sigma'_{XI}(X,D)$, where every element is isomorphic to the *X*-semilattice $Q_i\ (i=1,2,\cdots,8)$.

Let D' be an *XI*-subsemilattice of the semilattice *D*. By $I(D')$ we denoted the set of all right units of the semigroup $B_X(D')$, and

$$\left|I^*(Q_i)\right|=\sum_{D'\in Q_i\vartheta_{XI}}\left|I(D')\right|$$

where $i=1,2,\cdots,8$.

Lemma 4. *If X is a finite set, then the following equalities hold*

a) $\left|I(Q_1)\right|=1$

b) $\left|I(Q_2)\right|=\left(2^{|T'\setminus T|}-1\right)\cdot 2^{|X\setminus T'|}$

c) $\left|I(Q_3)\right|=\left(2^{|T'\setminus T|}-1\right)\cdot\left(3^{|T''\setminus T'|}-2^{|T''\setminus T'|}\right)\cdot 3^{|X\setminus T''|}$

d) $\left|I(Q_4)\right|=\left(2^{|T\setminus Z_9|}-1\right)\cdot\left(3^{|T'\setminus T|}-2^{|T'\setminus T|}\right)\cdot\left(4^{|\breve{D}\setminus T'|}-3^{|\breve{D}\setminus T'|}\right)\cdot 4^{|X\setminus\breve{D}|}$

e) $\left|I(Q_5)\right|=\left(2^{|T'\setminus T''|}-1\right)\cdot\left(2^{|T''\setminus T'|}-1\right)\cdot 4^{|X\setminus(T'\cup T'')|}$

f) $\left|I(Q_6)\right|=\left(2^{|T'\setminus T''|}-1\right)\cdot\left(2^{|T''\setminus T'|}-1\right)\cdot\left(5^{|\breve{D}\setminus(T\cup T'')|}-4^{|\breve{D}\setminus(T\cup T'')|}\right)\cdot 5^{|X\setminus\breve{D}|}$

g) $\left|I(Q_7)\right|=\left(2^{|Z_6\setminus Z_9|}-1\right)\cdot 2^{|(T\cap T')\setminus Z_6|}\cdot\left(3^{|T\setminus T'|}-2^{|T\setminus T'|}\right)\cdot\left(3^{|T'\setminus T|}-2^{|T'\setminus T|}\right)\cdot 5^{|X\setminus\breve{D}|}$

h) $\left|I(Q_8)\right|=\left(2^{|T\setminus Z|}-1\right)\cdot\left(2^{|T'\setminus T|}-1\right)\cdot\left(3^{|Z\setminus(T\cup T')|}-2^{|Z\setminus(T\cup T')|}\right)\cdot 6^{|X\setminus\breve{D}|}$

Proof. This lemma immediately follows from Theorem 13.1.2, 13.3.2, and 13.7.2 of the [1]. □

Theorem 10. *Let* $D\in\Sigma_1(X,10)$ *and* $\alpha\in B_X(D)$. *Binary relation* α *is an idempotent relation of the semmigroup* $B_X(D)$ *iff binary relation* α *satisfies only one conditions of the following conditions*:

a) $\alpha=X\times T$, *where* $T\in D$;

b) $\alpha=\left(Y_T^\alpha\times T\right)\cup\left(Y_{T'}^\alpha\times T'\right)$, *where* T, $T'\in D$, $T\subset T'$, Y_T^α, $Y_{T'}^\alpha\notin\{\varnothing\}$, *and satisfies the conditions*: $Y_T^\alpha\supseteq T$, $Y_{T'}^\alpha\cap T'\neq\varnothing$;

c) $\alpha=\left(Y_T^\alpha\times T\right)\cup\left(Y_{T'}^\alpha\times T'\right)\cup\left(Y_{T''}^\alpha\times T''\right)$, *where* T, T', $T''\in D$, $T\subset T'\subset T''$, Y_T^α, $Y_{T'}^\alpha$, $Y_{T''}^\alpha\notin\{\varnothing\}$, *and satisfies the conditions*: $Y_T^\alpha\supseteq T$, $Y_T^\alpha\cup Y_{T'}^\alpha\supseteq T'$, $Y_{T'}^\alpha\cap T'\neq\varnothing$, $Y_{T''}^\alpha\cap T''\neq\varnothing$;

d) $\alpha=\left(Y_9^\alpha\times Z_9\right)\cup\left(Y_T^\alpha\times T\right)\cup\left(Y_{T'}^\alpha\times T'\right)\cup\left(Y_0^\alpha\times\breve{D}\right)$, *where* $T,\ T'\in D$, $Z_9\subset T\subset T'\subset\breve{D}$, Y_9^α, Y_T^α, $Y_{T'}^\alpha$, $Y_0^\alpha\notin\{\varnothing\}$, *and satisfies the conditions*: $Y_9^\alpha\supseteq Z_9$, $Y_9^\alpha\cup Y_T^\alpha\supseteq T$, $Y_9^\alpha\cup Y_T^\alpha\cup Y_{T'}^\alpha\supseteq T'$, $Y_T^\alpha\cap T\neq\varnothing$, $Y_{T'}^\alpha\cap T'\neq\varnothing$, $Y_0^\alpha\cap\breve{D}\neq\varnothing$;

e) $\alpha=\left(Y_T^\alpha\times T\right)\cup\left(Y_{T'}^\alpha\times T'\right)\cup\left(Y_{T''}^\alpha\times T''\right)\cup\left(Y_{T'\cup T''}^\alpha\times\left(T'\cup T''\right)\right)$, *where* $T,\ T',\ T''\in D$, $T\subset T'$, $T\subset T''$, $T'\setminus T''\neq\varnothing$, $T''\setminus T'\neq\varnothing$, $Y_T^\alpha, Y_{T'}^\alpha, Y_{T''}^\alpha\notin\{\varnothing\}$ *and satisfies the conditions*: $Y_T^\alpha\cup Y_{T'}^\alpha\supseteq T'$, $Y_T^\alpha\cup Y_{T''}^\alpha\supseteq T''$, $Y_{T'}^\alpha\cap T'\neq\varnothing$, $Y_{T''}^\alpha\cap T''\neq\varnothing$;

f) $\alpha=\left(Y_9^\alpha\times Z_9\right)\cup\left(Y_T^\alpha\times T\right)\cup\left(Y_{T'}^\alpha\times T'\right)\cup\left(Y_{T\cup T'}^\alpha\times\left(T\cup T'\right)\right)\cup\left(Y_0^\alpha\times\breve{D}\right)$, *where* $Z_9\subset T$, $Z_9\subset T'$, $T\setminus T'\neq\varnothing$, $T'\setminus T\neq\varnothing$, $Y_T^\alpha, Y_{T'}^\alpha, Y_0^\alpha\notin\{\varnothing\}$ *and satisfies the conditions*: $Y_9^\alpha\cup Y_T^\alpha\supseteq T$, $Y_9^\alpha\cup Y_{T'}^\alpha\supseteq T'$, $Y_T^\alpha\cap T\neq\varnothing$, $Y_{T'}^\alpha\cap T'\neq\varnothing$, $Y_0^\alpha\cap\breve{D}\neq\varnothing$;

g) $\alpha=\left(Y_9^\alpha\times Z_9\right)\cup\left(Y_6^\alpha\times Z_6\right)\cup\left(Y_T^\alpha\times T\right)\cup\left(Y_{T'}^\alpha\times T'\right)\cup\left(Y_0^\alpha\times\breve{D}\right)$, *where* $T,\ T'\in D$, $Z_6\subset T$, $Z_6\subset T'$, $T\setminus T'\neq\varnothing$, $T'\setminus T\neq\varnothing$, $T\cup T'=\breve{D}$, $Y_6^\alpha, Y_T^\alpha, Y_{T'}^\alpha\notin\{\varnothing\}$ *and satisfies the conditions*: $Y_9^\alpha\supseteq Z_9$, $Y_9^\alpha\cup Y_6^\alpha\supseteq Z_6$, $Y_9^\alpha\cup Y_6^\alpha\cup Y_T^\alpha\supseteq T$, $Y_9^\alpha\cup Y_6^\alpha\cup Y_{T'}^\alpha\supseteq T'$, $Y_6^\alpha\cap Z_6\neq\varnothing$, $Y_T^\alpha\cap T\neq\varnothing$, $Y_{T'}^\alpha\cap T'\neq\varnothing$;

h) $\alpha=\left(Y_9^\alpha\times Z_9\right)\cup\left(Y_T^\alpha\times T\right)\cup\left(Y_{T'}^\alpha\times T'\right)\cup\left(Y_{T\cup T'}^\alpha\times\left(T\cup T'\right)\right)\cup\left(Y_Z^\alpha\times Z\right)\cup\left(Y_0^\alpha\times\breve{D}\right)$, *where* $Z_9\subset T'\subset Z$, $T\setminus T'\neq\varnothing$, $T'\setminus T\neq\varnothing$, $\left(T\cup T'\right)\setminus Z\neq\varnothing$, $Z\setminus\left(T\cup T'\right)\neq\varnothing$, $Y_T^\alpha, Y_{T'}^\alpha, Y_Z^\alpha\notin\{\varnothing\}$ *and satisfies the conditions*: $Y_9^\alpha\cup Y_T^\alpha\supseteq T$, $Y_9^\alpha\cup Y_{T'}^\alpha\supseteq T'$ $Y_9^\alpha\cup Y_{T'}^\alpha\cup Y_Z^\alpha\supseteq Z$, $Y_T^\alpha\cap T\neq\varnothing$, $Y_{T'}^\alpha\cap T'\neq\varnothing$, $Y_Z^\alpha\cap Z\neq\varnothing$.

Proof. By Lemma 3 we know that 1 to 8 are an *XI*-semilattices. We prove only statement *g*. Indeed, if

$$\alpha=\left(Y_9^\alpha\times Z_9\right)\cup\left(Y_6^\alpha\times Z_6\right)\cup\left(Y_T^\alpha\times T\right)\cup\left(Y_{T'}^\alpha\times T'\right)\cup\left(Y_0^\alpha\times\breve{D}\right),$$

where $Y_6^\alpha, Y_T^\alpha, Y_{T'}^\alpha\notin\{\varnothing\}$, then it is easy to see, that the set $D(\alpha)=\{Z_9,Z_6,T,T_1'\}$ is a generating set of the semilattice $\{Z_9,Z_6,T,T',\breve{D}\}$. Then the following equalities hold

$$\ddot{D}(\alpha)_{Z_9}=\{Z_9\},\ \ddot{D}(\alpha)_{Z_6}=\{Z_9,Z_6\},$$
$$\ddot{D}(\alpha)_T=\{Z_9,Z_6,T\},\ \ddot{D}(\alpha)_{T'}=\{Z_9,Z_6,T'\}.$$

By statement *a* of the Theorem 6.2.1 (see [1]) we have:

$$Y_9^\alpha\supseteq Z_9,\ Y_9^\alpha\cup Y_6^\alpha\supseteq Z_6,\ Y_9^\alpha\cup Y_6^\alpha\cup Y_T^\alpha\supseteq T,\ Y_9^\alpha\cup Y_6^\alpha\cup Y_{T'}^\alpha\supseteq T'.$$

Further, one can see, that the equalities are true:

$$l\left(\ddot{D}(\alpha)_{Z_6},Z_6\right)=\cup\left(\ddot{D}(\alpha)_{Z_6}\setminus\{Z_6\}\right)=Z_9,\ Z_6\setminus l\left(\ddot{D}(\alpha)_{Z_6},Z_6\right)=Z_6\setminus Z_9\neq\varnothing,$$
$$l\left(\ddot{D}(\alpha)_T,T\right)=\cup\left(\ddot{D}(\alpha)_T\setminus\{T\}\right)=Z_6,\ T\setminus l\left(\ddot{D}(\alpha)_T,T\right)=T\setminus Z_6\neq\varnothing,$$
$$l\left(\ddot{D}(\alpha)_{T'},T'\right)=\cup\left(\ddot{D}(\alpha)_{T'}\setminus\{T'\}\right)=Z_6,\ T'\setminus l\left(\ddot{D}(\alpha)_{T'},T'\right)=T'\setminus Z_6\neq\varnothing,$$

We have the elements Z_6, T, T' are nonlimiting elements of the sets $\ddot{D}(\alpha)_{Z_6}$, $\ddot{D}(\alpha)_T$, $\ddot{D}(\alpha)_{T'}$ respectively. By statement *b* of the Theorem 6.2.1 [1] it follows, that the conditions $Y_6^\alpha\cap Z_6\neq\varnothing$, $Y_T^\alpha\cap T\neq\varnothing$, $Y_{T'}^\alpha\cap T'\neq\varnothing$ hold. Therefore, the statement *g* is proved. Rest of statements can be proved analogously.

Lemma 5. *Let* $D\in\Sigma_1(X,10)$ *and* $Z_9\neq\varnothing$. *If X is a finite set, then the number* $\left|I^*(Q_1)\right|$ *may be calculated by the formula* $\left|I^*(Q_1)\right|=10$.

Lemma 6. *Let* $D\in\Sigma_1(X,10)$ *and* $Z_9\neq\varnothing$. *If X is a finite set, then the number* $\left|I^*(Q_2)\right|$ *may be calculated by formula*

$$\begin{aligned}\left|I^*(Q_2)\right|=&\left(2^{|Z_8\setminus Z_9|}-1\right)\cdot2^{|X\setminus Z_8|}+\left(2^{|Z_7\setminus Z_9|}-1\right)\cdot2^{|X\setminus Z_7|}+\left(2^{|Z_6\setminus Z_9|}-1\right)\cdot2^{|X\setminus Z_6|}+\left(2^{|Z_5\setminus Z_9|}-1\right)\cdot2^{|X\setminus Z_5|}\\&+\left(2^{|Z_4\setminus Z_9|}-1\right)\cdot2^{|X\setminus Z_4|}+\left(2^{|Z_3\setminus Z_9|}+2^{|Z_3\setminus Z_8|}+2^{|Z_3\setminus Z_7|}+2^{|Z_3\setminus Z_6|}-4\right)\cdot2^{|X\setminus Z_3|}\\&+\left(2^{|Z_2\setminus Z_9|}+2^{|Z_2\setminus Z_6|}-2\right)\cdot2^{|X\setminus Z_2|}+\left(2^{|Z_1\setminus Z_9|}+2^{|Z_1\setminus Z_6|}+2^{|Z_1\setminus Z_5|}+2^{|Z_1\setminus Z_4|}-4\right)\cdot2^{|X\setminus Z_1|}\\&+\left(2^{|\breve{D}\setminus Z_9|}+2^{|\breve{D}\setminus Z_8|}+2^{|\breve{D}\setminus Z_7|}+2^{|\breve{D}\setminus Z_6|}+2^{|\breve{D}\setminus Z_5|}+2^{|\breve{D}\setminus Z_4|}+2^{|\breve{D}\setminus Z_3|}+2^{|\breve{D}\setminus Z_2|}+2^{|\breve{D}\setminus Z_1|}-9\right)\cdot2^{|X\setminus\breve{D}|}.\end{aligned}$$

Lemma 7. *Let* $D \in \Sigma_1(X,10)$ *and* $Z_9 \neq \varnothing$. *If X is a finite set, then the number* $\left|I^*(Q_3)\right|$ *may be calculated by formula*

$$\begin{aligned}\left|I^*(Q_3)\right| &= \left(2^{|Z_8\setminus Z_9|}-1\right)\cdot\left(3^{|\bar{D}\setminus Z_8|}-2^{|\bar{D}\setminus Z_8|}\right)\cdot 3^{|X\setminus\bar{D}|}+\left(2^{|Z_7\setminus Z_9|}-1\right)\cdot\left(3^{|\bar{D}\setminus Z_7|}-2^{|\bar{D}\setminus Z_7|}\right)\cdot 3^{|X\setminus\bar{D}|}\\ &+\left(2^{|Z_6\setminus Z_9|}-1\right)\cdot\left(3^{|\bar{D}\setminus Z_6|}-2^{|\bar{D}\setminus Z_6|}\right)\cdot 3^{|X\setminus\bar{D}|}+\left(2^{|Z_5\setminus Z_9|}-1\right)\cdot\left(3^{|\bar{D}\setminus Z_5|}-2^{|\bar{D}\setminus Z_5|}\right)\cdot 3^{|X\setminus\bar{D}|}\\ &+\left(2^{|Z_4\setminus Z_9|}-1\right)\cdot\left(3^{|\bar{D}\setminus Z_4|}-2^{|\bar{D}\setminus Z_4|}\right)\cdot 3^{|X\setminus\bar{D}|}+\left(2^{|Z_3\setminus Z_9|}-1\right)\cdot\left(3^{|\bar{D}\setminus Z_3|}-2^{|\bar{D}\setminus Z_3|}\right)\cdot 3^{|X\setminus\bar{D}|}\\ &+\left(2^{|Z_2\setminus Z_9|}-1\right)\cdot\left(3^{|\bar{D}\setminus Z_2|}-2^{|\bar{D}\setminus Z_2|}\right)\cdot 3^{|X\setminus\bar{D}|}+\left(2^{|Z_1\setminus Z_9|}-1\right)\cdot\left(3^{|\bar{D}\setminus Z_1|}-2^{|\bar{D}\setminus Z_1|}\right)\cdot 3^{|X\setminus\bar{D}|}\\ &+\left(2^{|Z_8\setminus Z_9|}-1\right)\cdot\left(3^{|Z_3\setminus Z_8|}-2^{|Z_3\setminus Z_8|}\right)\cdot 3^{|X\setminus Z_3|}+\left(2^{|Z_7\setminus Z_9|}-1\right)\cdot\left(3^{|Z_3\setminus Z_7|}-2^{|Z_3\setminus Z_7|}\right)\cdot 3^{|X\setminus Z_3|}\\ &+\left(2^{|Z_6\setminus Z_9|}-1\right)\cdot\left(3^{|Z_3\setminus Z_6|}-2^{|Z_3\setminus Z_6|}\right)\cdot 3^{|X\setminus Z_3|}+\left(2^{|Z_6\setminus Z_9|}-1\right)\cdot\left(3^{|Z_2\setminus Z_6|}-2^{|Z_2\setminus Z_6|}\right)\cdot 3^{|X\setminus Z_2|}\\ &+\left(2^{|Z_6\setminus Z_9|}-1\right)\cdot\left(3^{|Z_1\setminus Z_6|}-2^{|Z_1\setminus Z_6|}\right)\cdot 3^{|X\setminus Z_1|}+\left(2^{|Z_5\setminus Z_9|}-1\right)\cdot\left(3^{|Z_1\setminus Z_5|}-2^{|Z_1\setminus Z_5|}\right)\cdot 3^{|X\setminus Z_1|}\\ &+\left(2^{|Z_4\setminus Z_9|}-1\right)\cdot\left(3^{|Z_1\setminus Z_4|}-2^{|Z_1\setminus Z_4|}\right)\cdot 3^{|X\setminus Z_1|}+\left(2^{|Z_3\setminus Z_8|}-1\right)\cdot\left(3^{|\bar{D}\setminus Z_3|}-2^{|\bar{D}\setminus Z_3|}\right)\cdot 3^{|X\setminus\bar{D}|}\\ &+\left(2^{|Z_3\setminus Z_7|}-1\right)\cdot\left(3^{|\bar{D}\setminus Z_3|}-2^{|\bar{D}\setminus Z_3|}\right)\cdot 3^{|X\setminus\bar{D}|}+\left(2^{|Z_3\setminus Z_6|}-1\right)\cdot\left(3^{|\bar{D}\setminus Z_3|}-2^{|\bar{D}\setminus Z_3|}\right)\cdot 3^{|X\setminus\bar{D}|}\\ &+\left(2^{|Z_2\setminus Z_6|}-1\right)\cdot\left(3^{|\bar{D}\setminus Z_2|}-2^{|\bar{D}\setminus Z_2|}\right)\cdot 3^{|X\setminus\bar{D}|}+\left(2^{|Z_1\setminus Z_6|}-1\right)\cdot\left(3^{|\bar{D}\setminus Z_1|}-2^{|\bar{D}\setminus Z_1|}\right)\cdot 3^{|X\setminus\bar{D}|}\\ &+\left(2^{|Z_1\setminus Z_5|}-1\right)\cdot\left(3^{|\bar{D}\setminus Z_1|}-2^{|\bar{D}\setminus Z_1|}\right)\cdot 3^{|X\setminus\bar{D}|}+\left(2^{|Z_1\setminus Z_4|}-1\right)\cdot\left(3^{|\bar{D}\setminus Z_1|}-2^{|\bar{D}\setminus Z_1|}\right)\cdot 3^{|X\setminus\bar{D}|}.\end{aligned}$$

Lemma 8. *Let* $D \in \Sigma_1(X,10)$ *and* $Z_9 \neq \varnothing$. *If X is a finite set, then the number* $\left|I^*(Q_4)\right|$ *may be calculated by formula*

$$\begin{aligned}\left|I^*(Q_4)\right| &= \left(2^{|Z_8\setminus Z_9|}-1\right)\cdot\left(3^{|Z_3\setminus Z_8|}-2^{|Z_3\setminus Z_8|}\right)\cdot\left(4^{|\bar{D}\setminus Z_3|}-3^{|\bar{D}\setminus Z_3|}\right)\cdot 4^{|X\setminus\bar{D}|}\\ &+\left(2^{|Z_7\setminus Z_9|}-1\right)\cdot\left(3^{|Z_3\setminus Z_7|}-2^{|Z_3\setminus Z_7|}\right)\cdot\left(4^{|\bar{D}\setminus Z_3|}-3^{|\bar{D}\setminus Z_3|}\right)\cdot 4^{|X\setminus\bar{D}|}\\ &+\left(2^{|Z_6\setminus Z_9|}-1\right)\cdot\left(3^{|Z_3\setminus Z_6|}-2^{|Z_3\setminus Z_6|}\right)\cdot\left(4^{|\bar{D}\setminus Z_3|}-3^{|\bar{D}\setminus Z_3|}\right)\cdot 4^{|X\setminus\bar{D}|}\\ &+\left(2^{|Z_6\setminus Z_9|}-1\right)\cdot\left(3^{|Z_2\setminus Z_6|}-2^{|Z_2\setminus Z_6|}\right)\cdot\left(4^{|\bar{D}\setminus Z_2|}-3^{|\bar{D}\setminus Z_2|}\right)\cdot 4^{|X\setminus\bar{D}|}\\ &+\left(2^{|Z_6\setminus Z_9|}-1\right)\cdot\left(3^{|Z_1\setminus Z_6|}-2^{|Z_1\setminus Z_6|}\right)\cdot\left(4^{|\bar{D}\setminus Z_1|}-3^{|\bar{D}\setminus Z_1|}\right)\cdot 4^{|X\setminus\bar{D}|}\\ &+\left(2^{|Z_5\setminus Z_9|}-1\right)\cdot\left(3^{|Z_1\setminus Z_5|}-2^{|Z_1\setminus Z_5|}\right)\cdot\left(4^{|\bar{D}\setminus Z_1|}-3^{|\bar{D}\setminus Z_1|}\right)\cdot 4^{|X\setminus\bar{D}|}\\ &+\left(2^{|Z_4\setminus Z_9|}-1\right)\cdot\left(3^{|Z_1\setminus Z_4|}-2^{|Z_1\setminus Z_4|}\right)\cdot\left(4^{|\bar{D}\setminus Z_1|}-3^{|\bar{D}\setminus Z_1|}\right)\cdot 4^{|X\setminus\bar{D}|}.\end{aligned}$$

Lemma 9. *Let* $D \in \Sigma_1(X,10)$ *and* $Z_9 \neq \varnothing$. *If X is a finite set, then the number* $\left|I^*(Q_5)\right|$ *may be calculated by formula*

$$\begin{aligned}\left|I^*\left(Q_5\right)\right| &= \left(2^{|Z_5\setminus Z_4|}-1\right)\cdot\left(2^{|Z_4\setminus Z_5|}-1\right)\cdot 4^{|X\setminus Z_1|}+\left(2^{|Z_6\setminus Z_4|}-1\right)\cdot\left(2^{|Z_4\setminus Z_6|}-1\right)\cdot 4^{|X\setminus Z_1|}\\ &+\left(2^{|Z_6\setminus Z_5|}-1\right)\cdot\left(2^{|Z_5\setminus Z_6|}-1\right)\cdot 4^{|X\setminus Z_1|}+\left(2^{|Z_7\setminus Z_6|}-1\right)\cdot\left(2^{|Z_6\setminus Z_7|}-1\right)\cdot 4^{|X\setminus Z_3|}\\ &+\left(2^{|Z_8\setminus Z_6|}-1\right)\cdot\left(2^{|Z_6\setminus Z_8|}-1\right)\cdot 4^{|X\setminus Z_3|}+\left(2^{|Z_8\setminus Z_7|}-1\right)\cdot\left(2^{|Z_7\setminus Z_8|}-1\right)\cdot 4^{|X\setminus Z_3|}\\ &+\left(2^{|Z_8\setminus Z_4|}-1\right)\cdot\left(2^{|Z_4\setminus Z_8|}-1\right)\cdot 4^{|X\setminus \bar{D}|}+\left(2^{|Z_8\setminus Z_5|}-1\right)\cdot\left(2^{|Z_5\setminus Z_8|}-1\right)\cdot 4^{|X\setminus \bar{D}|}\\ &+\left(2^{|Z_7\setminus Z_2|}-1\right)\cdot\left(2^{|Z_2\setminus Z_7|}-1\right)\cdot 4^{|X\setminus \bar{D}|}+\left(2^{|Z_7\setminus Z_4|}-1\right)\cdot\left(2^{|Z_4\setminus Z_7|}-1\right)\cdot 4^{|X\setminus \bar{D}|}\\ &+\left(2^{|Z_7\setminus Z_5|}-1\right)\cdot\left(2^{|Z_5\setminus Z_7|}-1\right)\cdot 4^{|X\setminus \bar{D}|}+\left(2^{|Z_8\setminus Z_1|}-1\right)\cdot\left(2^{|Z_1\setminus Z_8|}-1\right)\cdot 4^{|X\setminus \bar{D}|}\\ &+\left(2^{|Z_8\setminus Z_2|}-1\right)\cdot\left(2^{|Z_2\setminus Z_8|}-1\right)\cdot 4^{|X\setminus \bar{D}|}+\left(2^{|Z_4\setminus Z_2|}-1\right)\cdot\left(2^{|Z_2\setminus Z_4|}-1\right)\cdot 4^{|X\setminus \bar{D}|}\\ &+\left(2^{|Z_4\setminus Z_3|}-1\right)\cdot\left(2^{|Z_3\setminus Z_4|}-1\right)\cdot 4^{|X\setminus \bar{D}|}+\left(2^{|Z_5\setminus Z_2|}-1\right)\cdot\left(2^{|Z_2\setminus Z_5|}-1\right)\cdot 4^{|X\setminus \bar{D}|}\\ &+\left(2^{|Z_5\setminus Z_3|}-1\right)\cdot\left(2^{|Z_3\setminus Z_5|}-1\right)\cdot 4^{|X\setminus \bar{D}|}+\left(2^{|Z_7\setminus Z_1|}-1\right)\cdot\left(2^{|Z_1\setminus Z_7|}-1\right)\cdot 4^{|X\setminus \bar{D}|}\\ &+2\cdot\left(2^{|Z_2\setminus Z_1|}-1\right)\cdot\left(2^{|Z_1\setminus Z_2|}-1\right)\cdot 4^{|X\setminus \bar{D}|}+2\cdot\left(2^{|Z_3\setminus Z_1|}-1\right)\cdot\left(2^{|Z_1\setminus Z_3|}-1\right)\cdot 4^{|X\setminus \bar{D}|}\\ &+2\cdot\left(2^{|Z_3\setminus Z_2|}-1\right)\cdot\left(2^{|Z_2\setminus Z_3|}-1\right)\cdot 4^{|X\setminus \bar{D}|}.\end{aligned}$$

Lemma 10. *Let* $D\in\Sigma_1\left(X,10\right)$ *and* $Z_9\neq\varnothing$. *If X is a finite set, then the number* $\left|I^*\left(Q_6\right)\right|$ *may be calculated by formula*

$$\left|I^*\left(Q_6\right)\right| = 1+3+3+3+3+1=14$$

Lemma 11. *Let* $D\in\Sigma_1\left(X,10\right)$ *and* $Z_9\neq\varnothing$. *If X is a finite set, then the number* $\left|I^*\left(Q_7\right)\right|$ *may be calculated by formula*

$$\begin{aligned}\left|I^*\left(Q_7\right)\right| &= \left(2^{|Z_6\setminus Z_9|}-1\right)\cdot 2^{|(Z_2\cap Z_1)\setminus Z_6|}\cdot\left(3^{|Z_2\setminus Z_1|}-2^{|Z_2\setminus Z_1|}\right)\cdot\left(3^{|Z_1\setminus Z_2|}-2^{|Z_1\setminus Z_2|}\right)\cdot 5^{|X\setminus \bar{D}|}\\ &+\left(2^{|Z_6\setminus Z_9|}-1\right)\cdot 2^{|(Z_3\cap Z_1)\setminus Z_6|}\cdot\left(3^{|Z_3\setminus Z_1|}-2^{|Z_3\setminus Z_1|}\right)\cdot\left(3^{|Z_1\setminus Z_3|}-2^{|Z_1\setminus Z_3|}\right)\cdot 5^{|X\setminus \bar{D}|}\\ &+\left(2^{|Z_6\setminus Z_9|}-1\right)\cdot 2^{|(Z_3\cap Z_2)\setminus Z_6|}\cdot\left(3^{|Z_3\setminus Z_2|}-2^{|Z_3\setminus Z_2|}\right)\cdot\left(3^{|Z_2\setminus Z_3|}-2^{|Z_2\setminus Z_3|}\right)\cdot 5^{|X\setminus \bar{D}|}.\end{aligned}$$

Lemma 12. *Let* $D\in\Sigma_1\left(X,10\right)$ *and* $Z_9\neq\varnothing$. *If X is a finite set, then the number* $\left|I^*\left(Q_8\right)\right|$ *may be calculated by formula*

$$\begin{aligned}\left|I^*\left(Q_8\right)\right| &= \left(2^{|Z_8\setminus Z_2|}-1\right)\cdot\left(2^{|Z_6\setminus Z_8|}-1\right)\cdot\left(3^{|Z_2\setminus Z_3|}-2^{|Z_2\setminus Z_3|}\right)\cdot 6^{|X\setminus \bar{D}|}\\ &+\left(2^{|Z_8\setminus Z_1|}-1\right)\cdot\left(2^{|Z_6\setminus Z_8|}-1\right)\cdot\left(3^{|Z_1\setminus Z_3|}-2^{|Z_1\setminus Z_3|}\right)\cdot 6^{|X\setminus \bar{D}|}\\ &+\left(2^{|Z_7\setminus Z_2|}-1\right)\cdot\left(2^{|Z_6\setminus Z_7|}-1\right)\cdot\left(3^{|Z_2\setminus Z_3|}-2^{|Z_2\setminus Z_3|}\right)\cdot 6^{|X\setminus \bar{D}|}\\ &+\left(2^{|Z_7\setminus Z_1|}-1\right)\cdot\left(2^{|Z_6\setminus Z_7|}-1\right)\cdot\left(3^{|Z_1\setminus Z_3|}-2^{|Z_1\setminus Z_3|}\right)\cdot 6^{|X\setminus \bar{D}|}\\ &+\left(2^{|Z_5\setminus Z_3|}-1\right)\cdot\left(2^{|Z_6\setminus Z_5|}-1\right)\cdot\left(3^{|Z_3\setminus Z_1|}-2^{|Z_3\setminus Z_1|}\right)\cdot 6^{|X\setminus \bar{D}|}\\ &+\left(2^{|Z_5\setminus Z_2|}-1\right)\cdot\left(2^{|Z_6\setminus Z_5|}-1\right)\cdot\left(3^{|Z_2\setminus Z_1|}-2^{|Z_2\setminus Z_1|}\right)\cdot 6^{|X\setminus \bar{D}|}\\ &+\left(2^{|Z_4\setminus Z_3|}-1\right)\cdot\left(2^{|Z_6\setminus Z_4|}-1\right)\cdot\left(3^{|Z_3\setminus Z_1|}-2^{|Z_3\setminus Z_1|}\right)\cdot 6^{|X\setminus \bar{D}|}\\ &+\left(2^{|Z_4\setminus Z_2|}-1\right)\cdot\left(2^{|Z_6\setminus Z_4|}-1\right)\cdot\left(3^{|Z_2\setminus Z_1|}-2^{|Z_2\setminus Z_1|}\right)\cdot 6^{|X\setminus \bar{D}|}.\end{aligned}$$

Figure 6 shows all *XI*-subsemilattices with six elements.

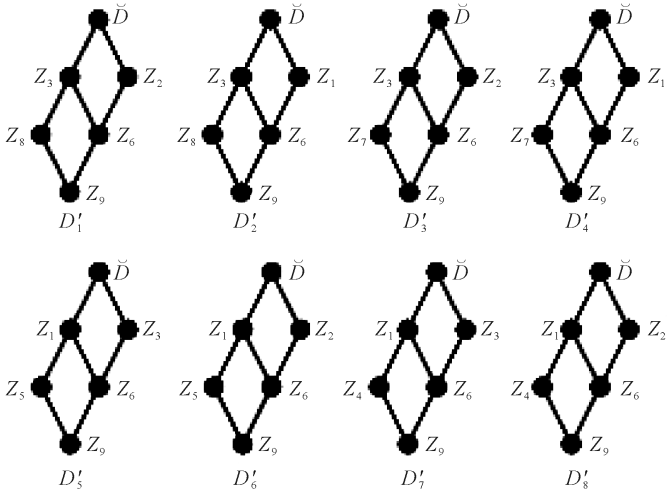

Figure 6. Diagram of all subsemilattices which are isomorphic.

Theorem 11. *Let* $D \in \Sigma_1(X,10)$, $Z_9 \neq \varnothing$. *If X is a finite set and* I_D *is a set of all idempotent elements of the semigroup* $B_X(D)$. *Then* $|I_D| = \sum_{i=1}^{8} |I^*(Q_i)|$.

Example 12. *Let* $X = \{1,2,3,4,5,6,7,8\}$,

$$P_0 = \{6\},\ P_1 = \{1\},\ P_2 = \{2\},\ P_3 = \{3\},\ P_4 = \{4\},$$
$$P_5 = \{5\},\ P_7 = \{7\},\ P_8 = \{8\},\ P_9 = P_6 = \varnothing.$$

Then $\breve{D} = \{1,2,3,4,5,6,7,8\}$, $Z_1 = \{2,3,4,5,6,7,8\}$, $Z_2 = \{1,3,4,5,6,7,8\}$, $Z_3 = \{1,2,4,5,6,7,8\}$, $Z_4 = \{2,3,5,6,7,8\}$, $Z_5 = \{2,3,4,6,7,8\}$, $Z_6 = \{4,5,6,7,8\}$, $Z_7 = \{1,2,4,5,6,8\}$, $Z_8 = \{1,2,4,5,6,7\}$ and $Z_9 = \{6\}$.

$$D = \{\{1,2,3,4,5,6,7,8\},\{2,3,4,5,6,7,8\},\{1,3,4,5,6,7,8\},\{1,2,4,5,6,7,8\},\{2,3,5,6,7,8\},$$
$$\{2,3,4,6,7,8\},\{4,5,6,7,8\},\{1,2,4,5,6,8\},\{1,2,4,5,6,7\},\{6\}\}$$

We have $Z_9 \neq \varnothing$. Where $|I^*(Q_1)| = 10$, $|I^*(Q_2)| = 1169$, $|I^*(Q_3)| = 2154$, $|I^*(Q_4)| = 349$, $|I^*(Q_5)| = 122$, $|I^*(Q_6)| = 14$, $|I^*(Q_7)| = 90$, $|I(Q_8)| = 8$, $|I_D| = 3916$.

3. Results

Lemma 13. *Let* $D \in \Sigma_1(X,10)$ *and* $Z_9 = \varnothing$. *Then the following sets exhaust all subsemilattices of the semilattice* $D = \{Z_9, Z_8, Z_7, Z_6, Z_5, Z_4, Z_3, Z_2, Z_1, \breve{D}\}$ *which contains the empty set*:

1) $\{\varnothing\}$
(*see diagram* 1 *of the* ***Figure 2***);

2) $\{\varnothing, \breve{D}\}$, $\{\varnothing, Z_8\}$, $\{\varnothing, Z_7\}$, $\{\varnothing, Z_6\}$, $\{\varnothing, Z_5\}$, $\{\varnothing, Z_4\}$, $\{\varnothing, Z_3\}$, $\{\varnothing, Z_2\}$, $\{\varnothing, Z_1\}$
(*see diagram* 2 *of the* ***Figure 2***);

3) $\{\varnothing, Z_8, \breve{D}\}$, $\{\varnothing, Z_7, \breve{D}\}$, $\{\varnothing, Z_6, \breve{D}\}$, $\{\varnothing, Z_5, \breve{D}\}$, $\{\varnothing, Z_4, \breve{D}\}$, $\{\varnothing, Z_3, \breve{D}\}$, $\{\varnothing, Z_2, \breve{D}\}$, $\{\varnothing, Z_1, \breve{D}\}$, $\{\varnothing, Z_8, Z_3\}$, $\{\varnothing, Z_7, Z_3\}$, $\{\varnothing, Z_6, Z_3\}$, $\{\varnothing, Z_6, Z_2\}$, $\{\varnothing, Z_6, Z_1\}$, $\{\varnothing, Z_5, Z_1\}$, $\{\varnothing, Z_4, Z_1\}$
(*see diagram* 3 *of the* ***Figure 2***);

4) $\{\varnothing, Z_4, Z_1, \breve{D}\}$, $\{\varnothing, Z_5, Z_1, \breve{D}\}$, $\{\varnothing, Z_6, Z_1, \breve{D}\}$, $\{\varnothing, Z_6, Z_2, \breve{D}\}$, $\{\varnothing, Z_6, Z_3, \breve{D}\}$, $\{\varnothing, Z_7, Z_3, \breve{D}\}$, $\{\varnothing, Z_8, Z_3, \breve{D}\}$
(*see diagram* 4 *of the* ***Figure 2***);

5) $\{\varnothing, Z_5, Z_4, Z_1\}$, $\{\varnothing, Z_6, Z_4, Z_1\}$, $\{\varnothing, Z_6, Z_5, Z_1\}$, $\{\varnothing, Z_7, Z_6, Z_3\}$, $\{\varnothing, Z_8, Z_6, Z_3\}$, $\{\varnothing, Z_8, Z_7, Z_3\}$, $\{\varnothing, Z_8, Z_4, \breve{D}\}$, $\{\varnothing, Z_8, Z_5, \breve{D}\}$, $\{\varnothing, Z_7, Z_2, \breve{D}\}$, $\{\varnothing, Z_7, Z_4, \breve{D}\}$, $\{\varnothing, Z_7, Z_5, \breve{D}\}$, $\{\varnothing, Z_8, Z_1, \breve{D}\}$, $\{\varnothing, Z_8, Z_2, \breve{D}\}$, $\{\varnothing, Z_4, Z_2, \breve{D}\}$, $\{\varnothing, Z_4, Z_3, \breve{D}\}$, $\{\varnothing, Z_5, Z_2, \breve{D}\}$, $\{\varnothing, Z_5, Z_3, \breve{D}\}$, $\{\varnothing, Z_7, Z_1, \breve{D}\}$, $\{\varnothing, Z_2, Z_1, \breve{D}\}$, $\{\varnothing, Z_3, Z_1, \breve{D}\}$, $\{\varnothing, Z_3, Z_2, \breve{D}\}$
(*see diagram* 5 *of the* ***Figure 2***);

6) $\{\varnothing, Z_5, Z_4, Z_1, \breve{D}\}$, $\{\varnothing, Z_6, Z_4, Z_1, \breve{D}\}$, $\{\varnothing, Z_6, Z_5, Z_1, \breve{D}\}$, $\{\varnothing, Z_7, Z_6, Z_3, \breve{D}\}$, $\{\varnothing, Z_8, Z_6, Z_3, \breve{D}\}$, $\{\varnothing, Z_8, Z_7, Z_3, \breve{D}\}$
(*see diagram* 6 *of the* ***Figure 2***);

7) $\{\varnothing, Z_6, Z_2, Z_1, \breve{D}\}$, $\{\varnothing, Z_6, Z_3, Z_1, \breve{D}\}$, $\{\varnothing, Z_6, Z_3, Z_2, \breve{D}\}$
(*see diagram* 7 *of the* ***Figure 2***);

8) $\{\varnothing, Z_8, Z_6, Z_3, Z_2, \breve{D}\}$, $\{\varnothing, Z_8, Z_6, Z_3, Z_1, \breve{D}\}$, $\{\varnothing, Z_7, Z_6, Z_3, Z_2, \breve{D}\}$, $\{\varnothing, Z_7, Z_6, Z_3, Z_1, \breve{D}\}$, $\{\varnothing, Z_6, Z_5, Z_3, Z_1, \breve{D}\}$, $\{\varnothing, Z_6, Z_5, Z_2, Z_1, \breve{D}\}$, $\{\varnothing, Z_6, Z_4, Z_3, Z_1, \breve{D}\}$, $\{\varnothing, Z_6, Z_4, Z_2, Z_1, \breve{D}\}$
(*see diagram* 8 *of the* ***Figure 2***);

Theorem 13. *Let* $D \in \Sigma_1(X, 10)$, $Z_9 = \varnothing$ *and* $\alpha \in B_X(D)$. *Binary relation* α *is an idempotent relation of the semmigroup* $B_X(D)$ *iff binary relation* α *satisfies only one conditions of the following conditions*:

a) $\alpha = \varnothing$;

b) $\alpha = \left(Y_9^\alpha \times \varnothing\right) \cup \left(Y_T^\alpha \times T\right)$, *where* $T \in D$, $\varnothing \neq T$, $Y_T^\alpha \neq \varnothing$, *and satisfies the conditions*: $Y_T^\alpha \cap T \neq \varnothing$;

c) $\alpha = \left(Y_9^\alpha \times \varnothing\right) \cup \left(Y_T^\alpha \times T\right) \cup \left(Y_{T'}^\alpha \times T'\right)$, *where* $T, T' \in D$, $\varnothing \neq T \subset T'$, $Y_T^\alpha, Y_{T'}^\alpha \notin \{\varnothing\}$, *and satisfies the conditions*: $Y_9^\alpha \cup Y_T^\alpha \supseteq T$, $Y_T^\alpha \cap T \neq \varnothing$, $Y_{T'}^\alpha \cap T' \neq \varnothing$;

d) $\alpha = \left(Y_9^\alpha \times \varnothing\right) \cup \left(Y_T^\alpha \times T\right) \cup \left(Y_{T'}^\alpha \times T'\right) \cup \left(Y_0^\alpha \times \breve{D}\right)$, *where* $T, T' \in D$, $\varnothing \neq T \subset T' \subset \breve{D}$, Y_T^α, $Y_{T'}^\alpha$, $Y_0^\alpha \notin \{\varnothing\}$, *and satisfies the conditions*: $Y_9^\alpha \cup Y_T^\alpha \supseteq T$, $Y_9^\alpha \cup Y_T^\alpha \cup Y_{T'}^\alpha \supseteq T'$, $Y_T^\alpha \cap T \neq \varnothing$, $Y_{T'}^\alpha \cap T' \neq \varnothing$, $Y_0^\alpha \cap \breve{D} \neq \varnothing$;

e) $\alpha = \left(Y_9^\alpha \times \varnothing\right) \cup \left(Y_T^\alpha \times T\right) \cup \left(Y_{T'}^\alpha \times T'\right) \cup \left(Y_{T \cup T'}^\alpha \times \left(T \cup T'\right)\right)$, *where* $T, T' \in D$, $T \setminus T' \neq \varnothing$, $T' \setminus T \neq \varnothing$, Y_T^α, $Y_{T'}^\alpha \notin \{\varnothing\}$ *and satisfies the conditions*: $Y_9^\alpha \cup Y_T^\alpha \supseteq T$, $Y_9^\alpha \cup Y_{T'}^\alpha \supseteq T'$, $Y_T^\alpha \cap T \neq \varnothing$, $Y_{T'}^\alpha \cap T' \neq \varnothing$;

f) $\alpha = \left(Y_9^\alpha \times \varnothing\right) \cup \left(Y_T^\alpha \times T\right) \cup \left(Y_{T'}^\alpha \times T'\right) \cup \left(Y_{T \cup T'}^\alpha \times \left(T \cup T'\right)\right) \cup \left(Y_0^\alpha \times \breve{D}\right)$, *where* $T \setminus T' \neq \varnothing$, $T' \setminus T \neq \varnothing$, Y_T^α, $Y_{T'}^\alpha$, $Y_0^\alpha \notin \{\varnothing\}$ *and satisfies the conditions*: $Y_9^\alpha \cup Y_T^\alpha \supseteq T$, $Y_9^\alpha \cup Y_{T'}^\alpha \supseteq T'$, $Y_T^\alpha \cap T \neq \varnothing$, $Y_{T'}^\alpha \cap T' \neq \varnothing$, $Y_0^\alpha \cap \breve{D} \neq \varnothing$.

g) $\alpha = \left(Y_9^\alpha \times \varnothing\right) \cup \left(Y_6^\alpha \times Z_6\right) \cup \left(Y_T^\alpha \times T\right) \cup \left(Y_{T'}^\alpha \times T'\right) \cup \left(Y_0^\alpha \times \breve{D}\right)$, *where* $T, T' \in D$, $Z_6 \subset T$, $Z_6 \subset T'$, $T \setminus T' \neq \varnothing$, $T' \setminus T \neq \varnothing$, $T \cup T' = \breve{D}$, Y_6^α, Y_T^α, $Y_{T'}^\alpha \notin \{\varnothing\}$ *and satisfies the conditions*: $Y_9^\alpha \cup Y_6^\alpha \supseteq Z_6$, $Y_9^\alpha \cup Y_6^\alpha \cup Y_T^\alpha \supseteq T$, $Y_9^\alpha \cup Y_6^\alpha \cup Y_{T'}^\alpha \supseteq T'$, $Y_6^\alpha \cap Z_6 \neq \varnothing$, $Y_T^\alpha \cap T \neq \varnothing$, $Y_{T'}^\alpha \cap T' \neq \varnothing$;

h) $\alpha = \left(Y_9^\alpha \times \varnothing\right) \cup \left(Y_T^\alpha \times T\right) \cup \left(Y_{T'}^\alpha \times T'\right) \cup \left(Y_{T \cup T'}^\alpha \times \left(T \cup T'\right)\right) \cup \left(Y_Z^\alpha \times Z\right) \cup \left(Y_0^\alpha \times \breve{D}\right)$, *where* $T' \subset Z$, $T \setminus T' \neq \varnothing$, $T' \setminus T \neq \varnothing$, $\left(T \cup T'\right) \setminus Z \neq \varnothing$, $Z \setminus \left(T \cup T'\right) \neq \varnothing$, Y_T^α, $Y_{T'}^\alpha$, $Y_Z^\alpha \notin \{\varnothing\}$ *and satisfies the conditions*: $Y_9^\alpha \cup Y_T^\alpha \supseteq T$, $Y_9^\alpha \cup Y_{T'}^\alpha \supseteq T'$, $Y_9^\alpha \cup Y_{T'}^\alpha \cup Y_Z^\alpha \supseteq Z$, $Y_T^\alpha \cap T \neq \varnothing$, $Y_{T'}^\alpha \cap T' \neq \varnothing$, $Y_Z^\alpha \cap Z \neq \varnothing$;

Lemma 14. *Let* $D \in \Sigma_1(X, 10)$ *and* $Z_9 = \varnothing$. *If X is a finite set, then* $\left|I^*\left(Q_1\right)\right| = 1$.

Lemma 15. *Let* $D \in \Sigma_1(X, 10)$ *and* $Z_9 = \varnothing$. *If X is a finite set, then the number* $\left|I^*\left(Q_2\right)\right|$ *may be calcu-*

lated by formula

$$\begin{aligned}\left|I^*\left(Q_2\right)\right| &= \left(2^{|\bar{D}|}-1\right)\cdot 2^{|X\setminus\bar{D}|}+\left(2^{|Z_8|}-1\right)\cdot 2^{|X\setminus Z_8|}+\left(2^{|Z_7|}-1\right)\cdot 2^{|X\setminus Z_7|}+\left(2^{|Z_6|}-1\right)\cdot 2^{|X\setminus Z_6|}\\ &+\left(2^{|Z_5|}-1\right)\cdot 2^{|X\setminus Z_5|}+\left(2^{|Z_4|}-1\right)\cdot 2^{|X\setminus Z_4|}+\left(2^{|Z_3|}-1\right)\cdot 2^{|X\setminus Z_3|}\\ &+\left(2^{|Z_2|}-1\right)\cdot 2^{|X\setminus Z_2|}+\left(2^{|Z_1|}-1\right)\cdot 2^{|X\setminus Z_1|}.\end{aligned}$$

Lemma 16. *Let* $D\in\Sigma_1\left(X,10\right)$ *and* $Z_9=\varnothing$. *If X is a finite set, then the number* $\left|I^*\left(Q_3\right)\right|$ *may be calculated by formula*

$$\begin{aligned}\left|I^*\left(Q_3\right)\right| &= \left(2^{|Z_8|}-1\right)\cdot\left(3^{|\bar{D}\setminus Z_8|}-2^{|\bar{D}\setminus Z_8|}\right)\cdot 3^{|X\setminus\bar{D}|}+\left(2^{|Z_7|}-1\right)\cdot\left(3^{|\bar{D}\setminus Z_7|}-2^{|\bar{D}\setminus Z_7|}\right)\cdot 3^{|X\setminus\bar{D}|}\\ &+\left(2^{|Z_6|}-1\right)\cdot\left(3^{|\bar{D}\setminus Z_6|}-2^{|\bar{D}\setminus Z_6|}\right)\cdot 3^{|X\setminus\bar{D}|}+\left(2^{|Z_5|}-1\right)\cdot\left(3^{|\bar{D}\setminus Z_5|}-2^{|\bar{D}\setminus Z_5|}\right)\cdot 3^{|X\setminus\bar{D}|}\\ &+\left(2^{|Z_4|}-1\right)\cdot\left(3^{|\bar{D}\setminus Z_4|}-2^{|\bar{D}\setminus Z_4|}\right)\cdot 3^{|X\setminus\bar{D}|}+\left(2^{|Z_3|}-1\right)\cdot\left(3^{|\bar{D}\setminus Z_3|}-2^{|\bar{D}\setminus Z_3|}\right)\cdot 3^{|X\setminus\bar{D}|}\\ &+\left(2^{|Z_2|}-1\right)\cdot\left(3^{|\bar{D}\setminus Z_2|}-2^{|\bar{D}\setminus Z_2|}\right)\cdot 3^{|X\setminus\bar{D}|}+\left(2^{|Z_1|}-1\right)\cdot\left(3^{|\bar{D}\setminus Z_1|}-2^{|\bar{D}\setminus Z_1|}\right)\cdot 3^{|X\setminus\bar{D}|}\\ &+\left(2^{|Z_8|}-1\right)\cdot\left(3^{|Z_3\setminus Z_8|}-2^{|Z_3\setminus Z_8|}\right)\cdot 3^{|X\setminus Z_3|}+\left(2^{|Z_7|}-1\right)\cdot\left(3^{|Z_3\setminus Z_7|}-2^{|Z_3\setminus Z_7|}\right)\cdot 3^{|X\setminus Z_3|}\\ &+\left(2^{|Z_6|}-1\right)\cdot\left(3^{|Z_3\setminus Z_6|}-2^{|Z_3\setminus Z_6|}\right)\cdot 3^{|X\setminus Z_3|}+\left(2^{|Z_6|}-1\right)\cdot\left(3^{|Z_2\setminus Z_6|}-2^{|Z_2\setminus Z_6|}\right)\cdot 3^{|X\setminus Z_2|}\\ &+\left(2^{|Z_6|}-1\right)\cdot\left(3^{|Z_1\setminus Z_6|}-2^{|Z_1\setminus Z_6|}\right)\cdot 3^{|X\setminus Z_1|}+\left(2^{|Z_5|}-1\right)\cdot\left(3^{|Z_1\setminus Z_5|}-2^{|Z_1\setminus Z_5|}\right)\cdot 3^{|X\setminus Z_1|}\\ &+\left(2^{|Z_4|}-1\right)\cdot\left(3^{|Z_1\setminus Z_4|}-2^{|Z_1\setminus Z_4|}\right)\cdot 3^{|X\setminus Z_1|}.\end{aligned}$$

Lemma 17. *Let* $D\in\Sigma_1\left(X,10\right)$ *and* $Z_9=\varnothing$. *If X is a finite set, then the number* $\left|I^*\left(Q_4\right)\right|$ *may be calculated by formula*

$$\begin{aligned}\left|I^*\left(Q_4\right)\right| &= \left(2^{|Z_4|}-1\right)\cdot\left(3^{|Z_1\setminus Z_4|}-2^{|Z_1\setminus Z_4|}\right)\cdot\left(4^{|\bar{D}\setminus Z_1|}-3^{|\bar{D}\setminus Z_1|}\right)\cdot 4^{|X\setminus\bar{D}|}\\ &+\left(2^{|Z_5|}-1\right)\cdot\left(3^{|Z_1\setminus Z_5|}-2^{|Z_1\setminus Z_5|}\right)\cdot\left(4^{|\bar{D}\setminus Z_1|}-3^{|\bar{D}\setminus Z_1|}\right)\cdot 4^{|X\setminus\bar{D}|}\\ &+\left(2^{|Z_6|}-1\right)\cdot\left(3^{|Z_1\setminus Z_6|}-2^{|Z_1\setminus Z_6|}\right)\cdot\left(4^{|\bar{D}\setminus Z_1|}-3^{|\bar{D}\setminus Z_1|}\right)\cdot 4^{|X\setminus\bar{D}|}\\ &+\left(2^{|Z_6|}-1\right)\cdot\left(3^{|Z_2\setminus Z_6|}-2^{|Z_2\setminus Z_6|}\right)\cdot\left(4^{|\bar{D}\setminus Z_2|}-3^{|\bar{D}\setminus Z_2|}\right)\cdot 4^{|X\setminus\bar{D}|}\\ &+\left(2^{|Z_6|}-1\right)\cdot\left(3^{|Z_3\setminus Z_6|}-2^{|Z_3\setminus Z_6|}\right)\cdot\left(4^{|\bar{D}\setminus Z_3|}-3^{|\bar{D}\setminus Z_3|}\right)\cdot 4^{|X\setminus\bar{D}|}\\ &+\left(2^{|Z_7|}-1\right)\cdot\left(3^{|Z_3\setminus Z_7|}-2^{|Z_3\setminus Z_7|}\right)\cdot\left(4^{|\bar{D}\setminus Z_3|}-3^{|\bar{D}\setminus Z_3|}\right)\cdot 4^{|X\setminus\bar{D}|}\\ &+\left(2^{|Z_8|}-1\right)\cdot\left(3^{|Z_3\setminus Z_8|}-2^{|Z_3\setminus Z_8|}\right)\cdot\left(4^{|\bar{D}\setminus Z_3|}-3^{|\bar{D}\setminus Z_3|}\right)\cdot 4^{|X\setminus\bar{D}|}.\end{aligned}$$

Lemma 18. *Let* $D\in\Sigma_1\left(X,10\right)$ *and* $Z_9=\varnothing$. *If X is a finite set, then the number* $\left|I^*\left(Q_5\right)\right|$ *may be calcu-*

lated by formula

$$\begin{aligned}\left|I^*\left(Q_5\right)\right| &= \left(2^{|Z_5\setminus Z_4|}-1\right)\cdot\left(2^{|Z_4\setminus Z_5|}-1\right)\cdot 4^{|X\setminus Z_1|}+\left(2^{|Z_6\setminus Z_4|}-1\right)\cdot\left(2^{|Z_4\setminus Z_6|}-1\right)\cdot 4^{|X\setminus Z_1|}\\ &+\left(2^{|Z_6\setminus Z_5|}-1\right)\cdot\left(2^{|Z_5\setminus Z_6|}-1\right)\cdot 4^{|X\setminus Z_1|}+\left(2^{|Z_7\setminus Z_6|}-1\right)\cdot\left(2^{|Z_6\setminus Z_7|}-1\right)\cdot 4^{|X\setminus Z_3|}\\ &+\left(2^{|Z_8\setminus Z_6|}-1\right)\cdot\left(2^{|Z_6\setminus Z_8|}-1\right)\cdot 4^{|X\setminus Z_3|}+\left(2^{|Z_8\setminus Z_7|}-1\right)\cdot\left(2^{|Z_7\setminus Z_8|}-1\right)\cdot 4^{|X\setminus Z_3|}\\ &+\left(2^{|Z_8\setminus Z_4|}-1\right)\cdot\left(2^{|Z_4\setminus Z_8|}-1\right)\cdot 4^{|X\setminus\bar{D}|}+\left(2^{|Z_8\setminus Z_5|}-1\right)\cdot\left(2^{|Z_5\setminus Z_8|}-1\right)\cdot 4^{|X\setminus\bar{D}|}\\ &+\left(2^{|Z_7\setminus Z_2|}-1\right)\cdot\left(2^{|Z_2\setminus Z_7|}-1\right)\cdot 4^{|X\setminus\bar{D}|}+\left(2^{|Z_7\setminus Z_4|}-1\right)\cdot\left(2^{|Z_4\setminus Z_7|}-1\right)\cdot 4^{|X\setminus\bar{D}|}\\ &+\left(2^{|Z_7\setminus Z_5|}-1\right)\cdot\left(2^{|Z_5\setminus Z_7|}-1\right)\cdot 4^{|X\setminus\bar{D}|}+\left(2^{|Z_8\setminus Z_1|}-1\right)\cdot\left(2^{|Z_1\setminus Z_8|}-1\right)\cdot 4^{|X\setminus\bar{D}|}\\ &+\left(2^{|Z_8\setminus Z_2|}-1\right)\cdot\left(2^{|Z_2\setminus Z_8|}-1\right)\cdot 4^{|X\setminus\bar{D}|}+\left(2^{|Z_4\setminus Z_2|}-1\right)\cdot\left(2^{|Z_2\setminus Z_4|}-1\right)\cdot 4^{|X\setminus\bar{D}|}\\ &+\left(2^{|Z_4\setminus Z_3|}-1\right)\cdot\left(2^{|Z_3\setminus Z_4|}-1\right)\cdot 4^{|X\setminus\bar{D}|}+\left(2^{|Z_5\setminus Z_2|}-1\right)\cdot\left(2^{|Z_2\setminus Z_5|}-1\right)\cdot 4^{|X\setminus\bar{D}|}\\ &+\left(2^{|Z_5\setminus Z_3|}-1\right)\cdot\left(2^{|Z_3\setminus Z_5|}-1\right)\cdot 4^{|X\setminus\bar{D}|}+\left(2^{|Z_7\setminus Z_1|}-1\right)\cdot\left(2^{|Z_1\setminus Z_7|}-1\right)\cdot 4^{|X\setminus\bar{D}|}\\ &+\left(2^{|Z_2\setminus Z_1|}-1\right)\cdot\left(2^{|Z_1\setminus Z_2|}-1\right)\cdot 4^{|X\setminus\bar{D}|}+\left(2^{|Z_3\setminus Z_1|}-1\right)\cdot\left(2^{|Z_1\setminus Z_3|}-1\right)\cdot 4^{|X\setminus\bar{D}|}\\ &+\left(2^{|Z_3\setminus Z_2|}-1\right)\cdot\left(2^{|Z_2\setminus Z_3|}-1\right)\cdot 4^{|X\setminus\bar{D}|}.\end{aligned}$$

Lemma 19. *Let* $D\in\Sigma_1\left(X,10\right)$ *and* $Z_9=\varnothing$. *If X is a finite set, then the number* $\left|I^*\left(Q_6\right)\right|$ *may be calculated by formula*

$$\begin{aligned}\left|I^*\left(Q_6\right)\right| &= \left(2^{|Z_5\setminus Z_4|}-1\right)\cdot\left(2^{|Z_4\setminus Z_5|}-1\right)\cdot\left(5^{|\bar{D}\setminus Z_1|}-4^{|\bar{D}\setminus Z_1|}\right)\cdot 5^{|X\setminus\bar{D}|}\\ &+\left(2^{|Z_6\setminus Z_4|}-1\right)\cdot\left(2^{|Z_4\setminus Z_6|}-1\right)\cdot\left(5^{|\bar{D}\setminus Z_1|}-4^{|\bar{D}\setminus Z_1|}\right)\cdot 5^{|X\setminus\bar{D}|}\\ &+\left(2^{|Z_6\setminus Z_5|}-1\right)\cdot\left(2^{|Z_5\setminus Z_6|}-1\right)\cdot\left(5^{|\bar{D}\setminus Z_1|}-4^{|\bar{D}\setminus Z_1|}\right)\cdot 5^{|X\setminus\bar{D}|}\\ &+\left(2^{|Z_7\setminus Z_6|}-1\right)\cdot\left(2^{|Z_6\setminus Z_7|}-1\right)\cdot\left(5^{|\bar{D}\setminus Z_3|}-4^{|\bar{D}\setminus Z_3|}\right)\cdot 5^{|X\setminus\bar{D}|}\\ &+\left(2^{|Z_8\setminus Z_6|}-1\right)\cdot\left(2^{|Z_6\setminus Z_8|}-1\right)\cdot\left(5^{|\bar{D}\setminus Z_3|}-4^{|\bar{D}\setminus Z_3|}\right)\cdot 5^{|X\setminus\bar{D}|}\\ &+\left(2^{|Z_8\setminus Z_7|}-1\right)\cdot\left(2^{|Z_7\setminus Z_8|}-1\right)\cdot\left(5^{|\bar{D}\setminus Z_3|}-4^{|\bar{D}\setminus Z_3|}\right)\cdot 5^{|X\setminus\bar{D}|}.\end{aligned}$$

Lemma 20. *Let* $D\in\Sigma_1\left(X,10\right)$ *and* $Z_9=\varnothing$. *If X is a finite set, then the number* $\left|I^*\left(Q_7\right)\right|$ *may be calculated by formula*

$$\begin{aligned}\left|I^*\left(Q_7\right)\right| &= \left(2^{|Z_6|}-1\right)\cdot 2^{|(Z_2\cap Z_1)\setminus Z_6|}\cdot\left(3^{|Z_2\setminus Z_1|}-2^{|Z_2\setminus Z_1|}\right)\cdot\left(3^{|Z_1\setminus Z_2|}-2^{|Z_1\setminus Z_2|}\right)\cdot 5^{|X\setminus\bar{D}|}\\ &+\left(2^{|Z_6|}-1\right)\cdot 2^{|(Z_3\cap Z_1)\setminus Z_6|}\cdot\left(3^{|Z_3\setminus Z_1|}-2^{|Z_3\setminus Z_1|}\right)\cdot\left(3^{|Z_1\setminus Z_3|}-2^{|Z_1\setminus Z_3|}\right)\cdot 5^{|X\setminus\bar{D}|}\\ &+\left(2^{|Z_6|}-1\right)\cdot 2^{|(Z_3\cap Z_2)\setminus Z_6|}\cdot\left(3^{|Z_3\setminus Z_2|}-2^{|Z_3\setminus Z_2|}\right)\cdot\left(3^{|Z_2\setminus Z_3|}-2^{|Z_2\setminus Z_3|}\right)\cdot 5^{|X\setminus\bar{D}|}.\end{aligned}$$

Lemma 21. *Let* $D\in\Sigma_1\left(X,7\right)$ *and* $Z_9=\varnothing$. *If X is a finite set, then the number* $\left|I^*\left(Q_8\right)\right|$ *may be calcu-*

lated by formula

$$\begin{aligned}\left|I^*\left(Q_8\right)\right| &= \left(2^{|Z_8\setminus Z_2|}-1\right)\cdot\left(2^{|Z_6\setminus Z_8|}-1\right)\cdot\left(3^{|Z_2\setminus Z_3|}-2^{|Z_2\setminus Z_3|}\right)\cdot 6^{|X\setminus \breve{D}|}\\ &+\left(2^{|Z_8\setminus Z_1|}-1\right)\cdot\left(2^{|Z_6\setminus Z_8|}-1\right)\cdot\left(3^{|Z_1\setminus Z_3|}-2^{|Z_1\setminus Z_3|}\right)\cdot 6^{|X\setminus \breve{D}|}\\ &+\left(2^{|Z_7\setminus Z_2|}-1\right)\cdot\left(2^{|Z_6\setminus Z_7|}-1\right)\cdot\left(3^{|Z_2\setminus Z_3|}-2^{|Z_2\setminus Z_3|}\right)\cdot 6^{|X\setminus \breve{D}|}\\ &+\left(2^{|Z_7\setminus Z_1|}-1\right)\cdot\left(2^{|Z_6\setminus Z_7|}-1\right)\cdot\left(3^{|Z_1\setminus Z_3|}-2^{|Z_1\setminus Z_3|}\right)\cdot 6^{|X\setminus \breve{D}|}\\ &+\left(2^{|Z_5\setminus Z_3|}-1\right)\cdot\left(2^{|Z_6\setminus Z_5|}-1\right)\cdot\left(3^{|Z_3\setminus Z_1|}-2^{|Z_3\setminus Z_1|}\right)\cdot 6^{|X\setminus \breve{D}|}\\ &+\left(2^{|Z_5\setminus Z_2|}-1\right)\cdot\left(2^{|Z_6\setminus Z_5|}-1\right)\cdot\left(3^{|Z_2\setminus Z_1|}-2^{|Z_2\setminus Z_1|}\right)\cdot 6^{|X\setminus \breve{D}|}\\ &+\left(2^{|Z_4\setminus Z_3|}-1\right)\cdot\left(2^{|Z_6\setminus Z_4|}-1\right)\cdot\left(3^{|Z_3\setminus Z_1|}-2^{|Z_3\setminus Z_1|}\right)\cdot 6^{|X\setminus \breve{D}|}\\ &+\left(2^{|Z_4\setminus Z_2|}-1\right)\cdot\left(2^{|Z_6\setminus Z_4|}-1\right)\cdot\left(3^{|Z_2\setminus Z_1|}-2^{|Z_2\setminus Z_1|}\right)\cdot 6^{|X\setminus \breve{D}|}.\end{aligned}$$

Theorem 14. *Let* $D\in\Sigma_1\left(X,10\right)$, $Z_9=\varnothing$. *If X is a finite set and* I_D *is a set of all idempotent elements of the semigroup* $B_X\left(D\right)$, *then* $\left|I_D\right|=\sum_{i=1}^{8}\left|I^*\left(Q_i\right)\right|$.

Example 15. *Let* $X=\{1,2,3,4,5,6,7\}$,

$$P_1=\{1\},\ P_2=\{2\},\ P_3=\{3\},\ P_4=\{4\},\ P_5=\{5\},\ P_7=\{6\},\ P_8=\{7\},\ P_0=P_6=P_9=\varnothing.$$

Then $\breve{D}=\{1,2,3,4,5,6,7\}$, $Z_1=\{2,3,4,5,6,7\}$, $Z_2=\{1,3,4,5,6,7\}$, $Z_3=\{1,2,4,5,6,7\}$, $Z_4=\{2,3,5,6,7\}$, $Z_5=\{2,3,4,6,7\}$, $Z_6=\{4,5,6,7\}$, $Z_7=\{1,2,4,5,7\}$, $Z_8=\{1,2,4,5,6\}$ and $Z_9=\varnothing$.

$$\begin{aligned}D=\big\{&\{1,2,3,4,5,6,7\},\{2,3,4,5,6,7\},\{1,3,4,5,6,7\},\{1,2,4,5,6,7\},\{2,3,5,6,7\},\\ &\{2,3,4,6,7\},\{4,5,6,7\},\{1,2,4,5,7\},\{1,2,4,5,6\},\varnothing\big\}\end{aligned}$$

We have $Z_9=\varnothing$. Where $\left|I^*\left(Q_1\right)\right|=1$, $\left|I^*\left(Q_2\right)\right|=1121$, $\left|I^*\left(Q_3\right)\right|=2141$, $\left|I^*\left(Q_4\right)\right|=349$, $\left|I^*\left(Q_5\right)\right|=119$, $\left|I^*\left(Q_6\right)\right|=14$, $\left|I^*\left(Q_7\right)\right|=90$, $\left|I\left(Q_8\right)\right|=8$, $\left|I_D\right|=3843$.

It was seen in ([4], Theorem 2) that if α and β are regular elements of $B_X\left(D\right)$ then $V\left(D,\alpha\circ\beta\right)$ is an *XI*-subsemilattice of *D*. Therefore $\alpha\circ\beta$ is regular elements of $B_X\left(D\right)$. That is the set of all regular elements of $B_X\left(D\right)$ is a subsemigroup of $B_X\left(D\right)$.

References

[1] Diasamidze, Ya. and Makharadze, Sh. (2013) Complete Semigroups of Binary Relations. Monograph. Kriter, Turkey, 620 p.

[2] Diasamidze, Ya. and Makharadze, Sh. (2010) Complete Semigroups of Binary Relations. Monograph. M., Sputnik+, 657 p. (In Russian)

[3] Diasamidze, Ya., Makharadze, Sh. and Diasamidze, Il. (2008) Idempotents and Regular Elements of Complete Semigroups of Binary Relations. *Journal of Mathematical Sciences, Plenum Publ. Cor., New York*, **153**, 481-499.

[4] Diasamidze, Ya. and Bakuridze, Al. (to appear) On Some Properties of Regular Elements of Complete Semigroups Defined by Semilattices of the Class $\Sigma_4\left(X,8\right)$.

Applied Mathematics, 2015, 6, 295-303
Published Online February 2015 in SciRes. http://www.scirp.org/journal/am
http://dx.doi.org/10.4236/am.2015.62027

Thermal Radiation Effects on MHD Boundary Layer Flow over an Exponentially Stretching Surface

Santosh Chaudhary[1], Sawai Singh[2], Susheela Chaudhary[2]

[1]Department of Mathematics, Malaviya National Institute of Technology, Jaipur, Rajasthan, India
[2]Department of Mathematics, S. K. Govt. (P.G.) College, Sikar, Rajasthan, India
Email: d11.santosh@yahoo.com, dhayal.sawaisingh@yahoo.com, susheelamaths@gmail.com

Received 11 January 2015; accepted 29 January 2015; published 5 February 2015

Abstract

The steady two-dimensional laminar boundary layer flow and heat transfer of a viscous incompressible electrically conducting fluid over an exponentially stretching surface in the presence of a uniform magnetic field with thermal radiation are investigated. The governing boundary layer equations are transformed to ordinary differential equations by taking suitable similarity transformation and solved numerically by shooting method. The effects of various parameters such as magnetic parameter, radiation parameter, Prandtl number and Eckert number on local skin-friction coefficient, local Nusselt number, velocity and temperature distributions are computed and represented graphically.

Keywords

Thermal Radiation, MHD, Boundary Layer Flow, Exponentially Stretching Surface

1. Introduction

The study of boundary layer flow and its applications are vital for advancement in the field of technology and engineering. The computation and computer coordinated applications of flow over a stretching surface are playing a pivotal role in different realm of industrial products of aerodynamics, polymers and metallurgy, such as liquid films in condensation process, artificial fibers, glass fiber, metal spinning, the cooling process of metallic plate in a cooling bath and glass, wire drawing, paper production, aerodynamic extrusion of plastic sheets, crystal growing, cable coating and many others, to get end product of desired quality and parameters. Sakiadis [1] probably was the first who investigated boundary layer flow on a moving continuous solid surface. Crane [2]

How to cite this paper: Chaudhary, S., Singh, S. and Chaudhary, S. (2015) Thermal Radiation Effects on MHD Boundary Layer Flow over an Exponentially Stretching Surface. *Applied Mathematics*, **6**, 295-303.
http://dx.doi.org/10.4236/am.2015.62027

extended this concept to a linearly stretching plate whose velocity is linearly proportional to the distance from the slit and produced an exact analytical solution for the steady two-dimensional flow problems. Gupta and Gupta [3], Carragher and Crane [4], Grubka and Bobba [5], Chen and Char [6], Ali [7], Andersson [8], Ariel *et al.* [9], Ishak *et al.* [10], Jat and Chaudhary [11] [12], Wang [13] and Nadeem *et al.* [14] analyzed the effects of heat transfer on a stretching surface taking into account different aspects of the problem.

Boundary layer flow and heat transfer over an exponentially stretching surface have wider applications in technology such as in case of annealing and thinning of copper wires. Magyari and Keller [15] obtained analytical and numerical solutions for boundary layer flow over an exponentially stretching continuous surface with an exponential temperature distribution. Many other problems on exponentially stretching surface under different physical situations were observed by Elbashbeshy [16], Partha *et al.* [17], Khan [18], Sanjayanand and Khan [19] and El-Aziz [20].

At higher operating temperature, the effects of thermal radiation and heat transfer play a pivotal role on the fluid flow problem of boundary layer. The application of controlled heat transfer in polymer industries is very important to get final product of desired parameters. The modern system of electric power generation, plasma, space vehicles, astrophysical flows and cooling of nuclear reactors are governed by applications of thermal radiation and heat transfer of fluid flow. Elbashbeshy [21] determined the effect of radiation on flow of an incompressible fluid along a heated horizontal stretching sheet. Sajid and Hayat [22] extended this concept by investigating the influence of thermal radiation on the boundary layer flow over an exponentially stretching sheet and solved the problem analytically. Recently, Bidin and Nazar [23], Jat and Chaudhary [24], Nadeem *et al.* [25] and Mukhopadhyay and Gorla [26] investigated various aspects of such problem either analytically or numerically.

With reference to above significant studies and in view of importance of MHD applications in various field of technologies, the objective of present paper is to investigate the effect of thermal radiation on an electrically conducting two-dimensional boundary layer incompressible viscous fluid flow over an exponentially stretching surface in the presence of uniform magnetic field by using Rosseland approximation. Numerical results of the momentum and energy equations are computed by using shooting method. The promising results of velocity and temperature distributions, local skin-friction coefficient and surface heat transfer are discussed for various physical parameters and simplified their effects for different conditions.

2. Problem Formulation

Consider the steady two-dimensional laminar boundary layer flow $(u,v,0)$ of a viscous incompressible electrically conducting radiative fluid over continuous exponentially stretching surface in the presence of an externally applied normal magnetic field of constant strength $(0,B_0,0)$. The *x*-axis is taken along the stretching surface in the direction of motion and *y*-axis is taken perpendicular to it. The stretching surface has a uniform temperature $T_w(x)=T_\infty+T_0\mathrm{e}^{x/2L}$ and a linear velocity $U_w(x)=U_0\mathrm{e}^{x/L}$ while temperature of flow external to the boundary layer is T_∞. The system of governing boundary layer equations (which model **Figure 1**) are given by:

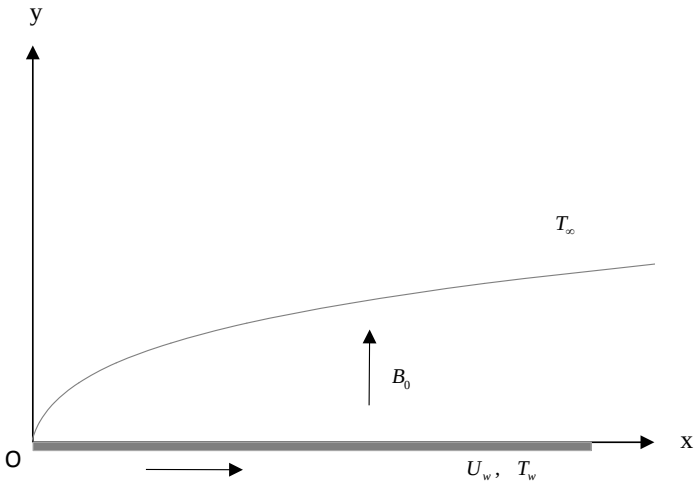

Figure 1. Sketch of the physical problem.

$$\frac{\partial u}{\partial x}+\frac{\partial v}{\partial y}=0 \tag{1}$$

$$u\frac{\partial u}{\partial x}+v\frac{\partial u}{\partial y}=\upsilon\frac{\partial^2 u}{\partial y^2}-\frac{\sigma B_0^2 u}{\rho} \tag{2}$$

$$\rho C_p\left(u\frac{\partial T}{\partial x}+v\frac{\partial T}{\partial y}\right)=\kappa\left(\frac{\partial^2 T}{\partial y^2}\right)+\mu\left(\frac{\partial u}{\partial y}\right)^2-\frac{\partial q_r}{\partial y} \tag{3}$$

where T_0 is the reference temperature, L is the reference length, U_0 is the reference velocity, $\upsilon=\frac{\mu}{\rho}$ is the coefficient of kinematic viscosity, μ is the coefficient of viscosity, ρ is the fluid density, σ is the electrical conductivity, C_p is the specific heat at constant pressure, T is the temperature, κ is the thermal conductivity and q_r is the radiative heat flux. The other symbols have their usual meanings.

The boundary conditions are:

$$\begin{aligned} &y=0: u=U_w(x),\ v=0;\ T=T_w(x)\\ &y\to\infty: u\to 0;\ T\to T_\infty. \end{aligned} \tag{4}$$

By using Rosseland approximation of the radiation for an optically thick boundary layer, the radiative heat flux q_r is expressed (Bidin and Nazar [23]) as:

$$q_r=-\frac{4\sigma^*}{3\kappa^*}\frac{\partial T^4}{\partial y} \tag{5}$$

where σ^* is the Stefan-Boltzmann constant and κ^* is the mean absorption coefficient. The above radiative heat flux q_r is effective at a point away from boundary layer surface in an intensive absorption flow. Considering that the temperature variation within the flow is very small, the T^4 may be expressed as a linear function of temperature T. Expanding T^4 by Taylor's series about temperature T_∞ and neglecting higher-order terms, hence

$$T^4\cong 4T_\infty^3 T-3T_\infty^4 \tag{6}$$

Using Equation (5) and (6), equation (3) is reduced to:

$$\rho C_p\left(u\frac{\partial T}{\partial x}+v\frac{\partial T}{\partial y}\right)=\left(\kappa+\frac{16\sigma^* T_\infty^3}{3\kappa^*}\right)\frac{\partial^2 T}{\partial y^2}+\mu\left(\frac{\partial u}{\partial y}\right)^2 \tag{7}$$

3. Similarity Analysis

The continuity Equation (1) is identically satisfied if we defined stream function $\psi(x,y)$ as:

$$u=\frac{\partial\psi}{\partial y},\quad v=-\frac{\partial\psi}{\partial x} \tag{8}$$

For the solution of momentum and energy Equations (2) and (7), introducing the following dimensionless variables:

$$\psi(x,y)=\sqrt{2\upsilon LU_w}\,f(\eta) \tag{9}$$

$$\eta=\sqrt{\frac{U_w}{2\upsilon L}}y \tag{10}$$

$$T=T_\infty+T_0 e^{x/2L}\theta(\eta) \tag{11}$$

Using Equations (8) to (11), Equations (2) and (7) are reduced to:

$$f'''+ff''-2f'^2-Mf'=0 \tag{12}$$

$$\left(1+\frac{4}{3}K\right)\theta'' + \Pr f\theta' - \Pr f'\theta + \Pr \mathrm{E}\mathrm{c} f''^2 = 0 \tag{13}$$

The boundary conditions are:

$$\begin{aligned} &\eta = 0: f = 0, \ f' = 1; \quad \theta = 1 \\ &\eta = \infty: f' = 0; \quad \theta = 0 \end{aligned} \tag{14}$$

where prime (′) denote differentiation with respect to η, $M = \frac{2\sigma B_0^2 L}{\rho U_w}$ is the Magnetic parameter, $K = \frac{4\sigma^* T_\infty^3}{\kappa^* \kappa}$ is the Radiation parameter, $\Pr = \frac{\mu C_p}{\kappa}$ is the Prandtl number and $\mathrm{E}\mathrm{c} = \frac{U_w^2}{C_p T_0 \mathrm{e}^{x/2L}}$ is the Eckert number.

4. Numerical Solution of the Problem

For numerical solution of the Equations (12) and (13), we use the following power series in terms of small magnetic parameter *M* as:

$$f(\eta) = \sum_{i=0}^{\infty} M^i f_i(\eta) \tag{15}$$

$$\theta(\eta) = \sum_{j=0}^{\infty} M^j \theta_j(\eta) \tag{16}$$

Substituting the values of $f(\eta)$ and $\theta(\eta)$ from Equations (15) and (16) and its derivatives in Equations (12) and (13), and then equating the coefficients of like powers of *M*, we get the following set of equations:

$$f_0''' + f_0 f_0'' - 2 f_0'^2 = 0 \tag{17}$$

$$\left(1+\frac{4}{3}K\right)\theta_0'' + \Pr f_0\theta_0' - \Pr f_0'\theta_0 = -\Pr \mathrm{E}\mathrm{c} f_0''^2 \tag{18}$$

$$f_1''' + f_0 f_1'' - 4 f_0' f_1' + f_0'' f_1 = f_0' \tag{19}$$

$$\left(1+\frac{4}{3}K\right)\theta_1'' + \Pr f_0\theta_1' - \Pr f_0'\theta_1 = -\Pr f_1\theta_0' + \Pr f_1'\theta_0 - 2\Pr \mathrm{E}\mathrm{c} f_0'' f_1'' \tag{20}$$

$$f_2''' + f_0 f_2'' - 4 f_0' f_2' + f_0'' f_2 = -f_1 f_1'' + 2 f_1'^2 + f_1' \tag{21}$$

$$\left(1+\frac{4}{3}K\right)\theta_2'' + \Pr f_0\theta_2' - \Pr f_0'\theta_2 = -\Pr f_1\theta_1' + \Pr f_1'\theta_1 - \Pr f_2\theta_0' + \Pr f_2'\theta_0 - 2\Pr \mathrm{E}\mathrm{c} f_0'' f_2'' - \Pr \mathrm{E}\mathrm{c} f_1''^2 \tag{22}$$

The corresponding boundary conditions are:

$$\begin{aligned} &\eta = 0: f_i = 0, \ f_0' = 1, \ f_j' = 0; \ \theta_0 = 1, \ \theta_j = 0 \\ &\eta = \infty: f_i' = 0; \ \theta_i = 0; \ i \geq 0, \ j > 0 \end{aligned} \tag{23}$$

The Equation (17) is same as that obtained by Bidin and Nazar [23] for non-magnetic case and the remaining equations from (18) to (22) are ordinary linear differential equations and have been solved numerically by Shooting method with boundary condition (23). The velocity and temperature distributions for various values of parameters are shown in **Figures 2-6** respectively.

5. Local Skin Friction Coefficient and Local Nusselt Number

The important physical quantities are the local skin-friction coefficient C_f and the local Nusselt number Nu, which are defined as:

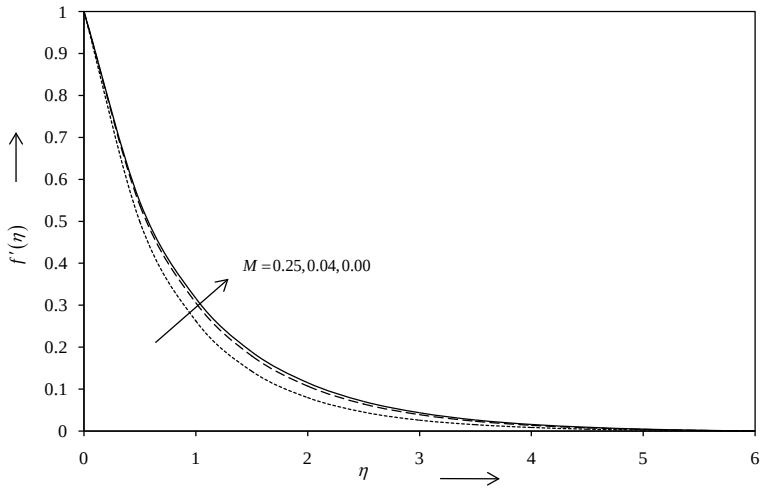

Figure 2. Velocity distribution against η for various values of M.

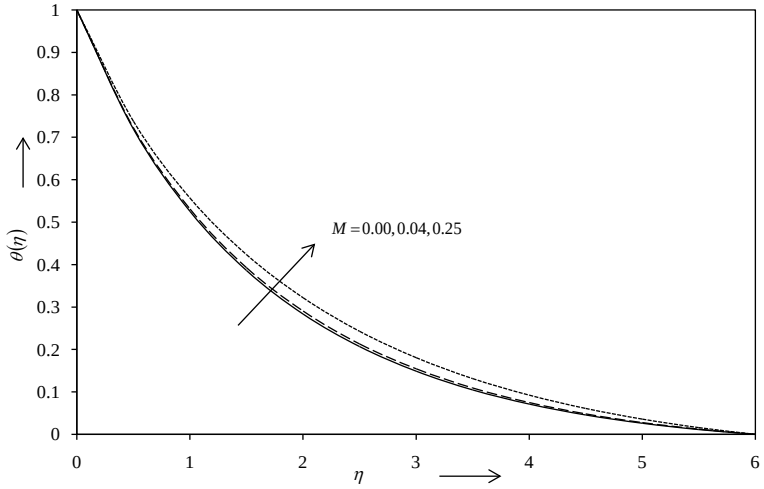

Figure 3. Temperature distribution against η for various values of M with K = 0.5, Pr = 1 and Ec = 0.0.

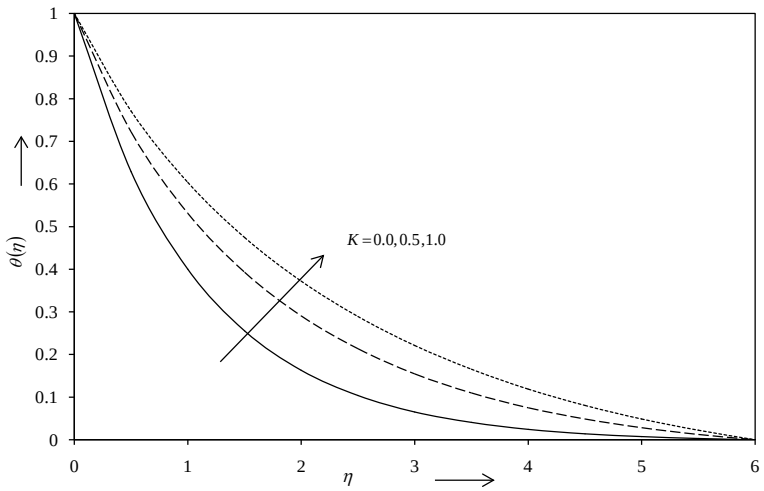

Figure 4. Temperature distribution against η for various values of K with M = 0.04, Pr = 1 and Ec = 0.0.

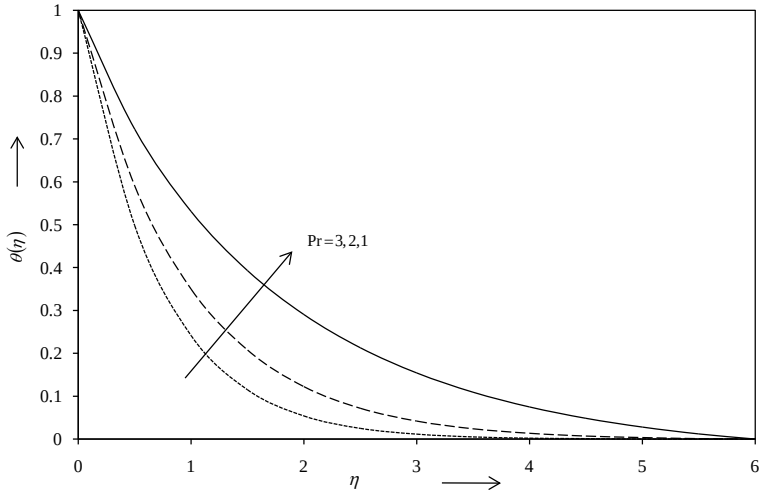

Figure 5. Temperature distribution against η for various values of Pr with M = 0.04, K = 0.5 and Ec = 0.0.

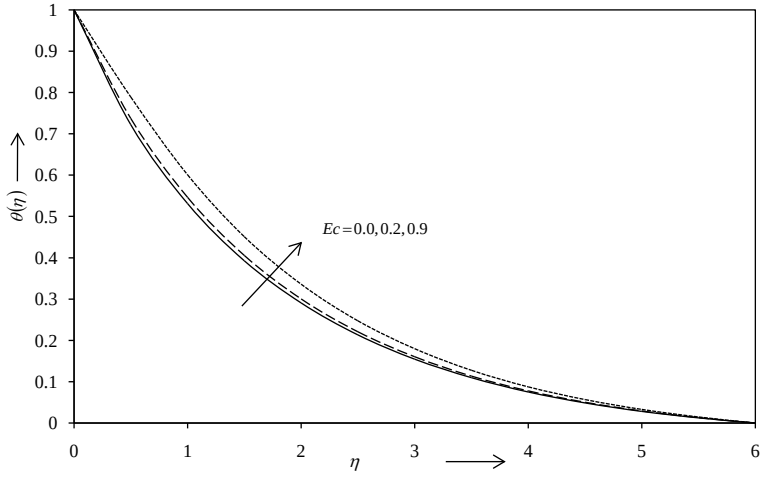

Figure 6. Temperature distribution against η for various values of Ec with M = 0.04, K = 0.5 and Pr = 1.

$$C_f = \frac{\tau_w}{\rho U_w^2/2} = \frac{\mu\left(\frac{\partial u}{\partial y}\right)_{y=0}}{\rho U_w^2/2} \tag{24}$$

and

$$\mathrm{Nu} = -\frac{L\left(\frac{\partial T}{\partial y}\right)_{y=0}}{T_w - T_\infty} \tag{25}$$

In the present case which can be expressed in dimensionless form as:

$$C_f = \sqrt{\frac{2}{\mathrm{Re}}} f''(0) = \sqrt{\frac{2}{\mathrm{Re}}}\left[\sum_{i=0}^{\infty} M^i f_i''(0)\right] \tag{26}$$

and

$$\mathrm{Nu} = -\sqrt{\frac{\mathrm{Re}}{2}}\theta'(0) = -\sqrt{\frac{\mathrm{Re}}{L}}\left[\sum_{j=0}^{\infty} M^{j}\theta_j'(0)\right] \tag{27}$$

where $\tau_w = \mu\left(\frac{\partial u}{\partial y}\right)_{y=0}$ is the surface shear stress and $\mathrm{Re} = \frac{U_w L}{\upsilon}$ is the local Reynolds number. The numerical values of $f''(0)$ and $\theta'(0)$ are proportional to the local skin-friction coefficient C_f and local Nusselt number Nu at the surface respectively and these are presented by **Table 1** for various values of the physical parameters.

6. Results and Discussion

Figure 2 shows variation of velocity distribution $f'(\eta)$ against η for various values of the magnetic parameter *M*. This figure shows that the fluid velocity decreases with increasing value of the magnetic parameter *M*, due to the effect of Lorentz force produced by transverse magnetic field causes deceleration of fluid velocity.

Figures 3-6 show the temperature distributions $\theta(\eta)$ against η for various values of the magnetic parameter *M*, the radiation parameter *K*, the Prandtl number Pr and the Eckert number Ec. It is observed from these figures that the temperature distribution $\theta(\eta)$ increases with increasing value of any parameter, such as the magnetic parameter *M*, the radiation parameter *K* and the Eckert number Ec. However, it decreases with increasing value of the Prandtl number Pr. An increasing Prandtl number Pr, causes decrease in thermal boundary layer of fluid flow.

The values of the local skin-friction coefficient C_f and the local Nusselt number Nu in terms of $f''(0)$ and $\theta'(0)$ respectively, are presented in the **Table 1**, for various values of the magnetic parameter *M*, the radiation parameter *K* and the Prandtl number Pr, with the Eckert number Ec = 0.0. It is significant that the local skin-friction coefficient C_f and the local Nusselt number Nu decreases with increasing value of the magnetic parameter *M*. Moreover, the local Nusselt number Nu decreases with increasing value of the radiation parameter *K*, whereas the reverse phenomena occurs for the Prandtl number Pr. Further, **Table 1** shows that all values of $f''(0)$ and $\theta'(0)$ are negative, corresponding to various values of physical parameters. A negative sign of $f''(0)$ implies the exertion of drag force on the surface and a negative sign of $\theta'(0)$ implies heat transfer from the surface.

Table 1. Variation of surface shear stress $f''(0)$ with *M* and surface heat transfer rate $\theta'(0)$ with *M*, *K*, Pr and Ec = 0.0.

$f''(0)$			
$M = 0.00$		$M = 0.04$	$M = 0.25$
−1.2821		−1.3135	−1.4642
$\theta'(0)$			
K	Pr	Ec = 0.0	
		M = 0.00	*M* = 0.04	*M* = 0.25
0.0	1	−0.9559	−0.9475	−0.9080
	2	−1.4712	−1.4627	−1.4217
	3	−1.8689	−1.8605	−1.8202
0.5	1	−0.6860	−0.6786	−0.6455
	2	−1.0737	−1.0652	−1.0246
	3	−1.3805	−1.3720	−1.3309
1.0	1	−0.5528	−0.5466	−0.5192
	2	−0.8653	−0.8571	−0.8190
	3	−1.1215	−1.1129	−1.0721

7. Conclusion

The characteristic relationships among various parameters influencing viscous incompressible electrically conducting fluid over an exponentially stretching surface in the presence of a uniform magnetic field with thermal radiation have been analyzed and illustrated graphically. The similarity equations are determined and solved numerically by shooting method. It is observed that thickness of the velocity boundary layer, the local skin-friction coefficient and the local Nusselt number decreases with increasing value of the magnetic parameter. However, thickness of the thermal boundary layer increases with increasing value of the magnetic parameter. Further, it is observed that thickness of thermal boundary layer increases with increasing value of the radiation parameter or the Eckert number, whereas, reverse phenomenon observed for the Prandtl number. Moreover, the local Nusselt number decreases with increasing value of the radiation parameter, while reverse behaviour observed for the Prandtl number.

References

[1] Sakiadis, B.C. (1961) Boundary-Layer Behavior on Continuous Solid Surfaces: I. Boundary-Layer Equations for Two-Dimensional and Axisymmetric Flow. *American Institute of Chemical Engineers Journal*, **7**, 26-28. http://dx.doi.org/10.1002/aic.690070108

[2] Crane, L.J. (1970) Flow past a Stretching Plate. *Zeitschrift für Angewandte Mathematik und Physik*, **21**, 645-647. http://dx.doi.org/10.1007/BF01587695

[3] Gupta, P.S. and Gupta, A.S. (1977) Heat and Mass Transfer on a Stretching Sheet with Suction or Blowing. *The Canadian Journal of Chemical Engineering*, **55**, 744-746. http://dx.doi.org/10.1002/cjce.5450550619

[4] Carragher, P. and Crane, L.J. (1982) Heat Transfer on a Continuous Stretching Sheet. *Zeitschrift für AngewandteMathematik und Mechanik*, **62**, 564-565. http://dx.doi.org/10.1002/zamm.19820621009

[5] Grubka, L.J. and Bobba, K.M. (1985) Heat Transfer Characteristics of a Continuous, Stretching Surface with Variable Temperature. *Journal of Heat Transfer*, **107**, 248-250. http://dx.doi.org/10.1115/1.3247387

[6] Chen, C.K. and Char, M.I. (1988) Heat Transfer of a Continuous, Stretching Surface with Suction or Blowing. *Journal of Mathematical Analysis and Applications*, **135**, 568-580. http://dx.doi.org/10.1016/0022-247X(88)90172-2

[7] Ali, M.E. (1994) Heat Transfer Characteristics of a Continuous Stretching Surface. *Heat and Mass Transfer*, **29**, 227-234.

[8] Andersson, H.I. (2002) Slip Flow past a Stretching Surface. *Acta Mechanica*, **158**, 121-125. http://dx.doi.org/10.1007/BF01463174

[9] Ariel, P.D., Hayat, T. and Asghar, S. (2006) The Flow of an Elastico-Viscous Fluid past a Stretching Sheet with Partial Slip. *Acta Mechanica*, **187**, 29-35. http://dx.doi.org/10.1007/s00707-006-0370-3

[10] Ishak, A., Nazar, R. and Pop, I. (2006) Mixed Convection Boundary Layers in the Stagnation-Point Flow toward a Stretching Vertical Sheet. *Meccanica*, **41**, 509-518. http://dx.doi.org/10.1007/s11012-006-0009-4

[11] Jat, R.N. and Chaudhary, S. (2008) Magnetohydrodynamic Boundary Layer Flow Near the Stagnation Point of a Stretching Sheet. *Il Nuovo Cimento della Società Italiana di Fisica B*: *General Physics*, **123**, 555-566.

[12] Jat, R.N. and Chaudhary, S. (2009) MHD Flow and Heat Transfer over a Stretching Sheet. *Applied Mathematical Sciences*, **3**, 1285-1294.

[13] Wang, C.Y. (2009) Analysis of Viscous Flow Due to a Stretching Sheet with Surface Slip and Suction. *Nonlinear Analysis*: *Real World Applications*, **10**, 375-380. http://dx.doi.org/10.1016/j.nonrwa.2007.09.013

[14] Nadeem, S., Hussain, A. and Khan, M. (2010) HAM Solutions for Boundary Layer Flow in the Region of the Stagnation Point towards a Stretching Sheet. *Communications in Nonlinear Science and Numerical Simulation*, **15**, 475-481. http://dx.doi.org/10.1016/j.cnsns.2009.04.037

[15] Magyari, E. and Keller, B. (1999) Heat and Mass Transfer in the Boundary Layers on an Exponentially Stretching Continuous Surface. *Journal of Physics D*: *Applied Physics*, **32**, 577-585. http://dx.doi.org/10.1088/0022-3727/32/5/012

[16] Elbashbeshy, E.M.A. (2001) Heat Transfer over an Exponentially Stretching Continuous Surface with Suction. *Archives of Mechanics*, **53**, 643-651.

[17] Partha, M.K., Murthy, P.V.S.N. and Rajasekhar, G.P. (2005) Effect of Viscous Dissipation on the Mixed Convection Heat Transfer from an Exponentially Stretching Surface. *Heat and Mass Transfer*, **41**, 360-366. http://dx.doi.org/10.1007/s00231-004-0552-2

[18] Khan, S.K. (2006) Boundary Layer Viscoelastic Fluid Flow over an Exponentially Stretching Sheet. *International Journal of Applied Mechanics and Engineering*, **11**, 321-335.

[19] Sanjayanand, E. and Khan, S.K. (2006) On Heat and Mass Transfer in a Viscoelastic Boundary Layer Flow over an Exponentially Stretching Sheet. *International Journal of Thermal Sciences*, **45**, 819-828. http://dx.doi.org/10.1016/j.ijthermalsci.2005.11.002

[20] El-Aziz, M.A. (2009) Viscous Dissipation Effect on Mixed Convection Flow of a Micropolar Fluid over an Exponentially Stretching Sheet. *Canadian Journal of Physics*, **87**, 359-368. http://dx.doi.org/10.1139/P09-047

[21] Elbashbeshy, E.M.A. (2000) Radiation Effect on Heat Transfer over a Stretching Surface. *Canadian Journal of Physics*, **78**, 1107-1112. http://dx.doi.org/10.1139/p00-085

[22] Sajid, M. and Hayat, T. (2008) Influence of Thermal Radiation on the Boundary Layer Flow Due to an Exponentially Stretching Sheet. *International Communications in Heat and Mass Transfer*, **35**, 347-356. http://dx.doi.org/10.1016/j.icheatmasstransfer.2007.08.006

[23] Bidin, B. and Nazar, R. (2009) Numerical Solution of the Boundary Layer Flow over an Exponentially Stretching Sheet with Thermal Radiation. *European Journal of Scientific Research*, **33**, 710-717.

[24] Jat, R.N. and Chaudhary, S. (2010) Radiation Effects on the MHD Flow Near the Stagnation Point of a Stretching Sheet. *Zeitschrift für angewandte Mathematik und Physik*, **61**, 1151-1154. http://dx.doi.org/10.1007/s00033-010-0072-5

[25] Nadeem, S., Zaheer, S. and Fang, T. (2011) Effects of Thermal Radiation on the Boundary Layer Flow of a Jeffrey Fluid over an Exponentially Stretching Surface. *Numerical Algorithms*, **57**, 187-205. http://dx.doi.org/10.1007/s11075-010-9423-8

[26] Mukhopadhyay, S. and Gorla, R.S.R. (2012) Effects of Partial Slip on Boundary Layer Flow past a Permeable Exponential Stretching Sheet in Presence of Thermal Radiation. *Heat and Mass Transfer*, **48**, 1773-1781. http://dx.doi.org/10.1007/s00231-012-1024-8

Applied Mathematics, 2015, 6, 304-311
Published Online February 2015 in SciRes. http://www.scirp.org/journal/am
http://dx.doi.org/10.4236/am.2015.62028

Scientific Research Publishing

Schur Complement Computations in Intel® Math Kernel Library PARDISO

Alexander Kalinkin, Anton Anders, Roman Anders

Intel Corporation, Software and Services Group (SSG), Novosibirsk, Russia
Email: alexander.a.kalinkin@intel.com, anton.anders@intel.com, roman.anders@intel.com

Received 11 January 2015; accepted 29 January 2015; published 5 February 2015

Abstract

This paper describes a method of calculating the Schur complement of a sparse positive definite matrix *A*. The main idea of this approach is to represent matrix *A* in the form of an elimination tree using a reordering algorithm like METIS and putting columns/rows for which the Schur complement is needed into the top node of the elimination tree. Any problem with a degenerate part of the initial matrix can be resolved with the help of iterative refinement. The proposed approach is close to the "multifrontal" one which was implemented by Ian Duff and others in 1980s. Schur complement computations described in this paper are available in Intel® Math Kernel Library (Intel® MKL). In this paper we present the algorithm for Schur complement computations, experiments that demonstrate a negligible increase in the number of elements in the factored matrix, and comparison with existing alternatives.

Keywords

Multifrontal Method, Direct Method, Sparse Linear System, Schur Complement, HPC, Intel® MKL

1. Introduction

According to F. Zhang [1], the term "Schur complement" was used first by E. Haynsworth [2]. Haynsworth chose this term because of the lemma (Schur determinant lemma) in the paper [3] that was edited by Schur himself. In spite of matrix $A - BD^{-1}C$ being used in this lemma as a secondary term, later this matrix came to play an important role in mathematical algorithms as the Schur complement. It is denoted as $\left(A\middle|D\right) = A_{loc} - BD^{-1}C$. For example, in mathematical statistics, the Schur complement matrix is important in computation of the probability density function of multivariate normal distribution, and in computational mechanics the Schur complement matrix correlates to media stiffness.

Partial solving of systems of linear equations plays an important role in linear algebra for implementation of

How to cite this paper: Kalinkin, A., Anders, A. and Anders, R. (2015) Schur Complement Computations in Intel® Math Kernel Library PARDISO. *Applied Mathematics*, **6**, 304-311. http://dx.doi.org/10.4236/am.2015.62028

efficient preconditioners based on domain decomposition algorithms. Partial solutions usually involve sparse matrices. For this reason Schur complement computations and partial solving have been implemented in Intel® Math Kernel Library (Intel® MKL) [4]. This paper covers the ideas behind the implementation.

There are a number of papers that focused on efficient implementation of the Schur complement. As example, Aleksandrov and Samuel [5] in their paper proposed algorithm to calcluate the Schur complement for Sparse system. Yamazaki and Li published an idea [6] of how to implement Schur complement efficiently on cluster. And we need to mention MUMPS solver [7] that integrated the Schur complement computation a few years ago.

Intel® MKL PARDISO [4] can be considered as one of the multifrontal methods that have been proposed by Duff [8] and further expanded by Liu [9]. This method is divided into three stages. First, the initial matrix undergoes a reordering procedure like the one developed by Karypis [10] [11] in order to represent it in the form of a dependency tree. Then symbolic factorization takes place, where the total number of nonzero elements is computed in LDU decomposition. And finally, factorization of the permuted matrix in the LDU form is performed like the factorization proposed in Amestoy [12]-[16]. In the last stage, both forward and backward substitutions are implemented to compute a solution for the two triangular systems.

The proposed implementation of the Schur complement continues the work of the authors in the area of multifrontal direct sparse solvers. In Kalinkin [17], the basic algorithm was implemented for symmetric, positive definite matrices. In the presentations [18] and [19], the proposed algorithm was significantly improved by balancing the dependency tree. In [20], the algorithm was expanded to non-positive definite matrices and non-symmetric matrices. In this paper, we propose to move all matrix elements that correlate to Schur complement to the top of the dependency tree in order to improve parallelization of computations.

Let A be a symmetric positive definite sparse matrix (the symmetry and positive definiteness of the matrix is set in order to simplify the algorithm description avoiding the case of degenerate matrix minors):

$$A = \begin{pmatrix} A_{loc} & B^{\mathrm{T}} \\ B & C \end{pmatrix}, \tag{1}$$

where A_{loc} and C are square sparse positive definite matrices, and B is a sparse rectangular matrix. Then we can make the following decomposition, which is similar to a Cholesky decomposition of matrix A:

$$A = \begin{pmatrix} L_{11} & 0 \\ L_{12} & I \end{pmatrix} * \begin{pmatrix} I & 0 \\ 0 & S \end{pmatrix} * \begin{pmatrix} L_{11}^{\mathrm{T}} & L_{12}^{\mathrm{T}} \\ 0 & I \end{pmatrix}, \tag{2}$$

where

$$A_{loc} = L_{11}L_{11}^{\mathrm{T}}; \quad B = L_{12}L_{11}^{\mathrm{T}}; \quad S = C - BA_{loc}^{-1}B^{\mathrm{T}}.$$

The matrix $S = \left(A \middle| A_{loc}\right)$ is the Schur complement. The general approach to computing the Schur complement based on this formula and mathematical kernels can be expressed in the form of pseudocode:

Algorithm 1. Simple Schur complement computational algorithm.

1) Calculate decomposition of $A_{loc} = L_{11}L_{11}^{\mathrm{T}}$ with the factorization step of the direct solver;

2) Calculate $B_{\text{temp}} = A_{loc}^{-1}B^{\mathrm{T}}$ with the solving step applied to multiple right-hand sides;

3) Calculate $C_{\text{temp}} = BB_{\text{temp}}$ as sparse-dense matrix-matrix multiplication;

4) Calculate $S = C - C_{\text{temp}}$ as a difference.

This algorithm has several significant disadvantages that can form barriers for its implementation for large sparse systems. The main disadvantage is in the step 2 of **Algorithm 1** involving the conversion of sparse matrix B^{T} into a dense matrix, which requires allocating a lot of memory for storing temporary data. Also, if we consider B^{T} as a dense matrix a large number of zero elements are processed in multiplication $A_{loc}^{-1}\ B^{\mathrm{T}}$, which would make this step one of the most computational intensive parts of the algorithm and would significantly increase the overall computational time. To prevent this, we propose the following algorithm based on the multifrontal approach which calculates the Schur complement matrix first, and then the factorization of the matrix A without significant memory requirements for the computations to proceed.

2. Schur Complement Computational Algorithm

As in the papers [17]-[20], consider a sparse symmetric matrix A_{loc} as in the left of **Figure 1**, where each shaded block is a sparse sub-matrix and each white block is a zero sub-matrix. Using reordering algorithm procedures [10] [11], this matrix can be rotated to the pattern shown in the right of **Figure 1**. A reordered matrix is more convenient for computations than the initial one since Cholesky decomposition can start simultaneously from several entry points (for the matrix on the right of **Figure 1**, the first, second, fourth, and fifth rows of the matrix L can be calculated independently.

Let us append the original matrix A_{loc} stored in the sparse format with zeroes so that its nonzero pattern matches completely that of the matrix L. The elements of L in row 3 can be computed only after the elements in rows 1 and 2 are computed; similarly, element in row 6 can be computed only after elements in rows 4 and 5 are computed. The elements in the 7th row can be computed last. This allows us to construct the dependency tree [10] [11]: a graph, where each node corresponds to a single row of the matrix and each graph node can be computed only if its children (nodes on which it depends) are computed. A deeper discussion of the algorithm with pseudocode of the distribution of nodes of the tree between processes can be found in [17]. The dependency tree for the matrix is given in **Figure 2** (the number in the center of a node shows the row number).

Such a representation allows us to modify **Algorithm 1** using the following notation: node Z_j is a child of Z_i if Z_j resides lower than Z_i in the dependency tree (**Figure 2**) and there is a connection from Z_j to Z_i.

Algorithm 2. LL^T decomposition based on the dependency tree.

```
1)  L = A_loc
2)  for i = 1, number_of_tree_nodes do
3)      Z_i = node of tree;
4)      for all Z_j child of Z_i do
5)          Z_{i,j} = Z_j * mask_i Z_j   prepare update of Z_i by j-th child;
6)          Z_i = Z_i − Z_{i,j} ;
7)      end
8)      Calculate LL^T decomposition of Z_i;
9)  end
```

where by $mask_iZ_j$ we denote a submatrix built as intersection of columns corresponding to node Z_i with rows corresponding to node Z_j. In terms of representation in the right of the **Figure 1** that would mean the ij-th square.

To calculate the Schur complement let us add to the representation in the columns and rows of matrices B, B^T, and C to achieve full representation of matrix A as in left part of the **Figure 3**. As one can see, we achieve similar representation to the **Figure 2** with additional rows corresponding to those of matrices B and C in **Figure 3**

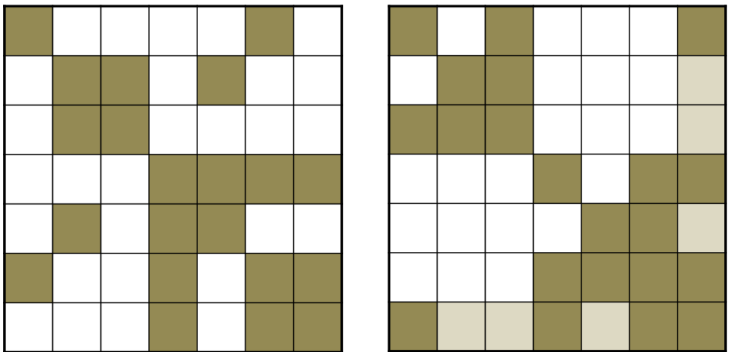

Figure 1. Nonzero pattern of the original matrix (left) and of the same matrix after reordering (right).

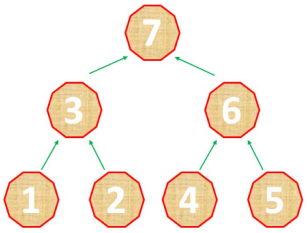

Figure 2. Dependency tree sample.

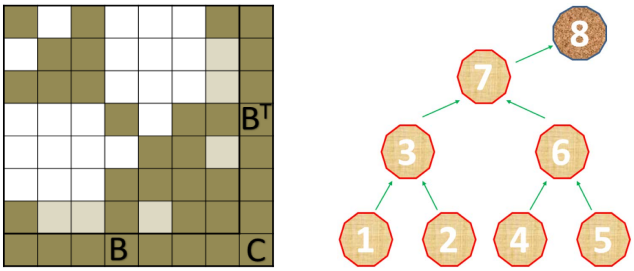

Figure 3. Nonzero pattern of matrix A after reordering of A_{loc} (left) and its tree representation (right).

(right). Note that blocks corresponding to the columns and rows of matrices B^{T}, B, and C are sparse. After factorization of the full matrix A the number of nonzero elements there increases significantly, but our experiments show that the blocks remain sparse and do not become dense.

Let's introduce the following notation: $\tilde{Z}_i$ is Z_i node of the tree expanded by the corresponding rows of the matrix B^{T}, Z_C is a node of the tree corresponding to the matrix C. Then we can modify **Algorithm 2** to take into account the elements of matrices B, B^{T}, and C.

Algorithm 3. LL^{T} decomposition based on the dependency tree.

1) $L = A$;
2) parallel **for** $i = 1$, *number_of_tree_nodes* **do**
3) $\quad \tilde{Z}_i$ = node of tree;
4) $\quad$ **for** *all* $\tilde{Z}_j$ *child of* $\tilde{Z}_i$ **do**
5) $\quad\quad \tilde{Z}_{i,j} = \tilde{Z}_j * mask_i \tilde{Z}_j$ prepare update of $\tilde{Z}_i$ by j-th child;
6) $\quad\quad \tilde{Z}_i = \tilde{Z}_i - \tilde{Z}_{i,j}$;
7) $\quad$ **end**
8) $\quad$ Calculate LL^{T} decomposition of $\tilde{Z}_i$;
9) **end**
10) **for** $j = 1$, *number_of_tree_node* **do**
11) $\quad Z_{C,j} = \tilde{Z}_j * mask_C \tilde{Z}_j$ prepare update of Z_C by j-th child;
12) $\quad Z_C = Z_C - Z_{C,j}$;
13) **end**

This algorithm produces $Z_C = S$. In fact, the **Algorithm 3** fully corresponds to the simple **Algorithm 2** without calculations of the LL^{T} decomposition of the last submatrix.

The approach proposed can be implemented on a parallel computers with a small modification of **Algorithm 3**.

Algorithm 4. Parallel implementation of LL^T decomposition based on the dependency tree.

1) $L = A$;
2) **for** $i = 1$, *number_of_tree_nodes* **do**
3) $\quad \tilde{Z}_i$ = node of tree;
4) $\quad$ **for** *all* $\tilde{Z}_j$ *child of* $\tilde{Z}_i$ **do**
5) $\quad\quad \tilde{Z}_{i,j} = \tilde{Z}_j * mask_i \tilde{Z}_j$ prepare update of $\tilde{Z}_i$ by j-th child;
6) $\quad\quad$ atomic $\tilde{Z}_i = \tilde{Z}_i - \tilde{Z}_{i,j}$;
7) $\quad$ **end**
8) $\quad$ Calculate LL^T decomposition of $\tilde{Z}_i$;
9) **end**
10) parallel **for** $j = 1$, *number_of_tree_node* **do**
11) $\quad Z_{C,j} = \tilde{Z}_j * mask_C \tilde{Z}_j$ prepare update of Z_C by j-th child;
12) $\quad$ atomic $Z_C = Z_C - Z_{C,j}$;
13) **end**

Approach presented in **Algorithm 4** allows us to implement the Schur complement of sparse matrix in Intel® Math Kernel Library.

3. Experiments

For all experiments we used a compute node with two Intel® Xeon® processors E5-2697 v3 (35MB cache, 2.60 GHz) with 64GB RAM, MUMPS version 4.10.0 [7], Intel MKL 11.2 Update 1 [4].

Figure 4 shows a cubic domain in which we apply seven-point approximation for a Laplace operator with mesh size $nx = ny = nz = 70$ to generate matrix A, and its cut-off through one of the axes as a domain for which we want to calculate the Schur complement (**Figure 4** (left)).

Figure 4 shows the portrait of matrix A before factorization (center) and the portrait of matrix L after factorization (right). One can see that the sparsity of L in the Schur complement columns decreased versus the sparsity of the part of L that corresponds to matrix A_{loc}, though it stays sparse and overall the number of nonzero elements increases slightly. For this test, we see that the number of nonzero elements is only five percent higher in the case when we calculate the Schur complement (**Algorithm 3**) compared to the case without Schur complement calculations (straight factorization).

In **Figure 5** and **Figure 6** we compare the performance of the implemented functionality with the similar functionality provided by the MUMPS package [7]. We compare the time needed to compute Schur complement matrix and return it in the dense format. The last 5000 rows and columns of the matrices presented are chosen for Schur complement computations.

For **Figure 5** we chose 2 matrices from Florida Matrix collection [21]: Fault_639 with about 600 K rows and columns and 27 M nonzero elements, and Serena with 1.3 M rows and columns and 64 M nonzero elements. On the x axis we plotted the number of threads on the compute node used for computation of the Schur complement. One can see that the time for computing Schur complement is almost the same for a small number of threads, but the time needed for Intel MKL PARDISO solver decreases when the number of threads increases.

For **Figure 6** we chose 2 matricesfrom Florida Matrix collection [21]: Geo_1438 with about 1.4 M rows and columns and 602 M nonzero elements, and Flan_1565 with 1.5 M rows and columns and 114 M nonzero elements. As before, on the x axis we plotted the number of threads on the compute node used for computation of the Schur complement. Notice that overall picture does not change significantly. The main difference between this set of matrices and the previous one is in sparsity—average number of nonzero elements per row. In the first set of experiments (Fault_639 and Serena) we used sparse matrices with fewer than 50 nonzero elements per

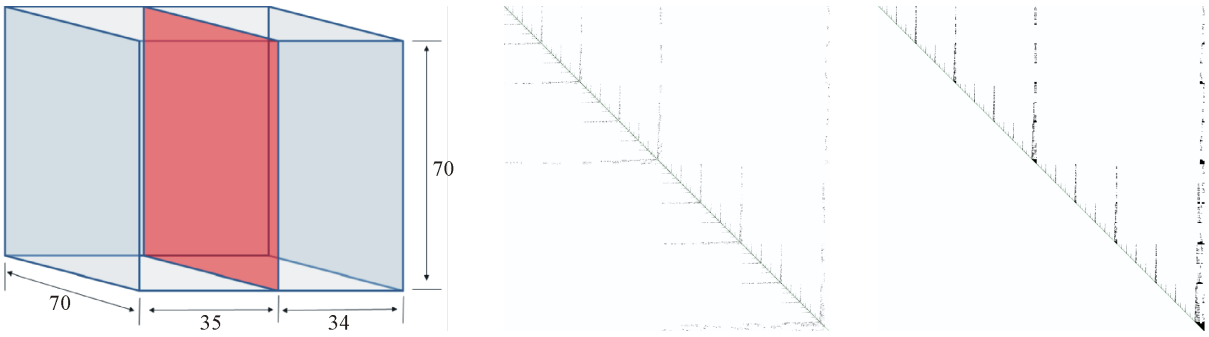

Figure 4. A domain with a dividing plane corresponding to Schur submatrix (left), portraits of the matrix before (center) and after factorization (right).

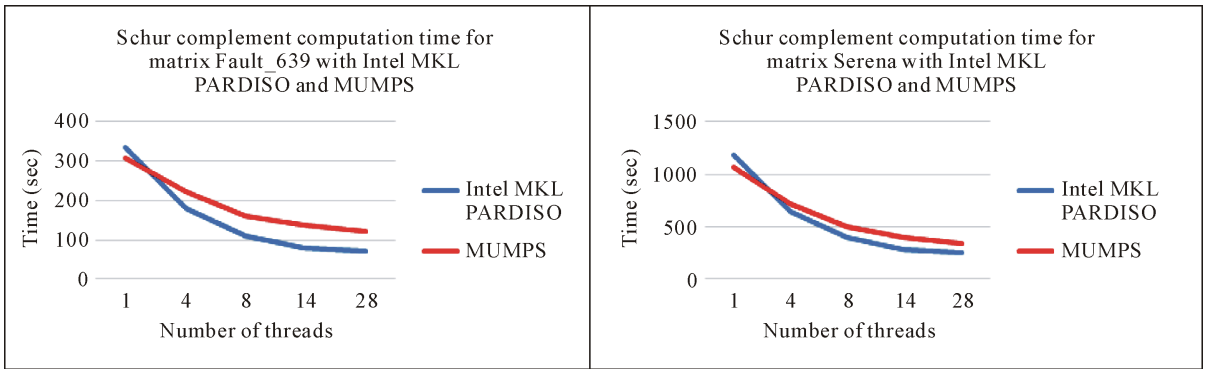

Figure 5. Schur complement computational time for matrices Fault 639 and Serena with Intel MKL PARDISO and MUMPS.

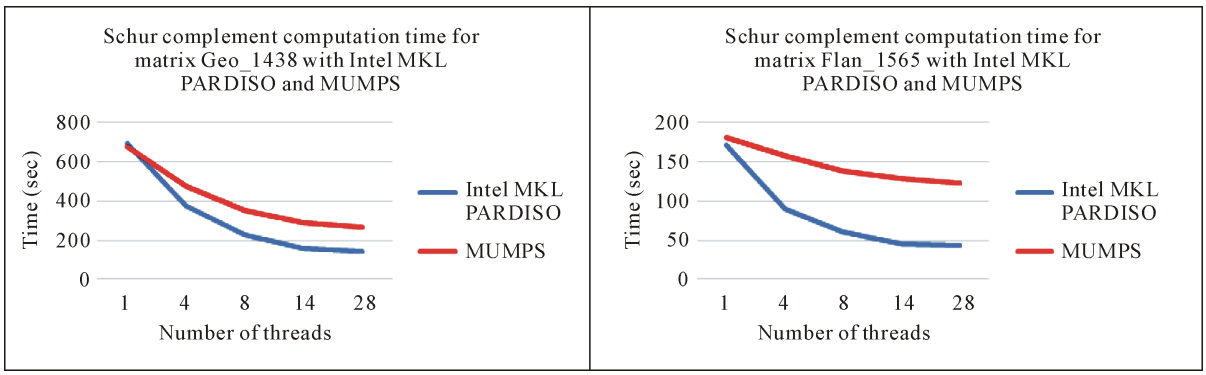

Figure 6. Schur complement computational time for matrices Geo 1438 and Flan 1565 with Intel® MKL PARDISO and MUMPS.

row on average, while the sparsity of Flan_1565 is about 70 nonzero elements per row and the sparsity of Geo_1438 is more than 400 nonzero elements per row. In both cases the time for Schur complement computations is almost the same when the number of threads is small for the Intel MKL and MUMPS, but the time needed for Intel MKL PARDISO solver significantly decreases when the number of threads increases. Moreover, comparison of **Figure 5** and **Figure 6** indicates that the performance of Intel MKL PARDISO becomes better if sparsity increases.

4. Conclusion

We demonstrated an approach that calculates the Schur complement for a sparse matrix implemented in Intel Math Kernel Library using the Intel MKL PARDISO interface. This implementation allows one to use a Schur complement for sparse matrices appearing in various mathematical applications, from statistical analysis to algebraic solvers. The proposed approach shows good scalability in terms of computational time and better performance than similar approaches proposed elsewhere.

References

[1] Zhang, F. (2005) The Schur Complement and Its Applications, Series: Numerical Methods and Algorithms, Vol. 4, Springer, USA.

[2] Haynsworth, E.V. (1968) On the Schur Complement. Basel Mathematical Notes, BMN 20, 17 p.

[3] Schur, I. (1986) On Power Series Which Are Bounded in the Interior of the Unit Circle, Series: Operator Theory: Advances and Applications, Birkhauser, Basel, Vol. 18, 31-59.

[4] Intel Math Kernel Library http://software.intel.com/en-us/intel-mkl

[5] Aleksandrov, V. and Samuel, H. (2010) The Schur Complement Method and Solution of Large-Scale Geophysical Problems. Bayerisches Geoinstitut (BGI). http://karel.troja.mff.cuni.cz/documents/2010-ML-Aleksandrov.pdf

[6] Yamazaki, I. and Li, S.X. (2010) On Techniques to Improve Robustness and Scalability of the Schur Complement Method. 9*th International Conference on High Performance Computing for Computational Science*, Berkeley, 22-25 June 2010, 14 p.

[7] MUMPS http://mumps.enseeiht.fr/

[8] Duff, I.S. and Reid, J.K. (1983) The Multifrontal Solution of Indefinite Sparse Symmetric Linear. *ACM Transactions on Mathematical Software*, **9**, 302-325. http://dx.doi.org/10.1145/356044.356047

[9] Liu, J.W.H. (1992) The Multifrontal Method for Sparse Matrix Solution: Theory and Practice. *SIAM Review*, **34**, 82-109. http://dx.doi.org/10.1137/1034004

[10] Karypis, G. and Kumar, V. (1996) Parallel Multilevel Graph Partitioning. *Proceedings of the* 10*th International Parallel Processing Symposium*, Honolulu, 15-19 April 1996, 314-319.

[11] Karypis, G. and Kumar, V. (1998) A Parallel Algorithm for Multilevel Graph Partitioning and Sparse Matrix Ordering. *Journal of Parallel and Distributed Computing*, **48**, 71-85 http://dx.doi.org/10.1006/jpdc.1997.1403

[12] Amestoy, P.R., Duff, I.S., Pralet, S. and Voemel, C. (2003) Adapting a Parallel Sparse Direct Solver to Architectures with Clusters of SMPs. *Parallel Computing*, **29**, 1645-1668. http://dx.doi.org/10.1016/j.parco.2003.05.010

[13] Amestoy, P.R., Duff, I.S. and Vomel, C. (2005) Task Scheduling in an Asynchronous Distributed Memory Multifrontal Solver. *SIAM Journal on Matrix Analysis and Applications*, **26**, 544-565. http://dx.doi.org/10.1137/S0895479802419877

[14] Amestoy, P.R., Guermouche, A., L'Excellent, J.-Y. and Pralet, S. (2006) Hybrid Scheduling for the Parallel Solution of Linear Systems. *Parallel Computing*, **32**, 136-156. http://dx.doi.org/10.1016/j.parco.2005.07.004

[15] Amestoy, P.R. and Duff, I.S. (1993) Memory Management Issues in Sparse Multifrontal Methods on Multiprocessors. *International Journal of High Performance Computing Applications*, **7**, 64-82. http://dx.doi.org/10.1177/109434209300700105

[16] Amestoy, P.R., Duff, I.S., L'Excellent, J.-Y. and Koster, J. (2001) A Fully Asynchronous Multifrontal Solver Using Distributed Dynamic Scheduling. *SIAM Journal on Matrix Analysis and Applications*, **23**, 15-41. http://dx.doi.org/10.1137/S0895479899358194

[17] Kalinkin, A. (2013) Intel Direct Sparse Solver for Clusters, a Research Project for Solving Large Sparse Systems of Linear Algebraic Equations on Clusters. *Sparse Days Meeting* 2013 *at CERFACS*, Toulouse, 17-18 June 2013. http://www.cerfacs.fr/6-27085-Sparse-Days-2013.php

[18] Kalinkin, A. (2013) Sparse Linear Algebra Support in Intel Math Kernel Library. *Sparse Linear Algebra Solvers for High Performance Computing Workshop*, Scarman House, University of Warwick, 8-9 July 2013. http://www2.warwick.ac.uk/fac/sci/dcs/research/pcav/linear solvers/programme/

[19] Kalinkin, A. and Arturov, K. (2013) Asynchronous Approach to Memory Management in Sparse Multifrontal Methods on Multiprocessors. *Applied Mathematics*, **4**, 33-39. http://dx.doi.org/10.4236/am.2013.412A004

[20] Kalinkin, A., Anders, A. and Anders, R. (2014) Intel® Math Kernel Library Parallel Direct Sparse Solver for Clusters. *EAGE Workshop on High Performance Computing for Upstream*, Chania, Crete, 7-10 September 2014. http://www.eage.org/events/index.php?evp=12682&ActiveMenu=2&Opendivs=s3 http://dx.doi.org/10.3997/2214-4609.20141926

[21] Davis, T.A. and Hu, Y. (2011) The University of Florida Sparse Matrix Collection. *ACM Transactions on Mathematical Software*, **38**, 1:1-1:25. http://www.cise.ufl.edu/research/sparse/matrices

Applied Mathematics, 2015, 6, 312-318
Published Online February 2015 in SciRes. http://www.scirp.org/journal/am
http://dx.doi.org/10.4236/am.2015.62029

Idempotent and Regular Elements of the Complete Semigroups of Binary Relations of the Class $\Sigma_3(X,9)$

Barış Albayrak, Neşet Aydın

Çanakkale Onsekiz Mart University, Çanakkale, Turkey
Email: balbayrak77@gmail.com, neseta@comu.edu.tr

Received 13 January 2015; accepted 1 February 2015; published 5 February 2015

Abstract

In this paper, we take Q_{16} subsemilattice of D and we will calculate the number of right unit, idempotent and regular elements α of $B_X(Q_{16})$ satisfied that $V(D,\alpha)=Q_{16}$ for a finite set X. Also we will give a formula for calculate idempotent and regular elements of $B_X(Q)$ defined by an X-semilattice of unions D.

Keywords

Semilattice, Semigroup, Binary Relation

1. Introduction

Let X be a nonempty set and B_X be semigroup of all binary relations on the set X. If D is a nonempty set of subsets of X which is closed under the union then D is called a complete X-semilattice of unions.

Let f be an arbitrary mapping from X into D. Then one can construct a binary relation α_f on X by $\alpha_f=\bigcup_{x\in X}(\{x\}\times f(x))$. The set of all such binary relations is denoted by $B_X(D)$ and called a complete semigroup of binary relations defined by an X-semilattice of unions D.

We use the notations, $y\alpha=\{x\in X\,|\,y\alpha x\}$, $Y\alpha=\bigcup_{y\in Y}y\alpha$, $V(D,\alpha)=\{Y\alpha\,|\,Y\in D\}$, $Y_T^{\alpha}=\{y\in X\,|\,y\alpha=T\}$.

A representation of a binary relation α of the form $\alpha=\bigcup_{T\in V(X^*,\alpha)}(Y_T^{\alpha}\times T)$ is called quasinormal. Note that,

How to cite this paper: Albayrak, B. and Aydın, N. (2015) Idempotent and Regular Elements of the Complete Semigroups of Binary Relations of the Class $\Sigma_3(X,9)$. *Applied Mathematics*, **6**, 312-318. http://dx.doi.org/10.4236/am.2015.62029

if $\alpha = \bigcup_{T \in V(X^*,\alpha)} \left(Y_T^\alpha \times T\right)$ is a quasinormal representation of the binary relation α, then $Y_T^\alpha \cap Y_{T'}^\alpha = \varnothing$ for T, $T' \in V\left(X^*,\alpha\right)$ and $T \neq T'$.

A complete X-semilattice of unions D is an XI-semilattice of unions if $\Lambda\left(D, D_t\right) \in D$ for any $t \in \breve{D}$ and $Z = \bigcup_{t \in Z} \Lambda\left(D, D_t\right)$ for any nonempty element Z of D.

Now, $\alpha \in B_X\left(D\right)$ is said to be right unit if $\beta \circ \alpha = \beta$ for all $\beta \in B_X\left(D\right)$. Also, $\alpha \in B_X\left(D\right)$ is idempotent if $\alpha \circ \alpha = \alpha$. And $\alpha \in B_X\left(D\right)$ is said to be regular if $\alpha \circ \beta \circ \alpha = \alpha$ for some $\beta \in B_X\left(D\right)$.

Let D', D'' be complete X-semilattices of unions and φ be a one-to-one mapping from D' to D''. A mapping $\varphi : D' \to D''$ is a complete isomorphism provided $\varphi\left(\cup D_1\right) = \bigcup_{T' \in D_1} \varphi\left(T'\right)$ for all nonempty subset D_1 of the semilattice D'. Besides that, if $\varphi : V\left(D,\alpha\right) \to D'$ is a complete isomorphism where $\alpha \in B_X\left(D\right)$, $\varphi\left(T\right)\alpha = T$ for all $T \in V\left(D,\alpha\right)$, φ is said to be a complete α-isomorphism.

Let Q and D' be respectively some XI and X-subsemilattices of the complete X-semilattice of unions D. Then

$$R_\varphi\left(Q, D'\right) = \left\{\alpha \in B_X\left(D\right) \middle| \alpha \text{ regular element, } \varphi \text{ complete } \alpha\text{-isomorphism}\right\}$$

where $\varphi : Q \to D'$ complete isomorphism and $V\left(D,\alpha\right) = Q$. Besides, let us denote

$$R\left(Q, D'\right) = \bigcup_{\varphi \in \Phi\left(Q, D'\right)} R_\varphi\left(Q, D'\right) \quad \text{and} \quad R\left(D'\right) = \bigcup_{Q' \in \Omega\left(Q\right)} R\left(Q', D'\right)$$

where

$$\Phi\left(Q, D'\right) = \left\{\varphi \mid \varphi : Q \to D' \text{ is a complete } \alpha\text{-isomorhism } \exists \alpha \in B_X\left(D\right)\right\}$$

$$\Omega\left(Q\right) = \left\{Q' \middle| Q' \text{ is } XI\text{-subsemilattices of } D \text{ which is complete isomorphic to } Q\right\}$$

This structure was comprehensively investigated in Diasamidze [1].

Lemma 1. [1] *If Q is complete X-semilattice of unions and $I\left(Q\right)$ is the set all right units of the semigroup $B_X\left(Q\right)$ then $I\left(Q\right) = R_{id_Q}\left(Q,Q\right)$.*

Lemma 2. [2] *Let X be a finite set, D be a complete X-semilattice of unions and $Q = \left\{T_1, T_2, T_3, T_4, T_5, T_6, T_7, T_8\right\}$ be X-subsemilattice of unions of D satisfies the following conditions*

$$\begin{aligned}
&T_1 \subset T_2 \subset T_3 \subset T_5 \subset T_6 \subset T_8, \quad T_1 \subset T_2 \subset T_3 \subset T_5 \subset T_7 \subset T_8,\\
&T_1 \subset T_2 \subset T_4 \subset T_5 \subset T_6 \subset T_8, \quad T_1 \subset T_2 \subset T_4 \subset T_5 \subset T_7 \subset T_8,\\
&T_4 \setminus T_3 \neq \varnothing, T_3 \setminus T_4 \neq \varnothing, \qquad T_6 \setminus T_7 \neq \varnothing, \quad T_7 \setminus T_6 \neq \varnothing,\\
&T_3 \cup T_4 = T_5, T_6 \cup T_7 = T_8 \qquad T_1 \neq \varnothing.
\end{aligned}$$

Q is XI-semilattice of unions.

Theorem 1. [2] *Let X be a finite set and Q be XI-semilattice. If $D' = \left\{\overline{T}_1, \overline{T}_2, \overline{T}_3, \overline{T}_4, \overline{T}_5, \overline{T}_6, \overline{T}_7, \overline{T}_8\right\}$ is α-isomorphic to Q and $\Omega\left(Q\right) = m_0$, then*

$$\begin{aligned}
\left|R\left(D'\right)\right| = m_0 \cdot 4 \cdot &\left(2^{\left|\left(\overline{T}_3 \cap \overline{T}_4\right) \setminus \overline{T}_1\right|}\left(2^{\left|\overline{T}_2 \setminus \overline{T}_1\right|} - 1\right)\right) \cdot \left(3^{\left|\overline{T}_4 \setminus \overline{T}_3\right|} - 2^{\left|\overline{T}_4 \setminus \overline{T}_3\right|}\right) \cdot \left(3^{\left|\overline{T}_3 \setminus \overline{T}_4\right|} - 2^{\left|\overline{T}_3 \setminus \overline{T}_4\right|}\right) \cdot 5^{\left|\left(\overline{T}_7 \cap \overline{T}_6\right) \setminus \overline{T}_5\right|}\\
&\cdot \left(6^{\left|\overline{T}_7 \setminus \overline{T}_6\right|} - 5^{\left|\overline{T}_7 \setminus \overline{T}_6\right|}\right) \cdot \left(6^{\left|\overline{T}_6 \setminus \overline{T}_7\right|} - 5^{\left|\overline{T}_6 \setminus \overline{T}_7\right|}\right) \cdot 8^{\left|X \setminus \overline{T}_8\right|}.
\end{aligned}$$

Theorem 2. [2] *Let $\alpha \in B_X\left(Q\right)$ be a quasinormal representation of the form $\alpha = \bigcup_{i=1}^{8}\left(Y_i^\alpha \times T_i\right)$ such that $V\left(D,\alpha\right) = Q$. $\alpha \in B_X\left(D\right)$ is a regular iff for some complete α-isomorphism $\varphi : Q \to D' \subseteq D$, the following conditions are satisfied*:

$$\begin{aligned}
&Y_1^\alpha \supseteq \varphi\left(T_1\right), \quad Y_1^\alpha \cup Y_2^\alpha \supseteq \varphi\left(T_2\right), \quad Y_1^\alpha \cup Y_2^\alpha \cup Y_3^\alpha \supseteq \varphi\left(T_3\right),\\
&Y_1^\alpha \cup Y_2^\alpha \cup Y_4^\alpha \supseteq \varphi\left(T_4\right), \quad Y_1^\alpha \cup Y_2^\alpha \cup Y_3^\alpha \cup Y_4^\alpha \cup Y_5^\alpha \cup Y_6^\alpha \supseteq \varphi\left(T_6\right),\\
&Y_1^\alpha \cup Y_2^\alpha \cup Y_3^\alpha \cup Y_4^\alpha \cup Y_5^\alpha \cup Y_7^\alpha \supseteq \varphi\left(T_7\right), \quad Y_2^\alpha \cap \varphi\left(T_2\right) \neq \varnothing,\\
&Y_3^\alpha \cap \varphi\left(T_3\right) \neq \varnothing, \quad Y_4^\alpha \cap \varphi\left(T_4\right) \neq \varnothing, \quad Y_6^\alpha \cap \varphi\left(T_6\right) \neq \varnothing, \quad Y_7^\alpha \cap \varphi\left(T_7\right) \neq \varnothing.
\end{aligned}$$

Let X be a finite set and $D=\{T_1,T_2,T_3,T_4,T_5,T_6,T_7,T_8,T_9\}$ be a complete X-semilattice of unions which satisfies the following conditions

$$T_1\subset T_3\subset T_5\subset T_6\subset T_8\subset T_9,$$
$$T_1\subset T_3\subset T_5\subset T_6\subset T_7\subset T_9,$$
$$T_1\subset T_3\subset T_4\subset T_6\subset T_8\subset T_9,$$
$$T_1\subset T_3\subset T_4\subset T_6\subset T_7\subset T_9,$$
$$T_2\subset T_3\subset T_5\subset T_6\subset T_8\subset T_9,$$
$$T_2\subset T_3\subset T_5\subset T_6\subset T_7\subset T_9,$$
$$T_2\subset T_3\subset T_4\subset T_6\subset T_8\subset T_9,$$
$$T_2\subset T_3\subset T_4\subset T_6\subset T_7\subset T_9,$$
$$T_1\setminus T_2\neq\varnothing,\ T_2\setminus T_1\neq\varnothing,\ T_4\setminus T_5\neq\varnothing,$$
$$T_5\setminus T_4\neq\varnothing,\ T_7\setminus T_8\neq\varnothing,\ T_8\setminus T_7\neq\varnothing,$$
$$T_1\cup T_2=T_3,\ T_4\cup T_5=T_6,$$
$$T_7\cup T_8=T_9,\ T_1\cap T_2\neq\varnothing$$

The diagram of the D is shown in **Figure 1**. By the symbol $\sum_3(X,9)$ we denote the class of all complete X-semilattice of unions whose every element is isomophic to an X-semilattice of the form D.

All subsemilattice of $D=\{T_1,T_2,T_3,T_4,T_5,T_6,T_7,T_8,T_9\}$ are given in **Figure 2**.

In Diasamidze [1], it has shown that subsemilattices 1 - 15 are XI-semilattice of unions and subsemilattices 17 - 24 are not XI-semilattice of unions. In Yeşil Sungur [3] and Albayrak [4], they have shown that subsemilattices 25 and 26 are XI-semilattice of unions if and only if $T_1\cap T_2=\varnothing$". Also they found that number of right unit, idempotent and regular elements in subsemilattices.

In this paper, we take in particular, $Q_{16}=\{T,T_3,T_4,T_5,T_6,T_7,T_8,T_9\}$ subsemilattice of D. We will calculate the number of right unit, idempotent and regular elements α of $B_X(Q_{16})$ satisfied that $V(D,\alpha)=Q_{16}$ for a finite set X. Also we will give a formula for calculate idempotent and regular elements of $B_X(D)$ defined by an X-semilattice of unions $D=\{T_1,T_2,T_3,T_4,T_5,T_6,T_7,T_8,T_9\}$.

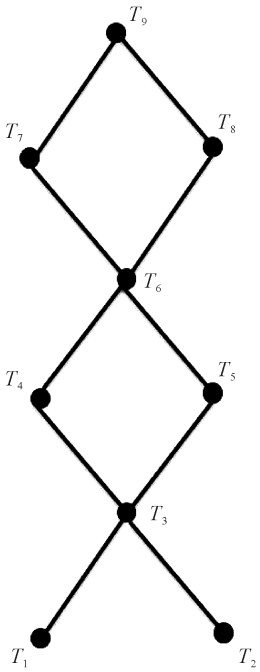

Figure 1. Diagram of D.

2. Results

Let $Q_{16}=\{T,T_3,T_4,T_5,T_6,T_7,T_8,T_9\}$ be complete X-subsemilattice of D satisfies the following conditions

$$T\subset T_3\subset T_4\subset T_6\subset T_7\subset T_9,$$
$$T\subset T_3\subset T_5\subset T_6\subset T_7\subset T_9,$$
$$T\subset T_3\subset T_4\subset T_6\subset T_8\subset T_9,$$
$$T\subset T_3\subset T_5\subset T_6\subset T_8\subset T_9,$$
$$T_4\setminus T_5\neq\varnothing,\quad T_5\setminus T_4\neq\varnothing,$$
$$T_7\setminus T_8\neq\varnothing,\quad T_8\setminus T_7\neq\varnothing,$$
$$T_4\cup T_5=T_6,\quad T_8\cup T_7=T_9$$
$$T\neq\varnothing.$$

The diagram of the Q_{16} is shown in **Figure 3**. From Lemma 2 Q_{16} is XI-semilattice of unions.

Let $Q_{16}\vartheta_{XI}$ denote the set of all XI-subsemilattice of the semilattice D which are isomorphic of the X-semilattice Q_{16}. Then we get

$$Q_{16}\vartheta_{XI}=\{\{T_1,T_3,T_4,T_5,T_6,T_7,T_8,T_9\},\{T_2,T_3,T_4,T_5,T_6,T_7,T_8,T_9\}\}$$

Let $\alpha\in B_X(Q_{16})$ be a idempotent element having a quasinormal representation of the form

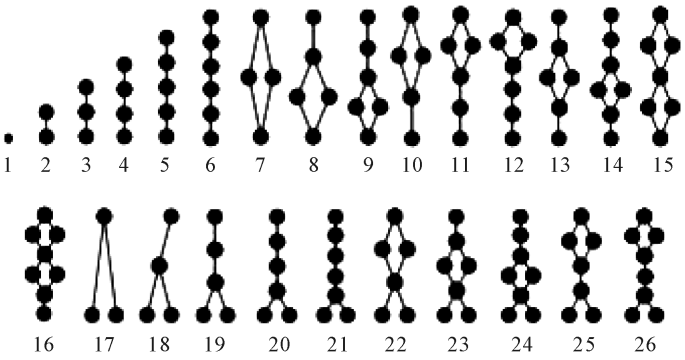

Figure 2. All subsemilattice of D.

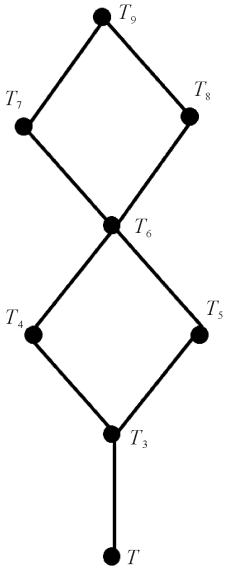

Figure 3. The diagram of the Q_{16}.

$\alpha=\left(Y_T^{\alpha}\times T\right)\cup\bigcup_{i=3}^{9}\left(Y_i^{\alpha}\times T_i\right)$, such that $V(D,\alpha)=Q_{16}$. First we calculate number of this idempotent elements in $B_X(Q_{16})$.

Lemma 3. *If X is a finite set and* $I(Q_{16})$ *is the set all right units of the semigroup* $B_X(Q_{16})$, *then the number* $\left|I(Q_{16})\right|$ *may be calculated by formula*:

$$\left|I(Q_{16})\right|=\left((2^{|T_3\setminus T|}-1)\cdot 2^{|(T_5\cap T_4)\setminus T_3|}\right)\cdot\left(3^{|T_5\setminus T_4|}-2^{|T_5\setminus T_4|}\right)\cdot\left(3^{|T_4\setminus T_5|}-2^{|T_4\setminus T_5|}\right)$$
$$\cdot 5^{|(T_7\cap T_8)\setminus T_6|}\cdot\left(6^{|T_8\setminus T_7|}-5^{|T_8\setminus T_7|}\right)\cdot\left(6^{|T_7\setminus T_8|}-5^{|T_7\setminus T_8|}\right)\cdot 8^{|X\setminus T_9|}.$$

Proof. From Lemma 1 we have $I(Q_{16})=R_{id_{Q_{16}}}(Q_{16},Q_{16})$ where $id_{Q_{16}}$ is identity mapping of the set Q_{16}. For this reason $D'=Q$ in Theorem 1. Then we obtain

$$\left|I(Q_{16})\right|=\left(\left(2^{|T_3\setminus T|}-1\right)\cdot 2^{|(T_5\cap T_4)\setminus T_3|}\right)\cdot\left(3^{|T_5\setminus T_4|}-2^{|T_5\setminus T_4|}\right)\cdot\left(3^{|T_4\setminus T_5|}-2^{|T_4\setminus T_5|}\right)$$
$$\cdot 5^{|(T_7\cap T_8)\setminus T_6|}\cdot\left(6^{|T_8\setminus T_7|}-5^{|T_8\setminus T_7|}\right)\cdot\left(6^{|T_7\setminus T_8|}-5^{|T_7\setminus T_8|}\right)\cdot 8^{|X\setminus T_9|}.$$

□

Theorem 3. *If X is a finite set and* $I^*(Q_{16})$ *is the set all idempotent elements of the semigroup* $B_X(Q_{16})$, *then the number* $\left|I^*(Q_{16})\right|$ *may be calculated by formula*:

$$\left|I^*(Q_{16})\right|=\left(\left(2^{|T_3\setminus T_2|}-1\right)\cdot 2^{|(T_5\cap T_4)\setminus T_3|}\right)\cdot\left(3^{|T_5\setminus T_4|}-2^{|T_5\setminus T_4|}\right)\cdot\left(3^{|T_4\setminus T_5|}-2^{|T_4\setminus T_5|}\right)$$
$$\cdot 5^{|(T_7\cap T_8)\setminus T_6|}\cdot\left(6^{|T_8\setminus T_7|}-5^{|T_8\setminus T_7|}\right)\cdot\left(6^{|T_7\setminus T_8|}-5^{|T_7\setminus T_8|}\right)\cdot 8^{|X\setminus T_9|}$$
$$+\left(\left(2^{|T_3\setminus T_1|}-1\right)\cdot 2^{|(T_5\cap T_4)\setminus T_3|}\right)\cdot\left(3^{|T_5\setminus T_4|}-2^{|T_5\setminus T_4|}\right)\cdot\left(3^{|T_4\setminus T_5|}-2^{|T_4\setminus T_5|}\right)$$
$$\cdot 5^{|(T_7\cap T_8)\setminus T_6|}\cdot\left(6^{|T_8\setminus T_7|}-5^{|T_8\setminus T_7|}\right)\cdot\left(6^{|T_7\setminus T_8|}-5^{|T_7\setminus T_8|}\right)\cdot 8^{|X\setminus T_9|}.$$

Proof. By using Lemma 3 we have number of right units of the semigroup $B_X(Q_{16})$ defined by $Q_{16}=\{T,T_3,T_4,T_5,T_6,T_7,T_8,T_9\}$ for $T\in\{T_1,T_2\}$. Then number of idempotent elements of $I^*(Q_{16})$ calculated by formula $I^*(Q_{16})=\sum_{D'\in Q_{16}\vartheta_{XI}}\left|I(D')\right|$. By using

$$Q_{16}\vartheta_{XI}=\left\{\{T_1,T_3,T_4,T_5,T_6,T_7,T_8,T_9\},\{T_2,T_3,T_4,T_5,T_6,T_7,T_8,T_9\}\right\}$$

we obtain above formula. □

Now we will calculate number of regular elements $\alpha\in B_X(Q_{16})$ having a quasinormal representation of the form $\alpha=\left(Y_T^{\alpha}\times T\right)\cup\bigcup_{i=3}^{9}\left(Y_i^{\alpha}\times T_i\right)$ such that $V(D,\alpha)=Q_{16}$. Let $R^*(Q_{16})$ be the set all regular elements of the semigroup $B_X(Q_{16})$. By using $Q_{16}\vartheta_{XI}=\left\{\{T_1,T_3,T_4,T_5,T_6,T_7,T_8,T_9\},\{T_2,T_3,T_4,T_5,T_6,T_7,T_8,T_9\}\right\}$ we get $\left|\Omega(Q_{16})\right|=2$. The number of all automorphisms of the semilattice Q_{16} is q = 4. These are

$$I_Q=\begin{pmatrix}T&T_3&T_4&T_5&T_6&T_7&T_8&T_9\\T&T_3&T_4&T_5&T_6&T_7&T_8&T_9\end{pmatrix}\quad\varphi=\begin{pmatrix}T&T_3&T_4&T_5&T_6&T_7&T_8&T_9\\T&T_3&T_5&T_4&T_6&T_7&T_8&T_9\end{pmatrix}$$
$$\theta=\begin{pmatrix}T&T_3&T_4&T_5&T_6&T_7&T_8&T_9\\T&T_3&T_4&T_5&T_6&T_8&T_7&T_9\end{pmatrix}\quad\tau=\begin{pmatrix}T&T_3&T_4&T_5&T_6&T_7&T_8&T_9\\T&T_3&T_5&T_4&T_6&T_8&T_7&T_9\end{pmatrix}$$

Then $\left|\Phi(Q_{16})\right|=4$. Also by using

$$D_1'=\{T_2,T_3,T_4,T_5,T_6,T_7,T_8,T_9\},\quad D_2'=\{T_2,T_3,T_5,T_4,T_6,T_7,T_8,T_9\}$$
$$D_3'=\{T_2,T_3,T_4,T_5,T_6,T_8,T_7,T_9\},\quad D_4'=\{T_2,T_3,T_5,T_4,T_6,T_8,T_7,T_9\}$$
$$D_5'=\{T_1,T_3,T_4,T_5,T_6,T_7,T_8,T_9\},\quad D_6'=\{T_1,T_3,T_5,T_4,T_6,T_7,T_8,T_9\}$$
$$D_7'=\{T_1,T_3,T_4,T_5,T_6,T_8,T_7,T_9\},\quad D_8'=\{T_1,T_3,T_5,T_4,T_6,T_8,T_7,T_9\}$$

we get $R^*(Q_{16}) = \bigcup_{i=1}^{8} R(D_i)$.

Theorem 4. *If X is a finite set and* $R^*(Q_{16})$ *is the set all regular elements of the semigroup* $B_X(Q_{16})$, *then the number* $\left|R^*(Q_{16})\right|$ *may be calculated by formula*:

$$\begin{aligned}\left|R^*(Q_{16})\right| &= 4\cdot 2\left(\left(2^{|T_3\setminus T_2|}-1\right)\cdot 2^{|(T_5\cap T_4)\setminus T_3|}\right)\cdot\left(3^{|T_5\setminus T_4|}-2^{|T_5\setminus T_4|}\right)\cdot 5^{|(T_7\cap T_8)\setminus T_6|}\\ &\cdot\left(3^{|T_4\setminus T_5|}-2^{|T_4\setminus T_5|}\right)\cdot\left(6^{|T_8\setminus T_7|}-5^{|T_8\setminus T_7|}\right)\cdot\left(6^{|T_7\setminus T_8|}-5^{|T_7\setminus T_8|}\right)\cdot 8^{|X\setminus T_9|}\\ &+ 4\cdot 2\cdot\left(\left(2^{|T_3\setminus T_1|}-1\right)\cdot 2^{|(T_5\cap T_4)\setminus T_3|}\right)\cdot\left(3^{|T_5\setminus T_4|}-2^{|T_5\setminus T_4|}\right)\cdot 5^{|(T_7\cap T_8)\setminus T_6|}\\ &\cdot\left(3^{|T_4\setminus T_5|}-2^{|T_4\setminus T_5|}\right)\cdot\left(6^{|T_8\setminus T_7|}-5^{|T_8\setminus T_7|}\right)\cdot\left(6^{|T_7\setminus T_8|}-5^{|T_7\setminus T_8|}\right)\cdot 8^{|X\setminus T_9|}.\end{aligned}$$

Proof. To account for the elements that are in $R^*(Q_{16})$, we first subtract out intersection of $R(D_i')$'s. Let $\alpha \in R(D_1')\cap R(D_2')$. By using Theorem 2 and $Q_{16} = \{T, T_3, T_4, T_5, T_6, T_7, T_8, T_9\}$

$$\begin{aligned}\alpha \in R(D_1')\cap R(D_2') &\Rightarrow \alpha \in R(D_1') \text{ and } \alpha \in R(D_2')\\ &\Rightarrow Y_T^\alpha \supseteq T_2,\ Y_T^\alpha \cup Y_3^\alpha \supseteq T_3,\ Y_T^\alpha \cup Y_3^\alpha \cup Y_5^\alpha \supseteq T_5\\ &\quad Y_T^\alpha \cup Y_3^\alpha \cup Y_4^\alpha \supseteq T_4,\ Y_T^\alpha \cup Y_3^\alpha \cup Y_4^\alpha \cup Y_5^\alpha \cup Y_6^\alpha \cup Y_8^\alpha \supseteq T_8,\\ &\quad Y_T^\alpha \cup Y_3^\alpha \cup Y_4^\alpha \cup Y_5^\alpha \cup Y_6^\alpha \cup Y_7^\alpha \supseteq T_7,\ Y_3^\alpha \cap T_3 \neq \varnothing,\\ &\quad Y_4^\alpha \cap T_4 \neq \varnothing,\ Y_5^\alpha \cap T_5 \neq \varnothing,\ Y_7^\alpha \cap T_7 \neq \varnothing,\ Y_8^\alpha \cap T_8 \neq \varnothing,\\ &\quad Y_T^\alpha \supseteq T_2,\ Y_T^\alpha \cup Y_3^\alpha \supseteq T_3,\ Y_T^\alpha \cup Y_3^\alpha \cup Y_5^\alpha \supseteq T_4,\\ &\quad Y_T^\alpha \cup Y_3^\alpha \cup Y_4^\alpha \supseteq T_5,\ Y_T^\alpha \cup Y_3^\alpha \cup Y_4^\alpha \cup Y_5^\alpha \cup Y_6^\alpha \cup Y_8^\alpha \supseteq T_8,\\ &\quad Y_T^\alpha \cup Y_3^\alpha \cup Y_4^\alpha \cup Y_5^\alpha \cup Y_6^\alpha \cup Y_7^\alpha \supseteq T_7,\ Y_3^\alpha \cap T_3 \neq \varnothing,\\ &\quad Y_5^\alpha \cap T_4 \neq \varnothing,\ Y_4^\alpha \cap T_5 \neq \varnothing,\ Y_7^\alpha \cap T_7 \neq \varnothing,\ Y_8^\alpha \cap T_8 \neq \varnothing.\end{aligned}$$

We get $\varnothing \neq Y_4^\alpha \cap T_4 \subseteq Y_4^\alpha \cap \left(Y_T^\alpha \cup Y_3^\alpha \cup Y_5^\alpha\right)$ which is a contradiction with Y_4^α, Y_T^α, Y_3^α, Y_5^α are disjoint sets. Then $R(D_1')\cap R(D_2') = \varnothing$. Smilarly $R(D_i')\cap R(D_j') = \varnothing$ for $i, j = 1,\cdots,6$. Thus we obtain

$$\left|R^*(Q_{16})\right| = \left|R(D_1')\right| + \left|R(D_2')\right| + \left|R(D_3')\right| + \left|R(D_4')\right| + \left|R(D_5')\right| + \left|R(D_6')\right| + \left|R(D_7')\right| + \left|R(D_8')\right|$$

From Theorem 1 we get above formula. □

Corollary 1. *If X is a finite set,* I_D *is the set all idempotent elements of the semigroup* $B_X(D)$ *and* R_D *is the set all regular elements of the semigroup* $B_X(D)$, *then the number* $|I_D|$ *and* $|R_D|$ *may be calculated by formula*:

$$\left|(I_D)\right| = \sum_{i=1}^{16}\left|I^*(Q_i)\right|, \quad \left|(R_D)\right| = \sum_{i=1}^{16}\left|R^*(Q_i)\right|$$

Proof. Let I_D be the set of all idempotent elements of the semigroup $B_X(D)$. Then number of idempotent element of $B_X(D)$ is equal to sum of idempotent elements of the subsemigroup defined by *XI*-subsemilattice of *D*. $\left|I^*(Q_i)\right|$ is given in Diasamidze [1] for $(i = 1,2,\cdots,15)$. From Theorem 3 we have number of idempotent elements of the subsemigroup $B_X(Q_{16})$. Then the number $|I_D|$ may be calculated by formula $\left|(I_D)\right| = \sum_{i=1}^{16}\left|I^*(Q_i)\right|$. Similarly the number $|R_D|$ may be calculated by formula $\left|(R_D)\right| = \sum_{i=1}^{16}\left|R^*(Q_i)\right|$. □

References

[1] Diasamidze, Ya. and Makharadze, Sh. (2013) Complete Semigroups of Binary Relations. Kriter Yayınevi, İstanbul, 524 p.

[2] Albayrak, B., Aydin, N. and Diasamidze, Ya. (2013) Reguler Elements of the Complete Semigroups of Binary Relations of the Class $\sum_7(X,8)$. *International Journal of Pure and Applied Mathematics*, **86**, 199-216. http://dx.doi.org/10.12732/ijpam.v86i1.13

[3] Yeşil Sungur, D. and Aydin, N. (2014) Reguler Elements of the Complete Semigroups of Binary Relations of the Class $\sum_8(X,7)$. *General Mathematics Notes*, **21**, 27-42.

[4] Albayrak, B., Aydin, N. and Yeşil Sungur, D. (2014) Regular Elements of Semigroups $B_X(D)$ Defined by the Generalized X-Semilattice. *General Mathematics Notes*, **23**, 96-107.

Applied Mathematics, 2015, 6, 319-325
Published Online February 2015 in SciRes. http://www.scirp.org/journal/am
http://dx.doi.org/10.4236/am.2015.62030

Semiparametric Estimator of Mean Conditional Residual Life Function under Informative Random Censoring from Both Sides

A. A. Abdushukurov, F. A. Abdikalikov

Department of Probability Theory and Mathematical Statistics, National University of Uzbekistan, Tashkent, Uzbekistan
Email: a_abdushukurov@rambler.ru

Received 14 January 2015; accepted 2 February 2015; published 5 February 2015

Abstract

In this paper we study estimator of mean residual life function in fixed design regression model when life times are subjected to informative random censoring from both sides. We prove an asymptotic normality of estimators.

Keywords

Informative Censoring, Power Estimator, Regression, Mean Residual Lifetime

1. Introduction

In survival data analysis, response random variable (r.v.) Z, the survival time of a individual (in medical study) or failure time of a machine (in industrial study) that usually can be influenced by r.v. X, is often called prognostic factor (or covariate). X represents e.g. the dose of a drug for individual or some environmental conditions of a machine (temperature, pressure,…). Moreover, in such practical situations it often occurs that not all of survival times $Z_1,\cdots,Z_n$ of n identical objects are complete observed, that they can be censored by other r.v.-s.

In this article we consider a regression model in which the response r.v.-s are subjected to random censoring from both sides.

We first introduce some notations. Let the support of covariate is the interval [0,1] and we describe our regression results in the situation of fixed design points $0 \le x_1 \le x_2 \le \cdots \le x_n \le 1$ at which we consider nonnegative independent responses $Z_1,\cdots,Z_n$. Suppose that these responses are censored from the left and right by

How to cite this paper: Abdushukurov, A.A. and Abdikalikov, F.A. (2015) Semiparametric Estimator of Mean Conditional Residual Life Function under Informative Random Censoring from Both Sides. *Applied Mathematics*, **6**, 319-325.
http://dx.doi.org/10.4236/am.2015.62030

nonnegative r.v.-s $L_1,\cdots,L_n$ and $Y_1,\cdots,Y_n$ and the observed r.v.-s at design points x_i are in fact $\left\{\xi_i,\chi_i^{(0)},\chi_i^{(1)},\chi_i^{(2)}\right\}$ with $\xi_i=\max\left(L_i,\min\left(Z_i,Y_i\right)\right)$, $\chi_i^{(0)}=I\left(\min\left(Z_i,Y_i\right)<L_i\right)$, $\chi_i^{(1)}=I\left(L_i\le Z_i\le Y_i\right)$ and $\chi_i^{(2)}=\left(L_i\le Y_i<Z_i\right)$, where $I(A)$ denote the indicator of event A. Hence the observed data is consist of n vectors:

$$S^{(n)}=\left\{\left(\xi_i,\chi_i^{(0)},\chi_i^{(1)},\chi_i^{(2)},X_i\right),i=1,\cdots,n\right\}.$$

Assume that components of vectors $\left(Z_i,L_i,Y_i\right)$ are independent for a given covariate $X_i=x_i$. In sample $S^{(n)}$ the r.v.-s of interest Z_i's are observable only when $\chi_i^{(1)}=1$. Denote by F_x, K_x and G_x the conditional distribution functions (d.f.-s) of r.v.-s Z_x, L_x and Y_x respectively, given that $X=x$ and suppose that they are continuous.

Let H_x and N_x are conditional d.f.-s of ξ_x and $\eta_x=\min\left(Z_x,Y_x\right)$ for $X=x$. Then it's easy to see that $H_x(t)=K_x(t)N_x(t)$ with $N_x(t)=1-\left(1-F_x(t)\right)\left(1-G_x(t)\right)$, $t\ge 0$. In particular, if for all $x\in[0,1]$, $P\left(L_x\le Y_x\right)=1$, then we obtain the interval random censoring model.

The main problem in considered fixed design regression model is consist on estimation the conditional d.f. F_x of lifetimes and its functionals from the samples $S^{(n)}$ under nuisance d.f.-s K_x and G_x. The first product-limit type estimators for F_x in the case of no censoring from the left (that is $P\left(L_x=-\infty\right)=1$ or $K_x(t)\equiv 1$) proposed by Beran [1] and has been investigated by many authors (see, for example [2] [3]). In this article supposing that the random censoring from both sides is informative we use twice power type estimator of F_x from [4] [5] for estimation the mean conditional residual life function. Suppose that d.f.-s K_x and G_x are expressed from F_x by following parametric relationships for all $t\ge 0$:

$$\begin{cases}1-G_x(t)=\left(1-F_x(t)\right)^{\theta_x},\\ K_x(t)=\left(N_x(t)\right)^{\beta_x},\end{cases}\tag{1.1}$$

where θ_x and β_x are positive unknown nuisance parameters, depending on the covariate value x. Informative model (1.1) include the well-known conditional proportional hazards model (PHM) of Koziol-Green, which follows under absence of left random censorship (that is $\beta_x\equiv 0$). Estimation of F_x in conditional PHM is considered in [6]. Model (1.1) one can considered as an extended two sided conditional PHM. In the case of no covariates, model (1.1) first is proposed in [7] [8].

It is not difficult to verify that from (1.1) one can obtain following expression of d.f. F_x:

$$1-F_x(t)=\left[1-\left(H_x(t)\right)^{\lambda_x}\right]^{\gamma_x},\quad t\ge 0,\tag{1.2}$$

where $\lambda_x=\dfrac{1}{1+\beta_x}=1-p_x^{(0)}$, $\gamma_x=\dfrac{1}{1+\theta_x}=\dfrac{p_x^{(1)}}{1-p_x^{(0)}}$ and $p_x^{(m)}=P\left(\chi_x^{(m)}=1\right)$, $m=0$, 1, 2, with $p_x^{(0)}+p_x^{(1)}+p_x^{(2)}=1$. Then estimator of F_x one can constructed by natural plugging method as follows:

$$1-F_{xh}(t)=\left\{1-\left[H_{xh}(t)\right]^{\lambda_{xh}}\right\}^{\gamma_{xh}},\quad t\ge 0.\tag{1.3}$$

Here $\gamma_{xh}=p_{xh}^{(1)}\left(1-p_{xh}^{(0)}\right)^{-1}$, $\lambda_{xh}=1-p_{xh}^{(0)}$,

$$p_{xh}^{(m)}=\sum_{i=1}^{n}\omega_{ni}\left(x;h_n\right)\chi_i^{(m)},\quad m=0,1,2,$$

and

$$H_{xh}(t)=\sum_{i=1}^{n}\omega_{ni}\left(x;h_n\right)I\left(\xi_i\le t\right),$$

are smoothed estimators of λ_x, γ_x, $p_x^{(m)}$ and $H_x(t)$, used Gasser-Müllers weights $\left\{\omega_{ni}\left(x;h_n\right)\right\}_{i=1}^{n}$:

$$\omega_{ni}\left(x;h_n\right)=\int_{x_{i-1}}^{x_i}\frac{1}{h_n}\pi\left(\frac{x-y}{h_n}\right)\mathrm{d}y\left(\int_0^{x_n}\frac{1}{h_n}\pi\left(\frac{x-y}{h_n}\right)\mathrm{d}y\right)^{-1},$$

$x_0 = 0$, $\pi(y)$ is a known probability density function (kernel), and $\{h_n\}$ is a sequence of positive constants tending to 0 as $n \to \infty$, called the bandwidth sequence. Note that in the case of no censoring from the left the estimator (1.3) is coincides with estimator in conditional Koziol-Green model in [6]. Note also that a class of power type estimators for conditional d.f.-s for several models authors have considered in book [9]. Estimator (1.3) was presented in [4] and its asymptotic properties have been investigated in [5]. Now we demonstrate some of these results.

2. Asymptotic Results for Estimator of Conditional Distribution Function

For asymptotic properties of estimator (1.3) we need some notations. For the design points $x_1, \cdots, x_n$ and kernel π we denote

$$\underline{\Delta}_n = \min_{1 \le i \le n}(x_i - x_{i-1}), \quad \overline{\Delta}_n = \max_{1 \le i \le n}(x_i - x_{i-1}),$$

$$\|\pi\|_2^2 = \int_{-\infty}^{\infty} \pi^2(y)\mathrm{d}y, \quad m_v(\pi) = \int_{-\infty}^{\infty} y^v \pi(y)\mathrm{d}y, \quad v = 1,2.$$

Let $\tau_{F_x} = \sup\{t \ge 0 : F_x(t) = 0\}$ and $T_{F_x} = \inf\{t \ge 0 : F_x(t) = 1\}$ are lower and upper bounds of support of d.f. F_x. Then by (1.1):

$$\tau_{F_x} = \tau_{G_x} = \tau_{N_x} = \tau_{K_x} = \tau_{H_x} \quad \text{and} \quad T_{F_x} = T_{G_x} = T_{N_x} = T_{K_x} = T_{H_x}.$$

In [4] authors have proved the following property of two sided conditional PHM (1.1).

Theorem 2.1 [5]**.** For a given covariate x, the model (1.1) holds if and only if r.v. ξ_x and the vector $\left(\chi_x^{(0)}, \chi_x^{(1)}, \chi_x^{(2)}\right)$ are independent.

This characterization of submodel (1.1) plays an important role for investigation the properties of estimator (1.3).

Let's introduce some conditions:

(C1) As $n \to \infty$, $x_n \to 1$, $\overline{\Delta}_n = O\left(\frac{1}{n}\right)$, $\overline{\Delta}_n - \underline{\Delta}_n = o\left(\frac{1}{n}\right)$.

(C2) π is a probability density function with compact support $[-M, M]$ for some $M > 0$, with $m_1(\pi) = 0$ and $|\pi(y) - \pi(y')| \le C_\pi |y - y'|$, where C_π is some constant.

(C3) $\dot{F}_x(t) = \frac{\partial}{\partial x} F_x(t)$ and $\ddot{F}_x(t) = \frac{\partial^2}{\partial x^2} F_x(t)$ exist and are continuous for $0 \le x \le 1$ and $\tau \le t \le T$, with $\tau_{F_x} < \tau < T < T_{F_x}$.

(C4) $\dot{\theta}_x = \frac{\mathrm{d}}{\mathrm{d}x}\theta_x$ and $\dot{\beta}_x = \frac{\mathrm{d}}{\mathrm{d}x}\beta_x$ exist and are continuous for $0 \le x \le 1$.

Let's also denote: $r^{-1} = \sup_{\tau \le t \le T}\left[\left(H_x(t)\right)^{p_x^{(0)}} - H_x(t)\right]^{-1}$,

$$\dot{H}_x(t) = \frac{\partial}{\partial x} H_x(t), \quad \ddot{H}_x(t) = \frac{\partial^2}{\partial x^2} H_x(t), \quad \left\|\dot{H}\right\| = \sup_{(x;t) \in [0,1] \times [\tau, T]} \left|\dot{H}_x(t)\right|, \quad \left\|\ddot{H}\right\| = \sup_{(x;t) \in [0,1] \times [\tau, T]} \left|\ddot{H}_x(t)\right|,$$

$$\dot{p}_x^{(m)} = \frac{\mathrm{d}}{\mathrm{d}x} p_x^{(m)}, \quad \ddot{p}_x^{(m)} = \frac{\mathrm{d}^2}{\mathrm{d}x^2} p_x^{(m)}, \quad \left\|\dot{p}_x^{(m)}\right\| = \sup_{0 \le x \le 1} \left|\dot{p}_x^{(m)}\right|, \quad \left\|\ddot{p}_x^{(m)}\right\| = \sup_{0 \le x \le 1} \left|\ddot{p}_x^{(m)}\right|, \quad m = 0,1.$$

Note that existence of all these derivatives follows from conditions (C3) and (C4). Now we state some asymptotic results for estimator (1.3), which have proved in [5].

Theorem 2.2 [5] **(uniform strong consistency with rate).** Assume (C1)-(C4), $\tau_{F_x} < \tau < T < T_{F_x}$. If $h_n \to 0$, $\frac{nh_n^5}{\log n} = O(1)$, as $n \to \infty$, then

$$\sup_{\tau \le t \le T} \left|F_{xh}(t) - F_x(t)\right| \overset{\text{a.s.}}{=} O\left(\left(\frac{\log n}{nh_n}\right)^{1/2}\right).$$

Theorem 2.3 [5] **(almost sure asymptotic representation with weighted sums).** Under the conditions of Theorem 2.2 with $r>0$, we have for $t\in\left(\tau_{F_x},T_{F_x}\right)$:

$$F_{xh}(t)-F_x(t)=\sum_{i=1}^{n}\omega_{ni}(x;h_n)\Psi_{tx}\left(\xi_i,\chi_i^{(0)},\chi_i^{(1)},\chi_i^{(2)}\right)+q_n(t,x),$$

where

$$\Psi_{tx}\left(\xi_i,\chi_i^{(0)},\chi_i^{(1)},\chi_i^{(2)}\right)=\left(1-F_x(t)\right)\Bigg\{p_x^{(1)}\left[\left(H_x(t)\right)^{p_x^{(0)}}-H_x(t)\right]^{-1}\left(I\left(\xi_i\le t\right)-H_x(t)\right)$$

$$-\left[\frac{p_x^{(1)}}{\left(1-p_x^{(0)}\right)^2}\log\left[1-\left(H_x(t)\right)^{1-p_x^{(0)}}\right]+\frac{p_x^{(1)}}{1-p_x^{(0)}}H_x(t)\log H_x(t)\left[\left(H_x(t)\right)^{p_x^{(0)}}-H_x(t)\right]^{-1}\right]$$

$$\times\left(\chi_i^{(0)}-p_x^{(0)}\right)-\frac{1}{1-p_x^{(0)}}\log\left[1-\left(H_x(t)\right)^{1-p_x^{(0)}}\right]\left(\chi_i^{(1)}-p_x^{(1)}\right)\Bigg\}.$$

and as $n\to\infty$,

$$\sup_{\tau\le t\le T}\left|q_n(t,x)\right|\overset{\text{a.s.}}{=}O\left(\frac{\log n}{nh_n}\right).$$

Corollary. Under the conditions of Theorem 2.3, and as $n\to\infty$, for $\tau\le t\le T$:

$$\left(nh_n\right)^{1/2}\left(F_{xh}(t)-F_x(t)\right)\overset{\text{a.s.}}{=}\left(nh_n\right)^{1/2}\sum_{i=1}^{n}\omega_{ni}(x;h_n)\Psi_{tx}\left(\xi_i,\chi_i^{(0)},\chi_i^{(1)},\chi_i^{(2)}\right)+O\left(\frac{\log n}{\left(nh_n\right)^{1/2}}\right).$$

Theorem 2.4 [5] **(asymptotic normality).** Assume (C1)-(C4). $\tau_{F_x}<\tau<T<T_{F_x}$.
(A) If $nh_n^5\to 0$ and $\left(nh_n\right)^{1/2}\log n\to 0$, then for $\tau\le t\le T$, as $n\to\infty$,

$$\left(nh_n\right)^{1/2}\left(F_{xh}(t)-F_x(t)\right)\xrightarrow{d}N\left(0,\sigma_x^2(t)\right);$$

(B) If $h_n=Cn^{-1/5}$ for some $C>0$, then for $\tau\le t\le T$, as $n\to\infty$,

$$\left(nh_n\right)^{1/2}\left(F_{xh}(t)-F_x(t)\right)\xrightarrow{d}N\left(a_x(t),\sigma_x^2(t)\right),$$

where

$$a_x(t)=\frac{1}{2}\left(1-F_x(t)\right)\Bigg\{p_x^{(1)}\left[\left(H_x(t)\right)^{p_x^{(0)}}-H_x(t)\right]^{-1}\ddot{H}_x(t)$$

$$-\left[\frac{p_x^{(1)}}{\left(1-p_x^{(0)}\right)^2}\log\left[1-\left(H_x(t)\right)^{1-p_x^{(0)}}\right]+\frac{p_x^{(1)}}{\left(1-p_x^{(0)}\right)}H_x(t)\log H_x(t)\left[\left(H_x(t)\right)^{p_x^{(0)}}-H_x(t)\right]^{-1}\right]\ddot{p}_x^{(0)}$$

$$-\frac{1}{1-p_x^{(0)}}\log\left[1-\left(H_x(t)\right)^{1-p_x^{(0)}}\right]\ddot{p}_x^{(1)}\Bigg\}m_2(\pi)C^{5/2},$$

$$\sigma_x^2(t)=\|\pi\|_2^2\left(1-F_x(t)\right)^2\gamma_x(t),$$

with

$$\gamma_x(t) = A_x^2(t)H_x(t)\left(1-H_x(t)\right) + B_x^2(t)\,p_x^{(0)}\left(1-p_x^{(0)}\right) + C_x^2(t)\,p_x^{(1)}\left(1-p_x^{(1)}\right) - 2B_x(t)C_x(t)\,p_x^{(0)}p_x^{(1)},$$

$$A_x(t) = p_x^{(1)}\left[\left(H_x(t)\right)^{p_x^{(0)}} - H_x(t)\right]^{-1},$$

$$B_x(t) = -\left[\frac{p_x^{(1)}}{\left(1-p_x^{(0)}\right)}C_x(t) + \frac{A_x(t)}{\left(1-p_x^{(0)}\right)}H_x(t)\log H_x(t)\right],$$

$$C_x(t) = -\frac{1}{\left(1-p_x^{(0)}\right)}\log\left[1-\left(H_x(t)\right)^{1-p_x^{(0)}}\right].$$

It is necessary to note that Theorems 2.1-2.4 are extended the corresponding theorems in conditional PHM of Koziol-Green from [6].

In the next Section 3 we use these theorems for investigation the properties of the estimator of mean conditional residual life function.

3. Asymptotic Normality of Estimator of Mean Conditional Residual Life Function

The conditional residual lifetime distribution defined as

$$F_x(s/t) = P\left(Z_x - t \le s/Z_x > t\right),$$

i.e. the d.f. of residual lifetime, conditional on survival upon a given time t and at a given value of the covariate x. Then for $0 < s < T_{F_x}$,

$$F_x(s/t) = \frac{F_x(t+s) - F_x(t)}{1-F_x(t)}. \tag{3.1}$$

One of main characteristics of d.f. (3.1) is its mean, *i.e.* mean conditional residual life function

$$\mu_x(t) = E\left(Z_x - t/Z_x > t\right) = \left(1-F_x(t)\right)^{-1}\int_t^\infty \left(1-F_x(s)\right)\mathrm{d}s, \quad t > 0. \tag{3.2}$$

We estimate functional $\mu_x(t)$ by plugging in estimator (1.3) instead of F_x in (3.2). But from section 2 we know that estimator (1.3) have consistent properties in some interval $[\tau, T]$ with $\tau_{F_x} < \tau < T < T_{F_x}$. Therefore, we will consider the following truncated version of (3.2):

$$\mu_x^T(t) = \left(1-F_x(t)\right)^{-1}\int_t^T \left(1-F_x(s)\right)\mathrm{d}s, \quad \tau < t < T. \tag{3.3}$$

Now we estimate (3.3) by statistics

$$\mu_{xh}^T(t) = \left(1-F_{xh}(t)\right)^{-1}\int_t^T \left(1-F_{xh}(s)\right)\mathrm{d}s, \quad \tau < t < T. \tag{3.4}$$

We have following asymptotic normality result.

Theorem 3.1. Assume (C1)-(C3) in $[\tau, T]$ with $\tau_{F_x} < \tau$, $T < T_{F_x}$.

(A) If $nh_n^5 \to 0$ and $\dfrac{\log n}{\left(nh_n\right)^{1/2}} \to 0$, as $n \to \infty$, then

$$\left(nh_n\right)^{1/2}\left(\mu_{xh}^T(t) - \mu_x^T(t)\right) \xrightarrow{d} N\left(0, \beta_x^2(t)\right);$$

(B) If $h_n = Cn^{-1/5}$ for some $C > 0$, then as $n \to \infty$,

$$\left(nh_n\right)^{1/2}\left(\mu_{xh}^T(t) - \mu_x^T(t)\right) \xrightarrow{d} N\left(\alpha_x(t), \beta_x^2(t)\right).$$

Here

$$\alpha_x(t)=\frac{1}{2}C^{5/2}m_2(\pi)\frac{1}{1-F_x(t)}\left\{\int_t^T a_x(s)\mathrm{d}s-a_x(t)\int_t^T\left(1-F_x(s)\right)\mathrm{d}s\right\},$$

$$\beta_x^2(t)=\|\pi\|_2^2\frac{1}{\left(1-F_x(t)\right)^2}\int_t^T\left(\int_t^T\left(1-F_x(s)\right)\mathrm{d}s\right)^2\mathrm{d}\gamma_x(s),$$

and $\gamma_x(t)$ from Theorem 2.4.

Proof of theorem 3.1. By standard manipulations and Theorem 2.3 we have that

$$\mu_{xh}^T(t)-\mu_x^T(t)=\int_t^T\left[\frac{1-F_{xh}(s)}{1-F_{xh}(t)}-\frac{1-F_x(s)}{1-F_x(t)}\right]\mathrm{d}s=M_{nx}(t)+\sum_{k=1}^4 Q_{nx}^{(k)}(t),$$

where

$$M_{nx}(t)=\sum_{i=1}^n\omega_{ni}(x;h_n)\left[-\frac{1}{1-F_x(t)}\int_t^T\Psi_{sx}\left(\xi_i,\chi_i^{(0)},\chi_i^{(1)},\chi_i^{(2)}\right)+\frac{\Psi_{tx}\left(\xi_i,\chi_i^{(0)},\chi_i^{(1)},\chi_i^{(2)}\right)}{\left(1-F_x(t)\right)^2}\int_t^T\left(1-F_x(s)\right)\mathrm{d}s\right],$$

$$Q_{nx}^{(1)}(t)=-\frac{1}{1-F_x(t)}\int_t^T q_n(s;x)\mathrm{d}s,$$

$$Q_{nx}^{(2)}(t)=\frac{q_n(t;x)}{\left(1-F_x(t)\right)^2}\int_t^T\left(1-F_x(s)\right)\mathrm{d}s,$$

$$Q_{nx}^{(3)}(t)=\frac{\left(F_{xh}(t)-F_x(t)\right)}{\left(1-F_x(t)\right)^2}\int_t^T\left(F_{xh}(s)-F_x(s)\right)\mathrm{d}s,$$

$$Q_{nx}^{(4)}(t)=\frac{\left(F_{xh}(t)-F_x(t)\right)^2}{\left(1-F_x(t)\right)^2}\int_t^T\left(1-F_{xh}(s)\right)\mathrm{d}s.$$

For $Q_{nx}^{(1)}$ and $Q_{nx}^{(2)}$ we use Theorem 2.3, for $Q_{nx}^{(3)}$ and $Q_{nx}^{(4)}$, Theorem 2.2. Then we see that all these remainder terms uniformly on $[\tau,T]$ almost surely have order $O\left((nh_n)^{-1}\log n\right)$.

Now statements (A) and (B) of theorem follows from corresponding statements of the theorem 2.4 by standard arguments.

Theorem 3.1 is proved.

Acknowledgements

This work is supported by Grant F4-01 of Fundamental Research Found of Uzbekistan.

References

[1] Beran, R (1981) Nonparametric Regression with Randomly Censored Survival Data. Technical Report, University of California, Berkeley, 19.

[2] Van Keilegom, I. and Veraverbeke, N. (1996) Uniform Strong Convergence for the Conditional Kaplan-Meir Estimator and Its Quantiles. *Communications in Statistics—Theory and Methods*, **25**, 2251-2265.

[3] Van Keilegom, I. and Veraverbeke, N. (1997) Estimation and Bootstrap with Censored Data in Fixed Design Nonparametric Regression. *Annals of the Institute of Statistical Mathematics*, **49**, 467-491. http://dx.doi.org/10.1023/A:1003166728321

[4] Abdikalikov, F.A. and Abdushukurov, A.A. (2012) Informative Regression Model under Random Censorship from Both Sides and Estimating of Survival Function. Book of Abstracts, *XXX Internet. Seminar on Stability Problems for stochastic Models*, Svetlogorsk, 24-28 September 2012, 3-4.

[5] Abdikalikov, F.A. and Abdushukurov, A.A. (2012) Semiparametrical Estimation of Conditional Survival Function in Informative Regression Model of Random Censorship from Both Sides. In: *Statistical Methods of Estimation and Hypothesis Testing*, Perm State University, Perm, Issue 24, 145-162. (In Russian)

[6] Veraverbeke, N. and Cadarso-Suárez, C. (2000) Estimation of the Conditional Distribution in a Conditional Koziol-Green Model. *Test*, **9**, 97-122.

[7] Abdushukurov, A.A. (1994) Model of Random Censoring from Both Sides and Independence Criterion for It. *Doclady Acad. Sci. Uzbekistan*, **11**, 8-9. (In Russian)

[8] Abdushukurov, A.A. (1998) Nonparametric Estimation of Distribution Function Based on Relative Risk Function. *Communications in Statistics—Theory and Methods*, **27**, 1991-2012. http://dx.doi.org/10.1080/03610929808832205

[9] Abdikalikov, F.A. and Abdushukurov, A.A. (2012) An Investigating of Power-Type Estimators of Lifetime Functions in Regression Models. LAMBERT Academic Publishing (LAP), Germany, 89. (In Russian)

Applied Mathematics, 2015, 6, 326-331
Published Online February 2015 in SciRes. http://www.scirp.org/journal/am
http://dx.doi.org/10.4236/am.2015.62031

Scientific Research Publishing

Optimum Maintenance Policy for a One-Shot System with Series Structure Considering Minimal Repair

Tomohiro Kitagawa, Tetsushi Yuge, Shigeru Yanagi

Department of Electrical and Electronic Engineering, National Defense Academy, Yokosuka, Japan
Email: em52001@nda.ac.jp, yuge@nda.ac.jp, shigeru@nda.ac.jp

Received 15 January 2015; accepted 2 February 2015; published 5 February 2015

Abstract

One-shot systems such as missiles and extinguishers are placed in storage for a long time and used only once during their lives. Their reliability deteriorates with time even when they are in storage, and their failures are detected only through inspections for their characteristics. Thus, we need to decide an appropriate inspection policy for such systems. In this paper, we deal with a system comprising non-identical units in series, where only minimal repairs are performed when unit failures are detected by periodic inspections. The system is replaced and becomes "as good as new" when the *n*th failure of the system is detected. Our objective is to find the optimal inspection interval and number of failures before replacement that minimize the expected total system cost per unit of time.

Keywords

One-Shot System, Maintenance Policy, Minimal Repair, Cost Rate

1. Introduction

Systems such as missiles and extinguishers are used only once during their lives. Once the system is placed in an operational position or a nearby depot, it spends almost its entire life in storage until it is used. Usually, such systems are not moved except for inspections or other special situations. Because of these characteristics, these systems are called one-shot systems or storage systems.

The reliability of a one-shot system decreases with time even if it is placed in storage. Hence, inspections should be carried out at appropriate times to ensure high reliability. Frequent inspections will ensure its high availability, while they sometimes incur a high cost that may not be acceptable to users.

How to cite this paper: Kitagawa, T., Yuge, T. and Yanagi, S. (2015) Optimum Maintenance Policy for a One-Shot System with Series Structure Considering Minimal Repair. *Applied Mathematics*, **6**, 326-331.
http://dx.doi.org/10.4236/am.2015.62031

Inspection policy problems for a one-shot system have been studied by numerous researchers. Barlow and Proschan [1] found an optimum inspection policy that minimized the cost rate in the case that a system was perfectly repaired upon failure detection. Ito and other researchers assumed that a system consisted of two and three types of unit [2]-[4]. They formulated the periodic inspection policy for a system requiring high reliability. Yun and other researchers considered the inspection policy for a system with two types of unit, where intrinsic replacement times for one type of unit were predetermined [5]-[7]. They determined the optimum inspection schedule of another type of unit by simulation to meet the goal of reliability.

All the above papers dealt with perfect repairs upon the detection of failures. On the other hand, there is another type of repair action. A minimal repair simply restores a failed unit to the working state. In this case, the hazard rate of the minimally repaired unit is the same as that immediately before the failure. Minimal repairs are useful for a complex one-shot system because they have a much lower cost than perfect repairs or replacements. Nakagawa [8] discussed an inspection policy for the case that the failures of a unit were detected instantly and minimally repaired. As we explained above, failures are not always detected instantly in a one-shot system. Thus, we have to take system down into account to develop a more practical model of a one-shot system.

In this paper, we deal with an inspection policy for a one-shot system that consists of m units in series. The system is not available when at least one unit is out of order. We assume that the system is inspected at periodic time intervals, T, and failures are detected only by inspections. A minimal repair is performed when a failure is detected, and all units in the system are replaced and become "as good as new" when a total of n failures are detected after the last replacement. The system has a predetermined limitation for the number of minimal repairs, N. We minimize the expected cost rate, which is expressed as a function of n and T. In Section 2, we explain the proposed model and derive the cost rate. A numerical example is shown in Section 3.

2. Model Assumptions and Analysis

2.1. Notations & Nomenclature

The following notations and nomenclature are used.
Cost rate: cost per unit time
N : limitation of number of minimal repairs for a system
n : number of failures until replacement, *i.e.*, $n \le N+1$.
T : inspection interval
m : number of units in a system
C_I : inspection cost of a system
C_{Ri} : minimal repair cost of unit i
C_D : risk (*i.e.*, cost) per unit of time resulting from system down
C_P : replacement cost of a system
$F_s^{(1)}$: failure distribution function of a system until first failure
$\bar{F}_s^{(1)}$: reliability function of a system between $(l-1)$ th failure and lth failure, which can be given by as the product of reliability function of each unit, where the 0th failure indicates the time that a system is in service.
$\mu_s^{(l)}$: mean operating time of a system between $(l-1)$ th failure and lth failure
H_i : cumulative hazard rate function of unit i
$\tau^{(l)}$: expected total time until detection of lth failure
$C_o^{(l)}$: expected total cost until detection of lth failure
$\rho_i^{(n)}$: ratio of the number of failures of unit i to n
$C(n,T)$: cost rate function, given by $C_o^{(l)} / \tau^{(l)}$

2.2. Model Assumptions

We consider a one-shot system that is described in the following. **Figure 1** shows an example of the process of the proposed model.

1) The system has a series structure of m units (unit 1, unit 2, …, unit m) and the system's hazard rate increases with time.

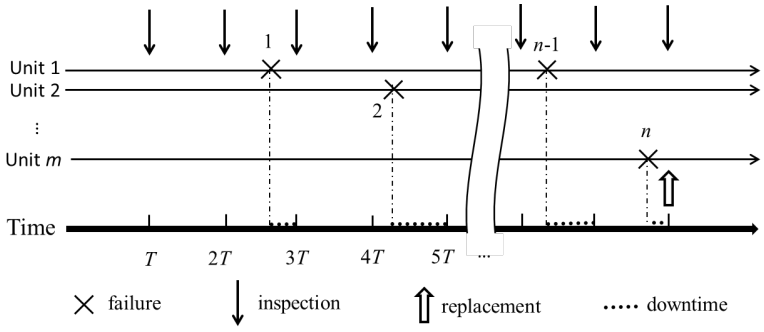

Figure 1. Example of process of the model.

2) All the units in the system are inspected periodically and simultaneously.

3) A failure of a unit is detected at the following inspection, and a minimal repair is performed upon the detection. The hazard rate of a failed unit is not changed by the minimal repair.

4) System down incurs some risk, which is the product of the system down probability and the incurred cost. In this paper, we regard the risk as the system down cost per unit of time for simplicity.

5) When a total of n failures are detected since the last replacement, all the units in the system are replaced and the system becomes "as good as new."

6) Times needed for inspections, minimal repairs, and replacements are negligible.

2.3. Model Analysis

Here we derive the cost rate function of the system. We can regard the time interval between replacements as one cycle because the system is renewed when n failures are detected after the last replacement. The expected cost rate is calculated from the expected cost per cycle and the expected time per cycle.

First, we consider the case that n = 1, which means that the system is replaced when the first failure is detected. In this case, the expected total cost until replacement is obtained as

$$\begin{aligned} C_o^{(1)} &= \sum_{k=1}^{\infty} \int_{(k-1)T}^{kT} \left[C_I k + C_D (kT - t) + C_P \right] \mathrm{d}F_s^{(1)}(t) \\ &= (C_I + C_D T) \sum_{k=0}^{\infty} \bar{F}_s^{(1)}(kT) - C_D \mu_s^{(1)} + C_P, \end{aligned} \tag{1}$$

where $\mu_s^{(1)} = \int_0^{\infty} \bar{F}_s^{(1)}(t)\,\mathrm{d}t$.

Similarly, we can derive $\tau^{(1)}$ as

$$\tau^{(1)} = \sum_{k=1}^{\infty} \int_{(k-1)T}^{kT} kT \mathrm{d}F_s^{(1)}(t) = T \sum_{k=0}^{\infty} \bar{F}_s^{(1)}(kT). \tag{2}$$

The cost rate function when $n = 1$ is

$$C(1,T) = \frac{C_o^{(1)}}{\tau^{(1)}} = C_D + \frac{C_I}{T} + \frac{C_P - C_D \mu_s^{(1)}}{T \sum_{k=0}^{\infty} \bar{F}_s^{(1)}(kT)}. \tag{3}$$

The result also can be derived using the results in [1].

To calculate the cost rate for $n \geq 2$, we use two approximations for the system parameters. One is used for the mean operating time and the other is used for the number of repairs of each unit. We have found that these approximations are useful in many cases, as shown in the numerical example in Section 3.

1) Mean operating time

The exact mean operating time until the second or a later failure is obtained by applying multiple integrals. It is not easy to calculate these integrals when n becomes large. Thus, we focus on the fact that the probability of detecting multiple failures at one inspection is very small. If we ignore the multiple failures and assume that the first failure of the system occurs at exactly $\mu_s^{(1)}$, we express $\bar{F}_s^{(2)}$ and $\mu_s^{(2)}$ as

$$\bar{F}_s^{(2)}(t)=\prod_{i=1}^{m}\exp\left\{-H_i\left(t+\mu_s^{(1)}\right)+H_i\left(\mu_s^{(1)}\right)\right\}, \tag{4}$$

$$\mu_s^{(2)}=\int_0^{\infty}\bar{F}_s^{(2)}(t)\,\mathrm{d}t. \tag{5}$$

$\mu_s^{(3)},\cdots,\mu_s^{(n)}$ are also obtained similarly. In other words, we assume that the system operating time between the $(k-1)$ th failure and the kth failure $(k<l)$ is exactly $\mu_s^{(k)}$. Then, $\bar{F}_s^{(l)}$ and $\mu_s^{(l)}\ (l\geq 2)$ are given by

$$\bar{F}_s^{(l)}(t)=\prod_{i=1}^{m}\exp\left\{-H_i\left(t+\sum_{j=1}^{l-1}\mu_s^{(j)}\right)+H_i\left(\sum_{j=1}^{l-1}\mu_s^{(j)}\right)\right\}, \tag{6}$$

$$\mu_s^{(l)}=\int_0^{\infty}\bar{F}_s^{(l)}(t)\,\mathrm{d}t. \tag{7}$$

2) Number of failures of unit *i*

We introduce $\rho_i^{(n)}$, which represents the ratio of the number of failures of unit *i* to *n*. Ignoring the downtime, the expected number of failures of unit *i* until a specific time would be calculated theoretically using the cumulative hazard rate function. We also use the cumulative hazard rate function and express $\rho_i^{(n)}$ as

$$\rho_i^{(n)}=\frac{H_i\left(\sum_{j=1}^{n}\mu_s^{(j)}\right)}{\sum_{i=1}^{m}H_i\left(\sum_{j=1}^{n}\mu_s^{(j)}\right)}. \tag{8}$$

Using these two approximations, we can obtain the expected cost and time until replacement as

$$C_o^{(n)}=(C_I+C_DT)\sum_{l=1}^{n}\sum_{k=0}^{\infty}\bar{F}_s^{(l)}(kT)-C_D\sum_{l=1}^{n}\mu_s^{(l)}+(n-1)\sum_{i=1}^{m}\rho_i^{(n)}C_{Ri}+C_P, \tag{9}$$

$$\tau^{(n)}=T\sum_{l=1}^{n}\sum_{k=0}^{\infty}\bar{F}_s^{(l)}(kT). \tag{10}$$

The expected cost rate until replacement, $C(n,T)$, is given by

$$C(n,T)=\frac{C_o^{(n)}}{\tau^{(n)}}=C_D+\frac{C_I}{T}+\frac{C_P-C_D\sum_{l=1}^{n}\mu_s^{(l)}+(n-1)\sum_{i=1}^{m}\rho_i^{(n)}C_{Ri}}{T\sum_{l=1}^{n}\sum_{k=0}^{\infty}\bar{F}_s^{(l)}(kT)}. \tag{11}$$

The larger *n* and *T* become, the longer the downtime becomes. However, too small value of *n* and *T* incur high replacement and inspection costs per unit of time. Thus, we have to determine the optimum values of *n* and *T* that minimize Equation (11).We determine the optimum values of *n* and *T* that minimize Equation (11) subject to $n\leq N+1$ by the steepest decent method.

3. Numerical Example

We show a numerical example of a missile system. The missile has three units; unit 1 is a blasting case, unit 2 is a guide and control unit, and unit 3 is an engine unit. Calculated results are compared with simulation results and errors are evaluated.

Parameters are given in **Table 1**, where Wei (η,β) indicates Weibull distributions whose reliability function is $\exp\left\{-(t/\eta)^{\beta}\right\}$. The unit of time is a day and the unit of cost is 1000 dollars. The optimum solutions and the errors are shown in **Table 2**. The sample number of the simulation is 1 million, and the error is estimated assuming that the simulation result is correct.

In this case, the optimum value of *n* is the same in both methods, but the optimum values of *T* and the minimum cost rate have some errors.

Figure 2 shows the cost rate plotted against *n* and *T*. It can be seen that the cost rate function is unimodal with respect to both *n* and *T* and the optimal policy can be determined uniquely.

Hence, we describe the tendency of the errors. First, we used the approximation for the mean operating times (Equation (7)). **Table 3** shows the errors for the example. The error increases as T or n increases in many cases. When T increases, the probability of detecting multiple failures at inspections increases, but this effect is ignored in Equations (6) and (7). That is why the mean operating time calculated using the approximation is longer than the value computed by simulation in many situations. Next, we also used the approximation for the number of repairs for each unit (Equation (8)). The errors are smaller than those for the mean operating time in many cases. In this example, the errors are about 1%. They also appear to depend on the values of n and T, but the behaviors are complex.

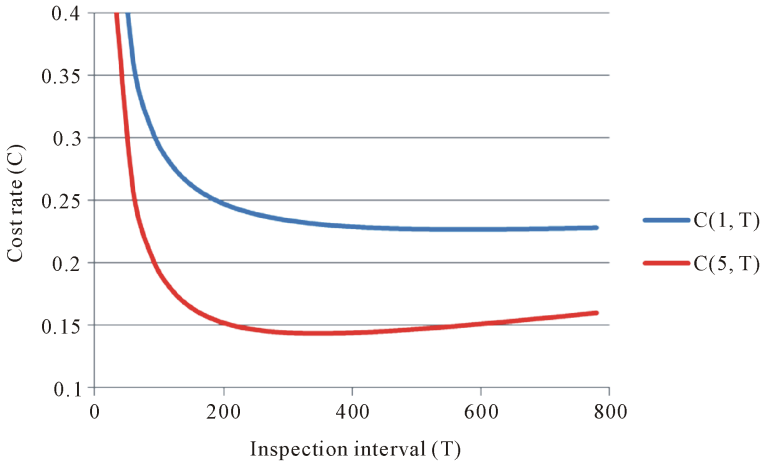

Figure 2. Cost rates plotted against inspection interval.

Table 1. Parameters.

N	m	Unit No.(i)	CDF	C_{Ri}	C_I	C_D	C_P
		1	Wei (4000, 1.2)	30			
4	3	2	Wei (5000, 1.5)	40	10	0.35	400
		3	Wei (6000, 2.0)	50			

Table 2. Optimum solutions and errors.

Method	n	T	$C(n,T)$
Proposed approximation	5	346	0.1433
Simulation	5	320	0.1451
Errors (%)	0	8.1	−1.2

Table 3. Errors of mean operating time (%).

T \ n	2	3	4	5
10	−1.93	−2.19	−2.11	−2.03
100	−1.17	−0.93	−0.71	−0.37
300	0.68	1.63	2.57	3.51
500	2.42	4.30	5.90	7.29

4. Conclusion

We considered a multiple-unit repairable system that is inspected periodically and whose failures are detected at the next inspection. We derived the cost rate function by using two approximations and determined the optimum number of failures until replacement and the inspection interval. We confirmed the effectiveness of our approximate method by a numerical example. Note that the proposed method does not always find the optimal solution. Establishing a search method to find global optimal solutions remains as a future work. Moreover, we assumed that no maintenance was performed before failure. However, in practice, not only repairs but also other preventive maintenance actions are performed for many types of systems. This should be considered when expanding the proposed model.

References

[1] Barlow, P.E. and Proschan, F. (1965) Mathematical Theory of Reliability. John Wiley & Sons, Hoboken.

[2] Ito, K. and Nakagawa, T. (1992) Optimal Inspection Policies for a System in Storage. *Computers and Mathematics with Applications*, **24**, 87-90. http://dx.doi.org/10.1016/0898-1221(92)90232-7

[3] Ito, K. and Nakagawa, T. (2000) Optimal Inspection Policies for a System with Degradation at Periodic Test. *Mathematical and Computer Modeling*, **31**, 191-195.

[4] Ito, K., Nakagawa, T. and Nishi, K. (1995) Extended Optimal Inspection Policies for a System in Storage. *Mathematical and Computer Modelling*, **22**, 83-78. http://dx.doi.org/10.1016/0895-7177(95)00184-4

[5] Yun, W.Y., Kim, H.W. and Han, Y.J. (2012) Simulation-Based Inspection Policies for a One-Shot System in Storage. *Proceedings of the* 5*th Asia-Pacific International Symposium*, Nanjing, 1-3 November 2012, 621-628.

[6] Yun, W.Y., Liu, K., Han, Y.J., Rhee, D.W. and Han, C.G. (2013) Simulation-Based Optimal Inspection Schedules for One-Shot Systems with Two Types of Units. *Proceedings of* 17th *International Conference on Industrial Engineering Theory, Applications and Practice*, Pusan, 6-9 October 2013, 314-320.

[7] Yun, W.Y., Zhao, Q. and Kim, H.W. (2014) Optimal Inspection Schedules for One-Shot Systems in Storage with Deployment Plan. *Proceedings of the* 6*th Asia-Pacific International Symposium*, Sapporo, 21-23 August, 578-585.

[8] Nakagawa, T. (2005) Maintenance Theory of Reliability. Springer, London.

Applied Mathematics, 2015, 6, 332-344
Published Online February 2015 in SciRes. http://www.scirp.org/journal/am
http://dx.doi.org/10.4236/am.2015.62032

Availability and Profit Optimization of Series-Parallel System with Linear Consecutive Cold Standby Units

Muhammad Sagir Aliyu[1*], Ibrahim Yusuf[2], U. A. Ali[1]

[1]Department of Mathematics, Usmanu Dan Fodio University, Sokoto, Nigeria
[2]Department of Mathematical Sciences, Bayero University, Kano, Nigeria
Email: [*]muhammadsagiraliyu@yahoo.com, iyusuf.mth@buk.edu.ng, ubahamad@yahoo.co.uk

Received 16 January 2015; accepted 6 February 2015; published 10 February 2015

Abstract

In this paper, we study availability and profit optimization of a series-parallel system consisting of three subsystems *A*, *B* and *C* in which *A* and *B* are cold standby. Subsystem *A* consists of linear consecutive *k*-out-of-*n* units while subsystems *B* and *C* consist of a single unit each. The system works if any of *A* or *B* and *C* work. The objective of this study is to maximize the steady-state availability and profit. To solve the optimization problem, different numbers of units for $n = 2, 3, 4, 5$ in subsystem *A* are considered. Explicit expressions for busy period of repairmen, steady-state availability and profit function are derived using linear first order differential equations. Several cases are analyzed graphically for $n = 2, 3, 4, 5$ to investigate the effects of various system parameters on availability and profit. The paper also presents graphical comparison for specific values of system parameters and finds that the optimal system configuration is when $n = 5$.

Keywords

Availability, Profit, Cold Standby, Optimization

1. Introduction

The series-parallel systems consist of subsystems connected in series where each subsystem consists of units arranged in parallel. Failure of any one of the subsystems leads to the failure of the system. These systems are used in industries, power stations, manufacturing, production and telecommunications. Due to their importance in promoting and sustaining industries and economy, reliability measures of such systems have become an area of interest. Among the reliability measures of interest there are the steady-state availability, busy period, profit

[*]Corresponding author.

How to cite this paper: Aliyu, M.S., Yusuf, I. and Ali, U.A. (2015) Availability and Profit Optimization of Series-Parallel System with Linear Consecutive Cold Standby Units. *Applied Mathematics*, **6**, 332-344.
http://dx.doi.org/10.4236/am.2015.62032

function and mean time to system failure (MTSF). Availability and profit of redundant systems can be enhanced using highly reliable structural system design. Improving the reliability and availability of system/subsystem leads to an increase in production and associated profit. Researches carried out on optimization problem for series-parallel/*k*-out-of-*n* *G* systems can be found in Hu *et al.* [1], Khatab *et al.* [2] who analyzed the availability of *k*-out-of-*n* *G* system with non identical components subject to repair priorities, Krishnan *et al.* [3] analyzed the reliability and profit analysis of repairable *k*-out-of-*n* system with sensor, Juang *et al.* [4], Levitin [5], Li *et al.* [6] and Wang *et al.* [7]. Wang *et al.* [8] performed comparative analysis of availability among three systems with general repair times, reboot delay and switching failure. Wang *et al.* [9] performed comparative analysis of availability between two systems with warm standby units and different imperfect coverage. The problem considered in the present paper is different from the work of the above mentioned authors in the sense that a number of units incorporated in subsystem *A* as a linear consecutive *k*-out-of-*n*. The contribution of this paper is twofold. First is to develop the explicit expressions for steady-state availability, busy period of repair man and profit function. Second is to perform numerical investigation on the effect of system parameters on reliability indices mentioned above. Models developed in this paper are found to be highly beneficial to engineers, maintenance managers, system designers and plant management for proper maintenance analysis, decision, and evaluation of performance. Comparisons are performed for n = 2, 3, 4, 5, for steady-state availability and profit based on assumed numerical values given to the system parameters.

The organization of the paper is as follows. Assumptions' of the study and states of the systems are presented in Section 2. Models formulations are given in Section 3. The results of our numerical simulations and discussions are presented in Section 4. Finally, we make a concluding remark in Section 5.

2. Assumptions and States of the Systems

2.1. Assumptions

1) The system is attended by three repairmen;
2) The failure and repair time are to be assumed exponential;
3) Units in subsystem *A* are linear consecutive *k*-out-of-*n*;
4) Subsystem *A* and *B* are in cold standby;
5) Repair is instantaneous;
6) Repaired unit is as good as new.

2.2. States of the System

System I

$$S_0\left(A_{1O}, A_{2S}, B_S, C_O\right),$$

$$S_1\left(A_{1R}, A_{2O}, B_S, C_O\right),$$

$$S_2\left(A_{1W}, A_{2R}, B_O, C_O\right),$$

$$S_3\left(A_{1G}, A_{2S}, B_S, C_R\right),$$

$$S_4\left(A_{1W}, A_{2G}, B_S, C_R\right),$$

$$S_5\left(A_{1W}, A_{2R}, B_W, C_G\right),$$

$$S_6\left(A_{1W}, A_{2R}, B_G, C_R\right).$$

System II

$$S_0\left(A_{1O}, A_{2O}, A_{3S}, B_S, C_O\right),$$

$$S_1\left(A_{1R}, A_{2O}, A_{3O}, B_S, C_O\right),$$

$$S_2\left(A_{1G}, A_{2R}, A_{3G}, B_O, C_O\right),$$

$$S_3\left(A_{1W}, A_{2R}, A_{3G}, B_O, C_O\right),$$
$$S_4\left(A_{1G}, A_{2G}, A_{3S}, B_S, C_R\right),$$
$$S_5\left(A_{1R}, A_{2G}, A_{3G}, B_S, C_R\right),$$
$$S_6\left(A_{1G}, A_{2R}, A_{3G}, B_R, C_G\right),$$
$$S_7\left(A_{1G}, A_{2R}, A_{3G}, B_G, C_R\right),$$
$$S_8\left(A_{1W}, A_{2R}, A_{3G}, B_R, C_G\right),$$
$$S_9\left(A_{1W}, A_{2R}, A_{3G}, B_G, C_R\right).$$

System III

$$S_0\left(A_{1O}, A_{2O}, A_{3S}, A_{4S}, B_S, C_O\right),$$
$$S_1\left(A_{1R}, A_{2O}, A_{3O}, A_{4S}, B_S, C_O\right),$$
$$S_2\left(A_{1G}, A_{2R}, A_{3O}, A_{4O}, B_S, C_O\right),$$
$$S_3\left(A_{1W}, A_{2R}, A_{3O}, A_{4O}, B_S, C_O\right),$$
$$S_4\left(A_{1W}, A_{2W}, A_{3R}, A_{4G}, B_O, C_O\right),$$
$$S_5\left(A_{1G}, A_{2W}, A_{3R}, A_{4G}, B_O, C_O\right),$$
$$S_6\left(A_{1R}, A_{2G}, A_{3G}, A_{4S}, B_S, C_R\right),$$
$$S_7\left(A_{1W}, A_{2R}, A_{3G}, A_{4G}, B_S, C_R\right),$$
$$S_8\left(A_{1W}, A_{2W}, A_{3R}, A_{4G}, B_R, C_G\right),$$
$$S_9\left(A_{1W}, A_{2W}, A_{3R}, A_{4G}, B_G, C_R\right),$$
$$S_{10}\left(A_{1G}, A_{2W}, A_{3R}, A_{4G}, B_R, C_G\right),$$
$$S_{11}\left(A_{1G}, A_{2W}, A_{3R}, A_{4G}, B_G, C_R\right),$$
$$S_{12}\left(A_{1G}, A_{2G}, A_{3S}, A_{4S}, B_S, C_R\right),$$
$$S_{13}\left(A_{1G}, A_{2R}, A_{3G}, A_{4G}, B_S, C_R\right).$$

System IV

$$S_0\left(A_{1O}, A_{2O}, A_{3S}, A_{4S}, A_{5S}, B_S, C_O\right),$$
$$S_1\left(A_{1R}, A_{2O}, A_{3O}, A_{4S}, A_{5S}, B_S, C_O\right),$$
$$S_2\left(A_{1G}, A_{2R}, A_{3O}, A_{4O}, A_{5S}, B_S, C_O\right),$$
$$S_3\left(A_{1W}, A_{2R}, A_{3O}, A_{4O}, A_{5S}, B_S, C_O\right),$$
$$S_4\left(A_{1W}, A_{2W}, A_{3R}, A_{4O}, A_{5O}, B_S, C_O\right),$$
$$S_5\left(A_{1W}, A_{2W}, A_{3W}, A_{4R}, A_{5S}, B_O, C_O\right),$$
$$S_6\left(A_{1G}, A_{2W}, A_{3R}, A_{4O}, A_{5O}, B_S, C_O\right),$$
$$S_7\left(A_{1G}, A_{2W}, A_{3W}, A_{4R}, A_{5G}, B_O, C_O\right),$$

$$S_8\left(A_{1G},A_{2G},A_{3G},A_{4S},A_5,B_S,C_R\right),$$

$$S_9\left(A_{1R},A_{2G},A_{3G},A_{4S},A_{5S},B_S,C_R\right),$$

$$S_{10}\left(A_{1W},A_{2R},A_{3G},A_{4S},A_{5S},B_S,C_R\right),$$

$$S_{11}\left(A_{1W},A_{2W},A_{3R},A_{4G},A_{5S},B_G,C_R\right),$$

$$S_{12}\left(A_{1W},A_{2W},A_{3W},A_{4R},A_{5G},B_R,C_G\right),$$

$$S_{13}\left(A_{1W},A_{2W},A_{3W},A_{4R},A_{5G},B_G,C_R\right),$$

$$S_{14}\left(A_{1G},A_{2R},A_{3G},A_{4G},A_{5S},B_S,C_R\right),$$

$$S_{15}\left(A_{1G},A_{2W},A_{3R},A_{4G},A_{5G},B_S,C_R\right),$$

$$S_{16}\left(A_{1G},A_{2W},A_{3W},A_{4R},A_{5G},B_R,C_R\right),$$

$$S_{17}\left(A_{1G},A_{2W},A_{3W},A_{4R},A_{5G},B_G,C_R\right).$$

3. Models Formulation

3.1. Availability, Busy Period and Profit Modeling for $n = 2$

Let $P(0)=\left[P_0(0),P_1(0),P_2(0),P_3(0),\cdots,P_6(0)\right]$ be the probability vector for system at time $t\geq 0$. Relating the state of the system at time t and $t+\mathrm{d}t$, the differential equations for the system when $n=2$ can be expressed in the form:

$$\frac{\mathrm{d}}{\mathrm{d}t}\left(P(t)\right)=A_1P(t) \tag{1}$$

where

$$A_1=\begin{bmatrix}-y_{11} & \alpha_{11} & 0 & \alpha_2 & 0 & 0 & 0\\ \beta_{11} & -y_{22} & \alpha_{12} & 0 & \alpha_2 & 0 & 0\\ 0 & \beta_{12} & -y_{33} & 0 & 0 & \alpha_1 & \alpha_2\\ \beta_2 & 0 & 0 & -\alpha_2 & 0 & 0 & 0\\ 0 & \beta_2 & 0 & 0 & -\alpha_2 & 0 & 0\\ 0 & 0 & \beta_1 & 0 & 0 & -\alpha_1 & 0\\ 0 & 0 & \beta_2 & 0 & 0 & 0 & -\alpha_2\end{bmatrix}$$

For the analysis of availability and busy period cases of system, we use the following procedure to obtain the steady-state availability, busy period and profit function. In steady-state, the derivatives of the state probabilities become zero and we obtain

$$\begin{bmatrix}-y_{11} & \alpha_{11} & 0 & \alpha_2 & 0 & 0 & 0\\ \beta_{11} & -y_{22} & \alpha_{12} & 0 & \alpha_2 & 0 & 0\\ 0 & \beta_{12} & -y_{33} & 0 & 0 & \alpha_1 & \alpha_2\\ \beta_2 & 0 & 0 & -\alpha_2 & 0 & 0 & 0\\ 0 & 0 & 0 & 0 & -\alpha_2 & 0 & 0\\ 0 & 0 & \beta_1 & 0 & 0 & -\alpha_1 & 0\\ 0 & \beta_2 & \beta_2 & 0 & 0 & 0 & -\alpha_2\end{bmatrix}\begin{bmatrix}P_0(t)\\ P_1(t)\\ P_2(t)\\ P_3(t)\\ P_4(t)\\ P_5(t)\\ P_6(t)\end{bmatrix}=\begin{bmatrix}0\\ 0\\ 0\\ 0\\ 0\\ 0\\ 0\end{bmatrix} \tag{2}$$

Replacing the last row of (2) with the normalizing condition below

$$\sum_{i=0}^{6}P_i(\infty)=1 \tag{3}$$

to obtain the states probabilities $P_0(\infty),\ P_1(\infty),\ \cdots,\ P_6(\infty)$.

Let T be the time to failure of the system for system.

The explicit expression for the steady-state availability is as follows:

The steady-state availability is given by

$$A_{T1} = P_0(\infty) + P_1(\infty) + P_2(\infty) = \frac{H_1}{D_1} \tag{4}$$

From state 1 to 6 the repairmen are busy in those states repairing the failed units. Let $B_{T1}(\infty)$ be the probabilities that the repairmen are busy in the states repairing the failed units. Using (2) and (3) above, the explicit expressions for the steady-state busy period of repairmen are as follows:

$$B_{T1} = P_1(\infty) + P_2(\infty) + P_3(\infty) + P_4(\infty) + P_5(\infty) + P_6(\infty) = \frac{H_2}{D_1} \tag{5}$$

The system/subsystems/units are subjected to corrective maintenance at failure as can be observed in states 1, 2, 3, 4, 5 and 6 of system I. In those states, the repairmen are busy performing corrective maintenance action to the system/subsystems/units at failure. The expected profit PF_1 per unit time incurred to the system in the steady-state is given by:

Profit = total revenue generated − accumulated cost incurred due corrective maintenance to the failed system/subsystems/units. Thus

$$PF_1 = C_0 A_{T1}(\infty) - C_1 B_{T1}(\infty) \tag{6}$$

3.2. Availability, Busy Period and Profit Modeling for $n = 3$

Let $P(0) = \left[P_1(0), P_2(0), P_3(0), \cdots, P_9(0)\right]$ be the probability vector for system at time $t \geq 0$. Relating the state of the system at time t and $t + \mathrm{d}t$ the differential equations for the system when $n = 3$ can be expressed in the form:

$$\frac{\mathrm{d}}{\mathrm{d}t}\left(P(t)\right) = A_2 P(t) \tag{7}$$

$$A_2 = \begin{bmatrix} -y_1 & \alpha_{11} & \alpha_{12} & 0 & \alpha_2 & 0 & 0 & 0 & 0 & 0 \\ \beta_{11} & -y_2 & 0 & \alpha_{12} & 0 & \alpha_2 & 0 & 0 & 0 & 0 \\ \beta_{12} & 0 & -y_3 & 0 & 0 & 0 & \alpha_1 & \alpha_2 & 0 & 0 \\ 0 & \beta_{12} & 0 & -y_4 & 0 & 0 & 0 & 0 & \alpha_1 & \alpha_2 \\ \beta_2 & 0 & 0 & 0 & -\alpha_2 & 0 & 0 & 0 & 0 & 0 \\ 0 & \beta_2 & 0 & 0 & 0 & -\alpha_2 & 0 & 0 & 0 & 0 \\ 0 & 0 & \beta_1 & 0 & 0 & 0 & -\alpha_1 & 0 & 0 & 0 \\ 0 & 0 & \beta_2 & 0 & 0 & 0 & 0 & -\alpha_2 & 0 & 0 \\ 0 & 0 & 0 & \beta_1 & 0 & 0 & 0 & 0 & -\alpha_1 & 0 \\ 0 & 0 & 0 & \beta_2 & 0 & 0 & 0 & 0 & 0 & -\alpha_2 \end{bmatrix}$$

$$y_1 = (\beta_2 + \beta_{11} + \beta_{12}),$$

$$y_2 = (\alpha_{11} + \beta_2 + \beta_{12}),$$

$$y_3 = (\alpha_{12} + \beta_1 + \beta_2),$$

$$y_4 = (\alpha_{12} + \beta_1 + \beta_2).$$

For the analysis of availability and busy period cases of system, we use the following procedure to obtain the

steady-state availability, busy period and profit function. In steady-state, the derivatives of the state probabilities become zero and we obtain

$$\begin{bmatrix} -y_1 & \alpha_{11} & \alpha_{12} & 0 & \alpha_2 & 0 & 0 & 0 & 0 & 0 \\ \beta_{11} & -y_2 & 0 & \alpha_{12} & 0 & \alpha_2 & 0 & 0 & 0 & 0 \\ \beta_{12} & 0 & -y_3 & 0 & 0 & 0 & \alpha_1 & \alpha_2 & 0 & 0 \\ 0 & \beta_{12} & 0 & -y_4 & 0 & 0 & 0 & 0 & \alpha_1 & \alpha_2 \\ \beta_2 & 0 & 0 & 0 & -\alpha_2 & 0 & 0 & 0 & 0 & 0 \\ 0 & \beta_2 & 0 & 0 & 0 & -\alpha_2 & 0 & 0 & 0 & 0 \\ 0 & 0 & \beta_1 & 0 & 0 & 0 & -\alpha_1 & 0 & 0 & 0 \\ 0 & 0 & \beta_2 & 0 & 0 & 0 & 0 & -\alpha_2 & 0 & 0 \\ 0 & 0 & 0 & \beta_1 & 0 & 0 & 0 & 0 & -\alpha_1 & 0 \\ 0 & 0 & 0 & \beta_2 & 0 & 0 & 0 & 0 & 0 & -\alpha_2 \end{bmatrix} \begin{bmatrix} P_0(t) \\ P_1(t) \\ P_2(t) \\ P_3(t) \\ P_4(t) \\ P_5(t) \\ P_6(t) \\ P_7(t) \\ P_8(t) \\ P_9(t) \end{bmatrix} = \begin{bmatrix} 0 \\ 0 \\ 0 \\ 0 \\ 0 \\ 0 \\ 0 \\ 0 \\ 0 \\ 0 \end{bmatrix} \tag{8}$$

Solving (8) and using the following normalizing condition

$$\sum_{i=0}^{9} P_i(\infty) = 1 \tag{9}$$

to obtain $P_0(\infty), P_1(\infty), P_2(\infty), \cdots, P_9(\infty)$.

The explicit expression for the steady-state availability is as follows:

$$A_{T2}(\infty) = P_0(\infty) + P_1(\infty) + P_2(\infty) + P_3(\infty) = \frac{H_3}{D_2} \tag{10}$$

where

$$H_3 = \alpha_1\alpha_2\alpha_{11}\alpha_{12} + \alpha_1\alpha_2\alpha_{12}\beta_{11} + \alpha_1\alpha_2\alpha_{11}\beta_{12} + \alpha_1\alpha_2\beta_{11}\beta_{12}$$

$$\begin{aligned} D_2 = {} & \alpha_1\alpha_2\alpha_{12}\beta_{11} + \alpha_1\alpha_2\beta_{11}\beta_{12} + \alpha_1\alpha_2\alpha_{11}\alpha_{12} + \alpha_1\alpha_2\alpha_{11}\beta_{12} + \alpha_1\alpha_{12}\beta_2\beta_{11} \\ & + \alpha_1\beta_2\beta_{11}\beta_{12} + \alpha_1\alpha_{11}\alpha_{12}\beta_2 + \alpha_1\alpha_{11}\beta_2\beta_{12} + \alpha_2\beta_1\beta_{11}\beta_{12} + \alpha_1\alpha_{11}\beta_1\beta_{12}. \end{aligned}$$

From state 1 to 9 the repairmen are busy in those states repairing the failed units. Let $B_{T2}(\infty)$ be the probabilities that the repairmen are busy in those states repairing the failed units. Using (8) and (9) above, the explicit expressions for the steady-state busy period of repairmen are as follows:

$$B_{T2}(\infty) = P_1(\infty) + P_2(\infty) + P_3(\infty) + \cdots + P_9(\infty) = \frac{H_4}{D_2} \tag{11}$$

The expected profit PF_2 per unit time incurred to the system in the steady-state is given by:

Profit = total revenue generated − accumulated cost incurred due corrective maintenance to the failed system/subsystems/units.

$$PF_2 = C_0 A_{T2}(\infty) - C_1 B_{T2}(\infty) \tag{12}$$

3.3. Availability, Busy Period and Profit Modeling for $n = 4$

Let $P(0) = \left[P_0(0), P_1(0), P_2(0), P_3(0), \cdots, P_{13}(0)\right]$ be the probability vector for system at time $t \geq 0$. Relating the state of the system at time t and $t + \mathrm{d}t$ the differential equations for the system when $n = 4$ can be expressed in the form:

$$\frac{\mathrm{d}}{\mathrm{d}t}\left(P(t)\right) = A_3 P(t) \tag{13}$$

where

$$A_3 = \begin{bmatrix}
-h_1 & \alpha_{11} & \alpha_{12} & 0 & 0 & 0 & 0 & 0 & 0 & 0 & 0 & 0 & \alpha_2 & 0 \\
\beta_{11} & -h_2 & 0 & \alpha_{12} & 0 & 0 & \alpha_2 & 0 & 0 & 0 & 0 & 0 & 0 & 0 \\
\beta_{12} & 0 & -h_3 & 0 & 0 & \alpha_{13} & 0 & 0 & 0 & 0 & 0 & 0 & 0 & \alpha_2 \\
0 & \beta_{12} & 0 & -h_4 & \alpha_{13} & 0 & 0 & \alpha_2 & 0 & 0 & 0 & 0 & 0 & 0 \\
0 & 0 & 0 & \beta_{13} & -h_5 & 0 & 0 & 0 & \alpha_1 & \alpha_2 & 0 & 0 & 0 & 0 \\
0 & 0 & \beta_{13} & 0 & 0 & -h_6 & 0 & 0 & 0 & 0 & \alpha_1 & \alpha_2 & 0 & 0 \\
0 & \beta_2 & 0 & 0 & 0 & 0 & -\alpha_2 & 0 & 0 & 0 & 0 & 0 & 0 & 0 \\
0 & 0 & 0 & \beta_2 & 0 & 0 & 0 & -\alpha_2 & 0 & 0 & 0 & 0 & 0 & 0 \\
0 & 0 & 0 & 0 & \beta_1 & 0 & 0 & 0 & -\alpha_1 & 0 & 0 & 0 & 0 & 0 \\
0 & 0 & 0 & 0 & \beta_2 & 0 & 0 & 0 & 0 & -\alpha_2 & 0 & 0 & 0 & 0 \\
0 & 0 & 0 & 0 & 0 & \beta_1 & 0 & 0 & 0 & 0 & -\alpha_1 & 0 & 0 & 0 \\
0 & 0 & 0 & 0 & 0 & \beta_2 & 0 & 0 & 0 & 0 & 0 & -\alpha_2 & 0 & 0 \\
\beta_2 & 0 & 0 & 0 & 0 & 0 & 0 & 0 & 0 & 0 & 0 & 0 & -\alpha_2 & 0 \\
0 & 0 & \beta_2 & 0 & 0 & 0 & 0 & 0 & 0 & 0 & 0 & 0 & 0 & -\alpha_2
\end{bmatrix}$$

$$h_1 = (\beta_2 + \beta_{11} + \beta_{12}),$$

$$h_2 = (\alpha_{11} + \beta_2 + \beta_{12}),$$

$$h_3 = (\alpha_{12} + \beta_2 + \beta_{13}),$$

$$h_4 = (\alpha_{12} + \beta_2 + \beta_{13}),$$

$$h_5 = (\alpha_{13} + \beta_1 + \beta_2),$$

$$h_6 = (\alpha_{13} + \beta_1 + \beta_2).$$

In steady-state, the derivatives of the state probabilities become zero and we obtain

$$\begin{bmatrix}
-h_1 & \alpha_{11} & \alpha_{12} & 0 & 0 & 0 & 0 & 0 & 0 & 0 & 0 & 0 & \alpha_2 & 0 \\
\beta_{11} & -h_2 & 0 & \alpha_{12} & 0 & 0 & \alpha_2 & 0 & 0 & 0 & 0 & 0 & 0 & 0 \\
\beta_{12} & 0 & -h_3 & 0 & 0 & \alpha_{13} & 0 & 0 & 0 & 0 & 0 & 0 & 0 & \alpha_2 \\
0 & \beta_{12} & 0 & -h_4 & \alpha_{13} & 0 & 0 & \alpha_2 & 0 & 0 & 0 & 0 & 0 & 0 \\
0 & 0 & 0 & \beta_{13} & -h_5 & 0 & 0 & 0 & \alpha_1 & \alpha_2 & 0 & 0 & 0 & 0 \\
0 & 0 & \beta_{13} & 0 & 0 & -h_6 & 0 & 0 & 0 & 0 & \alpha_1 & \alpha_2 & 0 & 0 \\
0 & \beta_2 & 0 & 0 & 0 & 0 & -\alpha_2 & 0 & 0 & 0 & 0 & 0 & 0 & 0 \\
0 & 0 & 0 & \beta_2 & 0 & 0 & 0 & -\alpha_2 & 0 & 0 & 0 & 0 & 0 & 0 \\
0 & 0 & 0 & 0 & \beta_1 & 0 & 0 & 0 & -\alpha_1 & 0 & 0 & 0 & 0 & 0 \\
0 & 0 & 0 & 0 & \beta_2 & 0 & 0 & 0 & 0 & -\alpha_2 & 0 & 0 & 0 & 0 \\
0 & 0 & 0 & 0 & 0 & \beta_1 & 0 & 0 & 0 & 0 & -\alpha_1 & 0 & 0 & 0 \\
0 & 0 & 0 & 0 & 0 & \beta_2 & 0 & 0 & 0 & 0 & 0 & -\alpha_2 & 0 & 0 \\
\beta_2 & 0 & 0 & 0 & 0 & 0 & 0 & 0 & 0 & 0 & 0 & 0 & -\alpha_2 & 0 \\
0 & 0 & \beta_2 & 0 & 0 & 0 & 0 & 0 & 0 & 0 & 0 & 0 & 0 & -\alpha_2
\end{bmatrix}
\begin{bmatrix} P_0(t) \\ P_1(t) \\ P_2(t) \\ P_3(t) \\ P_4(t) \\ P_5(t) \\ P_6(t) \\ P_7(t) \\ P_8(t) \\ P_9(t) \\ P_{10}(t) \\ P_{11}(t) \\ P_{12}(t) \\ P_{13}(t) \end{bmatrix} =
\begin{bmatrix} 0 \\ 0 \\ 0 \\ 0 \\ 0 \\ 0 \\ 0 \\ 0 \\ 0 \\ 0 \\ 0 \\ 0 \\ 0 \\ 0 \end{bmatrix}$$

Solving (8) and using the following normalizing condition

$$\sum_{i=0}^{13} P_i(\infty) = 1 \tag{15}$$

and obtain $P_0(\infty), P_1(\infty), P_2(\infty), \cdots, P_{12}(\infty), P_{13}(\infty)$.

The explicit expression for the steady-state availability is as

$$A_{T3}(\infty) = P_0(\infty) + P_1(\infty) + P_2(\infty) + P_3(\infty) + P_4(\infty) + P_5(\infty) = \frac{H_5}{D_3} \tag{16}$$

From state 1 to 13 the repairmen are busy in those states repairing the failed units. Let $B_{T3}(\infty)$ be the probabilities that the repairmen are busy in those states repairing the failed units. Using (14) and (15) above, the explicit expressions for the steady-state busy period of repairmen are as follows:

$$B_{T3}(\infty) = P_1(\infty) + P_2(\infty) + P_3(\infty) + P_4(\infty) + \cdots + P_{13}(\infty) = \frac{H_6}{D_3} \tag{17}$$

The expected profit PF_3 per unit time incurred to the system in the steady-state is given by:

Profit = total revenue generated − accumulated cost incurred due corrective maintenance to the failed system/subsystems/units.

$$PF_3 = C_0 A_{T3}(\infty) - C_1 B_{T3}(\infty) \tag{18}$$

3.4. Availability, Busy Period and Profit Modeling for $n = 5$

Let $P(0) = \left[P_1(0), P_2(0), P_3(0), \cdots, P_{17}(0)\right]$ be the probability vector for system at time $t \geq 0$. Relating the state of the system at time t and $t + \mathrm{d}t$ the differential equations for $n = 5$ can be expressed in the form:

$$\frac{\mathrm{d}}{\mathrm{d}t}\left(P(t)\right) = A_4 P(t) \tag{19}$$

where

$$A_4 = \begin{bmatrix}
-k_1 & \alpha_{11} & \alpha_{12} & 0 & 0 & 0 & 0 & 0 & \alpha_2 & 0 & 0 & 0 & 0 & 0 & 0 & 0 & 0 & 0 \\
\beta_{11} & -k_2 & 0 & \alpha_{12} & 0 & 0 & 0 & 0 & 0 & \alpha_2 & 0 & 0 & 0 & 0 & 0 & 0 & 0 & 0 \\
\beta_{12} & 0 & -k_3 & 0 & 0 & 0 & \alpha_{13} & 0 & 0 & 0 & 0 & 0 & 0 & 0 & \alpha_2 & 0 & 0 & 0 \\
0 & \beta_{12} & 0 & -k_4 & \alpha_{13} & 0 & 0 & 0 & 0 & 0 & \alpha_2 & 0 & 0 & 0 & 0 & 0 & 0 & 0 \\
0 & 0 & 0 & \beta_{13} & -k_5 & \alpha_{14} & 0 & 0 & 0 & 0 & 0 & \alpha_2 & 0 & 0 & 0 & 0 & 0 & 0 \\
0 & 0 & 0 & 0 & \beta_{14} & -k_6 & 0 & 0 & 0 & 0 & 0 & 0 & \alpha_1 & \alpha_2 & 0 & 0 & 0 & 0 \\
0 & 0 & \beta_{13} & 0 & 0 & 0 & -k_7 & \alpha_{14} & 0 & 0 & 0 & 0 & 0 & 0 & 0 & \alpha_2 & 0 & 0 \\
0 & 0 & 0 & 0 & 0 & 0 & \beta_{14} & -k_8 & 0 & 0 & 0 & 0 & 0 & 0 & 0 & 0 & \alpha_1 & \alpha_2 \\
\beta_2 & 0 & 0 & 0 & 0 & 0 & 0 & 0 & -\alpha_2 & 0 & 0 & 0 & 0 & 0 & 0 & 0 & 0 & 0 \\
0 & \beta_2 & 0 & 0 & 0 & 0 & 0 & 0 & 0 & -\alpha_2 & 0 & 0 & 0 & 0 & 0 & 0 & 0 & 0 \\
0 & 0 & 0 & \beta_2 & 0 & 0 & 0 & 0 & 0 & 0 & -\alpha_2 & 0 & 0 & 0 & 0 & 0 & 0 & 0 \\
0 & 0 & 0 & 0 & \beta_2 & 0 & 0 & 0 & 0 & 0 & 0 & -\alpha_2 & 0 & 0 & 0 & 0 & 0 & 0 \\
0 & 0 & 0 & 0 & 0 & \beta_1 & 0 & 0 & 0 & 0 & 0 & 0 & -\alpha_1 & 0 & 0 & 0 & 0 & 0 \\
0 & 0 & 0 & 0 & 0 & \beta_2 & 0 & 0 & 0 & 0 & 0 & 0 & 0 & -\alpha_2 & 0 & 0 & 0 & 0 \\
0 & 0 & \beta_2 & 0 & 0 & 0 & 0 & 0 & 0 & 0 & 0 & 0 & 0 & 0 & -\alpha_2 & 0 & 0 & 0 \\
0 & 0 & 0 & 0 & 0 & 0 & \beta_2 & 0 & 0 & 0 & 0 & 0 & 0 & 0 & 0 & -\alpha_2 & 0 & 0 \\
0 & 0 & 0 & 0 & 0 & 0 & 0 & \beta_1 & 0 & 0 & 0 & 0 & 0 & 0 & 0 & 0 & -\alpha_1 & 0 \\
0 & 0 & 0 & 0 & 0 & 0 & 0 & \beta_2 & 0 & 0 & 0 & 0 & 0 & 0 & 0 & 0 & 0 & -\alpha_2
\end{bmatrix}$$

$$k_1 = (\beta_{11} + \beta_{12} + \beta_2),$$

$$k_2 = (\alpha_{11} + \beta_{12} + \beta_2),$$

$$k_3 = (\alpha_{12} + \beta_{13} + \beta_2),$$

$$k_4 = (\alpha_{12} + \beta_{13} + \beta_2),$$

$$k_5 = (\alpha_{13} + \beta_{14} + \beta_2),$$

$$k_6 = (\alpha_{14} + \beta_1 + \beta_2),$$

$$k_7 = (\alpha_{13} + \beta_{14} + \beta_2),$$

$$k_8 = (\alpha_{14} + \beta_1 + \beta_2).$$

In steady-state, the derivatives of the state probabilities become zero and we obtain

$$\begin{bmatrix}
-k_1 & \alpha_{11} & \alpha_{12} & 0 & 0 & 0 & 0 & 0 & \alpha_2 & 0 & 0 & 0 & 0 & 0 & 0 & 0 & 0 & 0 \\
\beta_{11} & -k_2 & 0 & \alpha_{12} & 0 & 0 & 0 & 0 & 0 & \alpha_2 & 0 & 0 & 0 & 0 & 0 & 0 & 0 & 0 \\
\beta_{12} & 0 & -k_3 & 0 & 0 & 0 & \alpha_{13} & 0 & 0 & 0 & 0 & 0 & 0 & 0 & \alpha_2 & 0 & 0 & 0 \\
0 & \beta_{12} & 0 & -k_4 & \alpha_{13} & 0 & 0 & 0 & 0 & 0 & \alpha_2 & 0 & 0 & 0 & 0 & 0 & 0 & 0 \\
0 & 0 & 0 & \beta_{13} & -k_5 & \alpha_{14} & 0 & 0 & 0 & 0 & 0 & \alpha_2 & 0 & 0 & 0 & 0 & 0 & 0 \\
0 & 0 & 0 & 0 & \beta_{14} & -k_6 & 0 & 0 & 0 & 0 & 0 & 0 & \alpha_1 & \alpha_2 & 0 & 0 & 0 & 0 \\
0 & 0 & \beta_{13} & 0 & 0 & 0 & -k_7 & \alpha_{14} & 0 & 0 & 0 & 0 & 0 & 0 & 0 & \alpha_2 & 0 & 0 \\
0 & 0 & 0 & 0 & 0 & 0 & \beta_{14} & -k_8 & 0 & 0 & 0 & 0 & 0 & 0 & 0 & 0 & \alpha_1 & \alpha_2 \\
\beta_2 & 0 & 0 & 0 & 0 & 0 & 0 & 0 & -\alpha_2 & 0 & 0 & 0 & 0 & 0 & 0 & 0 & 0 & 0 \\
0 & \beta_2 & 0 & 0 & 0 & 0 & 0 & 0 & 0 & -\alpha_2 & 0 & 0 & 0 & 0 & 0 & 0 & 0 & 0 \\
0 & 0 & 0 & \beta_2 & 0 & 0 & 0 & 0 & 0 & 0 & -\alpha_2 & 0 & 0 & 0 & 0 & 0 & 0 & 0 \\
0 & 0 & 0 & 0 & \beta_2 & 0 & 0 & 0 & 0 & 0 & 0 & -\alpha_2 & 0 & 0 & 0 & 0 & 0 & 0 \\
0 & 0 & 0 & 0 & 0 & \beta_1 & 0 & 0 & 0 & 0 & 0 & 0 & -\alpha_1 & 0 & 0 & 0 & 0 & 0 \\
0 & 0 & 0 & 0 & 0 & \beta_2 & 0 & 0 & 0 & 0 & 0 & 0 & 0 & -\alpha_2 & 0 & 0 & 0 & 0 \\
0 & 0 & \beta_2 & 0 & 0 & 0 & 0 & 0 & 0 & 0 & 0 & 0 & 0 & 0 & -\alpha_2 & 0 & 0 & 0 \\
0 & 0 & 0 & 0 & 0 & 0 & \beta_2 & 0 & 0 & 0 & 0 & 0 & 0 & 0 & 0 & -\alpha_2 & 0 & 0 \\
0 & 0 & 0 & 0 & 0 & 0 & 0 & \beta_1 & 0 & 0 & 0 & 0 & 0 & 0 & 0 & 0 & -\alpha_1 & 0 \\
0 & 0 & 0 & 0 & 0 & 0 & 0 & \beta_2 & 0 & 0 & 0 & 0 & 0 & 0 & 0 & 0 & 0 & -\alpha_2
\end{bmatrix}
\begin{bmatrix} P_0(t) \\ P_1(t) \\ P_2(t) \\ P_3(t) \\ P_4(t) \\ P_5(t) \\ P_6(t) \\ P_7(t) \\ P_8(t) \\ P_9(t) \\ P_{10}(t) \\ P_{11}(t) \\ P_{12}(t) \\ P_{13}(t) \\ P_{14}(t) \\ P_{15}(t) \\ P_{16}(t) \\ P_{17}(t) \end{bmatrix}
= \begin{bmatrix} 0 \\ 0 \\ 0 \\ 0 \\ 0 \\ 0 \\ 0 \\ 0 \\ 0 \\ 0 \\ 0 \\ 0 \\ 0 \\ 0 \\ 0 \\ 0 \\ 0 \\ 0 \end{bmatrix} \tag{20}$$

$$\sum_{i=0}^{17} P_i(\infty) = 1 \tag{21}$$

to obtain $P_i(\infty)$, $i = 1, 2, 3, \cdots, 17$.

States 0, 1, 2, 3, 4, 5, 6 and 7 in the states of the system IV above are operational states and states 1, 2, 3, ···, 17 are busy period states, putting (21) in the last rows of (20), the system availability, busy period and profit function are given by:

$$A_{T4}(\infty) = P_0(\infty) + P_1(\infty) + P_2(\infty) + P_3(\infty) + P_4(\infty) + P_5(\infty) + P_6(\infty) + P_7(\infty) = \frac{H_7}{D_4} \tag{22}$$

$$B_{T4}(\infty) = P_1(\infty) + P_2(\infty) + P_3(\infty) + P_4(\infty) + P_5(\infty) + P_6(\infty) + \cdots + P_{17}(\infty) = \frac{H_8}{D_4} \tag{23}$$

The expected profit PF_4 per unit time incurred to the system in the steady-state is given by:

Profit = total revenue generated − accumulated cost incurred due corrective maintenance to the failed system/subsystems/units.

Thus

$$PF_4 = C_0 A_{T4}(\infty) - C_1 B_{T4}(\infty) \tag{24}$$

4. Numerical Illustration

In this section, we numerically obtained and compared the results for system availability and profit function for the developed models. The objectives here are to analyze graphically the effects of system parameters on availability and profit and make comparison for different values of *n*. For each model the following set of parameters values are fixed throughout the simulations for consistency.

$$\beta_1 = 0.4,\ \beta_2 = 0.3,\ \beta_{11} = 0.3,\ \beta_{12} = 0.1,\ \beta_{13} = 0.2,\ \beta_{14} = 0.3,$$

$$\alpha_1 = 0.2,\ \alpha_{11} = 0.3,\ \alpha_2 = 0.3,\ \alpha_{12} = 0.4,\ \alpha_{13} = 0.4,\ \alpha_{14} = 0.5,$$

$$C_0 = 100,000,\ C_1 = 20,000.$$

It is can be seen from **Figure 1**, that availability increases with increase in repair rate α_1 for n = 2, 3, 4, 5 and also the availability increases as n increases. It is evident from **Figure 1** that as n increases, the steady state availability also increases. The result in **Figure 1** also shows that steady state availability increases with increase in repair and provision of more standby units. **Figure 2** shows that the availability decreases with increase in failure rate β_1. However, availability for n = 2, n = 3, n = 4 decreases more compared to when n = 5. Here the optimal availability result with respect to β_1 is when n = 5. The result here indicates that the availability of the system with more standby units tend to decrease slightly than the system with less standby units. **Figure 3** shows that the generated profit increases with increase in repair rate α_1 for n = 2, 3, 4, 5. The profit is higher when n = 5 than when n = 2, 3, 4. It is evident here that provision of more standby units lead to increase in the generated profit. **Figure 4** shows that the generated profit decreases with increase in failure rate β_1. However, the generated profit for n = 2, n = 3, n = 4 decreases more compared to when n = 5. Here the optimal profit with respect to β_1 is when n = 5. This indicates that the generated profit of the system with more standby units tend to decrease slightly than the system with less standby units. These numerical results are summarized in **Table 1**.

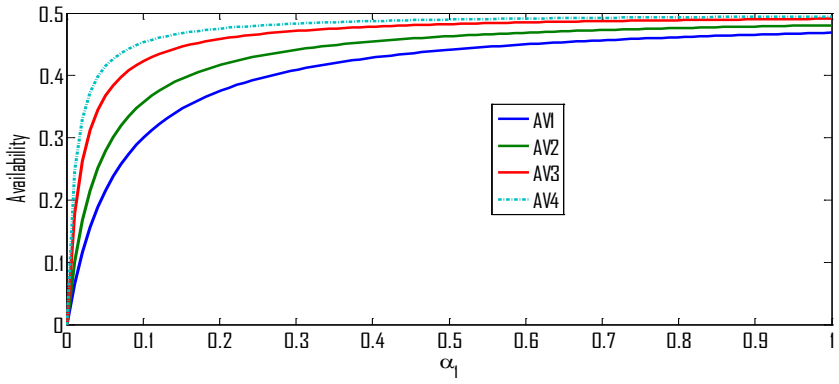

Figure 1. Availability against α_1.

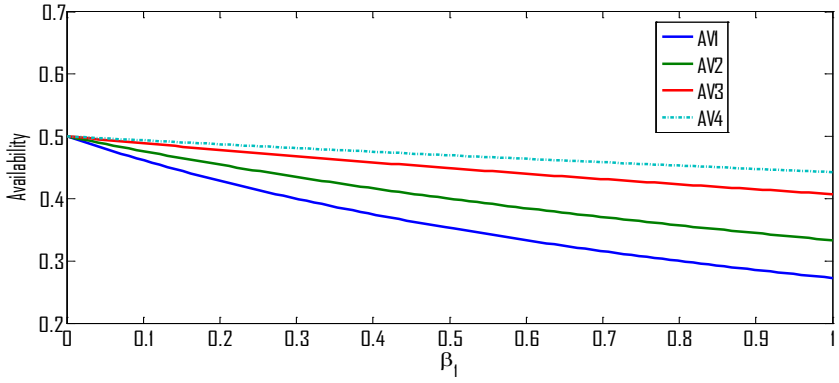

Figure 2. Availability against β_1.

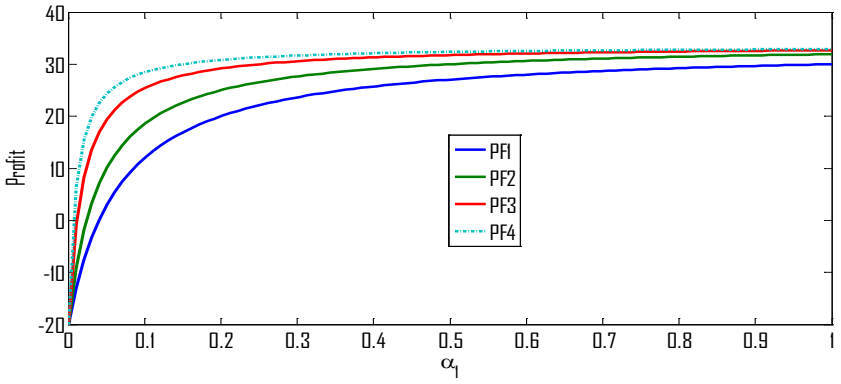

Figure 3. Profit against α_1.

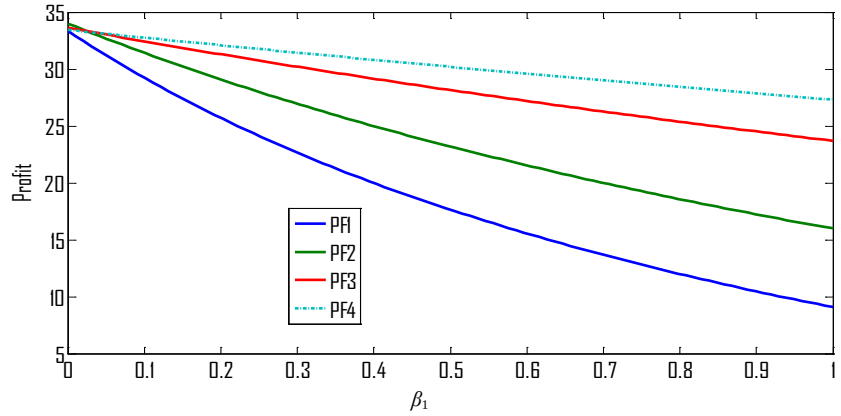

Figure 4. Profit against β_1.

Table 1. Comparison of availability and profit for n = 2, 3, 4, 5.

Parameter	Range of parameter	Results
β_1	$0 \le \beta_1 \le 1$	$A_{T4} > A_{T3}(\infty) > A_{T2}(\infty) > A_{T1}$ $PF_4 > PF_3(\infty) > PF_2(\infty) > PF_1$
α_1	$0 \le \alpha_1 \le 1$	$A_{T4} > A_{T3}(\infty) > A_{T2}(\infty) > A_{T1}$ $PF_4 > PF_3(\infty) > PF_2(\infty) > PF_1$

5. Conclusion

In this paper, we constructed four different series-parallel systems consisting of subsystems *A*, *B* and *C*. Subsystems *A* and *B* are cold standby with subsystem *A* containing linear consecutive *k*-out-of-*n* units while subsystem *B* and *C* consist of a single unit each. We developed the explicit expressions for the availability, busy period and profit for the four systems and performed a comparative analysis. It is interesting to see that as the number of units in subsystem *A* increases, the availability and profit also increase. Parametric investigation of various system parameters on system availability and profit function has been captured. It is evident from **Table 1** that the system with n = 5 units in subsystem *A* is optimal. The results of this paper are found to be highly beneficial to maintenance managers, reliability engineers, plant management and system designers for the proper maintenance analysis, decision making, system safety, and performance evaluation.

References

[1] Hu, l., Yue, D. and Li, J. (2012) Availability Analysis and Design Optimization for a Repairable Series-Parallel System

with Dependencies, *International Journal of Innovative Computing, Information and Control*, **8**, 6693-6705.

[2] Khatab, A., Nahas, N. and Nourelfath, M. (2009) Availbilty of *K-Out-of-N*: *G* Systems with Non-Identical Components Subject to Repair Priorities. *Reliability Engineering & System Safety*, **94**, 142-151. http://dx.doi.org/10.1016/j.ress.2008.02.017

[3] Krishnan, R. and Somasundaram, S. (2012) Reliability and Profit Analysis of Repairable *K-Out-of-N* System with Sensor. *European Journal of Scientific Research*, **67**, 215-222.

[4] Juang, Y.-S., Lin, S.-S. and Kao, H.-P. (2008) A Knowledge Management System for Series-Parallel Availability Optimization and Design. *Expert Systems with Applications*, **34**, 181-193. http://dx.doi.org/10.1016/j.eswa.2006.08.023

[5] Levitin, G. (2002) Optimal Series-Parallel Topology of Multi-State System with Two Failure Modes. *Reliability Engineering & System Safety*, **77**, 93-107. http://dx.doi.org/10.1016/S0951-8320(02)00034-0

[6] Li, C.Y., Chen, X., Yi, X.S. and Tao, J.Y. (2010) Heterogeneous Redundancy Optimization for Multi-State Series-Parallel Systems Subject to Common Cause Failures. *Reliability Engineering and System Safety*, **95**, 202-207. http://dx.doi.org/10.1016/j.ress.2009.09.011

[7] Wang, S. and Wadata, J. (2009) Reliability Optimization of a Series-Parallel System with Fuzzy Random Lifetimes. *International Journal of Innovative Computing, Information and Control*, **5**, 1547-1558.

[8] Wang, K.H. and Chen, Y.J. (2009) Comparative Analysis of Availability between Three Systems with General Repair Times, Reboot Delay and Switching Failures. *Applied Mathematics and Computation*, **215**, 384-394. http://dx.doi.org/10.1016/j.amc.2009.05.023

[9] Wang, K.-H., Yen, T.-C. and Fang, Y.-C. (2012) Comparison of Availability between Two Systems with Warm Standby Units and Different Imperfect Coverage. *Quality Technology and Quantitative Management*, **9**, 265-282.

Appendix

Notations

A_{jS}, A_{jO}, A_{jR}, A_{jW}, A_{jG} : Unit in subsystem A is in standby, in operation, failed and under repair, failed and waiting for repair, idle for $j=1,2,3,4,5$

B_S, B_O, B_R, B_G : Subsystem B is in standby, operation, failed and is under repair, is idle

C_O, C_R, C_G : Subsystem C is in operation, failed and is under repair, is idle

T : Time to failure of the system

A_{Ti}, B_{Ti}, PF_i : Steady-state availability, Busy period and Profit function for $i=1,2,3,4$

$P_m(t)$: Probability that the system is in state S_m at $t\geq 0$ for $m=0,1,2,3,\cdots,17$

β_{1w}, α_{1w} : Failure and repair rate of unit A_{1w} in subsystem A for $w=1,2,3,4$

β_1, α_1 : Failure and repair rate of subsystem B

β_2, α_2 : Failure and repair rates of subsystem C

n : Total number of units in subsystem A

C_0 : Revenue generated when the system is in working state and no income when in failed state

C_1 : Cost of each repair for failed system/subsystems/units

$$D_1=\alpha_2\beta_1\beta_{11}\beta_{12}+\alpha_1\alpha_2\beta_{11}\beta_{12}+\alpha_2\beta_1\beta_2\beta_{11}+\alpha_1\alpha_2\alpha_{12}\beta_{11}+\alpha_1\alpha_2\beta_2\beta_{11}+\alpha_1\alpha_2\alpha_{11}\alpha_{12}+\alpha_1\beta_2\beta_{11}\beta_{12}+\alpha_1\alpha_{12}\beta_2\beta_{11}+\alpha_1\beta_2^2\beta_{11}+\alpha_1\alpha_{11}\alpha_{12}\beta_2,$$

$$D_2=\alpha_1\alpha_2\alpha_{12}\beta_{11}+\alpha_1\alpha_2\beta_{11}\beta_{12}+\alpha_1\alpha_2\alpha_{11}\alpha_{12}+\alpha_1\alpha_2\alpha_{11}\beta_{12}+\alpha_1\alpha_{12}\beta_2\beta_{11}+\alpha_1\beta_2\beta_{11}\beta_{12}+\alpha_1\alpha_{11}\alpha_{12}\beta_2+\alpha_1\alpha_{11}\beta_2\beta_{12}+\alpha_2\beta_1\beta_{11}\beta_{12}+\alpha_1\alpha_{11}\beta_1\beta_{12},$$

$$D_3=\alpha_1\alpha_2\alpha_{11}\alpha_{13}\beta_{12}+\alpha_1\alpha_2\alpha_{11}\beta_{12}\beta_{13}+\alpha_1\alpha_2\alpha_{11}\alpha_{12}\alpha_{13}+\alpha_1\alpha_2\alpha_{13}\beta_{11}\beta_{12}+\alpha_1\alpha_2\alpha_{12}\alpha_{13}\beta_{11}+\alpha_1\alpha_2\beta_{11}\beta_{12}\beta_{13}+\alpha_1\alpha_{11}\alpha_{13}\beta_2\beta_{12}+\alpha_1\alpha_{11}\beta_2\beta_{12}\beta_{13}+\alpha_1\alpha_{11}\alpha_{12}\alpha_{13}\beta_2+\alpha_1\alpha_{13}\beta_2\beta_{11}\beta_{12}+\alpha_1\alpha_{12}\alpha_{13}\beta_2\beta_{11}+\alpha_1\beta_2\beta_{11}\beta_{12}\beta_{13}+\alpha_2\alpha_{11}\beta_1\beta_{12}\beta_{13}+\alpha_2\beta_1\beta_{11}\beta_{12}\beta_{13},$$

$$D_4=\alpha_1\alpha_2\beta_{11}\beta_{12}\beta_{13}\beta_{14}+\alpha_1\alpha_2\beta_{11}\beta_{12}\beta_{13}\beta_{14}+\alpha_1\alpha_2\alpha_{13}\alpha_{14}\beta_{11}\beta_{12}+\alpha_1\alpha_2\alpha_{12}\alpha_{13}\alpha_{14}\beta_{11}+\alpha_1\alpha_2\alpha_{11}\beta_{12}\beta_{13}\beta_{14}+\alpha_1\alpha_2\alpha_{11}\alpha_{14}\beta_{12}\beta_{13}+\alpha_1\alpha_2\alpha_{11}\alpha_{13}\alpha_{14}\beta_{12}+\alpha_1\alpha_2\alpha_{11}\alpha_{12}\alpha_{13}\alpha_{14}+\alpha\beta_2\beta_{11}\beta_{12}\beta_{13}\beta_{14}+\alpha_1\alpha_{14}\beta_2\beta_{11}\beta_{12}\beta_{13}+\alpha_1\alpha_{13}\alpha_{14}\beta_2\beta_{11}\beta_{12}+\alpha_1\alpha_{12}\alpha_{13}\alpha_{14}\beta_2\beta_{11}+\alpha_1\alpha_{11}\beta_2\beta_{12}\beta_{13}\beta_{14}+\alpha_1\alpha_{11}\alpha_{14}\beta_2\beta_{12}\beta_{13}+\alpha_1\alpha_{11}\alpha_{13}\alpha_{14}\beta_2\beta_{12}+\alpha_1\alpha_{11}\alpha_{12}\alpha_{13}\alpha_{14}\beta_2+\alpha_2\beta_1\beta_{11}\beta_{12}\beta_{13}\beta_{14}+\alpha_2\alpha_{11}\beta_1\beta_{12}\beta_{13}\beta_{14},$$

$$H_1=\alpha_1\alpha_2\alpha_{11}\alpha_{12}+\alpha_1\alpha_2\alpha_{12}\beta_{11}+\alpha_1\alpha_2\beta_{11}(\beta_{12}+\beta_2)$$

$$H_2=\alpha_1\alpha_2\alpha_{12}\beta_{11}+\alpha_1\alpha_2\beta_{11}(\beta_2+\beta_{12})+\alpha_1\alpha_{11}\alpha_{12}\beta_2+\alpha_2\beta_1\beta_{11}(\beta_2+\beta_{12})+\alpha_1\beta_2\beta_{11}(\alpha_{12}+\beta_{12}+\beta_2)$$

$$H_3=\alpha_1\alpha_2\alpha_{11}\alpha_{12}+\alpha_1\alpha_2\alpha_{12}\beta_{11}+\alpha_1\alpha_2\alpha_{11}\beta_{12}+\alpha_1\alpha_2\beta_{11}\beta_{12}$$

$$H_4=\alpha_1\alpha_2\alpha_{12}\beta_{11}+\alpha_1\alpha_2\alpha_{11}\beta_{12}+\alpha_1\alpha_2\beta_{11}\beta_{12}+\alpha_1\alpha_{11}\alpha_{12}\beta_2+\alpha_1\alpha_{12}\beta_2\beta_{11}+\alpha_2\alpha_{11}\beta_1\beta_{12}+\alpha_1\alpha_{11}\beta_2\beta_{12}+\alpha_2\alpha_1\beta_{11}\beta_{12}+\alpha_1\alpha_2\beta_{11}\beta_{12},$$

$$H_5=\alpha_1\alpha_2\alpha_{11}\alpha_{12}\alpha_{13}+\alpha_1\alpha_2\alpha_{12}\alpha_{13}\beta_{11}+\alpha_1\alpha_2\alpha_{11}\alpha_{13}\beta_{12}+\alpha_1\alpha_2\alpha_{13}\beta_{11}\beta_{12}+\alpha_1\alpha_2\beta_{11}\beta_{12}\beta_{13}+\alpha_1\alpha_2\alpha_{11}\beta_{12}\beta_{13}$$

$$H_6=\alpha_1\alpha_2\alpha_{12}\alpha_{13}\beta_{11}+\alpha_1\alpha_2\alpha_{11}\alpha_{13}\beta_{12}+\alpha_1\alpha_2\alpha_{13}\beta_{11}\beta_{12}+\alpha_1\alpha_2\beta_{11}\beta_{12}\beta_{13}+\alpha_1\alpha_2\alpha_{11}\beta_{12}\beta_{13}+\alpha_1\alpha_{12}\alpha_{13}\beta_2\beta_{11}+\alpha_1\alpha_{13}\beta_2\beta_{11}\beta_{12}+\alpha_2\beta_1\beta_{11}\beta_{12}\beta_{13}+\alpha_1\beta_2\beta_{11}\beta_{12}\beta_{13}+\alpha_2\alpha_{11}\beta_1\beta_{12}\beta_{13}+\alpha_1\alpha_{11}\beta_2\beta_{12}\beta_{13}+\alpha_1\alpha_{11}\alpha_{12}\alpha_{13}\beta_2+\alpha_1\alpha_2\alpha_{11}\beta_2\beta_{12},$$

$$H_7=\alpha_1\alpha_2\alpha_{11}\alpha_{12}\alpha_{13}\alpha_{14}+\alpha_1\alpha_2\alpha_{12}\alpha_{13}\alpha_{14}\beta_{11}+\alpha_1\alpha_2\alpha_{11}\alpha_{13}\alpha_{14}\beta_{12}+\alpha_1\alpha_2\alpha_{13}\alpha_{14}\beta_{11}\beta_{12}+\alpha_1\alpha_2\alpha_{14}\beta_{11}\beta_{12}\beta_{13}+\alpha_1\alpha_2\beta_{11}\beta_{12}\beta_{13}\beta_{14}+\alpha_1\alpha_2\alpha_{11}\alpha_{14}\beta_{12}\beta_{13}+\alpha_1\alpha_2\alpha_{11}\beta_{12}\beta_{13}\beta_{14},$$

$$H_8=\alpha_1\alpha_2\alpha_{12}\alpha_{13}\alpha_{14}\beta_{11}+\alpha_1\alpha_2\alpha_{11}\alpha_{13}\alpha_{14}\beta_{12}+\alpha_1\alpha_2\alpha_{13}\alpha_{14}\beta_{11}\beta_{12}+\alpha_1\alpha_2\alpha_{14}\beta_{11}\beta_{12}\beta_{13}+\alpha_1\alpha_2\beta_{11}\beta_{12}\beta_{13}\beta_{14}+\alpha_1\alpha_2\alpha_{11}\alpha_{14}\beta_{12}\beta_{13}+\alpha_1\alpha_2\alpha_{11}\beta_{12}\beta_{13}\beta_{14}+\alpha_1\alpha_{11}\alpha_{12}\alpha_{13}\alpha_{14}\beta_2+\alpha_1\alpha_{12}\alpha_{13}\alpha_{14}\beta_2\beta_{11}+\alpha_1\alpha_{13}\alpha_{14}\beta_2\beta_{11}\beta_{12}+\alpha_1\alpha_{14}\beta_2\beta_{11}\beta_{12}\beta_{13}+\alpha_2\beta_1\beta_{11}\beta_{12}\beta_{13}\beta_{14}+\alpha_1\beta_2\beta_{11}\beta_{12}\beta_{13}\beta_{14}+\alpha_1\alpha_{11}\alpha_{13}\alpha_{14}\beta_2\beta_{12}+\alpha_1\alpha_{11}\alpha_{14}\beta_2\beta_{12}\beta_{13}+\alpha_2\alpha_{11}\beta_1\beta_{12}\beta_{13}\beta_{14}+\alpha_1\alpha_{11}\beta_2\beta_{12}\beta_{13}\beta_{14}.$$

Applied Mathematics, 2015, 6, 345-358
Published Online February 2015 in SciRes. http://www.scirp.org/journal/am
http://dx.doi.org/10.4236/am.2015.62033

Scientific Research Publishing

Homotopy Approach to Fractional Quantum Hall Effect

Janusz Jacak, Patrycja Łydżba, Lucjan Jacak

Institute of Physics, Wroclaw University of Technology, Wrocław, Poland
Email: lucjan.jacak@pwr.edu.pl

Received 16 January 2015; accepted 6 February 2015; published 10 February 2015

Abstract

The topology-based explanation of the origin of the fractional quantum Hall effect is summarized. The cyclotron braid subgroups crucial for this approach are introduced in order to identify the origin of Laughlin correlations in 2D Hall systems. The so-called composite fermions are explained in terms of the homotopy cyclotron braids. Some new concept for fractional Chern insulator states is formulated in terms of the homotopy condition applied to the Berry field flux quantization.

Keywords

Quantum Hall Effects, Braid Groups, Homotopy Methods

1. Introduction

Topology plays increasing role in the development of current understanding of fundamentals in physics [1]. The field theory employs homotopy methods, even the classical electro-magnetics by Maxwell is formulated in terms of topological defects for vector fields in 3D. The notion of the spin is also closely related with the topological concepts visible in related covering symmetry groups or in the odd manifestation of the time reversion for spin expressed by $i\sigma_y$ operator with the square −1 and not identity. The homotopy methods [2] [3] have found application in condensed matter structures with multicomponent phase parameters, as for superfluid He^3 or for liquid crystals [4]. Recently, the strong increase of the interest in topological methods is related with so-called topological insulators [5]-[7]. The topological insight starts to be dominant in current understanding of Integer Quantum Hall Effect (IQHE) [8] and in rich applications of geometrical phase by Berry in various condensed matter problems [9] [10]. Application of the simple methods of the topological algebra in two dimensional spaces and also in locally two dimensional ones, like a sphere or torus, is linked with the exceptional richness of the topological structure for multiparticle planar systems which is expressed by the π_1 group of the related configuration spaces, called the braid groups [11]. For the indistinguishable N-particle planar systems the braid

How to cite this paper: Jacak, J., Łydżba, P. and Jacak, L. (2015) Homotopy Approach to Fractional Quantum Hall Effect. *Applied Mathematics*, **6**, 345-358. http://dx.doi.org/10.4236/am.2015.62033

groups are infinite in contrary to 3D systems where the full braid groups are finite permutation groups. The fundamental role of one dimensional unitary representations (1DURs) of the related full braid groups is noticeable in using of the path integrals by Feynman to determine statistics of quantum particles [12]. In the present paper we summarize the topological approach to Fractional Quantum Hall Effect (FQHE) via introduction of so-called cyclotron braid subgroups which help us in understanding of the Laughlin correlations specific for FQHE [13] [14].

2. FQHE Revisted

Shortly after discovery of the integer quantum Hall effect (IQHE) in two dimensional electron system (2DEG) upon strong magnetic fields corresponding to complete fillings of succeeding Landau levels (LLs), the surprising observation of the fractional quantum Hall effect (FQHE) was reported at stronger magnetic fields resulting in the fractional fillings of the lowest Landau level (LLL). Both discoveries were awarded with Nobel prizes, with regard to IQHE for K. von Klitzing (1985) and to FQHE for D. Tsui, H. Störmer and R. Laughlin (1989). While IQHE can be understood within single particle approach including topology arguments [16], the FQHE is a collective phenomenon regarded as a manifestation of strong interparticle correlations. The crucial prerequisite for FQHE is the flat band with quenched kinetic energy, as in the almost degenerated LLL in the presence of interaction (and massively degenerated without the interaction). Reducing of the kinetic energy allows for the subtle interaction effects resulting in the organization of correlated multiparticle states. The special role plays the very special 2D topology, what is convincingly supported by the absence of FQHE in 3D samples.

In order to describe correlations in 2D charged multi-particle systems in the presence of strong perpendicular magnetic field corresponding to fractional LLL fillings $\frac{1}{q}$ (q odd integer), the famous Laughlin wave-function (LF) was introduced [16]. The representation of the Coulomb interaction of particles in terms of the so-called Haldane pseudopotential allowed then for an observation [17]-[19] that the LF describes exactly the ground state for N charged 2D particles at the LLL filling $\frac{1}{q}$, if one neglects the long-range part of the Coulomb forces. Division of the interaction for the near- and long-range parts is expressed by the projection of the interaction onto the relative angular momenta of particle pairs and for chosen q the values of relative angular momenta greater than $q-2$ correspond to the long-range tail of interaction, whereas lower than $q-2$, to the near-range part of the field. It has been proved that the long-range part of the interaction only weekly influences the exact ground state given by LF for the near-range interaction only. The LF was a generalization of the Slater function for N noninteracting electrons completely filling LLL, written in this case in the form of the Vandermonde determinant multiplied by the Gaussian factor [20]. The LF has the same structure but with the Vandermonde determinant substituted by the Jastrow polynomial [16],

$$\Psi_L\left(z_1,\cdots,z_N\right)=\prod_{i,j=1,i>j}^{N}\left(z_i-z_j\right)^q \mathrm{e}^{-\sum_{i=1}^{N}\frac{|z_i|^2}{4l^2}}, \tag{1}$$

where, $z_i=x_i+iy_i$ is the complex representation of the position of i-th particle on a plane, $l=\sqrt{\frac{\hbar c}{\mathrm{e}B}}$ is a "magnetic" distance scale (magnetic length). For $q=1$ the above function is the Slater function with the Vandermonde determinant. This function (1) expresses correlations in the system, called Laughlin correlations. The main property is here the phase shift acquired by the LF if two particles interchange on the plane. This phase shift is $q\pi$ for interchange of two neighboring particles, which differentiates Laughlin correlations from ordinary fermion correlations corresponding to the phase shift π when these particles interchange. Note that a simple permutation of indices coincides with algebraic properties of the multi-argument wave function and corresponds to the fact, that in 3D (and in higher dimensions) the full braid group is the permutation group. For 2D manifolds association of the algebraic properties of multi-argument functions with exchanges of particles described by these functions may be misleading and exchanges of function arguments must be referred as to the braid group distinct than the permutation group. The unitary factor $\mathrm{e}^{iq\pi}=-1$ equals, however, to $\mathrm{e}^{i\pi}=-1$ and this property does not allow for distinguishing of Laughlin correlated particles from the ordinary fermions though they

are distinguished with the phase shift. This coincidence of exponential factors masks to some extent the topological difference between 2D and 3D and lies in foundations of using simplified and confusing analogies from 3D case to 2D one. Of that type is an assertion that the particles creating the correlated Laughlin state can be modeled as ordinary electrons dressed with the Coulomb interaction in analogy to quasiparticles common in solids [21]. Along this line the Laughlin correlations were modeled by so-called composite fermions (CFs) [22], *i.e.*, by electrons dressed with quantized magnetic field flux-tubes attached to particles as the result of the Coulomb interaction. By virtue of the Aharonov-Bohm effect, these flux-tubes, of $q-1$ flux quanta each, attached to particles produce the required by the LF phase shift when the composite particles interchange. The advantage of the CF construction was recognized in possibility of interpretation of the FQHE in an external magnetic field as IQHE in resultant field diminished by the averaged field of the auxiliary field flux-tubes [22]. However, neither the origin of the auxiliary magnetic field nor the mechanism of fixing flux-tubes to particles were not explained and the assertion that magnetic flux tubes are result of the Coulomb interaction was not demonstrated. Moreover the hierarchy of LLL fractional fillings obtained by mapping of FQHE on IGHE in resultant magnetic field does not cover all fractional states, cf. **Figure 1**.

The role of topology in creation of the strongly correlated state of FQHE was noticed [23]-[25] in the context of exceptional topological properties of 2D plane or of locally 2D manifolds like sphere or torus. This special topology of planar systems is linked with the exceptionally rich structure of the braid groups for 2D manifolds (R^2, or sphere and torus) in comparison to braid groups for higher dimensional spaces (R^d, $d > 2$) [11]. The full braid group is defined as π_1 homotopy group of the configuration space for N indistinguishable particles, *i.e.*, the group of multi-particle closed trajectory classes, disjoint and topologically nonequivalent (trajectories from various classes cannot be continuously deformed one into another one). The full braid group is infinite for 2D case while this group is finite (and equal to the ordinary permutation group S_N) in higher dimensions of the manifold on which particles can be located [11]. This property makes two dimensional systems exceptional in geometry-topology sense which inherently lies in foundations of FQHE.

For matching the topological properties with quantum system properties, the quantization according to the Feynman path integral method is useful [12] [23] [24]. Due to a fundamental ideas of path integral quantization in the case of not simply-connected configuration spaces (distinguished by the nontrivial π_1 groups), like for the multi-particle systems, additional phase factors—the weights of nonequivalent (nonhomotopic) trajectory classes and summation over these classes must be included in the path integral definition. It means that a measure in the trajectory space is distributed over separated disjoint homotopy classes of π_1 because in general this measure cannot be defined uniformly over the domain consisting of disjoint pieces owing to the continuity requirements. As it was proved [12], these weight factors form a one-dimensional unitary representation (1DUR) of the related braid group. Different 1DURs of the full braid group give rise to distinct types of quantum particles corresponding to the same classical ones. In this manner one can get fermions and bosons corresponding

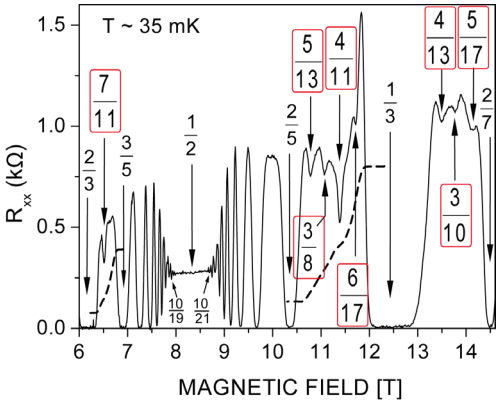

Figure 1. FQHE features in a quantum well GaAs/AlGaAs with electron density of 10^{11} 1/cm^{-2}; *Rxx* for $\frac{2}{3} > \nu > \frac{2}{7}$ at the temperature equal $T \sim 35$ mK (after Ref. [15]); the fractions outside the standard CF hierarchy are indicated in color.

to only possible 1DURs of the permutation group S_N, $\sigma_i \to e^{i\pi}$ and $\sigma_i \to e^{i0}$, respectively (the permutation group S_N is the full braid group in 3D and in higher dimensions, σ_i, $i = 1, \cdots, N$ denote generators of S_N, *i.e.*, the exchanges between elements—particles *i*-th and *i* + 1-th). For the far more rich braid groups in 2D one encounters, however, the infinite number of possible so-called anyons (including bosons an fermions) related to 1DURs, $\sigma_i \to e^{i\Theta}$, $\Theta \in [0, 2\pi)$ (σ_i are here generators of the full braid group in 2D, cf. **Figure 2**) [11] [23]-[25].

We will develop the topological approach to Hall systems and recover Laughlin correlations by employing geometry properties of the so-called cyclotron braids [13] [14] in the framework of formal braid group approach and without invoking to any auxiliary elements inherent to the CF concepts. We will demonstrate that particles with statistics properties familiar in the CF model are 2D quantum particles characterized by appropriate 1DURs of the cyclotron braid subgroups.

3. Too-Short for Interchanges Cyclotron Trajectories in FQHE

3.1. 2D Full Braid Group without Magnetic Field—Anyons

One-dimensional unitary representations (1DURs) of the full braid group [11], *i.e.*, of π_1 homotopy group of the configuration space for indistinguishable *N* particles define weights for the path integral summation over trajectories [12] [24]. All trajectories fall into separated homotopy classes that are distinguished by non-equivalent closed loops (from π_1) attached to open trajectories $\lambda_{a,b}$ (linking in the configuration space points, *a* and *b*). Then an additional summation over these classes with an appropriate unitary factor (the weight of the particular trajectory class) should be included in the path integral (for transition from the point *a* at the time moment $t = t_1$ to the point *b* at $t = t_2$) [23] [24]:

$$I_{a,t_1 \to b,t_2} = \sum_{l \in \pi_1} e^{i\alpha_l} \int d\lambda_l e^{iS\left[\lambda^l_{(a,b)}\right]}, \tag{2}$$

where π_1 stands for the full braid group and the index *l* enumerates π_1 group elements, λ^l indicates an open trajectory $\lambda_{(a,b)}$ between *a* and *b* with added *l*th loop from π_1 (the full braid group here). The factors $e^{i\alpha_l}$ form a 1DUR of the full braid group and the distinct representations correspond to the distinct types of quantum particles [12] [24]. The closed loops from the full braid group describe exchanges of identical particles, thus, the full braid group 1DURs indicate the statistics of particles [23]-[25]. The full braid group for 2D manifold has infinite number of 1DURs, $e^{i\alpha}$, with $\alpha \in [0, 2\pi)$. The corresponding particles are called anyons, including bosons for $\alpha = 0$ and fermions for $\alpha = \pi$.

Nevertheless, it is impossible to relate CFs with the 1DURs of the full braid group in 2D, because 1DURs are periodic with a period of 2π, whereas the CFs require the statistics phase shift *q*π, *q*-odd integer. In order to solve this problem, we propose to associate CFs with the appropriately constructed braid subgroups instead of the full braid group and in this way to distinguish CFs from the ordinary fermions.

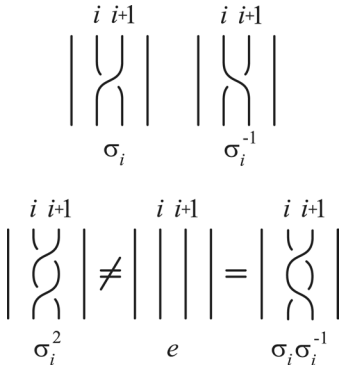

Figure 2. The geometrical presentation of the generator σ_i of the full braid group for R^2 and its inverse σ_i^{-1} (left); in 2D $\sigma_i^2 \neq e$ (right).

3.2. Cyclotron Structure of Braid Group in 2D Charged Systems at Strong Magnetic Field Presence

The full braid group contains all accessible closed multi-particle classical trajectories, *i.e.*, braids (with initial and final orderings of particles that may differ by permutation as is admitted for indistinguishable particles). One can, however, notice that inclusion of a strong magnetic field may substantially change trajectories—a classical cyclotron motion may confine a variety of accessible braids if magnetic field is strong enough and the manifold is two-dimensional. When the separation of particles is greater than twice the cyclotron radius, which situation occurs at fractional LLL fillings, the exchanges of particles along single-looped cyclotron trajectories are *precluded*, because the cyclotron orbits are *too short* for particle interchanges in this case. Interaction cannot enhance cyclotron orbit size in the uniform multiparticle system.

Particles must, however, interchange in the braid picture for the reason of defining the statistics and creation of the collective correlated state. Therefore, in order to allow exchanges again, the cyclotron radius must somehow be enhanced. This can be achieved by screening the external field, like in the construction of the CFs with flux tubes oppositely oriented with respect to the external field [22]. We suppose that the natural way to enhance the range of cyclotronic movement is to exclude inaccessible braids from the full braid group. We will show that remaining braids would be sufficiently large in size for particle exchanges realization [13] [14]. We will demonstrate below that at high magnetic fields in 2D charged N-particle systems, the *multi-looped braids* allow for the effective enlargement of cyclotron orbits, thus restoring particle exchanges in a natural way.

4. Cyclotron Braid Subgroups—Restitution of Particle Interchanges in 2D

The multi-looped braids form the *cyclotron braid subgroups* which are generated by the following generators:

$$b_i^{(q)} = \sigma_i^q, \quad (q = 3,5\cdots), \quad i = 1,\cdots,N-1, \tag{3}$$

where each q corresponds to a different type of the cyclotron subgroup and σ_i are the generators of the full braid group. The group element $b_i^{(q)}$ represents the interchanges of the ith and (i + 1)th particles with $\frac{q-1}{2}$ loops, which is clear by virtue of the definition of the single interchange σ_i (cf. **Figure 3**, e.g., for q = 3 one

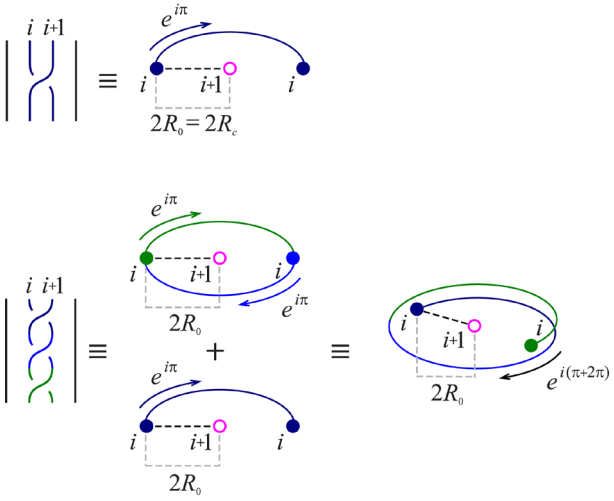

Figure 3. The generator σ_i of the full braid group and the corresponding relative trajectory of the ith and (i + 1)th particles exchange (upper); the generator of the cyclotron braid subgroup, $b_i^{(q)} = \sigma_i^q$ (in the figure, q = 3), corresponds to additional $\frac{q-1}{2}$ loops when the ith particle interchanges with the (i + 1)th one (lower) ($2R_0$ is the inter-particle separation, R_c is the cyclotron radius, 3D view added for better visualization).

deals with elementary particle exchange braid with one additional loop). It is clear that $b_i^{(q)}$ generate a subgroup of the full braid group as they are expressed by the full braid group generators σ_i.

The 1DURs of the full group confined to the cyclotron subgroup (they do not depend on *i* as 1DURs of the full braid group do not depend on *i* by virtue of the σ_i generators property, $\sigma_i\sigma_{i+1}\sigma_i=\sigma_{i+1}\sigma_i\sigma_{i+1}$, $1\le i\le N-1$, [11]) are 1DURs of the cyclotron subgroup:

$$b_i^{(q)}\to \mathrm{e}^{iq\alpha},\quad i=1,\cdots,N-1, \tag{4}$$

where *q* is an odd integer and $\alpha\in(-\pi,\pi]$. We argue, that these 1DURs, enumerated by the *pairs* (q,α), describe composite anyons (CFs, for $\alpha=\pi$). Thus in order to distinguish various types of composite particles one has to consider (q,α) 1DURs of cyclotron braid subgroups.

In agreement with the general rules of quantization [25], the *N*-particle wave function must transform according to the 1DUR of an appropriate element of the braid group, when the particles traverse, in classical terms, a closed loop in the configuration space corresponding to this particular braid element. In this way the wave function acquires an appropriate phase shift due to particle interchanges (*i.e.*, due to exchanges of its positions as arguments of the wave function, according to the prescription given by braids in 2D configuration space). Using 1DURs as given by (4), the Aharonov-Bohm phase of CFs fictitious fluxes is replaced by the contribution of additional loops (each loop adds 2π to the total phase shift, if one considers 1DUR with $\alpha=\pi$ related to CFs, cf. **Figure 3** (right)). Let us emphasize that the real particles do not traverse the braid trajectories, as quantum particles do not have any trajectories, but the exchanges of arguments of the *N*-particle wave function can be represented by braid group elements; in 2D an exchange of particle positions described by coordinates on the plane does not resolve itself to the permutation only, as it was in 3D, but must be performed according to an appropriate element of the braid group, being in 2D not the same as the permutation group [25]. Hence, for the braid cyclotron subgroup generated by $b_i^{(q)}$, $i=1,\cdots,N-1$, we obtain the statistics phase shifts $q\pi$ for CFs (*i.e.*, for $\alpha=\pi$ in Equation (4)), as required by Laughlin correlations, without the need to model them with the auxiliary field flux tubes.

Each additional loop of a relative trajectory for the particle pair interchange (as defined by the generators $b_i^{(q)}$) reproduces an additional loop in the individual cyclotron trajectories for both interchanging particles—cf. **Figure 4**. The cyclotron trajectories are repeated in the relative trajectory (*c*, *d*) with twice the radius of the individual particle trajectories (*a*, *b*). In quantum language, with regards to classical multi-looped cyclotron trajectories, one can conclude only about the number, $\frac{BS}{N}\Big/\frac{hc}{\mathrm{e}}$, of flux quanta per single particle in the system, which for the filling $\frac{1}{q}$ is *q* (for odd integer *q*), *i.e.*, the same as the number of individual particle cyclotron loops (which equals to $q=2n+1$, where $n=1,2,\cdots$ indicates the number of additional braid-loops for particle interchange trajectories). From this observation it follows a simple rule: for $\nu=\frac{1}{q}$ (*q* odd), each additional loop of a cyclotron braid corresponding to particle interchange, results in two additional flux quanta piercing the individual particle cyclotron trajectories. This rule follows immediately from the definition of the cyclotron trajectory, which must be a *closed* individual particle trajectory related to a double interchange of the particle pair (cf. **Figure 5**). In this way, the cyclotron trajectories of both interchanging particles are closed, just like the closed relative trajectory for the double interchange (the braid trajectory for the elementary exchange of the indistinguishable particles is open in the geometrical presentation, and therefore the double interchange is needed to close this trajectory in this presentation). If the interchange is simple, *i.e.*, without any additional loops, the corresponding individual particle cyclotron trajectories are also simple, *i.e.*, single-looped. Nevertheless, when the interchange of particles is multi-looped, as associated with the *q*-type cyclotron subgroup $(q>1)$, the double interchange relative trajectory has $2\frac{q-1}{2}+1=q$ closed loops, and the individual cyclotron trajectories are also multi-looped, with *q* loops [14].

In 2D additional loops cannot enhance the total surface of the system. In this regard, it is important to emphasize the basic difference between the circumvolutions of a 3D winding (e.g., of a wire) and of multi-looped 2D cyclotron trajectories. 2D multi-looped trajectories do not enhance the surface of the system and therefore do

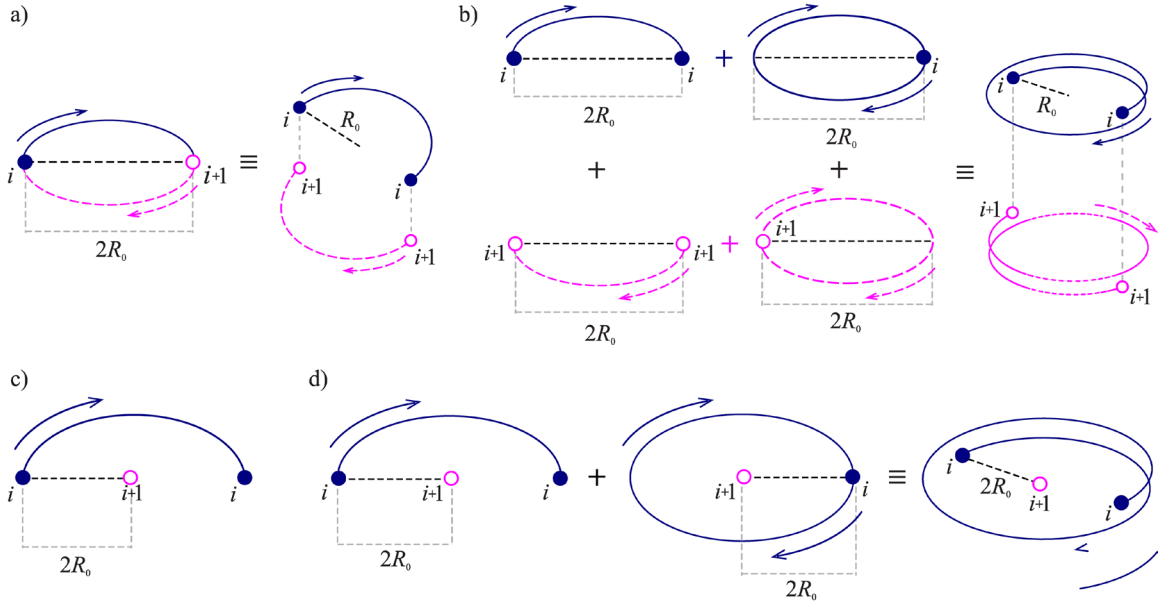

Figure 4. Half of the individual particle cyclotron trajectories of the *i*th and (*i* + 1)th particles (top) and the corresponding relative trajectories (bottom) for interchanges of the *i*th and (*i* + 1)th 2D-particles under a strong magnetic field, for $\nu = 1$ (left) and for $\nu = \frac{1}{3}$ (right), respectively (R_c—cyclotron radius, $2R_0$—particle separation, 3D added for better visualization).

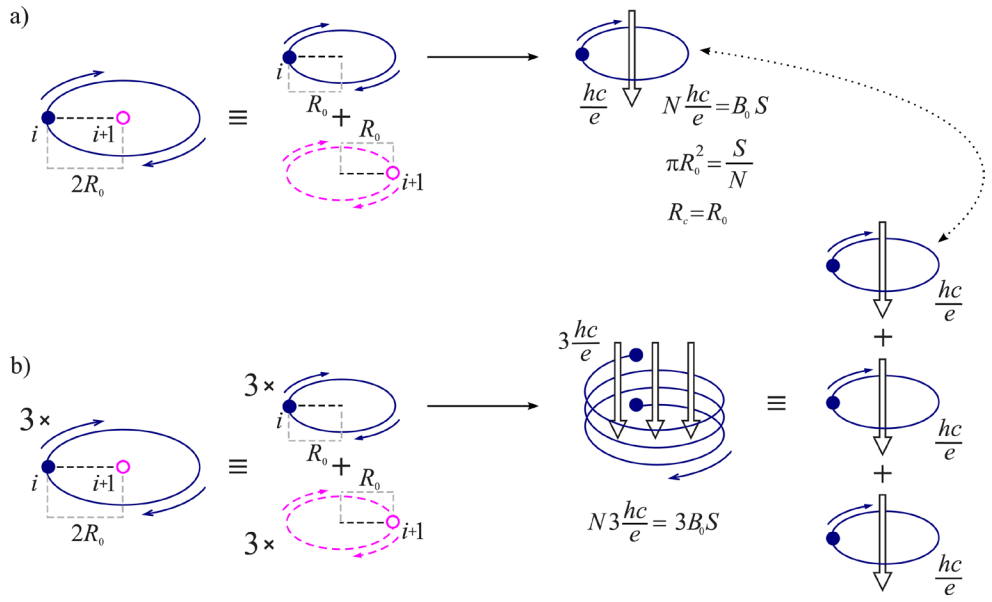

Figure 5. Cyclotron trajectories of individual particles must be closed, therefore they correspond to *double* exchange braids, for both, simple exchanges (upper) and exchanges with additional loops (lower), in the right part, quantization of flux per particle, for $\nu = 1$ and $\nu = \frac{1}{3}$, is indicated.

not enhance the total magnetic field flux *BS* piercing the system, in opposition to 3D case. In 3D case, each circumvolution of the winding adds a new portion of the flux, just as a new circumvolution adds a new surface, which is, however, impossible in 2D. Thus in 2D all loops must share the same total flux, which results in *diminishing* flux-portion per a single loop and, effectively, in longer cyclotron radius (allowing again particle inter-

changes).

The additional loops in 2D take away the flux-portions (equal to $q-1$ flux quanta just at $\nu=\frac{1}{q}$, q odd) simultaneously diminishing the effective field; this gives an explanation for Jain's auxiliary fluxes screening the external field B. Thus, it is clear that the CFs are actually not compositions of particles with flux-tubes, but are rightful particles in 2D corresponding to 1DURs of the cyclotron subgroups instead of the full braid group, which is unavoidably forced by too short ordinary single-looped cyclotron trajectories. The original name "composite fermions" can be, however, still used for history reason. Moreover, one can use a similar name, "composite anyons", for particles associated with fractional 1DURs (*i.e.*, with fractional α) of the cyclotron subgroup instead of the full braid group, the latter linked rather with ordinary anyons (without magnetic field).

How Additional Loops Enhance the Cyclotron Radius in 2D Hall System

It is important to emphasize that braid group approach in terms of trajectories does not describe detailed classical trajectories of particles in the system but only determines classes of trajectories which are available upon topological constraints. Thus, if one considers physical factors which restrict availability of particular classes of trajectories (e.g., specific topology of configuration space of N particles system located on specified manifold), one should describe a condition upon which one can determine whether a specific trajectory class is possible or not. In the case of N particles system on 2D plane in the presence of a perpendicular strong magnetic field such a condition can be based on the cyclotron radius. Although cyclotron radius is properly defined for free particles one can still consider some kind of focusing of charged particle motion on the cyclotron radius scale even in the presence of interaction, especially in homogeneous planar system with isotropic interaction. One can also observe that for noninteracting fermions we have in the case of completely filled LLL exactly one external field flux quantum $\frac{hc}{\mathrm{e}}$ per particle which means that the cyclotron radius is defined by the single flux quantum. Here must be emphasized that in the case of the degenerated LLL all particles have the same cyclotron radius. Even though the velocity is not well determined in the LLL (their coordinates do not commute as the operators), all particles have, however, the same kinetic energy, thus all particles have the same averaged velocity and the same cyclotron radius. In order to determine whether a trajectory class is available for particles in the system can be brought to comparison of cyclotron orbit size with distance between particles, which for homogeneous system is defined from density and blocked by Coulomb repulsion preventing approaching one particle onto another one. The distance between particles in homogeneous system is protected by the short-range part of the Coulomb interaction. Thus potentially available trajectory must ensure reaching neighboring particles, *i.e.*, the trajectory must fit to the minimal distance between particles. The rigorous requirement to keep minimal distance intact leads to the observation that in too strong magnetic field (when the cyclotron radius is smaller than half of the minimal distance) some trajectory classes are unavailable for particles—as shown in **Figure 6**.

In 2D charged system in the presence of the perpendicular magnetic field only cyclotron trajectories are available for particles. Thus if one increases the magnetic field magnitude then the cyclotron radius will decrease causing the trajectory of particles exchange impossible. The simplest exchange was the implementation

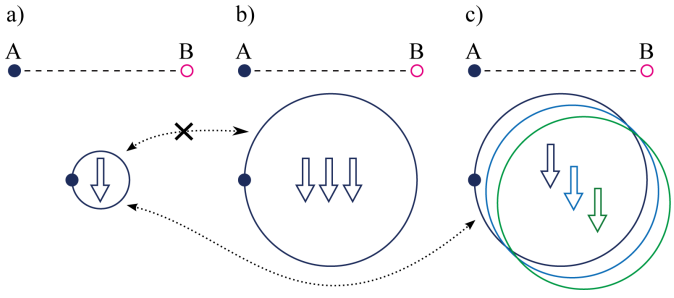

Figure 6. Schematic presentation of effective growth of cyclotron radius in 2D case for multi-looped cyclotron trajectory in comparison to single-looped trajectory (length $A-B$ means uniform separation between particles in the system).

of the generators of the full braid group and now they cannot be defined. If one excludes unavailable trajectories too short for exchanges, the rest of the full braid group occurs a subgroup generated by new generators describing in 2D multi-looped braids and corresponding to multi-looped cyclotron trajectories. These multi-looped cyclotron trajectories have the larger effective size allowing to match neighboring particles at strong magnetic field presence. This subgroup we call cyclotron braid group (or subgroup).

The exchange trajectories of neighboring particles—the generators of braid group—are open trajectories i the geometrical presentation (in fact for indistinguishable particles the initial and final particle ordering are bound despite remunerations, but for geometrical presentation of braid group some selected, arbitrary ordering of particles is assumed). Nevertheless, the cyclotron trajectories are closed trajectories despite the enumeration of particles (only for closed trajectories one can define the piercing flux of the magnetic field). Thus, one must consider closed cyclotron trajectories. The smallest closed trajectory is a double exchange (two semicircles create closed circle in the simplest case of single-looped exchanges). If now one considers multi-looped exchanges (for $\nu = 1/q$, q—odd), one has to take also into account closed trajectories related to cyclotron trajectories—each particle traverses a closed cyclotron trajectory with $q-1$ additional loops. Closed loops can be added only by one, therefore the simplest exchange with one additional loop results in three-looped cyclotron trajectory of individual particles. This explains why FQHE manifests in simplest case for $\nu = 1/3$. Summarizing this argumentation, we emphasize that additional loops can be added to single exchange trajectory (braid group generator) one by one (in order to keep the exchange character of the trajectory). Then to the closed trajectories (double exchange) must be added the double number of the additional loops, two in the case of $\nu = 1/3$. That is why braid trajectories are odd-looped trajectories (1, 3, 5, 7, etc. for respectively $\nu = 1$, $\nu = 1/3$, $nu = 1/5$ etc.) and not even-looped closed trajectories (such trajectories divided on half will not give an exchange trajectory). For $\nu = 1/q$ LLL fillings particles traverse the closed individual cyclotron trajectories with $q-1$ additional loops and simultaneously open exchange trajectories with $(q-1)/2$ additional loops.

Those multi-looped closed trajectories in case of 2D have enhanced effective cyclotron radius which allows particles to exchange and to define the statistics. Each additional loop cannot add any new surface in 2D space. For e.g., $\nu = 1/3$ the cyclotron radius is too short for exchanges. For each particle at corresponding magnetic field we have 3 flux quanta $3hc/\mathrm{e}$. But the cyclotron trajectory is defined by a single flux quantum. However, if one considers 3-looped cyclotron trajectory in 2D with the size as trajectory corresponding to $3hc/\mathrm{e}$ then the total flux of external field does not change. The surface of the multi-looped trajectory also fits to the particle separation distance, but through every loop passes only single flux quantum because in 2D the total flux must be shared between all loops, which means that in the multi-looped case the effective cyclotron radius is greater than for single-looped trajectory. It is illustrated in **Figure 6** for $\nu = 1/3$ case and the arrow represents the single flux quantum defining the cyclotron radius.

The Coulomb interaction plays a central role in the collective state with Laughlin correlations [17]-[19] protecting the uniform equidistant distribution of particles. Nevertheless, in 2D systems upon the quantized magnetic field, the interaction of charges cannot be accounted for in a manner of the standard dressing of particles with the interaction as it was typical for quasiparticles in solids, because in 2D Hall regime this interaction does not have a continuous spectrum with respect to particle separation expressed by relative angular momentum projection [17] [18]. This non-continuous character of the interaction contribution in 2D charged systems upon sufficiently strong magnetic fields precludes the continuity of the mass operator which prevents the quasiparticle definition (as a pole of the retarded single-particle Green function).

5. Topological Chern Insulators

Investigation of IQHE and then of FQHE in 2D charged systems opened a broad area of topologically conditioned effects [26]. Especially deeply developed with this regard is the present understanding of IQHE treated in single-particle and topological terms [7]. This is based on the observation that the IQHE states protected by Landau quantization gaps are not connected with symmetry breaking as many other condensed matter phases in scenario of ordinary phase transitions, but rather with some topological invariants associated to a particular geometry and matter organization [6] [27]. These invariants are better and better recognized currently in terms of homotopy groups related to specially defined multidimensional transformations of physically conditioned objects like Green functions and their derivatives [28] [29], previously developed for description of topology of textures in multicomponent condensed matter states with rich matrix order parameter, including superfluid He^3

or liquid crystals [4]. The role of various factors protecting gaps separating flat bands (almost degenerated, as LLs at the interaction presence, and massively degenerated in the absence of the interaction) are of particular interest in view of the role of the magnetic field breaking time reversion or other effects like spin-orbit interaction or special type (time-reversion breaking) traversing around the closed loop inside an elementary cell with complex hopping constants. Generalization of the familiar in mathematics Chern invariants [5] is developed in order to grasp the essential topology of various multiparticle structures [5]-[7]. The mappings of the Brillouin zone into the state related objects can be in that manner classified by disjoint classes corresponding to topologically nonequivalent band organizations protected by energy gaps conditioned by various physical factors and leading to distinct incompressible states in analogy to their prototype in the form of IQHE. The distinctive character of 2D space is linked in the latter case with the magnetic field flux quantization.

Topological notions allow for definition of a new state of crystal called topological insulator. Despite of the local similarity between the gapped states of the ordinary and the topological insulator, the global arrangement of the band, noticeable only non-locally (on the Brillouin zone as a whole), induces different overall behavior of the system. In the case of topological insulator one deals with insulating state inside the sample, whereas with conducting non-dissipative state on the sample edge, protected topologically, what is, however, no case for ordinary insulating state. This surprising phenomenon was confirmed experimentally, which was a strong stimulus to the rapid and enormous great growth of the interest.

The topological insulators from point of view of band organization must be characterized by flat bands which meet in summits of locally cone shaped valleys resembling Dirac points in graphene. These Dirac points changes the topology and allow Chern-type invariant to attain nonzero value, indicating the emergence of the different global state. Spin degrees of freedom are of high significance with regard to topological arrangement and related spin-type topological insulators are referred as to spin IQHE.

Commonly accepted definition of the topological insulator emphasizes the robust metallic character of the edge or surface states and extended bulk insulating states that are also robust against disorder. This is an extraordinary behavior, especially in two-dimensional models—when an edge or a surface is cut in a sample of topological insulator, the emerging edge states seem to be connected to these bulk states. The edge states can be viewed as these extended bulk states terminating at the boundary. For this reason, the bulk and the edge properties of the topological insulators are equally important and mutually dependent. This is the development of the interpretation of IQHE revealed a spectacular emergence of non-dissipative charge currents flowing around the edges of any finite IQHE sample. The IQHE was observed only in the presence of an externally applied magnetic field.

In 1988 Haldane presented a model of a condensed matter phase that exhibits IQHE without the need of a macroscopic magnetic field [30]. The general idea of this effect can be sketched by writing a model Hamiltonian, for the system of spinless particles occupying a honeycomb-type planar lattice with one state $|n\rangle$ per site,

$$\hat{H} = \sum_{\langle n,m\rangle} |n\rangle\langle m| + \sum_{\langle\langle n,m\rangle\rangle} \left[\xi_n |n\rangle\langle m| + h.c.\right], \tag{5}$$

where $\langle n,m\rangle$ indicates summation over nearest neighbors, whereas the symbol $\langle\langle n,m\rangle\rangle$ indicates that the summation includes also next-nearest neighbors, the hopping factor $\xi_n = 0.5(t+i\eta)\alpha_n$ is assumed artificially as a complex number, and $\alpha_n = \pm 1$ depending on how n is positioned in the unit cell (equivalently an isospin can be introduced here), as is shown in **Figure 7**. The essence of the topological effect is linked with imaginary contribution to hopping factor given by η. The band structure corresponding to this Hamiltonian depends on parameters t, η and exhibits nontrivial topological properties (expressed by the Chern number C) for various values t, η.

The difference between a quantum Hall state and an ordinary insulator is a matter of topology [8]. A 2D band structure consists of a mapping from the momentum $\boldsymbol{k}$ defined on a torus of the Brillouin zone to the Bloch Hamiltonian $H(\boldsymbol{k})$. Gapped band structures can be classified topologically by considering the equivalence classes of this mapping that can not be continuously deformed into one another without closing the energy gap. These classes are distinguished by integer topological invariants—the Chern numbers. The Chern numbers were introduced in the theory of fiber bundles [10], and they can be understood physically in terms of the Berry phase [9] associated with the Bloch wave functions $|u_m(\boldsymbol{k})\rangle$. When $\boldsymbol{k}$ traverses a closed loop, the Bloch function acquires a Berry phase given by the line integral of $\boldsymbol{A}_m = i\langle u_m|\nabla_k|u_m\rangle$, or by a surface integral of the Berry field $\boldsymbol{F}_m = \nabla\times\boldsymbol{A}_m$. The Chern invariant is the total Berry field flux for the Brillouin zone,

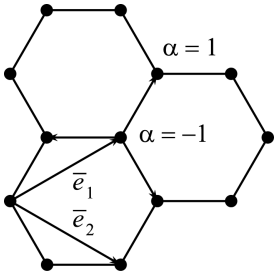

Figure 7. The honeycomb structure (similar as in graphene) for the Haldane model [30]; e_1, e_2 are Bravais lattice vectors, nonequivalent site positions in the unit cell are indicated by $\alpha = \pm 1$.

$$C = \frac{1}{2\pi}\int \mathrm{d}^2 k \boldsymbol{F}_m \in Z\,, \tag{6}$$

C is integer for reasons analogous to the quantization of the Dirac magnetic monopole. The Chern number, C, is a topological invariant in the sense that it cannot change when the Hamiltonian varies smoothly and this explains the quantization of conductivity in IQHE [8]. Helpful would be here a simple analogy. Rather than maps from the Brillouin zone to a Hilbert space, one can consider maps from two to three dimensions, which describe surfaces. 2D surfaces can be topologically classified by their genus g, which counts the number of holes. For instance, a sphere has $g = 0$, while a torus has $g = 1$. A theorem in mathematics states that the integral of the Gaussian curvature over a closed surface is a quantized topological invariant, and its value is related to g. The Chern number is an integral of a related curvature.

Change of the Chern number requires closing the insulating gap. This happens for the Hamiltonian (5) in the Dirac-like points when the locally cone shaped valleys of conduction and valence bands touch together. This allows for the change of the Chern number and for the metallic boundary states protected by still insulating phase inside the sample [6] [7].

The systems that behave like the one described by Haldane are now called Chern insulators. The time reversal symmetry in these systems is broken like in the IQHE, but it is broken by the presence of a net magnetic moment in each unit cell rather than by an external magnetic field, as it was the case for IQHE. The Chern insulators were never found experimentally as of yet.

Fractional Chern Insulators

Recently grew up a new field related to IQHE and its fractional version, namely Chern insulators and fractional Chern insulators, respectively. There is linked with development of Haldane model of IQHE effect without Landau levels, but with time-braking imaginary part of hopping factors for carries on planar lattice instead of the external magnetic field. The quantization of carrier orbit along elementary cell is given in this case by the quantization of the Berry field flux which can be expressed by the Chern numbers. Even though neither Chern insulator nor its fractional state is not observed experimentally, the theoretical studies are currently extensively developing [31] [32]. From exact diagonalization of corresponding Hamiltonians, provided they give sufficiently flat bends, it follows that the interaction causes collective state analogous to FQHE, though without any magnetic field and with the dynamics assigned by nontrivial Chern number. What is especially challenging, the fractional Chern insulator is predicted for fractional ($\frac{1}{p}$, p—odd integer) fillings of planar crystal lattice, analogously to ordinary FQHE. Again arises a question of how single particle trajectories ranged by Berry field flux quantization to the elementary cell can match every third cell (for 1/3 filling). The concept of CFs with auxiliary field flux-tubes is not useful here, due to absence of the magnetic field. The trajectories must be, however, enlarged somehow to allow organization of the collective state with the determined statistics via particle interchanges.

Again here the multi-looped braid subgroup might be the solution of the problem with too short orbits, especially in this case which is without any other conceptual competition (composite fermions are associated with

magnetic field flux tubes, but here no magnetic field presents). This supports the topological attitude to fractional correlated 2D states which is robust against details of quantized field flux and explains the occurrence of such states only at specific fractions for fillings, surprisingly coinciding for FQHE and for fractional Chern insulators.

To be more specific with this regard, the recent analyzes of FQHE in model systems without Landau levels [33] [34] are worth emphasizing also. In the paper [33] there is constructed a class of model Hamiltonians on 2D lattice which give nearly-flat bands with nontrivial topology. This property is regarded as a required prerequisite for organization of FQHE-like states when interaction would be next included. For flat band the kinetic energy is frozen which allows the interaction to dominate and create strongly correlated state of FQHE type. This has been theoretically verified in the paper [34] for a checkerboard lattice including nearest and next-nearest interaction in model Hamiltonian of the form,

$$H = -H_0 + U\sum_{\langle i,j\rangle} n_i n_j + V\sum_{\langle\langle i,j\rangle\rangle} n_i n_j , \tag{7}$$

where H_0 is a two-band checkerboard lattice model with nonzero Chern number implemented by complex hopping factors of the type,

$$H_0 = -t\sum_{\langle i,j\rangle} \mathrm{e}^{i\psi_{ij}} \left(c_i^+ c_j + h.c.\right) + H_1 , \tag{8}$$

and H_1 describes ordinary real-number-assigned hopping between next and next-next nearest neighbors [33]. Some attributes characteristic for FQHE have been indicated within this model for fractional fillings 1/3 and 1/5 (in the latter case repulsion V was required above a certain threshold value, unless U enhances strongly) [34]. This observation supports an idea of multi-looped structure of quasiclassical wave packets which in this way can reach equidistantly separated 2D particles (in every third cell for $\nu = 1/3$) due to repulsion interaction in almost flat band with suppressed kinetic energy, quite similarly as in the described above 2DEG system in the magnetic field. Though any links can be here drawn toward CF model with auxiliary magnetic field flux quanta attached to hypothetical composite particles, the multi-looped requirements in order to enhance orbits still hold. As number of loops can be only integer, this explains the fractional structure of fillings exactly in the same manner as in the case of 2DEG upon strong magnetic field. The role of cyclotron orbit quantization is substituted here by the orbit quantization due to Chern number invariant conservation (*i.e.*, the quantization of the Berry field flux instead of the magnetic field flux).

6. Conclusions

By means of braid group approach it is possible to select appropriate braid subgroups of the full braid group of which one dimensional unitary representations (1DURs) define effective particles in the correlated states referred to FQHE. The argumentation is linked with the simple observation that at fractional fillings of the LLL the cyclotron trajectories which build braids in equidistantly distributed 2D charged system are too short in comparison to particle separation when the magnetic field is sufficiently strong. This precludes particle exchanges which is, however, necessary for organization of the collective multiparticle state with the determined statistics according to 1DURs of related braid group. One can observe that only at these filling fractions at which FQHE occurs the multi-looped braid structure recover exchanges along enhanced cyclotron trajectories. This enhancement is an exclusive property of 2D system when additional loops of cyclotron trajectory cannot add a surface (oppositely to 3D multi-looped trajectory), but must share the same total external magnetic field flux, which leads to effective enlargement of cyclotron orbits. For $1/q$ fillings of the LLL, the braid trajectories must be q-looped and then corresponding cyclotron orbits match neighboring particles without any artificial constructions. This unavoidable property of braids directly gives Laughlin correlations in the natural way and simultaneously explains the underlying spirit and structure of composite fermions phenomenologically introduced to illustrate Laughlin correlations. The flux tubes attached to composite fermions do not actually exist and they model the result of additional cyclotron loops presence. Recently developed theoretical studies of the fractional Chern insulators support correlated states with similar fractional hierarchy as in FQHE but without any magnetic field. This apparently goes beyond the explanation ability of the standard CF concept due to absence of the magnetic field in such systems, but still admit the multi-looped braid group explanation. Instead of the magnetic field quantization in fractional topological Chern insulators one can consider quantization of the Berry field flux which selects orbits similarly to magnetic field flux quantization. Multi-looped trajectories are here responsible

for the same hierarchy of fillings as in FQHE. This evidences some advantages of the homotopy braid group approach to correlations in various 2D systems.

Acknowledgements

The support from the NCN Project UMO-2011/02/A/ST3/00116 is acknowledged.

References

[1] Ryder, L.H. (1996) Quantum Field Theory. 2nd Edition, Cambridge University Press, Cambridge. http://dx.doi.org/10.1017/CBO9780511813900

[2] Spanier, E. (1966) Algebraic Topology. Springer-Verlag, Berlin.

[3] Hatcher, A. (2002) Algebraic Topology. Cambridge University Press, Cambridge.

[4] Mermin, N. (1979) The Topological Theory of Defects in Ordered Media. *Reviews of Modern Physics*, **51**, 591. http://dx.doi.org/10.1103/RevModPhys.51.591

[5] Prodan, E. (2011) Disordered Topological Insulators: A Non-Commutative Geometry Perspective. *Journal of Physics A*: *Mathematical and Theoretical*, **44**, Article ID: 113001. http://dx.doi.org/10.1088/1751-8113/44/11/113001

[6] Hasan, M.Z. and Kane, C.L. (2010) Colloquium: Topological Insulators. *Reviews of Modern Physics*, **82**, 3045-3067.

[7] Qi, X.L. and Zhang, S.C. (2011) Topological Insulators and Superconductors. *Reviews of Modern Physics*, **83**, 1057. http://dx.doi.org/10.1103/RevModPhys.83.1057

[8] Thouless, D.J., Kohmoto, M., Nightingale, M.P. and den Nijs, M. (1982) Quantized Hall Conductance in a Two-Dimensional Periodic Potential. *Physical Review Letters*, **49**, 405. http://dx.doi.org/10.1103/PhysRevLett.49.405

[9] Berry, M.V. (1984) Quantal Phase Factors Accompanying Adiabatic Changes. *Proceedings of the Royal Society of London. Series A, Mathematical and Physical Sciences*, **392**, 45-57.

[10] Nakahara, M. (1990) Geometry, Topology and Physics. Adam Hilger, Bristol.

[11] Birman, J.S. (1974) Braids, Links and Mapping Class Groups. Princeton University Press, Princeton.

[12] Laidlaw, M.G. and DeWitt, C.M. (1971) Feynman Functional Integrals for Systems of Indistinguishable Particles. *Physical Review D*, **3**, 1375-1378. http://dx.doi.org/10.1103/PhysRevD.3.1375

[13] Jacak, J., Jóźwiak, I. and Jacak, L. (2009) New Implementation of Composite Fermions in Terms of Subgroups of a Braid Group. *Physics Letters A*, **374**, 346-350. http://dx.doi.org/10.1016/j.physleta.2009.10.075

[14] Jacak, J., Jóźwiak, I., Jacak, L. and Wieczorek, K. (2010) Cyclotron Braid Group Structure for Composite Fermions. *Journal of Physics*: *Condensed Matter*, **22**, Article ID: 355602. http://dx.doi.org/10.1088/0953-8984/22/35/355602

[15] Pan, W., Störmer, H.L., Tsui, D.C., Pfeiffer, L.N., Baldwin, K.W. and West, K.W. (2003) Fractional Quantum Hall Effect of Composite Fermions. *Physical Review Letters*, **90**, Article ID: 016801. http://dx.doi.org/10.1103/PhysRevLett.90.016801

[16] Laughlin, R.B. (1983) Anomalous Quantum Hall Effect: An Incompressible Quantum Fluid with Fractionally Charged Excitations. *Physical Review Letters*, **50**, 1395-1398. http://dx.doi.org/10.1103/PhysRevLett.50.1395

[17] Haldane, F.D.M. (1983) Fractional Quantization of the Hall Effect: A Hierarchy of Incompressible Quantum Fluid States. *Physical Review Letters*, **51**, 605-608. http://dx.doi.org/10.1103/PhysRevLett.51.605

[18] Prange, R.E. and Girvin, S.M. (1990) The Quantum Hall Effect. Springer-Verlag, New York. http://dx.doi.org/10.1007/978-1-4612-3350-3

[19] Laughlin, R.B. (1983) Quantized Motion of Three Two-Dimensional Electrons in a Strong Magnetic Field. *Physical Review B*, **27**, 3383-3389. http://dx.doi.org/10.1103/PhysRevB.27.3383

[20] Landau, L.D. and Lifshitz, E.M. (1972) Quantum Mechanics: Non-Relativistic Theory. Nauka, Moscow.

[21] Abrikosov, A.A., Gorkov, L.P. and Dzialoshinskii, I.E. (1975) Methods of Quantum Field Theory in Statistical Physics. Dover Publications Inc., Dover.

[22] Jain, J.K. (1989) Composite-Fermion Approach for the Fractional Quantum Hall Effect. *Physical Review Letters*, **63**, 199-202. http://dx.doi.org/10.1103/PhysRevLett.63.199

[23] Wilczek, F. (1990) Fractional Statistics and Anyon Superconductivity. World Scientific, Singapore City. http://dx.doi.org/10.1142/0961

[24] Wu, Y.S. (1984) General Theory for Quantum Statistics in Two Dimensions. *Physical Review Letters*, **52**, 2103-2106. http://dx.doi.org/10.1103/PhysRevLett.52.2103

[25] Sudarshan, E.C.G., Imbo, T.D. and Govindarajan, T.R. (1988) Configuration Space Topology and Quantum Internal

Symmetries. *Physics Letters B*, **213**, 471-476. http://dx.doi.org/10.1016/0370-2693(88)91294-4

[26] Avron, J.E., Osadchy, D. and Seiler, R. (2003) A Topological Look at the Quantum Hall Effect. *Physics Today*, **56**, 38-42.

[27] Qi, X.L. and Zhang, S.C. (2010) The Quantum Spin Hall Effect and Topological Insulators. arXiv:1001.1602v1 [cond-mat.mtrl-sci]

[28] Wang, Z., Qi, X.L. and Zhang, S.C. (2010) Topological Order Parameters for Interacting Topological Insulators. *Physical Review Letters*, **105**, Article ID: 256803. http://dx.doi.org/10.1103/PhysRevLett.105.256803

[29] Qi, X.L. (2011) Generic Wave-Function Description of Fractional Quantum Anomalous Hall States and Fractional Topological Insulators. *Physical Review Letters*, **107**, Article ID: 126803. http://dx.doi.org/10.1103/PhysRevLett.107.126803

[30] Haldane, F.D.M. (1988) Model of Quantum Hall Effect without Landau Levels: Condensed Matter Realization of the "Parity Anomaly". *Physical Review Letters*, **61**, 2015-2018. http://dx.doi.org/10.1103/PhysRevLett.61.2015

[31] Kourtis, S., Venderbos, J.W.F. and Daghofer, M. (2012) Fractional Chern Insulator on a Triangular Lattice of Strongly Correlated t2g Electrons. *Physical Review B*, **86**, Article ID: 235118. http://dx.doi.org/10.1103/PhysRevB.86.235118

[32] Parameswaran, S.A., Roy, R. and Sondhi, S.L. (2013) Fractional Quantum Hall Physics in Topological Flat Bands. *Comptes Rendus Physique*, **14**, 816-839. http://dx.doi.org/10.1016/j.crhy.2013.04.003

[33] Sun, K., Gu, Z., Katsura, H. and Das Sarma, S. (2011) Nearly Flatbands with Nontrivial Topology. *Physical Review Letters*, **106**, Article ID: 236803. http://dx.doi.org/10.1103/PhysRevLett.106.236803

[34] Sheng, D.N., Gu, Z.C., Sun, K. and Sheng, L. (2011) Fractional Quantum Hall Effect in the Absence of Landau Levels. arXiv:1102.2658v1 [cond-mat.str-el]

Applied Mathematics, 2015, 6, 359-372
Published Online February 2015 in SciRes. http://www.scirp.org/journal/am
http://dx.doi.org/10.4236/am.2015.62034

Scientific Research Publishing

Availability Importance Measures for Virtualized System with Live Migration

Junjun Zheng, Hiroyuki Okamura, Tadashi Dohi

Department of Information Engineering, Graduate School of Engineering, Hiroshima University, Higashi-Hiroshima, Japan
Email: z1023@s.rel.hiroshima-u.ac.jp, okamu@rel.hiroshima-u.ac.jp, dohi@rel.hiroshima-u.ac.jp

Received 16 January 2015; accepted 6 February 2015; published 10 February 2015

Abstract

This paper presents component importance analysis for virtualized system with live migration. The component importance analysis is significant to determine the system design of virtualized system from availability and cost points of view. This paper discusses the importance of components with respect to system availability. Specifically, we introduce two different component importance analyses for hybrid model (fault trees and continuous-time Markov chains) and continuous-time Markov chains, and show the analysis for existing probabilistic models for virtualized system. In numerical examples, we illustrate the quantitative component importance analysis for virtualized system with live migration.

Keywords

Virtualized System, Live Migration, System Availability, Component Importance Analysis, Fault Tree, Continuous-Time Markov Chain

1. Introduction

Virtualization is one of the key technologies to deploy cloud computing, which provides a variety of system resources as a service over the Internet [1]. The virtualization is to create software components that emulate behavior of hardware units and platform, and is to control them in a software platform. The virtualization can be classified to several classes. For example, VMware, Xen and KVM can provide virtual machines that emulate physical computers as software. Also Docker offers more lightweight virtual machines than VMware, Xen and KVM as processes. From the reliability point of view, the virtualization is promising to deploy high-availability (HA) system. As is well known, the most popular virtualization is to create virtual machines (VMs) as software components that behave actual computers. However, since VMs are essentially software processes on platform,

How to cite this paper: Zheng, J., Okamura, H. and Dohi, T. (2015) Availability Importance Measures for Virtualized System with Live Migration. *Applied Mathematics*, **6**, 359-372. http://dx.doi.org/10.4236/am.2015.62034

they can be migrated to another physical server running the virtualization platform. In particular, if two physical servers have the same platform that can drive virtual machines, we exploit the live migration between them [2]. The live migration is a technique that allows a server administrator to move a running virtual machine of application between different physical machines without disconnecting the client or application. The live migration drastically improves the system availability by migrating a failed virtual machine on a platform to another platform.

Although the virtualization is a promising way for HA services, the design of system architecture is not so easy, compared to non-virtual system. For example, the system availability can easily be improved by increasing physical servers which run the virtualization platform. However, from the points of cost and energy consumption, it is not always the best design. That is, towards the best design of virtualized system, we should consider the method to evaluate the system performance beforehand.

On the performance index, Kundu *et al.* [3] presented statistical models using regression and artificial Neural networks. Also, Okamura *et al.* [4] proposed a queueing model to evaluate energy efficiency of virtualized system design. On the system index for reliability and availability, Cully *et al.* [5] and Farr *et al.* [6] built and evaluated their schemes to enhance the system availability in virtualized system design. Myint and Thein [7] also evaluated a system architecture combining virtualization and rejuvenation. Vishwanath and Nagappan [8] collected operation data of virtualized system and performed statistical analysis to reveal a causal relationship between server failures and hardware repairs. Kim *et al.* [9] focused on failure modes of virtualized system and presented availability evaluation using fault trees and continuous-time Markov chains (CTMCs). Also Matos *et al.* [10] developed the CTMC model representing the dynamic behaviors of live migration in the virtualized system. Zheng *et al.* [11] considered the component importance analysis for non-virtualized and virtualized system based on the model by Kim *et al.* [9].

This paper is an extension work of [11]. In [11], we have developed a method to evaluate the importance (the effect of a component's availability on the system availability) of components for hybrid models. The hybrid model consists of fault trees (FTs) and CTMCs. The FTs are top level descriptions for the system failure and represent causal relationship between component failures and system failures. The disadvantage of FT is not to describe the dynamic behaviors. To address this problem, dynamic FT is also proposed in [12]. On the other hand, CTMC can well describe the dynamic behaviors of system. In the hybrid model, CTMCs are used for defining the behavior of components. The advantage of hybrid model is to obtain the structure function of system failure with respect to component failures from FT and to be able to define the dynamic behaviors of components. Based on this feature, we have proposed the component importance analysis for hybrid model in [11]. However, the hybrid model had a limitation for the model expression. For example, when two or more components have interactions between them, the structure function cannot always be explicitly expressed. In such cases, we cannot use the hybrid model. Instead of using the hybrid model, we should use a CTMC describing whole the system behavior. In the component analysis of virtualized system, the behavior of live migration is this case. In fact, Matos *et al.* [10] presented only a CTMC for the live migration. Since the structure function cannot be obtained from the CTMC, we cannot also apply the component importance analysis by [11] to the live migration model. In this paper, we introduce the state-of-art component importance analysis [13] and apply it to the CTMC-based live migration model to reveal the component importance in the context of live migration.

The rest of this paper is organized as follows. Section 2 presents the hybrid model for virtualized system design in [11], and introduces the component importance analysis for the hybrid model from the availability point of view. In Section 3, we explain the CTMC model for live migration presented in [10], and show the component importance analysis by using only CTMCs. In Section 4, we illustrate the component importance analysis of hybrid model and live migration model for virtualized system. Section 5 concludes this paper with some remarks.

2. Availability Importance Analysis for Hybrid Model

2.1. Fault Trees

In this section, we introduce the availability model for virtualized system which was presented in [9]. For example, the system under consideration provides two different services such as Web and SQL servers to clients. When one of the servers has been stopped, the system also causes a system failure. In [9], they assumed that a host equips not only hardware units; CPU, memory (Mem), power subsystem (Pow), network device (Net),

cooling subsystem (Cool) but also a software component; virtual machine manager (VMM).

Figure 1 illustrates the fault tree (FT) for virtualized system when there are two physical hosts. In the system design, each host provides a specific service, and is supposed to install the same VMM where the virtual machines (VMs) run and provide the services. One of the important features provided by the VMM is the live migration [2]. The live migration is a technique that can enhance the system availability by migrating the VMs when system failure occurs. More precisely, when a physical host is stopped, all the VMs running on the host can migrate to another physical host without the down time. In fact, most of the VMM products such as Xen, VMware and Hyper-V provide the live migration. However, in order to use the live migration, the two hosts are required to share a common storage area network (SAN) which is a service to provide hard disk drives through a high-speed network using Fiber Channel or iSCSI technologies. In **Figure 1**, the top event means the system failure and the leaf nodes correspond to the events that respective components are failed. The nodes, H1 (H2) and HW1 (HW2) represent the events that the host 1 (host 2) is failed and the hardware failure occurs in the host 1 (host 2), respectively. The failure of the system is given by an AND gate because of the live migration. In addition, the VM failure (VM1 or VM2) is connected to the failure of another host (H2 or H1) with an AND gate. This is because even if the VM is failed on one VMM, it can be migrated to another VMM. On the other hand, the failure of SAN causes the system failure directly, and therefore the top event is given by an OR gate connected to these events.

2.2. Continuous-Time Markov Chain (CTMC) Models

In [9], Kim *et al.* defined the continuous-time Markov chain (CTMC) models to represent behavior of hardware and software components. This section briefly introduces the CTMC models presented in [9].

In the availability modeling, the state of system can be classified into two sets: $\mathcal{U}$, the set of up (operational) states in which the system is available; and $\mathcal{D}$, the set of down (or failure) states in which the system is unavailable. **Figure 2** shows the 3-state CTMC availability models of CPU and Mem components proposed in [9]. In the figure, the states UP, DN and RP mean that the component is available, the component is failed, and the component is under repair, respectively. Hence the states DN and RP are classified into $\mathcal{D}$ set in the availability model. Moreover, λ and μ denote failure and repair rates of the component. For example, if the host equips 2-way CPUs, the failure rate is given by $\lambda = 2\lambda_{\text{CPU}}$ by using the failure rate of a single CPU because both processors are needed for the operation. Also, the transition from DN to RP corresponds to the event that a repair person is summoned and its mean time is given by $1/\alpha$ using the rate of summoning inherent in the component.

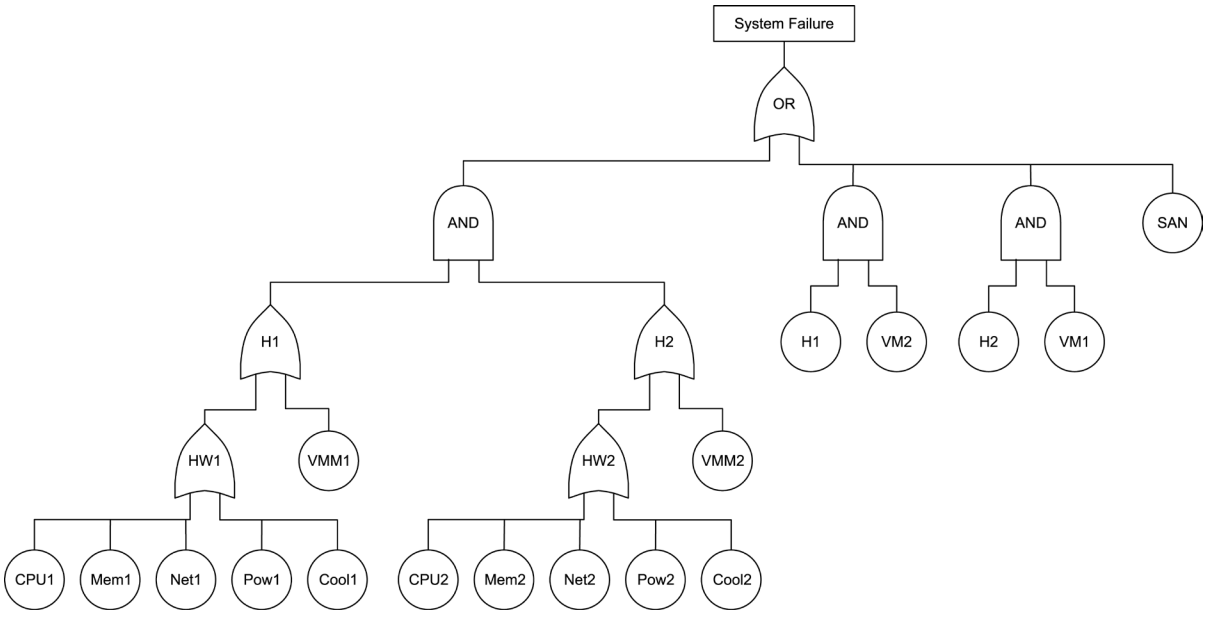

Figure 1. The FT diagram of virtualized system.

As seen in **Figure 3**, Kim *et al.* [9] applied the 5-state availability model to describe the dynamic behaviors of components Pow and Net which are described as 2-unit redundant (parallel) subsystems. In the figure, white and gray nodes represent up and down states respectively. The main difference from the 3-state availability model is to add the state U1 representing that only one unit is failed, since the component failure is caused when both of two units are failed. Moreover, the model adds a repair state RP2 where two units are failed. For the components, Cool and SAN, the CTMC models are extended from the 5-state availability model. Concretely, in the CTMC for Cool as shown in **Figure 4**, they added a transition from RP to RP2, namely, the Cool availability model allows the event occurrence that one unit fails while another unit is under repair. In the CTMC for SAN as shown in **Figure 5**, a state CP is put to the transition between the states UP and RP, which means the mirrored data is copied from a working disk unit to the repaired disk unit under RAID1 design. The transition rate from CP to UP is given by χ_{SAN}. Additionally, since the working disk unit may fail in the CP state, they added a transition from CP to RP2 with the failure rate of a disk unit λ_{SAN}.

The CTMC model for VMM is given by **Figure 6**. As seen in this figure, since the software failure cannot be detected immediately, the state DT is added, which means the failure is detected. In [9], after the failure detection, the system takes an action to reboot VMM with mean time $1/\beta$. It is empirically known that most of transient failures in software can be recovered by the system reboot [14]. In this CTMC model, the reboot will be unsuccessful with probability $(1-b)$. Hence the state DW indicates that the failure is not recovered by a failed system reboot, and a repair person is summoned.

In [9], based on the CTMC model in **Figure 6**, they built the CTMC model for VM which takes account of the dynamic behaviors of the live migration. Thus the CTMC model for VM was quite complicated so that the

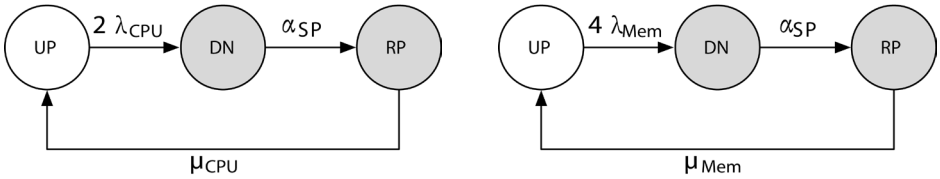

Figure 2. State transition diagram of the CPU and memory availability models.

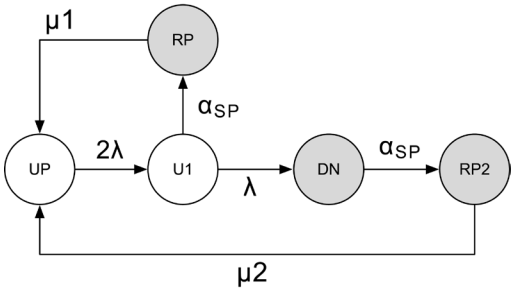

Figure 3. State transition diagram of the power (or network card) availability model.

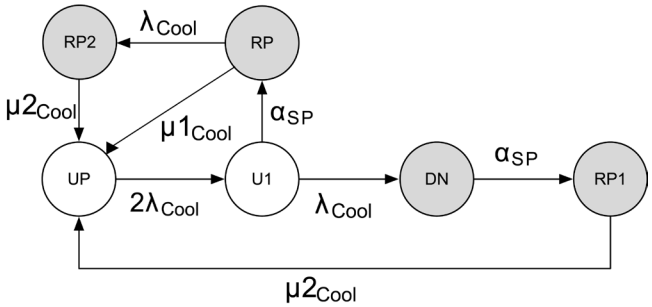

Figure 4. State transition diagram of the cooling system availability model.

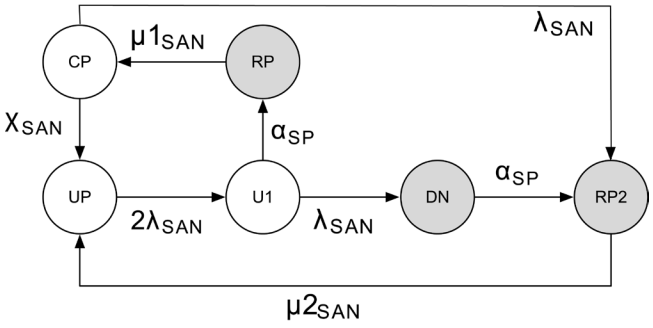

Figure 5. State transition diagram of the SAN availability model.

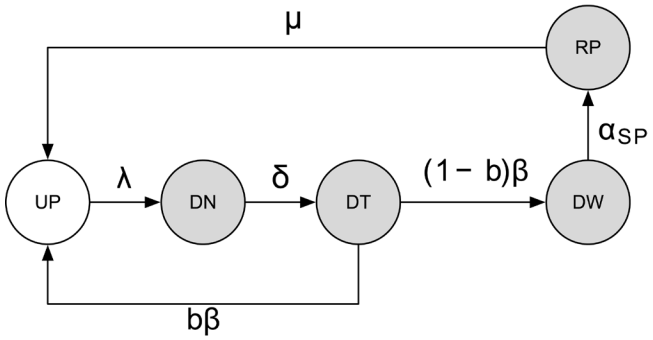

Figure 6. State transition diagram of the VMM/VM availability model.

system failure in the virtualized system cannot be represented by the FT. Since this paper describes the correlation between the failures of VM and host by the AND gate in the FT representation, the CTMC model simply becomes the same model as VMM, *i.e.*, the model of **Figure 6** can also represent the availability for VM.

Based on these CTMC models, the steady-state availability for component *x* can be calculated as follows.

$$A_x = \lim_{t\to\infty} \frac{\text{the cumulative available time during } [0,t)}{t} = \sum_{k\in\mathcal{U}} \pi_k \tag{1}$$

where π_k is the steady-state probability of state *k* in the availability model and $\mathcal{U}$ is the set of up states. The steady-state probability π_k is computed by numerical methods given in [15].

2.3. Importance Measures

Let A_i be the steady-state availability of component *i*. Then we have the following steady-state availability for a host in the virtualized system according to the FT analysis:

$$A_H = A_{\text{VMM}} \prod_{i\in\text{HW}} A_i, \tag{2}$$

where HW is the set of $\{\text{CPU}, \text{Mem}, \text{Net}, \text{Pow}, \text{Cool}\}$. Then the system availability can be obtained

$$A_S = 1 - \left(\bar{A}_{\text{H1}}\bar{A}_{\text{H2}} + \bar{A}_{\text{H1}}\bar{A}_{\text{VM2}} + \bar{A}_{\text{H2}}\bar{A}_{\text{VM1}} - \bar{A}_{\text{H1}}\bar{A}_{\text{H2}}\left(\bar{A}_{\text{VM2}} + \bar{A}_{\text{VM1}}\right)\right)\left(1 - A_{\text{SAN}}\right), \tag{3}$$

where $\bar{A}_i = 1 - A_i$. The above equation is often called the structure function which represents the effect of component availability on the system availability.

In [15], Cassady *et al.* proposed the importance measures of components in terms of availability. They assumed the FT model with the events that are described by the 2-state availability model. The 2-state availability model is a CTMC model with only two states: up and down. In such modeling, Cassady *et al.* [16] defined two importance measures as the derivatives of the system availability:

$$I_{\lambda,i} = \frac{1}{A_S}\left|\frac{\partial A_S}{\partial \lambda_i}\right|, \quad I_{\mu,i} = \frac{1}{A_S}\left|\frac{\partial A_S}{\partial \mu_i}\right|, \tag{4}$$

where λ_i and μ_i are the failure and repair rates of component *i*, *i.e.*, the transition rates from up to down and from down to up in the 2-state availability model, respectively. These measures come from the idea behind the Birnbaum measure [17].

In this paper, since we do not treat the 2-state availability model to represent the component availability, the importance measures proposed in [16] cannot directly be applied to evaluating the virtualized system. This paper proposes a preprocessing based on the aggregation of CTMC-based availability model [18] before applying the availability importance measures.

The aggregation is a technique to transform CTMC-based availability models into a equivalent 2-state, 2-transition availability model which has the same availability as the original model. As mentioned before, the states of CTMC-based availability models can be classified into $\mathcal{U}$ (up states) and $\mathcal{D}$ (down states) sets. The aggregation technique converts the $\mathcal{U}$ and $\mathcal{D}$ sets to the up and down states of the equivalent 2-state, 2-transition availability model. The essential problem of the aggregation is to find the transition rates; failure and repair rates that ensure the steady-state probability of the up (down) set in the original model equals that of the up (down) state in the equivalent 2-state, 2-transition model. From the argument of CTMC, such failure and repair rates can be computed as follows.

$$\tilde{\lambda} = \frac{\sum_{(i,j)\in\mathcal{U}\times\mathcal{D}} \pi_i t_{i,j}}{\sum_{i\in\mathcal{U}} \pi_i}, \quad \tilde{\mu} = \frac{\sum_{(i,j)\in\mathcal{D}\times\mathcal{U}} \pi_i t_{i,j}}{\sum_{i\in\mathcal{D}} \pi_i}, \tag{5}$$

where the set $\mathcal{U}\times\mathcal{D}$ indicates the transitions from up to down state in the original model. Also, $t_{i,j}$ denotes the transition rate from state *i* to state *j* in the original model. For simplification, $t_{i,j} = 0$ if there is no transition from state *i* to state *j*. The calculated failure and repair rates $\tilde{\lambda}$ and $\tilde{\mu}$ in the equivalent 2-state, 2-transition availability model are called the equivalent failure and repair rates [18]. In this paper, we call the equivalent failure and repair rates as the effective failure and repair rates.

By applying the aggregation to the component availability models as preprocessing, the availability importance measures of the component *i* can be rewritten by

$$I_{\tilde{\lambda},i} = \frac{1}{A_S}\left|\frac{\partial A_S}{\partial \tilde{\lambda}_i}\right|, \quad I_{\tilde{\mu},i} = \frac{1}{A_S}\left|\frac{\partial A_S}{\partial \tilde{\mu}_i}\right|, \tag{6}$$

where $\tilde{\lambda}_i$ and $\tilde{\mu}_i$ are the effective failure and repair rates of component *i*.

3. Component Importance for Live Migration

In the previous section, we have introduced the component importance for the structure function given by the FT model. The model considered the live migration as a static structure. However, since the live migration is essentially described by a dynamic behavior, the previous method cannot analyze how effect of components on the dynamic behaviors of live migration. Thus in this section, we consider the component importance on live migration from the viewpoint of dynamic behaviors, that is, we apply the component importance analysis for a CTMC representing the dynamic behaviors of live migration presented in [10].

3.1. Model Description

Matos *et al.* [10] presented the CTMC for live migration in the virtualized system. This availability model does not consider the detailed behavior of hardware components (e.g., CPU, Mem, Pow) and the VMM, but only the components of VMs (VM1 and VM2), hosts (H1 and H2) and applications (App1 and App2).

Table 1 shows notations for the state of system which are based on the current conditions of components. Concretely, each state is indicated by six characters. The first character means the state of H1. The notations "U", "F" and "D" correspond to the conditions where H1 is up, H1 fails and the failure is detected, respectively. The second character represents the state of VM1 and its application (App1). When both are up, the character is given by "U". If VM1 fails, it is "Fv". When the failure is detected, the character becomes "Dv". Also, when a manual repair is applied, the character is "Pv". If App1 fails, it is "Fa". When the failure of App1 is detected, the

Table 1. The states of system.

State	Description
UUXUUX	VM1 is running on H1, VM2 is running on H2.
FXXUUX	H1 is failed, VM1 is failed due to the failure of H1. VM2 is running on H2.
DXXUUR	H1 failure is detected, VM1 is restarting on H2.
DXXUUU	H1 is down, VM1 and VM2 are running on H2.
UXXUUU	H1 is up, VM1 and VM2 are running on H2.
UXXFXX	H1 is up, H2 is failed. VM1 and VM2 are failed due to the failure of H2.
URXDXX	H2 failure is detected. VM1 is restarting on H1.
DXXFXX	H1 is down, H2 is failed.
DXXDXX	H1 is down, H2 failure is detected.
DXXURX	H1 is down, H2 is up, VM2 is restarting on H2.
UXXURX	H1 is up, H2 is up, VM2 is restarting on H2.
UXXUUR	H1 is up, VM2 is running on H2. VM1 is restarting on H2.
UFaXUUX	App1 is failed, both VMs and Hosts are up.
UDaXUUX	App1 failure is detected.
UPaXUUX	App1 failure is not covered. Additional recovery step is started.
UFvXUUX	H1 is up, VM1 is failed, VM2 is running on H2.
UDvXUUX	VM1 failure is detected.
UPvXUUX	VM1 failure is not covered.
	Manual repair is started.

state of system is represented by “Da”. If App1 requires an additional repair in the case where the application restart cannot solve the problem, the character is given by “Pa”. Also, when VM1 and App1 are restarting, the state is given by “R”. If VM1 and App1 are not running on the H1, then the character is “X”. The third character represents whether or not VM2 and App2 are running on H1. If VM2 and App2 run on H1, the character is given by “U”. If they are restarting on H1, the character is “R”. Otherwise, if they are not running on H1, the character is “X”. The fourth through sixth characters represent the state of H2 in the same manner as the first through third characters. **Figure 7** shows the state transition diagram for live migration in the virtualized system which is described by the CTMC model in [10]. Also, **Table 2** presents the parameters of the CTMC model. For example, $1/\lambda_h$ is MTTF (mean time to failure) of host H1 and H2, and then λ_h is a failure rate which is a transition rate in the CTMC.

3.2. Importance Analysis

Dissimilar to the case of FT model, we do not know the structure function in the CTMC. We consider the component importance analysis by only using the parameter sensitivity analysis.

Let $\boldsymbol{Q}$ be the infinitesimal generator of CTMC described in **Figure 7**. Then the steady-state probability vector $\boldsymbol{\pi}_s$ is given by the linear equations;

$$\boldsymbol{\pi}_s \boldsymbol{Q} = \boldsymbol{0}, \quad \boldsymbol{\pi}_s \boldsymbol{1} = 1, \tag{7}$$

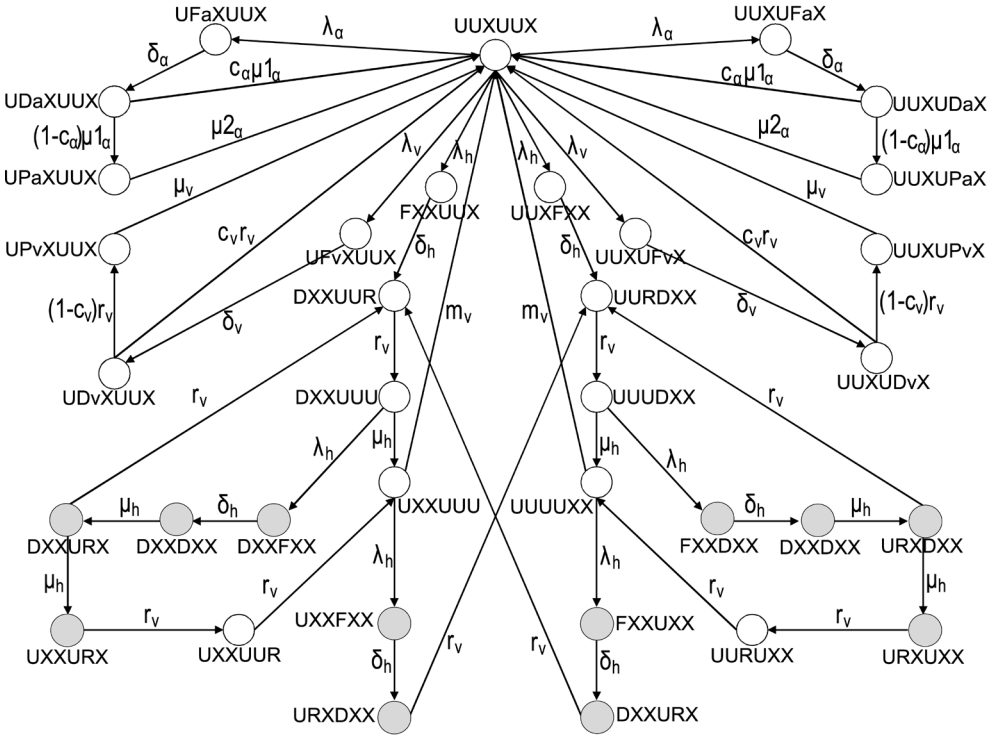

Figure 7. CTMC availability model for live migration.

Table 2. Model parameters.

Params	Description
$1/\lambda_h$	Mean time to host failure
$1/\lambda_v$	Mean time to VM failure
$1/\lambda_a$	Mean time to Application failure
$1/\delta_h$	Mean time for host failure detection
$1/\delta_v$	Mean time for VM failure detection
$1/\delta_a$	Mean time for App failure detection
$1/m_v$	Mean time to migrate a VM
$1/r_v$	Mean time to restart a VM
$1/\mu_h$	Mean time to repair a host
$1/\mu_v$	Mean time to repair a VM
$1/\mu 1_a$	Mean time to App first repair (covered case)
$1/\mu 2_a$	Mean time to App second repair (not covered case)
c_v	coverage factor for VM repair
c_a	coverage factor for application repair

where **1** is a column vector whose elements are 1. Also we define the following vectors:

- $\xi_{hi,i\in\{1,2\}}$: a 0 - 1 vector whose elements are 1 in the state where H1 or H2 is up.
- $\xi_{vi,i\in\{1,2\}}$: a 0 - 1 vector whose elements are 1 in the state where VM1 or VM2 is up.
- $\xi_{ai,i\in\{1,2\}}$: a 0 - 1 vector whose elements are 1 in the state where App1 or App2 is up.

- $\boldsymbol{\xi}_{sys}$: a 0 - 1 vector whose elements are 1 in the state where the system is up.

Then the component availability is given by a inner product of $\boldsymbol{\pi}_s$ and $\boldsymbol{\xi}_{\cdot}$; for example, the component availability of H1 becomes

$$A_{h1} = \boldsymbol{\pi}_s \boldsymbol{\xi}_{h1}. \tag{8}$$

On the other hand, the system availability can be obtained by

$$A_S = \boldsymbol{\pi}_s \boldsymbol{\xi}_{sys}. \tag{9}$$

Similar to the case of FT model, we define the importance measures of component *i* as follows.

$$I_{\tilde{\lambda},i} = \frac{1}{A_S}\left|\frac{\partial A_S}{\partial \tilde{\lambda}_i}\right|, \quad I_{\tilde{\mu},i} = \frac{1}{A_S}\left|\frac{\partial A_S}{\partial \tilde{\mu}_i}\right|, \tag{10}$$

where $\tilde{\lambda}_i$ and $\tilde{\mu}_i$ are the effective failure and repair rates of component *i*. They can be computed by the aggregation technique introduced in Section 2.3. Also, we have

$$I_{\tilde{\lambda},i} = \frac{1}{A_S}\left|\frac{\partial A_S}{\partial \tilde{\lambda}_i}\right| = \frac{1}{A_S}\left|\frac{\partial A_S}{\partial A_i}\right|\left|\frac{\partial A_i}{\partial \tilde{\lambda}_i}\right| = \frac{1}{A_S}\left|\frac{\partial A_S}{\partial A_i}\right|\frac{\tilde{\mu}_i}{\left(\tilde{\lambda}_i + \tilde{\mu}_i\right)^2}. \tag{11}$$

Similarly, the importance measure with respect to repair rate is given by

$$I_{\tilde{\mu},i} = \frac{1}{A_S}\left|\frac{\partial A_S}{\partial A_i}\right|\frac{\tilde{\lambda}_i}{\left(\tilde{\lambda}_i + \tilde{\mu}_i\right)^2}. \tag{12}$$

Thus the problem is to estimate the sensitivity $\partial A_S / \partial A_i$ without the structure function.

To estimate the sensitivities for all the component availabilities, we consider the sensitivities of system and component availabilities with respect to model parameters. Suppose that $\theta_1, \cdots, \theta_m$ are model parameters of the underlying CTMC. Here we define a matrix $\boldsymbol{J}$ and a column vector $\boldsymbol{z}$ whose elements are the sensitivities for all the component availabilities and the system availability with respect to the model parameters, *i.e.*,

$$\boldsymbol{J} = \begin{pmatrix} \frac{\partial A_1}{\partial \theta_1} & \frac{\partial A_2}{\partial \theta_1} & \cdots & \frac{\partial A_n}{\partial \theta_1} \\ \frac{\partial A_1}{\partial \theta_2} & \frac{\partial A_2}{\partial \theta_2} & \cdots & \frac{\partial A_n}{\partial \theta_2} \\ \vdots & \vdots & \ddots & \vdots \\ \frac{\partial A_1}{\partial \theta_m} & \frac{\partial A_2}{\partial \theta_m} & \cdots & \frac{\partial A_n}{\partial \theta_m} \end{pmatrix}, \quad \boldsymbol{z} = \begin{pmatrix} \frac{\partial A_S}{\partial \theta_1} \\ \frac{\partial A_S}{\partial \theta_2} \\ \vdots \\ \frac{\partial A_S}{\partial \theta_m} \end{pmatrix}, \tag{13}$$

where $A_1, \cdots, A_n$ represent component availabilities for all the components. These sensitivities can be obtained by solving the following linear equations:

$$\boldsymbol{s}\left(\theta_j\right) = \frac{\partial}{\partial \theta_j}\boldsymbol{\pi}_s, \quad \boldsymbol{s}\left(\theta_j\right)\boldsymbol{Q} = -\boldsymbol{\pi}_s \frac{\partial}{\partial \theta_j}\boldsymbol{Q}, \quad \boldsymbol{s}\left(\theta_j\right)\boldsymbol{1} = 0. \tag{14}$$

By using the vector $\boldsymbol{s}\left(\theta_j\right)$, the sensitivities are given by

$$\frac{\partial A_i}{\partial \theta_j} = \boldsymbol{s}\left(\theta_j\right)\boldsymbol{\xi}_i, \quad \frac{\partial A_S}{\partial \theta_j} = \boldsymbol{s}\left(\theta_j\right)\boldsymbol{\xi}_{sys}. \tag{15}$$

According to [19], the estimates of $\partial A_S / \partial A_i$ can be obtained by

$$\begin{pmatrix} \frac{\partial A_S}{\partial A_1} & \frac{\partial A_S}{\partial A_2} & \cdots & \frac{\partial A_S}{\partial A_n} \end{pmatrix}^{\mathrm{T}} = \left(\boldsymbol{J}^{\mathrm{T}}\boldsymbol{J}\right)^{-1}\boldsymbol{J}^{\mathrm{T}}\boldsymbol{z}, \tag{16}$$

where *T* is the transpose operator. By substituting the estimates of the sensitivities into Equations (11) and (12), we have the component importance measures for live migration.

4. Numerical Illustration

4.1. Hybrid Model

In this section, we illustrate the quantitative component importance analysis of hybrid model for virtualized system. **Table 3** presents the parameters of the CTMC models for all components. For example, $1/\lambda_{CPU}$ is mean time for CPU failure, and $1/\mu_{Mem}$ is mean time to repair one memory (*i.e.*, MTTR of one memory). Also we give other model parameters in **Table 4**.

Using the aggregation technique, we first transform the availability models for all components into the equivalent 2-state, 2-transition models, then compute the effective failure and repair rates for components based on the model parameters. We also compute the component availabilities, and these results are shown in **Table 5**. From this table, we can see the availabilities of hardware units are relatively high by the comparison to the availabilities of software components, especially for SAN, the availability is quite high.

We then compute the system availabilities based on the structure functions and the component availabilities. The availabilities of a hardware unit and a host, and the system availability are presented in **Table 6**. From this table, the sufficiently high availability of the virtualized system implies that the live migration is considerably effective to enhance the system availability.

Next we derive the importance measures of components in the virtualized system by using Equation (6), and the effective failure and repair rates shown in **Table 5**. The importance measures of components in terms of the system availability are shown in **Table 7**. Note that this table presents the importance measures of components only in a host, because the components of the host 1 and 2 are assumed to be the same in the system design, and the importance measures of same components in the host 1 and 2 are identical.

Table 3. MTTF/MTTR of components.

Params	Description	Value (hours)
$1/\lambda_{CPU}$	MTTF of CPU	2,500,000
$1/\lambda_{Mem}$	MTTF of Mem	480,000
$1/\lambda_{Pow}$	MTTF of Pow	670,000
$1/\lambda_{Net}$	MTTF of Net	120,000
$1/\lambda_{Cool}$	MTTF of Cool	3,100,000
$1/\lambda_{SAN}$	MTTF of SAN	20,000,000
$1/\lambda_{VMM}$	MTTF of VMM	2880
$1/\lambda_{VM}$	MTTF of VM	2880
$1/\mu_{CPU}$	MTTR of CPU	0.5
$1/\mu_{Mem}$	MTTR of Mem	0.5
$1/\mu 1_{Pow}$	MTTR of one power module	0.5
$1/\mu 2_{Pow}$	MTTR of two power modules	1
$1/\mu 1_{Net}$	MTTR of one network device	0.5
$1/\mu 2_{Net}$	MTTR of two network devices	1
$1/\mu 1_{Cool}$	MTTR of one cooler module	0.5
$1/\mu 2_{Cool}$	MTTR of two cooler modules	1
$1/\mu 1_{SAN}$	MTTR of one disk unit	0.5
$1/\mu 2_{SAN}$	MTTR of two disk units	1
$1/\mu_{VMM}$	MTTR of VMM	1
$1/\mu_{VM}$	MTTR of VM	0.5

Table 4. Other model parameters.

Params	Description	Value
$1/\alpha_{SP}$	Mean time to repair person summoned	30 minutes
$1/\chi_{SAN}$	Mean time to copy data	20 minutes
$1/\delta_{VMM}$	Mean time for VMM failure detection	30 seconds
$1/\delta_{VM}$	Mean time for VM failure detection	30 seconds
$1/\beta_{VMM}$	Mean time to reboot VMM	10 minutes
$1/\beta_{VM}$	Mean time to reboot VM	5 minutes
b_{VMM}	Coverage factor for VMM reboot	0.9
b_{VM}	Coverage factor for VM reboot	0.95

Table 5. Effective failure and repair rates and component availabilities.

Component	$\tilde{\lambda}_i$	$\tilde{\mu}_i$	A_i
CPU	8.0000000e−7	1.0000000	0.99999920
Mem	8.3333333e−6	1.0000000	0.99999167
Net	1.6666528e−5	1.9999833	0.99999167
Pow	2.9850702e−6	1.9999970	0.99999851
Cool	6.4516108e−7	1.9999990	0.99999968
VMM	3.4722222e−4	3.0769231	0.99988717
VM	3.4722222e−4	7.0588235	0.99995081
SAN	9.9999992e−8	1.9999999	0.99999995

Table 6. Availabilities of hardware units, host and system.

System	Availability
HW1 and HW2	0.99998072
H1 and H2	0.99986789
System availability	0.99999992

Table 7. Component importance measures in the virtualized system.

Component	$I_{\tilde{\lambda},i}$	$I_{\tilde{\mu},i}$
CPU	1.8126415e−4	1.4501132e−10
Mem	1.8126278e−4	1.5105232e−09
Net	9.0632147e−5	7.5526790e−10
Pow	9.0632147e−5	1.3527186e−10
Cool	9.0632162e−5	2.9236186e−11
VMM	5.8904249e−5	6.6471808e−09
VM	1.8711815e−5	9.2043069e−10
SAN	0.5000000000	2.4999999e−08

Table 7 shows that the importance measure with respect to failure rate is higher than that with respect to repair rate for any component. The importance measure regarding failure rate, $I_{\tilde{\lambda},i}$, indicates the relative improvement in system availability resulting from a decrease to the component failure rate. Similarly, the importance measure regarding repair rate, $I_{\tilde{\mu},i}$, indicates the relative improvement in system availability resulting from an increase to the component repair rate. Thus, to improve the system availability, the more efficient way is to decrease the failure rates of components. Also, as seen in this table, it is easy to find that the importance measures of SAN are much higher than those of the other components, especially the importance measure with respect to failure rate, $I_{\tilde{\lambda},\mathrm{SAN}}$. The highest importance of SAN indicates that the improvement of failure rate of SAN is the most efficient way to improve the system availability. In other words, SAN is a bottleneck of availability, though its availability seems to be high. Besides, from **Table 5**, we find the repair rates of CPU and Mem are not so high. This implies that the failures of CPU and Mem cause long down time. Hence their importance measures with respect to failure rate are relatively higher than the others except SAN. Moreover, we find that the importance measures of VM and VMM are not high in **Table 7**. This is caused by the fact that VM and VMM can be migrated when a failure of a host occurs. Therefore, VM and VMM are not critical components, compared to SAN.

4.2. Dynamic Model for Live Migration

This section illustrates the quantitative component importance analysis of the CTMC for live migration in the virtualized system. Based on these parameters shown in **Table 8**, we first compute the availabilities for all components and system which are shown in **Table 9**. From this table, we find that the availability of VM is the highest among those of the other components because of the live migration.

Next we compute the effective failure and repair rates for all components based on the aggregation of CTMC model, and the results are shown in **Table 10**. From this table, it is found that the repair rate of VM are much higher than that in **Table 5**. As mentioned before, the FT model considered the live migration as a static structure which cannot represent the dynamic behaviors of system. However, since the live migration is essentially described by a dynamic behavior, the dynamic behaviors have been taken into account in the CTMC model for live migration. The higher repair rate of VM confirms the effectiveness of live migration in the virtualized system. **Table 11** presents the importance measures for components in the virtualized system. As observed in **Table 10**

Table 8. Model parameters.

Params	Description	Value
$1/\lambda_h$	Mean time for host failure	2654 hr
$1/\lambda_v$	Mean time for VM failure	2893 hr
$1/\lambda_a$	Mean time to Application failure	175 hr
$1/\delta_h$	Mean time for host failure detection	30 sec
$1/\delta_v$	Mean time for VM failure detection	30 sec
$1/\delta_a$	Mean time for App failure detection	30 sec
$1/m_v$	Mean time to migrate a VM	330 sec
$1/r_v$	Mean time to restart a VM	50 sec
$1/\mu_h$	Mean time to repair a host	100 min
$1/\mu_v$	Mean time to repair a VM	30 min
$1/\mu 1_a$	Mean time to App first repair (covered case)	1 min
$1/\mu 2_a$	Mean time to App second repair (not covered case)	20 min
c_v	Coverage factor for VM repair	0.95
c_a	Coverage factor for application repair	0.8

Table 9. Availabilities of host, VM, application components and system.

System	Availability
H1 and H2	0.9993644
VM1 and VM2	0.9999746
App1 and App2	0.9994520
System availability	0.9999992

Table 10. Effective failure and repair rates.

Component	$\tilde{\lambda}_i$	$\tilde{\mu}_i$
H1 and H2	3.763673e−4	0.5917368
VM1 and VM2	7.212219e−4	28.351750
App1 and App2	6.425198e−3	11.718790

Table 11. Component importance measures in the dynamic model for live migration.

Component	$I_{\tilde{\lambda},i}$	$I_{\tilde{\mu},i}$
H1 and H2	2.118715e−03	1.347584e−06
VM1 and VM2	1.675414e−12	4.261977e−17
App1 and App2	9.438502e−13	5.174957e−16

and **Table 11**, we find that, although the failure rate of VM is higher than that of host, the importance measures of VM are much lower than those of host. This is because the repair rate of VM is very high. Also, comparing **Table 9** with **Table 10**, we can see that the availability of host is the lowest among those of others, because the repair rate of host is also the lowest. This indicates that, the component host is important, and any change in its associated parameters will have a large effect on the system availability. And this conclusion also can be confirmed from **Table 11**.

Table 11 shows that the importance measures of host is the most highest. Moreover, by comparing between the importance measure with respect to failure and repair rates for each component, it is found that the importance measure with respect to failure rate is higher than that with respect to repair rate. Therefore, it indicates that the improvement of failure rate of host is more efficient to enhance the system availability.

5. Conclusions

In this paper, we have dealt with quantitative component importance analysis of virtualized system with live migration in terms of availability. In [11], we have developed a method to evaluate the importance of components for hybrid model which consists of fault trees (FTs) and CTMCs. However, the hybrid model had a limitation for the model expression in the situation where two or more components have interactions between them. Instead of using the hybrid model, we considered a CTMC model for live migration presented in [10]. This paper introduced the state-of-art component importance analysis [13] and applied it to the CTMC-based live migration model to reveal the component importance in the context of live migration. More precisely, our method is based on the aggregation techniques of CTMC-based availability models [18] and the importance measures with respect to failure and repair rates [16]. Also, we proposed a method to estimate the sensitivities of system availability with respect to component availabilities. In numerical examples, we illustrated the quantitative component importance analysis of hybrid model and live migration model for virtualized system, and compared the importance of components. In future, we intend to improve our method so that it can be applied to more complicated event models. Also, we will focus on the component importance analysis for Markov chain in terms

of reliability.

References

[1] Furht, B. and Escalante, A. (2010) Cloud Computing Fundamentals. In *Handbook of Cloud Computing*, Springer, 3-19. http://dx.doi.org/10.1007/978-1-4419-6524-0_1

[2] Clark, C., Fraser, K., Hand, S., Hansen, J.G., Jul, E., Limpach, C., Pratt, I. and Warfield, A. (2005) Live Migration of Virtual Machines. In: *Proceedings of the* 2*nd Conference on Symposium on Networked Systems Design & Implementation—Volume* 2, USENIX Association, Berkeley, 273-286.

[3] Kundu, S., Rangaswami, R., Dutta, K. and Zhao, M. (2010) Application Performance Modeling in a Virtualized Environment. *Proceedings of the* 16*th IEEE International Symposium on High-Performance Computer Architecture*, Bangalore, 9-14 January 2010, 1-10.

[4] Okamura, H., Shigeoka, K., Yamasaki, K., Dohi, T. and Kihara, H. (2012) Performance Evaluation of Cloud Computing in PaaS Environments. *Supplemental Proceedings of* 42*nd Annual IEEE/IFIP International Conference on Dependable Systems and Networks* (*DSN*2012), **36**, 122-127.

[5] Cully, B., Lefebvre, G., Meyer, D., Feeley, M., Hutchinson, N. and Warfield, A. (2008) Remus: High Availability via Asynchronous Virtual Machine Replication. *Proceedings of the* 5*th USENIX Symposium on Networked Systems Design and Implementation*, USENIX Association, Berkeley, 161-174.

[6] Farr, E., Harper, R., Spainhower, L. and Xenidis, J. (2008) A Case for High Availability in a Virtualized Environment (HAVEN). *Proceedings of the* 2008 *Third International Conference on Availability, Reliability and Security* (*ARES*'08), Barcelona, 4-7 March 2008, 675-682.

[7] Hla Myint, M.T. and Thein, T. (2010) Availability Improvement in Virtualized Multiple Servers with Software Rejuvenation and Virtualization. *Proceedings of* 4*th International Conference on Secure Software Integration and Reliability Improvement*, Singapore, 9-11 June 2010, 156-162.

[8] Vishwanath, K.V. and Nagappan, N. (2010) Characterizing Cloud Computing Hardware Reliability. *Proceedings of the first ACM Symposium on Cloud Computing* (*SoCC*'10), Indianapolis, 10-11 June 2010, 193-204.

[9] Kim, D.S., Machida, F. and Trivedi, K.S. (2009) Availability Modeling and Analysis of a Virtualized System. *Proceedings of the* 15*th IEEE Pacific Rim International Symposium on Dependable Computing* (*PRDC*-2009), Shanghai, 16-18 November 2009, 365-371.

[10] Matos, R.D.S., Maciel, P.R.M., Machida, F., Kim, D.S. and Trivedi, K.S. (2012) Sensitivity Analysis of Server Virtualized System Availability. *IEEE Transactions on Reliability*, **61**, 994-1006.

[11] Zheng, J., Okamura, H. and Dohi, T. (2012) Component Importance Analysis of Virtualized System. *Proceedings of the* 9*th IEEE International Conference on Autonomic & Trusted Computing* (*ATC*2012), Fukuoka, 4-7 September 2012, 462-469.

[12] Cepin, M. and Mavko, B. (2002) A Dynamic Fault Tree. *Reliability Engineering & System Safety*, **75**, 83-91. http://dx.doi.org/10.1016/S0951-8320(01)00121-1

[13] Okamura, H., Zheng, J. and Dohi, T. (2015) Sensitivity Estimation for Markov Reward Models and Its Application to Component Importance Analysis. (In Submission)

[14] Castelli, V., Harper, R.E., Heidelberger, P., Hunter, S.W., Trivedi, K.S., Vaidyanathan, K. and Zeggert, W.P. (2001) Proactive Management of Software Aging. *IBM Journal of Research and Development*, **45**, 311-332. http://dx.doi.org/10.1147/rd.452.0311

[15] Trivedi, K.S. (2001) Probability and Statistics with Reliability, Queueing, and Computer Sciences Applications. 2nd Edition, John Wiley & Sons, New York.

[16] Cassady, C.R., Pohl, E.A. and Jin, S. (2004) Managing Availability Improvement Efforts with Importance Measures and Optimization. *IMA Journal of Management Mathematics*, **15**, 161-174. http://dx.doi.org/10.1093/imaman/15.2.161

[17] Birnbaum, Z.W. (1969) On the Importance of Different Components in a Multicomponent System. In: Krishnaiah, P.R., Ed., *Multivariate Analysis—II*, Academic Press, New York, 581-592.

[18] Lanus, M., Yin, L. and Trivedi, K.S. (2003) Hierarchical Composition and Aggregation of State-Based Availability and Performability Models. *IEEE Transactions on Reliability*, **52**, 44-52. http://dx.doi.org/10.1109/TR.2002.805781

[19] Strang, G. (2009) Introduction to Linear Algebra. 4th Edition, Wellesley Cambridge Press, Wellesley.

Applied Mathematics, 2015, 6, 373-381
Published Online February 2015 in SciRes. http://www.scirp.org/journal/am
http://dx.doi.org/10.4236/am.2015.62035

Regular Elements and Right Units of Semigroup $B_X(D)$ Defined Semilattice D for Which $V(D,\alpha)=Q\in\Sigma_3(X,8)$

Giuli Tavdgiridze, Yasha Diasamidze

Department of Mathematics, Faculty of Physics, Mathematics and Computer Sciences, Shota Rustaveli Batumi State University, Batumi, Georgia
Email: g.tavdgiridze@mail.ru, diasamidze_ya@mail.ru

Received 16 January 2015; accepted 6 February 2015; published 10 February 2015

Abstract

In this paper we take $Q=\{T_7,T_6,T_5,T_4,T_3,T_2,T_1,T_0\}$ subsemilattice of X-semilattice of unions D which satisfies the following conditions:

$$T_7\subset T_5\subset T_3\subset T_1\subset T_0,\ T_7\subset T_6\subset T_4\subset T_2\subset T_0,\ T_7\subset T_5\subset T_4\subset T_1\subset T_0,\ T_7\subset T_5\subset T_4\subset T_2\subset T_0,$$
$$T_7\subset T_6\subset T_4\subset T_1\subset T_0,\ T_5\setminus T_6\neq\varnothing,\ T_6\setminus T_5\neq\varnothing,\ T_4\setminus T_3\neq\varnothing,\ T_3\setminus T_4\neq\varnothing,\ T_2\setminus T_1\neq\varnothing,$$
$$T_1\setminus T_2\neq\varnothing,\ T_6\cup T_5=T_4,\ T_4\cup T_3=T_1,\ T_2\cup T_1=T_0.$$

We will investigate the properties of regular elements of the complete semigroup of binary relations $B_X(D)$ satisfying $V(D,\alpha)=Q$. For the case where X is a finite set we derive formulas by means of which we can calculate the numbers of regular elements and right units of the respective semigroup.

Keywords

Semilattice, Semigroup, Regular Element, Right Unit, Binary Relation

1. Introduction

Let X be an arbitrary nonempty set and D be an X-semilattice of unions, which means a nonempty set of subsets of the set X that is closed with respect to the set-theoretic operations of unification of elements from D. Let's denote an arbitrary mapping from X into D by f. For each f there exists a binary relation α_f on the set X that

How to cite this paper: Tavdgiridze, G. and Diasamidze, Y. (2015) Regular Elements and Right Units of Semigroup $B_X(D)$ Defined Semilattice D for Which $V(D,\alpha)=Q\in\Sigma_3(X,8)$. *Applied Mathematics*, **6**, 373-381.
http://dx.doi.org/10.4236/am.2015.62035

satisfies the condition $\alpha_f = \bigcup_{x\in X}\left(\{x\}\times f(x)\right)$. Let denote the set of all such α_f $\left(f: X \to D\right)$ by $B_X(D)$. It is not hard to prove that $B_X(D)$ is a semigroup with respect to the operation of multiplication of binary relations. $B_X(D)$ is called a complete semigroup of binary relations defined by a *X*-semilattice of unions *D* (see [1], Item 2.1), ([2], Item 2.1]).

An empty binary relation or an empty subset of the set *X* is denoted by $\varnothing$. The form $x\alpha y$ is used to express that $(x,y)\in\alpha$. Also, in this paper following conditions are used $x, y \in X$, $Y \subseteq X$, $\alpha \in B_X(D)$, $T \in D$, $\varnothing \neq D' \subseteq D$ and $t \in \breve{D} = \bigcup_{Y\in D} Y$. Moreover, following sets are denoted by given symbols:

$$y\alpha = \{x \in X \mid y\alpha x\}, \quad Y\alpha = \bigcup_{y\in Y} y\alpha, \quad V(D,\alpha) = \{Y\alpha \mid Y \in D\},$$

$$X^* = \{T \mid \varnothing \neq T \subseteq X\}, \quad D'_t = \{Z' \in D' \mid t \in Z'\}, \quad D'_T = \{Z' \in D' \mid T \subseteq Z'\}.$$

$$\ddot{D}'_T = \{Z' \in D' \mid Z' \subseteq T\}, \quad l(D',T) = \cup(D' \setminus D'_T), \quad Y^\alpha_T = \{x \in X \mid x\alpha = T\}.$$

And $\wedge(D, D_t)$ is an exact lower bound of the set D_t in the semilattice *D*.

Definition 1.1. Let $\varepsilon \in B_X(D)$. If $\varepsilon\circ\varepsilon = \varepsilon$ or $\alpha\circ\varepsilon = \alpha$ for any $\alpha \in B_X(D)$, then ε is called an idempotent element or called right unit of the semigroup $B_X(D)$ respectively (see [1]-[3]).

Definition 1.2. An element α taken from the semigroup $B_X(D)$ called a regular element of the semigroup $B_X(D)$ if in $B_X(D)$ there exists an element β such that $\alpha\circ\beta\circ\alpha = \alpha$ (see [1]-[4]).

Definition 1.3. We say that a complete *X*-semilattice of unions *D* is an *XI*-semilattice of unions if it satisfies the following two conditions:

1) $\wedge(D, D_t) \in D$ for any $t \in \breve{D}$;

2) $Z = \bigcup_{t\in Z} \wedge(D, D_t)$ for any nonempty element *Z* of *D* (see [1], definition 1.14.2), ([2] definition 1.14.2), [5] or [6].

Definition 1.4. Let *D* be an arbitrary complete *X*-semilattice of unions, $\alpha \in B_X(D)$ and $Y^\alpha_T = \{x \in X \mid x\alpha = T\}$. If

$$V[\alpha] = \begin{cases} V(X^*,\alpha), & \text{if } \varnothing \notin D, \\ V(X^*,\alpha), & \text{if } \varnothing \in V(X^*,\alpha), \\ V(X^*,\alpha)\cup\{\varnothing\}, & \text{if } \varnothing \notin V(X^*,\alpha) \text{ and } \varnothing \in D, \end{cases}$$

then it is obvious that any binary relation α of a semigroup $B_X(D)$ can always be written in the form $\alpha = \bigcup_{T\in V[\alpha]} \left(Y^\alpha_T \times T\right)$ the sequel, such a representation of a binary relation α will be called quasinormal.

Note that for a quasinormal representation of a binary relation α, not all sets Y^α_T $\left(T \in V[\alpha]\right)$ can be different from an empty set. But for this representation the following conditions are always fulfilled:

1) $Y^\alpha_T \cap Y^\alpha_{T'} = \varnothing$, for any $T, T' \in D$ and $T \neq T'$;

2) $X = \bigcup_{T\in V[\alpha]} Y^\alpha_T$ (see [1], definition 1.11.1), ([2], definition 1.11.1).

Definition 1.5. We say that a nonempty element *T* is a nonlimiting element of the set *D'* if $T \setminus l(D',T) \neq \varnothing$ and a nonempty element *T* is a limiting element of the set *D'* if $T \setminus l(D',T) = \varnothing$ (see [1], definition 1.13.1 and definition 1.13.2), ([2], definition 1.13.1 and definition 1.13.2).

Definition 1.6. The one-to-one mapping φ between the complete *X*-semilattices of unions $\phi(Q,Q)$ and D'' is called a complete isomorphism if the condition

$$\varphi(\cup D_1) = \bigcup_{T=D_1} \varphi(T')$$

is fulfilled for each nonempty subset D_1 of the semilattice D' (see [1], definition 6.3.2), ([2] definition 6.3.2) or [5]).

Definition 1.7. Let α be some binary relation of the semigroup $B_X(D)$. We say that the complete iso-

morphism φ between the complete semilattices of unions Q and D' is a complete α-isomorphism if

1) $Q = V(D,\alpha)$;

2) $\varphi(\varnothing) = \varnothing$ for $\varnothing \in V(D,\alpha)$ and $\varphi(T)\alpha = T$ for eny $T \in V(D,\alpha)$ (see [1], definition 6.3.3), ([2], definition 6.3.3).

Lemma 1.1. Let $Y = \{y_1, y_2, \cdots, y_k\}$ and $D_j = \{T_1, \cdots, T_j\}$ be any two sets. Then the number $s(k, j)$ of all possible mappings of Y into any subset D'_j of the set that D_j such that $T_j \in D'_j$ can be calculated by the formula $s(k, j) = j^k - (j-1)^k$ (see [1], Corollary 1.18.1), ([2], Corollary 1.18.1).

Lemma 1.2. Let D by a complete X-semilattice of unions. If a binary relation ε of the form $\varepsilon = \bigcup_{t \in \breve{D}} (\{t\} \times \wedge(D, D_t)) \cup \left((X \setminus \breve{D}) \times \breve{D} \right)$ is right unit of the semigroup $B_X(D)$, then ε is the greatest right unit of that semigroup (see [1], Lemma 12.1.2), ([2], Lemma 12.1.2).

Theorem 1.1. Let $D_j = \{T_1, T_2, \cdots, T_j\}$, X and Y- be three such sets, that $\varnothing \neq Y \subseteq X$. If f is such mapping of the set X, in the set D_j, for which $f(y) = T_j$ for some $y \in Y$, then the number s of all those mappings f of the set X in the set D_j is equal to $s = j^{|X \setminus Y|} \cdot \left(j^{|Y|} - (j-1)^{|Y|} \right)$ (see [1], Theorem 1.18.2), ([2], Theorem 1.18.2).

Theorem 1.2. Let $D = \{\breve{D}, Z_1, Z_2, \cdots, Z_{m-1}\}$ be some finite X-semilattice of unions and $C(D) = \{P_0, P_1, P_2, \cdots, P_{m-1}\}$ be the family of sets of pairwise nonintersecting subsets of the set X. If φ is a mapping of the semilattice D on the family of sets $C(D)$ which satisfies the condition $\varphi(\breve{D}) = P_0$ and $\varphi(Z_i) = P_i$ for any $i = 1, 2, \cdots, m-1$ and $\hat{D}_Z = D \setminus \{T \in D \mid Z \subseteq T\}$, then the following equalities are valid:

$$\breve{D} = P_0 \cup P_1 \cup P_2 \cup \cdots \cup P_{m-1}, \quad Z_i = P_0 \cup \bigcup_{T \in \hat{D}_{Z_i}} \varphi(T). \tag{*}$$

In the sequel these equalities will be called formal.

It is proved that if the elements of the semilattice D are represented in the form (*), then among the parameters P_i $(i = 0,1,2,\cdots,m-1)$ there exist such parameters that cannot be empty sets for D. Such sets P_i $(0 < i \leq m-1)$ are called basis sources, whereas sets P_i $(0 \leq j \leq m-1)$ which can be empty sets too are called completeness sources.

It is proved that under the mapping φ the number of covering elements of the pre-image of a basis source is always equal to one, while under the mapping φ the number of covering elements of the pre-image of a completeness source either does not exist or is always greater than one (see [1], Item 11.4), ([2], Item 11.4) or [4]).

Theorem 1.3. Let D be a complete X-semilattice of unions. The semigroup $B_X(D)$ possesses a right unit iff D is an XI-semilattice of unions (see [1], Theorem 6.1.3, [2], Theorem 6.1.3, [7] or [8]).

Theorem 1.4. Let $\beta \in B_X(D)$. A binary relation β is a regular element of the semigroup $B_X(D)$ iff the complete X-semilattice of unions $D' = V(D,\beta)$ satisfies the following two conditions:

1) $V(X^*, \beta) \subseteq D'$;

2) D' is a complete XI-semilattice of unions (see [1] Theorem 6.3.1), ([2], Theorem 6.3.1).

Theorem 1.5. Let D be a finite X-semilattice of unions and $\alpha \circ \sigma \circ \alpha = \alpha$ for some α and σ of the semigroup $B_X(D)$; $D(\alpha)$ be the set of those elements T of the semilattice $Q = V(D,\alpha) \setminus \{\varnothing\}$ which are nonlimiting elements of the set $\ddot{Q}_T$. Then a binary relation α having a quasinormal representation of the form $\alpha = \bigcup_{T \in V(D,\alpha)} \left(Y_T^{\alpha} \times T \right)$ is a regular element of the semigroup $B_X(D)$ iff the set $V(D,\alpha)$ is a XI-semilattice of unions and for α-isomorphism φ of the semilattice $V(D,\alpha)$ on some X-subsemilattice D' of the semilattice D the following conditions are fulfilled:

1) $\varphi(T) = T\sigma$ for any $T \in V(D,\alpha)$;

2) $\bigcup_{T \in \breve{D}(\alpha)_T} Y_T^{\alpha} \supseteq \varphi(T)$ for any $T \in D(\alpha)$;

3) $Y_T^{\alpha} \cap \varphi(T) \neq \varnothing$ for any element T of the set $\ddot{D}(\alpha)_T$ (see [1], Theorem 6.3.3), ([2], Theorem 6.3.3) or [5]).

2. Results

Let D be arbitrary X-semilattice of unions and $Q = \{T_7, T_6, T_5, T_4, T_3, T_2, T_1, T_0\} \subseteq D$, which satisfies the following conditions:

$$\begin{aligned}
&T_7 \subset T_5 \subset T_3 \subset T_1 \subset T_0,\ \ T_7 \subset T_6 \subset T_4 \subset T_2 \subset T_0,\\
&T_7 \subset T_5 \subset T_4 \subset T_1 \subset T_0,\ \ T_7 \subset T_5 \subset T_4 \subset T_2 \subset T_0,\\
&T_7 \subset T_6 \subset T_4 \subset T_1 \subset T_0,\ \ T_5 \setminus T_6 \neq \varnothing,\ \ T_6 \setminus T_5 \neq \varnothing,\\
&T_4 \setminus T_3 \neq \varnothing,\ \ T_3 \setminus Z_4 \neq \varnothing,\ \ T_2 \setminus T_1 \neq \varnothing,\ \ T_1 \setminus T_2 \neq \varnothing,\\
&T_6 \cup T_5 = T_4,\ \ T_4 \cup T_3 = T_1,\ \ T_2 \cup T_1 = T_0.
\end{aligned} \tag{1}$$

Figure 1 is a graph of semilattice Q, where the semilattice Q satisfies the conditions (1). The symbol $\Sigma_3(X,8)$ is used to denote the set of all X-semilattices of unions, whose every element is isomorphic to Q.

P_7, P_6, P_5, P_4, P_3, P_2, P_1, P_0 are pairwise disjoint subsets of the set X and let $C(Q)=\{P_7,P_6,P_5,P_4,P_3,P_2,P_1,P_0\}$ be a family sets, also

$$\psi = \begin{pmatrix} T_7 & T_6 & T_5 & T_4 & T_3 & T_2 & T_1 & T_0 \\ P_7 & P_6 & P_5 & P_4 & P_3 & P_2 & P_1 & P_0 \end{pmatrix}$$

is a mapping from the semilattice Q into the family sets $C(Q)$. Then we have following formal equalities of the semilattice Q:

$$\begin{aligned}
T_0 &= P_0 \cup P_1 \cup P_2 \cup P_3 \cup P_4 \cup P_5 \cup P_6 \cup P_7,\\
T_1 &= P_0 \cup P_2 \cup P_3 \cup P_4 \cup P_5 \cup P_6 \cup P_7,\\
T_2 &= P_0 \cup P_1 \cup P_3 \cup P_4 \cup P_5 \cup P_6 \cup P_7,\\
T_3 &= P_0 \cup P_2 \cup P_4 \cup P_5 \cup P_6 \cup P_7,\\
T_4 &= P_0 \cup P_3 \cup P_5 \cup P_6 \cup P_7,\\
T_5 &= P_0 \cup P_6 \cup P_7,\\
T_6 &= P_0 \cup P_3 \cup P_5 \cup P_7,\\
T_7 &= P_0.
\end{aligned} \tag{2}$$

Note that the elements P_1, P_2, P_3, P_6 are basis sources, the element P_0, P_4, P_5, P_7 is sources of completenes of the semilattice Q. Therefore $|X| \geq 4$ and $\delta = 4$ (see Theorem 1.2).

Theorem 2.1. *Let* $Q=\{T_7,T_6,T_5,T_4,T_3,T_2,T_1,T_0\} \in \Sigma_3(X,8)$. *Then Q is XI-semilattice*

Proof. Let $t \in T_0$, $Q_t=\{T \in Q \mid t \in T\}$ and $\wedge(Q,Q_t)$ is the exact lower bound of the set Q_t in Q. Then from the formal equalities (2) we get that

$$Q_t = \begin{cases} T_0, & \text{if } t \in P_0,\\ \{T_2,T_0\}, & \text{if } t \in P_1,\\ \{T_3,T_1,T_0\}, & \text{if } t \in P_2,\\ \{T_6,T_4,T_2,T_1,T_0\}, & \text{if } t \in P_3,\\ \{T_3,T_2,T_1,T_0\}, & \text{if } t \in P_4,\\ \{T_6,T_4,T_3,T_2,T_1,T_0\}, & \text{if } t \in P_5,\\ \{T_5,T_4,T_3,T_2,T_1,T_0\}, & \text{if } t \in P_6,\\ \{T_6,T_5,T_4,T_3,T_2,T_1,T_0\}, & \text{if } t \in P_7, \end{cases} \qquad \wedge(Q,Q_t) = \begin{cases} T_7, & \text{if } t \in P_0,\\ T_2, & \text{if } t \in P_1,\\ T_3, & \text{if } t \in P_2,\\ T_6, & \text{if } t \in P_3,\\ T_5, & \text{if } t \in P_4,\\ T_7, & \text{if } t \in P_5,\\ T_5, & \text{if } t \in P_6,\\ T_7, & \text{if } t \in P_7, \end{cases}$$

We have $Q^{\wedge}=\{T_7,T_6,T_5,T_3,T_2\}$, $\wedge(Q,Q_t) \in Q$ for all t and $T_4 = T_6 \cup T_5$, $T_1 = T_6 \cup T_3$, $T_0 = T_3 \cup T_2$. The semilattice Q, which has diagram of **Figure 1**, is *XI*-semilattice, which follows from the Definition 1.3.

Theorem is proved.

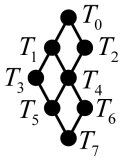

Figure 1. Diagram of Q.

Lemma 2.1. Let $Q=\{T_7,T_6,T_5,T_4,T_3,T_2,T_1,T_0\}\in\sum_3(X,8)$. Then following equalities are true:

$$P_0\cup P_5\cup P_7=T_6\cap T_3,\ \ P_3=T_6\setminus T_3,\ \ P_4\cup P_6=\big((T_3\cap T_2)\setminus T_6\big),$$
$$P_2=(T_3\setminus T_2),\ \ P_1=(T_2\setminus T_1).$$

Proof. This Lemma follows directly from the formal equalities (2) of the semilattice Q.
Lemma is proved.

Lemma 2.2. Let $Q=\{T_7,T_6,T_5,T_4,T_3,T_2,T_1,T_0\}\in\sum_3(X,8)$. Then the binary relation

$$\varepsilon=\big((T_6\cap T_3)\times T_7\big)\cup\big((T_6\setminus T_3)\times T_6\big)\cup\big(\big((T_3\cap T_2)\setminus T_6\big)\times T_5\big)$$
$$\cup\big((T_3\setminus T_2)\times T_3\big)\cup\big((T_2\setminus T_1)\times T_2\big)\cup\big((X\setminus T_0)\times T_0\big)$$

is the largest right unit of the semigroup $B_X(D)$.

Proof. From preposition and from Theorem 2.1 we get that Q is XI-semilattice. To prove this Lemma we will use Lemma 1.2, lemma 2.1, and Theorem 1.3, from where we have that the following binary relation

$$\begin{aligned}\varepsilon&=\bigcup_{t\in D}\big(\{t\}\times\wedge(Q,Q_t)\big)\cup\big((X\setminus T_0)\times T_0\big)\\&=\big((P_0\cup P_5\cup P_7)\times T_7\big)\cup(P_3\times T_6)\cup\big((P_4\cup P_6)\times T_5\big)\cup(P_2\times T_3)\cup(P_1\times T_2)\cup\big((X\setminus T_0)\times T_0\big)\\&=\big((T_6\cap T_3)\times T_7\big)\cup\big((T_6\setminus T_3)\times T_6\big)\cup\big(\big((T_3\cap T_2)\setminus T_6\big)\times T_5\big)\cup\big((T_3\setminus T_2)\times T_3\big)\\&\quad\cup\big((T_2\setminus T_1)\times T_2\big)\cup\big((X\setminus T_0)\times T_0\big).\end{aligned}$$

is the largest right unit of the semigroup $B_X(D)$.
Lemma is proved.

Lemma 2.3. Let $Q=\{T_7,T_6,T_5,T_4,T_3,T_2,T_1,T_0\}\in\sum_3(X,8)$. Binary relation α having quazinormal representation of the form

$$\alpha=\big(Y_7^\alpha\times T_7\big)\cup\big(Y_6^\alpha\times T_6\big)\cup\big(Y_5^\alpha\times T_5\big)\cup\big(Y_4^\alpha\times T_4\big)\cup\big(Y_3^\alpha\times T_3\big)\cup\big(Y_2^\alpha\times T_2\big)\cup\big(Y_1^\alpha\times T_1\big)\cup\big(Y_0^\alpha\times T_0\big)$$

where $Y_7^\alpha,\ Y_6^\alpha,\ Y_5^\alpha,\ Y_3^\alpha,\ Y_2^\alpha\notin\{\varnothing\}$ and $V(D,\alpha)=Q\in\sum_3(X,8)$ is a regular element of the semigroup $B_X(D)$ iff for some complete α-isomorphism $\varphi=\begin{pmatrix}T_7&T_6&T_5&T_4&T_3&T_2&T_1&T_0\\\overline{T}_7&\overline{T}_6&\overline{T}_5&\overline{T}_4&\overline{T}_3&\overline{T}_2&\overline{T}_1&\overline{T}_0\end{pmatrix}$ of the semilattice Q on some X-subsemilattice $Q'=\{\overline{T}_7,\overline{T}_6,\overline{T}_5,\overline{T}_4,\overline{T}_3,\overline{T}_2,\overline{T}_1,\overline{T}_0\}$ of the semilattice Q satisfies the following conditions:

$$Y_7^\alpha\supseteq\overline{T}_7,\ \ Y_7^\alpha\cup Y_6^\alpha\supseteq\overline{T}_6,\ \ Y_7^\alpha\cup Y_5^\alpha\supseteq\overline{T}_5,\ \ Y_7^\alpha\cup Y_5^\alpha\cup Y_3^\alpha\supseteq\overline{T}_3,$$
$$Y_7^\alpha\cup Y_6^\alpha\cup Y_5^\alpha\cup Y_4^\alpha\cup Y_2^\alpha\supseteq\overline{T}_2,\ \ Y_6^\alpha\cap\overline{T}_6\neq\varnothing,\ \ Y_5^\alpha\cap\overline{T}_5\neq\varnothing,$$
$$Y_3^\alpha\cap\overline{T}_3\neq\varnothing,\ \ Y_2^\alpha\cap\overline{T}_2\neq\varnothing.$$

Proof. It is easy to see, that the set $Q(\alpha)=\{T_7,T_6,T_5,T_4,T_3,T_2,T_1\}$ is a generating set of the semilattice Q. Then the following equalities are hold:

$$\ddot{Q}(\alpha)_{T_7}=\{T_7\},\ \ \ddot{Q}(\alpha)_{T_6}=\{T_7,T_6\},\ \ \ddot{Q}(\alpha)_{T_5}=\{T_7,T_5\},\ \ \ddot{Q}(\alpha)_{T_4}=\{T_7,T_6,T_5,T_4\},$$
$$\ddot{Q}(\alpha)_{T_3}=\{T_7,T_5,T_3\},\ \ \ddot{Q}(\alpha)_{T_2}=\{T_7,T_6,T_5,T_4,T_2\},\ \ \ddot{Q}(\alpha)_{T_1}=\{T_7,T_6,T_5,T_4,T_3,T_1\}.$$

If we follow statement *b*) of the Theorem 1.5 we get that followings are true:

$$Y_7^\alpha\supseteq\overline{T}_7,\ \ Y_7^\alpha\cup Y_6^\alpha\supseteq\overline{T}_6,\ \ Y_7^\alpha\cup Y_5^\alpha\supseteq\overline{T}_5,\ \ Y_7^\alpha\cup Y_6^\alpha\cup Y_5^\alpha\cup Y_4^\alpha\supseteq\overline{T}_4$$
$$Y_7^\alpha\cup Y_5^\alpha\cup Y_3^\alpha\supseteq\overline{T}_3,\ \ Y_7^\alpha\cup Y_6^\alpha\cup Y_5^\alpha\cup Y_4^\alpha\cup Y_2^\alpha\supseteq\overline{T}_2,$$
$$Y_7^\alpha\cup Y_6^\alpha\cup Y_5^\alpha\cup Y_4^\alpha\cup Y_3^\alpha\cup Y_1^\alpha\supseteq\overline{T}_1,$$

From the last conditions we have that following is true:

$$Y_7^\alpha\cup Y_6^\alpha\cup Y_5^\alpha\cup Y_4^\alpha=\big(Y_7^\alpha\cup Y_6^\alpha\big)\cup\big(Y_7^\alpha\cup Y_5^\alpha\big)\cup Y_4^\alpha\supseteq\overline{T}_6\cup\overline{T}_5\cup Y_4^\alpha=\overline{T}_4\cup Y_4^\alpha\supseteq\overline{T}_4,$$

$$Y_7^\alpha \cup Y_6^\alpha \cup Y_5^\alpha \cup Y_4^\alpha \cup Y_3^\alpha \cup Y_1^\alpha = \left(Y_7^\alpha \cup Y_5^\alpha \cup Y_3^\alpha\right) \cup \left(Y_7^\alpha \cup Y_6^\alpha\right) \cup Y_4^\alpha \cup Y_1^\alpha$$
$$\supseteq \overline{T}_3 \cup \overline{T}_6 \cup Y_4^\alpha \cup Y_1^\alpha = \overline{T}_1 \cup Y_4^\alpha \cup Y_1^\alpha \supseteq \overline{T}_1.$$

Moreover, the following conditions are true:

$$l\left(\ddot{Q}_{T_6}, T_6\right) = \cup\left(\ddot{Q}_{T_6} \setminus \{T_6\}\right) = T_7, \quad T_6 \setminus l\left(\ddot{Q}_{T_6}, T_6\right) = T_6 \setminus T_7 \neq \varnothing;$$

$$l\left(\ddot{Q}_{T_5}, T_5\right) = \cup\left(\ddot{Q}_{T_5} \setminus \{T_5\}\right) = T_7, \quad T_5 \setminus l\left(\ddot{Q}_{T_5}, T_5\right) = T_5 \setminus T_7 \neq \varnothing;$$

$$l\left(\ddot{Q}_{T_4}, T_4\right) = \cup\left(\ddot{Q}_{T_4} \setminus \{T_4\}\right) = \cup\{T_7, T_6, T_5\} = T_4, \quad T_4 \setminus l\left(\ddot{Q}_{T_4}, T_4\right) = T_4 \setminus T_4 = \varnothing;$$

$$l\left(\ddot{Q}_{T_3}, T_3\right) = \cup\left(\ddot{Q}_{T_3} \setminus \{T_3\}\right) = \cup\{T_7, T_5\} = T_5, \quad T_3 \setminus l\left(\ddot{Q}_{T_3}, T_3\right) = T_3 \setminus T_5 \neq \varnothing;$$

$$l\left(\ddot{Q}_{T_2}, T_2\right) = \cup\left(\ddot{Q}_{T_2} \setminus \{T_2\}\right) = \cup\{T_7, T_6, T_5, T_4\} = T_4, \quad T_2 \setminus l\left(\ddot{Q}_{T_2}, T_2\right) = T_2 \setminus T_4 \neq \varnothing;$$

$$l\left(\ddot{Q}_{T_1}, T_1\right) = \cup\left(\ddot{Q}_{T_1} \setminus \{T_1\}\right) = \cup\{T_7, T_6, T_5, T_4, T_3\} = T_1, \quad T_1 \setminus l\left(\ddot{Q}_{T_1}, T_1\right) = T_1 \setminus T_1 = \varnothing;$$

The elements T_6, T_5, T_3, T_2 are nonlimiting elements of the sets $\ddot{Q}(\alpha)_{T_6}$, $\ddot{Q}(\alpha)_{T_5}$, $\ddot{Q}(\alpha)_{T_3}$ and $\ddot{Q}(\alpha)_{T_2}$ respectively. The proof of condition $Y_6^\alpha \cap \overline{T}_6 \neq \varnothing$, $Y_5^\alpha \cap \overline{T}_5 \neq \varnothing$, $Y_3^\alpha \cap \overline{T}_3 \neq \varnothing$ and $Y_2^\alpha \cap \overline{T}_2 \neq \varnothing$ comes from the statement *c*) of the Theorem 1.5

Therefore the following conditions are hold:

$$Y_7^\alpha \supseteq \overline{T}_7, \quad Y_7^\alpha \cup Y_6^\alpha \supseteq \overline{T}_6, \quad Y_7^\alpha \cup Y_5^\alpha \supseteq \overline{T}_5, \quad Y_7^\alpha \cup Y_5^\alpha \cup Y_3^\alpha \supseteq \overline{T}_3,$$
$$Y_7^\alpha \cup Y_6^\alpha \cup Y_5^\alpha \cup Y_4^\alpha \cup Y_2^\alpha \supseteq \overline{T}_2, \quad Y_6^\alpha \cap \overline{T}_6 \neq \varnothing, \quad Y_5^\alpha \cap \overline{T}_5 \neq \varnothing,$$
$$Y_3^\alpha \cap \overline{T}_3 \neq \varnothing, \quad Y_2^\alpha \cap \overline{T}_2 \neq \varnothing.$$

Lemma is proved.

Definition 2.1. Assume that $Q' \in \Sigma_3(X, 8)$. Denote by the symbol $R(Q')$ the set of all regular elements α of the semigroup $B_X(D)$, for which the semilattices Q' and Q are mutually α -isomorphic and $V(D, \alpha) = Q'$.

Note that, $q = 1$, where q is the number of automorphism of the semilattice Q.

Theorem 2.2. Let $Q = \{T_7, T_6, T_5, T_4, T_3, T_2, T_1, T_0\} \in \Sigma_3(X, 8)$ and $|\Sigma_3(X, 8)| = m_0$. If X be finite set, and the *XI*-semilattice Q and $Q' = \{\overline{T}_7, \overline{T}_6, \overline{T}_5, \overline{T}_4, \overline{T}_3, \overline{T}_2, \overline{T}_1, \overline{T}_0\}$ (see **Figure 2**) are α -isomorphic, then

$$\left|R(Q')\right| = m_0 \cdot \left(2^{|\overline{T}_6 \setminus \overline{T}_3|} - 1\right) \cdot 2^{\left|(\overline{T}_3 \cap \overline{T}_2) \setminus \overline{T}_4\right|} \cdot \left(2^{|\overline{T}_5 \setminus \overline{T}_6|} - 1\right) \cdot \left(3^{|\overline{T}_3 \setminus \overline{T}_2|} - 2^{|\overline{T}_3 \setminus \overline{T}_2|}\right) \cdot \left(5^{|\overline{T}_2 \setminus \overline{T}_1|} - 4^{|\overline{T}_2 \setminus \overline{T}_1|}\right) \cdot 8^{|X \setminus \overline{T}_0|}$$

Proof. Assume that $\alpha \in R(Q')$. Then a quasinormal representation of a regular binary relation α has the form

$$\alpha = \left(Y_7^\alpha \times T_7\right) \cup \left(Y_6^\alpha \times T_6\right) \cup \left(Y_5^\alpha \times T_5\right) \cup \left(Y_4^\alpha \times T_4\right) \cup \left(Y_3^\alpha \times T_3\right) \cup \left(Y_2^\alpha \times T_2\right) \cup \left(Y_1^\alpha \times T_1\right) \cup \left(Y_0^\alpha \times T_0\right)$$

where Y_7^α, Y_6^α, Y_5^α, Y_3^α, $Y_2^\alpha \notin \{\varnothing\}$ and by Lemma 2.2 satisfies the conditions:

$$Y_7^\alpha \supseteq \overline{T}_7, \quad Y_7^\alpha \cup Y_6^\alpha \supseteq \overline{T}_6, \quad Y_7^\alpha \cup Y_5^\alpha \supseteq \overline{T}_5, \quad Y_7^\alpha \cup Y_5^\alpha \cup Y_3^\alpha \supseteq \overline{T}_3,$$
$$Y_7^\alpha \cup Y_6^\alpha \cup Y_5^\alpha \cup Y_4^\alpha \cup Y_2^\alpha \supseteq \overline{T}_2, \quad Y_6^\alpha \cap \overline{T}_6 \neq \varnothing, \quad Y_5^\alpha \cap \overline{T}_5 \neq \varnothing, \tag{3}$$
$$Y_3^\alpha \cap \overline{T}_3 \neq \varnothing, \quad Y_2^\alpha \cap \overline{T}_2 \neq \varnothing.$$

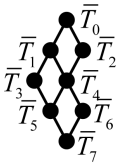

Figure 2. Diagram of Q'.

Father, let f_α is a mapping the set X in the semilattice Q satisfying the conditions $f_\alpha(t)=t\alpha$ for all $t\in X$. $f_{0\alpha}$, $f_{1\alpha}$, $f_{2\alpha}$, $f_{3\alpha}$, $f_{4\alpha}$ and $f_{5\alpha}$ are the restrictions of the mapping f_α on the sets $\overline{T}_6\cap\overline{T}_3$, $\overline{T}_6\setminus\overline{T}_3$, $\left(\overline{T}_3\cap\overline{T}_2\right)\setminus\overline{T}_6$, $\overline{T}_3\setminus\overline{T}_2$, $\overline{T}_2\setminus\overline{T}_1$, $X\setminus\overline{T}_0$ respectively. It is clear, that the intersection disjoint elements of the set $\left\{\overline{T}_6\cap\overline{T}_3,\overline{T}_6\setminus\overline{T}_3,\left(\overline{T}_3\cap\overline{T}_2\right)\setminus\overline{T}_6,\overline{T}_3\setminus\overline{T}_2,\overline{T}_2\setminus\overline{T}_1,X\setminus\overline{T}_0\right\}$ are empty set and

$\overline{T}_6\cap\overline{T}_3\cup\overline{T}_6\setminus\overline{T}_3\cup\left(\overline{T}_3\cap\overline{T}_2\right)\setminus\overline{T}_6\cup\overline{T}_3\setminus\overline{T}_2\cup\overline{T}_2\setminus\overline{T}_1\cup X\setminus\overline{T}_0=X$.

We are going to find properties of the maps $f_{1\alpha}$, $f_{2\alpha}$, $f_{3\alpha}$, $f_{4\alpha}$, $f_{5\alpha}$, $f_{6\alpha}$.

1) $t\in\overline{T}_6\cap\overline{T}_3$. Then by properties (3) we have $t\in\overline{T}_6\cap\overline{T}_3\subseteq\left(Y_7^\alpha\cup Y_6^\alpha\right)\cap\left(Y_7^\alpha\cup Y_5^\alpha\cup Y_3^\alpha\right)=Y_7^\alpha$, *i.e.*, $t\in Y_7^\alpha$ and $t\alpha=\overline{T}_7$ by definition of the set Y_7^α. Therefore $f_{1\alpha}(t)=T_7$ for all $t\in\overline{T}_6\cap\overline{T}_3$.

2) $t\in\overline{T}_6\setminus\overline{T}_3$. Then by properties (3) we have $t\in\overline{T}_6\setminus\overline{T}_3\subseteq Y_7^\alpha\cup Y_6^\alpha$, *i.e.*, $t\in Y_7^\alpha\cup Y_6^\alpha$ and $t\alpha=\left\{\overline{T}_7,\overline{T}_6\right\}$ by definition of the set Y_7^α and Y_6^α. Therefore $f_{2\alpha}(t)=\left\{T_7,T_6\right\}$ for all $t\in\overline{T}_6\setminus\overline{T}_3$.

By suppose we have that $Y_6^\alpha\cap\overline{T}_6\neq\varnothing$, *i.e.* $t_1\alpha=T_6$ for some $t_1\in\overline{T}_6$. If $t_1\in\overline{T}_3$. Then $t_1\in Y_7^\alpha\cup Y_5^\alpha\cup Y_3^\alpha$. Therefore $t_1\alpha\in\left\{\overline{T}_7,\overline{T}_5,\overline{T}_3\right\}$. That is contradict of the equality $t_1\alpha=T_6$, while $T_6\neq T_7$, $T_6\neq T_5$ and $T_6\neq T_3$ by definition of the semilattice Q. Therefore $f_{1\alpha}(t_1)=T_6$ for some $t\in\overline{T}_6\setminus\overline{T}_3$.

3) $t\in\left(\overline{T}_3\cap\overline{T}_2\right)\setminus\overline{T}_6$. Then by properties (3) we have

$$\left(\overline{T}_3\cap\overline{T}_2\right)\setminus\overline{T}_6\subseteq\overline{T}_3\cap\overline{T}_2\subseteq\left(Y_7^\alpha\cup Y_5^\alpha\cup Y_3^\alpha\right)\cap\left(Y_7^\alpha\cup Y_6^\alpha\cup Y_5^\alpha\cup Y_4^\alpha\cup Y_2^\alpha\right)=Y_7^\alpha\cup Y_5^\alpha$$

i.e., $t\in Y_7^\alpha\cup Y_5^\alpha$ and $t\alpha\in\left\{\overline{T}_7,\overline{T}_5\right\}$ by definition of the sets Y_7^α and Y_5^α. Therefore $f_{3\alpha}(t)\in\left\{T_7,T_5\right\}$ for all $t\in\left(\overline{T}_3\cap\overline{T}_2\right)\setminus\overline{T}_6$.

By suppose we have, that $Y_5^\alpha\cap\overline{T}_5\neq\varnothing$, *i.e.* $t_3\alpha=T_5$ for some $t_3\in\overline{T}_5$. If $t_3\in\overline{T}_6$ then $t_2\in\overline{T}_6\subseteq Y_7^\alpha\cup Y_6^\alpha$. Therefore $t_3\alpha\in\left\{T_7,T_6\right\}$. We have contradict of the equality $t_2\alpha=T_5$, since $T_5\notin\left\{T_7,T_6\right\}$.

Therefore $f_{3\alpha}(t_3)=T_5$ for some $t_3\in\overline{T}_5\setminus\overline{T}_6$.

4) $t\in\overline{T}_3\setminus\overline{T}_2$. Then by properties (3) we have $\overline{T}_3\setminus\overline{T}_2\subseteq\overline{T}_3\subseteq Y_7^\alpha\cup Y_5^\alpha\cup Y_3^\alpha$, *i.e.*, $t\in Y_7^\alpha\cup Y_5^\alpha\cup Y_3^\alpha$ and $t\alpha\in\left\{\overline{T}_7,\overline{T}_5,\overline{T}_3\right\}$ by definition of the sets Y_7^α, Y_5^α, and Y_3^α. Therefore $f_{4\alpha}(t)\in\left\{T_7,T_5,T_3\right\}$ for all $t\in\overline{T}_3\setminus\overline{T}_2$.

By suppose we have, that $Y_3^\alpha\cap\overline{T}_3\neq\varnothing$, *i.e.* $t_4\alpha=T_3$ for some $t_4\in\overline{T}_3$. If $t_4\in\overline{T}_2$. Then $t_4\in\overline{T}_2\subseteq Y_7^\alpha\cup Y_6^\alpha\cup Y_5^\alpha\cup Y_4^\alpha\cup Y_2^\alpha$. Therefore $t_4\alpha\in\left\{T_7,T_6,T_5,T_4,T_2\right\}$. We have contradict of the equality $t_4\alpha=T_3$, since $T_3\notin\left\{T_7,T_6,T_5,T_4,T_2\right\}$.

Therefore $f_{4\alpha}(t_4)=T_3$ for some $t\in\overline{T}_3\setminus\overline{T}_2$.

5) $t\in\overline{T}_2\setminus\overline{T}_1$. Then by properties (3) we have $\overline{T}_2\setminus\overline{T}_1\subseteq\overline{T}_2\subseteq Y_7^\alpha\cup Y_6^\alpha\cup Y_5^\alpha\cup Y_4^\alpha\cup Y_2^\alpha$, *i.e.*, $t\in Y_7^\alpha\cup Y_6^\alpha\cup Y_5^\alpha\cup Y_4^\alpha\cup Y_2^\alpha$ and $t\alpha\in\left\{\overline{T}_7,\overline{T}_6,\overline{T}_5,\overline{T}_4,\overline{T}_2\right\}$ by definition of the sets Y_7^α, Y_6^α, Y_5^α, Y_4^α and Y_2^α. Therefore $f_{5\alpha}(t)\in\left\{T_7,T_6,T_5,T_4,T_2\right\}$ for all $t\in\overline{T}_2\setminus\overline{T}_1$.

By suppose we have, that $Y_2^\alpha\cap\overline{T}_2\neq\varnothing$, *i.e.* $t_5\alpha=T_2$ for some $t_5\in\overline{T}_2$. If $t_5\in\overline{T}_1$. Then $t_5\in\overline{T}_1\subseteq Y_7^\alpha\cup Y_6^\alpha\cup Y_5^\alpha\cup Y_4^\alpha\cup Y_3^\alpha\cup Y_1^\alpha$. Therefore $t_5\alpha\in\left\{T_7,T_6,T_5,T_4,T_3,T_1\right\}$. We have contradict of the equality $t_5\alpha=T_2$, since $T_2\notin\left\{T_7,T_6,T_5,T_4,T_3,T_1\right\}$.

Therefore $f_{5\alpha}(t_5)=T_2$ for some $t\in\overline{T}_2\setminus\overline{T}_1$.

6) $t\in X\setminus T_0$. Then by definition quasinormal representation binary relation α and by property (3) we have $t\in X\setminus T_0\subseteq X=Y_7^\alpha\cup Y_6^\alpha\cup Y_5^\alpha\cup Y_4^\alpha\cup Y_3^\alpha\cup Y_2^\alpha\cup Y_1^\alpha\cup Y_0^\alpha$, *i.e.* $t\alpha\in\left\{\overline{T}_7,\overline{T}_6,\overline{T}_5,\overline{T}_4,\overline{T}_3,\overline{T}_2,\overline{T}_1,\overline{T}_0\right\}$ by definition of the sets Y_7^α, Y_6^α, Y_5^α, Y_4^α, Y_3^α, Y_2^α, Y_1^α, Y_0^α. Therefore $f_{6\alpha}(t)\in\left\{T_7,T_6,T_5,T_4,T_3,T_2,T_1,T_0\right\}$ for all $t\in X\setminus\breve{D}$.

Therefore for every binary relation α exist ordered system $\left(f_{1\alpha},f_{2\alpha},f_{3\alpha},f_{4\alpha},f_{5\alpha},f_{6\alpha}\right)$. It is obvious that for disjoint binary relations exist disjoint ordered systems.

Father, let

$$f_1:\overline{T}_6\cap\overline{T}_3\to T_7,\qquad f_2:\overline{T}_6\setminus\overline{T}_3\to\left\{T_7,T_6\right\},$$
$$f_3:\left(\overline{T}_3\cap\overline{T}_2\right)\setminus\overline{T}_6\to\left\{T_7,T_5\right\},\qquad f_4:\overline{T}_3\setminus\overline{T}_2\to\left\{T_7,T_5,T_3\right\},$$
$$f_5:\overline{T}_2\setminus\overline{T}_1\to\left\{T_7,T_6,T_5,T_4,T_2\right\},\quad f_6:X\setminus\overline{T}_0\to\left\{T_7,T_6,T_5,T_4,T_3,T_2,T_1,T_0\right\}.$$

are such mappings, which satisfying the conditions:

7) $f_1(t)=T_7$ for all $t\in\overline{T}_6\cap\overline{T}_3$;

8) $f_2(t)\in\{T_7,T_6\}$ for all $t\in\overline{T}_6\setminus\overline{T}_3$ and $f_2(t_1)=T_6$ for some $t_1\in\overline{T}_6\setminus\overline{T}_3$;

9) $f_3(t)\in\{T_7,T_5\}$ for all $t\in(\overline{T}_3\cap\overline{T}_2)\setminus\overline{T}_6$ and $f_3(t_2)=T_5$ for some $t_2\in\overline{T}_5\setminus\overline{T}_6$;

10) $f_4(t)\in\{T_7,T_5,T_3\}$ for all $t\in\overline{T}_3\setminus\overline{T}_2$ and $f_4(t_3)=T_3$ for some $t_3\in\overline{T}_3\setminus\overline{T}_2$;

11) $f_5(t)\in\{T_7,T_6,T_5,T_4,T_2\}$ for all $t\in\overline{T}_2\setminus\overline{T}_1$ and $f_5(t_4)=T_2$ for some $t_4\in\overline{T}_2\setminus\overline{T}_1$;

12) $f_6(t)\in\{T_6,T_5,T_4,T_3,T_2,T_1,T_0\}$ for all $t\in X\setminus\overline{T}_0$.

Now we define a map f of a set X in the semilattice D, which satisfies the condition:

$$f(t)=\begin{cases}f_1(t), & \text{if } t\in\overline{T}_6\cap\overline{T}_3,\\ f_2(t), & \text{if } t\in\overline{T}_6\setminus\overline{T}_3,\\ f_3(t), & \text{if } t\in(\overline{T}_3\cap\overline{T}_2)\setminus\overline{T}_6,\\ f_4(t), & \text{if } t\in\overline{T}_3\setminus\overline{T}_2,\\ f_5(t), & \text{if } \overline{T}_2\setminus\overline{T}_1,\\ f_6(t), & \text{if } X\setminus\overline{T}_0.\end{cases}$$

Father, let $\beta=\bigcup_{x\in X}(\{x\}\times f(x))$, $Y_i^{\beta}=\{t\,|\,t\beta=T_i\}$ $(i=1,2,\cdots,6)$. Then binary relation β my be representation by form

$$\beta=(Y_7^{\beta}\times T_7)\cup(Y_6^{\beta}\times T_6)\cup(Y_5^{\beta}\times T_5)\cup(Y_4^{\beta}\times T_4)\cup(Y_3^{\beta}\times T_3)\cup(Y_2^{\beta}\times T_2)\cup(Y_1^{\beta}\times T_1)\cup(Y_0^{\beta}\times T_0)$$

and satisfying the conditions:

$$Y_7^{\beta}\supseteq\overline{T}_7,\ Y_7^{\beta}\cup Y_6^{\beta}\supseteq\overline{T}_6,\ Y_7^{\beta}\cup Y_5^{\beta}\supseteq\overline{T}_5,\ Y_7^{\beta}\cup Y_5^{\beta}\cup Y_3^{\beta}\supseteq\overline{T}_3,$$
$$Y_7^{\beta}\cup Y_6^{\beta}\cup Y_5^{\beta}\cup Y_4^{\beta}\cup Y_2^{\beta}\supseteq\overline{T}_2,\ Y_6^{\beta}\cap\overline{T}_6\neq\varnothing,\ Y_5^{\beta}\cap\overline{T}_5\neq\varnothing,$$
$$Y_3^{\beta}\cap\overline{T}_3\neq\varnothing,\ Y_2^{\beta}\cap\overline{T}_2\neq\varnothing.$$

(By suppose $f_2(t_1)=T_6$ for some $t_1\in\overline{T}_6\setminus\overline{T}_3$; $f_3(t_2)=T_5$ for some $t_2\in\overline{T}_5\setminus\overline{T}_6$; $f_4(t_3)=T_3$ for some $t_3\in\overline{T}_3\setminus\overline{T}_2$; $f_5(t_4)=T_2$ for some $t_4\in\overline{T}_2\setminus\overline{T}_1$. From this and by lemma 2.3 we have that $\beta\in R(Q')$.

Therefore for every binary relation $\alpha\in R(Q')$ and ordered system $(f_{1\alpha},f_{2\alpha},f_{3\alpha},f_{4\alpha},f_{5\alpha},f_{6\alpha})$ exist one to one mapping.

By Theorem 1.1 the number of the mappings $f_{0\alpha},f_{1\alpha},f_{2\alpha},f_{3\alpha},f_{4\alpha},f_{5\alpha}$ are respectively:

$$1,\ 2^{|\overline{T}_6\setminus\overline{T}_3|}-1,\ 2^{|(\overline{T}_3\cap\overline{T}_2)\setminus(\overline{T}_5\cup\overline{T}_6)|}\cdot\left(2^{|\overline{T}_5\setminus\overline{T}_6|}-1\right),\ 3^{|\overline{T}_3\setminus\overline{T}_2|}-2^{|\overline{T}_3\setminus\overline{T}_2|},\ 5^{|\overline{T}_2\setminus\overline{T}_1|}-4^{|\overline{T}_2\setminus\overline{T}_1|},\ 8^{|X\setminus\overline{T}_0|}$$

(see Lemma 1.1). The number of ordered system $(f_{1\alpha},f_{2\alpha},f_{3\alpha},f_{4\alpha},f_{5\alpha},f_{6\alpha})$ or number idempotent elements of this case we my be calculated by formula

$$|R(Q')|=m_0\cdot\left(2^{|\overline{T}_6\setminus\overline{T}_3|}-1\right)\cdot2^{|(\overline{T}_3\cap\overline{T}_2)\setminus\overline{T}_4|}\cdot\left(2^{|\overline{T}_5\setminus\overline{T}_6|}-1\right)\cdot\left(3^{|\overline{T}_3\setminus\overline{T}_2|}-2^{|\overline{T}_3\setminus\overline{T}_2|}\right)\cdot\left(5^{|\overline{T}_2\setminus\overline{T}_1|}-4^{|\overline{T}_2\setminus\overline{T}_1|}\right)\cdot8^{|X\setminus\overline{T}_0|}$$

Theorem is proved.

Corollary 2.1. Let $Q=\{T_7,T_6,T_5,T_4,T_3,T_2,T_1,T_0\}\in\sum_3(X,8)$, If X be a finite set and $E_X^{(r)}(Q)$ be the set of all right units of the semigroup $B_X(Q)$, then the following formula is true

$$\left|E_X^{(r)}(Q)\right|=\left(2^{|T_6\setminus T_3|}-1\right)\cdot2^{|(T_3\cap T_2)\setminus T_4|}\cdot\left(2^{|T_5\setminus T_6|}-1\right)\cdot\left(3^{|T_3\setminus T_2|}-2^{|T_3\setminus T_2|}\right)\cdot\left(5^{|T_2\setminus T_1|}-4^{|T_2\setminus T_1|}\right)\cdot8^{|X\setminus T_0|}$$

Proof: This Corollary directly follows from the Theorem 2.2 and from the [2, 3 Theorem 6.3.7].

Corollary is proved.

References

[1] Diasamidze, Ya. and Makharadze, Sh. (2010) Complete Semigroups of Binary Relations. Monograph. M., Sputnik+, 657 p. (In Russian)

[2] Diasamidze, Ya. and Makharadze, Sh. (2013) Complete Semigroups of Binary Relations. Monograph. Kriter, Turkey, 1-520.

[3] Lyapin, E.S. (1960) Semigroups. Fizmatgiz, Moscow. (In Russian)

[4] Diasamidze, Ya.I. (2003) Complete Semigroups of Binary Relations. *Journal of Mathematical Sciences*, **117**, 4271-4319.

[5] Diasamidze, Ya.I., Makharadze, Sh.I. and Diasamidze, I.Ya. (2008) Idempotents and Regular Elements of Complete Semigroups of Binary Relations. *Journal of Mathematical Sciences*, **153**, 481-499.

[6] Diasamidze, Ya., Makharadze, Sh. and Rokva, N. (2008) On *XI*-Semilattices of Union. *Bull. Georg. Nation. Acad. Sci.*, **2**, 16-24.

[7] Diassamidze, Ya., Erdogan, A. and Aydm, N. (2014) Some Regular Elements, Idempotents and Right Units of Complete Semigroups of Binary Relations Defined by Semilattices of the Class Lower Incomplete Nets. *International Journal of Pure and Applied Mathematics*, **93**, 549-566. http://dx.doi.org/10.12732/ijpam.v93i4.6

[8] Diasamidze, Ya. (2009) The Properties of Right Units of Semigroups Belonging to Some Classes of Complete Semigroups of Binary Relations. *Proc. of A. Razmadze Math. Inst.*, **150**, 51-70.

Applied Mathematics, 2015, 6, 382-402
Published Online February 2015 in SciRes. http://www.scirp.org/journal/am
http://dx.doi.org/10.4236/am.2015.62036

Scientific Research Publishing

The Barone-Adesi Whaley Formula to Price American Options Revisited

Lorella Fatone[1], Francesca Mariani[2], Maria Cristina Recchioni[3], Francesco Zirilli[4]

[1]Dipartimento di Matematica e Informatica, Università di Camerino, Camerino, Italy
[2]Dipartimento di Scienze Economiche, Università degli Studi di Verona, Verona, Italy
[3]Dipartimento di Management, Università Politecnica delle Marche, Ancona, Italy
[4]Dipartimento di Matematica "G. Castelnuovo", Università di Roma "La Sapienza", Roma, Italy
Email: lorella.fatone@unicam.it, francesca.mariani@univr.it, m.c.recchioni@univpm.it, zirilli@mat.uniroma1.it

Received 22 January 2015; accepted 10 February 2015; published 13 February 2015

Abstract

This paper presents a method to solve the American option pricing problem in the Black Scholes framework that generalizes the Barone-Adesi, Whaley method [1]. An auxiliary parameter is introduced in the American option pricing problem. Power series expansions in this parameter of the option price and of the corresponding free boundary are derived. These series expansions have the Baroni-Adesi, Whaley solution of the American option pricing problem as zero-th order term. The coefficients of the option price series are explicit formulae. The partial sums of the free boundary series are determined solving numerically nonlinear equations that depend from the time variable as a parameter. Numerical experiments suggest that the series expansions derived are convergent. The evaluation of the truncated series expansions on a grid of values of the independent variables is easily parallelizable. The cost of computing the *n*-th order truncated series expansions is approximately proportional to *n* as *n* goes to infinity. The results obtained on a set of test problems with the first and second order approximations deduced from the previous series expansions outperform in accuracy and/or in computational cost the results obtained with several alternative methods to solve the American option pricing problem [1]-[3]. For example when we consider options with maturity time between three and ten years and positive cost of carrying parameter (*i.e.* when the continuous dividend yield is smaller than the risk free interest rate) the second order approximation of the free boundary obtained truncating the series expansions improves substantially the Barone-Adesi, Whaley free boundary [1]. The website: http://www.econ.univpm.it/recchioni/finance/w20 contains material including animations, an interactive application and an app that helps the understanding of the paper. A general reference to the work of the authors and of their coauthors in mathematical finance is the website: http://www.econ.univpm.it/recchioni/finance.

How to cite this paper: Fatone, L., Mariani, F., Recchioni, M.C. and Zirilli, F. (2015) The Barone-Adesi Whaley Formula to Price American Options Revisited. *Applied Mathematics*, **6**, 382-402. http://dx.doi.org/10.4236/am.2015.62036

Keywords

American Option Pricing, Perturbation Expansion

1. Introduction

American call and put options are one of the most traded products in financial markets. They are traded either standing alone or embedded in a variety of financial contracts such as, for example, convertible bonds, mortgages or life insurance policies. The fast and accurate evaluation of American option prices and of the corresponding free boundaries is an important problem in mathematical finance. Let us restrict our attention to the American option pricing problem in the Black Scholes framework. Many methods have been suggested to solve this problem. In particular several hybrid methods have been suggested. These methods combine analytical and numerical approximations. For example let us mention the hybrid methods proposed by Geske, Johnson (1984) [4], Barone-Adesi, Whaley (1987) [1], Kim (1990) [5], Bunch, Johnson, (1992) [6], Bjerksund, Stensland (1993) [7], Ju, Zhong (1999) [2], Barone-Adesi (2005) [8] and Zhu (2006) [9].

In [1] Barone-Adesi and Whaley write the American option price as the sum of the price of the corresponding European option and of a quantity called early exercise premium. The European option price is given by the Black Scholes formula and the early exercise premium is approximated with the solution of a free boundary value problem for an ordinary differential equation. This ordinary differential equation is obtained dropping the time derivative term in the partial differential equation satisfied by the early exercise premium. Barone-Adesi and Whaley [1] give a simple formula for the solution of this free boundary value problem for an ordinary differential equation. Moreover they determine an approximation of the free boundary solving numerically a nonlinear equation that depends from the time variable as a parameter. This approximate solution of the American option pricing problem is called Barone-Adesi, Whaley formula and is widely used in the financial markets by practitioners. An exhaustive review of the methods used to solve the American option pricing problem and of the developments of the Barone-Adesi, Whaley method during the period 1987-2005 can be found in Barone-Adesi (2005) [8]. For example in 1999 Ju, Zhong [2] reconsidered the Barone-Adesi, Whaley formula of the early exercise premium. The Ju, Zhong formula [2] introduces a correction to the Barone-Adesi, Whaley approximation of the early exercise premium. This correction consists in writing the early exercise premium as the product of the Barone-Adesi, Whaley early exercise premium times a time-independent function determined solving an ordinary differential equation. When long dated options are considered, the Ju, Zhong formula improves the approximate option price obtained with the Barone-Adesi, Whaley formula.

Given a positive integer n, Geske and Johnson [4] approximate the price of an American put option using an n-fold compound option. They assume that exercise decisions are taken only at some known time values. These time values are a set of n points. In [4] Geske and Johnson deduce a formula to approximate the American put option price with a piecewise solution of the Black Scholes partial differential equation subject to boundary conditions imposed at the decision times. Moreover, using Richardson extrapolation, they show how to approximate the Geske, Johnson formula with a simple polynomial expression. Bunch and Johnson [6] refine the results obtained in [4] determining the n exercise times that maximize the accuracy of the option prices obtained.

In [7] Bjerksund and Stensland approximate the solution of the American option pricing problem assuming a flat early exercise boundary and using a trigger price. Bjerksund and Stensland reduce the evaluation of an American call option with exercise price E and maturity time T to the evaluation of a European call up-and-out barrier option with knock-out barrier X, strike price E and maturity time T. A rebate given by $X - E$ is received by the holder of the option at the knock-out time when the option is exercised prior to maturity time. The barrier X is the flat boundary that approximates the free boundary of the American option pricing problem. In [7] the problem of choosing X is studied. In [10] the approximation of the free boundary used in [7] is refined. In fact in [10] the time interval where the problem is studied is divided in two disjoint subintervals and a flat early exercise boundary is used in each subinterval.

Zhu (2006) [9] considers the American put option pricing problem and derives an explicit formula of the American put option price associated to a numerically approximated free boundary. This formula is a Taylor's series expansion with infinitely many terms. Each term of this Taylor's expansion considered contains several

integrals that must be evaluated numerically. In [11] I. J. Kim, Jang, K. T. Kim show that the numerical evaluation of Zhu's formula is cumbersome and suggest a method to approximate the free boundary of the American option pricing problem. This method consists in the numerical solution of the integral equation satisfied by the free boundary deduced in [3] by Little, Pant, Hou. The solution of the American put option pricing problem suggested in [11] combines the integral formula of the option price obtained by I. J. Kim [5] with the approximation of the corresponding free boundary obtained solving numerically the integral equation presented in [3]. Note that in the option price formula contained in [5] there are several integrals that must be evaluated numerically.

To solve the American option pricing problem instead of using hybrid methods it is possible to use only numerical methods. For example the finite differences method (see [12]), the Monte Carlo method (see [13]-[18]), and the regression method (see [19] [20]) can be used to solve the American option pricing problem.

Usually hybrid methods are computationally cheaper than numerical methods. However in many circumstances numerical methods provide approximate solutions of the American option pricing problem that are more accurate than those obtained with hybrid methods. In fact, at least in principle, the solutions provided by numerical methods can be made arbitrarily accurate choosing appropriately the values of the parameters that define the approximation computed. Instead many hybrid methods have a certain accuracy that depends from the problem under consideration and this accuracy cannot be changed choosing parameter values. That is most of the solutions found with hybrid methods do not converge to the exact solution of the American option pricing problem when a suitable limit is taken. Moreover most hybrid methods give satisfactory results when pricing problems with short maturity times are considered. The results obtained with these methods deteriorate when problems with medium or long maturity times are considered.

This paper presents a hybrid method to solve the American option pricing problem. We introduce an auxiliary parameter in the American option pricing problem and we deduce power series expansions in this parameter of the option price and of the corresponding free boundary. Explicit formulae (depending from the free boundary) are given for the coefficients of the option price series. The partial sums of the free boundary series are determined solving numerically nonlinear equations that depend from the time variable as a parameter. These series expansions are a formal solution of the American option pricing problem. Numerical experiments suggest that the series obtained are convergent. The zero-th order term of the series expansions is the Barone-Adesi, Whaley solution of the American option pricing problem [1] (*i.e.* the Barone-Adesi, Whaley formula). The first order approximation of the option price deduced from the expansions developed here has some similarities with the early exercise premium formula suggested by Ju, Zhong [2].

Test problems taken from [1] [2] and [3] are studied. The behaviour of the truncated series expansions on these test problems is studied. In particular in the numerical experiments presented we use the n-th order approximate solutions deduced from the expansions when $n = 0, 1, 2$ to solve the test problems considered. These experiments show that each approximation order of the solution deduced from the expansions adds roughly one correct significant digit to the results obtained. Moreover for $n = 0, 1, \cdots$ the computation of the n-th order approximation deduced from the expansions of the solution of the American option pricing problem on a grid of values of the independent variables is easily parallelizable and its computational cost is "substantially" linear in n as n goes to infinity. In particular the numerical experiments show that when we consider options with intermediate maturity times (*i.e.*: maturity times ranging in the interval 3 - 10 years) the first and the second order approximations of the solution obtained from the series expansions improve substantially the approximate solution obtained using the Barone-Adesi, Whaley formula (see in Section 4, **Table 1**, **Table 3**, **Table 4** and **Figure 2**). For example the improvement obtained with the higher order terms of the expansions is significant when we compare the approximations of the free boundary of the American option pricing problem obtained using the Barone-Adesi, Whaley formula with those obtained using the n-th order truncated power series expansions, $n = 1, 2$ (see Section 4, **Table 1**, **Table 4** and **Figure 2**). Note that the Barone-Adesi, Whaley formula gives excellent results when we consider options with short or with long maturity times and that in these circumstances there is no room for improvements of practical value (see [1]).

The website: http://www.econ.univpm.it/recchioni/finance/w20 contains material including animations, an interactive application and an app that helps the understanding of the paper. More general references to the work of the authors and of their coauthors in mathematical finance are available in the website: http://www.econ.univpm.it/recchioni/finance.

The paper is organized as follows. In Section 2 we formulate the American call option pricing problem in the

Black Scholes framework and we introduce the auxiliary parameter that is used to solve it. In Section 3 we deduce the perturbation expansions in this auxiliary parameter of the American call option price and of the corresponding free boundary. The analysis of Sections 2 and 3 can be easily extended from the case of the American call option pricing problem to the case of the American put option pricing problem. This extension is omitted for simplicity. In Section 4 we present the results obtained with the method developed in Sections 2 and 3 on a set of test problems involving American call and put options. These results are compared with those discussed in the scientific literature obtained with some alternative methods to solve the American option pricing problem.

2. The American Option Pricing Problem in the Black Scholes Framework

We follow Barone-Adesi and Whaley [1] and we consider the problem of pricing American call and put options on commodities in the Black Scholes framework.

Let t be a real variable that denotes time and S_t, $t > 0$, be a real stochastic process that models the commodity price, that is for $t > 0$ the random variable S_t represents the commodity price at time t. We assume that under the risk neutral measure the commodity price satisfies the following stochastic differential equation:

$$\mathrm{d}S_t = bS_t\mathrm{d}t + \sigma S_t\mathrm{d}z_t,\ t > 0, \tag{1}$$

where b, σ are real parameters, z_t, $t > 0$, is the standard Wiener process such that $z_0 = 0$ and $\mathrm{d}z_t$ is its stochastic differential. Equation (1) is known as Black Scholes asset price equation. The parameter $\sigma > 0$ is the volatility or instantaneous standard deviation and b is the cost of carrying parameter. In the most common situations we have $b = r - d$ where $r > 0$ is the risk free interest rate and $d > 0$ is the continuous dividend yield, see [1]. When needed Equation (1) is equipped with an initial condition.

To keep the exposition simple we study only the American call option pricing problem. The American put option pricing problem can be studied analogously. However in the test problems presented in Section 4 the method developed here to solve the American option pricing problem is used to evaluate both call and put options.

Let $t = 0$ be the current time, consider the problem of pricing an American call option having exercise price $E > 0$ and maturity time $T > 0$ written on a commodity whose price S_t, $t > 0$, satisfies (1). The price $V_A(S,t)$, $0 < S < S_f(t)$, $0 < t < T$, of this option and the corresponding free boundary $S_f(t)$, $0 < t < T$, solve the following problem [21]:

$$\frac{\partial V_A}{\partial t} + \frac{\sigma^2}{2}S^2\frac{\partial^2 V_A}{\partial S^2} + bS\frac{\partial V_A}{\partial S} - rV_A = 0,\ 0 < S < S_f(t),\ 0 < t < T, \tag{2}$$

with boundary conditions:

$$V_A(0,t) = 0,\ 0 < t < T, \tag{3}$$

$$V_A(S_f(t),t) = S_f(t) - E,\ 0 < t < T, \tag{4}$$

$$\frac{\partial V_A}{\partial S}(S_f(t),t) = 1,\ 0 < t < T, \tag{5}$$

and final condition:

$$V_A(S,T) = \max(S - E, 0),\ 0 < S < S_f(T). \tag{6}$$

Problem (2), (3), (4), (5), (6) is the American call option pricing problem in the Black Scholes framework. It is a free boundary value problem for the partial differential Equation (2) whose unknowns are: the option price $V_A(S,t)$, $0 < S < S_f(t)$, $0 < t < T$, and the free boundary $S_f(t)$, $0 < t < T$, see [22]. Note that the boundary condition (3) can be omitted. In fact condition (3) follows from the degeneracy in $S = 0$ of (2) and from the fact that in mathematical finance only bounded solutions of (2) are meaningful (see [21] Chapter 3, p. 48-49). However to make easier the understanding of some choices made later (see Section 3) we prefer to state (3) explicitly.

Let us consider the change of variable: $\tau = T - t$, $0 \le t \le T$, the variable τ is called time to maturity, and let us define: $C_A(S,\tau) = V_A(S,T-\tau)$, $0 < S < S^*(\tau)$, $0 \le \tau \le T$, $S^*(\tau) = S_f(T-\tau)$, $0 \le \tau \le T$. Problem (2), (3), (4), (5), (6) rewritten in the variables S, τ for the unknowns C_A, S^* becomes:

$$-\frac{\partial C_A}{\partial \tau}+\frac{\sigma^2}{2}S^2\frac{\partial^2 C_A}{\partial S^2}+bS\frac{\partial C_A}{\partial S}-rC_A=0,\ 0<S<S^*(\tau),\ 0<\tau<T, \tag{7}$$

with boundary conditions:

$$C_A(0,\tau)=0,\ 0<\tau<T, \tag{8}$$

$$C_A\left(S^*(\tau),\tau\right)=S^*(\tau)-E,\ 0<\tau<T, \tag{9}$$

$$\frac{\partial C_A}{\partial S}\left(S^*(\tau),\tau\right)=1,\ 0<\tau<T, \tag{10}$$

and initial condition:

$$C_A(S,0)=\max(S-E,0),\ 0<S<S^*(0). \tag{11}$$

Let $C_E(S,\tau)$, $S>0$, $0<\tau<T$, be the Black Scholes price of the European call option having strike price E, maturity time T and parameters r, b, σ. The price $C_E(S,\tau)$, $S>0$, $0<\tau<T$, has a simple expression given by the Black Scholes formula [21]. Note that C_E is defined for $S>0$, $0<\tau<T$. As done in [1] we seek a solution of problem (7), (8), (9), (10), (11) given by the sum of $C_E(S,\tau)$, $0<S<S^*(\tau)$, $0<\tau<T$, and of a quantity called early exercise premium denoted with $e(S,\tau)$, $0<S<S^*(\tau)$, $0<\tau<T$. That is we assume that:

$$C_A(S,\tau)=C_E(S,\tau)+e(S,\tau),\ 0<S<S^*(\tau),\ 0<\tau<T, \tag{12}$$

Substituting (12) in (7), (8), (9), (10), (11) and using the fact that C_E satisfies the Black Scholes partial differential Equation (7), the boundary condition (8) and the initial condition (11) we obtain the following problem:

$$-\frac{\partial e}{\partial \tau}+\frac{\sigma^2}{2}S^2\frac{\partial^2 e}{\partial S^2}+bS\frac{\partial e}{\partial S}-re=0,\ 0<S<S^*(\tau),\ 0<\tau<T, \tag{13}$$

with boundary conditions:

$$e(0,\tau)=0,\ 0<\tau<T, \tag{14}$$

$$e\left(S^*(\tau),\tau\right)=S^*(\tau)-E-C_E\left(S^*(\tau),\tau\right),\ 0<\tau<T, \tag{15}$$

$$\frac{\partial e}{\partial S}\left(S^*(\tau),\tau\right)=1-\frac{\partial C_E}{\partial S}\left(S^*(\tau),\tau\right),\ 0<\tau<T, \tag{16}$$

and initial condition:

$$e(S,0)=0,\ 0<S<S^*(0). \tag{17}$$

Problem (13), (14), (15), (16), (17) is a free boundary value problem for the partial differential Equation (13) in the unknowns $e(S,\tau)$, $0<S<S^*(\tau)$, $0<\tau<T$, and $S^*(\tau)$, $0<\tau<T$.

We assume that the early exercise premium e has the following form (see [1]):

$$e(S,\tau)=K(\tau)\,f\left(S,K(\tau)\right),\ 0<S<S^*(\tau),\ 0\le\tau\le T, \tag{18}$$

where $K(\tau)$, $0<\tau<T$, is a sufficiently regular function that will be chosen later and $f\left(S,K(\tau)\right)$, $0<S<S^*(\tau)$, $0<\tau<T$, is an auxiliary unknown that must be determined solving (13), (14), (15), (16), (17), (18). Substituting (18) in (13) we have:

$$S^2\frac{\partial^2 f}{\partial S^2}+NS\frac{\partial f}{\partial S}-Mf\left[1+\frac{1}{rK}\frac{\partial K}{\partial \tau}\left(1+\frac{K}{f}\frac{\partial f}{\partial K}\right)\right]=0,\ 0<S<S^*(\tau),\ K=K(\tau),\ 0<\tau<T, \tag{19}$$

where $M=2r/\sigma^2$ and $N=2b/\sigma^2$. Choosing $K(\tau)=1-\mathrm{e}^{-r\tau}$, $0\le\tau\le T$, (see [1]), Equation (19) becomes:

$$S^2\frac{\partial^2 f}{\partial S^2}+NS\frac{\partial f}{\partial S}-\left(\frac{M}{K}\right)f-(1-K)M\frac{\partial f}{\partial K}=0,\ 0<S<S^*(\tau),\ K=K(\tau),\ 0<\tau<T, \tag{20}$$

Equation (18) and the previous choice of K imply that the boundary conditions (14), (15), (16) can be rewritten respectively as:

$$f\left(0,K\left(\tau\right)\right)=0,\ \ 0<\tau<T, \tag{21}$$

$$f\left(S^*\left(\tau\right),K\left(\tau\right)\right)=\left(S^*\left(\tau\right)-E-C_E\left(S^*\left(\tau\right),\tau\right)\right)\frac{1}{K\left(\tau\right)},\ \ 0<\tau<T, \tag{22}$$

$$\frac{\partial f}{\partial S}\left(S^*\left(\tau\right),K\left(\tau\right)\right)=\left(1-\frac{\partial C_E}{\partial S}\left(S^*\left(\tau\right),\tau\right)\right)\frac{1}{K\left(\tau\right)},\ \ 0<\tau<T. \tag{23}$$

Note that in the formulation of problem (20), (21), (22), (23) we use the two variables τ and K, and recall that these two variables are linked by the condition $K=K\left(\tau\right)=1-\mathrm{e}^{-r\tau}$, $0<\tau<T$. Moreover from the choice $K\left(\tau\right)=1-\mathrm{e}^{-r\tau}$, $0\le\tau\le T$, it follows that $K\left(0\right)=0$. This implies that when the function f is well behaved in $\tau=0$ the function e defined in (18) satisfies the initial condition (17).

In [1] Barone-Adesi and Whaley dropped the term $\left(1-K\right)M\left(\partial f/\partial K\right)$ in Equation (20) and solved the problem that remains. This is an ingenious and fruitful idea. In fact after dropping the term $\left(1-K\right)M\left(\partial f/\partial K\right)$ in (20) the problem that remains is easy to solve, see [1], moreover the term dropped tends to zero when τ goes to zero and when τ goes to T and T goes to infinity. Let f_0, S_0^* be the solution of the problem obtained from (20), (21), (22), (23) dropping the term $\left(1-K\right)M\left(\partial f/\partial K\right)$ in (20) determined by Barone-Adesi and Whaley in [1]. The function f_0 has a closed form expression that contains the free boundary $S_0^*\left(\tau\right)$, $0<\tau<T$. The free boundary $S_0^*\left(\tau\right)$ is defined implicitly as solution of the nonlinear Equation (23) when we have $f=f_0$, $0<\tau<T$. The approximation of the free boundary of Barone-Adesi and Whaley [1] is obtained solving numerically the nonlinear equation (23) when $f=f_0$, $0<\tau<T$. Note that the nonlinear Equation (23) that defines S_0^* depends from f_0. The approximate solution of the American option pricing problem given by the functions f_0, S_0^* is called Barone-Adesi, Whaley formula. With abuse of notation in this paper $S_0^*\left(\tau\right)$, $0<\tau<T$, denotes both the Barone-Adesi, Whaley free boundary defined implicitly by the nonlinear equation (23) when $f=f_0$, $0<\tau<T$, and its numerical approximation.

In problem (20), (21), (22), (23) we introduce a real parameter ϵ, $0\le\epsilon\le1$. The parameter ϵ is the auxiliary parameter mentioned in the introduction that is used to solve the American call option pricing problem. That is instead of problem (20), (21), (22), (23) we consider problem:

$$S^2\frac{\partial^2 f_\epsilon}{\partial S^2}+NS\frac{\partial f_\epsilon}{\partial S}-\left(\frac{M}{K}\right)f_\epsilon-\epsilon\left(1-K\right)M\frac{\partial f_\epsilon}{\partial K}=0,\ \ 0<S<S_\epsilon^*\left(\tau\right),\ \ K=K\left(\tau\right),\ \ 0<\tau<T,\ \ 0\le\epsilon\le1, \tag{24}$$

$$f_\epsilon\left(0,K\left(\tau\right)\right)=0,\ \ 0<\tau<T,\ \ 0\le\epsilon\le1, \tag{25}$$

$$f\left(S_\epsilon^*\left(\tau\right),K\left(\tau\right)\right)=\left(S_\epsilon^*\left(\tau\right)-E-C_E\left(S_\epsilon^*\left(\tau\right),\tau\right)\right)\frac{1}{K\left(\tau\right)},\ \ 0<\tau<T,\ \ 0\le\epsilon\le1, \tag{26}$$

$$\frac{\partial f_\epsilon}{\partial S}\left(S_\epsilon^*\left(\tau\right),K\left(\tau\right)\right)=\left(1-\frac{\partial C_E}{\partial S}\left(S_\epsilon^*\left(\tau\right),\tau\right)\right)\frac{1}{K\left(\tau\right)},\ \ 0<\tau<T,\ \ 0\le\epsilon\le1, \tag{27}$$

in the unknowns f_ϵ, S_ϵ^*, $0\le\epsilon\le1$. The initial condition (17) and Equation (18) rewritten for the functions f_ϵ, S_ϵ^* become respectively:

$$e\left(S,0\right)=0,\ \ 0<S<S_\epsilon^*\left(0\right),\ \ 0\le\epsilon\le1, \tag{28}$$

and

$$e\left(S,\tau\right)=K\left(\tau\right)f_\epsilon\left(S,K\left(\tau\right)\right),\ \ 0<S<S_\epsilon^*\left(\tau\right),\ \ 0\le\tau\le T,\ \ 0\le\epsilon\le1. \tag{29}$$

Note that when $\epsilon=1$ Equation (24) reduces to Equation (20), that is when $\epsilon=1$ problem (24), (25), (26), (27), (28), (29) reduces to the American call option pricing problem (20), (21), (22), (23), (17), (18). Moreover when $\epsilon=0$ problem (24), (25), (26), (27) reduces to the problem obtained from (20), (21), (22), (23) dropping the term $\left(1-K\right)M\frac{\partial f_\epsilon}{\partial K}$ in (20), that is when $\epsilon=0$ problem (24), (25), (26), (27) reduces to the problem con-

sidered by Barone-Adesi and Whaley in [1]. Note that the solution determined in [1] of (24), (25), (26), (27) when $\epsilon = 0$ satisfies the conditions (28), (29) with $\epsilon = 0$.

Moreover problem (24), (25), (26), (27), (28), (29) when $\epsilon \to 0^+$ is a singular perturbation problem. In fact when $\epsilon = 0$ in Equation (24) the term containing the higher order derivative with respect to K is multiplied by zero. This fact suggests that when $\epsilon \to 0^+$ an expansion of f_ϵ, S_ϵ^* in powers of ϵ with base point $\epsilon = 0$ cannot hold uniformly in K and S when $0 < K < 1 - \mathrm{e}^{-rT}$, $0 < S < S_\epsilon^*(\tau)$, $0 \le \tau \le T$, due to the presence of a boundary layer in $K = 0$. In singular perturbation theory this kind of problems is approached using the method of matched asymptotic expansions [23]. The matched asymptotic expansion method builds a uniform approximation of the solution of problem (24), (25), (26), (27), (28), (29) when $0 < K < 1 - \mathrm{e}^{-rT}$, $0 < S < S_\epsilon^*(\tau)$, $0 < \tau < T$, and $\epsilon \to 0^+$ matching two series (called inner and outer expansions). Let $O(\cdot)$ be the Landau symbol, roughly speaking in the K variable the inner expansion of the option price holds when $K \in [0, \eta_1]$, $\eta_1 = O(\epsilon)$, $\epsilon \to 0^+$, and the outer expansion of the option price holds when $K > \eta_2$, $\eta_2 = O(\epsilon)$, $\epsilon \to 0^+$, and only the matched expansion holds uniformly in the entire solution domain (see [23] for further details). However it is important to point out that in problem (24), (25), (26), (27), (28), (29) ϵ is not a parameter of the model, ϵ is only an auxiliary parameter added to the model and that in finance only the solution of the previous problem when $\epsilon = 1$ is meaningful. The behaviour of the solution of problem (24), (25), (26), (27), (28), (29) when $\epsilon \to 0^+$ is of no interest in finance. This observation suggests that in the solution of the problem (24), (25), (26), (27), (28), (29) it should be possible to avoid the study of the boundary layer in $K = 0$ that appears when $\epsilon \to 0^+$. That is it should be possible to solve problem (24), (25), (26), (27), (28), (29) when $\epsilon = 1$ with an ad hoc procedure avoiding the matched asymptotic expansions of singular perturbation theory needed to study the problem when $\epsilon \to 0^+$. In fact in Section 3 we build a kind of outer series expansion of the solution of problem (24), (25), (26), (27), (28), (29). More specifically in Section 3 we neglect the initial condition (28) and we impose Equation (24) and the boundary conditions (25), (26), (27) in $\epsilon = 1$ order by order in perturbation theory to a series expansion of the solution of problem (4), (25), (26), (27), (28), (29). This procedure is a straightforward generalization of the procedure followed by Barone-Adesi and Whaley in [1] to solve problem (24), (25), (26), (27), (28), (29) when $\epsilon = 0$.

The zero-th order term of the expansions in powers of ϵ of f_ϵ, S_ϵ^* obtained in Section 3 when $\epsilon = 1$ are the functions f_0, S_0^* determined by Barone-Adesi and Whaley in [1]. Moreover the expansions developed in Section 3 rewritten in the variables S, τ evaluated in $\epsilon = 1$ and (29) are a formal series expansion of the solution of the American option pricing problem (13), (14), (15), (16), (17).

Let us recall that in [24] a similar approach has been used in the study of barrier options. In fact in [24] it is considered the problem of pricing (put up-and-out) barrier options with time-dependent parameters in the Black Scholes framework. An auxiliary parameter is introduced in the barrier option pricing problem and a perturbation expansion in this parameter of the barrier option price is deduced. Note that the perturbation problem studied in [24] is a regular perturbation problem, while the perturbation problem considered here when $\epsilon \to 0^+$ is a singular perturbation problem.

3. A Series Expansion of the Solution of the American Option Pricing Problem

Let us drop the initial condition (28) from problem (24), (25), (26), (27), (28), (29). That is let us consider the equation:

$$S^2 \frac{\partial^2 f_\epsilon}{\partial S^2} + NS \frac{\partial f_\epsilon}{\partial S} - \left(\frac{M}{K}\right) f_\epsilon = \epsilon (1 - K) M \frac{\partial f_\epsilon}{\partial K}, \quad 0 < S < S_\epsilon^*(\tau), \quad K = K(\tau), \quad 0 < \tau < T, \quad 0 \le \epsilon \le 1, \tag{30}$$

with the boundary conditions:

$$f_\epsilon\left(0, K(\tau)\right) = 0, \quad 0 < \tau < T, \quad 0 \le \epsilon \le 1, \tag{31}$$

$$f_\epsilon\left(S_\epsilon^*(\tau), K(\tau)\right) = \left(S_\epsilon^*(\tau) - E - C_E\left(S_\epsilon^*(\tau), \tau\right)\right) \frac{1}{K(\tau)}, \quad 0 < \tau < T, \quad 0 \le \epsilon \le 1, \tag{32}$$

$$\frac{\partial f_\epsilon}{\partial S}\left(S_\epsilon^*(\tau), K(\tau)\right) = \left(1 - \frac{\partial C_E}{\partial S}\left(S_\epsilon^*(\tau), \tau\right)\right) \frac{1}{K(\tau)}, \quad 0 < \tau < T, \quad 0 \le \epsilon \le 1. \tag{33}$$

Recall that once determined f_ϵ, S_ϵ^* as solution of (30), (31), (32), (33) we will recover the function e using (29) and that when f_ϵ is well behaved in $\tau = 0$ the function e determined in this way will satisfy the initial condition (28) as a consequence of the choice $K(\tau) = 1 - \mathrm{e}^{-r\tau}$, $0 < \tau < T$, that implies $K(0) = 0$. Let us assume that the following expansions in powers of ϵ of the functions f_ϵ, S_ϵ^*, $0 \le \epsilon \le 1$, hold:

$$f_\epsilon\left(S, K(\tau)\right) = \sum_{j=0}^{+\infty} \epsilon^j \hat{f}_j\left(S, K(\tau)\right),\ 0 < S < S_\epsilon^*(\tau),\ 0 \le \tau \le T,\ 0 \le \epsilon \le 1, \tag{34}$$

$$S_\epsilon^*(\tau) = \sum_{j=0}^{+\infty} \epsilon^j \hat{S}_j^*(\tau),\ 0 \le \tau \le T,\ 0 \le \epsilon \le 1, \tag{35}$$

where the functions $\hat{f}_j$, $\hat{S}_j^*$, $j = 0,1,\cdots$ are independent of ϵ.

For later convenience we define the partial sums $b_{n,\epsilon}$, $S_{n,\epsilon}^*$, $0 \le \epsilon \le 1$, $n = 0,1,\cdots$, of the series (34), (35), that is:

$$b_{n,\epsilon}(S,\tau) = \sum_{j=0}^{n} \epsilon^j \hat{f}_j\left(S, K(\tau)\right),\ 0 < S < S_{n,\epsilon}^*(\tau),\ 0 \le \tau \le T,\ 0 \le \epsilon \le 1,\ n = 0,1,\cdots, \tag{36}$$

$$S_{n,\epsilon}^*(\tau) = \sum_{j=0}^{n} \epsilon^j \hat{S}_j^*(\tau),\ 0 \le \tau \le T,\ 0 \le \epsilon \le 1,\ n = 0,1,\cdots. \tag{37}$$

Note that for $j = 0,1,\cdots$ the problems that follow define the function $\hat{f}_j$ for $0 < S < S_{j,\epsilon=1}^*(\tau)$, $0 < \tau < T$. To give a meaning to the sums contained in (34) and (36) we extend with zero the function $\hat{f}_j$ when $S > S_{j,\epsilon=1}^*(\tau)$, $0 < \tau < T$, $j = 0,1,\cdots$. With abuse of notation $\hat{f}_j$ denotes both the original function and the extended function $j = 0,1,\cdots$.

We impose (30), (31), (32), (33) to the series expansions (34), (35), order by order in powers of ϵ. For n = 0, 1, ⋯ the unknowns of the n-th order problem are the functions $\hat{f}_n$, $S_{n,\epsilon=1}^*$. Note that as unknown of the n-th order problem, we use $S_{n,\epsilon=1}^*$ instead of $\hat{S}_n^*$, n = 0, 1, ⋯. This is due to the fact that since we are interested only in the solution of problem (30), (31), (32), (33) when $\epsilon = 1$ we impose the boundary conditions (32), (33) in $\epsilon = 1$ instead of imposing them in $\epsilon = 0$. This is what has been done by Barone-Adesi and Whaley [1] in the solution of the zero-th order problem. We simply extend the idea of Barone-Adesi and Whaley from the zero-th order problem to the n-th order problem, n = 1, 2, ⋯. Proceeding in this way we obtain:

For n = 0 the zero-th order problem is:

$$S^2 \frac{\partial^2 \hat{f}_0}{\partial S^2} + NS \frac{\partial \hat{f}_0}{\partial S} - \left(\frac{M}{K}\right)\hat{f}_0 = 0,\ 0 < S < S_{0,\epsilon=1}^*(\tau),\ K = K(\tau),\ 0 < \tau < T, \tag{38}$$

with boundary conditions:

$$\hat{f}_0\left(0, K(\tau)\right) = 0,\ 0 < \tau < T, \tag{39}$$

$$\hat{f}_0\left(S_{0,\epsilon=1}^*(\tau), K(\tau)\right) = \left(S_{0,\epsilon=1}^*(\tau) - E - C_E\left(S_{0,\epsilon=1}^*(\tau), \tau\right)\right)\frac{1}{K(\tau)},\ 0 < \tau < T, \tag{40}$$

$$\frac{\partial \hat{f}_0}{\partial S}\left(S_{0,\epsilon=1}^*(\tau), K(\tau)\right) = \left(1 - \frac{\partial C_E}{\partial S}\left(S_{0,\epsilon=1}^*(\tau), \tau\right)\right)\frac{1}{K(\tau)},\ 0 < \tau < T, \tag{41}$$

for n = 1, 2, ⋯ the n-th order problem is:

$$S^2 \frac{\partial^2 \hat{f}_n}{\partial S^2} + NS \frac{\partial \hat{f}_n}{\partial S} - \frac{M}{K}\hat{f}_n - (1-K)M \frac{\partial \hat{f}_{n-1}}{\partial K} = 0,\ 0 < S < S_{n,\epsilon=1}^*(\tau),\ K = K(\tau),\ 0 < \tau < T, \tag{42}$$

with boundary conditions:

$$\hat{f}_n\left(0, K(\tau)\right) = 0,\ 0 < \tau < T, \tag{43}$$

$$\hat{f}_n\left(S_{n,\epsilon=1}^*(\tau), K(\tau)\right) = \left(S_{n,\epsilon=1}^*(\tau) - E - C_E\left(S_{n,\epsilon=1}^*(\tau), \tau\right)\right)\frac{1}{K(\tau)} - b_{n-1,\epsilon=1}\left(S_{n,\epsilon=1}^*(\tau), \tau\right)\frac{1}{K(\tau)},\ 0 < \tau < T, \tag{44}$$

$$\frac{\partial \hat{f}_n}{\partial S}\left(S^*_{n,\epsilon=1}(\tau),K(\tau)\right)=\left(1-\frac{\partial C_E}{\partial S}\left(S^*_{n,\epsilon=1}(\tau),\tau\right)-\frac{\partial b_{n-1,\epsilon=1}}{\partial S}\left(S^*_{n,\epsilon=1}(\tau),\tau\right)\right)\frac{1}{K(\tau)},\ 0<\tau<T. \tag{45}$$

The problems (38), (39), (40), (41) and (42), (43), (44), (45) are respectively free boundary value problems for the ordinary differential Equations (38) and (42). These problems depend from the parameter τ, $0<\tau<T$. The boundary conditions (40), (41) and (44), (45) are the boundary conditions imposed in $\epsilon=1$ derived from (32), (33). Note that we have: $f_0=\hat{f}_0$, $S_0^*=\hat{S}_0^*=S^*_{0,\epsilon=1}$ where f_0, S_0^* is the Barone-Adesi, Whaley solution of the American option pricing problem deduced in [1]. Numerical experiments have shown that the approximations of the first few orders of f and S^* deduced from the series expansions (34), (35) with the boundary conditions (40), (41) and (44), (45) imposed to the partial sums (37) evaluated in $\epsilon=1$ are of higher quality than the corresponding approximations of the same order in ϵ obtained imposing the boundary conditions (32), (33) order by order in powers of ϵ in $\epsilon=0$. In particular these numerical experiments show that the approximations of $S^*_{n,\epsilon=1}$, $n=1,2$, obtained solving problem (42), (43), (44), (45) are more accurate than the corresponding approximations obtained evaluating in $\epsilon=1$ the partial sums $\sum_{i=0}^{n}\epsilon^i\hat{S}_i^*$, $0\le\epsilon\le1$, $n=1,2$, where $\hat{S}_i^*$, $i=1,2$ are the terms obtained imposing in $\epsilon=0$ the boundary conditions (32), (33) at the first and at the second order in powers of ϵ.

Let us consider the zero-th order problem (38), (39), (40), (41).

From now on instead of using the notation $\hat{f}_0$, $S^*_{0,\epsilon=1}$ introduced previously we denote the solution of the zero-th order problem (38), (39), (40), (41) with the notation f_0, S_0^*. This choice emphasizes the fact that the zero-th order term of the expansions (34), (35) determined solving the previous problems is the Barone-Adesi, Whaley solution of the American option pricing problem. As done in [1] we seek a solution f_0 of (38), (39), (40), (41) of the following form:

$$f_0\left(S,K(\tau)\right)=A_{0,0}\left(K(\tau)\right)S^{q(K(\tau))},\ 0<S<S_0^*(\tau),\ 0\le\tau\le T, \tag{46}$$

where in (46) the functions $A_{0,0}$ and q are auxiliary unknowns that must be determined. Substituting (46) in (38) we have:

$$A_{0,0}\left(K(\tau)\right)(S)^{q(K(\tau))}\left(q\left(K(\tau)\right)^2+(N-1)q\left(K(\tau)\right)-\frac{M}{K(\tau)}\right)=0,\ 0<S<S_0^*(\tau),\ 0\le\tau\le T. \tag{47}$$

Equation (47) is satisfied if we impose that:

$$q^2\left(K(\tau)\right)+(N-1)q\left(K(\tau)\right)-\frac{M}{K(\tau)}=0,\ 0<\tau<T, \tag{48}$$

the quadratic Equation (48) in the unknown q is easily solved, and one of its solutions is:

$$q\left(K(\tau)\right)=\frac{1}{2}\left(1-N+\sqrt{(N-1)^2+4M/K(\tau)}\right),\ 0<\tau<T. \tag{49}$$

From (49) it follows that $q(K)$ is positive when K is positive. This means that when $q(k)$ is given by (49) the function $f_0\left(S,K(\tau)\right)$, $0<S<S_0^*(\tau)$, $0<\tau<T$, given by (46) satisfies (39). The second solution of (48) is negative when K is positive and must be discarded since the corresponding function f_0 given by (46) does not satisfy (39).

Substituting the formulae (46), (49) in the Equations (40), (41) we obtain respectively:

$$A_{0,0}\left(K(\tau)\right)=S_0^*(\tau)^{\left(1-q(K(\tau))\right)}\left(1-\frac{\partial C_E}{\partial S}\left(S_0^*(\tau),\tau\right)\right)\frac{1}{K(\tau)q\left(K(\tau)\right)},\ 0<\tau<T, \tag{50}$$

and

$$\left(q\left(K(\tau)\right)-1\right)S_0^*(\tau)=q\left(K(\tau)\right)\left(E+C_E\left(S_0^*(\tau),\tau\right)\right)-S_0^*\frac{\partial C_E}{\partial S}\left(S_0^*(\tau),\tau\right),\ 0<\tau<T. \tag{51}$$

For $0<\tau<T$ Equation (50) defines $A_{0,0}$ as a function of $S_0^*(\tau)$ and Equation (51) is a nonlinear equation in the unknown $S_0^*(\tau)$ that depends from the parameter τ. Given τ this last equation is easily trans-

formed in a fixed point problem and solved numerically using Banach iteration, $0 \le \tau \le T$. The approximate solution of (51) determined in this way is substituted in (50) to obtain $A_{0,0}$. The zero-th order term f_0 given by (46), (49), (50) with the numerical approximation of S_0^* substituted in $A_{0,0}$ multiplied by K (see (18)) is the Baroni-Adesi, Whaley formula of the early exercise premium (see [1] formula (20)). The numerical approximation of S_0^* obtained solving numerically (51) is the Barone-Adesi, Whaley approximation of the free boundary (see [1], formula (19)). Note that as already said with abuse of notation in the previous formulae $S_0^*(\tau)$, $0 < \tau < T$, denotes both the unknown of the nonlinear Equation (51) and its numerical approximation. This ambiguity is reflected in the functions $A_{0,0}$ and f_0.

Let $n = 1, 2, \cdots$ we seek a solution $\hat{f}_n$ of the n-th order problem (42), (43), (44), (45) of the following form:

$$\hat{f}_n\left(S, K(\tau)\right) = \left(A_{n,0}\left(K(\tau)\right) + \sum_{j=1}^{2n} A_{n,j}\left(K(\tau)\right)\left(\ln S\right)^j \right) S^{q(K(\tau))}, \quad 0 < S < S^*_{n,\epsilon=1}(\tau), \quad 0 \le \tau \le T, \quad n = 1, 2, \cdots, \tag{52}$$

where the functions $A_{j,n}$, $j = 0, 1, \cdots, 2n$, $n = 1, 2, \cdots$, are auxiliary unknowns that must be determined imposing (42), (43), (44), (45). Substituting formula (52) in Equation (42) it is easy to see that in order to satisfy (42) it is sufficient to impose that the functions $A_{n,j}$, $j = 1, 2, \cdots, 2n$, $n = 1, 2, \cdots$, satisfy the following systems of linear equations:

$$2n\left(2q - 1 + N\right) A_{n,2n} = \left(1 - K\right) M \frac{\partial q}{\partial K} A_{n-1,2(n-1)}, \quad n = 1, 2, \cdots, \tag{53}$$

$$\left(2q - 1 + N\right) j A_{n,j} + j\left(j+1\right) A_{n,j+1} = \left(1 - K\right) M \left(\frac{\partial q}{\partial K} A_{n-1,j-2} + \frac{\partial A_{n-1,j-1}}{\partial K} \right), \quad j = 2, 3, \cdots, 2n-1, \quad n = 1, 2, \cdots, \tag{54}$$

$$\left(2q - 1 + N\right) A_{n,1} + 2A_{n,2} = \left(1 - K\right) M \frac{\partial A_{n-1,0}}{\partial K}, \quad n = 1, 2, \cdots. \tag{55}$$

To keep the notation simple in (53), (54), (55) we have omitted the dependence from K of the functions $A_{n,j}$, $j = 1, 2, \cdots, 2n$, $n = 1, 2, \cdots$. For $n = 1, 2, \cdots$ the unknowns $A_{n,j}$, $j = 1, 2, \cdots, 2n$, are determined solving the n-th linear system of linear equations contained in (53), (54), (55). In fact for $n = 1, 2, \cdots$ the n-th system of linear equations contained in (53), (54), (55) is a system of $2n$ linear equations in the $2n$ unknowns $A_{n,j}$, $j = 1, 2, \cdots, 2n$, that can be solved by backward substitution starting from the n-th Equation (53). Note that due to its special form the computational cost of solving these linear systems obtained in (53), (54), (55) grows linearly in n when n goes to infinity. Finally for $n = 1, 2, \cdots$ the coefficient $A_{n,0}$ and the unknown $S^*_{n,\epsilon=1}$ are determined imposing the boundary conditions (44), (45), that is imposing respectively:

$$\begin{aligned} A_{n,0}(K) = {} & \frac{1}{Kq(K)} \frac{1}{\left(S^*_{n,\epsilon=1}\right)^{q-1}} \left(1 - \frac{\partial C_E}{\partial S}\left(S^*_{n,\epsilon=1}, \tau\right) - \frac{\partial b_{n-1,\epsilon=1}}{\partial S}\left(S^*_{n,\epsilon=1}, \tau\right) \right) - \sum_{j=1}^{2n} A_{n,j} \left(\ln S^*_{n,\not=1}\right)^j \\ & - \frac{1}{q(K)} \sum_{j=1}^{2n} j A_{n,j} \left(\ln S^*_{n,\not=1}\right)^{j-1}, \quad 0 < \tau < T, \quad n = 1, 2, \cdots, \end{aligned} \tag{56}$$

and

$$\begin{aligned} \left(1 - \frac{1}{q(K)}\right) S^*_{n,\epsilon=1} = {} & E + C_E\left(S^*_{n,\epsilon=1}, \tau\right) + b_{n-1,\epsilon=1}\left(S^*_{n,\epsilon=1}, \tau\right) + \frac{S^*_{n,\epsilon=1}}{q(K)} \left(- \frac{\partial C_E}{\partial S}\left(S^*_{n,\epsilon=1}, \tau\right) - \frac{\partial b_{n-1,\epsilon=1}}{\partial S}\left(S^*_{n,\epsilon=1}, \tau\right) \right) \\ & - \frac{\left(S^*_{n,\epsilon=1}\right)^q K}{q(K)} \sum_{j=1}^{2n} j A_{n,j} \left(\ln S^*_{n,\not=1}\right)^{j-1}, \quad 0 < \tau < T, \quad n = 1, 2, \cdots. \end{aligned} \tag{57}$$

To keep the notation simple in (56), (57) we have omitted the dependence from τ of $S_{n,\epsilon=1}$, $n = 1, 2, \cdots$. For $n = 1, 2, \cdots$ Equation (56) defines $A_{n,0}$ as a function of $S^*_{n,\epsilon=1}$ and of the solution of the n-th linear system contained in (53), (54), (55), $0 < \tau < T$. Equation (57) is a nonlinear equation in the unknown $S^*_{n,\epsilon=1}(\tau)$, $0 < \tau < T$, depending from the parameter τ, that defines implicitly $S^*_{n,\epsilon=1}(\tau)$, $0 < \tau < T$, $n = 1, 2, \cdots$. In the numerical experiments of Section 4 this equation is transformed in a fixed point problem and solved numerically using Banach iteration. The numerical approximation of $S^*_{n,\epsilon=1}(\tau)$, $n = 1, 2, \cdots$, obtained from the solution of

(57) is substituted in (56) and together with the solution of the *n*-th linear system contained in (53), (54), (55) determines (56). Note that when $n=1,2,\cdots$, for simplicity with abuse of notation we denote with $S^*_{n,\epsilon=1}(\tau)$, $0<\tau<T$, both the unknown of (57) and its numerical approximation.

A careful inspection of formulae (46), (51) and (52), (57) shows that for $n=0,1,\cdots$ the numerical evaluation on a grid of values of the *S* and τ variables of the *n*-th order approximations $\hat{f}_n$, $S^*_{n,\epsilon=1}$ of the solution of the American call option pricing problem is easily parallelized.

4. Numerical Results

Let us discuss the numerical results obtained on a set of test problems with the solution method of the American option pricing problem developed in Sections 2 and 3.

We use the trinomial tree method [17] with n_T = 1000 time steps to compute the "true value" of the option prices considered in our experiments. The choice n_T = 1000 guarantees four correct significant digits in the option prices computed in this Section. The "true value" of the corresponding free boundaries of the American call options considered in our experiments is computed solving numerically the following integral equation (see [25], [3] and the reference therein):

$$\begin{aligned} S^*(\tau) = {} & E + S^*(\tau)\mathrm{e}^{-(r-b)\tau}N\left(d\left(S^*(\tau),\tau\right)\right) - E\mathrm{e}^{-r\tau}N\left(d\left(S^*(\tau),\tau\right)-\sigma\sqrt{\tau}\right) \\ & + \int_0^\tau (r-b)S^*(\tau)\mathrm{e}^{-(r-b)\xi}N\left(d_\xi\left(S^*(\tau),S^*(\tau-\xi)\right)\right) - rE\mathrm{e}^{-r\xi}N\left(d_\xi\left(S^*(\tau),S^*(\tau-\xi)\right)-\sigma\sqrt{\xi}\right)\mathrm{d}\xi, \quad (58) \\ & 0<\tau\le T. \end{aligned}$$

The free boundary $S^*(\tau)$, $0<\tau<T$, is the unknown of the integral Equation (58), moreover in (58) the function $\mathcal{N}(x)=\frac{1}{\sqrt{2\pi}}\int_{-\infty}^{x}\mathrm{e}^{-u^2/2}\mathrm{d}u$ is the standard normal cumulative distribution and the functions *d* and d_ξ are given by:

$$d\left(S^*(\tau),\tau\right)=\frac{1}{\sigma\sqrt{\tau}}\ln\left(\frac{S^*(\tau)}{E}\right)+\left(\frac{b}{\sigma}-\frac{\sigma}{2}\right)\sqrt{2\tau},\ 0<\tau\le T,\ \sigma>0, \quad (59)$$

$$d_\xi\left(S^*(\tau),S^*(\tau-\xi)\right)=\frac{1}{\sigma\sqrt{\xi}}\ln\left(\frac{S^*(\tau)}{S^*(\tau-\xi)}\right)+\left(\frac{b}{\sigma}-\frac{\sigma}{2}\right)\sqrt{2\xi},\ 0<\tau\le T,\ \sigma>0, \quad (60)$$

where in (58), (59), (60) *T* is the maturity time and *E* is the strike price of the American call option considered. The integral operator contained in (58) is approximated with the composite rectangular rule with time step $\Delta\tau>0$ and $S^*(\tau)$, $0<\tau<T$, is approximated on the set of evenly spaced nodes of step $\Delta\tau>0$ used to discretize the integral operator. This discretized version of the integral Equation (58) is solved as a fixed point problem using Banach iteration. Let $\lfloor\ \rfloor$ denote the integer part of ·, for $\Delta\tau>0$ let $\tau_\nu=\nu\Delta\tau$ and $S^a_{\Delta\tau}(\tau_\nu)$ be the solution of the discretized version of the integral Equation (58) at the node τ_ν, $\nu=1,2,\cdots,\lfloor T/\Delta\tau\rfloor$. For $0<\tau<T$ let $S^*(\tau)$ be the solution of (58) it is easy to see that we have: $\lim_{\Delta\tau\to0}\lim_{\nu\to+\infty}S^a_{\Delta\tau}(\nu\Delta\tau)=S^*(\tau)$, when $\tau=\nu\Delta\tau$ is fixed. When we consider an American call option and we have $b<r$ the algorithm that solves the discretized version of (58) starts from $\tau=0$ choosing $S^a_{\Delta\tau}(0)=S^*(0)=E$ when $0<r\le r-b$ or choosing $S^a_{\Delta\tau}(0)=S^*(0)=rE/(r-b)$ when $r>r-b$. Recall that when $b\ge r$ (*i.e.* when the continuous dividend yield *d* is smaller or equal to zero) in [1] page 307 it is shown that the American call option price reduces to the corresponding European call option price. In fact in this case the free boundary is "at infinity" and the American call option must be exercised at maturity time, that is the value of the early exercise premium is identically zero.

The integral Equation (58) must be modified to deal with American put options (see [3]). Moreover in the case of put options the algorithm that solves the corresponding discretized integral equation starts from $\tau=0$ choosing $S^a_{\Delta\tau}(0)=S^*(0)=E$ when $r\le r-b$ or choosing $S^a_{\Delta\tau}(0)=S^*(0)=rE/(r-b)$ when $r>r-b$.

In the numerical experiments discussed below the discretized versions of Equation (58) for call options and of the analogous equation for put options (see [3]) are solved iteratively at the points $\tau=\tau_\nu=\nu\Delta\tau$, $\nu=1,2,\cdots,m$, when $m=\lfloor T/\Delta\tau\rfloor$ and $\Delta\tau=0.001$. That is we consider the unknowns $S^a_{\nu,\Delta\tau}=S^a_{\Delta\tau}(\tau_\nu)$, $\nu=1,2,\cdots,m$,

implicitly defined as solution of the following set of equations (see [25] for further details):

$$S^a_{\nu,\Delta\tau} = F\left(S^a_{\nu,\Delta\tau}\right),\ \nu = 1,2,\cdots,m, \tag{61}$$

where in the case of call options from Equation (58) we have:

$$\begin{aligned} F\left(S^a_{\nu,\Delta\tau}\right) &= E + S^a_{\nu,\Delta\tau}\mathrm{e}^{-(r-b)\nu\Delta\tau}N\left(d\left(S^a_{\nu,\Delta\tau},\nu\Delta\tau\right)\right) - E\mathrm{e}^{-r\nu\Delta\tau}N\left(d\left(S^a_{\nu,\Delta\tau},\nu\Delta\tau\right) - \sigma\sqrt{\nu\Delta\tau}\right) \\ &+ \Delta\tau\sum_{i=0}^{\nu-1}\left[(r-b)S^a_{\nu,\Delta\tau}\mathrm{e}^{-(r-b)i\Delta\tau}N\left(d_{i\Delta\tau}\left(S^a_{\nu,\Delta\tau},S^a_{(\nu-i),\Delta\tau}\right)\right) - rE\mathrm{e}^{-ri\Delta\tau}N\left(d_{i\Delta\tau}\left(S^a_{\nu,\Delta\tau},S^a_{\nu-i,\Delta\tau}\right) - \sigma\sqrt{i\Delta\tau}\right)\right], \\ &\nu = 1,2,\cdots,m, \end{aligned} \tag{62}$$

and $S^a_{0,\Delta\tau}$ is assigned as specified above. Of course when we consider put options Equation (58) must be substituted with a different integral equation, see [3], and as a consequence Equation (62) must be modified coherently. Equations (61), (62) (and their analogous for put options) are solved using Banach iteration. For $\nu = 1,2,\cdots,m$ and $j = 0,1,\cdots$ let $S^{a,j}_{\nu,\Delta\tau}$ be the *j*-th element of the sequence generated by Banach iteration applied to (61), (62), $\nu = 1,2,\cdots,m$. The Banach iteration associated to (61) is stopped at the smallest value of the index *j* that satisfies the condition:

$$\frac{\left|S^{a,j+1}_{\nu,\Delta\tau} - F\left(S^{a,j}_{\nu,\Delta\tau}\right)\right|}{E} < 0.001,\ \nu = 1,2,\cdots,m. \tag{63}$$

Note that in general the stopping value of the index *j* defined by (63) depends from ν, $\nu = 1,2,\cdots,m$. The "true values" of the option prices and of the corresponding free boundaries defined previously are used as benchmarks to test the approximate solutions of the American option pricing problem computed with the method developed in Sections 2 and 3 and with some alternative methods taken from the scientific literature.

We begin our numerical experiments studying some test problems taken from [1] Section C.4. These test problems consider options on long-term U.S. Treasury bonds (time to maturity up to three years) and long term care insurance inflation options (time to maturity up to ten years and beyond).

In the first experiment we use the values of the Black Scholes parameters of Table V in [1]. That is we consider the following three sets of parameter values: $r = 0.08$, $\sigma = 0.2$, and $b = -0.04$, or $b = 0.0$ or $b = 0.04$. For each set of Black Scholes parameters we consider three call options with strike price $E = 100$ and maturity time $T = 3$, or $T = 5$, or $T = 10$. The maturity time *T* is expressed in years.

Table 1 shows several free boundary approximations of the American call option pricing problems specified above when $\tau = T = 3$, 5, 10. From left to right **Table 1** shows the free boundary $S^*(T)$ computed solving iteratively the discretized version of the integral Equation (58) (*i.e.* $S^*(T)$ is the "true free boundary" used as benchmark) and the approximations $S^*_{n,\epsilon=1}(T)$, when $n = 0,1,2$, discussed in Sections 2 and 3. Recall that $S^*_{0,\epsilon=1} = S^*_0$ is the Barone-Adesi Whaley approximation of the free boundary. **Table 1** shows that for $n = 0,1$ going from the *n*-th order approximation to $(n+1)$-th order approximation of the free boundary roughly adds one correct significant digit to the approximation of the free boundary found. This effect is particularly evident when $b > 0$, in fact in this case the Barone-Adesi, Whaley approximation of the free boundary is poor and has no correct significant digits. Note that positive values of *b* correspond to values of the continuous dividend yield $d = r - b$ smaller than the risk free interest rate *r*. Recall that for American call options when $b > 0$ and $r - b > 0$ the integral Equation (58) becomes singular as $\tau \to 0^+$, see [25].

When $\tau = T$ (*i.e.* when $t = 0$) **Table 2** shows the asset price *S*, the European call option price C_E obtained evaluating the Black Scholes formula, the approximations of the American call option price obtained using the trinomial tree method C_T (*i.e.* C_T is the "true value" of the option price used as benchmark), the Barone-Adesi, Whaley option price C_{BW} obtained from (12), (18) when $f = f_0$, $S^* = S^*_0$ and the *n*-th order approximation $C_{A,n,\epsilon=1}$, derived from (12), (18) and the series expansions presented in Sections 2 and 3 truncated after $n+1$ terms, $n = 1,2$. Furthermore **Table 2** shows the relative errors: $re_{\mathrm{BW}}(S,T) = \left|C_{\mathrm{BW}}(S,T) - C_T(S,T)\right| / C_T(S,T)$ and $re^C_{n,\epsilon=1}(S,T) = \left|C_{A,n,\epsilon=1}(S,T) - C_T(S,T)\right| / C_T(S,T)$, $n = 1,2$.

Table 1 and **Table 2** suggest that increasing the approximation order of the solution of the American call option pricing problem that has been deduced from the expansions in powers of ϵ developed in Sections 2 and 3 (that is increasing *n*) it is possible to improve substantially the results obtained with the Barone-Adesi, Whaley

formula (*i.e.* the result obtained when $n = 0$).

Figure 1 shows the "true" free boundaries of the American call option pricing problem as a function of τ that have been obtained solving numerically the discretized version of the integral Equation (58) when E = 100,

Table 1. Approximations of the free boundary of an American call option with intermediate maturity T and strike price E = 100.

$r = 0.08$, $\sigma = 0.2$, $b = -0.04$				
T	$S^*(T)$	$S^*_{0,\epsilon=1}(T)$	$S^*_{1,\epsilon=1}(T)$	$S^*_{2,\epsilon=1}(T)$
3	129.065	128.588	129.036	128.951
5	131.064	130.701	131.154	130.973
10	132.687	132.207	132.862	132.705
$r = 0.08$, $\sigma = 0.2$, $b = 0.00$				
T	$S^*(T)$	$S^*_{0,\epsilon=1}(T)$	$S^*_{1,\epsilon=1}(T)$	$S^*_{2,\epsilon=1}(T)$
3	149.676	150.206	149.017	149.617
5	155.051	156.917	154.473	154.823
10	160.505	164.206	160.463	160.129
$r = 0.08$, $\sigma = 0.2$, $b = 0.04$				
T	$S^*(T)$	$S^*_{0,\epsilon=1}(T)$	$S^*_{1,\epsilon=1}(T)$	$S^*_{2,\epsilon=1}(T)$
3	241.191	255.316	236.006	242.394
5	251.915	273.499	246.402	252.762
10	265.960	304.187	260.422	265.212

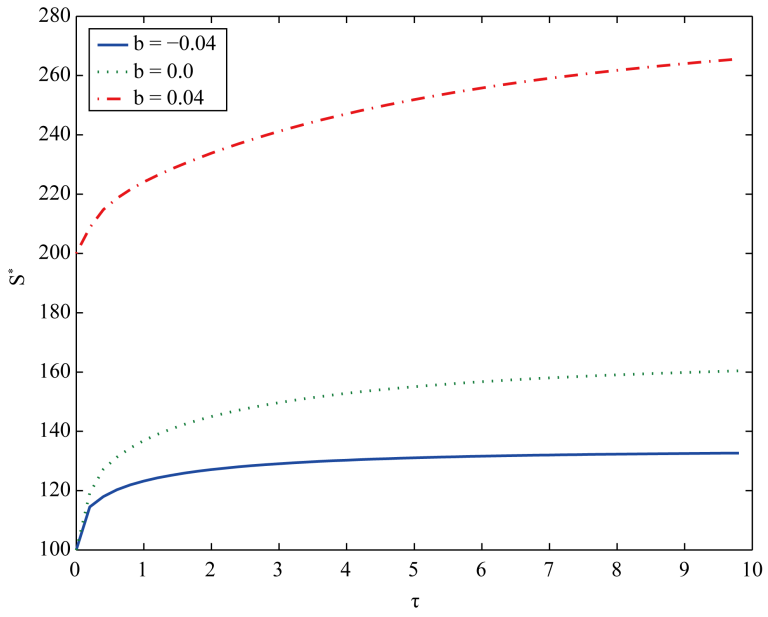

Figure 1. American call option "true" free boundary S^* as a function of the time to maturity τ when E = 100, T = 10, r = 0.08, σ = 0.2 and b = −0.04 (solid line $S^*(0) = E$, $r \le r - b$), b = 0.0 (dotted line $S^*(0) = E$, $r \le r - b$), b = 0.04 (dash-dotted line $S^*(0) = rE/(r-b)$, $r > r - b$).

Table 2. Approximations of the price of an American call option with intermediate maturity T, strike price E = 100 and negative cost of carrying.

$r=0.08$, $\sigma=0.2$, $b=-0.04$								
maturity $T=3$								
S	$C_E(S,T)$	$C_T(S,T)$	$C_{BW}(S,T)$	$C_{A,1,\epsilon=1}(S,T)$	$C_{A,2,\epsilon=1}(S,T)$	$re^C_{BW}(S,T)$	$re^C_{1,\epsilon=1}(S,T)$	$re^C_{2,\epsilon=1}(S,T)$
70	0.8211	0.9587	1.0861	0.9258	0.9617	1.33×10^{-1}	3.38×10^{-2}	3.58×10^{-3}
80	1.9285	2.3414	2.5258	2.3068	2.3334	7.87×10^{-2}	1.47×10^{-2}	3.41×10^{-3}
90	3.7480	4.7585	4.9706	4.7193	4.7336	4.45×10^{-2}	8.24×10^{-3}	5.23×10^{-3}
100	6.3571	8.4921	8.6777	8.4453	8.4504	2.18×10^{-2}	5.49×10^{-3}	4.91×10^{-3}
110	9.7526	13.792	13.896	13.746	13.748	7.52×10^{-3}	3.34×10^{-3}	3.18×10^{-3}
120	13.872	20.886	20.906	20.878	20.882	1.04×10^{-3}	2.88×10^{-4}	1.11×10^{-4}
maturity $T=5$								
S	$C_E(S,T)$	$C_T(S,T)$	$C_{BW}(S,T)$	$C_{A,1,\epsilon=1}(S,T)$	$C_{A,2,\epsilon=1}(S,T)$	$re^C_{BW}(S,T)$	$re^C_{1,\epsilon=1}(S,T)$	$re^C_{2,\epsilon=1}(S,T)$
70	1.1410	1.5349	1.7261	1.5612	1.4912	1.24×10^{-1}	1.71×10^{-2}	2.84×10^{-2}
80	2.2026	3.1467	3.3887	3.1927	3.1021	7.68×10^{-2}	1.46×10^{-2}	1.14×10^{-2}
90	3.7323	5.6921	5.9446	5.7503	5.6506	4.43×10^{-2}	1.02×10^{-2}	7.28×10^{-3}
100	5.7491	9.4043	9.6129	9.4629	9.3695	2.21×10^{-2}	6.22×10^{-3}	3.70×10^{-3}
110	8.2416	14.523	14.640	14.570	14.498	8.05×10^{-3}	3.27×10^{-3}	1.71×10^{-3}
120	11.178	21.302	21.319	21.330	21.288	8.13×10^{-4}	1.32×10^{-3}	6.15×10^{-4}
maturity $T=10$								
S	$C_E(S,T)$	$C_T(S,T)$	$C_{BW}(S,T)$	$C_{A,1,\epsilon=1}(S,T)$	$C_{A,2,\epsilon=1}(S,T)$	$re^C_{BW}(S,T)$	$re^C_{1,\epsilon=1}(S,T)$	$re^C_{2,\epsilon=1}(S,T)$
70	1.0638	2.1845	2.3679	2.2715	2.1878	8.39×10^{-2}	3.98×10^{-2}	1.47×10^{-3}
80	1.7276	3.9387	4.1329	4.0428	3.9483	4.93×10^{-2}	2.64×10^{-2}	2.43×10^{-3}
90	2.5807	6.5377	6.7081	6.6482	6.5526	2.60×10^{-2}	1.68×10^{-2}	2.26×10^{-3}
100	3.6212	10.201	10.312	10.302	10.216	1.08×10^{-2}	9.94×10^{-3}	1.51×10^{-3}
110	4.8422	15.166	15.198	15.246	15.179	2.11×10^{-2}	5.29×10^{-3}	8.71×10^{-4}
120	6.2334	21.690	21.666	21.746	21.705	1.11×10^{-3}	2.59×10^{-3}	7.02×10^{-4}

T = 10, r = 0.08, $\sigma=0.2$, and b = −0.04, or b = 0.0, or b = 0.04, and $0<\tau<T$. **Figure 2** shows the "true" free boundary, the Barone-Adesi, Whaley free boundary, the first and the second order approximations of the free boundary obtained from the expansions of Sections 2 and 3 as a function of the time to maturity τ, $0<\tau<T$, when E = 100, T = 10, r = 0.08, $\sigma=0.2$, b = 0.04. In particular **Figure 2** shows that the first order approximation of the free boundary improves significantly the zero-th order approximation of the free boundary (*i.e.* the Barone-Adesi, Whaley free boundary) and that the second order approximation of the free boundary refines the result obtained with the first order approximation. **Figure 3(a)** and **Figure 3(b)** show the "true" and the approximated prices of the American call option corresponding to the free boundaries shown in **Figure 2** as a function of the time to maturity τ, $0<\tau<T$, T = 10, when the asset price S takes the values S = 90 (**Figure 3(a)**) and S = 110 (**Figure 3(b)**). The approximated option prices are obtained using (12), (18) and the zero-th, first and second order approximations of the sum the series expansions developed in Sections 2 and 3. **Figure 2** and **Figure 3** suggest that the second order corrections of the option price and of the free boundary are necessary to obtain satisfactory approximations of the solution of the American call option pricing problem when we consider

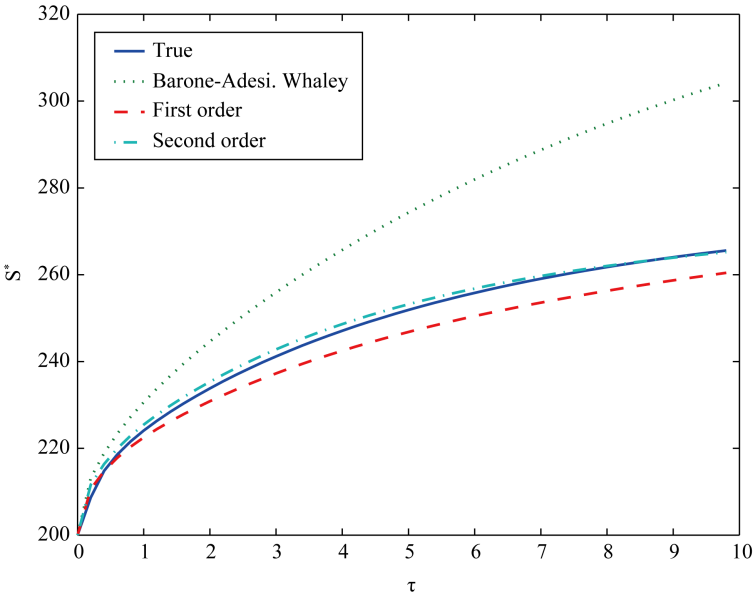

Figure 2. American call option free boundary S^* as a function of the time to maturity τ when $E = 100$, $T = 10$, $r = 0.08$, $\sigma = 0.2$, $b = 0.04$: "true" free boundary (solid line), Barone-Adesi, Whaley free boundary (dotted line), first order approximation of the free boundary (dashed line), second order approximation of the free boundary (dash-dotted line).

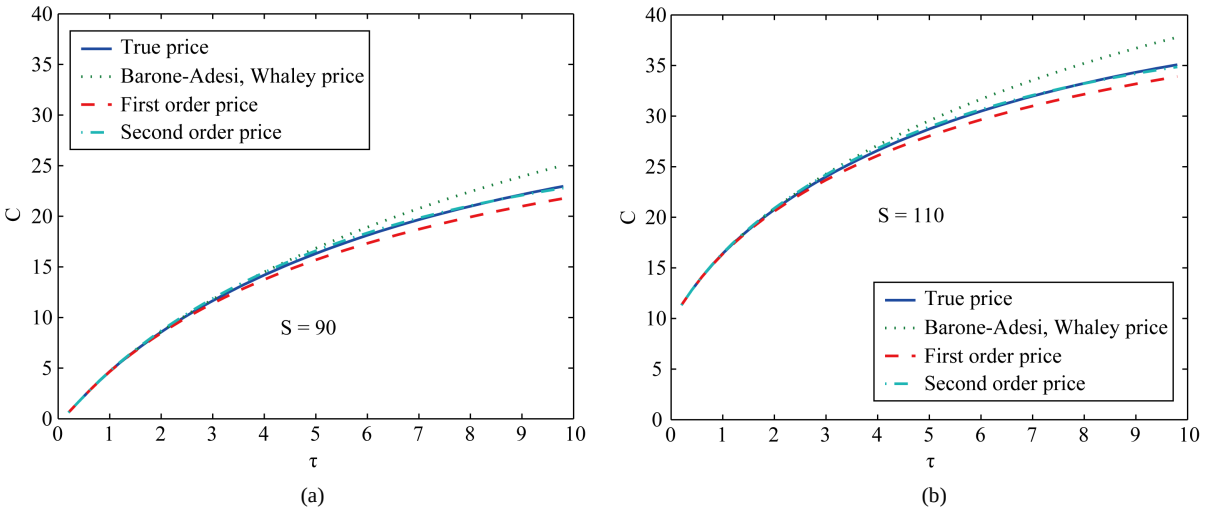

Figure 3. American call option price C as a function of the time to maturity τ for two values of the asset price $S = 90$ (a), $S = 110$ (b), when $E = 100$, $T = 10$, $r = 0.08$, $\sigma = 0.2$, $b = 0.04$. "True" price C_T (solid line), Barone-Adesi, Whaley price C_{BW} (dotted line), first order approximation $C_{A,1,\epsilon=1}$ of the price (dashed line), second order approximation $C_{A,2,\epsilon=1}$ of the price (dash-dotted line).

options with intermediate maturity times (*i.e.* when $3 \le T \le 10$) at time $t = 0$ (*i.e.* $\tau = T$) or at time t close to zero.

Figure 4 shows the American call option price C when $\tau = T$ (*i.e.* when $t = 0$), $T = 10$, $E = 100$, $r = 0.08$, $\sigma = 0.2$, $b = 0.04$ as a function of the asset price S. Note that the option price approximation obtained using the zero-th order term (*i.e.* the Barone-Adesi, Whaley price) is not accurate (see **Figure 4** dotted line). This is a consequence of the fact that the zero-th order approximation of the free boundary is unsatisfactory (see **Figure 2**, **Figure 4**). Note that in **Figure 4** the payoff function (solid line) is a lower bound for the "true" American call

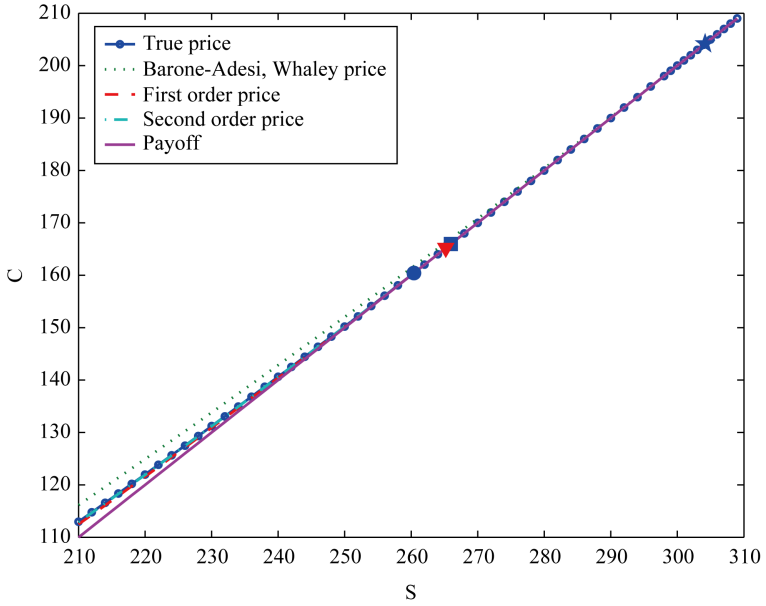

Figure 4. American call option price C as a function of the asset price S when $\tau = T = 10$, $E = 100$, $r = 0.08$, $\sigma = 0.2$, $b = 0.04$. "True" price C_T (square-solid line), Barone-Adesi, Whaley price C_{BW} (dotted line), first order approximation $C_{A,1,\epsilon=1}$ of the price (dashed line), second order approximation $C_{A,2,\epsilon=1}$ of the price (dash-dotted line), and payoff function (solid line). The abscissae of the four marked points show the location of the free boundary: square mark—true free boundary, star mark Barone-Adesi, Whaley free boundary, circle mark—first order approximation of the free boundary, triangle mark—second order approximation of the free boundary.

option price C_T and that the first order (dashed line) and the second order (dash-dotted line) approximations obtained using (12), (18) and the series expansions developed in Sections 2 and 3 and the "true" option price C_T (square-solid line) overlap while the zero-th order approximation (*i.e.* the Barone-Adesi, Whaley solution) (dotted line) is not accurate. The abscissae of the four points marked in **Figure 4** are the location of the free boundaries: square mark—"true" free boundary, star mark—zero-th order approximation of the free boundary (*i.e.* Barone-Adesi, Whaley free boundary), circle mark—first order approximation of the free boundary, triangle mark—second order approximation of the free boundary. Note that in **Figure 4** the true free boundary and its second order approximation overlap. In **Figure 5** we present the relative errors with respect to the "true" option price of the approximated option prices shown in **Figure 4** as a function of the asset price. That is **Figure 5** shows as a function of the asset price S the relative errors with respect to the "true" option price of the Barone-Adesi, Whaley option price (dotted line), of the first order approximation of the option price (dashed line) and of the second order approximation of the option price (dashed-dotted line) obtained from (12), (18) and the series expansions introduced in Sections 2 and 3. Recall that in **Figure 4** and **Figure 5** the parameters of the American call option problem considered are: $\tau = T = 10$, $E = 100$, $r = 0.08$, $\sigma = 0.2$, $b = 0.04$.

Let us consider the American put option pricing problem. We study a set of test problems similar to those discussed in [2] [3].

The first test problem involving American put options is taken from Table 5 of [2] and consists in evaluating at time $t = 0$ the prices of the American put options having $E = 100$, $T = 3$ when the underlying asset price ranges from $S = 80$ to $S = 120$, that is when $S = S_j = 80 + (j-1)*10$, $j = 1, 2, \cdots, 5$, and the Black Scholes parameters have the following values: $\sigma = 0.2$, $r = 0.05$, $b = b_j = -0.04 + (j-1)*0.04$, $j = 1, 2, 3, 4$.

In analogy with the notation introduced previously in the study of the American call option pricing problem we denote with $P_T(S,T)$, $P_{\mathrm{BW}}(S,T)$, $P_{A,n,\epsilon=1}(S,T)$, $n = 1, 2$, respectively the values of the American put option prices obtained using the trinomial tree method (*i.e.* the "true value" of the option price used as benchmark), the Barone-Adesi, Whaley formula (for put options) and the n-th order approximation, $n = 1, 2$, obtained from

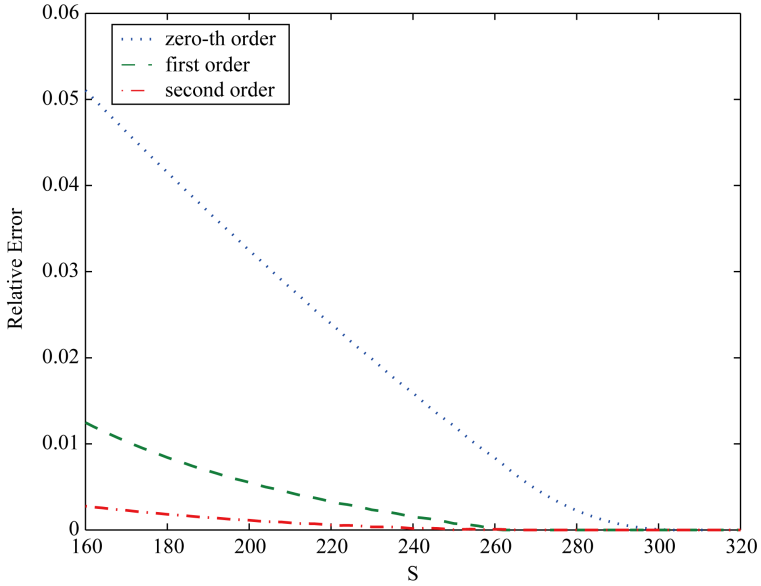

Figure 5. Relative errors of the approximations of an American call option price with respect to the "true value" of the price as a function of the asset price S when $\tau = T = 10$, $E = 100$, $r = 0.08$, $\sigma = 0.2$, $b = 0.04$: relative error of the Barone-Adesi, Whaley price (dotted line), relative error of the first order approximation of the price (dashed line), relative error of the second order approximation of the price (dashed-dotted line).

the analogous (for put options) of (12), (18) and of the series expansions introduced in Sections 2, 3. For later convenience to emphasize the dependence from the parameter $b = b_j$, $j = 1, 2, \cdots, 4$, of the put option prices and we write b as an argument of the put option price, that is we write $P_T(S,T,b)$, $P_{\mathrm{BW}}(S,T,b)$, $P_{A,n,\epsilon=1}(S,T,b)$, instead of writing respectively $P_T(S,T)$, $P_{\mathrm{BW}}(S,T)$, $P_{A,n,\epsilon=1}(S,T)$, $n = 1, 2$. Moreover let re^P_{BW} and $re^P_{A,n,\epsilon=1}$, $n = 1, 2$, be the following relative errors:

$$re^P_{\mathrm{BW}}(S,T,b) = \left|P_T(S,T,b) - P_{\mathrm{BW}}(S,T,b)\right| \Big/ \left|P_T(S,T,b)\right|, \tag{64}$$

$$re^P_{n,\epsilon=1}(S,T,b) = \left|P_T(S,T,b) - P_{A,n,\epsilon=1}(S,T,b)\right| \Big/ \left|P_T(S,T,b)\right|, \quad n = 1,2. \tag{65}$$

Table 3 shows the results obtained in this experiment. In the attempt of making **Table 3** comparable with **Table 5** of [2] we show in **Table 3** the values of the following Root Mean Square Errors (RMSE):

$$\mathrm{RMSE-BW} = \sqrt{\frac{1}{20}\sum_{i=1}^{5}\sum_{j=1}^{4}\left(P_T(S_i,T,b_j) - P_{\mathrm{BW}}(S_i,T,b_j)\right)^2}, \tag{66}$$

$$\mathrm{RMSE}-E_{n,\epsilon=1} = \sqrt{\frac{1}{20}\sum_{i=1}^{5}\sum_{j=1}^{4}\left(P_T(S_i,T,b_j) - P_{A,n,\epsilon=1}(S_i,T,b_j)\right)^2}, \quad n = 1,2, \tag{67}$$

and the values of the following Maximum Absolute Errors (MAE):

$$\mathrm{MAE-BW} = \max_{i,j}\left|P_T(S_i,T,b_j) - P_{\mathrm{BW}}(S_i,T,b_j)\right|, \tag{68}$$

$$\mathrm{MAE}-E_{n,\epsilon=1} = \max_{i,j}\left|P_T(S_i,T,b_j) - P_{A,n,\epsilon=1}(S_i,T,b_j)\right|, \quad n = 1,2, \tag{69}$$

where in (68), (69) i takes the values $1, 2, \cdots, 5$ and j takes values $1, 2, \cdots, 4$.

Table 5 of [2] compares on the test problems considered the accuracy of the put option prices computed with some well known methods used to solve the American put option pricing problem including the methods of Geske and Johnson [4], Bunch and Johnson [6], Brodie and Detemple [19] (see [2] for further details). **Table 3**

Table 3. Approximations of the price of an American put option with $T = 3$, $E = 100$, $r = 0.08$, $\sigma = 0.2$ and relative and absolute errors committed.

b	S	P_T	P_{BW}	$P_{A,1,\epsilon=1}$	$P_{A,2,\epsilon=1}$	re^P_{BW}	$re^P_{1,\epsilon=1}$	$re^P_{2,\epsilon=1}$
−0.04	80	25.658	26.245	25.462	25.648	2.289×10^{-2}	7.628×10^{-3}	3.973×10^{-4}
−0.04	90	20.083	20.641	19.833	20.079	2.778×10^{-2}	1.244×10^{-2}	1.809×10^{-4}
−0.04	100	15.497	15.990	15.208	15.509	3.183×10^{-2}	1.866×10^{-2}	7.861×10^{-4}
−0.04	110	11.803	12.221	11.486	11.834	3.545×10^{-2}	2.679×10^{-2}	2.683×10^{-3}
−0.04	120	8.8854	9.2345	8.5561	8.9411	3.928×10^{-2}	3.707×10^{-2}	6.265×10^{-3}
0.0	80	22.205	22.395	22.127	22.196	8.575×10^{-3}	3.502×10^{-3}	3.767×10^{-4}
0.0	90	16.207	16.498	16.099	16.194	1.795×10^{-2}	6.601×10^{-3}	7.556×10^{-4}
0.0	100	11.702	12.030	11.578	11.692	2.801×10^{-2}	1.065×10^{-2}	8.832×10^{-4}
0.0	110	8.3667	8.6871	8.2272	8.3597	3.829×10^{-2}	1.667×10^{-2}	8.393×10^{-4}
0.0	120	5.9299	6.2222	5.7804	5.9293	4.928×10^{-2}	2.522×10^{-2}	1.166×10^{-4}
0.04	80	20.347	20.325	20.337	20.342	1.062×10^{-3}	4.765×10^{-4}	2.613×10^{-4}
0.04	90	13.495	13.563	13.469	13.473	5.021×10^{-3}	1.972×10^{-3}	1.659×10^{-3}
0.04	100	8.9423	9.1076	8.9138	8.9116	1.847×10^{-2}	3.187×10^{-3}	3.436×10^{-3}
0.04	110	5.9111	6.1225	5.8799	5.8757	3.576×10^{-2}	5.262×10^{-3}	5.982×10^{-3}
0.04	120	3.8972	4.1153	3.8612	3.8604	5.595×10^{-2}	9.251×10^{-3}	9.448×10^{-3}
0.08	80	20.000	20.000	20.000	20.000	0.000	0.000	0.000
0.08	90	11.696	11.634	11.709	11.687	5.300×10^{-3}	1.066×10^{-3}	8.073×10^{-4}
0.08	100	6.9298	6.9621	6.9581	6.9137	4.672×10^{-3}	4.083×10^{-3}	2.324×10^{-4}
0.08	110	4.1536	4.2574	4.1881	4.1319	2.499×10^{-2}	8.311×10^{-3}	5.230×10^{-3}
0.08	120	2.5096	2.6402	2.5414	2.4840	5.205×10^{-2}	1.266×10^{-2}	1.018×10^{-2}

$\mathrm{RMSE-BW} = 0.2971$, $\mathrm{RMSE} - E_{1,\epsilon=1} = 0.1541$, $\mathrm{RMSE} - E_{2,\epsilon=1} = 0.0227$

$\mathrm{MAE-BW} = 0.5875$, $\mathrm{MAE} - E_{1,\epsilon=1} = 0.3294$, $\mathrm{MAE} - E_{2,\epsilon=1} = 0.0557$

shows that the root mean square errors and the maximum absolute errors of the put option prices obtained using the second order approximation of the solution of the American put option pricing problem deduced from the analogous for put options of (12), (18) and of the expansions introduced in Sections 2 and 3 outperform those shown in Table 5 of [2]. In particular note that the second order approximation of the put option price obtained with the method developed in Sections 2 and 3 outperforms in accuracy the best approximation of the American put option price obtained with the Brodie and Detemple method shown in Table 5 of [2].

Moreover **Table 3** shows that the behaviour of the series expansions developed in Sections 2 and 3 applied to the put option pricing problem is similar to their behaviour in the case of the call option pricing problem shown in **Table 2**. In fact in **Table 3** when $n = 0, 1$ going from the n-th order approximation to the $(n+1)$-th order approximation of the American put option price we gain roughly one correct significant digit in the approximate solution found. A similar behaviour has already been observed in the call option case in **Table 2**.

The last test problem studied is taken from Little, Pant, Hou [3]. We consider the American put option pricing problem when $T = 1$, $E = 100$, $r = 0.07$, $\sigma = 0.25$, $d = r - b = 0.0$ (*i.e.* $b = 0.07$) or $d = r - b = 0.03$ (*i.e.* $b = 0.04$). We compare the free boundaries obtained using the approximations shown in Table 5 and Table 6 of [3] and the first three order approximations, $S^*_{0,\epsilon=1} = S^*_0$, $S^*_{1,\epsilon=1}$, $S^*_{2,\epsilon=1}$ of the free boundary obtained with the method developed in Sections 2 and 3 (adapted for put options) shown in **Table 4**. In **Table 4** $S^*(\tau)$, $0 < \tau < T$, denotes the "true" free boundary of the American put option pricing problem obtained solving numerically the

integral equation for the put free boundary presented in [3]. Note that the second order approximation of the free boundary obtained with the method developed in Sections 2 and 3 (adapted for put options) (shown in **Table 4**) is roughly of the same quality of the numerically computed free boundary obtained in [3] solving the integral equation analogous to (58) satisfied by the free boundary of the American put option pricing problem (see Table 4, Table 5 of [3]).

Finally let us compare the computational times needed to obtain the approximations of the solution of the American option pricing problem that have been considered in this Section. Let us consider the American call option pricing problem defined by $S = 70$, $\tau = T = 10$, $E = 100$, $b = -0.04$, $\sigma = 0.02$, $r = 0.08$, **Table 5** shows the time (in seconds) required to compute for $n = 0, 1, 2$ the coefficients $A_{n,j}$, $j = 0,1,\cdots,2n$, the option price approximation $C_{A,n,\epsilon=1}$ and the corresponding free boundary approximation $S^*_{n,\epsilon=1}$, and the time (in seconds) required to compute the same option price and the corresponding free boundary with the trinomial tree method when $n_T = 1000$ steps and solving numerically the integral equation satisfied by the free boundary. These computational times have been obtained using an Intel CORE 3i processor. **Table 5** shows that the time required to compute the first three order approximations of the solution of the American call option pricing problem ($n = 0, 1, 2$) deduced from (12), (18) and the series expansions of Sections 2, 3 is negligible when compared to the time required to compute the same quantities (price and free boundary) with the trinomial tree method and the numerical solution of the integral equation. Furthermore, as already said, it is easy to see that for $n = 0,1,\cdots$ the computation on a grid of values of the S and τ variables of the n-th order approximation of the option price and of the corresponding free boundary derived from (12), (18) and the series expansions introduced in Sections 2, 3 can be easily parallelized. In fact the computation of the free boundary at a given order on a grid of maturity times can be done in parallel since at each order in ϵ the condition that defines the free boundary in the method developed Sections 2 and 3 is a local condition. Furthermore for any fixed maturity time the evaluation of the

Table 4. Approximations of the free boundary of an American put option with maturity $T = 1$ and strike price $E = 100$.

$r = 0.07$, $\sigma = 0.25$, $b = 0.04$				
τ	$S^*(\tau)$	$S^*_{0,\epsilon=1}(\tau)$	$S^*_{1,\epsilon=1}(\tau)$	$S^*_{2,\epsilon=1}(\tau)$
0.04	90.3991	90.9985	90.0245	90.3994
0.4	79.5573	80.5337	79.7225	79.5589
0.6	77.2021	78.1801	77.2351	77.2055
1	74.1860	74.1027	74.2529	74.1801
$r = 0.07$, $\sigma = 0.25$, $b = 0.07$				
τ	$S^*(\tau)$	$S^*_{0,\epsilon=1}(\tau)$	$S^*_{1,\epsilon=1}(\tau)$	$S^*_{2,\epsilon=1}(\tau)$
0.04	91.3962	91.9431	91.1940	91.3925
0.4	82.2619	83.1359	82.2465	82.2614
0.6	80.3417	81.2235	80.3608	80.3414
1	77.9201	78.7683	77.9707	77.9202

Table 5. Computational times (Intel Core i3 processor).

American call option $E = 100$, $T = 10$, $r = 0.08$, $\sigma = 0.2$				
b	zero-th order appr. (sec)	first order appr. (sec)	second order appr: (sec)	trinomial appr. (sec)
−0.04	2.12×10^{-4}	7.85×10^{-4}	1.79×10^{-3}	6.302
0.00	2.08×10^{-4}	8.40×10^{-4}	1.82×10^{-3}	6.318
0.04	2.08×10^{-4}	8.03×10^{-4}	1.89×10^{-3}	6.303

option price at a given order on a grid of asset prices can be done in parallel, in fact this is simply the evaluation of a closed form formula on a set of points.

A rough comparison of the computing times of the iterative method of [11] to solve the American option pricing problem (see Tables 3-5 of [11]) and of our approximated solutions (see **Table 5**), that takes into account the difference between the two CPU employed in the computations (*i.e.* the Intel Core i3 in our numerical experiments and the 3.0-GHz Pentium in the numerical experiments of [11]), shows that these computing times are similar and are (on both CPUs) of the order of 2 - 3 milliseconds for the evaluation of the option price and of the corresponding free boundary given the values of the independent variables S, τ. However it must be noted that when the American option pricing problem must be solved on a grid in the S and τ variables the method developed in Sections 2 and 3 can be fully parallelized while the method developed in [11] due to the nonlocal character of the integral equation used to determine the free boundary cannot be fully parallelized.

The experiments presented in this Section show that the approximate solutions of the American option pricing problem obtained using the method introduced in Sections 2 and 3 are a natural and useful extension of the Barone-Adesi, Whaley formula and that these approximate solutions can be used fruitfully to obtain at a very competitive computational cost accurate solutions of the American option pricing problem.

The website: http://www.econ.univpm.it/recchioni/finance/w20 contains material including animations, an interactive application and an app that helps the understanding of the paper. A general reference to the work of the authors and of their coauthors in mathematical finance is the website: http://www.econ.univpm.it/recchioni/finance.

References

[1] Barone-Adesi, G. and Whaley, R.E. (1987) Efficient Analytic Approximation of American Option Values. *The Journal of Finance*, **42**, 301-320. http://dx.doi.org/10.1111/j.1540-6261.1987.tb02569.x

[2] Ju, N.J. and Zhong, R. (1999) An Approximate Formula for Pricing American Options. *The Journal of Derivatives*, **7**, 31-40. http://dx.doi.org/10.3905/jod.1999.319140

[3] Little, T., Pant, V. and Hou, C. (2000) A New Integral Representation of the Early Exercise Boundary for American Put Options. *Journal of Computational Finance*, **3**, 73-96.

[4] Geske, R. and Johnson, H.E. (1984) The American Put Option Valued Analytically. *Journal of Finance*, **39**, 1511-1524. http://dx.doi.org/10.1111/j.1540-6261.1984.tb04921.x

[5] Kim, I.N. (1990) The Analytic Valuation of American Options. *Review of Financial Studies*, **3**, 547-572. http://dx.doi.org/10.1093/rfs/3.4.547

[6] Bunch, D.S. and Johnson, H. (1992) A Simple and Numerically Efficient Valuation Method for American Puts Using a Modified Geske-Johnson Approach. *Journal of Finance*, **47**, 809-816. http://dx.doi.org/10.1111/j.1540-6261.1992.tb04412.x

[7] Bjerksund, P. and Stensland, G. (1993) Closed-Form Approximation of American Options. *Scandinavian Journal of Management*, **9**, S87-S99. http://dx.doi.org/10.1016/0956-5221(93)90009-H

[8] Barone-Adesi, G. (2005) The Saga of the American Put. *Journal of Banking & Finance*, **29**, 2909-2918. http://dx.doi.org/10.1016/j.jbankfin.2005.02.001

[9] Zhu, S.P. (2006) An Exact and Explicit Solution for the Valuation of American Put Options. *Quantitative Finance*, **6**, 229-242. http://dx.doi.org/10.1080/14697680600699811

[10] Bjerksund, P. and Stensland, G. (2002) Closed Form Valuation of American Options. Technical Report, Norwegian School of Economics and Business Administration, Bergen.

[11] Kim, I.J., Jang, B.G. and Kim, K.T. (2013) A Simple Iterative Method for the Valuation of American Options. *Quantitative Finance*, **13**, 885-895. http://dx.doi.org/10.1080/14697688.2012.696780

[12] Brennan, M. and Schwartz, E. (1977) The Valuation of American Put Options. *The Journal of Finance*, **32**, 449-462. http://dx.doi.org/10.2307/2326779

[13] Cox, J.C., Ross, S.A. and Rubinstein, M. (1979) Option Pricing: A Simplified Approach. *Journal of Financial Economics*, **7**, 229-263. http://dx.doi.org/10.1016/0304-405X(79)90015-1

[14] Figlwski, S. and Gao, B. (1999) The Adaptive Mesh Model: A New Approach to Efficient Option Pricing. *Journal of Financial Economics*, **53**, 313-351. http://dx.doi.org/10.1016/S0304-405X(99)00024-0

[15] Jiang, L. and Dai, M. (2004) Convergence of Binomial Tree Methods for European/American Path-Dependent Options. *SIAM Journal on Numerical Analysis*, **42**, 1094-1109. http://dx.doi.org/10.1137/S0036142902414220

[16] Breen, R. (1991) The Accelerated Binomial Option Pricing Model. *The Journal of Financial and Quantitative Analysis*, **26**, 153-164. http://dx.doi.org/10.2307/2331262

[17] Boyle, P. (1986) Option Valuation Using Three-Jump Process. *International Options Journal*, **3**, 7-12.

[18] Ahn, J. and Song, M. (2007) Convergence of the Trinomial Tree Method for Pricing European/American Options. *Applied Mathematics and Computation*, **189**, 575-582. http://dx.doi.org/10.1016/j.amc.2006.11.132

[19] Brodie, M. and Detemple, J. (1996) American Option Valuation: New Bounds Approximations, and a Comparison of Existing Methods. *Review of Financial Studies*, **9**, 1211-1250. http://dx.doi.org/10.1093/rfs/9.4.1211

[20] Longstaff, F.A. and Schwartz, E.S. (2001) Valuing American Options by Simulation: A Simple Least-Squares Approach. *Review of Financial Studies*, **14**, 113-147. http://dx.doi.org/10.1093/rfs/14.1.113

[21] Wilmott, P., Dewynne, J.N. and Howison, S.D. (1993) Option Pricing: Mathematical Models and Computation. Oxford Financial Press, Oxford.

[22] Dewynne, J.N., Howison, S.D., Rupf, I. and Wilmott, P. (1993) Some Mathematical Results in the Pricing of American Options. *European Journal of Applied Mathematics*, **4**, 381-398. http://dx.doi.org/10.1017/S0956792500001194

[23] Verhulst, F. (2005) Methods and Applications of Singular Perturbations: Boundary Layers and Multiple Timescale Dynamics. Springer, Berlin.

[24] Fatone, L., Recchioni, M.C. and Zirilli, F. (2007) A Perturbative Formula to Price Barrier Options with Time-Dependent Parameters in the Black and Scholes World. *Journal of Risk*, **10**, 131-146.

[25] Šečovic, D. (2001) Analysis of the Free Boundary for the Pricing of an American Call Option. *European Journal of Applied Mathematics*, **12**, 25-37.

Applied Mathematics, 2015, 6, 403-413
Published Online February 2015 in SciRes. http://www.scirp.org/journal/am
http://dx.doi.org/10.4236/am.2015.62037

Scientific Research Publishing

Wave Iterative Method for Patch Antenna Analysis

Pinit Nuangpirom, Surasak Inchan, Somsak Akatimagool

Department of Teacher Training in Electrical Engineering, King Mongkut's University of Technology North Bangkok, Bangkok, Thailand
Email: ssa@kmutnb.ac.th, hs5qab@hotmail.com, Surasak.inchan@gmail.com

Received 22 January 2015; accepted 10 February 2015; published 13 February 2015

Abstract

Wave Iterative Method (WIM) is a numerical modeling for electromagnetic field analysis of microwave circuits. Theories of transmission line, four terminal network and boundary condition are applied to developing WIM simulation that the physical electromagnetic wave is described to a mathematical model using GUI function of MATLAB. In applying, the microstrip patch antenna was analyzed and implemented. The research result shows that the WIM simulation can be used correctly to analyze the electric field, magnetic field theory and return lose of sample patch antenna. The comparison of the WIM calculation agrees well with the measurement and the classical simulation.

Keywords

Wave Iterative Method, Electromagnetic Field Analysis, Patch Antenna

1. Introduction

Presently, numerical methods are important for scientists, engineers and researchers. The development and research are necessary for technical problem solving [1]-[4]. The basic Wave Iterative Method (WIM) is a full wave analysis that has been developed since 2001, and is suitable for microwave circuit analysis [5]-[9]. Evolution of the WIM was developed to support microwave circuits such as waveguides [10] [11], filter circuits [7] and applied in telecommunication engineering education [8] [12]. The advantages of WIM algorithm are the integration of theories of transmission line, two ports network and boundary conditions and iterative method that are weak definition to study.

2. Wave Iterative Method

The WIM concept based on iterative method is to calculate amplitude and direction of incident wave, reflected

wave and transmitted wave in the multi-layers planar structure. The electric field, magnetic field and network parameters of equivalent circuit are results that we want to solve and display.

2.1. Wave Equations

Transmission line is represented by equivalent circuit, as shown in **Figure 1**, where V_{in} and I_{in} are the voltage and current variables at the input ports, V_{in}^{+} and I_{in}^{+} are incident voltage and current wave, V_{in}^{-} and I_{in}^{-} are reflected voltage and current wave, respectively. The relationship between incident wave and reflected wave is defined as [13]

$$V_{\text{in}} = V_{\text{in}}^{+} + V_{\text{in}}^{-}, \tag{1}$$

$$I_{\text{in}} = I_{\text{in}}^{+} - I_{\text{in}}^{-}. \tag{2}$$

Considering the input port, as shown in **Figure 1**, normalized waves in Equations (1) and (2) are divided by $\sqrt{Z_0}$, thus we have

$$\frac{V_{\text{in}}}{\sqrt{Z_0}} = \frac{V_{\text{in}}^{+}}{\sqrt{Z_0}} + \frac{V_{\text{in}}^{-}}{\sqrt{Z_0}}, \tag{3}$$

$$\sqrt{Z_0} I_{\text{in}} = \sqrt{Z_0} I_{\text{in}}^{+} - \sqrt{Z_0} I_{\text{in}}^{-}. \tag{4}$$

The relation equation base on the incident wave (A) and reflected wave (B) is presented by

$$\frac{V_{\text{in}}}{\sqrt{Z_0}} = A + B, \tag{5}$$

and

$$\sqrt{Z_0} I_{\text{in}} = A - B \tag{6}$$

where $A = \dfrac{V_{\text{in}}^{+}}{\sqrt{Z_0}} = \sqrt{Z_0} I_{\text{in}}^{+}$ and $B = \dfrac{V_{\text{in}}^{-}}{\sqrt{Z_0}} = \sqrt{Z_0} I_{\text{in}}^{-}$.

Then, the input voltage and current equation can be written as

$$V_{\text{in}} = \sqrt{Z_0}\left(A + B\right), \tag{7}$$

$$I_{\text{in}} = \frac{1}{\sqrt{Z_0}}\left(A - B\right). \tag{8}$$

Rewrite the equations in the form of an electric field and current density that are as

$$E = \sqrt{Z_0}\left(A + B\right), \tag{9}$$

$$J = \frac{1}{\sqrt{Z_0}}\left(A - B\right). \tag{10}$$

Equation (9) and (10) are the electric field and current density (or magnetic field) in following the wave equation. The variable A (incident wave) and B (reflected wave) are the key parameters used in the WIM algorithm.

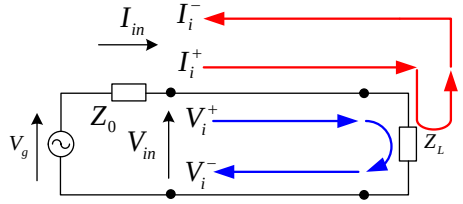

Figure 1. Transmission line circuit.

Considering, the scattering parameter (*S*) of a two ports network as shown in **Figure 2**, is defined in terms of wave variables as [14]

$$B_1 = S_{11}A_1 + S_{12}A_2 , \tag{11}$$

$$B_2 = S_{21}A_1 + S_{22}A_2 . \tag{12}$$

The *S* parameters defined by the incident and reflected wave are expressed as

$$\begin{aligned} S_{11} &= \frac{B_1}{A_1} \text{ when } A_2 = 0, \; S_{12} = \frac{B_1}{A_2} \text{ when } A_1 = 0 \\ S_{21} &= \frac{B_2}{A_1} \text{ when } A_2 = 0, \; S_{22} = \frac{B_2}{A_2} \text{ when } A_1 = 0, \end{aligned} \tag{13}$$

where A_n, B_n are the wave variables and $A_n = 0$ that implies a perfect impedance match at port *n*. The wave definition is written as

$$\begin{bmatrix} B_1 \\ B_2 \end{bmatrix} = \begin{bmatrix} S_{11} & S_{12} \\ S_{21} & S_{22} \end{bmatrix} \begin{bmatrix} A_1 \\ A_2 \end{bmatrix}. \tag{14}$$

The parameters variable S_{ii} is called the reflection coefficients at port $i = 1,2$, whereas S_{ij} is the transmission coefficients of two ports network, where $i \neq j$ and $j = 1,2$.

2.2. Wave Iterative Method (WIM)

Wave propagation described by incident, reflected and transmitted waves is represented in the planar structure. We see that the waves will be reflected continuously, as shown in **Figure 3**.

In iterative procedure, the excited wave $\left(B_{(x,y)}\right)$ in the real domain (Pixel) of planar source is converted to the wave $B^i_{(m,n)}$ in the spectrum domain (Modes) by using the Fast Fourier Transform (FFT). Considering the upper and bottom side of metallic box, we obtain the wave $A^i_{(m,n)}$ form reflection of the wave $B^i_{(m,n)}$ by the reflection coefficient $\left(\Gamma_i\right)$. The wave $A^i_{(m,n)}$ in the spectrum domain will be transformed to the wave $A^i_{(x,y)}$ in the real domain by using the Invert Fast Fourier Transform (IFFT). At the planar structure situated between

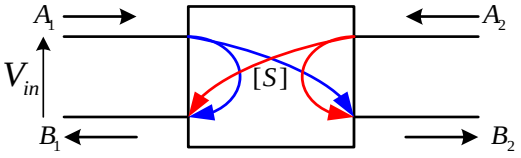

Figure 2. Two ports network.

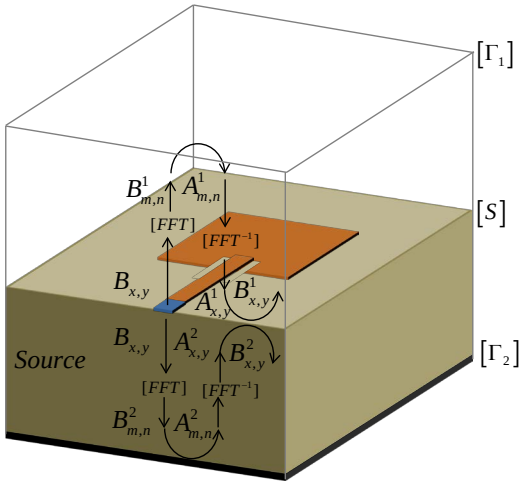

Figure 3. Wave propagation in planar circuit.

dielectric region (i) 1 and 2, the wave $A^i_{(x,y)}$ will reflect to the wave $B^i_{(x,y)}$ by the scattering parameter (S) of two ports equivalent network. Finally, the process of wave propagation will be repeated until the convergence of waves is solved.

The WIM procedure, as shown in **Figure 4**, is summarized by the following steps:

1) Define the excited wave $B_{(x,y)}$ of planar source.

2) Convert the waves in the real domain to the spectrum domain by the FFT: $B^i_{(m,n)} = [\text{FFT}]\left(B^i_{(x,y)}\right)$.

3) Apply the reflection coefficient (Γ_n) for reflected waves to obtain incident waves: $A^{(i)}_{(m,n)} = [\Gamma_i]\left(B^{(i)}_{(m,n)}\right)$.

4) Transform the waves in the spectrum domain to the real domain by the IFFT: $A^{(i)}_{(x,y)} = \left[\text{FFT}^{-1}\right]\left(A^{(i)}_{(m,n)}\right)$.

5) Calculate the reflected waves using the scattering parameters of planar circuit: $B^{(i)}_{(x,y)} = [S]\left(A^{(i)}_{(x,y)}\right)$.

6) Repeat step 2 to step 5 until the convergence of the network parameters are obtained.

After testing the convergence at the k iterations, the tangential electric field and current density in the discontinuity using Equations (9) and (10), can be written as

$$E^k_{(x,y)} = \sqrt{Z_{0i}}\left(A^k_i + B^k_i\right), \tag{15}$$

$$J^k_{(x,y)} = \left(A^k_i + B^k_i\right)\Big/\sqrt{Z_{0i}}\,. \tag{16}$$

Thus, the admittance parameter of two ports network are obtained as

$$Y = \sum_{x,y}\left(\frac{J_{(x,y)}}{E_{(x,y)}}\right), \tag{17}$$

also, the impedance parameter can be written as

$$Z = \sum_{x,y}\left(\frac{E_{(x,y)}}{J_{(x,y)}}\right). \tag{18}$$

Finally, the scattering parameter of planar circuit is given by

$$S = [Z_0 - Z][Z_0 + Z]^{-1}. \tag{19}$$

The detail of mathematical operator in the WIM procedure, as shown in **Figure 4** is represented as following.

2.2.1. Source Excitation Definition

The excited wave $\left(B_{(x,y)}\right)$ in the real domain of planar source can be written as

$$B_{x,y} = \frac{1}{1+n_1+n_2}\begin{bmatrix}1\Big/\sqrt{Z_{01}}\\ 1\Big/\sqrt{Z_{02}}\end{bmatrix}, \tag{20}$$

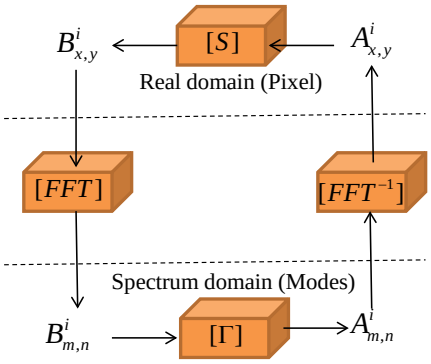

Figure 4. Iterative procedure.

where $n_1 = \frac{Z_0}{Z_{01}}$, $n_2 = \frac{Z_0}{Z_{02}}$, $Z_{0i} = \sqrt{\frac{\mu_0 \mu_{ri}}{\varepsilon_0 \varepsilon_{ri}}}$ that is the characteristic impedance of dielectric layer $i = 1, 2$.

2.2.2. The Modal FFT and Modal IFFT Transform

For simplify the calculation of the generalized $TE_{m,n}$, $TM_{m,n}$ mode wave description, the Modal FFT pair permits movement the transverse filed components from the real domain to the spectrum domain, the modal wave equation in x direction can be defined as

$$B_{x(m,n)}^{TE/TM} = \sum_{j=1}^{M}\sum_{k=1}^{N} B_{x(j,k)} \cos\left(\frac{m\pi x_j}{a}\right) \sin\left(\frac{n\pi y_k}{b}\right), \tag{21}$$

And also, the equation in y direction is defined as

$$B_{y(m,n)}^{TE/TM} = \sum_{j=1}^{M}\sum_{k=1}^{N} B_{y(j,k)} \sin\left(\frac{m\pi x_k}{a}\right) \cos\left(\frac{n\pi y_k}{b}\right). \tag{22}$$

Thus, the modal transform matrix using WIM algorithm can be represented as

$$\begin{bmatrix} B_{(m,n)}^{TE} \\ B_{(m,n)}^{TM} \end{bmatrix} = Q_{m,n} \begin{bmatrix} n/b & -m/a \\ m/a & n/b \end{bmatrix} \mathrm{FFT} \begin{bmatrix} B_x \\ B_y \end{bmatrix}. \tag{23}$$

Similar, the Modal IFFT pair permits movement the modal filed components from the spectrum domain comeback to the real domain, the spatial wave equation in x direction can be defined as

$$A_x = \sum_{m=1}^{M}\sum_{n=1}^{N} A_{x(m,n)}^{TE/TM} \cos\left(\frac{m\pi x}{M}\right) \sin\left(\frac{n\pi y}{N}\right), \tag{24}$$

And also, the wave equation in y direction is defined as

$$A_y = \sum_{m=1}^{M}\sum_{n=1}^{N} A_{y(m,n)}^{TE/TM} \sin\left(\frac{m\pi x}{M}\right) \cos\left(\frac{n\pi y}{N}\right). \tag{25}$$

Thus, the spatial wave matrix using WIM algorithm can be represented as

$$\begin{bmatrix} A_x \\ A_y \end{bmatrix} = \mathrm{FFT}^{-1} \left\{ \frac{1}{Q_{m,n}} \begin{bmatrix} n/b & -m/a \\ m/a & n/b \end{bmatrix}^{-1} \begin{bmatrix} A_{(m,n)}^{TE} \\ A_{(m,n)}^{TM} \end{bmatrix} \right\}, \tag{26}$$

where $Q_{m,n} = \sqrt{\frac{ab}{2\Phi_{m,n}}} \frac{1}{\sqrt{(m/a)^2 + (n/b)^2}}$, $\Phi_{m,n} = \begin{cases} 2, & \text{if } m,n \neq 0; \\ 1, & \text{if } m,n \neq 0. \end{cases}$ M, N refer the pixel or modes number, a, b refer the metallic box dimension.

2.2.3. Reflection Coefficient (Γ_i) in the Spectrum Domain

The expression of reflection coefficient at the upper and bottom side of box in the spectrum domain is given by

$$\Gamma_i^{TE/TM} = \frac{1 - Z_{0i} Y_{m,n}^{TE/TM}}{1 + Z_{0i} Y_{m,n}^{TE/TM}}, \tag{27}$$

where the $TE_{m,n}$, $TM_{m,n}$ mode admittances in the metallic box are $Y_{m,n}^{TE} = \frac{\gamma}{j\omega\mu_0\mu_r}$, $Y_{m,n}^{TM} = \frac{j\omega\varepsilon_0\varepsilon_r}{\gamma}$ respectively, $\gamma = \sqrt{(m\pi/a)^2 + (n\pi/b)^2 - k_0^2 \varepsilon_r}$, and $k_0 = \omega\sqrt{\mu_0\varepsilon_0}$.

2.2.4. Scattering Parameter (S) in the Real Domain

At the printed surface of the discontinuity, the boundary conditions of fields, as shown in **Figure 5**, are expressed in terms of waves that consist of 3 conditions as

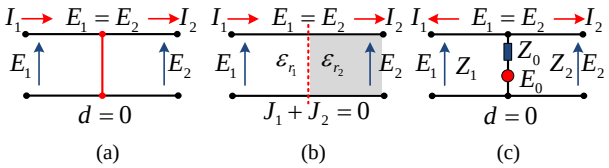

Figure 5. Equivalent circuit of discontinuity. (a) Metal region; (b) Dielectric region; (c) Source region.

Case 1, on the metal regions (*M*), we have the condition; $E_1 = E_2 = 0$, thus the wave relation in the region 1 and 2 can be represented as

$$\begin{bmatrix} B_1 \\ B_2 \end{bmatrix}_M = \begin{bmatrix} -1 & 0 \\ 0 & -1 \end{bmatrix} \begin{bmatrix} A_1 \\ A_2 \end{bmatrix}_M . \tag{28}$$

Case 2, on the dielectric regions (*D*), we have the conditions; $E_1 = E_2$ and $J_1 + J_2 = 0$, the wave relation can be represented as

$$\begin{bmatrix} B_1 \\ B_2 \end{bmatrix}_D = \begin{bmatrix} \dfrac{1-n^2}{n^2+1} & \dfrac{2n}{n^2+1} \\ \dfrac{2n}{n^2+1} & \dfrac{n^2-1}{n^2+1} \end{bmatrix} \begin{bmatrix} A_1 \\ A_2 \end{bmatrix}_D . \tag{29}$$

Case 3, on the planar source regions (*P*), we have the condition; $E_1 = E_2 = E_0 - Z_0\left(J_1 + J_2\right)$, the wave relation can be represented as

$$\begin{bmatrix} B_1 \\ B_2 \end{bmatrix}_P = \begin{bmatrix} \dfrac{-1+n_1-n_2}{1+n_1+n_2} & \dfrac{2n_{12}}{1+n_1+n_2} \\ \dfrac{2n_{12}}{1+n_1+n_2} & \dfrac{-1-n_1+n_2}{1+n_1+n_2} \end{bmatrix} \begin{bmatrix} A_1 \\ A_2 \end{bmatrix}_P , \tag{30}$$

where E_0 refers the excited electric field and the Z_0 refers the source internal impedance, and $n = \sqrt{\dfrac{Z_{01}}{Z_{02}}}$, $n_1 = \dfrac{z_0}{Z_{01}}$, $n_2 = \dfrac{z_0}{Z_{02}}$, and $n_{12} = \dfrac{z_0}{\sqrt{Z_{01}Z_{02}}}$.

Finally, at the planar circuit in the real domain, the scattering parameters of wave equation are summarized on each printed surface region using Equations (23)-(25). The wave relation equation can be expressed as

$$\begin{bmatrix} B_1 \\ B_2 \end{bmatrix} = \begin{bmatrix} T & U \\ V & W \end{bmatrix} \begin{bmatrix} A_1 \\ A_2 \end{bmatrix}. \tag{31}$$

where

$$T = -M + \frac{\left(1-n^2\right)D}{1+n^2} + \frac{\left(-1+n_1-n_2\right)P}{1+n_1+n_2},$$

$$U = V = M + \frac{\left(2n\right)D}{1+n^2} + \frac{\left(2n_{12}\right)P}{1+n_1+n_2},$$

$$W = -M + \frac{\left(n^2-1\right)D}{1+n^2} + \frac{\left(-1-n_1+n_2\right)P}{1+n_1+n_2}.$$

When considering the condition of each region, on the dielectric region: $D = 1$, metal region: $M = 1$ and source region: $P = 1$, and $D = M = P = 0$ when elsewhere.

3. WIM Simulation Design

Computer aided design based on a graphical user interface (GUI) function of MATLAB® is developed using the Wave Iterative Method (WIM) algorithm. The WIM scheme consists of four parts as 1) setup the initial values, 2) design the patch antenna structures, 3) calculate the waves propagated in the spectrum (Modes) and real domain (Pixel) using WIM algorithm, and 4) analysis the network parameters and electromagnetic distributions. The WIM simulation process can be presented in **Figure 6**.

The WIM simulation applied to simple patch antenna works in the following steps.

1) Start the WIM simulation program base on GUI function of the MATLAB, as shown in **Figure 7**.

2) Setup the usable values of calculation by using the "Setup" menu such as; operating frequency, desired printed circuit, dielectric constant value, characteristic impedance, etc.

3) Select the "Analysis" menu to design the microstrip patch antenna parameters using conventional antenna theories approach [14] [15].

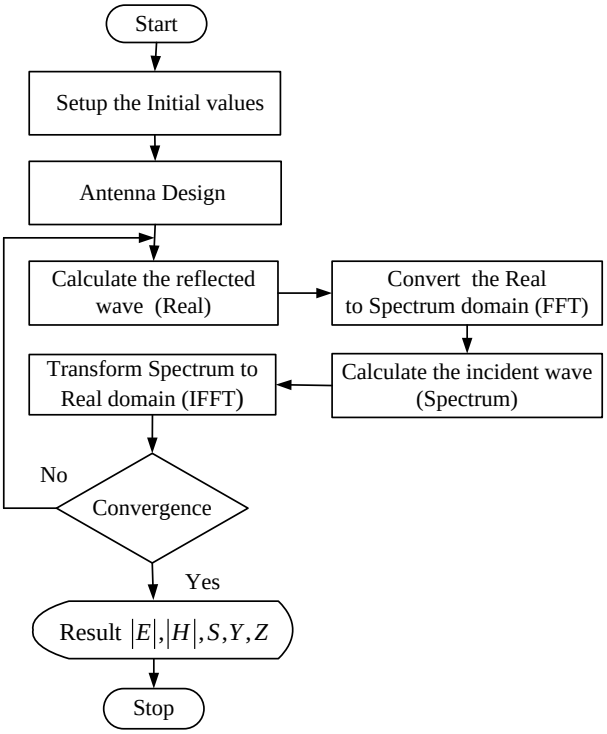

Figure 6. Flowchart of the WIM simulation.

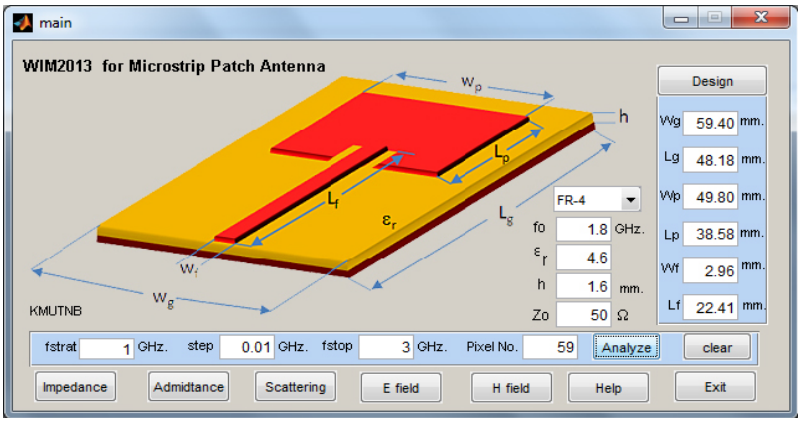

Figure 7. WIM simulation program.

4) Select the "Scattering" or "Impedance" or "Admittance" menu to calculate the scattering parameters of two ports network using the WIM algorithm for designed antenna analysis, an example is shown in **Figure 8(a)**.

5) Select the "E- Field" menu to represent the electric field distributions using the WIM algorithm on the printed interface of planar circuit, as shown in **Figure 8(b)**.

6) Select the "H- Field" menu to represent the magnetic field or current density distributions using the WIM algorithm on the printed interface of planar circuit, as illustrated in **Figure 8(c)**.

7) Select the "Exit" menu to quit form the program.

4. Simulated and Experimented Results

An example of simple microstrip patch antenna is presented using the electromagnetic simulation base on the proposed Wave Iterative Method (WIM) algorithm. In this topic, we will introduce an antenna design tool, an efficiently WIM simulated results to compare to the IE3D software and measurement.

4.1. Microstrip Antenna Design

The optimal parameters of the simple microstrip patch antenna are designed at 1.8 GHz operating frequency. The FR4 printed board was implemented with the relative permittivity (ε_r) equal to 4.6, and the thickness of

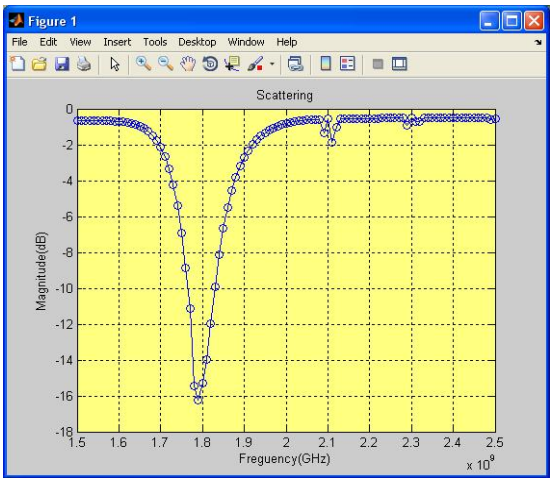

(a)

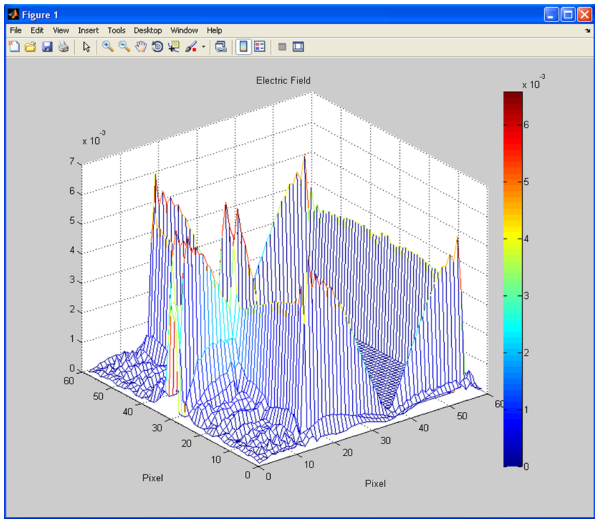

(c)

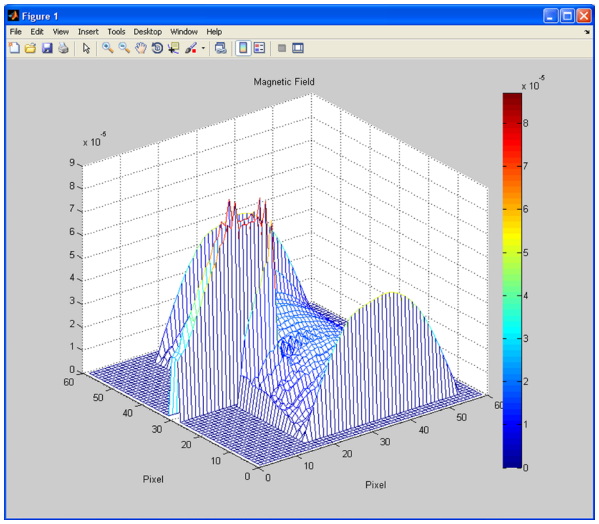

(d)

Figure 8. Display windows. (a) Scattering parameter (S11) window; (b) E-Field display; (c) H-Field display.

dielectric layer is1.6 mm., The analyzed results using the WIM simulation program can be obtained correctly to compare the conventional antenna theories approaches [14] [15]. The printed circuit dimension of designed antenna is 49.8 × 38.58 mm^2, as shown in **Figure 9**.

4.2. Electromagnetic Field Distributions

The simulation program has been developed using the WIM algorithm. Determination of the input E-filed of source excitation on the planar circuit, the computing electromagnetic field distribution will be propagated gradually on the planar structure. The evaluation of the electric and magnetic field distributions in term of iteration number at 1, 5, 10 and 200 rounds is appeared on the antenna structure, as shown in **Figure 10**. It was found that small iteration number, the electromagnetic field distributions on the planar structure are not completely and exactly. After testing the convergence with reasonable number of iterations, on the printed circuit, the normalized electric field peak is at the conductor edge, and minimum values are occurred in remote areas. On the other hand, the current density distributions on $\lambda/2$ long of conductor of each calculation have spread from source in to conductor area and will stabilize when the calculation is convergence (Approximately 200 rounds or more that depends on the designed circuit resolutions).

4.3. Return Loss Analysis of Patch Antenna

In the order to confirm the efficiency of the WIM simulation to compare the IE3D software and measurement, we will analyze and measure the return loss of the simple patch antenna using the N5230C network analyzer of

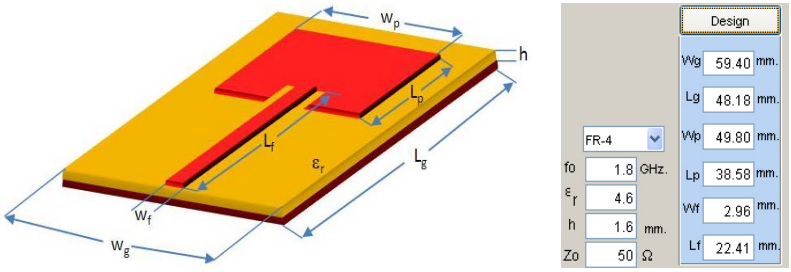

Figure 9. Microstrip patch antenna structure, where Wp = 49.8 mm; Lp = 38.58 mm; Wg = 59.40 mm; Lg = 48.18 mm; Wf = 2.96mm; Lf = 22.41 mm.

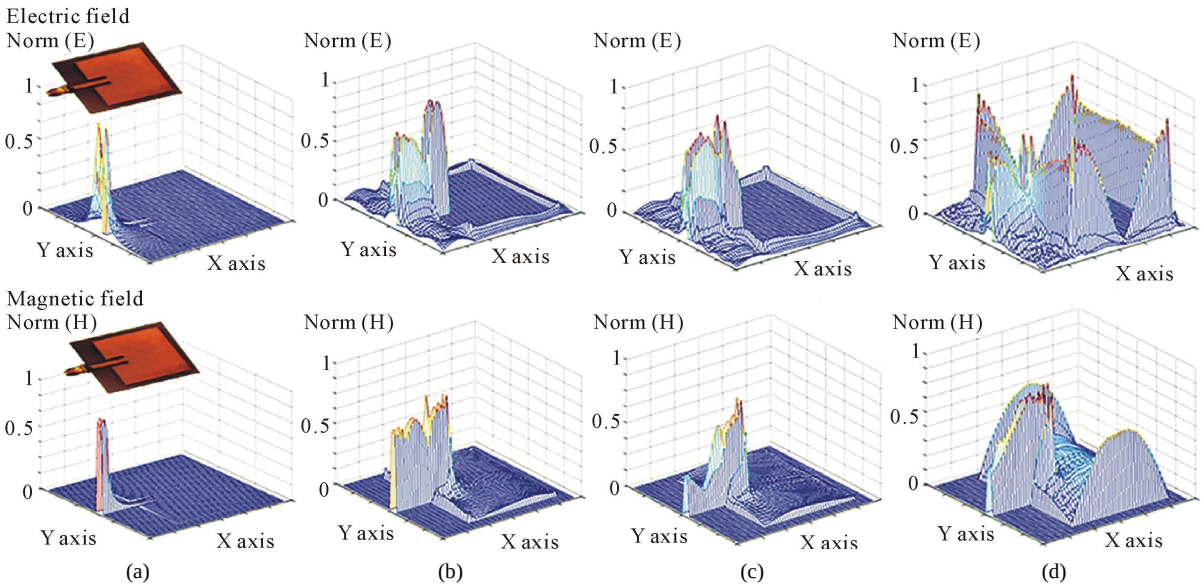

Figure 10. Comparison of electromagnetic field in term of iteration number. (a) n = 1 round; (b) n = 5 rounds; (c) n = 10 rounds; (d) n =200 rounds.

Figure 11. Experiment of the patch antenna.

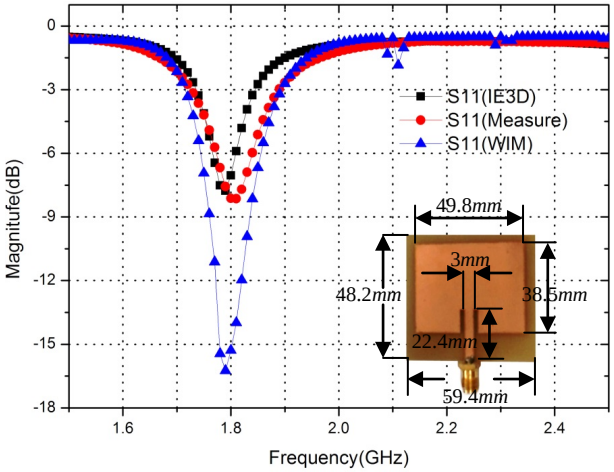

Figure 12. Simulated and measured results of return loss.

Agilent Technologies, as shown in **Figure 11**.

The WIM simulated result of return loss of the designed patch antenna as shown in **Figure 12**, found that the center frequency is obtained at 1.8 GHz, and the −3 dB bandwidth is 180 MHz. Compared to the WIM simulation, theIE3D software and measurement of designed antenna are good agreement. Therefore, a little measurement errors were occurred, it may be the limitation of the experiment set, the interface between coaxial probe and conductor strip, and also the planar structure different in the implemented process.

5. Conclusions

We have demonstrated the full wave analysis based on the developed Wave Iterative Method (WIM) algorithm to analyze the simple microstip patch antenna. The novel WIM algorithm can provide a reasonably good approximation to the correct values of circuit parameters, and its accuracy is dependent on usable pixel size and mode number. Additionally, this algorithm has the advantage of representing the electromagnetic field on circuit structure. Finally, the contribution in this paper indicates the development of the novel WIM algorithm based on iterative method that can be used to analyze effectively in arbitrarily inhomogeneous region formations.

In the future, the proposed WIM algorithm will be also applied to MMICs, various planar circuit structures, passive circuit in the waveguide, and the electromagnetic solving for EMI/EMC problems.

References

[1] Carrasco, J.A. and Sune, V. (2011) A Numerical Method for the Evaluation of the Distribution of Cumulative Reward

till Exit of a Subset of Transient States of a Markov Reward Model. *IEEE Transactions on Dependable and Secure Computing*, **8**, 798-809. http://dx.doi.org/10.1109/TDSC.2010.49

[2] Lezar, E. and Davidson, D.B. (2011) GPU-Accelerated Method of Moments by Example: Monostatic Scattering. *IEEE Antennas and Propagation Magazine*, **52**, 120-135.

[3] Li, H., *et al.* (2010) Multi-Target Scattering Analysis Based on Generalized Higher-Order Finite-Difference Time-Domain Method. *International Conference on Microwave and Millimeter Wave Technology* (*ICMMT*), Chengdu, 8-11 May 2010, 88-90.

[4] Gao, X.-K., Chua, E.-K. and Li, E.-P. (2011) Application of Integrated Transmission Line Modeling and Behavioral Modeling on Electromagnetic Immunity Synthesis. *IEEE International Symposium on Electromagnetic Compatibility* (*EMC*), Long Beach, 14-19 August 2011, 910-915. http://dx.doi.org/10.1109/ISEMC.2011.6038438

[5] Akatimagool, S., Bajon, D. and Baudrand, H. (2001) Analysis of Multi-Layer Integrated Inductors with Wave Concept Iterative Procedure (WCIP). *IEEE MTT-S International in Microwave Symposium Digest*, **3**, 1941-1944.

[6] Tellache, M. and Baudrand, H. (2011) Efficient Iterative Method for Characterization of Microwave Planar Circuits. 11*th Mediterranean Microwave Symposium* (*MMS*), Phoenix, 20-24 May 2001, 265-272.

[7] Hajlaoui, E.A., Glaoui, M. and Trabelsi, H. (2006) Analysis of Multilayer Microstrip Filter by Wave Concept Iterative Process. *International Conference on Design and Test of Integrated Systems in Nanoscale Technology*, Tunis, 5-7 September 2006, 150-153.

[8] Raveu, N., Prigent, G., Pigaglio, O. and Baudrand, H. (2010) Different Spectral Scale Level in the Wave Concept Iterative Procedure to Solve Multi-Scale Problems. *IET Microwaves, Antennas & Propagation*, **4**, 1247-1255. http://dx.doi.org/10.1049/iet-map.2008.0416

[9] Ji, W.-S., Luo, Q.-Z. and Yang F. (2010) Analysis of H-shaped Patch Antenna by Wave Concept Iterative Procedure (WCIP). *International Conference on Microwave and Millimeter Wave Technology* (*ICMMT*), Chengdu, 8-11 May 2010, 797-800.

[10] Akatimagool, S. and Choocadee, S. (2013) Wave Iterative Method for Electromagnetic Simulation. In: Zheng, Y., Ed., *Wave Propagation Theories and Applications*, InTech, Charpter14, 331-352.

[11] Tao, Q., Nie, Z.P. and Zong, X.Z. (2012) Numerical Solution of the Horn Antenna with Complex Structure. *International Symposium on Antennas, Propagation & EM Theory* (*ISAPE*), Xi'an, 22-26 October 2012, 562-565.

[12] Husoy, J.H. (2003) Making a Case for Iterative Linear Equation Solvers in DSP Education. *IEEE International Conference on Acoustics, Speech, and Signal Processing* (*ICASSP*'03), 6-10 April 2003, Vol. 3, 765-768.

[13] Liao, S.Y. (1988) Microwave Circuit Analysis and Amplifier Design. Prentice-Hall International Inc., Upper Saddle River.

[14] Hong, J.G. and Lancaster, M.J. (2001) Microstrip Filters for RF/Microwave Applications. Wiley, Hoboken.

[15] Ramesh, G., *et al.* (2001) Microstrip Antenna Design Handbook. Artech House Inc, Boston.

Applied Mathematics, 2015, 6, 414-420
Published Online February 2015 in SciRes. http://www.scirp.org/journal/am
http://dx.doi.org/10.4236/am.2015.62038

Scientific Research Publishing

Skeletons of 3D Surfaces Based on the Laplace-Beltrami Operator Eigenfunctions

Adolfo Horacio Escalona-Buendia[1], Lucía Ivonne Hernández-Martínez[2], Rafael Martínez-Vega[2], Julio Roberto Murillo-Torres[2], Omar Nieto-Crisóstomo[1]

[1]Academia de Informática, Universidad Autónoma de la Ciudad de México, Mexico City, Mexico
[2]Academia de Matemáticas, Universidad Autónoma de la Ciudad de México, Mexico City, Mexico
Email: aheb@xanum.uam.mx

Received 25 January 2015; accepted 13 February 2015; published 17 February 2015

Abstract

In this work we describe the algorithms to construct the skeletons, simplified 1D representations for a 3D surface depicted by a mesh of points, given the respective eigenfunctions of the Discrete Laplace-Beltrami Operator (LBO). These functions are isometry invariant, so they are independent of the object's representation including parameterization, spatial position and orientation. Several works have shown that these eigenfunctions provide topological and geometrical information of the surfaces of interest [1] [2]. We propose to make use of that information for the construction of a set of skeletons, associated to each eigenfunction, which can be used as a fingerprint for the surface of interest. The main goal is to develop a classification system based on these skeletons, instead of the surfaces, for the analysis of medical images, for instance.

Keywords

Skeleton, Centerline, Discrete Laplace-Beltrami Operator Eigenfunctions, Graph Theory

1. Skeletons

A curve-skeleton is a 1D model of a 3D object that captures the general characteristics of the original object, and it is also known as centerline. They are useful for visualization and virtual navigation. Another application is registration of 3D objects: given a query object, the task is to find similar objects in a database by using the curve-skeleton as a fingerprint. A great variety of algorithms for the generation of skeletons have been developed in recent years [3] [4].

Shape intrinsic information should not depend on the given representation of the object. However, many of the current methods of skeleton construction have the weakness of being sensitive to changes on scale factors,

How to cite this paper: Escalona-Buendia, A.H., Hernández-Martínez, L.I., Martínez-Vega, R., Murillo-Torres, J.R. and Nieto-Crisóstomo, O. (2015) Skeletons of 3D Surfaces Based on the Laplace-Beltrami Operator Eigenfunctions. *Applied Mathematics*, **6**, 414-420. http://dx.doi.org/10.4236/am.2015.62038

changes in the surface's triangulation, orientation, etcetera. It is desirable that the curve-skeletons have certain properties in order to be used as fingerprints [1]:

- Topology preserving. Two objects have the same topology if they have the same number of connected components and cavities. Though a 1D curve cannot have cavities, skeletons must be able to grasp objects characteristics related to its genus.
- Scaling invariant. It is necessary for the skeletons to be measurement unit independent; *i.e.* that it does not depend on the way in which the object could be measured.
- Isometry invariant. The skeleton of an object should be independent of the object's given depiction and location.
- Rotation invariant. Therefore, checking if two objects are similar needs no prior alignment.
- Similarity. Similar objects should have similar fingerprints.

In particular, it is known, that the eigenfunctions of the Laplace-Beltrami Operator satisfy several of the properties required for a fingerprint [1], for instance:

The eigenfunctions depend only on the gradient and divergence which are dependent on the Riemannian structure of the manifold, so they are clearly isometry invariant.

The eigenfunctions are normalizable, therefore, there is no need to concern about scale factors.

Recently, several methods have been developed making use of these eigenfunctions to construct the curve-skeletons of objects of interest [5].

2. Surfaces Representation

Object File Format (.off) files are used to represent the geometry of a model by specifying a triangulation of the model's surface. The OFF files in the Princeton Shape Benchmark [6] conform to the following standard:

OFF files are text files.

It has a header line with the string OFF.

The second line states the number of vertices, the number of faces, and the number of edges; however the number of edges can be ignored for our purpose.

The next lines describe the Cartesian coordinates of each vertex, written one per line. The enumeration of the vertices is given by the order they occurred in the file, starting with 0.

After the list of vertices, the faces are listed; starting with the number of sides and followed by the oriented list of vertices included. All the faces are oriented in the same direction.

The faces can have any number of vertices, although they usually are triangles. For example, **Table 1** shows the description of a unitary cube in this format.

Case of Study

Our present case of study are surfaces of rat-hippocampus, obtained from MRI images. On reported works, a relation between morphological changes in the hippocampus and Alzheimer disease in early stages has been found; nowadays there are many studies in image analysis of this and other different brain structures [7].

As many works have shows, the first eigenfunction of the Laplace-Beltrami operator clearly identifies a principal direction of the surfaces of interest, so it is very useful to build a skeleton. Besides that, we noticed that the second eigenfunction reveals additional geometrical information, such as localization of protuberance. Thus, we decided to build a skeleton based on the second eigenfunction also. The construction of both skeletons will be described in detail in section 4. We expect that the properties of these skeletons will provide important information regarding the geometry of objects of interest in order to classify them in a more detailed manner.

3. Laplace-Beltrami Operator

Let $f \in C^2$ be a real-valued function defined on a Riemannian manifold M:

$$f : M \to \mathbf{R}. \tag{1}$$

The Laplace-Beltrami operator is defined as

$$\Delta f = \operatorname{div}(\nabla f) \tag{2}$$

This operator appears in several equations in physics:

Table 1. Unitary cube.

OFF				
8	6	0		
0.0	0.0	0.0		
1.0	0.0	0.0		
0.0	1.0	0.0		
1.0	1.0	0.0		
0.0	0.0	1.0		
1.0	0.0	1.0		
0.0	1.0	1.0		
1.0	1.0	1.0		
4	0	1	3	2
4	0	4	5	1
4	0	2	6	4
4	3	1	5	7
4	3	7	6	2
4	6	7	5	4

$$\text{wave equation}: \Delta u = u_{tt} / c^2 \tag{3}$$

$$\text{diffusion equation}: \Delta u = u_t / \alpha^2 \tag{4}$$

The method of separation of variables allows us to isolate the spatial dependence of u from the temporal dependence. Let $u(r,t) = f(r)a(t)$, substituting this into the wave equation produces

$$c^2 \frac{\Delta f}{f} = \frac{a_{tt}}{a} = \lambda \tag{5}$$

$$\Delta f = \lambda f \tag{6}$$

The substitution into diffusion equation leads to the same result. The solution of Equation (6) is a set of eigenvalues $\lambda_1, \lambda_2, \cdots$ and a set of eigenfunctions $f_1, f_2, \cdots$ which can be thought as fundamental vibration modes.

Finite Element Method

We do not have an equation describing a differentiable variety M, thus we work with a discrete representation of a triangulated surface S described by an OFF file. We need a numerical integration method to solve Equation (6) on S. We have opted to use the Finite Element Method [2].

First of all, we choose N linearly independent form functions $F_1, F_2, \cdots, F_N$ as a basis of a vector space. These base functions $F_i : S \to \mathbf{R}$ are chosen to simplify the calculations, so they are constructed as linear functions that "sample" function f at each vertex of the triangulated surface:

$$F_i(j) = \begin{cases} 1 & \text{for } i = j, \\ 0 & \text{for } i \neq j. \end{cases} \tag{7}$$

The function f then can be written as a linear combination of these base functions

$$f = \sum U_i F_i \tag{8}$$

The substitution of this approximation in (6) reduces the equation to a generalized eigenvalue problem.

$$AU = \lambda BU \tag{9}$$

where the entry U_i is the contribution of f at vertex i on S. The components of matrix A are given by:

$$A_{ij} = \oint_S \nabla F_i \cdot \nabla F_j \mathrm{d}s \tag{10}$$

and the components of matrix B are:

$$B_{ij} = \oint_S F_i \cdot F_j \mathrm{d}s \tag{11}$$

Figure 1(a) and **Figure 1(b)** show the first and second eigenfunctions, respectively, of Equation (9) applied on a triangulated surface of a rat-hippocampus. The lower values are colored in blue and the higher ones in red. We can see the monotonous behavior of the first function whereas the second function grows from the middle of the surface through its extremes.

4. The Construction of the Skeletons

The first step is to transform the OFF format into a graph, in this way we can use standard Graph Theory methods. Let be $\mathbf{G} = \{\mathbf{V}, \mathbf{E}\}$, the vertices **V** are indexed as they are in the OFF file, and the edges **E** can be easily obtained from the list of faces.

We chose the adjacency lists representation for simplicity and efficiency on a triangulated surface with thousands of vertices, usually each one is adjacent only up to five or six vertices; although that number depends on the triangulation and the surfaces. **Table 2** shows the adjacency lists of the unitary cube above.

Although the graph is undirected, we allow redundancy of edges in order to simplify the search for local maxima and minima of the eigenfunctions.

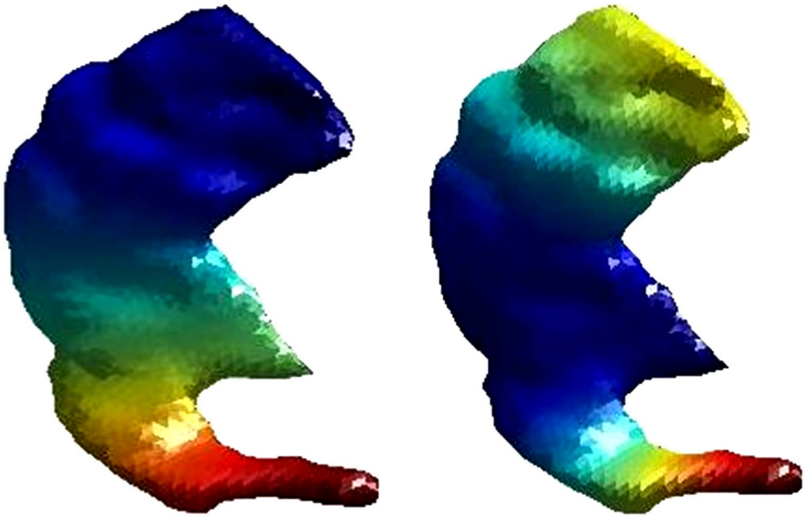

(a) (b)

Figure 1. First (a) and second (b) eigenfunctions on a hippocampus surface.

Table 2. Adjacency lists for the unitary cube.

0:	1	4	2
1:	3	5	0
2:	0	6	3
3:	2	1	7
4:	5	0	6
5:	1	7	4

We do not want to modify the OFF files, so we use an auxiliary file with the values of the first eigenfunctions calculated for each vertex, this is done with the method described in the previous section. On the surfaces studied, we have observed that each eigenfunction gives different information:

- The first eigenfunction f_1 has one maximum and one minimum at opposite points of the surface, these extreme points give us a principal axis, and a main direction (**Figure 1(a)**). So we decide to use this function to build a polygonal skeleton, which can give us information about curvature and torsion.
- The second eigenfunction f_2 has several local maxima and minima at the prominent protuberances of the surface (**Figure 1(b)**). So we decide to use this function to build a tree-based skeleton that captures the arborescent structure of the surface.

So we need two variations of the same algorithm, one for each eigenvalue.

4.1. First Eigenfunction Skeleton

Let M and m be the vertices with the absolute maximum and minimum values of the first eigenfunction: $f_1(M)=e_M$ and $f_1(m)=e_m$, respectively. We define a set of energy levels $\{e_0,e_1,\cdots,e_n\}$ equally spaced:

$$e_i = e_m + (e_M - e_m)\frac{i}{n},\ i=0,1,\cdots,n \tag{12}$$

The vertices fall between these energy levels, however there are some edges with one vertex in one level and the other in the following, so we define a boundary as a subgraph $\mathbf{B}_i=\{\mathbf{V}_i,\mathbf{E}_i\}$:

$$\begin{aligned}\mathbf{E}_i &= \left\{(j,k)\in\mathbf{E}\,\middle|\, f_1(j)\le e_i \wedge f_1(k)\ge e_i\right\}\\ \mathbf{V}_i &= \text{All vertices of } \mathbf{E}_i\end{aligned} \tag{13}$$

These boundaries generate a partition of the original graph.

We perform a deep-first search to find one vertex in the boundary $\mathbf{B}_i$, and a second deep-first search to get all the vertices in it. It is possible that for some energy levels these are so close to each other that the algorithm cannot find a definite boundary; in this case we skip to the next level.

Each boundary $\mathbf{B}_i$ is a "ring" of vertices, which must be reduced into a centroid c_i that can be calculated as a "center of mass":

$$c_i = \frac{1}{N_i}\sum_{j\in\mathbf{V}_i} r_j,\ \text{for } i=1,2,\cdots,n-1;\ N_i=|V_i| \tag{14}$$

where r_j represents the coordinates of the vector of vertex j. Obviously, the boundaries for e_m and e_M have just one vertex, so $c_0=r_m$ and $c_n=r_M$.

Finally we connect these centroids to build the skeleton; this last step is performed by the Prim's algorithm [8]. This algorithm finds the minimum cost-spanning tree of the set of centroids c_i, using their Euclidean distances as the costs function. Although the skeleton for the first eigenfunction is a polygonal, it can be seen as a degenerated tree (a one-degree tree).

Figure 2(a) and **Figure 2(b)** show the first eigenfunction skeletons of two surfaces for 32 energy levels.

4.2. The Second Eigenfunction Skeleton

As we exposed for the first eigenfunction, we search for the absolute maximum and minimum points $f_2(M)=e_M$ and $f_2(m)=e_m$ and, in this case, we also search for local minima and maxima. A local maximum (or minimum) is a vertex l which is surrounded by vertices of lower (or upper) values of f_2.

$$\mathbf{L}=\left\{l\in\mathbf{V}\,\middle|\,\forall u\in\mathbf{V},\ (l,u)\in\mathbf{E}\Rightarrow f_2(l)>f_2(u)\vee\forall u\in\mathbf{V},\ (l,u)\in\mathbf{E}\Rightarrow f_2(l)<f_2(u)\right\} \tag{15}$$

The search can be easily done in the adjacency lists of $\mathbf{E}$.

We use the coordinates vectors of these vertices as the base of the centroids set:

$$\begin{aligned}&c_0 = r_m;\\ &c_{i(l)} = r_l,\ \forall l\in\mathbf{L},\ i(l)\ \text{an enumeration of } \mathbf{L};\\ &c_{p+1} = r_M,\ \text{where } p=|\mathbf{L}|.\end{aligned} \tag{16}$$

We define the energy levels e_i as in (12) and the boundaries $\mathbf{B}_i$ as in (13). However each one of these boundaries could have k connected components $\mathbf{B}_{i1}, \mathbf{B}_{i2}, \cdots, \mathbf{B}_{ik}$, each one has its own centroid $c_{i1}, c_{i2}, \cdots, c_{ik}$, as defined in (14). The algorithm for the second eigenfunction process the surface as a tree structure: it performs a deep-first search for a set of boundaries with their respective branch of centroids, and then it performs a second search to find a second branch, an so on. The partition of the surface defined by the first search avoids the algorithm to fall into the same boundaries.

In this case, the Prim's algorithm shows all its performance in the construction of the skeleton, connecting the set of centroids as a minimum-cost spanning tree. In order to avoid that the skeleton cuts the surface, we add directions to the distances between centroids. We associate the information of the energy level to each centroid:

$$h\left(c_{i(l)}\right) = f_2(l) \text{ for the centers defined in } (16), \tag{17}$$

$$h\left(c_{ik}\right) = e_i \text{ for the centroid of } \mathbf{B}_{ik}. \tag{18}$$

The algorithm connects the centroids in increasing order of $h(c)$. **Figure 3(a)** and **Figure 3(b)** show the second eigenfunction skeletons of the same surfaces as **Figure 2** and **Figure 3**.

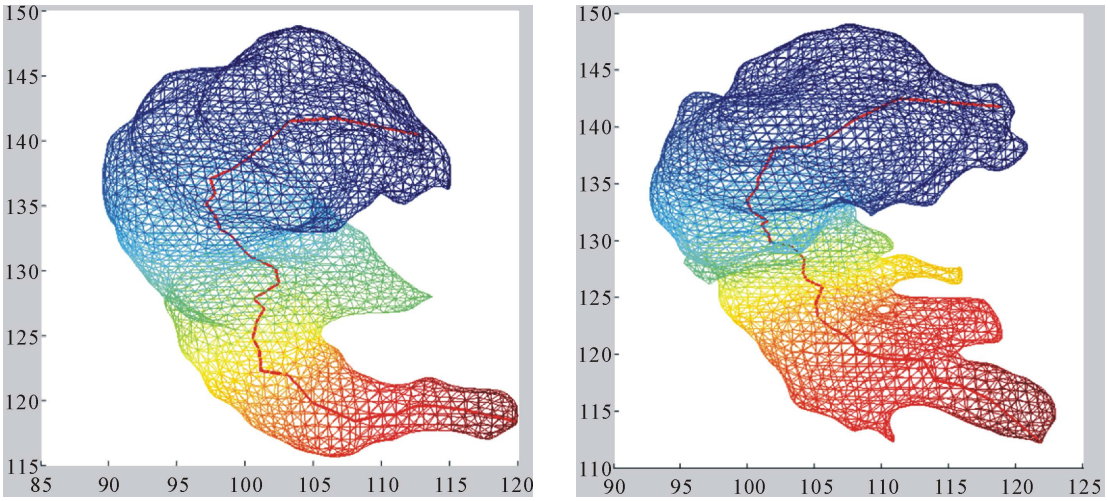

(a) (b)

Figure 2. Skeletons of the first eigenfunction on hippocampus (a) and hippocampus (b).

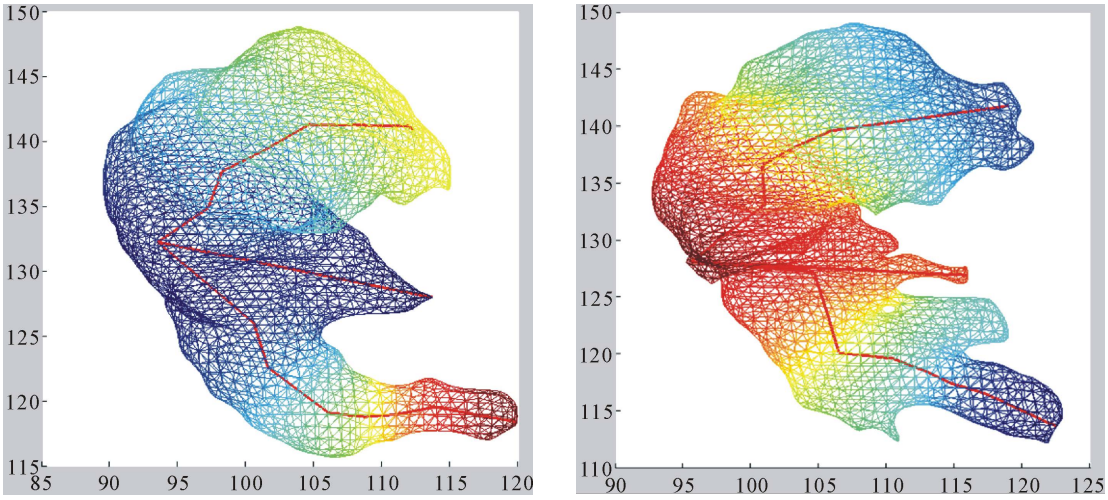

(a) (b)

Figure 3. Skeletons of the second eigenfunction on hippocampus (a) and hippocampus (b).

5. Conclusions and Further Work

We have developed the algorithms for building the skeletons for the first and second eigefunctions of the Laplace-Beltrami operator calculated on an rat-hippocampus surface depicted by an OFF file.

The skeleton for the first eigenfunction is built as a polygonal structure along the main axis of the surface. The skeleton for the second eigenfunction has a tree-structure with two main branches, each one with a similar structure to the first skeleton, and small branches for some local maxima at prominent protuberances.

This is a first step for the developing of a classification system. The next steps are to generalize these results for different anatomical structures, and define characterization methods for these skeletons based on their geometrical and topological properties, such as critical points of curvature and torsion, bifurcation points, number of branches, etcetera.

References

[1] Reuter, M., Wolter, F.E. and Peinecke, N. (2006) Laplace-Beltrami Spectra as "Shape-DNA" of Surfaces and Solids. *Computer-Aided Design*, **38**, 342-366. http://dx.doi.org/10.1016/j.cad.2005.10.011

[2] Reuter, M., Biasotii, S., Patanè, G. and Spagnulo, M. (2009) Discrete Laplace-Beltrami Operators for Shape Analysis and Segmentation. *Computer & Graphics*, **33**, 381-390. http://dx.doi.org/10.1016/j.cag.2009.03.005

[3] Sadleir, R.J.T. and Whelan, P.F. (2005) Fast Colon Centerline Calculation Using Optimized 3D Topological Thinning. *Computerized Medical Imaging and Graphics*, **29**, 251-318. http://dx.doi.org/10.1016/j.compmedimag.2004.10.002

[4] Cornea, H.D., Siver, D. and Min, P. (2005) Curve-Skeleton Applications. *IEEE Visualization*, 23-28 October 2005, 95-102.

[5] Seo, S., Chung, M.K., Whyms, B.J. and Vorperian, H.K. (2011) Mandible Shape Modeling Using the Second Eigenfunction of the Laplace-Beltrami Operator. *Proceedings of SPIE, Medical Imaging*, 2011: *Image Processing*, **7962**, 79620Z. http://dx.doi.org/10.1117/12.877537

[6] Object File Format (2005) Princeton Shape Benchmark. http://shape.cs.princeton.edu/benchmark/documentation/off_format.html

[7] Thompson, P.M., Hayashi, K.M., *et al.* (2004) Mapping Hippocampal and Ventricular Change in Alzheimer Disease. *Neuroimage*, **22**, 1754-1766. http://dx.doi.org/10.1016/j.neuroimage.2004.03.040

[8] Aho, A.V., Hopcfort, J.E. and Ullman, J.D. (1983) Data Structures and Algorithms. Addison-Welsey, Boston.

Applied Mathematics, 2015, 6, 421-429
Published Online February 2015 in SciRes. http://www.scirp.org/journal/am
http://dx.doi.org/10.4236/am.2015.62039

Scientific Research Publishing

Generalized Spectrum of Steklov-Robin Type Problem for Elliptic Systems

Alzaki Fadlallah, Kwadwo Antwi-Fordjour, Marius N. Nkashama

Department of Mathematics, University of Alabama at Birmingham, Birmingham, USA
Email: zakima99@uab.edu, kantwi@uab.edu, nkashama@math.uab.edu

Received 25 January 2015; accepted 13 February 2015; published 17 February 2015

Abstract

We will study the generalized Steklov-Robin eigenproblem (with possibly matrix weights) in which the spectral parameter is both in the system and on the boundary. The weights may be singular on subsets of positive measure. We prove the existence of an increasing unbounded sequence of eigenvalues. The method of proof makes use of variational arguments.

Keywords

Steklov-Robin, Variational Arguments, Matrix Weights

1. Introduction

We study the generalized Steklov-Robin eigenproblem. This spectrum includes the Steklov, Neumann and Robin spectra. We therefore generalize the results in [1]-[4].

Consider the elliptic system

$$\begin{aligned} -\Delta U + A(x)U &= \mu M(x)U \quad \text{in } \Omega, \\ \frac{\partial U}{\partial \nu} + \Sigma(x)U &= \mu P(x)U \quad \text{on } \partial\Omega, \end{aligned} \tag{1}$$

where $\Omega \subset \mathbb{R}^N$, $N \geq 2$ is a bounded domain with boundary $\partial\Omega$ of class $C^{0,1}$, $U = [u_1, \cdots, u_k]^{\mathrm{T}} \in H(\Omega) := \left[H^1(\Omega)\right]^k = H^1(\Omega) \times H^1(\Omega) \times \cdots \times H^1(\Omega)$. Throughout this paper all matrices are symmetric. The matrix

$$A(x) = \begin{bmatrix} a_{11}(x) & a_{12}(x) & \cdots & a_{1k}(x) \\ a_{21}(x) & a_{22}(x) & \cdots & a_{2k}(x) \\ \vdots & \vdots & \ddots & \vdots \\ a_{k1}(x) & a_{k2}(x) & \cdots & a_{kk}(x) \end{bmatrix},$$

How to cite this paper: Fadlallah, A., Antwi-Fordjour, K. and Nkashama, M.N. (2015) Generalized Spectrum of Steklov-Robin Type Problem for Elliptic Systems. *Applied Mathematics*, **6**, 421-429. http://dx.doi.org/10.4236/am.2015.62039

verifies the following conditions:

($A1$) The functions $a_{ij}:\Omega\to\mathbb{R}$.

($A2$) $A(x)$ is positive semidefinite a.e. on Ω with $a_{ij}\in L^{p}(\Omega)\ \forall i,j=1,\cdots,k,$ for $p>\frac{N}{2}$ when $N\geq 3$, and $p>1$ when $N=2$.

The matrix

$$M(x)=\begin{bmatrix} m_{11}(x) & m_{12}(x) & \cdots & m_{1k}(x)\\ m_{21}(x) & m_{22}(x) & \cdots & m_{2k}(x)\\ \vdots & \vdots & \ddots & \vdots\\ m_{k1}(x) & m_{k2}(x) & \cdots & m_{kk}(x)\end{bmatrix}$$

satisfies the following conditions:

($M1$) $M(x)$ is positive semidefinite a.e. on Ω The functions $m_{ij}:\Omega\to\mathbb{R},$ for $p\geq\frac{N}{2}$ when $N\geq 3$, and $p>1$ when $N=2$.

$\partial/\partial\nu:=\nu\cdot\nabla$ is the outward (unit) normal derivative on $\partial\Omega$. The matrix

$$\Sigma(x)=\begin{bmatrix} \sigma_{11}(x) & \sigma_{12}(x) & \cdots & \sigma_{1k}(x)\\ \sigma_{21}(x) & \sigma_{22}(x) & \cdots & \sigma_{2k}(x)\\ \vdots & \vdots & \ddots & \vdots\\ \sigma_{k1}(x) & \sigma_{k2}(x) & \cdots & \sigma_{kk}(x)\end{bmatrix},$$

verifies the following conditions:

($S1$) The functions $\sigma_{ij}:\partial\Omega\to\mathbb{R}$.

($S2$) $\Sigma(x)$ is positive semidefinite a.e. on $\partial\Omega$ with $\sigma_{ij}\in L^{q}(\partial\Omega)\ \forall i,j=1,\cdots,k,$ for $q\geq N-1$ when $N\geq 3$, and $q>1$ when $N=2$,
and the matrix

$$P(x)=\begin{bmatrix} \rho_{11}(x) & \rho_{12}(x) & \cdots & \rho_{1k}(x)\\ \rho_{21}(x) & \rho_{22}(x) & \cdots & \rho_{2k}(x)\\ \vdots & \vdots & \ddots & \vdots\\ \rho_{k1}(x) & \rho_{k2}(x) & \cdots & \rho_{kk}(x)\end{bmatrix}.$$

($P1$) $P(x)$ is positive semidefinite a.e. on $\partial\Omega$ for $q\geq N-1$ when $N\geq 3$, and $q>1$ when $N=2$.

We assume that $A(x),\Sigma(x),M(x),P(x)$ verify the following assumptions:

Assumption 1. *$A(x)$ is positive definite on a set of positive measure of Ω,*
or *$\Sigma(x)$ is positive definite on a set of positive measure of $\partial\Omega$.*
And *$M(x)$ is positive definite on a set of positive measure of Ω,*
or *$P(x)$ is positive definite on a set of positive measure of $\partial\Omega$.*

Remark 2. *Assumption* 1 *is equivalent to*

$$\int_{\Omega}\langle A(x)U,U\rangle\mathrm{d}x+\int_{\partial\Omega}\langle\Sigma(x)U,U\rangle\mathrm{d}x>0\quad\forall U\neq 0.$$

Remark 3. *Since $A(x),\Sigma(x),M(x),P(x)$ satisfy* (A2), (S2), (M1), (P1) *respectively, then we can write them in the following form* (*i.e.*; *eigen-decomposition of a positive semi-definite matrix or diagonalization*)

$$J(x)=Q_{J}^{\mathrm{T}}(x)D_{J}(x)Q_{J}(x).$$

where $Q_{J}(x)^{\mathrm{T}}Q_{J}(x)=I$ ($Q_{J}^{\mathrm{T}}(x)=Q_{J}^{-1}(x)$ i.e.; are orthogonal matrices) are the normalized eigenvectors, I is the identity matrix, $D_{J}(x)$ is diagonal matrix and in the diagonal of $D_{J}(x)$ are the eigenvalues of J (i.e.; $D(x)_{J}=\mathrm{diag}\left(\lambda_{1}^{J}(x),\cdots,\lambda_{k}^{J}(x)\right)$) and $J=\{A,\Sigma,M,P\}$.

Remark 4. *The weight matrices $M(x)$ and $P(x)$ may vanish on subsets of positive measure.*

Definition 1. *The generalized Steklov-Robin eigensystem is to find a pair $(\mu,\varphi)\in\mathbb{R}\times H(\Omega)$ with $\varphi\not\equiv 0$*

such that

$$\begin{aligned}&\int_\Omega \nabla\varphi\cdot\nabla U\mathrm{d}x+\int_\Omega\langle A(x)\varphi,U\rangle\mathrm{d}x+\int_{\partial\Omega}\langle\Sigma(x)\varphi,U\rangle\mathrm{d}x\\&=\mu\left[\int_\Omega\langle M(x)\varphi,U\rangle\mathrm{d}x+\int_{\partial\Omega}\langle P(x)\varphi,U\rangle\mathrm{d}x\right]\quad\forall U\in H(\Omega).\end{aligned}\tag{2}$$

Remark 5. *Let* $U=\varphi$ *in* (2) *if there is such an eigenpair, then* $\mu>0$ *and*

$$\int_\Omega\langle M(x)\varphi,\varphi\rangle\mathrm{d}x+\int_{\partial\Omega}\langle P(x)\varphi,\varphi\rangle\mathrm{d}x>0.$$

Indeed, if $\int_\Omega\langle M(x)\varphi,\varphi\rangle\mathrm{d}x+\int_{\partial\Omega}\langle P(x)\varphi,\varphi\rangle\mathrm{d}x=0,$ or $\mu=0,$ then

$$\int_\Omega|\nabla\varphi|^2\,\mathrm{d}x+\int_\Omega\langle A(x)\varphi,\varphi\rangle\mathrm{d}x+\int_{\partial\Omega}\langle\Sigma(x)\varphi,\varphi\rangle\mathrm{d}x=0.$$

We have that $\int_\Omega|\nabla\varphi|^2\,\mathrm{d}x=0$ which implies that $\varphi=\text{constant},$ and $\int_\Omega\langle A(x)\varphi,\varphi\rangle\mathrm{d}x=0$ this implies that $\langle A(x)\varphi,\varphi\rangle=0,$ a.e. (with $\varphi\neq0$) in Ω. This implies that $A(x)$ is not positive definite on a subset of Ω of positive measure, and $\int_{\partial\Omega}\langle\Sigma(x)\varphi,\varphi\rangle\mathrm{d}x=0,$ then $\langle\Sigma(x)\varphi,\varphi\rangle=0,$ a.e. with $(\varphi\neq0)$ on $\partial\Omega.$ This implies that $\Sigma(x)$ is not positive definite on subset of $\partial\Omega$ of positive measure. So we have that, φ would be a constant vector function; which would contradict the assumptions (Assumption 1) imposed on $A(x)$ and $\Sigma(x).$

Remark 6. *If* $A(x)\equiv0$ *and* $\Sigma(x)\equiv0$ *then* $\mu=0$ *is an eigenvalue of the system* (1) *with eigenfunction* $\varphi=\text{constant}$ *vector function on* $\overline{\Omega}$.

It is therefore appropriate to consider the closed linear subspace (to be shown below) of $H(\Omega)$ under Assumption 1 defined by

$$\mathbb{H}_{(M,P)}(\Omega):=\left\{U\in H(\Omega):\int_\Omega\langle M(x)U,U\rangle\mathrm{d}x+\int_{\partial\Omega}\langle P(x)U,U\rangle\mathrm{d}x=0\right\}.$$

Now all the eigenfunctions associated with (2) must belong to the (A,Σ)-orthogonal complement $H_{(M,P)}(\Omega):=\left[\mathbb{H}_{(M,P)}(\Omega)\right]^\perp$ of this subspace in $H(\Omega).$ We will show that indeed $\mathbb{H}_{(M,P)}(\Omega)$ is subspace of $H(\Omega).$ Let $U,V\in\mathbb{H}_{(M,P)}(\Omega)$ and $\alpha\in\mathbb{R}$ we wish to show that $\alpha U\in\mathbb{H}_{(M,P)}(\Omega)$ and $U+V\in\mathbb{H}_{(M,P)}(\Omega).$

$$\begin{aligned}&\left(\int_\Omega\langle M(x)(\alpha U),\alpha U\rangle\mathrm{d}x+\int_{\partial\Omega}\langle P(x)(\alpha U),\alpha U\rangle\mathrm{d}x\right)\\&=\alpha^2\left(\int_\Omega\langle M(x)U,U\rangle\mathrm{d}x+\int_{\partial\Omega}\langle P(x)U,U\rangle\mathrm{d}x\right)=^{U\in\mathbb{H}_{(M,P)}(\Omega)}0.\end{aligned}$$

Therefore $\alpha U\in\mathbb{H}_{(M,P)}(\Omega).$ Now we show that $U+V\in\mathbb{H}_{(M,P)}(\Omega).$

$$\begin{aligned}&\int_\Omega\langle M(x)(U+V),(U+V)\rangle\mathrm{d}x+\int_{\partial\Omega}\langle P(x)(U+V),(U+V)\rangle\mathrm{d}x\\&=\int_\Omega\langle M(x)U,U\rangle\mathrm{d}x+\int_{\partial\Omega}\langle P(x)U,U\rangle\mathrm{d}x+\int_\Omega\langle M(x)V,V\rangle\mathrm{d}x\\&\quad+\int_{\partial\Omega}\langle P(x)V,V\rangle\mathrm{d}x+2\int_\Omega\langle M(x)U,V\rangle\mathrm{d}x+2\int_{\partial\Omega}\langle P(x)U,V\rangle\mathrm{d}x.\end{aligned}$$

Since $U\in\mathbb{H}_{(M,P)}(\Omega),$ it follows that

$$\begin{aligned}0&=\int_\Omega\langle M(x)U,U\rangle\mathrm{d}x=\int_\Omega\langle Q_M^{\mathrm{T}}(x)D_M(x)Q_M(x)U,U\rangle\mathrm{d}x\\&=\int_\Omega\langle D_M(x)Q_M(x)U,Q_M(x)U\rangle\mathrm{d}x.\end{aligned}$$

By setting $y(x):=Q_M(x)U,$ we get

$$0=\int_\Omega\langle D_M(x)y(x),y(x)\rangle\mathrm{d}x=\sum_{i=1}^k\int_\Omega\lambda_i^M(x)y_i^2(x)\mathrm{d}x.$$

Since $\lambda_i^M(x)\geq0$ for *a.e.* $x\in\Omega,$ it readily follows that

$$\lambda_i^M(x)y_i(x)=0\quad\text{for a.e. } x\in\Omega;$$

that is, the vector $D_M(x)y(x)$ satisfies

$$D_M(x)y(x)=0 \quad \text{for } a.e.\ x\in\Omega,$$

or equivalently

$$D_M(x)Q_M(x)U=0 \quad \text{for } a.e. \text{ on } \Omega.$$

Hence,

$$\begin{aligned}2\int_\Omega\langle M(x)U,V\rangle dx &= 2\int_\Omega\langle Q_M^{\mathrm{T}}(x)D_M(x)Q_M(x)U,V\rangle dx\\ &= 2\int_\Omega\langle D_M(x)Q_M(x)U,Q_M(x)V\rangle dx=0,\end{aligned}$$

since $D_M(x)Q_M(x)U=0$ *a.e.* on Ω. A similar arguments shows that

$$2\int_{\partial\Omega}\langle P(x)U,V\rangle dx=0.$$

Therefore $U+V\in\mathbb{H}_{(M,P)}(\Omega)$, so we have that $\mathbb{H}_{(M,P)}(\Omega)$ is a subspace of $H(\Omega)$. Thus, one can split the Hilbert space $H(\Omega)$ as a direct (A,Σ)-orthogonal sum in the following way

$$H(\Omega)=\mathbb{H}_{(M,P)}(\Omega)\oplus_{(A,\Sigma)}\left[\mathbb{H}_{(M,P)}(\Omega)\right]^{\perp}.$$

Remark 7. 1) *If* $M(x)\equiv 0$ *in* Ω, *then the subspace* $\mathbb{H}_{(M,P)}(\Omega)=H_0(\Omega):=\left[H_0^1\right]^k=H_0^1(\Omega)\times H_0^1(\Omega)\times\cdots\times H_0^1(\Omega)$, *provided* $P(x)>0$ *on* $\partial\Omega$.
2) *If* $P(x)\equiv 0$ *in* $\partial\Omega$ *and* $x\in\Omega(M)$, *then the subspace* $\mathbb{H}_{(M,P)}(\Omega)=\{0\}$, *provided* $M(x)>0$ *on* Ω.

- We shall make use in what follows the real Lebesgue space $L_k^q(\partial\Omega)$ for $1\le q\le\infty$, and of the continuity and compactness of the trace operator

$$\Gamma: H(\Omega)\to L_k^q(\partial\Omega) \quad \text{for } 1\le q<\frac{2(N-1)}{N-2},$$

is well-defined, it is a Lebesgue integrable function with respect to Hausdorff $N-1$ dimensional measure. Sometimes we will just use U in place of ΓU when considering the trace of a function on $\partial\Omega$. Throughout, this work we denote the $L_k^2(\partial\Omega)$-inner product by

$$\langle U,V\rangle_\partial:=\int_{\partial\Omega}U\cdot V dx$$

and the associated norm by

$$\|U\|_\partial^2:=\int_{\partial\Omega}U\cdot U \quad \forall U,V\in H(\Omega)$$

(see [5], [6] and the references therein for more details).

- The trace mapping $\Gamma: H(\Omega)\to L_k^2(\partial\Omega)$ is compact (see [7]).

$$\langle U,V\rangle_{(M,P)}=\int_\Omega\langle M(x)U,V\rangle dx+\int_{\partial\Omega}\langle P(x)U,V\rangle dx, \tag{3}$$

defines an inner product for $H(\Omega)$, with associated norm

$$\|U\|_{(M,P)}^2:=\int_\Omega\langle M(x)U,U\rangle dx+\int_{\partial\Omega}\langle P(x)U,U\rangle dx. \tag{4}$$

Now, we state some auxiliary result, which will be need in the sequel for the proof of our main result. Using the Hölder inequality, the continuity of the trace operator, the Sobolev embedding theorem and lower semicontinuity of $\|.\|_{(A,\Sigma)}$, we deduce that $\|.\|_{(A,\Sigma)}$ is equivalent to the standard $H(\Omega)$-norm. This observation enables us to prove the existence of an unbounded and discrete spectrum for the Steklov-Robin eigenproblem (1) and discuss some of its properties.

Definition 2. *Define the functional*

$$\Lambda_{A,\Sigma}: H(\Omega)\to[0,\infty),$$

$$\Lambda_{A,\Sigma}(U):=\int_\Omega\left[\nabla U\cdot\nabla U+\langle A(x)U,U\rangle\right]dx+\int_{\partial\Omega}\langle\Sigma(x)U,U\rangle dx=\|U\|_{(A,\Sigma)}^2, \quad \forall U\in H(\Omega),$$

and

$$\Upsilon_{M,P}: H(\Omega) \to [1,\infty),$$

$$\Upsilon_{M,P}(U) := \int_{\Omega} \langle M(x)U,U\rangle \mathrm{d}x + \int_{\partial\Omega} \langle P(x)U,U\rangle \mathrm{d}x - 1 = \|U\|^2_{(M,P)} - 1, \ \forall U \in H(\Omega).$$

Lemma 1. *Suppose* (A2), (S2), (M1), (P1) *are met. Then the functionals* $\Lambda_{A,\Sigma}$ *and* $\Upsilon_{M,P}$ *are* C^1*-functional* (*i.e.*; *continuously differentiable*).

See [8] *for the proof of Lemma* 1.

Theorem 8. $\Lambda_{A,\Sigma}$ *is G-differentiable and convex. Then* $\Lambda_{A,\Sigma}$ *is weakly lower-semi-continuous.*

See [8] *for the proof of Theorem* 8.

2. Main Result

Theorem 9. *Assume Assumption* 1 *as above, then we have the following.*

1) *The eigensystem* (1) *has a sequence of real eigenvalues*

$$0 < \mu_1 \le \mu_2 \le \mu_3 \le \cdots \le \mu_j \le \cdots \to \infty \quad \text{as } j \to \infty,$$

and each eigenvalue has a finite-dimensional eigenspace.

2) *The eigenfunctions* φ_j *corresponding to the eigenvalues* μ_j *from an* (A,Σ)*-orthogonal and* (M,P)*-orthonormal family in* $\left[\mathbb{H}_{M,P}(\Omega)\right]^{\perp}$ (*a closed subspace of* $H(\Omega)$).

3) *The normalized eigenfunctions provide a complete* (A,Σ)*-orthonormal basis of* $\left[\mathbb{H}_{M,P}(\Omega)\right]^{\perp}$. *Moreover, each function* $U \in \left[\mathbb{H}_{M,P}(\Omega)\right]^{\perp}$ *has a unique representation of the from*

$$\begin{aligned} U &= \sum_{j=1}^{\infty} c_j \varphi_j \quad \text{with } c_j := \frac{1}{\mu_j}\langle U,\varphi_j\rangle_{(A,\Sigma)} = \langle U,\varphi_j\rangle_{(M,P)}, \\ \|U\|^2_{(A,\Sigma)} &= \sum_{j=1}^{\infty} \mu_j |c_j|^2. \end{aligned} \tag{5}$$

In addition,

$$\|U\|^2_{(M,P)} = \sum_{j=1}^{\infty} |c_j|^2.$$

Proof of Theorem 9. We will prove the existence of a sequence of real eigenvalues μ_j and the eigenfunctions φ_j corresponding to the eigenvalues that from an orthogonal family in $\left[\mathbb{H}_{M,P}(\Omega)\right]^{\perp}$.

We show that $\Lambda_{A,\Sigma}$ attains its minimum on the constraint set

$$W_0 = \left\{U \in \left[\mathbb{H}_{M,P}(\Omega)\right]^{\perp} : \Upsilon_{M,P}(U) = 0\right\}.$$

Let $\alpha := \inf_{U \in W_0} \Lambda_{(A,\Sigma)}(U)$, by using the continuity of the trace operator, the Sobolev embedding theorem and the lower-semi-continuity of $\Lambda_{A,\Sigma}$.

Let $\{U_l\}_{l=1}^{\infty}$ be a minimizing sequence in W_0 for $\Lambda_{A,\Sigma}$, since $\lim_{l\to\infty} \Lambda_{A,\Sigma}(U_l) = \alpha$, we have that $\Lambda_{A,\Sigma}(U_l) = \|U_l\|_{(A,\Sigma)}$, by the definition of α we have that for all $\epsilon > 0$ and for all sufficiently large *l*, then $\|U_l\|^2_{A,\Sigma} \le \alpha + \epsilon$ by using the equivalent norm we have that, there is exist β, such that

$$\|U_l\|^2_{H(\Omega)} \le \beta \|U_l\|^2_{A,\Sigma},$$

so we have that

$$\|U_l\|^2_{H(\Omega)} \le \beta \|U_l\|^2_{A,\Sigma} \le \beta(\alpha + \epsilon).$$

Therefore, this sequence is bounded in $H(\Omega)$. Thus it has a weakly convergent subsequence $\{U_{l_j} : j \ge 1\}$

which convergent weakly to $\hat{U}$ in $H(\Omega)$. From Rellich-Kondrachov theorem this subsequence converges strongly to $\hat{U}$ in $L_k^2(\Omega)$, so $\hat{U}$ in W_0. Thus $\Lambda_{A,\Sigma}(\hat{U}) = \alpha$ as the functional is weakly l.s.c. (see Theorem 8).

There exists φ_1 such that $\Lambda_{A,\Sigma}(\varphi_1) = \alpha$. Hence, $\Lambda_{A,\Sigma}$ attains its minimum at φ_1 and φ_1 satisfies the following

$$\begin{aligned} &\int_\Omega \langle \nabla\varphi_1 \cdot \nabla V\rangle \mathrm{d}x + \int_\Omega \langle A(x)\varphi_1, V\rangle \mathrm{d}x + \int_{\partial\Omega} \langle \Sigma(x)\varphi_1, V\rangle \\ &= \mu_1 \left(\int_\Omega \langle M(x)\varphi_1, V\rangle \mathrm{d}x + \int_{\partial\Omega} \langle P(x)\varphi_1, V\rangle \mathrm{d}x \right). \end{aligned} \tag{6}$$

for all $V \in \left[\mathbb{H}_{(M,P)}(\Omega)\right]^\perp$. We see that (μ_1, φ_1) satisfies Equation (2) in a weak sense and $\varphi_1 \in W_0$ this implies that $\varphi_1 \in \left[\mathbb{H}_{(M,P)}(\Omega)\right]^\perp$ by the definition of W_0. Now take $V = \varphi_1$ in Equation (6), we obtain that the eigenvalue μ_1 is the infimum $\alpha = \Lambda_{A,\Sigma}(\varphi_1) = \mu_1$. This means that we could define μ_1 by the Rayleigh quotient

$$\mu_1 = \inf_{\substack{U \in W_0 \\ U \neq 0}} \frac{\Lambda_{A,\Sigma}(U)}{\|U\|^2_{(M,P)}}.$$

Clearly, $\mu_1 = \Lambda_{A,\Sigma}(\varphi_1) > 0$. Indeed assume that $\Lambda_{A,\Sigma}(\varphi_1) = 0$ then $|\nabla\varphi_1| = 0$ on Ω, hence φ_1 must be a constant and $\langle A(x)\varphi, \varphi\rangle = 0$ with $\varphi \neq 0$ that contradicts the assumptions imposed on $A(x)$. Thus $\mu_1 > 0$.

Now we show the existence of higher eigenvalues.

Define

$$\mathbb{F}_1 : W_0 \to \mathbb{R} \text{ by } \mathbb{F}_1(U) := \langle U, \varphi_1\rangle_{M,P}.$$

We know that the kernel of $\mathbb{F}_1$

$$ker\mathbb{F}_1 = \{U \in W_0 : \mathbb{F}_1(U) = 0\} =: W_1.$$

Since W_1 is the null-space of the continuous functional $\langle ., \varphi_1\rangle_{M,P}$ on $\left[\mathbb{H}_{(M,P)}(\Omega)\right]^\perp$, W_1 is a closed subspace of $\left[\mathbb{H}_{(M,P)}(\Omega)\right]^\perp$, and it is therefore a Hilbert space itself under the same inner product $\langle .,.\rangle_{(M,P)}$. Now we define

$$\mu_2 = \inf\{\Lambda_{A,\Sigma}(U) : U \in W_1\} = \inf_{\substack{U \in W_1 \\ U \neq 0}} \frac{\Lambda_{A,\Sigma}(U)}{\|U\|^2_{(M,P)}}.$$

Since $W_1 \subset W_0$ then we have that $\mu_1 \leq \mu_2$. Now we define

$$\mathbb{F}_2 : W_1 \to \mathbb{R} \text{ by } \mathbb{F}_2(U) = \langle U, \varphi_2\rangle_{M,P}$$

we know that the kernel of $\mathbb{F}_2$

$$ker\mathbb{F}_2 = \{U \in W_1 : \mathbb{F}_2(U) = 0\} =: W_2.$$

Since W_2 is the null-space of the continuous functional $\langle ., \varphi_2\rangle_{M,P}$ on $\left[\mathbb{H}_{(M,P)}(\Omega)\right]^\perp$, W_2 is a closed subspace of $\left[\mathbb{H}_{(M,P)}(\Omega)\right]^\perp$, and it is therefore a Hilbert space itself under the same inner product $\langle .,.\rangle_{(M,P)}$. Now we define

$$\mu_3 = \inf\{\Lambda_{A,\Sigma}(U) : U \in W_2\} = \inf_{\substack{U \in W_2 \\ U \neq 0}} \frac{\Lambda_{A,\Sigma}(U)}{\|U\|^2_{(M,P)}}.$$

Since $W_2 \subset W_1$ then we have that $\mu_2 \leq \mu_3$. Moreover, we can repeat the above arguments to show that μ_3 is achieved at some $\varphi_3 \in \left[\mathbb{H}_{(M,P)}(\Omega)\right]^\perp$.

We let

$$W_3 = \left\{u \in W_2 : \langle U, \varphi_3\rangle_{(M,P)} = 0\right\}$$

and

$$\mu_4 = \inf\left\{\Lambda_{A,\Sigma}(U) : U \in W_3\right\} = \inf_{\substack{U\in W_3\\ U\neq 0}} \frac{\Lambda_{A,\Sigma}(U)}{\|U\|^2_{(M,P)}}.$$

Since $W_3 \subset W_2$ then we have that $\mu_3 \le \mu_4$. Moreover, we can repeat the above arguments to show that μ_4 is achieved at some $\varphi_4 \in \left[\mathbb{H}_{(M,P)}(\Omega)\right]^{\perp}$.

Proceeding inductively, in general we can define

$$\mathbb{F}_j : W_{j-1} \to \mathbb{R} \text{ by } \mathbb{F}_j(U) = \left\langle U, \varphi_j \right\rangle_{M,P},$$

we know that the kernel of $\mathbb{F}_2$

$$ker\mathbb{F}_j = \left\{U \in W_{j-1} : \mathbb{F}_j(U) = 0\right\} =: W_j.$$

Since W_j is the null-space of the continuous functional $\left\langle ., \varphi_j \right\rangle_{M,P}$ on $\left[\mathbb{H}_{(M,P)}(\Omega)\right]^{\perp}$, W_j is a closed subspace of $\left[\mathbb{H}_{(M,P)}(\Omega)\right]^{\perp}$, and it is therefore a Hilbert space itself under the same inner product $\left\langle .,. \right\rangle_{(M,P)}$. Now we define

$$\mu_{j+1} = \inf\left\{\Lambda_{A,\Sigma}(U) : U \in W_j\right\} = \inf_{\substack{U\in W_j\\ U\neq 0}} \frac{\Lambda_{A,\Sigma}(U)}{\|U\|^2_{(M,P)}}.$$

In this way, we generate a sequence of eigenvalues

$$0 < \mu_1 \le \mu_2 \le \mu_3 \le \cdots \le \mu_j \le \cdots$$

whose associated φ_j are c-orthogonal and (M,P)-orthonormal in $\left[H_0^1(\Omega)\right]^{\perp}$.

Claim 1 $\mu_j \to \infty$ as $j \to \infty$.

Proof of claim 1. By way of contradiction, assume that the sequence is bounded above by a constant. Therefore, the corresponding sequence of eigenfunctions φ_j is bounded in $H(\Omega)$. By Rellich-Kondrachov theorem and the compactness of the trace operator, there is a Cauchy subsequence (which we again denote by φ_j), such that

$$\|\varphi_j - \varphi_k\|^2_{(M,P)} \to 0. \tag{7}$$

Since the φ_j are (M,P)-orthonormal, we have that $\|\varphi_j - \varphi_k\|^2_{(M,P)} = \|\varphi_j\|^2_{(M,P)} + \|\varphi_k\|^2_{(M,P)} = 2 > 0$, if $j \neq k$, which contradicts Equation (7). Thus, $\mu_j \to \infty$. We have that each μ_j occurs only finitely many times.

Claim 2

Each eigenvalue μ_j has a finite-dimensional eigenspace.

See [8] *for the proof of claim* 2.

We will now show that the normalized eigenfunctions provide a complete orthonormal basis of $\left[H_0^1(\Omega)\right]^{\perp}$. Let

$$\psi_j = \frac{1}{\sqrt{\mu_j}}\varphi_j,$$

so that $\|\psi_j\|^2_{(A,\Sigma)} = 1$.

Claim 3

The sequence $\{\psi_j\}_{j\ge 1}$ is a maximal (A,Σ)-orthonormal family of $\left[\mathbb{H}_{(M,P)}(\Omega)\right]^{\perp}$. (We know that the set is maximal (A,Σ)-orthonormal if and only if it is a complete orthonormal basis).

Proof of Claim 3. By way of contradiction, assume that the sequence $\{\psi_j\}_{j\ge 1}$ is not maximal, then there exists a $\xi \in \left[\mathbb{H}_{(M,P)}(\Omega)\right]^{\perp}$, and $\xi \notin \{\psi_j\}_{j\ge 1}$, such that $\|\xi\|^2_{(A,\Sigma)} = 1$ and $\left\langle \xi, \psi_j \right\rangle_{(A,\Sigma)} = 0 \ \forall j$, *i.e.*;

$$0=\left\langle \xi,\psi_j\right\rangle_{(A,\Sigma)}=\left\langle \xi,\frac{1}{\sqrt{\mu_j}}\varphi_j\right\rangle_{(A,\Sigma)}=\frac{1}{\sqrt{\mu_j}}\left\langle \xi,\varphi_j\right\rangle_{(A,\Sigma)}$$

$$=^{(\text{by }(6))}\frac{\mu_j}{\sqrt{\mu_j}}\left\langle \xi,\varphi_j\right\rangle_{(M,P)}=\mu_j\left\langle \xi,\frac{1}{\sqrt{\mu_j}}\varphi_j\right\rangle_{(M,P)}=\mu_j\left\langle \xi,\psi_j\right\rangle_{\partial},$$

since $\mu_j>0\ \forall j$. Therefore $\left\langle \xi,\psi_j\right\rangle_{(M,P)}=0$. We have that $\xi\in W_j\ \forall j\geq 1$. It follows from the definition of μ_j that

$$\mu_j\leq\frac{\|\xi\|^2_{(A,\Sigma)}}{\|\xi\|^2_{(M,P)}}=\frac{1}{\|\xi\|^2_{(M,P)}}\quad\forall j\geq 1.$$

Since we know from Claim 1 that $\mu_j\to\infty$ as $j\to\infty$, we have that $\|\xi\|^2_{(M,P)}=0$. Therefore $\xi=0$ a.e in Ω, which contradicts the definition of ξ. Thus the sequence $\{\psi_j\}_{j\geq 1}$ is a maximal (A,Σ)-orthonormal family of $\left[H_{(M,P)}(\Omega)\right]^{\perp}$, so the sequence $\{\psi_j\}_{j\geq 1}$ provides a complete orthonormal basis of $\left[H_{(M,P)}(\Omega)\right]^{\perp}$; that is, for any $U\in\left[\mathbb{H}_{(A,\Sigma)}(\Omega)\right]^{\perp}$, $U=\sum_{j=1}^{\infty}d_j\psi_j$ with $d_j=\left\langle U,\psi_j\right\rangle_{(A,\Sigma)}=\frac{1}{\sqrt{\mu_j}}\left\langle U,\kappa_j\right\rangle_{(A,\Sigma)}$, and

$$\|U\|^2_{(A,\Sigma)}=\sum_{j=1}^{\infty}|d_j|^2,$$

$$U=\sum_{j=1}^{\infty}d_j\frac{1}{\sqrt{\mu_j}}\varphi_j.$$

Now let

$$c_j=d_j\frac{1}{\sqrt{\mu_j}}=\frac{1}{\mu_j}\left\langle U,\varphi_j\right\rangle_{(A,\Sigma)}=^{(6)}\left\langle U,\varphi_j\right\rangle_{(M,P)}.$$

Therefore,

$$U=\sum_{j=1}^{\infty}c_j\varphi_j$$

and

$$\|U\|^2_{(A,\Sigma)}=\sum_{j=1}^{\infty}|c_j|^2\|\varphi_j\|^2_{(A,\Sigma)}=\sum_{j=1}^{\infty}\mu_j|c_j|^2.$$

Claim 4
We shall show that

$$\|U\|^2_{(M,P)}=\sum_{j=1}^{\infty}|c_j|^2.$$

Proof of Claim 4.

$$\|U\|^2_{(M,P)}=\langle u,u\rangle_{(M,P)}=\left\langle\sum_{j=1}^{\infty}c_j\varphi_j,\sum_{k=1}^{\infty}c_k\varphi_k\right\rangle_{(M,P)}$$

$$=\sum_{j=1}^{\infty}c_j\sum_{k=1}^{\infty}c_k\left\langle\varphi_j,\varphi_k\right\rangle_{(M,P)}=\sum_{j=1}^{\infty}|c_j|^2.$$

Thus

$$\|U\|^2_{(M,P)} = \sum_{j=1}^{\infty} |c_j|^2 .$$

References

[1] Auchmuty, G. (2012) Bases and Comparison Results for Linear Elliptic Eigenproblems. *Journal of Mathematical Analysis and Applications*, **390**, 394-406. http://dx.doi.org/10.1016/j.jmaa.2012.01.051

[2] Mavinga, N. (2012) Generalized Eigenproblem and Nonlinear Elliptic Equations with Nonlinear Boundary Conditions. *Proceedings of the Royal Society of Edinburgh*: *Section A Mathematics*, **142**, 137-153.

[3] de Godoi, J.D.B., Miyagaki, O.H. and Rodrigues, R.S. (2013) Steklov-Neumann Eigenvalue Problems for a Class of Elliptic System. SP-Brazil.

[4] Steklov, L.M.W. (1902) Sur les problèmes fundamentaux de la physique mathématique. *Annali Scuola Norm. Sup. Pisa*, **19**, 455-490.

[5] Küfner, A., John, O. and Fučik, S. (1977) Function Spaces. Noordhoff International Publishing, Leyden.

[6] Nečas, J. (1967) Les Mèthodes directes en thèorie des equations elliptiques. Masson, Paris.

[7] Grisvard, P. (1985) Elliptic Problems in Nonsmooth Domains. Pitman, Boston.

[8] Fadlallah, A. (2015) Elliptic Equations and Systems with Nonlinear Boundary Conditions. Ph.D. Dissertation, University of Alabama at Birmingham (UAB), Birmingham.

Applied Mathematics, 2015, 6, 430-439
Published Online February 2015 in SciRes. http://www.scirp.org/journal/am
http://dx.doi.org/10.4236/am.2015.62040

The Rotationally Symmetric Flow of Micropolar Fluids in the Presence of an Infinite Rotating Disk

Atif Nazir[1], Sajjad Hussain[2], Mohammad Shafique[3*]

[1]Mathematics Group Coordinator, Yanbu Industrial College, Yanbu, Saudi Arabia
[2]Department of Mathematics, College of Science, Al-Zulfi, Saudi Arabia
[3]Ex-AP Department of Mathematics, Gomal University, D. I. Khan, Pakistan
Email: profatif@hotmail.com, s.nawaz@mu.edu.sa, *mshafique6161@yahoo.com

Received 5 February 2015; accepted 23 February 2015; published 27 February 2015

Abstract

The rotationally symmetric flow of a micropolar fluid in the presence of an infinite rotating disk has been studied numerically. The equations of motion are reduced to a system of ordinary differential equations, which in turn are solved numerically using SOR method and Simpson's (1/3) rule. The results are calculated for different values of the parameter *s* (the ratio of angular velocities of disc and fluid) and the suction parameter *a*. Moreover, three different sets of the values of non-dimensional material constants related to micropolar behavior of the fluid have been chosen arbitrarily. The calculations have been carried out using three different grid sizes to check the accuracy of the results. The research concludes that the micropolar fluids flow resembles with that of Newtonian fluids when the material constants become close to zero. The comparison of these results is presented for possible values of the parameter *s*.

Keywords

Micropolar Fluids, Rotating Disk and Numerical Study

1. Introduction

Eringen [1] introduced the theory of micropolar fluids, a sub class of microfluid [2]. The theory fully explains the internal characteristics of the substructure particles which are also allowed to undergo rotation and deformation. Airman *et al*. [3] concluded that the micropolar fluid serves a better model for animal blood. Guram and

*Corresponding author.

How to cite this paper: Nazir, A., Hussain, S. and Shafique, M. (2015) The Rotationally Symmetric Flow of Micropolar Fluids in the Presence of an Infinite Rotating Disk. *Applied Mathematics*, **6**, 430-439. http://dx.doi.org/10.4236/am.2015.62040

Smith [4] considered the flow of a micropolar fluid which is steady relative to a frame of reference rotating with small uniform angular velocity when the velocity and spin are two dimensional and depend on the depth whereas pressure is independent of the horizontal coordinates. Anwar and Guram [5] considered the flow of a micropolar fluid contained between a rotating and a stationary disk. Narayana and Rudraiah [6] discussed the flow of a viscous fluid between two disks, one rotating and the other at rest. The same problem in micropolar fluid has been studied numerically taking either suction or blowing at the stationary disk by Agrawal Dhanapal [7].

The laminar flow due to an infinite rotating disk was first theoretically investigated with an approximate method by Von Karman [8]. Later on, Cochran [9] presented accurate numerical solutions of the Von Karman's problem. Dolidge [10], Sparrow & Gregg [11] and Benton [12] studied the related problems for different physical situations. Rogers and Lance [13] presented numerical solution for the flow produced by an infinite rotating disk when the fluid at infinity is in a state of solid rotation. Balaram and Luthra [14] obtained numerical solution of the steady flow produced by an infinite rotating disk when the second-order fluid at infinity is in a state of solid rotation. Sajjad *et al*. [15] obtained numerical solution for accelerated rotating disk in a viscous fluid. Ram and Kumar [16] analyzed three dimensional rotationally symmetric boundary layer flow of field dependent viscous fluid saturating porous medium due to the rotation of an infinite disk. Evans [17] studied the effect of uniform suction on the rotationally symmetric flow produced by an infinite rotating disc with the fluid at infinity is rotating in the same sense as the disc.

In this research, the numerical solutions of the rotationally symmetric slow of micropolar fluids in the presence of an infinite rotating disk have been discussed. In order to find the numerical solution of the problem, the Navier Stokes equations are reduced to ordinary differential equations by using similarity transformations [17]. The finite difference scheme is solved numerically by using SOR Iterative Procedure with Simpson (1/3) Rule [18]. The calculations have been carried out using three different grid sizes to check the accuracy of the results. The numerical results have been discussed both in tabular and graphically.

The purpose of using these numerical techniques for numerical solution is that, the finite difference approximations are found to be discrete techniques wherein the domain of interest is represented by a set of points or nodes and information among these points is commonly obtained by using Taylor series expansions while the finite element method employs piecewise continuous polynomials to interpolate among nodal points. The finite difference techniques are very easy to understand and straight forward for computational analysis.

2. Mathematical Analysis

The cylindrical polar coordinates (r,φ,z) are used, r being the radial distance from the axis, φ, the polar angle and z the normal distance from the disk. We assume that the flow is steady and incompressible. The body force and body couples are neglected. With these assumptions the equations of motion become:

$$\nabla\cdot\underline{\mathbf{V}}=0 \tag{1}$$

$$-(\mu+k)\nabla\times(\nabla\times\underline{\mathbf{V}})+k(\nabla\times\underline{\mathbf{v}})-\nabla p+=\rho(\underline{\mathbf{V}}\cdot\nabla)\underline{\mathbf{V}} \tag{2}$$

$$(\alpha+\beta+\gamma)\nabla(\nabla\cdot\underline{\mathbf{v}})-\gamma(\nabla\times\nabla\times\underline{\mathbf{v}})+k(\nabla\times\underline{\mathbf{V}})-2k\underline{\mathbf{v}}=\rho j(\underline{\mathbf{V}}\cdot\nabla)\underline{\mathbf{v}} \tag{3}$$

where ρ is the density, $\underline{\mathbf{V}}$ the velocity, $\underline{\mathbf{v}}$ the micro-rotation or spin, p the pressure, μ is dynamic viscosity coefficient, j the micro-inertia, α, β, γ and k are material constants.

The following similarity transformations are used:

$$u=r\Omega F(\zeta),\quad v=r\Omega G(\zeta),\quad w=\sqrt{\Omega\upsilon}H(\zeta) \tag{4}$$

$$v_1=-\left(r\Omega^{3/2}/\upsilon^{1/2}\right)L(\zeta),\quad v_2=\left(r\Omega^{3/2}/\upsilon^{1/2}\right)M(\zeta),\quad \text{and}\quad v_3=2\Omega N(\zeta)$$

where $\zeta=\sqrt{\dfrac{\Omega}{\upsilon}}z$ is the dimensionless variable, υ being kinematics viscosity. The Equations (1) to (3) in dimensionless form become:

$$2F+H'=0 \tag{5}$$

$$F''=F^2-G^2+HF'+s^2+C_1M' \tag{6}$$

$$2FG + HG' - G'' + M_1 G + C_1 L' = 0 \tag{7}$$

$$L'' + C_2 G' - 2C_2 L + C_3 \left(L^2 - 2LN' - M^2 \right) = 0 \tag{8}$$

$$M'' + C_2 F' - 2C_2 M - 2C_3 \left(NM' - LM \right) = 0 \tag{9}$$

$$N'' - L' + C_4 L' + C_5 G - 2C_5 N - 2C_6 NN' = 0 \tag{10}$$

where primes denote differentiation with respect to ζ. The constants C_1, C_2, C_3, C_4, C_5 and C_6 all are non dimensional.

The boundary conditions are

$$\begin{aligned} &\zeta = 0 : F = 0,\ G = 1,\ H = 0,\ L = 0,\ M = 0,\ N = 0; \\ &\zeta \to \infty : F = 0,\ G = s,\ L = 0,\ M = 0,\ N = 0. \end{aligned} \tag{11}$$

3. Finite Difference Equations

In order to obtain the numerical solution of nonlinear ordinary differential Equations (6) to (10), we approximate these equations by central difference approximation at a typical point $\zeta = \zeta_n$ of the interval $[0, \infty)$, we obtain

$$\left(1 - \frac{h}{2} H_n\right) F_{n+1} - \left(2 + M_1 h^2 + 2h^2 F_n\right) F_n + \left(1 + \frac{h}{2} H_n\right) F_{n-1} + h^2 \left(G_n^2 - s^2\right) - C_1 \frac{h}{2} \left(M_{n+1} - M_{n-1}\right) = 0 \tag{12}$$

$$\left(1 - \frac{h}{2} H_n\right) G_{n+1} - 2\left(1 + h^2 F_n\right) G_n + \left(1 + \frac{h}{2} H_n\right) G_{n-1} - C_1 \frac{h}{2} \left(L_{n+1} - L_{n-1}\right) = 0 \tag{13}$$

$$\left(1 - C_3 h N_n\right) L_{n+1} - 2\left(1 + C_2 h^2 - C_3 \frac{h^2}{2} L_n\right) L_n + \left(1 + C_3 h N_n\right) L_{n-1} - C_3 h^2 M_n^2 + C_2 \frac{h}{2} \left(G_{n+1} - G_{n-1}\right) = 0 \tag{14}$$

$$\left(1 - C_3 h N_n\right) M_{n+1} - 2\left(1 + C_2 h^2 - C_3 h^2 L_n\right) M_n + \left(1 + C_3 h N_n\right) M_{n-1} + C_2 \frac{h}{2} \left(F_{n+1} - F_{n-1}\right) = 0 \tag{15}$$

$$\left(1 - C_6 h N_n\right) N_{n+1} - 2\left(1 - C_5 h^2\right) N_n + \left(1 + C_6 h N_n\right) N_{n-1} + C_5 h^2 G_n - \frac{h}{2} \left(1 - C_4\right) \left(L_{n+1} - L_{n-1}\right) = 0 \tag{16}$$

where h denotes a grid size, $F_n = F(\zeta_n)$, $G_n = G(\zeta_n)$ and $H_n = H(\zeta_n)$. For computational purposes, we replace the interval $[0, \infty)$ by $[0, t)$, where t is sufficiently large.

4. Computational Procedure

We now solve numerically the finite difference Equations (12) to (16) by using SOR method subject to the appropriate boundary conditions (11). The first order ordinary differential Equation (5) integrate by Simpson's (1/3) rule subject to the initial condition $H = -a$ when $\zeta = 0$ where a is the suction parameter.

The computation has been checked for different of the relaxation parameter between $1 < \omega < 2$. The optimum value of the relaxation parameter for the problem under consideration is 1.5. The SOR procedure is terminated when the following condition is satisfied:

$$\max \left| U_i^{n+1} - U_i^n \right| < 10^{-6}$$

where n denotes the number of iterations and U stands for each of F, G, L, M and N. The above procedure is repeated for higher grid levels $\frac{h}{2}$ and $\frac{h}{4}$.

5. Discussion on Numerical Results

Numerical results have been found to observe the effect of parameters s and a on velocity field and microrota-

tion. In order to check the accuracy of the results for velocity components F, G and H and the microrotation components L, M and N, the calculations have been carried out on three different grid sizes namely $h = 0.1$, 0.05 and 0.025. The three different sets of the material constants C_1, C_2, C_3, C_4, C_5 and C_6 in the **Table 1** below have been chosen arbitrarily and calculations have been carried out for each set.

The velocity derivatives at the surface of the disc are given in **Table 2** for micropolar fluids results with the results for Newtonian fluids. In **Table 3** to **Table 5**, the numerical results are presented for $s = 0.0, -0.1, -0.16$ and $a = 0.0$, 1.5 for the material constants case I. The radial and transverse velocity components F and G are respectively depicted in **Figure 1** and **Figure 2** for different values of the suction parameter a when $s = 0$. The velocity components show a reduction in magnitude with increasing values of a. The boundary layer is clearly indicated near the surface of the disk.

Figure 3 and **Figure 4** present velocity components F and G for various values of suction parameter a when $s = -0.1$. The figure indicates the effect of the outer flow for the first time. Some radial flow reversal is occurring in the outer flow but there is stability for the boundary layer. Thus for increasing s negatively and then the radial flow development will cause the boundary layer to leave the disk.

Table 1. Three sets of material constants used in calculations of micropolar fluids.

Cases	C_1	C_2	C_3	C_4	C_5	C_6
I	0.1	0.3	0.4	0.5	0.7	0.8
II	0.5	1.5	2.0	3.0	3.5	4.0
III	0.3	0.5	1.5	2.5	3.0	3.5

Table 2. The comparison of Micropolar fluids and Newtonian fluids for $F'(0)$ and $G'(0)$.

s	$F'(0)$		$G'(0)$	
	Micropolar fluids	Newtonian fluids [17]	Micropolar fluids	Newtonian fluids [17]
0.0	0.51022801	0.51022912	−0.61592027	−0.61591916
−0.10	0.49130449	0.49130550	−0.60825160	−0.60825056
−0.15	0.47627299	0.47627301	−0.58762407	−0.58761507
−0.16	0.47332786	0.47332988	−0.57766843	−0.57766748

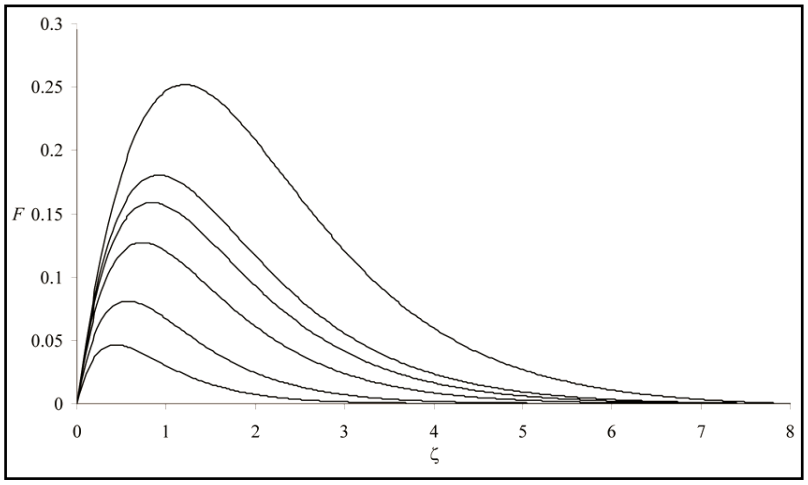

Figure 1. Graph of F for different values of parameter $a = 0$, 0.2, 0.5, 1.0 and 1.5 from top to bottom when $s = 0$.

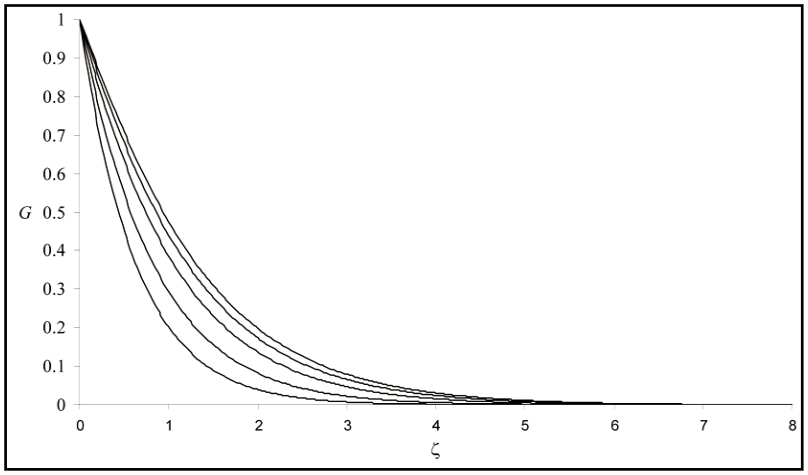

Figure 2. Graphs of G for different values of parameter a = 0, 0.2, 0.5, 1.0 and 1.5 from top to bottom when s = 0.

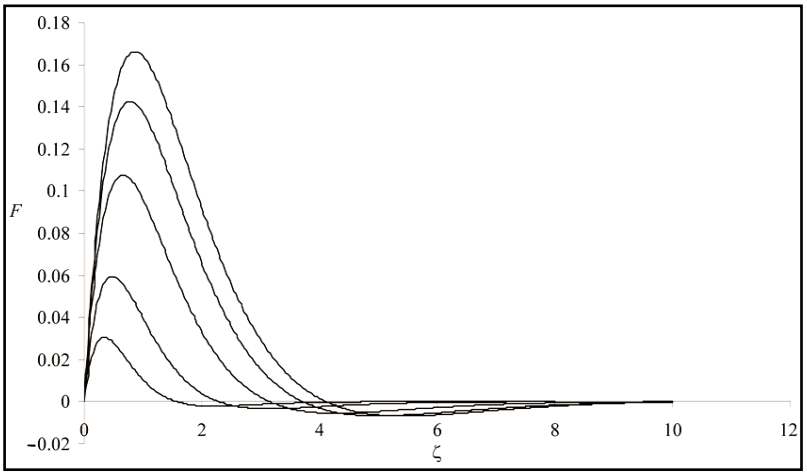

Figure 3. Graph of F for different values of parameter a = 0, 0.3, 0.5, 1.0 and 1.5 from top to bottom when s = −0.1.

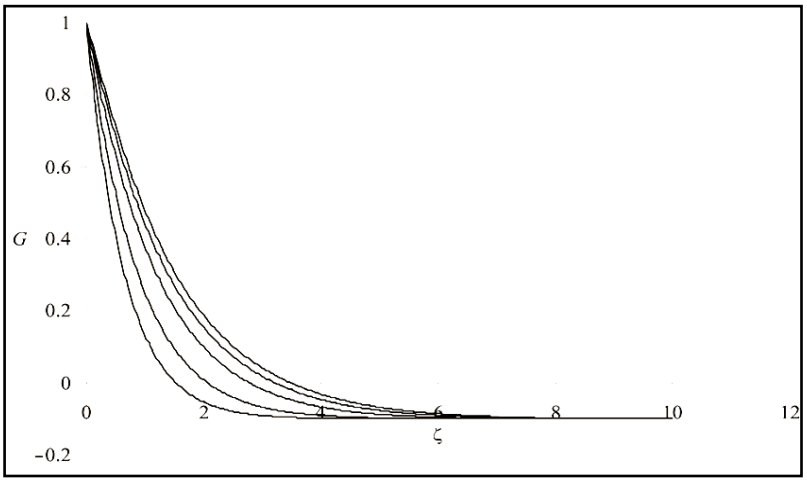

Figure 4. Graph of G for different values of parameter a = 0, 0.2, 0.5, 0.7, 1.0 and 1.5 from top to bottom when s = −0.1.

Table 3. The numerical results for velocity components F, G and H and the microrotation components L, M and N when s = 0.0 and a = 0.0.

h	ζ	F	G	H	L	M	N
	0.000	0.000000	1.000000	0.000000	0.000000	0.000000	0.000000
	1.000	0.179240	0.475672	−0.264748	−0.132547	−0.005065	0.061811
	2.000	0.116682	0.198637	−0.569258	−0.100132	−0.017006	0.030972
	3.000	0.055710	0.079067	−0.736567	−0.055573	−0.015614	0.009449
0.05	4.000	0.023615	0.030491	−0.811870	−0.027335	−0.010107	0.001537
	5.000	0.009307	0.011294	−0.842782	−0.012569	−0.005525	−0.000480
	6.000	0.003340	0.003853	−0.854550	−0.005392	−0.002665	−0.000683
	7.000	0.000936	0.001029	−0.858460	−0.001912	−0.001024	−0.000438
	8.000	0.000000	0.000000	−0.859246	0.000000	0.000000	0.000000
	0.000	0.000000	1.000000	0.000000	0.000000	0.000000	0.000000
	1.000	0.179756	0.475490	−0.265459	−0.132669	−0.005076	0.061869
	2.000	0.116687	0.198008	−0.570529	−0.100185	−0.017102	0.030837
	3.000	0.055505	0.078594	−0.737561	−0.055501	−0.015655	0.009322
0.025	4.000	0.023472	0.030247	−0.812501	−0.027248	−0.010100	0.001480
	5.000	0.009235	0.011179	−0.843204	−0.012505	−0.005508	−0.000501
	6.000	0.003306	0.003803	−0.854869	−0.005355	−0.002651	−0.000689
	7.000	0.000925	0.001015	−0.858737	−0.001898	−0.001017	−0.000438
	8.000	0.000000	0.000000	−0.859515	0.000000	0.000000	0.000000
	0.000	0.000000	1.000000	0.000000	0.000000	0.000000	0.000000
	1.000	0.179545	0.475495	−0.265239	−0.132672	−0.005128	0.061799
	2.000	0.116731	0.198355	−0.570108	−0.100151	−0.017086	0.030901
	3.000	0.055642	0.078881	−0.737367	−0.055528	−0.015651	0.009401
0.012	4.000	0.023554	0.030398	−0.812532	−0.027287	−0.010111	0.001519
	5.000	0.009270	0.011246	−0.843348	−0.012534	−0.005518	−0.000486
	6.000	0.003321	0.003830	−0.855060	−0.005372	−0.002658	−0.000685
	7.000	0.000930	0.001023	−0.858946	−0.001904	−0.001020	−0.000437
	8.000	0.000000	0.000000	−0.859728	0.000000	0.000000	0.000000

Table 4. The numerical results for velocity components F, G and H and the microrotation components L, M and N when $s = -0.01$ and $a = 0.0$.

h	ζ	F	G	H	L	M	N
	0.000	0.000000	1.000000	0.000000	0.000000	0.000000	0.000000
	1.000	0.163850	0.477984	−0.248418	−0.136301	−0.006879	0.061170
	2.000	0.091781	0.186209	−0.511450	−0.107574	−0.017863	0.026623
	3.000	0.029148	0.040950	−0.625998	−0.065370	−0.014898	−0.000802
	4.000	0.001462	−0.032056	−0.651904	−0.037765	−0.008380	−0.014413
0.05	5.000	−0.006261	−0.068608	−0.645015	−0.022444	−0.003547	−0.020480
	6.000	−0.006178	−0.086359	−0.631914	−0.014246	−0.000984	−0.022865
	7.000	−0.004098	−0.094583	−0.621554	−0.009695	0.000058	−0.023092
	8.000	−0.002131	−0.098170	−0.615414	−0.006718	0.000315	−0.021139
	9.000	−0.000784	−0.099592	−0.612605	−0.003921	0.000229	−0.015200
	10.000	0.000000	−0.100000	−0.611900	0.000000	0.000000	0.000000
	0.000	0.000000	1.000000	0.000000	0.000000	0.000000	0.000000
	1.000	0.163982	0.477946	−0.248625	−0.136390	−0.006934	0.061146
	2.000	0.091849	0.186099	−0.511859	−0.107607	−0.017903	0.026584
	3.000	0.029187	0.040848	−0.626508	−0.065366	−0.014914	−0.000831
	4.000	0.001495	−0.032127	−0.652484	−0.037750	−0.008385	−0.014430
0.025	5.000	−0.006233	−0.068650	−0.645656	−0.022430	−0.003549	−0.020489
	6.000	−0.006157	−0.086381	−0.632605	−0.014236	−0.000986	−0.022869
	7.000	−0.004083	−0.094593	−0.622282	−0.009688	0.000056	−0.023094
	8.000	−0.002124	−0.098174	−0.616163	−0.006714	0.000313	−0.021140
	9.000	−0.000781	−0.099593	−0.613365	−0.003919	0.000228	−0.015201
	10.000	0.000000	−0.100000	−0.612663	0.000000	0.000000	0.000000
	0.000	0.000000	1.000000	0.000000	0.000000	0.000000	0.000000
	1.000	0.164012	0.477938	0.248672	0.136410	0.006948	0.061140
	2.000	0.091861	0.186080	−0.511947	−0.107613	−0.017915	0.026576
	3.000	0.029189	0.040832	−0.626607	−0.065365	−0.014920	−0.000836
	4.000	0.001493	−0.032137	−0.652584	−0.037747	−0.008387	−0.014431
0.012	5.000	−0.006235	−0.068656	−0.645753	−0.022427	−0.003549	−0.020488
	6.000	−0.006158	−0.086385	−0.632699	−0.014233	−0.000986	−0.022868
	7.000	−0.004084	−0.094595	−0.622374	−0.009687	0.000056	−0.023093
	8.000	−0.002124	−0.098174	−0.616255	−0.006714	0.000313	−0.021139
	9.000	−0.000781	−0.099593	−0.613456	−0.003919	0.000228	−0.015201
	10.000	0.000000	−0.100000	−0.612754	0.000000	0.000000	0.000000

Table 5. The numerical results for velocity components F, G and H and the microrotation components L, M and N when $s = -0.16$ and $a = 1.5$.

h	ζ	F	G	H	L	M	N
	0.000	0.000000	1.000000	−1.500000	0.000000	0.000000	0.000000
	1.000	−0.002528	0.088033	−1.522923	−0.082486	−0.002232	−0.010100
	2.000	−0.008317	−0.109105	−1.507162	−0.049570	−0.000038	−0.035059
	3.000	−0.003198	−0.150499	−1.495820	−0.029503	0.000588	−0.040513
	4.000	−0.000582	−0.158720	−1.492485	−0.020994	0.000374	−0.040488
0.05	5.000	0.000199	−0.160254	−1.492282	−0.017493	0.000139	−0.039504
	6.000	0.000329	−0.160529	−1.492864	−0.015606	0.000020	−0.038042
	7.000	0.000272	−0.160560	−1.493479	−0.013809	−0.000022	−0.035449
	8.000	0.000170	−0.160498	−1.493923	−0.011234	−0.000028	−0.030365
	9.000	0.000069	−0.160330	−1.494159	−0.007036	−0.000018	−0.020215
	10.000	0.000000	−0.160000	−1.494221	0.000000	0.000000	0.000000
	0.000	0.000000	1.000000	−1.500000	0.000000	0.000000	0.000000
	1.000	−0.011205	0.060019	−1.506979	−0.089021	−0.000175	−0.016609
	2.000	−0.005664	−0.144366	−1.484961	−0.057573	0.003504	−0.044292
	3.000	0.006414	−0.180500	−1.487086	−0.035908	0.003608	−0.049458
	4.000	0.009843	−0.179762	−1.504564	−0.025014	0.002249	−0.047525
0.025	5.000	0.008359	−0.173125	−1.523221	−0.019566	0.001041	−0.044332
	6.000	0.005517	−0.167406	−1.537139	−0.016459	0.000315	−0.041014
	7.000	0.002973	−0.163677	−1.545512	−0.014051	−0.000021	−0.037073
	8.000	0.001260	−0.161617	−1.549599	−0.011245	−0.000115	−0.031068
	9.000	0.000352	−0.160591	−1.551095	−0.006991	−0.000082	−0.020325
	10.000	0.000000	−0.160000	−1.551378	0.000000	0.000000	0.000000
	0.000	0.000000	1.000000	−1.500000	0.000000	0.000000	0.000000
	1.000	−0.067561	0.195665	−1.454176	−0.078957	−0.009610	0.012609
	2.000	−0.108889	−0.008283	−1.266693	−0.045617	−0.003901	−0.010169
	3.000	−0.108214	−0.076914	−1.045830	−0.025831	0.001519	−0.019670
	4.000	−0.093475	−0.109525	−0.842828	−0.018374	0.004688	−0.024761
0.012	5.000	−0.073748	−0.129694	−0.675170	−0.016381	0.006288	−0.028789
	6.000	−0.053074	−0.143288	−0.548445	−0.016000	0.006704	−0.032064
	7.000	−0.034184	−0.152062	−0.461664	−0.015355	0.006121	−0.033907
	8.000	−0.018827	−0.157114	−0.409328	−0.013376	0.004737	−0.032798
	9.000	−0.007588	−0.159491	−0.383588	−0.008934	0.002729	−0.024962
	10.000	0.000000	−0.160000	−0.376529	0.000000	0.000000	0.000000

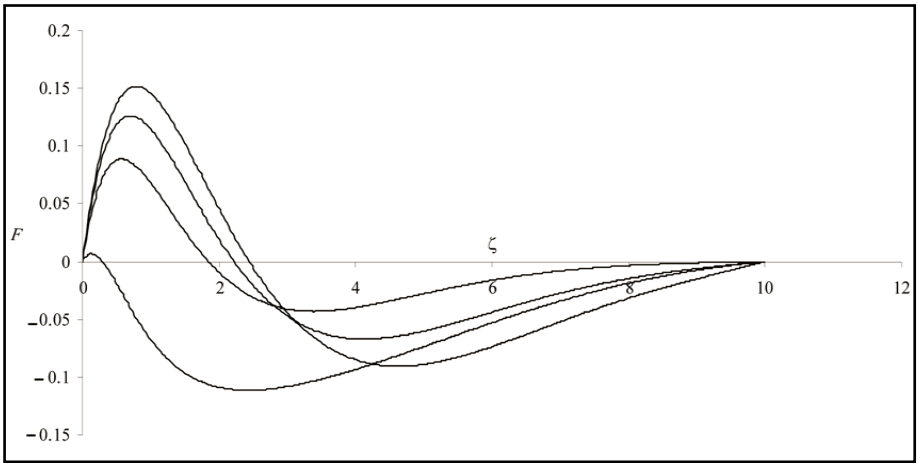

Figure 5. Graph of F for different values of parameter a = 0, 0.3, 0.5 and 1.5 from top to bottom when s = −0.16.

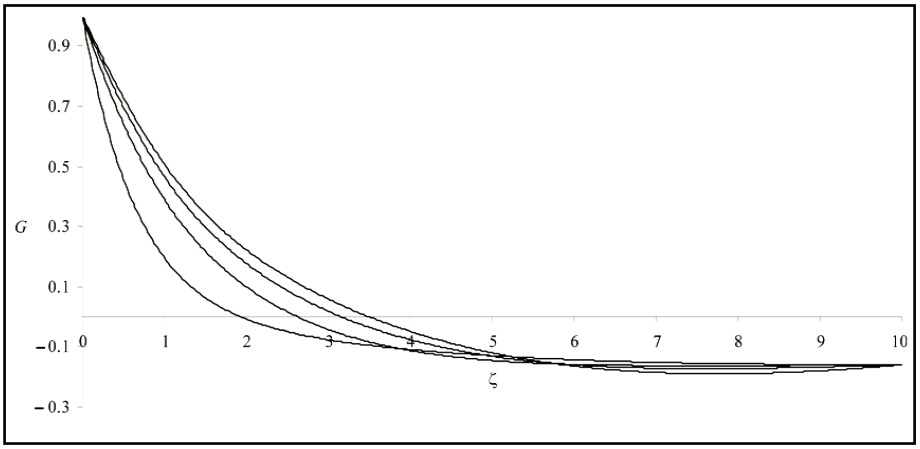

Figure 6. Graphs of G for different values of parameter a = 0, 0.2, 0.5 and 1.5 from top to bottom when s = −0.16.

Figure 5 and **Figure 6** show velocity profiles for F and G for different values of the parameter a when s = −0.16. It is noted that this value of s is limiting for which a solution for a = 0 can be found and a large value of suction is required to reduce the radial flow traversal as amount of the outflow in the boundary layer is increased. Some oscillatory behavior is seen for transverse velocity component. The flow pattern changes quickly.

References

[1] Eringen, A.C. (1966) Theory of Micropolar Fluids. *Journal of Mathematics and Mechanics*, **16**, 1-16.

[2] Eringen, A.C. (1964) Simple Microfluids. *International Journal of Engineering Science*, **2**, 205-217. http://dx.doi.org/10.1016/0020-7225(64)90005-9

[3] Ariman, T., Turk, M.A. and Sylvester, N.D. (1974) Applications of Microcontinuum Fluid Mechanics. *International Journal of Engineering Science*, **12**, 273-293. http://dx.doi.org/10.1016/0020-7225(74)90059-7

[4] Guram, G.S. and Anwar, M. (1981) Micropolar Flow Due to a Rotating Disc with Suction and Injection. *ZAMM—Journal of Applied Mathematics and Mechanics*, **61**, 589-595. http://dx.doi.org/10.1002/zamm.19810611107

[5] Guram, G.S. and Smith, A.C. (1980) Stagnation Flows of Micropolar Fluids with Strong and Weak Interactions. *Computers & Mathematics with Applications*, **6**, 213-233. http://dx.doi.org/10.1016/0898-1221(80)90030-9

[6] Narayana, C.L. and Rudraiah, N. (1972) On the Steady Flow between a Rotating and a Stationary Disk with a Uniform Suction at the Stationary Disk. *Zeitschrift für angewandte Mathematik und Physik—ZAMP*, **23**, 96-104. http://dx.doi.org/10.1007/BF01593206

[7] Agarwal, R.S. and Dhanapal, C. (1988) Stagnation Point Micropolar Fluid Flow between Porous Discs with Uniform Blowing. *International Journal of Engineering Science*, **26**, 293-300. http://dx.doi.org/10.1016/0020-7225(88)90078-X

[8] Von Karaman, T. (1921) Uberlaminare und Turbulent Reibung. *Zeitschrift für Angew and te Mathematik und Mechanik*, **1**, 233-252. http://dx.doi.org/10.1002/zamm.19210010401

[9] Cochran, W.G. (1934) The Flow Due to a Rotating Disk. *Mathematical Proceedings of the Cambridge Philosophical Society*, **30**, 365-375. http://dx.doi.org/10.1017/S0305004100012561

[10] Dolidge, D.E. (1954) Unsteady Motion of a Viscous Liquid Produced by a Rotating Disk. *Prikladnaya Matematika i Mekhanika*, **18**, 371-378.

[11] Sparrow, E.M. and Gregg, J.L. (1960) Flow about an Unsteadily Rotating Disk. *Journal of the Aeronautical Sciences*, **27**, 252-257.

[12] Benton, E.R. (1966) On the Flow Due to a Rotating Disk. *Journal of Fluid Mechanics*, **24**, 781-800.

[13] Rogers, M.H. and Lance, G.N. (1960) The Rotationally Symmetric Flow of a Viscous Fluid in the Presence of an Infinite Rotating Disk. *Journal of Fluid Mechanics*, **7**, 617-631. http://dx.doi.org/10.1017/S0022112060000335

[14] Balaram, M. and Luthra, B.R. (1973) A Numerical Study of Rotationally Symmetric Flow of Second-Order Fluid. *Journal of Applied Mechanics*, **40**, 685-687. http://dx.doi.org/10.1115/1.3423073

[15] Hussain, S., Kamal, M.A., Ahmad, F., Ali, M., Shafique, M. and Hussain, S. (2013) Numerical Solution for Accelerated Rotating Disk in a Viscous Fluid. *Applied Mathematics*, **4**, 899-902.

[16] Ram, P. and Kumar, V. (2014) Rotationally Symmetric Ferrofluid Flow and Heat Transfer in Porous Medium with Variable Viscosity and Viscous Dissipation. *Journal of Applied Fluid Mechanics*, **7**, 357-366.

[17] Evans, D.J. (1969) The Rotationally Symmetric Flow of a Viscous Fluid in the Presence of an Infinite Rotating Disc with Uniform Suction. *Quarterly Journal of Mechanics and Applied Mathematics*, **22**, 467-485. http://dx.doi.org/10.1093/qjmam/22.4.467

[18] Burden, R.L. (1985) Numerical Analysis. Prindle, Weber & Schmidt, Boston.

Applied Mathematics, 2015, 6, 440-446
Published Online February 2015 in SciRes. http://www.scirp.org/journal/am
http://dx.doi.org/10.4236/am.2015.62041

Temperature Fluctuations in Photoionized Nebulae in Case of Oxygen and Nitrogen Abundances

S. Belay Goshu[1], Derck P. Smits[2]

[1]Department of Physics, Dire-Dawa University, Dire-Dawa, Ethiopia
[2]Department of Mathematics, Astronomy and Computing Science, UniSA, Pretoria, South Africa
Email: belaysitotaw@gmail.com, Smitsdp@unisa.ac.za

Received 5 February 2015; accepted 24 February 2015; published 27 February 2015

Abstract

We present the dependence of electron temperature fluctuations of O^{++} and H^{+} by the chemical abundances of oxygen and nitrogen. Models assume that hydrogen density is uniform in one case and non uniform in the second case, which vary with the distance from the central star. The abundances of oxygen and nitrogen change by scale factor 5 and 1/5. Our analysis suggests that temperature fluctuations are consistent with photoionization. Using the cloudy photoionization code, we found a reasonable close agreement of the computed value with the one that was done before this work. Our simulation also shows that how change of abundances affects temperature fluctuations and its value is less than 0.01.

Keywords

H II Region, Planetary Nebulae, Abundances

1. Introduction

Accurate abundances of heavy metals are essential for solving astrophysical problems, including stellar and galactic chemical evolution. This was tested by different authors like [1]. The problem of the existence of temperature fluctuations in H II regions was first noted by [2], suggested that those measured in ionized gaseous nebulae depend on the ionization radiation field, hydrogen density and elemental abundances.

The gas temperature obtained from the observed O[III] line ratio is greater than the one from the Balmer discontinuity [3]. Different authors like [4] [5] tried to estimate the value of temperature fluctuations t^2 on pho-

toionization in H II region. These values in H II region varying from 0.02 to 0.09 were found and yielded significant effects on element abundances.

The abundance determination in H II region and the planetary nebula have positive impacts of temperature fluctuations given by [2]. The abundances of H, He, C, O, N, Ne, S, and Ar are included to determine the temperature fluctuations of electron by changing the abundances of oxygen and nitrogen elements by scale factor 5 and 0.2. These are the most important elements which have a great impact on cooling.

Cloudy is an impressive code offering a vast amount of possibilities to model wide variety of objects. The contents of physics and the basic numerical framework of the codes are explained in the documents given by [6] with the version of C10.00 to explain all the phenomena.

In this paper, we will try to analyze the effect of hydrogen density and chemical abundances on temperature structure of electrons and its temperature fluctuations of both hydrogen and oxygen ions. In §2, we present the problem formulation of temperature fluctuations. In §3 we describe the models and present our calculations. In §4 we present the results and finally we present the conclusion.

2. Formulation of the Problem

Temperature in homogeneities on the emission lines, based on statistical approximation introduced by [2], which quantifies the brightness increase or decrease of each line in terms of the departure of the temperature from the average temperature T_0 and is given by

$$T_0 = \frac{\int_V n_e^2 T \mathrm{d}V}{\int_V n_e^2 \mathrm{d}V} \tag{1}$$

For homogeneous metalicity nebulae characterized by small temperature in homogeneities, n_e is the electron density, T is the electron temperature, and V is the volume over which the integration is carried out. The rms amplitude t of the temperature in homogeneities is defined as

$$t^2 = \frac{\int_V n_e^2 \left(T - T_0\right)^2 \mathrm{d}V}{T_0^2 \int_V n_e^2 \mathrm{d}V} \tag{2}$$

We simplified the expression presented by [2], in which t^2 depends on the density of ionic species considered while in the above equation. We implicitly consider only ionized H (by setting $n_i = n_H = n_e^2$).

The nature of temperature fluctuations is one of the important question in nebular astrophysics. CLOUDY predicts that they should be very small because of the abundance of cooling function of temperature, while some observations indicate a very large value of t^2 [7]. Density fluctuations could be a source of temperature fluctuations, due to increased collisional deexcitation in zones of higher density, but photoionization models including such density fluctuations also fail to return large enough values of t^2 [1] and [8].

3. Model Parameters

We consider two different models for this photoionized region in H II regions. The first one correspond to a dense nebulae ionized by a star that is very hot and its temperature is $T_\star$ = 75,000 K and its density n(H) = 10^4 cm^{-3}. The second correspond to a more diluted nebulae ionized by a hot star. We assumed the density of the gas in neutral medium within the galaxy is that of power law decrease in the gas density with the distance from the center given by

$$n = n_o \left(\frac{r}{r_o}\right)^{-\alpha} \tag{3}$$

where n_o is the gas density at $r = r_o$ and r_o is the scale length describing the rate of decay of this with radius. We have chosen hydrogen density, n(H) = 10^3 cm^{-3}, change by $\alpha = -0.5$, and $T_\star$ = 10^5 K. The stars are assumed to radiate as a blackbody. The inner radius of the nebulae is chosen to be 10^{16} cm for the former case and 5 × 10^{16} cm for the latter one. In both cases we assume that the total number of H Lyman continuum photons emitted by the star, Q(H) = 10^{48} photons per second and the filling factor is unit.

An additional set of a nebular parameters is the chemical composition of gas, usually taken to be 10^5, 776,

437, 182, 110, 75, and 36 atoms of He, C, O, N, Ne, S, and Ar, respectively per 10^6 H atoms is shown in **Table 1**. This is taken from the average composition of elements are taken from [9], whereas the chemical composition of Ar and S are taken from the solar composition given by [10]. The most important of these abundances are that of C, O, which we assume that these elements as the principal coolant [11] and [12]. This model is constructed with different values of oxygen and nitrogen. To investigate the temperature fluctuations of electron, we vary the total abundances of both oxygen and nitrogen by scale factor 5 and 1/5 to test separately. When the abundance of oxygen vary by scale factor 5 and 1/5 in H II region helps to estimate temperature of electron and very useful for obtaining estimates of abundance gradients in spiral galaxies and of oxygen abundances of star-forming regions in the distant universe [13]. The parameters are given in **Table 2** and **Table 3**.

4. Result and Discussion

We can easily observe from the result given in **Table 4** and **Table 5**, variations of temperature with inhomogeneities abundances of O and N. This result of this paper strongly suggests that abundances change produce temperature fluctuations. When the abundances of O rises by scale factor 5, the magnitude of its temperature is

Table 1. Elemental abundances used in the nebular model.

H	He	O	C	N	Ne	S	Ar
10^6	10^5	437	776	182	110	18	16
0.00	−1.00	−3.36	−3.11	−3.74	−3.96	−4.75	−4.79

Table 2. First model parameters.

$Q(\mathrm{H})$ ph s^{-1}	$T_\star$	$n(\mathrm{H})$ cm^{-3}	R_{in} cm	O (abundance) increase scale by 5	N (abundance) increase scale by 5
10^{48}	75,000 K	10^4	10^{16}	2188 $\log(\mathrm{O/H}) = -2.66$	912 $\log(\mathrm{N/H}) = -3.04$
	100,000 K	10^3	5×10^{16}	$\log(\mathrm{O/H}) = -2.66$	$\log(\mathrm{N/H}) = -3.04$

Table 3. Second model parameters.

$Q(\mathrm{H})$ ph s^{-1}	$T_\star$	$n(\mathrm{H})$ cm^{-3}	R_{in} cm	O (abundance by scale factor of 1/5)	N (abundance by scale factor 1/5)
10^{48}	100,000 K	10^4	5×10^{16}	689 $\log(\mathrm{O/H}) = -4.06$	145.6 $\log(\mathrm{N/H}) = -4.439$
	75,000 K	10^3	10^{16}	$\log(\mathrm{O/H}) = -4.06$	$\log(\mathrm{N/H}) = -4.439$

Table 4. Elemental abundances used in the model and the result obtained.

	$T_\star = 75{,}000$ K, $n(\mathrm{H}) = 10^4$ cm^{-3}, $Q(\mathrm{H}) = 10^{48}$ phs^{-1} and $R = 10^{16}$ cm			
Abundances	$T(\mathrm{O^{++}})$	$T(\mathrm{H^+})$	$t^2(\mathrm{H^+})$	$t^2(\mathrm{O^{++}})$
$\log(\mathrm{O/H}) = -3.66$	9760 K	9340 K	0.0083	0.006
$\log(\mathrm{O/H}) = -2.66$	7430 K	6860 K	0.01	0.007
$\log(\mathrm{O/H}) = -4.06$	11,200 K	10,900 K	0.0036	0.004
$\log(\mathrm{N/H}) = -3.74$	9760 K	9340 K	0.0083	0.006
$\log(\mathrm{N/H}) = -4.4$	9850 K	9410 K	0.01	0.007
$\log(\mathrm{N/H}) = -3.04$	9410 K	9050 K	0.005	0.0032

lower than the normal abundances given by [9]. Whereas the abundances decreases by scale factor 1/5, its peak temperature greater than the normal one. Similarly, when the abundances increases, $t^2 \approx 0.007$ whereas $t^2 \approx 0.004$ when the O abundances decrease by scale factor 1/5. This result shows that there is slight variation with the result obtained by [3] for uniform density distribution. This shows that when the abundances increases, its temperature fluctuations increases. In similar way $T(O^{++})$, the rise of the abundances and temperature of ionized O are in the contrary. When it increases by scale factor its temperature is 7430 K and drops by 1/5, its temperature rises to 11,200 K.

When the abundances of O is increased by a scale factor 5, the temperature of H ($T(H^+)$) is decreased by 26.5% and its temperature fluctuation $t^2(O^{++})$ is slightly increased by 0.001. But it drops by scale factor 1/5, temperature of H rises to 10 900 K and its fluctuation is $t^2(H^+) = 0.004$.

Similarly, when the abundance of nitrogen increases by scale factor 5, its temperature of $T(O^{++})$ decreases by 3.7%. This is much smaller than the previous one. Its temperature fluctuation $t^2(H^+)$ of H and O when the abundances of N increases by scale factor 5 are 0.05 and 0.0032 respectively. But when the abundance of nitrogen drops by scale factor 1/5, its temperature is slightly greater than the normal abundances given by [9].

In the first model, we have more diluted nebulae ionized by a hot star. We have chosen hydrogen density $n(H) = 10^4$ cm^{-3}, change by $\alpha = -0.5$, and $T_\star = 75{,}000$ K. The result is shown in **Figure 1** describes the

Table 5. Elemental abundances used in the this model and the result obtained.

	$T_\star = 100{,}000$ K, $n(H) = 10^3$ cm^{-3}, $\alpha = -0.5$, $Q(H) = 10^{48}$ phs^{-1} and $R = 10^{16}$ cm			
Abundances	$T(O^{++})$	$T(H^+)$	$t^2(H^+)$	$t^2(O^{++})$
$\log(O/H) = -3.66$	9476 K	8950 K	0.013	0.008
$\log(O/H) = -2.66$	7550 K	5270 K	0.043	0.003
$\log(O/H) = -4.06$	11,100 K	10,800 K	0.006	0.003
$\log(N/H) = -3.74$	9470 K	8950 K	0.001	0.008
$\log(N/H) = -4.4$	9710 K	9210 K	0.02	0.007
$\log(N/H) = -3.04$	8490 K	7830 K	0.0013	0.009

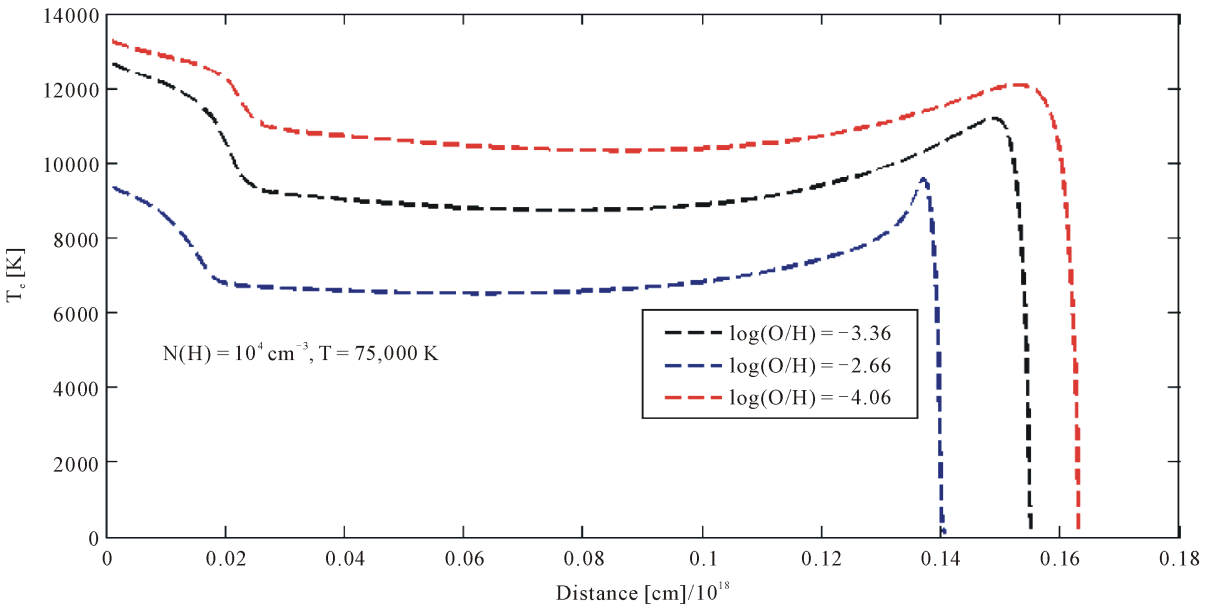

Figure 1. Temperature structure for the first model. Green broken line is the abundances of oxygen increase by scale factor 5, whereas black dot line is the abundances decrease by scale factor 1/5 and red broken line is for the normal abundances given by [9], $T_\star = 75{,}000$ K, and $n(H) = 10^3$, $\alpha = -0.5$.

temperature of electrons drops when the abundances of the most cooling elements increase by scale factor 5. The higher the abundances of oxygen elements, its peak temperature drops faster than the other two cases. Similarly the abundances of nitrogen shown in **Figure 2** increase by the scale factor 5, its variation of temperature fluctuation is significant relative to oxygen abundances. But this does not mean that, nitrogen abundances have not impacts on changing the temperature. At a distance around 0.145 pc, the variations of temperature are high relative to other points.

In the second model, we have more diluted nebulae ionized by a hot star and we have chosen hydrogen density $n(\mathrm{H}) = 10^3$ cm^{-3}, change by $\alpha = -0.5$, and $T_\star = 10^5$ K. The result shown in **Figure 3** and **Figure 4**

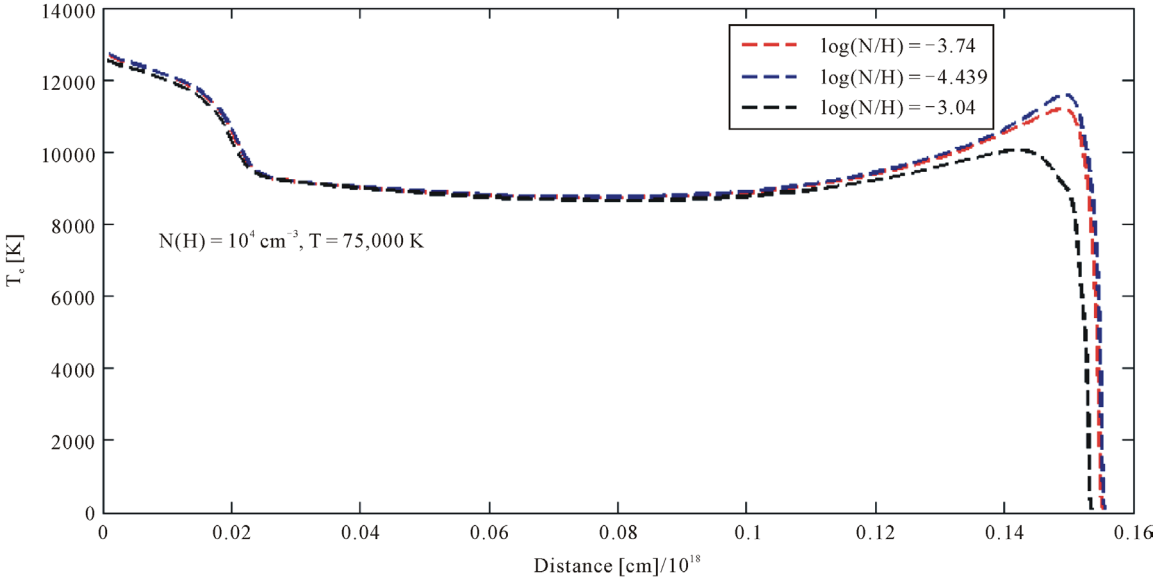

Figure 2. Temperature structure for the first model. Green broken line is the abundances of nitrogen decrease by scale factor 1/5, whereas black dot line is the abundances increase by scale factor 5 and red broken line is for the normal abundances given by [9] $T_\star$ = 75,000 K, and $n(\mathrm{H}) = 10^3$, $\alpha = -0.5$.

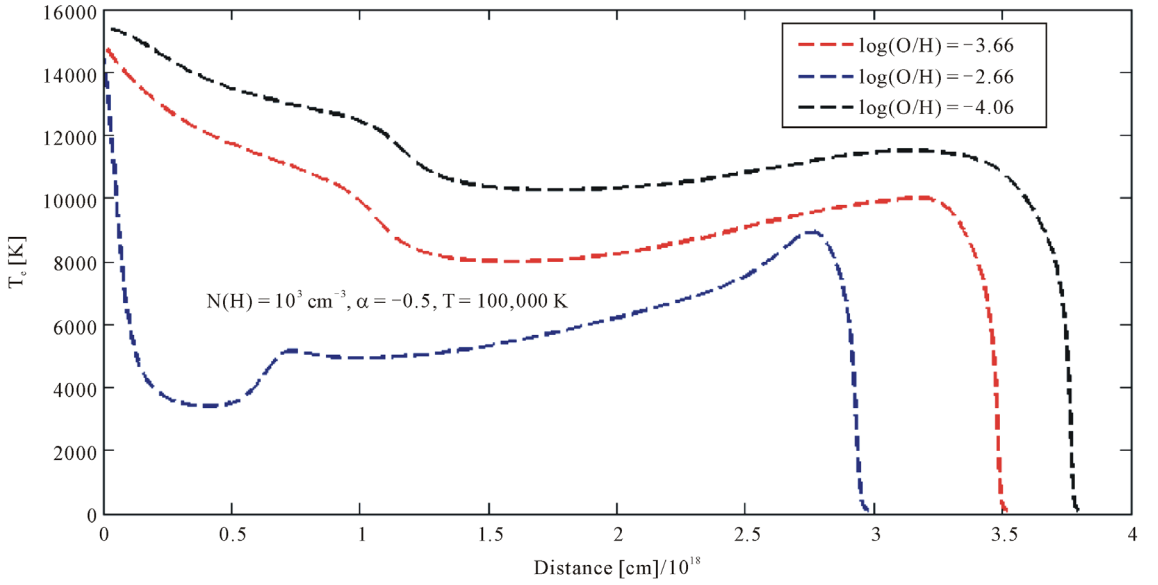

Figure 3. Temperature structure for the second model. Green broken line is the abundances of oxygen increase by scale factor 5, whereas black dot line is the abundances decrease by scale factor 1/5 and red broken line is for the normal abundances given by [9], $T_\star$ = 100,000 K, and $n(\mathrm{H}) = 10^4$.

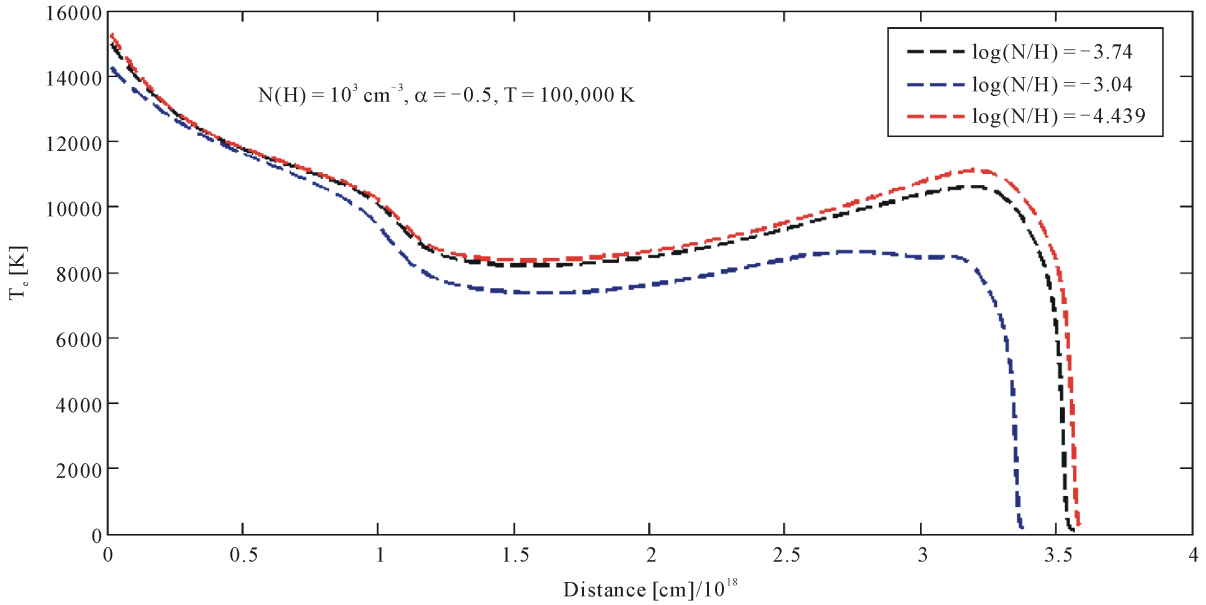

Figure 4. Temperature structure for the first model. Green broken line is the abundances of oxygen increase by scale factor 5, whereas black dot line is the abundances decrease by scale factor 1/5 and red broken line is for the normal abundances given by [9], $T_\star$ = 100,000 K, and n(H) = 10^4.

describe the temperature of electron is greatest when the abundances of both O and N are smallest. Since these elements are the main cooling agents, its temperature structure shows that through the processes temperature drops in both cases. Temperature fluctuations of O and N are smaller in this model.

5. Conclusion

In this paper we present a study of temperature fluctuation on two different cases, for uniform and non uniform hydrogen density at two different temperatures of 75,000 and 100,000 K. This was done by in homogeneities on the emission lines, based on statistical approximation introduced by [11], which quantities the brightness increase or decrease of each line in terms of the departure of the temperature from the average temperature T_0 described by Equation (1). The main results are based on the analysis of chemical abundances of oxygen and nitrogen on different mechanism to test such change. Temperature fluctuations are obtained from the photoionization models generated by the spectral synthesis code CLOUDY (C10.00), calculated using the recombination theory for hydrogenic ions. Accurate t^2 values have been obtained by comparing the O^{++} abundances derived from recombination lines with those derived from collisionally excited lines. It is clear from the result that temperature variations $t^2 < 0.01$ value as described in [14]. The main causes of temperature fluctuations are chemical inhomogeneities of heavy metals, density variations and temperature of central stars.

Acknowledgements

We thank our supervisor Prof. Dreck Smith, the Editor and the referee for their comments. This research is funded by the Dire-Dawa University and My Friend Mr. Yared Ayele who arrived at the right time. This support is greatly appreciated.

References

[1] Knigdon, J. and Ferland, G. (1998) Temperature Fluctuations in Photoionized Nebulae. II. The Effect of Inhomogeneous Abundances. *The Astrophysical Journal*, **506**, 323-328.

[2] Peimbert, M. and Torres-Poembert, S. (1971) Planetary Nebulae III. Chemical Abundances. *The Astrophysical Journal*, **168**, 413-421. http://dx.doi.org/10.1086/151097

[3] Gruenwald, R. and Viegas, S.M. (1995) Temperature Fluctuations in Planetary Nebulae. *A & A*, **303**, 535.

[4] Gonzalez-Delgado, R.M., *et al.* (1994) Temperature Fluctuations in H II Region. *ApJ*, **287**, 116.

[5] Esteban, RevMexAA(Sc) (2002) Temperature Fluctuations in H Regions.

[6] Ferland, G.J. (2011) Hazy: Introduction to Cloudy c10.00.

[7] Knigdon, J. and Ferland, G. (1995) Temperature Fluctuations in Photoionized Nebulae I. *The Astrophysical Journal*, **450**, 691-704.

[8] Giammanco, C. and Beckman, J.E. (2005) Temperature Fluctuations in H Regions: Ionization by Cosmic Rays as a Key Mechanism. *A & A*, **437**, L11-L14.

[9] Smith, D. (2011) Model of Hydrogen Deficient Nebulae. *Astrophysics Journal*.

[10] Grevesse, N.A.E. (1989) Solar System Abundances of the Elements. In: AIP conf. proc.183. Cosmic Abundances od Matter.

[11] Torres-Peimbert A & A, 223-540, 1990.

[12] Pequignot.D, J.F.M.M..M.P., W.J. (2002) Henney Ionized Gaseous Nebulae. In: Editors, Eds., *Conference Series of the Revisita Mexican de Astrnomiya Y Astrofisica*, in Press.

[13] Bresolin, F., Garnett, D.R. and Kennicutt Jr., R.C. (2004) Abundances of Metal-Rich H II Regions in M51. *The Astrophysical Journal*, **615**, 228-241.

[14] Torres-Peimbert, S. and Peimbert, M. (2002) Temperature Variations and Abundances Determinations in Planetary Nebulae. Instituto de Astronom'ia, Universidad Nacional Auto'noma de Me'xico.

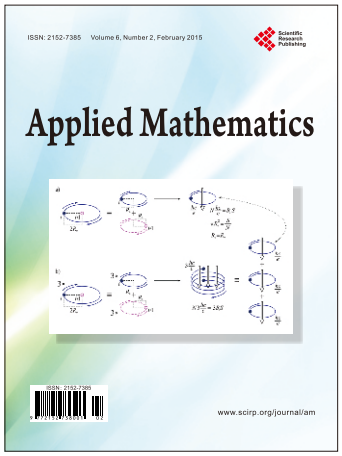

Call for Papers

Applied Mathematics (AM)

ISSN Print: 2152-7385 ISSN Online: 2152-7393
http://www.scirp.org/journal/am

Applied Mathematics **(AM)** is an international journal dedicated to the latest advancement of applied mathematics. The goal of this journal is to provide a platform for scientists and academicians all over the world to promote, share, and discuss various new issues and developments in different areas of applied mathematics.

Subject Coverage

All manuscripts must be prepared in English, and are subject to a rigorous and fair peer-review process. Accepted papers will immediately appear online followed by printed hard copy. The journal publishes original papers including but not limited to the following fields:

- Applied Probability
- Applied Statistics
- Approximation Theory
- Chaos Theory
- Combinatorics
- Complexity Theory
- Computability Theory
- Computational Methods in Mechanics and Physics
- Continuum Mechanics
- Control Theory
- Cryptography
- Discrete Geometry
- Dynamical Systems
- Elastodynamics
- Evolutionary Computation
- Financial Mathematics
- Fuzzy Logic
- Game Theory
- Graph Theory
- Information Theory
- Inverse Problems
- Linear Programming
- Mathematical Biology
- Mathematical Chemistry
- Mathematical Economics
- Mathematical Physics
- Mathematical Psychology
- Mathematical Sociology
- Matrix Computations
- Neural Networks
- Nonlinear Processes in Physics
- Numerical Analysis
- Operations Research
- Optimal Control
- Optimization
- Ordinary Differential Equations
- Partial Differential Equations
- Probability Theory
- Statistical Finance
- Stochastic Processes
- Theoretical Statistics

We are also interested in: 1) Short Reports—2-5 page papers where an author can either present an idea with theoretical background but has not yet completed the research needed for a complete paper or preliminary data; 2) Book Reviews—Comments and critiques.

Notes for Intending Authors

Submitted papers should not have been previously published nor be currently under consideration for publication elsewhere. Paper submission will be handled electronically through the website. All papers are refereed through a peer review process. For more details about the submissions, please access the website.

Website and E-mail

http://www.scirp.org/journal/am **E-mail: am@scirp.org**

What is SCIRP?

Scientific Research Publishing (SCIRP) is one of the largest Open Access journal publishers. It is currently publishing more than 200 open access, online, peer-reviewed journals covering a wide range of academic disciplines. SCIRP serves the worldwide academic communities and contributes to the progress and application of science with its publication.

What is Open Access?

All original research papers published by SCIRP are made freely and permanently accessible online immediately upon publication. To be able to provide open access journals, SCIRP defrays operation costs from authors and subscription charges only for its printed version. Open access publishing allows an immediate, worldwide, barrier-free, open access to the full text of research papers, which is in the best interests of the scientific community.

- High visibility for maximum global exposure with open access publishing model
- Rigorous peer review of research papers
- Prompt faster publication with less cost
- Guaranteed targeted, multidisciplinary audience

Scientific Research Publishing

Website: http://www.scirp.org

Subscription: sub@scirp.org

Advertisement: service@scirp.org